frontiers | Research Topics

Vascular immunity and ischemic stroke

Edited by
Yanlin Zhang, Xia Wang and Jie Lu

Published in
Frontiers in Neurology

ISSN 1664-8714
ISBN 978-2-8325-5692-4
DOI 10.3389/978-2-8325-5692-4

About Frontiers

Frontiers is more than just an open access publisher of scholarly articles: it is a pioneering approach to the world of academia, radically improving the way scholarly research is managed. The grand vision of Frontiers is a world where all people have an equal opportunity to seek, share and generate knowledge. Frontiers provides immediate and permanent online open access to all its publications, but this alone is not enough to realize our grand goals.

Frontiers journal series

The Frontiers journal series is a multi-tier and interdisciplinary set of open-access, online journals, promising a paradigm shift from the current review, selection and dissemination processes in academic publishing. All Frontiers journals are driven by researchers for researchers; therefore, they constitute a service to the scholarly community. At the same time, the *Frontiers journal series* operates on a revolutionary invention, the tiered publishing system, initially addressing specific communities of scholars, and gradually climbing up to broader public understanding, thus serving the interests of the lay society, too.

Dedication to quality

Each Frontiers article is a landmark of the highest quality, thanks to genuinely collaborative interactions between authors and review editors, who include some of the world's best academicians. Research must be certified by peers before entering a stream of knowledge that may eventually reach the public - and shape society; therefore, Frontiers only applies the most rigorous and unbiased reviews. Frontiers revolutionizes research publishing by freely delivering the most outstanding research, evaluated with no bias from both the academic and social point of view. By applying the most advanced information technologies, Frontiers is catapulting scholarly publishing into a new generation.

What are Frontiers Research Topics?

Frontiers Research Topics are very popular trademarks of the *Frontiers journals series*: they are collections of at least ten articles, all centered on a particular subject. With their unique mix of varied contributions from Original Research to Review Articles, Frontiers Research Topics unify the most influential researchers, the latest key findings and historical advances in a hot research area.

Find out more on how to host your own Frontiers Research Topic or contribute to one as an author by contacting the Frontiers editorial office: frontiersin.org/about/contact

Vascular immunity and ischemic stroke

Topic editors

Yanlin Zhang — Second Affiliated Hospital of Soochow University, China

Xia Wang — University of New South Wales, Australia

Jie Lu — Nanjing Brain Hospital Affiliated to Nanjing Medical University, China

Citation

Zhang, Y., Wang, X., Lu, J., eds. (2024). *Vascular immunity and ischemic stroke*. Lausanne: Frontiers Media SA. doi: 10.3389/978-2-8325-5692-4

Table of contents

frontiers | Frontiers in Neurology

TYPE Review
PUBLISHED 08 November 2022
DOI 10.3389/fneur.2022.1048113

OPEN ACCESS

EDITED BY
Yanlin Zhang,
Second Affiliated Hospital of Soochow University, China

REVIEWED BY
Chengyan Chu,
Dalian Municipal Central Hospital, China
Yimei Hong,
Guangdong Provincial People's Hospital, China

*CORRESPONDENCE
Min Huang
hmwalkman@163.com
Yuling Mao
maovuling0121@126.com

SPECIALTY SECTION
This article was submitted to Stroke, a section of the journal Frontiers in Neurology

RECEIVED 19 September 2022
ACCEPTED 17 October 2022
PUBLISHED 08 November 2022

CITATION
Tan N, Xin W, Huang M and Mao Y (2022) Mesenchymal stem cell therapy for ischemic stroke: Novel insight into the crosstalk with immune cells. *Front. Neurol.* 13:1048113. doi: 10.3389/fneur.2022.1048113

Mesenchymal stem cell therapy for ischemic stroke: Novel insight into the crosstalk with immune cells

Nana Tan[1], Wenqiang Xin[2], Min Huang[1]* and Yuling Mao[3,4]*

[1]Department of Health Management, The Third Affiliated Hospital of Guangzhou Medical University, Guangzhou, China, [2]Department of Neurosurgery, Tianjin Medical University General Hospital, Tianjin, China, [3]Department of Obstetrics and Gynecology, Center for Reproductive Medicine, Guangdong Provincial Key Laboratory of Major Obstetric Diseases, The Third Affiliated Hospital of Guangzhou Medical University, Guangzhou, China, [4]Key Laboratory for Reproductive Medicine of Guangdong Province, The Third Affiliated Hospital of Guangzhou Medical University, Guangzhou, China

Stroke, a cerebrovascular accident, is prevalent and the second highest cause of death globally across patient populations; it is as a significant cause of morbidity and mortality. Mesenchymal stem cell (MSC) transplantation is emerging as a promising treatment for alleviating neurological deficits, as indicated by a great number of animal and clinical studies. The potential of regulating the immune system is currently being explored as a therapeutic target after ischemic stroke. This study will discuss recent evidence that MSCs can harness the immune system by interacting with immune cells to boost neurologic recovery effectively. Moreover, a notion will be given to MSCs participating in multiple pathological processes, such as increasing cell survival angiogenesis and suppressing cell apoptosis and autophagy in several phases of ischemic stroke, consequently promoting neurological function recovery. We will conclude the review by highlighting the clinical opportunities for MSCs by reviewing the safety, feasibility, and efficacy of MSCs therapy.

KEYWORDS

ischemic stroke, mesenchymal stem cells, immunomodulation, preclinical study, clinical trials

Introduction

Stroke is responsible for almost six million deaths, at least 10% of all mortalities yearly, and two-thirds of stroke survivors remain disabled (1). Worldwide, over 80 million people have survived a stroke; 70% of incident strokes are ischemic (1). Although recent evolutions of thrombectomy technology, as well as improvements in imaging devices, have achieved ground-breaking changes in ischemic stroke therapy (2), given its narrow therapeutic time window and the concern of hemorrhagic complications (3), thrombolysis is still not performed routinely (4). In this context, it is urgent to yield neurorestorative treatments for abrogating stroke-induced neurological deficits for both basic scientists and clinical researchers. Cell therapy is emerging as a promising novel modality for facilitating neurologic recovery after a stroke (5). Harnessing the immune

system to function and effectively boost neurologic recovery has transitioned from a theoretical possibility to a viable therapeutic option for ischemic stroke. Mesenchymal stem cells (MSCs) transplantation is an attractive therapy method because they have the potential for proliferation, differentiation, and immunomodulatory properties (6, 7). While the MSCs can be derived from any type of tissue beyond the bone marrow, adipose, and placenta, these MSCs share the same core attributes of ability to cell migration patterns and behave as immunomodulatory cells (8–10). In addition to immunomodulation, growing evidence demonstrates that MSCs are involved in multiple pathological processes by targeting series downstream. Such downstream activities include the inhibition of apoptosis and autophagy and the promotion of angiogenesis, neurogenesis, and synaptic remodeling in several phases of ischemic stroke (11, 12). MSCs may also be an ideal candidate for cell transplantation therapy for ischemic stroke. Despite growing evidence indicating that MSCs may improve neurological function under pathological conditions, including stroke (13, 14), data on the interaction between MSCs and immunomodulation is limited. In this review, we summarize the therapeutic effects of MSCs both in preclinical studies and in clinical stroke trials. We also consider the mutual crosstalk between MSCs and immune cells under stroke conditions.

Mesenchymal stem cells

Rodent bone marrow cells were first ectopically transplanted into the kidney capsule by Friedenstein et al. in the 1960s and 1970s, showing an osteogenic effect (15). Given the potential to differentiate into various cell lineages, Caplan et al. suggested the "mesenchymal stem cells" term in 1991 (16, 17). MSCs are multipotent fibroblast-like cells that, interestingly, exist in various adult tissues, including adipose tissue, periosteum, liver, spleen, muscle connective tissue, placenta, umbilical cord blood, dental pulp, and aborted fetal tissues (18–20). Further, The Mesenchymal and Tissue Stem Cell Committee of the International Society for Cellular Therapy (ISCT) recommended specific minimum MSC criteria to distinguish them from other cell types by expression of many cell surface markers, including CD73, CD90, and CD105, and the absence of expression of CD45, CD34, CD14, CD19, CD11b, or Human Leukocyte Antigen–DR isotype (21–23). Recently, a significant number of novel cell surface markers associated with the stemness within MSCs, namely SSEA1/4, CD44, CD146, and CD271, have been revealed as well (23–26). A further two criteria are that isolated cells show adherence to plastic in culture and the capacity to differentiate into adipocytes, osteoblasts, and chondroblasts *in vitro* (21–23). To date, MSCs have become the most widely studied stem cell population and are studied in various preclinical models and clinical settings alike. And these studies have focused on the vital roles in coordinating tissue responses to ischemic stroke in acute and post-acute stroke settings, in which MSCs modulate cell survival, cell apoptosis, autophagy angiogenesis, and immunosuppression (23), consequently supporting neurological recovery.

Therapeutic application of MSCs in preclinical ischemic stroke study

MSCs promote post-stroke cell survival

Upon an ischemic stroke, the cerebral artery occlusion influences the survival of various brain cells, such as brain neurons, glial cells, and vascular cells. Among these cells, the neurons are the most vulnerable, and neuronal viability plays a crucial role in neurological recovery after ischemic stroke (27, 28). Studies in experimental models mimicking ischemic stroke imply that MSCs can abrogate ischemia-induced neuronal survival and neurological function recovery. As such, under such conditions, MSCs derived from bone marrow, adipose tissue, and umbilical cord can significantly reduce neuronal death (29–31). In addition, neurological recovery is also associated with the successful restitution of vascular and glial functions. During the ischemic lesion remodeling, neurons, glial cells, and vascular cells can strongly interact with each other, contributing to neurological recovery (27). Interestingly, it is demonstrated that MSCs are involved in promoting the survival of microglia, astrocyte, and endotheliocyte survival via regulating many pathways (32–35). Notably, white matter demyelination predates axonal injury in the early stage of ischemic stroke, indicating a time window for stroke intervention focusing on preventing or postponing axonal injury through myelin regeneration (36). Meanwhile, Bagdasarian et al. (37) applied therapeutic MSC to a rodent stroke model and demonstrated their efficacy in white matter by comparison of Diffusion tensor imaging and Neurite Orientation Dispersion and Density Imaging metrics. MSCs exert many unique biological effects, including self-recovery via promoting post-stroke cell survival, providing a promising cellular therapeutic approach for treating white matter injury (38).

MSCs suppress post-stroke cell apoptosis

Among the many cell death pathways (39), apoptosis accounts for a large proportion of cell death under such a condition (40), a rational and reactive performance made to sacrifice specific cells for the benefit of the tissue. Researchers have indicated that MSCs have vital roles in regulating cell apoptosis. For example, Kong et al. (41) demonstrated MSCs potentially protect the cortical neurons from OGD injury *in vitro* by rescuing neurons from apoptosis. Xiao et al. (42) indicated that bone marrow-derived MSC-exosomes repressed

oligodendrocyte apoptosis via releasing exosomal miR-134, in turn negatively regulating the caspase-8-dependent apoptosis pathway. In addition to apoptosis, MSCs can promote cell survival by alleviating parthanatos and necroptosis. By co-culturing MSCs with hypoxic neurons, Kong et al. indicated that MSCs prevented neurons from parthanatos by suppressing the expression of nuclear translocation of apoptosis-inducing factors (41). The reduction of neuronal necrosis kinase RIP1 and RIP3 levels caused by MSCs, meanwhile, was tightly related to the suppression of neuronal necroptosis (41).

MSCs suppress post-stroke cell autophagy

Autophagy, another type of cell death, is an evolutionarily conserved cellular mechanism that balances cellular nerve homeostasis. It is a process that results from the injury in cells' internal conditions, including starvation, hypoxia, and infection (43). MSCs can inhibit autophagy and, in turn, promote cell survival. Kuang et al. (31) illustrated that the application of adipose-derived MSC-exosomes suppressed the autophagic response under both *in vitro* hypoxia and *in vivo* cerebral ischemia regarding cell survival through transferring of miR-25, as a consequence, supporting post-stroke neurological function recovery. Moreover, the knockdown of SNHG12 in MSCs boosted the effects of MSCs in suppressing hypoxia-induced autophagy in brain microvascular endothelial cells and MCAO rats by interacting with the PI3K/AKT/mTOR signaling pathway (44). By contrast, MSCs can reverse ischemic injury by enhancing autophagy as well (45, 46). Likewise, Zeng et al. indicated that PC12 cells were exposed to oxygen-glucose deprivation (OGD) and cocultured with MSCs secreted extracellular vesicles (EVs). Under such conditions, MSC-secreted EVs significantly attenuated pyroptosis mediated by NLRP3 inflammasome by promoting AMPK-dependent autophagy flux (47).

MSCs promote post-stroke angiogenesis

During post-stroke conditions, capillaries are dysfunctional, and blood-brain barrier permeability is increased, consequently aggravating the inflammatory reaction and neuronal necrosis. In addition to rescuing and restoring neuronal cells, increasing evidence has shown that increasing the survival of endothelial cells, ameliorating brain angiogenesis, and mediating the recanalization of brain collaterals are great therapeutic targets. MSCs transplantation has been revealed to migrate to the peri-infarct region and differentiate into neuronal, glial, and endothelial cells to enhance neuroplasticity (30). Moreover, MSCs act in an indirect paracrine way as well. MSCs have also been shown to induce regenerative processes by increasing the level of insulin-like growth factor 1 (IGF-1) and inducing vascular endothelial growth factor (VEGF), angiopoietin-1 (Ang-1), essential fibroblast growth factor (bFGF), and neurotrophic factors in the host brain (48–51). These bioactive factors of VEGF and Ang-1 are the most essential in promoting neurological recovery by boosting neurogenesis. Besides that, the hypoxia and 0.04 MHz ultrasound-modified MSCs and MSCs-derived exosomes have been illustrated to have the capacity to achieve angiogenic effects (14, 52–54). Significantly, implantation of MSCs promoted angiogenesis and increased neurogenesis by releasing these angiogenic and neurotrophic factors. By conducting a three-dimensional analysis of the neovascularization in the peri-infarct region, Toyama et al. (55) and Chen et al. (56) demonstrated that the capillary-like tube formation was significantly induced in stroke mice treated with MSCs, suggesting a direct effect of MSCs on facilitating angiogenesis.

MSCs support the post-stroke immunomodulatory effects

MSCs-microglia interactions

Microglia, which comprise a significant immune cell population in the central nervous system, appear as a ramified structure with a small soma in the resting form under physiological conditions (57, 58). When activated by ischemic stroke, microglia increase in number and transform to amoeboid forms characterized by the larger microglial cell body and shorter bumps. The activation of microglia activation is the first step in response to inflammation; further, the other immune cells, such as T cells, neutrophils, and natural killer cells, are activated (59, 60). While MSCs in microglial activation have been widely studied, there is not enough research on transplantation in ischemic stroke. Plenty of studies investigating various donor cell-derived MSCs identified a novel insight into crosstalk in ischemic stroke, and the role of MSCs in microglial activation has begun to be recognized (14, 61–63). For example, Yang et al. (64) indicated that bone marrow-MSCs can shift the microglia phenotype from M1 to M2, contributing to MSCs-induced brain repair. As a paracrine interaction between MSCs and microglia, the synergistic effect of MANF and PDGF-AA pathway governed M2 polarization. Furthermore, despite peripheral LPS treatment before the stroke, increased CD16/32-M1 microglia boosted the number of microglia surrounding the peri-infarct region and diminished CD206-M2 microglia on the post-stroke seventh day; they were rectified by the administration of human umbilical cord MSCs (65). Moreover, a series of researchers have accessed the effects of MSCs on microglial activation (14, 61–75); more details are shown in

TABLE 1 Preclinical stroke studies assessing the effect of MSCs on the activation of microglia.

Author	Year	Country	Species	Dosage	Route	MSCs source	The main effects on microglia	References
Cunningham et al.	2020	UK.	Mice	1.4×10^6	Sub	BM	Have no effect microglial Iba1 expression	(61)
Narantuya et al.	2010	Japan	Rats	NA	IV	BM	Reduce microglial activation and MMP level	(66)
Ishizaka et al.	2013	Japan	Rats	1×10^6	IA	NA	Suppress microglia activation in the peri-infarct and core lesion	(67)
Yamaguchi et al.	2018	Japan	Rats	1×10^6	IA	Blood	Suppress microglia activation in the peri-infarct cortex	(62)
Wang et al.	2014	China	Rats	2×10^6	IV	BM	Inhibit macrophages/microglia activation in the ischemic brain	(68)
Wei et al.	2012	America	Rats	1×10^6	IV	BM	Inhibit microglia activation in the ischemic brain	(14)
Nakajima et al.	2017	Japan	Rats	1×10^6	IV	BM	Inhibit microglia activation and proinflammatory levels	(69)
McGuckin et al.	2013	France	Rats	NA	Stereotaxis	UC.	Decrease markers of microglial activation (lower ED1 and Iba)	(63)
Li et al.	2018	China	Rats	1×10^6	IV	BM	Inhibit microglia activation	(70)
Lv et al.	2016	China	Cells	NA	NA	BM.	Inhibit hypoxia-activated rat microglia	(71)
Sheikh et al.	2019	Japan	Rats	3×10^6	IV	BM	Inhibit microglia activation	(72)
Wang et al.	2013	Japan	Rats	3×10^6	IV	BM	Inhibit microglia activation and proinflammatory gene levels	(73)
Yoo et al.	2013	South Korea	Rats	5×10^5	Stereotaxis	BM.	Inhibit microglia activation	(74)
Sheikh et al.	2011	Japan	Rats	3×10^6	IV	BM	Decrease the accumulation of Iba-1+ microglia	(75)
Feng et al.	2020	China	Mice	1×10^6/20 g	IV	UC	Inhibit CD16/32-M1 microglia, Promote CD206-M2 microglia	(65)
Yang et al.	2020	China	Rats	1×10^6	IV	BM	Induce M2 microglia polarization through PDGF-AA/MANF	(64)

NA, not available; IA, intraarterial; IV, intravenous; Sub, subcutaneous; BM, bone marrow; UC, umbilical cord; OGD, oxygen-glucose deprivation; MSCs, mesenchymal stem cell; IL, interleukin.

Table 1. To sum up, the application of MSCs appears to inhibit microglial activation and promote M2 polarization.

MSCs-neutrophils interactions

Neutrophils are the essential infiltrating cell type in the ischemic brain the first few days after stroke (76), tightly correlating with ischemic stroke-induced BBB disruption. The preclinical stroke studies have implied that MSCs' administration can reduce neutrophil accumulation in the brain. Vehicle or EVs (the equivalent of 2 × 106 MSCs) were intravenously administered to mice after transient intraluminal middle cerebral artery occlusion (77). MSC-EVs decreased specifically polymorphonuclear neutrophil infiltration in ischemic brains of aged mice. Moreover, MSCs can boost the beneficial effects of neutrophils on the brain. Bone marrow-MSCs can potentially induce interleukin-17 (IL-17) production in memory $CD4^+$ T cells that, in turn, promote the enhanced phagocytic activity of neutrophils (78). Still, bone marrow-MSCs may also protect resting and interleukin-8-activated neutrophils from apoptosis, preserving their effector functions and suppressing the reactive oxygen species production (79).

MSCs-natural killer (NK) cells interactions

NK cells, one type of lymphocyte, belong to a part of the innate immune system that is well-known for the potential to mediate cytotoxicity and produce cytokines (80).

The immunomodulatory effects of MSCs on NK cells have been extensively studied in the peripheral regions. MSCs are involved in inhibiting the differentiation, proliferation, cytotoxicity, and activation of the NK cells through a variety of cytokines (81). These cytokines may include prostaglandin E2 (PGE2), soluble human leukocyte antigen-G5 (sHLA-G5), and transforming growth factor-β (TGF-β), which is partly linked to glycoprotein A repetitions predominant on the surface of

MSCs (82). Additionally, hypoxic MSCs can also repress NK cell cytotoxicity and reduce the accumulation of host-derived NK cells when transplanted *in vivo*, as a result, contributing to ameliorating limb ischemia in allogeneic recipients (83).

MSCs-dendritic cells (DCs) interactions

The immune response to ischemic stroke consists of inflammatory and regulatory processes. DC is one of the cell types involved in innate and adaptive immunity. Upon an ischemic condition, the brain DCs are increased at 24- and 72-h post-stroke and accumulated in the peri-infarct region near invading T cells (84). Peripheral DC appearing in the brain was apparent at 72-h post-stroke and was confined primarily to the lesion core (84). MSCs are revealed to have capacities to suppress DCs differentiation and maturation and even reverse mature DCs to immature states (85–88). Gao et al. (85) indicated that MSCs inhibited the differentiation of human monocyte-derived DCs through both releasing IL-10 and direct cell contact. Likewise, Zhao et al. (87) showed that MSCs can differentiate mature DCs into a distinct regulatory DC population characterized by a lower expression of CD1a, CD80, CD86, and CD40 and a higher expression of CD11b. Importantly, such an effect on inhibiting DCs differentiation and maturity is demonstrated to be linked to both maintaining homeostasis of regulatory T cells and lower levels of proinflammatory cytokines TNF-α and MHC II surface antigens (86, 87).

MSCs-T cells interactions

T cells, which are involved in both innate and adaptive immune responses, can be divided into the αβ subset and the unconventional γδ subset (89). The αβ subset includes $CD4^+$ T helper cells (Th1, Th2, Th17) that mainly modulate the functions of phagocytes and granulocytes, $CD8^+$ T cells that have a cytotoxic role, and regulatory T cells (Treg) that regulate immune responses (89). After the ischemia-onset, T cells are revealed at the border of the infarct, where they appear within days (90, 91). More specifically, $CD8^+$ T cells are recruited as early as 3 h post-ischemia onset, with $CD4^+$ T cells and NK T cells following within 24 h, and accumulation of these T cells peaks 3 to 4 days after ictus (76, 92, 93). There is solid evidence that MSCs are linked to direct immunosuppressive properties via suppressing the activation and proliferation of $CD4^+$ and $CD8^+$ T cells while promoting activation, differentiation, and proliferation of Tregs through direct cell-to-cell communication or releasing of various factors. Upon a hypoxic-ischemic encephalopathy condition, MSCs can induce persistent peripheral T-cell tolerance and inhibit the invasion of T-cells into the preterm brain (94). During a critical limb ischemia condition, MSCs showed effective prevention of Th1 priming, which was strongly related to an altered IL-12/IL-10 production (95). Likewise, in renal ischemia/reperfusion rats, by releasing TGF-β, MSCs can not only suppress $CD8^+$ T cells but boost the development of Tregs, as a result, repressing T cell-related inflammation (96). As such, MSCs might therefore contribute to suppressing the activation and proliferation of $CD4^+$ and $CD8^+$ T cells and promoting the proliferation of Tregs during an ischemic condition. However, information regarding this aspect of the interaction between MSCs and T cells upon an ischemic stroke condition appears to be limited. It is scarce, so additional and reliable data is urgently needed.

MSCs-B cells interactions

B cells, one part of the adaptive immune response, have the capacity to present antigens, produce antibodies, and activate the immune system (97). These cells are detectable in insufficient quantities in the brain under normoxic conditions; however, they are trafficked in larger quantities to the brain tissues in response to injury (98, 99). B cell adoptive transfer to mice does not contribute to acute pathology but can support post-stroke recovery, independent of changing immune populations in recipient mice (100). Completed and ongoing clinical trials and preclinical studies on the therapeutic effects of MSCs transplantation against immune-mediated diseases have demonstrated an increased generation of B cells (101). The effectiveness of related MSCs-B cell interaction-based treatments dramatically depends on the functions of Bregs, as MSCs can increase the secretion of IL-10 by Bregs (101). On the contrary, several studies identified that MSCs are involved in suppressing the activation and proliferation of B cells. For instance, human adipose tissue-derived MSCs can inhibit the proliferation and chemotaxis of B cells by inducing cell cycle arrest in G0/G1 phase and regulating CXCR4 and CXCR5 expression, respectively (102). As such, *in vitro*, by secreting various factors, MSCs decreased the proliferation of B cells and the production of immunoglobulin (103). Taken together, the combined effects on the proliferation and activation of B cells are found in MSCs. However, the precise effect of inhibition/promotion on B cells modulated under ischemic stroke conditions is not fully clear yet. An overview of how MSCs interact with immune cells is shown in Figure 1.

MSCs improve the post-stroke neurological function recovery

The size of the infarct volume is tightly correlated with ischemic stroke severity. *In vivo* experiments on MCAO rats demonstrated that MSCs derived from bone marrow, adipose tissue, and the umbilical cord could reduce the post-stroke infarct volume (104). However, many conditions, such as the source of MSCs, species injected, and the timing and dose of MSC injection, can affect specific effects on decreasing

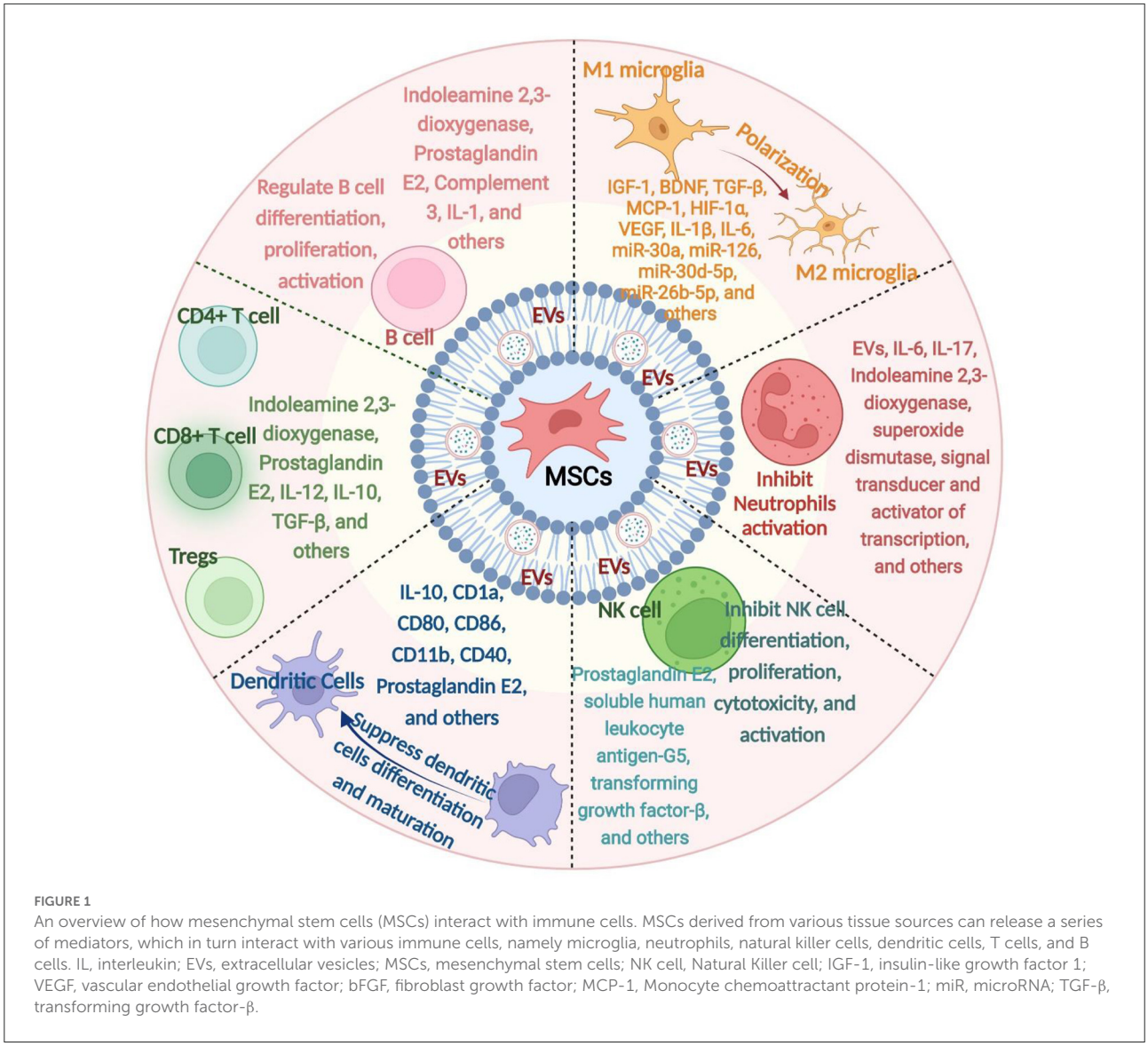

FIGURE 1
An overview of how mesenchymal stem cells (MSCs) interact with immune cells. MSCs derived from various tissue sources can release a series of mediators, which in turn interact with various immune cells, namely microglia, neutrophils, natural killer cells, dendritic cells, T cells, and B cells. IL, interleukin; EVs, extracellular vesicles; MSCs, mesenchymal stem cells; NK cell, Natural Killer cell; IGF-1, insulin-like growth factor 1; VEGF, vascular endothelial growth factor; bFGF, fibroblast growth factor; MCP-1, Monocyte chemoattractant protein-1; miR, microRNA; TGF-β, transforming growth factor-β.

infarct volume after stroke. Along with such a reduction of infarct volume, the behavioral test analyses illustrated better test scores of mice/rats transplanted with MSCs at either time. Of note, this better test performance in the corner turn test, the rotarod test, balance beam test, tightrope test, and paw slips recording was long-lasting and stable until the end of the observation period (31, 105–107). It is suggested that MSCs can potentially mitigate postischemic motor coordination impairment in preclinical stroke experiments. Significantly, post-stroke impairment of the blood-brain barrier and perifocal vasogenic edema are also alleviated by endovascular MSCs administration. Post-stroke edema, impairment of the blood-brain barrier, as well as upregulation of aquaporin 4 (AQP4) water transport channels, play an essential role in the progression of ischemia and deteriorating disease recovery. Datta et al. (108) presented preliminary evidence that 1×10^5 endovascular MSCs at 6 h post-stroke down-regulates AQP4 expression and alleviates vasogenic edema toward neuroprotection. Likewise, MSCs protected blood-brain barrier integrity by inhibiting the ischemia-induced astrocyte apoptosis, owing to the downregulation of AQP4 expression via the p38 signaling pathway (109).

The underlying patterns of how MSCs exhibit the therapeutic effects

MSC-EVs are critical players in treating ischemic stroke

EVs, the membrane-enclosed nanoscale particles secreted by all eukaryotes, always serve as a variety of molecular cargoes,

such as peptides, lipids, proteins, and noncoding RNAs (43, 110). Based on the size of EVs, they can be divided into three subtypes: exosomes, microvesicles, and apoptotic bodies (111). Exosomes with a diameter of 30–150 nm form via the fusion of multivesicular bodies with membrane and are further released into the extracellular matrix (112, 113). Microvesicles with a diameter of 200–1,000 nm are produced owing to the outward budding of the plasma membrane (112, 113). Conversely, apoptotic bodies with a diameter of 1,000–5,000 nm are produced by dying cells and are even more abundant than the two other particles (111). Only exosomes and microvesicles are relevant to the therapeutic effects imparted by MSC-EVs. When these nanosized vesicles are released from donor cells into the extracellular matrix, they can be internalized by numerous recipient cells. In turn, they transfer the above bioactive cargos into recipient cells, including near and far from the secreting cell, further serving as messengers and performing biological functions. This cargo mix is revealed to mediate the biological properties of EVs and, indirectly, the treatment of MSCs under ischemic stroke conditions. The EVs derived from MSCs are emerging to be an appealing therapeutic tool for ischemic stroke, with the MSC-derived properties and the characteristics of effortless storage, lower immunogenicity, higher safety profile, and nature delivery vehicles. Previous research works indicated that EVs derived from MSCs promoted post-stroke recovery. They have the capacity to regulate the expression of recipient cell genes, alter cell properties involved in ischemic stroke, and mediate restorative effects, including cell survival, cell apoptosis, cell autophagy, angiogenesis, neurological function recovery, and immunomodulation, through a variety of molecular cargoes transfer (13, 31, 33, 34, 42, 53, 114–142). Moreover, by inhibiting the release of EVs, the beneficial effect on these aspects is also suppressed. For example, by establishing a coculture model that MSCs cocultured with hypoxic neurons and brain microvascular endothelial cells, the results showed that the MSCs treatment could inhibit the apoptosis of hypoxic neurons and restore the tube formation of brain microvascular endothelial cells (143). However, an inhibitor, GW4869, of EVs secretion can reverse these beneficial effects, indicating that these EVs are the key players that serve as the central mediator of the neuroprotective and angiogenic effects of MSCs (143). Currently, studies are paying attention to the function of the EVs isolated from bone marrow, adipose tissue, and, sometimes, umbilical cord-MSCs (144).

The critical role of noncoding RNAs (NcRNAs) in treating ischemic stroke

Despite being well-established that most human RNA transcripts cannot encode proteins, the emerging evidence demonstrates that ncRNAs regulate cell physiology and shape cellular functions (145, 146). ncRNAs can be divided into long [namely long noncoding RNA (lncRNA) and circRNA] and small ncRNAs [including microRNAs (miRNAs), tRNAs, and piRNAs] by taking 200 nucleotides as the limit (147). miRNAs, ∼18–24 nucleotides in size, are much earlier reported and the most discussed. lncRNAs are a large and heterogeneous kind of ncRNAs with more than 200 nucleotides and are involved in the modulation of transcription, translation, RNA metabolism, as well as homeostasis (148–150). CircRNAs are defined as circular covalently bonded structures associated with a higher tolerance to exonucleases (151), which serve as a scaffold for chromatin-modifying complexes, regulating the expression level of parental genes, modulating mRNA splicing, and acting as miRNA sponges (152, 153). Notably, the aberrant expression of many noncoding RNAs has been associated with aggressive pathologies. A variety of ncRNAs are reduced in the ischemic brain or blood after ischemic stroke, as previously reported for circSCMH1, miR-124-3p, miR-126, miR-221-3p, and miR-132 (114–119, 154), whereas other ncRNAs, namely miR-98 and miR-494, are increased at defined follow-up (155–157). MSC-based therapies offer an attractive approach because they promote cell survival, angiogenesis, and neurological function recovery, suppress cell apoptosis and autophagy, and regulate immunomodulation, where ncRNAs play an essential role. Interestingly, these ncRNAs were mainly derived from EVs, including lncRNA MALAT1, miR-1-3p, miR-17-92, miR-22-3p, miR-25, miR-26a, miR-26b-5p, miR-31, miR-124, miR-126, miR-132, miR-133b, miR-134, miR-138-5p, miR-146a-5p, miR-181b, miR-206, miR-210, miR-221-3p, miR-223-3p, miR-542-3p, and miR-1290 (31, 33, 34, 42, 114, 115, 117, 119, 121–125, 129–133, 135, 136, 138, 158). These EVs are isolated from bone marrow and adipose tissue, as well as umbilical cord-MSCs. Additionally, MSCs can regulate the expression of ncRNA directly, in turn, to support neuroprotection. For instance, Yang et al. indicated that MSCs-mediated mesencephalic astrocyte-derived neurotrophic factor paracrine signaling, the PDGF-AA/miR-30a*/XBP1/MANF pathway, synergistically mediates MSC-induced M2 polarization (64). Likewise, Huang et al. found that, with enhanced cell homing, MSCs can be applied to deliver miR-133b to boost the expression level of miR-133b in an ischemic lesion and further improve therapeutic effects (159). To sum up, MSCs can not only directly regulate the level of ncRNA but also indirectly regulate the level of ncRNA in the form of secreting exosomes, thus promoting the improvement of neurological function recovery. More details regarding preclinical studies that evaluate the effect of MSC-ncRNA on treating ischemic stroke are shown in Table 2 (31, 33, 34, 42, 64, 114, 115, 117, 119, 121–125, 129–133, 135, 136, 138, 158, 159).

TABLE 2 Preclinical studies evaluating the effect of MSC-non-coding RNA on treating ischemic stroke.

Authors	Country, year	ncRNA	Expression	Source	Donor cell	Recipient cell	Main function
Zhong and Luo (135)	China, 2021	miR-1-3p	Upregulation	EVs	ucMSCs	Primary neurons	Promote cell viability and inhibit apoptosis
El Bassit et al. (158)	USA, 2017	lncR MALAT1	Upregulation	EVs	MSCs	HT22 neuronal cells	Promote cell viability
Xin et al. (131)	China, 2017	miR-17-92	Upregulation	EVs	MSCs	Neurons, glial cells	Promote neuroplasticity
Zhang et al. (123)	China, 2021	miR-22-3p	Upregulation	EVs	ADSCs	Primary neurons	Promote cell viability and inhibit apoptosis
Kuang et al. (31)	Germany, 2020	miR-25	Upregulation	EVs	ADSCs	Primary neurons	Inhibit autophagy
Hou et al. (124)	China, 2021	miR-26a	Upregulation	EVs	ADSCs	Primary neurons	Promote cell viability and inhibit apoptosis
Ling et al. (132)	China, 2020	miR-26a	Upregulation	EVs	USCs	NSCs	Promote neurogenesis
Li et al. (122)	China, 2020	miR-26b-5p	Upregulation	EVs	ucMSCs	SH-SY5Y, PC12, microglia	Inhibit apoptosis and inflammation
Lv et al. (125)	China, 2020	miR-31	Upregulation	EVs	ADSCs	Primary neurons	Promote cell viability and inhibit apoptosis
Yang et al. (133)	China, 2017	miR-124	Upregulation	EVs	BMSCs	NPCs	Promote neurogenesis
Geng et al. (119)	China, 2019	miR-126	Upregulation	EVs	ADSCs	Neurons, ECs, BV2	Promote neurogenesis and inhibit inflammation
Feng et al. (114)	China, 2018	miR-132	Upregulation	EVs	BMSCs	Primary neurons	Promote cell viability and inhibit apoptosis
Xin et al. (121)	China, 2013	miR-133b	Upregulation	EVs	BMSCs	Neurons, AS	Promote neurite outgrowth
Xiao et al. (42)	China, 2018	miR-134	Downregulation	EVs	BMSCs	OLs	Inhibit apoptosis
Deng et al. (34)	China, 2019	miR-138-5p	Upregulation	EVs	BMSCs	Primary AS	Inhibit apoptosis
Zhang et al. (33)	China, 2021	miR-146a-5p	Upregulation	E.V.s	ucMSCs	BV2 microglia	Inhibit inflammation
Yang et al. (129)	China, 2018	miR-181b	Upregulation	EVs	ADSCs	BMECs	Promote angiogenesis
Zhong and Luo (135)	China, 2021	miR-206	Upregulation	EVs	ucMSCs	Primary neurons	Promote cell viability and inhibit apoptosis
Zhang et al. (130)	China, 2019	miR-210	Upregulation	EVs	BMSCs	BMECs	Promote angiogenesis
Ai et al. (115)	China, 2021	miR-221-3p	Upregulation	EVs	BMSCs	Primary neurons	Inhibit apoptosis and inflammation
Zhao et al. (136)	China, 2020	miR-223-3p	Upregulation	EVs	MSCs	BV2	Inhibit inflammation
Cai et al. (117)	China, 2021	miR-542-3p	Upregulation	EVs	MSCs	HA1800 AS	Inhibit apoptosis and inflammation
Yue et al. (138)	China, 2019	miR-1290	Upregulation	EVs	ucMSCs	Primary neurons	Inhibit apoptosis
Yang et al. (64)	China, 2020	miR-30a*	Upregulation	Cells	MSCs	Microglia	Inhibit inflammation
Huang et al. (159)	China, 2017	miR-133b	Upregulation	Cells	MSCs	Neurons/Astrocytes	Promote cell viability

BMSCs, Bone marrow-derived mesenchymal stem cells; ADSCs, adipose-derived stem cells; ucMSCs, umbilical cord mesenchymal stem cells; USCs, human urine-derived stem cells; EVs, Extracellular vesicles.

The critical role of trophic factors and cytokines in treating ischemic stroke

Preclinical studies in rodent models of ischemic stroke have uncovered the potential effectiveness of the administration of trophic factors in ischemic brain injury recovery. The brain-derived neurotrophic factor (BDNF), glial cell line-derived neurotrophic factor (GDNF), and vascular endothelial growth factor (VEGF) are the most described (160). MSCs released or stimulated the release of three aforementioned neurotrophic factors associated with the contribution of ischemic stroke recovery. After administration, MSCs migrated from the vascular system outside the lesion to the area of the lesion core or peri-lesion to reduce the infarct volume by secreting BDNF, GDNF, and VEGF (161, 162). BDNF protein, highly expressed in the hippocampus, is known to affect the survival and proliferation of several neural cells, including cerebellar and cortical neurons (163). BDNF rapidly boosts in response to ischemic brain injury, contributing to reducing neuronal apoptosis and promoting neuronal survival (163). GDNF, produced by glial cells after brain injury, accelerates the survival and recovery of several types of mature neurons, including motor and dopaminergic neurons (164). VEGF, produced by neurons and astrocytes, is involved in

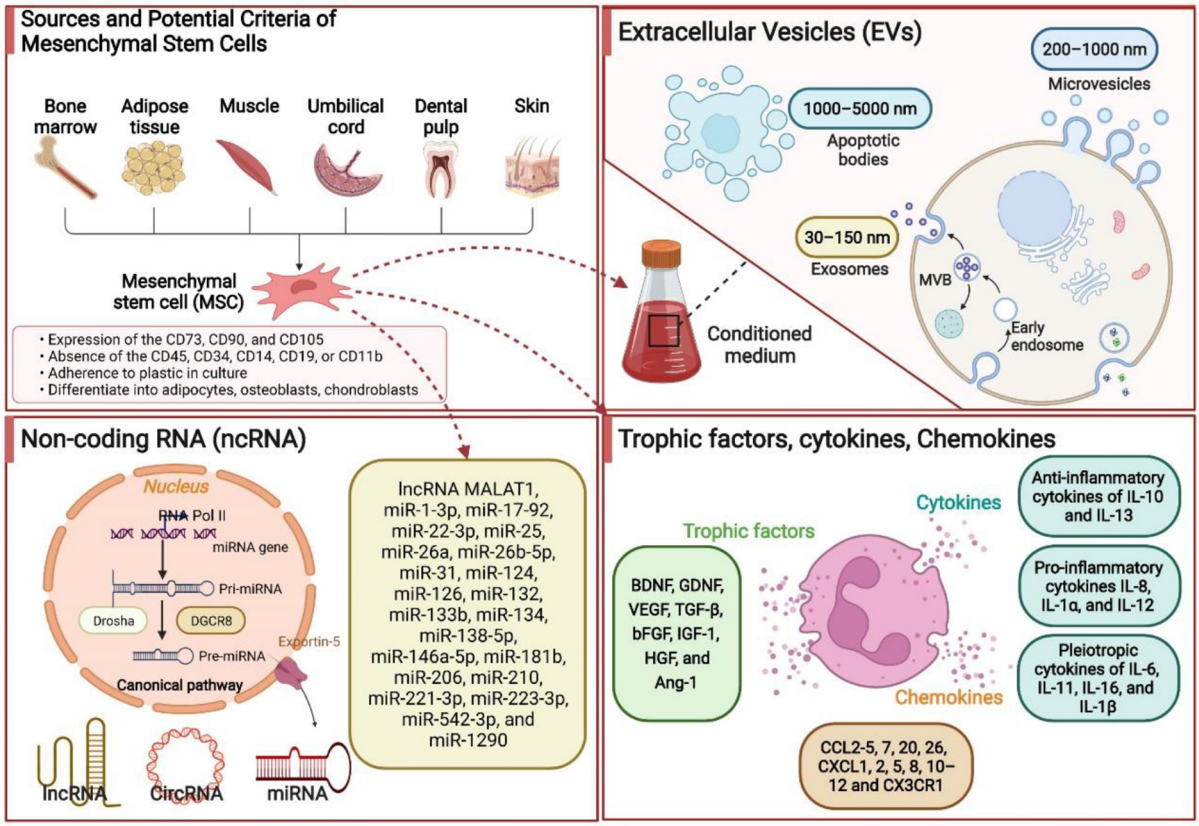

FIGURE 2
Some of the underlying therapeutic mechanisms associated with the mesenchymal stem cells (MSCs) in ischemic stroke. MSCs are isolated and identified from various tissue sources. These MSCs produce extracellular vesicles (EVs), noncoding RNAs (ncRNAs), trophic factors, chemokines, and cytokines by paracrine mechanisms to promote neurological recovery. Based on the EVs size, they can be divided into three subtypes, namely exosomes (30–150 nm), microvesicles (200–1,000 nm), and apoptotic bodies (1,000–5,000 nm). ncRNAs primarily include microRNA, long noncoding RNA, and circRNA. BDNF, brain-derived neurotrophic factor; GDNF, glial cell line-derived neurotrophic factor; VEGF, vascular endothelial growth factor; bFGF, basic fibroblast growth factor; IL, interleukin; TGF-β, transforming growth factor-β; HGF, hepatocyte growth factor; miR, microRNA.

various stages of neurodevelopment (proliferation, migration, differentiation, synaptogenesis, myelination (160). Additionally, VEGF stimulates angiogenesis by stimulating endothelial cell proliferation and migration and increases blood-brain barrier integrity (160). Notably, further growth and trophic factors, namely TGF-β, bFGF, IGF-1, HGF, and HGF, released or regulated by MSCs, are also involved in post-stroke neurological recovery. The types of cytokines released directly by MSCs or indirectly modulated in response to neuroinflammation due to stem cell transplantation are huge. They cannot be discussed in full detail here. Briefly, anti-inflammatory cytokines of IL-10 and IL-13, proinflammatory cytokines IL-8, IL-1α, and IL-12, and pleiotropic cytokines of IL-6, IL-11, IL-16, and IL-1β, correlated to immune function modulation after ischemic stroke, are revealed to be directly or indirectly produced by MSCs (165). In summary, MSCs played diverse therapeutic roles by secreting a series of trophic factors and cytokines. Hence, gene modification could be performed to enhance the therapeutic effects of MSCs by modulating the trophic factors and cytokines. However, attention should be given to the adverse effects of trophic factors and cytokines due to the adverse concentration. Some of the underlying therapeutic mechanisms associated with MSCs in ischemic stroke are summarized in Figure 2.

Therapeutic application of stem cells in clinical ischemic stroke study

Meta-analysis: The clinical application of MSCs in treating ischemic stroke

A comprehensive literature search of several electronic databases, namely PubMed, Cochrane Library, EMBASE,

TABLE 3 Main characteristics of the clinical study assessing stem cells in treating ischemic stroke.

References	Country	Study design	Sample size	Stem cell type	Cell dosage	Injection route	Follow-up
Bhatia et al. (166)	India	RCT	20	Autologous BMMNCs	6.1×10^8	IV	1 year
Bang et al. (181)	South Korea	RCT	30	Autologous MSCs	5×10^7/2 times	IV	12 months
Meng et al. (179)	China	Non-RCT	120	Autologous MSCs	2.97×10^9	IV	Half a year
Lee et al. (171)	South Korea	RCT	52	Autologous MSCs	5×10^7/2 times	IV	5 years
Bhasin et al. (174)	India	Non-RCT	24	Autologous BMMNCs	5.46×10^7	IV	24 weeks
Bhasin et al. (175)	India	Non-RCT	40	Autologous BMMNCs and MSCs	5.54×10^7	IV	24 weeks
Prasad et al. (172)	India	RCT	120	Autologous MSCs	2.8×10^8	IV	1 year
Chen et al. (167)	China	RCT	30	Autologous PBSCs	$3–8 \times 10^6$	IA.	Half a year
Bhasin et al. (176)	India	Non-RCT	20	Autologous BMMNCs	6.28×10^7	IV	8 weeks
Ghali et al. (178)	Egypt	Non-RCT	39	Autologous BMMNCs	1×10^6	IA	1 year
Bhasin et al. (177)	India	Non-RCT	12	Autologous MSCs	$5–6 \times 10^7$	IV	4 years
Hess et al. (169)	UK/USA	RCT	129	Allogeneic MAPC	1.2×10^9	IV	1 year
Jin et al. (170)	China	RCT	20	Autologous BMMNCs	1×10^7	Subarachnoid	7 years
Fang et al. (168)	China	RCT	16	Autologous EPSs and MSCs	2.5×10^6/kg/2 times	IV	4 years
Savitz et al. (173)	USA	RCT	48	Autologous BM ALDHbr Cells	3.08×10^6	IA	1 year
Moniche et al. (180)	Spain	Non-RCT	20	Autologous BMMNCs	3.38×10^6	IA	Half a year

ALDHbr, aldehyde dehydrogenase; BMMNC, bone marrow-derived mononuclear cell; EPS, endothelial progenitor cell; IA, intra-arterial infusion; IV, intravenous infusion; MSCs, mesenchymal stem cells; PBSC, peripheral blood stem cell; MAPC, multipotent adult progenitor cells; RCT, randomized controlled trial.

and Web of Science, was performed by two researchers independently from the inception of these databases to 30 June 2022. We retrieved studies assessing stem cells in treating ischemic stroke by adopting the following keywords: "stem cell" together with "ischemia," "stroke," "middle cerebral artery occlusion," or "MCAO." References from the identified reports were manually searched to identify other potential qualifying studies. The specific screening process is shown in Supplementary Figure 1. A total of 16 reports were included in this section from South Korea, India, the UK, China, the United States, Egypt, and Spain, which were conducted varied from 2005 to 2019 (166–181). Table 3, Supplementary Table 1 described the characteristics and quality assessment of included studies, respectively. The Stata, version 12.0, was used for endpoint analyses. When $I^2 > 50\%$, the data were deemed to have apparent heterogeneity, and a random-effect model was adopted. Otherwise, a fixed-effects model was adopted. Among all outcomes, weighted mean differences (WMD) or rate differences (RDs) with 95% CIs were applied for the assessment.

First, this study analyzed the efficacy of MSCs on patients with ischemic stroke through the modified Rankin Scale (mRS), National Institutes of Health Stroke Scale (NIHSS), and Barthel index (BI). Data on mRS were provided by night studies. There are 219 and 227 participants in the MSCs and control groups. The patients treated with MSCs were associated with a statistically significant lower mRS value (WMD, −0.354; 95% CI, −0.681 to −0.027; $P = 0.034$, Figure 3A). Similarly, seven and nine studies reported the data of NIHSS and BI, respectively. The cross-sectional data from various studies were plotted and demonstrated that the NIHSS was statistically lower (WMD, −1.538; 95% CI, −2.506 to −0.571; $P = 0.002$, Figure 3B) and BI was statistically higher (WMD, 7.444; 95% CI, −4.488 to 10.401; $P < 0.001$, Figure 3C) in the MSCs group than that of the control group. Second, we also evaluated the safety of MSCs on patients with ischemic stroke; 15 studies (356 and 354

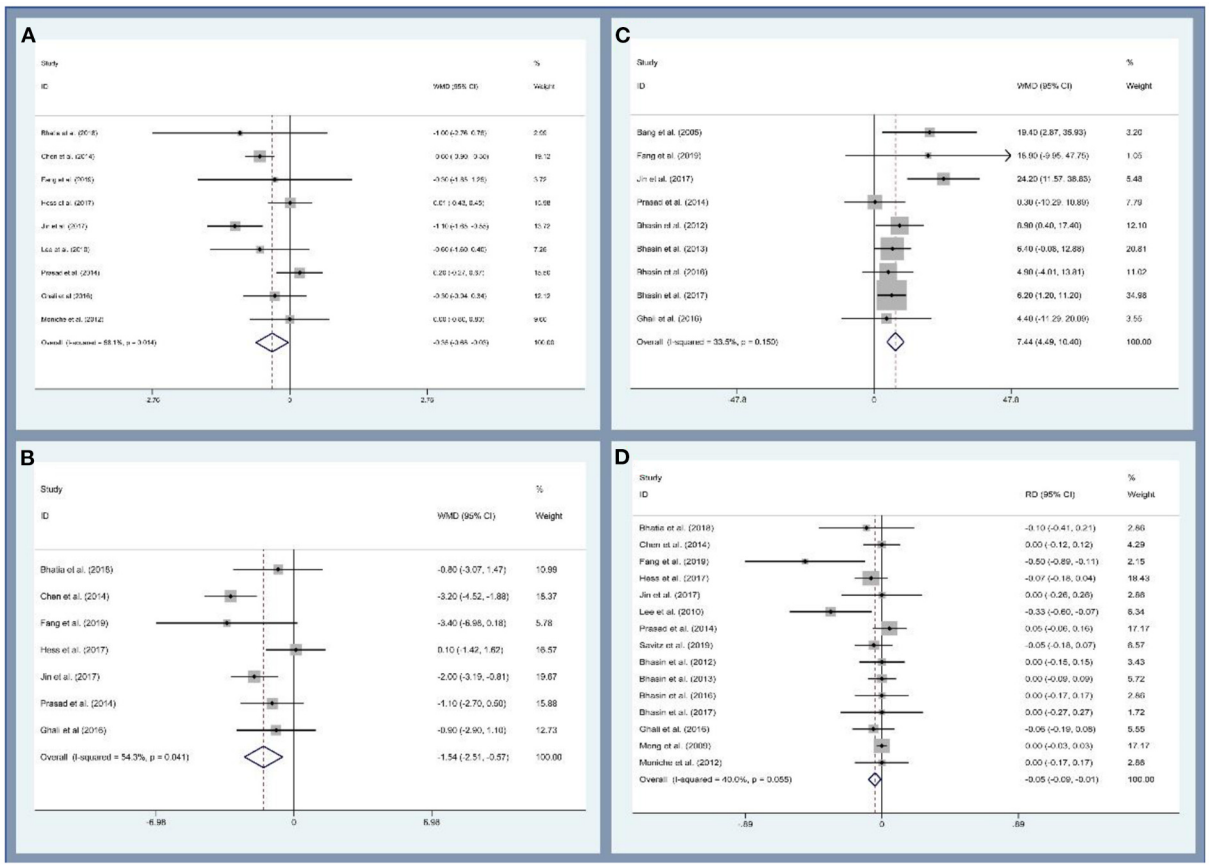

FIGURE 3
Forest plot for meta-analysis of the modified Rankin Scale (mRS) **(A)**, National Institute of Health Stroke Scale (NIHSC) **(B)**, Barthel index (BI) **(C)**, and death rate **(D)**.

patients in the MSCs and control group, respectively) reported the death rate. No significant heterogeneity was observed, and a fix-effect model was used (I^2 = 40%, P = 0.055). The death rate between the experimental and control groups was statistically significant (RD, −0.046; 95% CI, −0.086 to −0.005; P = 0.026, Figure 3D). More details regarding the results are described in Supplementary Table 2. Altogether, stem cell-based therapies have the capacity to improve neurological deficits and activities of daily living in patients with ischemic stroke. However, several common limitations exist for current studies, such as small sample size, long-term waiting for MSC culture, age of participants, heterogeneity of ischemic brain injury site, and severity (155, 156).

The clinical translation of MSC-based therapy for ischemic stroke is booming, and MSCs are expected to improve the sequence of ischemic stroke in patients. Nevertheless, this treatment has led to some controversy as well. (I) Stem cell translation has the potential to result in tumor formation (157). For example, stem cells derived from embryonic stem cells may have the potential for tumorigenicity. Moreover, a reduction of genetic modification of stem cells will be associated with a lower risk of tumor formation. (II) the controlled treatment of transplanted exogenous stem cells to regulate differentiation and achieve the desired therapeutic effect has yet to be studied (157, 182). (III) the insufficient brain delivery and retention and the invasiveness of current administration routes prevent MSCs from fully exerting their clinical therapeutic potential (183). (IV) the issue of immune rejection is also necessary to be addressed. Although MSCs rarely express the major histocompatibility complex, they can still cause some immunological issues (182).

Conclusion

The application of MSCs in treating ischemic stroke is vast. In preclinical settings, the transplantation of MSCs offers an excellent opportunity for adjuvant ischemic stroke treatment, participating in multiple pathological processes, such as increasing cell survival angiogenesis and suppressing cell apoptosis and autophagy. Importantly, immunomodulation

is another excellent target of MSCs by interacting with a variety of immune cells, namely microglia, neutrophils, NK cells, DCs, T cells, and B cells. However, no large-scale randomized, double-blind, multicenter clinical study exists to prove their effectiveness. In clinic, MSCs have many advantages: they are easy to harvest, expand, and store for a long time and are convenient to manage in many ways. Additionally, their clinical use does not raise many ethical issues. Increasing evidence supports the potential of MSCs to treat stroke, and autologous stem cell-based therapies can improve post-stroke neurological deficits and daily living activities in patients with minimal clinical adverse events. Nevertheless, the heterogeneity of MSCs is the primary barrier to their clinical application and therapeutic effect. Nonetheless, despite these issues, the application of MSCs appears to achieve neuroprotective effects, which result from the release of EVs and modification of various signaling pathways, such as ncRNAs, trophic factors, and cytokines.

Author contributions

NT, MH, and YM designed and conceptualized the article. NT prepared the figures and tables. All authors significantly contributed to writing the paper and provided important intellectual content.

Conflict of interest

The authors declare that the research was conducted in the absence of any commercial or financial relationships that could be construed as a potential conflict of interest.

Publisher's note

All claims expressed in this article are solely those of the authors and do not necessarily represent those of their affiliated organizations, or those of the publisher, the editors and the reviewers. Any product that may be evaluated in this article, or claim that may be made by its manufacturer, is not guaranteed or endorsed by the publisher.

Supplementary material

The Supplementary Material for this article can be found online at: https://www.frontiersin.org/articles/10.3389/fneur.2022.1048113/full#supplementary-material

References

1. Phipps MS, Cronin CA. Management of acute ischemic stroke. *BMJ.* (2020) 368:l6983. doi: 10.1136/bmj.l6983

2. Khandelwal P, Yavagal DR, Sacco RL. Acute ischemic stroke intervention. *J Am Coll Cardiol.* (2016) 67:2631–44. doi: 10.1016/j.jacc.2016.03.555

3. Del Zoppo GJ, Saver JL, Jauch EC, Adams HP Jr. Expansion of the time window for treatment of acute ischemic stroke with intravenous tissue plasminogen activator: a science advisory from the American Heart Association/American Stroke Association. *Stroke.* (2009) 40:2945–8. doi: 10.1161/STROKEAHA.109.192535

4. Liu X. Beyond the time window of intravenous thrombolysis: standing by or by stenting? *Interv Neurol.* (2012) 1:3–15. doi: 10.1159/000338389

5. Savitz SI, Chopp M, Deans R, Carmichael ST, Phinney D, Wechsler L. Stem cell therapy as an emerging paradigm for stroke (STEPS) II. *Stroke.* (2011) 42:825–9. doi: 10.1161/STROKEAHA.110.601914

6. Sui BD, Zheng CX, Li M, Jin Y, Hu CH. Epigenetic regulation of mesenchymal stem cell homeostasis. *Trends Cell Biol.* (2020) 30:97–116. doi: 10.1016/j.tcb.2019.11.006

7. Fu X, Liu G, Halim A, Ju Y, Luo Q, Song AG. Mesenchymal stem cell migration and tissue repair. *Cells.* (2019) 8:784. doi: 10.3390/cells8080784

8. Chamberlain G, Fox J, Ashton B, Middleton J. Concise review: mesenchymal stem cells: their phenotype, differentiation capacity, immunological features, and potential for homing. *Stem Cells.* (2007) 25:2739–49. doi: 10.1634/stemcells.2007-0197

9. Djouad F, Plence P, Bony C, Tropel P, Apparailly F, Sany J, et al. Immunosuppressive effect of mesenchymal stem cells favors tumor growth in allogeneic animals. *Blood.* (2003) 102:3837–44. doi: 10.1182/blood-2003-04-1193

10. Song N, Scholtemeijer M, Shah K. Mesenchymal stem cell immunomodulation: mechanisms and therapeutic potential. *Trends Pharmacol Sci.* (2020) 41:653–64. doi: 10.1016/j.tips.2020.06.009

11. Kim HY, Kim TJ, Kang L, Kim YJ, Kang MK, Kim J, et al. Mesenchymal stem cell-derived magnetic extracellular nanovesicles for targeting and treatment of ischemic stroke. *Biomaterials.* (2020) 243:119942. doi: 10.1016/j.biomaterials.2020.119942

12. Wang F, Tang H, Zhu J, Zhang JH. Transplanting mesenchymal stem cells for treatment of ischemic stroke. *Cell Transpl.* (2018) 27:1825–34. doi: 10.1177/0963689718795424

13. Zhao Y, Gan Y, Xu G, Yin G, Liu D. MSCs-derived exosomes attenuate acute brain injury and inhibit microglial inflammation by reversing CysLT2R-ERK1/2 mediated microglia M1 polarization. *Neurochem Res.* (2020) 45:1180–90. doi: 10.1007/s11064-020-02998-0

14. Wei L, Fraser JL, Lu ZY, Hu X, Yu SP. Transplantation of hypoxia preconditioned bone marrow mesenchymal stem cells enhances angiogenesis and neurogenesis after cerebral ischemia in rats. *Neurobiol Dis.* (2012) 46:635–45. doi: 10.1016/j.nbd.2012.03.002

15. Friedenstein AJ, Petrakova KV, Kurolesova AI, Frolova GP. Heterotopic of bone marrow. Analysis of precursor cells for osteogenic and hematopoietic tissues. *Transplantation.* (1968) 6:230–47. doi: 10.1097/00007890-196803000-00009

16. Andrzejewska A, Lukomska B, Janowski M. Concise review: mesenchymal stem cells: from roots to boost. *Stem Cells.* (2019) 37:855–64. doi: 10.1002/stem.3016

17. Xin WQ, Wei W, Pan YL, Cui BL, Yang XY, Bähr M, et al. Modulating poststroke inflammatory mechanisms: novel aspects of mesenchymal stem cells, extracellular vesicles and microglia. *World J Stem Cells.* (2021) 13:1030–48. doi: 10.4252/wjsc.v13.i8.1030

18. Kern S, Eichler H, Stoeve J, Klüter H, Bieback K. Comparative analysis of mesenchymal stem cells from bone marrow, umbilical cord blood, or adipose tissue. *Stem Cells.* (2006) 24:1294–301. doi: 10.1634/stemcells.2005-0342

19. In 't Anker PS, Noort WA, Scherjon SA, Kleijburg-Van Der Keur C, Kruisselbrink AB, Van Bezooijen RL, et al. Mesenchymal stem cells in human second-trimester bone marrow, liver, lung, and spleen exhibit a similar immunophenotype but a heterogeneous multilineage differentiation potential. *Haematologica.* (2003) 88:845–52.

20. Yeo RW, Lai RC, Zhang B, Tan SS, Yin Y, Teh BJ, et al. Mesenchymal stem cell: an efficient mass producer of exosomes for drug delivery. *Adv Drug Deliv Rev.* (2013) 65:336–41. doi: 10.1016/j.addr.2012.07.001

21. Horwitz EM, Le Blanc K, Dominici M, Mueller I, Slaper-Cortenbach I, Marini FC, et al. Clarification of the nomenclature for MSC: the International Society for Cellular Therapy position statement. *Cytotherapy.* (2005) 7:393–5. doi: 10.1080/14653240500319234

22. Dominici M, Le Blanc K, Mueller I, Slaper-Cortenbach I, Marini F, Krause D, et al. Minimal criteria for defining multipotent mesenchymal stromal cells. The International Society for Cellular Therapy position statement. *Cytotherapy.* (2006) 8:315–17. doi: 10.1080/14653240600855905

23. Li J, Zhang Q, Wang W, Lin F, Wang S, Zhao J. Mesenchymal stem cell therapy for ischemic stroke: a look into treatment mechanism and therapeutic potential. *J Neurol.* (2021) 268:4095–107. doi: 10.1007/s00415-020-10138-5

24. Lv FJ, Tuan RS, Cheung KM, Leung VY. Concise review: the surface markers and identity of human mesenchymal stem cells. *Stem Cells.* (2014) 32:1408–19. doi: 10.1002/stem.1681

25. Camilleri ET, Gustafson MP, Dudakovic A, Riester SM, Garces CG, Paradise CR, et al. Identification and validation of multiple cell surface markers of clinical-grade adipose-derived mesenchymal stromal cells as novel release criteria for good manufacturing practice-compliant production. *Stem Cell Res Ther.* (2016) 7:107. doi: 10.1186/s13287-016-0370-8

26. Pachón-Peña G, Donnelly C, Ruiz-Cañada C, Katz A, Fernández-Veledo S, Vendrell J, et al. A glycovariant of human CD44 is characteristically expressed on human mesenchymal stem cells. *Stem Cells.* (2017) 35:1080–92. doi: 10.1002/stem.2549

27. Hermann DM, Chopp M. Promoting brain remodelling and plasticity for stroke recovery: therapeutic promise and potential pitfalls of clinical translation. *Lancet Neurol.* (2012) 11:369–80. doi: 10.1016/S1474-4422(12)70039-X

28. Reitmeir R, Kilic E, Kilic U, Bacigaluppi M, Elali A, Salani G, et al. Post-acute delivery of erythropoietin induces stroke recovery by promoting perilesional tissue remodelling and contralesional pyramidal tract plasticity. *Brain.* (2011) 134(Pt. 1):84–99. doi: 10.1093/brain/awq344

29. Xiao X, Li W, Xu Z, Sun Z, Ye H, Wu Y, et al. Extracellular vesicles from human umbilical cord mesenchymal stem cells reduce lipopolysaccharide-induced spinal cord injury neuronal apoptosis by mediating miR-29b-3p/PTEN. *Connect Tissue Res.* (2022) 63:634–49. doi: 10.1080/03008207.2022.2060826

30. De Simone U, Spinillo A, Caloni F, Gribaldo L, Coccini T. Neuron-like cells generated from human umbilical cord lining-derived mesenchymal stem cells as a new *in vitro* model for neuronal toxicity screening: using magnetite nanoparticles as an example. *Int J Mol Sci.* (2019) 21:271. doi: 10.3390/ijms21010271

31. Kuang Y, Zheng X, Zhang L, Ai X, Venkataramani V, Kilic E, et al. Adipose-derived mesenchymal stem cells reduce autophagy in stroke mice by extracellular vesicle transfer of miR-25. *J Extracell Vesicles.* (2020) 10:e12024. doi: 10.1002/jev2.12024

32. Liu X, Zhang M, Liu H, Zhu R, He H, Zhou Y, et al. Bone marrow mesenchymal stem cell-derived exosomes attenuate cerebral ischemia-reperfusion injury-induced neuroinflammation and pyroptosis by modulating microglia M1/M2 phenotypes. *Exp Neurol.* (2021) 341:113700. doi: 10.1016/j.expneurol.2021.113700

33. Zhang Z, Zou X, Zhang R, Xie Y, Feng Z, Li F, et al. Human umbilical cord mesenchymal stem cell-derived exosomal miR-146a-5p reduces microglial-mediated neuroinflammation via suppression of the IRAK1/TRAF6 signaling pathway after ischemic stroke. *Aging.* (2021) 13:3060–79. doi: 10.18632/aging.202466

34. Deng Y, Chen D, Gao F, Lv H, Zhang G, Sun X, et al. Exosomes derived from microRNA-138–5p-overexpressing bone marrow-derived mesenchymal stem cells confer neuroprotection to astrocytes following ischemic stroke via inhibition of LCN2. *J Biol Eng.* (2019) 13:71. doi: 10.1186/s13036-019-0193-0

35. Liu K, Guo L, Zhou Z, Pan M, Yan C. Mesenchymal stem cells transfer mitochondria into cerebral microvasculature and promote recovery from ischemic stroke. *Microvasc Res.* (2019) 123:74–80. doi: 10.1016/j.mvr.2019.01.001

36. Li S, Rao JH, Lan XY, Li X, Chu CY, Liang Y, et al. White matter demyelination predates axonal injury after ischemic stroke in cynomolgus monkeys. *Exp Neurol.* (2021) 340:113655. doi: 10.1016/j.expneurol.2021.113655

37. Bagdasarian FA, Yuan X, Athey J, Bunnell BA, Grant SC. NODDI highlights recovery mechanisms in white and gray matter in ischemic stroke following human stem cell treatment. *Magn Reson Med.* (2021) 86:3211–23. doi: 10.1002/mrm.28929

38. Li J, Xiao L, He D, Luo Y, Sun H. Mechanism of white matter injury and promising therapeutic strategies of MSCs after intracerebral hemorrhage. *Front Aging Neurosci.* (2021) 13:632054. doi: 10.3389/fnagi.2021.632054

39. Datta A, Sarmah D, Mounica L, Kaur H, Kesharwani R, Verma G, et al. Cell death pathways in ischemic stroke and targeted pharmacotherapy. *Transl Stroke Res.* (2020) 11:1185–202. doi: 10.1007/s12975-020-00806-z

40. Radak D, Katsiki N, Resanovic I, Jovanovic A, Sudar-Milovanovic E, Zafirovic S, et al. Apoptosis and acute brain ischemia in ischemic stroke. *Curr Vasc Pharmacol.* (2017) 15:115–22. doi: 10.2174/1570161115666161104095522

41. Kong D, Zhu J, Liu Q, Jiang Y, Xu L, Luo N, et al. Mesenchymal stem cells protect neurons against hypoxic-ischemic injury via inhibiting parthanatos, necroptosis, and apoptosis, but not autophagy. *Cell Mol Neurobiol.* (2017) 37:303–13. doi: 10.1007/s10571-016-0370-3

42. Xiao Y, Geng F, Wang G, Li X, Zhu J, Zhu W. Bone marrow-derived mesenchymal stem cells-derived exosomes prevent oligodendrocyte apoptosis through exosomal miR-134 by targeting caspase-8. *J Cell Biochem.* (2018) 120:2109–18. doi: 10.1002/jcb.27519

43. Wei W, Pan Y, Yang X, Chen Z, Heng Y, Yang B, et al. The emerging role of the interaction of extracellular vesicle and autophagy-novel insights into neurological disorders. *J Inflamm Res.* (2022) 15:3395–407. doi: 10.2147/JIR.S362865

44. Li Y, Guo S, Liu W, Jin T, Li X, He X, et al. Silencing of SNHG12 enhanced the effectiveness of MSCs in alleviating ischemia/reperfusion injuries via the PI3K/AKT/mTOR signaling pathway. *Front Neurosci.* (2019) 13:645. doi: 10.3389/fnins.2019.00645

45. Huang X, Ding J, Li Y, Liu W, Ji J, Wang H, et al. Exosomes derived from PEDF modified adipose-derived mesenchymal stem cells ameliorate cerebral ischemia-reperfusion injury by regulation of autophagy and apoptosis. *Exp Cell Res.* (2018) 371:269–77. doi: 10.1016/j.yexcr.2018.08.021

46. Yang BO, Duan WU, Wei L, Zhao Y, Han Z, Wang J, et al. Bone marrow mesenchymal stem cell-derived hepatocyte-like cell exosomes reduce hepatic ischemia/reperfusion injury by enhancing autophagy. *Stem Cells Dev.* (2020) 29:372–9. doi: 10.1089/scd.2019.0194

47. Zeng Q, Zhou Y, Liang D, He H, Liu X, Zhu R, et al. Exosomes secreted from bone marrow mesenchymal stem cells attenuate oxygen-glucose deprivation/reoxygenation-induced pyroptosis in PC12 cells by promoting AMPK-dependent autophagic flux. *Front Cell Neurosci.* (2020) 14:182. doi: 10.3389/fncel.2020.00182

48. Wakabayashi K, Nagai A, Sheikh Am Shiota Y, Narantuya D, Watanabe T, Masuda J, et al. Transplantation of human mesenchymal stem cells promotes functional improvement and increased expression of neurotrophic factors in a rat focal cerebral ischemia model. *J Neurosci Res.* (2010) 88:1017–25. doi: 10.1002/jnr.22279

49. Kurozumi K, Nakamura K, Tamiya T, Kawano Y, Kobune M, Hirai S, et al. BDNF gene-modified mesenchymal stem cells promote functional recovery and reduce infarct size in the rat middle cerebral artery occlusion model. *Mol Ther.* (2004) 9:189–97. doi: 10.1016/j.ymthe.2003.10.012

50. Nomura T, Honmou O, Harada K, Houkin K, Hamada H, Kocsis JD. IV. Infusion of brain-derived neurotrophic factor gene-modified human mesenchymal stem cells protects against injury in a cerebral ischemia model in adult rat. *Neuroscience.* (2005) 136:161–9. doi: 10.1016/j.neuroscience.2005.06.062

51. Onda T, Honmou O, Harada K, Houkin K, Hamada H, Kocsis JD. Therapeutic benefits by human mesenchymal stem cells (hMSCs) and Ang-1 gene-modified hMSCs after cerebral ischemia. *J Cereb Blood Flow Metab.* (2008) 28:329–40. doi: 10.1038/sj.jcbfm.9600527

52. Jeong CH, Kim SM, Lim JY, Ryu CH, Jun JA, Jeun SS. Mesenchymal stem cells expressing brain-derived neurotrophic factor enhance endogenous neurogenesis in an ischemic stroke model. *BioMed Res Int.* (2014) 2014:129145. doi: 10.1155/2014/129145

53. Xin H, Li Y, Cui Y, Yang JJ, Zhang ZG, Chopp M. Systemic administration of exosomes released from mesenchymal stromal cells promote functional recovery and neurovascular plasticity after stroke in rats. *J Cereb Blood Flow Metab.* (2013) 33:1711–15. doi: 10.1038/jcbfm.2013.152

54. Cho SE, Kim YM, Jeong JS, Seo YK. The effect of ultrasound for increasing neural differentiation in hBM-MSCs and inducing neurogenesis in ischemic stroke model. *Life Sci.* (2016) 165:35–42. doi: 10.1016/j.lfs.2016.08.029

55. Toyama K, Honmou O, Harada K, Suzuki J, Houkin K, Hamada H, et al. Therapeutic benefits of angiogenetic gene-modified human mesenchymal stem cells after cerebral ischemia. *Exp Neurol.* (2009) 216:47–55. doi: 10.1016/j.expneurol.2008.11.010

56. Chen J, Zhang ZG, Li Y, Wang L, Xu YX, Gautam SC, et al. Intravenous administration of human bone marrow stromal cells induces angiogenesis in the ischemic boundary zone after stroke in rats. *Circ Res.* (2003) 92:692–9. doi: 10.1161/01.RES.0000063425.51108.8D

57. Guruswamy R, Elali A. Complex roles of microglial cells in ischemic stroke pathobiology: new insights and future directions. *Int J Mol Sci.* (2017) 18:496. doi: 10.3390/ijms18030496

58. Qin C, Zhou LQ, Ma XT, Hu ZW, Yang S, Chen M, et al. Dual functions of microglia in ischemic stroke. *Neurosci Bull.* (2019) 35:921–33. doi: 10.1007/s12264-019-00388-3

59. Iadecola C, Anrather J. The immunology of stroke: from mechanisms to translation. *Nat Med.* (2011) 17:796–808. doi: 10.1038/nm.2399

60. Jin R, Yang G, Li G. Inflammatory mechanisms in ischemic stroke: role of inflammatory cells. *J Leukoc Biol.* (2010) 87:779–89. doi: 10.1189/jlb.1109766

61. Cunningham CJ, Wong R, Barrington J, Tamburrano S, Pinteaux E, Allan SM. Systemic conditioned medium treatment from interleukin-1 primed mesenchymal stem cells promotes recovery after stroke. *Stem Cell Res Ther.* (2020) 11:1–12. doi: 10.1186/s13287-020-1560-y

62. Yamaguchi S, Horie N, Satoh K, Ishikawa T, Mori T, Maeda H, et al. Age of donor of human mesenchymal stem cells affects structural and functional recovery after cell therapy following ischaemic stroke. *J Cereb Blood Flow Metab.* (2018) 38:1199–212. doi: 10.1177/0271678X17731964

63. McGuckin CP, Jurga M, Miller AM, Sarnowska A, Wiedner M, Boyle NT, et al. Ischemic brain injury: a consortium analysis of key factors involved in mesenchymal stem cell-mediated inflammatory reduction. *Arch Biochem Biophys.* (2013) 534:88–97. doi: 10.1016/j.abb.2013.02.005

64. Yang F, Li WB, Qu YW, Gao JX, Tang YS, Wang DJ, et al. Bone marrow mesenchymal stem cells induce M2 microglia polarization through PDGF-AA/MANF signaling. *World J Stem Cells.* (2020) 12:633–58. doi: 10.4252/wjsc.v12.i7.633

65. Feng YW, Wu C, Liang FY, Lin T, Li WQ, Jing YH, et al. hUCMSCs mitigate LPS-induced trained immunity in ischemic stroke. *Front Immunol.* (2020) 11:1746. doi: 10.3389/fimmu.2020.01746

66. Narantuya D, Nagai A, Sheikh AM, Wakabayashi K, Shiota Y, Watanabe T, et al. Microglia transplantation attenuates white matter injury in rat chronic ischemia model via matrix metalloproteinase-2 inhibition. *Brain Res.* (2010) 1316:145–52. doi: 10.1016/j.brainres.2009.12.043

67. Ishizaka S, Horie N, Satoh K, Fukuda Y, Nishida N, Nagata I. Intra-arterial cell transplantation provides timing-dependent cell distribution and functional recovery after stroke. *Stroke.* (2013) 44:720–26. doi: 10.1161/STROKEAHA.112.677328

68. Wang LQ, Lin ZZ, Zhang HX, Shao B, Xiao L, Jiang HG, et al. Timing and dose regimens of marrow mesenchymal stem cell transplantation affect the outcomes and neuroinflammatory response after ischemic stroke. *CNS Neurosci Ther.* (2014) 20:317–26. doi: 10.1111/cns.12216

69. Nakajima M, Nito C, Sowa K, Suda S, Nishiyama Y, Nakamura-Takahashi A, et al. Mesenchymal stem cells overexpressing interleukin-10 promote neuroprotection in experimental acute ischemic stroke. *Mol Ther Methods Clin Dev.* (2017) 6:102–111. doi: 10.1016/j.omtm.2017.06.005

70. Li X, Huang M, Zhao R, Zhao C, Liu Y, Zou H, et al. Intravenously delivered allogeneic mesenchymal stem cells bidirectionally regulate inflammation and induce neurotrophic effects in distal middle cerebral artery occlusion rats within the first 7 days after stroke. *Cell Physiol Biochem.* (2018) 46:1951–70. doi: 10.1159/000489384

71. Lv B, Li F, Fang J, Xu L, Sun C, Han J, et al. Activated microglia induce bone marrow mesenchymal stem cells to produce glial cell-derived neurotrophic factor and protect neurons against oxygen-glucose deprivation injury. *Front Cell Neurosci.* (2016) 10:283. doi: 10.3389/fncel.2016.00283

72. Sheikh AM, Yano S, Mitaki S, Haque MA, Yamaguchi S, Nagai A. A mesenchymal stem cell line (B10) increases angiogenesis in a rat MCAO model. *Exp Neurol.* (2019) 311:182–93. doi: 10.1016/j.expneurol.2018.10.001

73. Wang H, Nagai A, Sheikh AM, Liang XY, Yano S, Mitaki S, et al. Human mesenchymal stem cell transplantation changes proinflammatory gene expression through a nuclear factor-κB-dependent pathway in a rat focal cerebral ischemic model. *J Neurosci Res.* (2013) 91:1440–49. doi: 10.1002/jnr.23267

74. Yoo SW, Chang DY, Lee HS, Kim GH, Park JS, Ryu BY, et al. Immune following suppression mesenchymal stem cell transplantation in the ischemic brain is mediated by TGF-β. *Neurobiol Dis.* (2013) 58:249–57. doi: 10.1016/j.nbd.2013.06.001

75. Sheikh AM, Nagai A, Wakabayashi K, Narantuya D, Kobayashi S, Yamaguchi S, et al. Mesenchymal stem cell transplantation modulates neuroinflammation in focal cerebral ischemia: contribution of fractalkine and IL-5. *Neurobiol Dis.* (2011) 41:717–24. doi: 10.1016/j.nbd.2010.12.009

76. Gelderblom M, Leypoldt F, Steinbach K, Behrens D, Choe CU, Siler DA, et al. Temporal and spatial dynamics of cerebral immune cell accumulation in stroke. *Stroke.* (2009) 40:1849–57. doi: 10.1161/STROKEAHA.108.534503

77. Wang C, Börger V, Mohamud Yusuf A, Tertel T, Stambouli O, Murke F, et al. Postischemic neuroprotection associated with anti-inflammatory effects by mesenchymal stromal cell-derived small extracellular vesicles in aged mice. *Stroke.* (2022) 53:e14–18. doi: 10.1161/STROKEAHA.121.035821

78. Hsu SC, Wang LT, Yao CL, Lai HY, Chan KY, Liu BS, et al. Mesenchymal stem cells promote neutrophil activation by inducing IL-17 production in CD4+ CD45RO+ T cells. *Immunobiology.* (2013) 218:90–95. doi: 10.1016/j.imbio.2012.02.007

79. Raffaghello L, Bianchi G, Bertolotto M, Montecucco F, Busca A, Dallegri F, et al. Human mesenchymal stem cells inhibit neutrophil apoptosis: a model for neutrophil preservation in the bone marrow niche. *Stem Cells.* (2008) 26:151–62. doi: 10.1634/stemcells.2007-0416

80. Vivier E, Tomasello E, Baratin M, Walzer T, Ugolini S. Functions of natural killer cells. *Nat Immunol.* (2008) 9:503–10. doi: 10.1038/ni1582

81. Wang Y, Chen X, Cao W, Shi Y. Plasticity of mesenchymal stem cells in immunomodulation: pathological and therapeutic implications. *Nat Immunol.* (2014) 15:1009–16. doi: 10.1038/ni.3002

82. Carrillo-Galvez Ab Cobo M, Cuevas-Ocaña S, Gutiérrez-Guerrero A, Sánchez-Gilabert A, Bongarzone P, García-Pérez A, et al. Mesenchymal stromal cells express GARP/LRRC32 on their surface: effects on their biology and immunomodulatory capacity. *Stem Cells.* (2015) 33:183–95. doi: 10.1002/stem.1821

83. Huang WH, Chen HL, Huang PH, Yew TL, Lin MW, Lin SJ, et al. Hypoxic mesenchymal stem cells engraft and ameliorate limb ischaemia in allogeneic recipients. *Cardiovasc Res.* (2014) 101:266–76. doi: 10.1093/cvr/cvt250

84. Felger JC, Abe T, Kaunzner UW, Gottfried-Blackmore A, Gal-Toth J, Mcewen BS, et al. Brain dendritic cells in ischemic stroke: time course, activation state, and origin. *Brain Behav Immunity.* (2010) 24:724–37. doi: 10.1016/j.bbi.2009.11.002

85. Gao WX, Sun YQ, Shi J, Li CL, Fang SB, Wang D, et al. Effects of mesenchymal stem cells from human induced pluripotent stem cells on differentiation, maturation, and function of dendritic cells. *Stem Cell Res Ther.* (2017) 8:48. doi: 10.1186/s13287-017-0499-0

86. Jo H, Eom YW, Kim HS, Park HJ, Kim HM, Cho MY. Regulatory dendritic cells induced by mesenchymal stem cells ameliorate dextran sodium sulfate-induced chronic colitis in mice. *Gut Liver.* (2018) 12:664–73. doi: 10.5009/gnl18072

87. Zhao Zg Xu W, Sun L, You Y, Li F, Li Qb Zou P. Immunomodulatory function of regulatory dendritic cells induced by mesenchymal stem cells. *Immunol Investig.* (2012) 41:183–98. doi: 10.3109/08820139.2011.607877

88. Zhang B, Liu R, Shi D, Liu X, Chen Y, Dou X, et al. Mesenchymal stem cells induce mature dendritic cells into a novel Jagged-2-dependent regulatory dendritic cell population. *Blood.* (2009) 113:46–57. doi: 10.1182/blood-2008-04-154138

89. Rich Robert R, Fleisher Thomas A, Shearer William T, Schroeder Jr Harry W, Frew Anthony J, Weyand Cornelia M. *Clinical Immunology E-Book: Principles and Practice*. Elsevier Health Sciences (2012).

90. Selvaraj UM, Stowe AM. Long-term T cell responses in the brain after an ischemic stroke. *Discov Med.* (2017) 24:323–33.

91. Zhang D, Ren J, Luo Y, He Q, Zhao R, Chang J, et al. T Cell response in ischemic stroke: from mechanisms to translational insights. *Front Immunol.* (2021) 12:707972. doi: 10.3389/fimmu.2021.707972

92. Chu HX, Kim HA, Lee S, Moore JP, Chan CT, Vinh A, et al. Immune cell infiltration in malignant middle cerebral artery infarction: comparison with transient cerebral ischemia. *J Cereb Blood Flow Metab.* (2014) 34:450–59. doi: 10.1038/jcbfm.2013.217

93. Liesz A, Suri-Payer E, Veltkamp C, Doerr H, Sommer C, Rivest S, et al. Regulatory T cells are key cerebroprotective immunomodulators in acute experimental stroke. *Nat Med.* (2009) 15:192–9. doi: 10.1038/nm.1927

94. Jellema RK, Wolfs TG, Lima Passos V, Zwanenburg A, Ophelders DR, Kuypers E, et al. Mesenchymal stem cells induce T-cell tolerance and protect the preterm brain after global hypoxia-ischemia. *PLoS ONE.* (2013) 8:e73031. doi: 10.1371/journal.pone.0073031

95. Consentius C, Akyüz L, Schmidt-Lucke Ja Tschöpe C, Pinzur L, Ofir R, Reinke P, et al. Mesenchymal stromal cells prevent allostimulation *in vivo* and control checkpoints of Th1 priming: migration of human DC to lymph nodes and NK cell activation. *Stem Cells.* (2015) 33:3087–99. doi: 10.1002/stem.2104

96. Cai J, Jiao X, Zhao S, Liang Y, Ning Y, Shi Y, et al. Transforming growth factor-β1-overexpressing mesenchymal stromal cells induced local tolerance in rat renal ischemia/reperfusion injury. *Cytotherapy.* (2019) 21:535–45. doi: 10.1016/j.jcyt.2018.12.003

97. Boothby M, Rickert RC. Metabolic regulation of the immune humoral response. *Immunity.* (2017) 46:743–55. doi: 10.1016/j.immuni.2017.04.009

98. Anthony IC, Crawford DH, Bell JE. B lymphocytes in the normal brain: contrasts with HIV-associated lymphoid infiltrates and lymphomas. *Brain.* (2003) 126:1058–67. doi: 10.1093/brain/awg118

99. Funaro MG, Messina M, Shabbir M, Wright P, Najjar S, Tabansky I, et al. The role of B cells in multiple sclerosis: more than antibodies. *Discov Med.* (2016) 22:251–5.

100. Ortega SB, Torres VO, Latchney SE, Whoolery CW, Noorbhai IZ, Poinsatte K, et al. B cells migrate into remote brain areas and support neurogenesis and functional recovery after focal stroke in mice. *Proc Natl Acad Sci USA.* (2020) 117:4983–93. doi: 10.1073/pnas.1913292117

101. Liu J, Liu Q, Chen X. The immunomodulatory effects of mesenchymal stem cells on regulatory B cells. *Front Immunol.* (2020) 11:1843. doi: 10.3389/fimmu.2020.01843

102. Shin TH, Lee BC, Choi SW, Shin JH, Kang I, Lee JY, et al. Human adipose tissue-derived mesenchymal stem cells alleviate atopic dermatitis via regulation of B lymphocyte maturation. *Oncotarget.* (2017) 8:512–22. doi: 10.18632/oncotarget.13473

103. Rosado MM, Bernardo ME, Scarsella M, Conforti A, Giorda E, Biagini S, et al. Inhibition of B-cell proliferation and antibody production by mesenchymal stromal cells is mediated by T cells. *Stem Cells Dev.* (2015) 24:93–103. doi: 10.1089/scd.2014.0155

104. Noh JE, Oh SH, Park IH, Song J. Intracerebral transplants of GMP-grade human umbilical cord-derived mesenchymal stromal cells effectively treat subacute-phase ischemic stroke in a rodent model. *Front Cell Neurosci.* (2020) 14:546659. doi: 10.3389/fncel.2020.546659

105. Kurozumi K, Nakamura K, Tamiya T, Kawano Y, Ishii K, Kobune M, et al. Mesenchymal stem cells that produce neurotrophic factors reduce ischemic damage in the rat middle cerebral artery occlusion model. *Mol Ther.* (2005) 11:96–104. doi: 10.1016/j.ymthe.2004.09.020

106. Vu Q, Xie K, Eckert M, Zhao W, Cramer SC. Meta-analysis of preclinical studies of mesenchymal stromal cells for ischemic stroke. *Neurology.* (2014) 82:1277–86. doi: 10.1212/WNL.0000000000000278

107. Haupt M, Zheng X, Kuang Y, Lieschke S, Janssen L, Bosche B, et al. Lithium modulates miR-1906 levels of mesenchymal stem cell-derived extracellular vesicles contributing to poststroke neuroprotection by toll-like receptor 4 regulation. *Stem Cells Transl Med.* (2021) 10:357–73. doi: 10.1002/sctm.20-0086

108. Datta A, Sarmah D, Kaur H, Chaudhary A, Mounica Kl Kalia K, Borah A, et al. Post-stroke impairment of the blood-brain barrier and perifocal vasogenic edema is alleviated by endovascular mesenchymal stem cell administration: modulation of the PKCδ/MMP9/AQP4-mediated pathway. *Mol Neurobiol.* (2022) 59:2758–75. doi: 10.1007/s12035-022-02761-2

109. Tang G, Liu Y, Zhang Z, Lu Y, Wang Y, Huang J, et al. Mesenchymal stem cells maintain blood-brain barrier integrity by inhibiting aquaporin-4 upregulation after cerebral ischemia. *Stem Cells.* (2014) 32:3150–62. doi: 10.1002/stem.1808

110. Akbar N, Azzimato V, Choudhury RP, Aouadi M. Extracellular vesicles in metabolic disease. *Diabetologia.* (2019) 62:2179–87. doi: 10.1007/s00125-019-05014-5

111. Li F, Kang X, Xin W, Li X. The emerging role of extracellular vesicle derived from neurons/neurogliocytes in central nervous system diseases: novel insights into ischemic stroke. *Front Pharmacol.* (2022) 13:890698. doi: 10.3389/fphar.2022.890698

112. Théry C, Ostrowski M, Segura E. Membrane vesicles as conveyors of immune responses. *Nat Rev Immunol.* (2009) 9:581–93. doi: 10.1038/nri2567

113. Saltarella I, Lamanuzzi A, Apollonio B, Desantis V, Bartoli G, Vacca A, et al. Role of extracellular vesicle-based cell-to-cell communication in multiple myeloma progression. *Cells.* (2021) 10:3185. doi: 10.3390/cells10113185

114. Feng B, Meng L, Luan L, Fang Z, Zhao P, Zhao G. viaUpregulation of extracellular vesicles-encapsulated mir-132 released from mesenchymal stem cells attenuates ischemic neuronal injury by inhibiting Smad2/c-jun pathway Acvr2b suppression. *Front Cell Dev Biol.* (2020) 8:568304. doi: 10.3389/fcell.2020.568304

115. Ai Z, Cheng C, Zhou L, Yin S, Wang L, Liu Y. Bone marrow mesenchymal stem cells-derived extracellular vesicles carrying microRNA-221–3p protect against ischemic stroke via ATF3. *Brain Res Bull.* (2021) 172:220–28. doi: 10.1016/j.brainresbull.2021.04.022

116. Venkat P, Cui C, Chopp M, Zacharek A, Wang F, Landschoot-Ward J, et al. MiR-126 mediates brain endothelial cell exosome treatment-induced neurorestorative effects after stroke in type 2 diabetes mellitus mice. *Stroke.* (2019) 50:2865–74. doi: 10.1161/STROKEAHA.119.025371

117. Cai G, Cai G, Zhou H, Zhuang Z, Liu K, Pei S, et al. Mesenchymal stem cell-derived exosome miR-542–3p suppresses inflammation and prevents cerebral infarction. *Stem Cell Res Ther.* (2021) 12:2. doi: 10.1186/s13287-020-02030-w

118. Qi Z, Zhao Y, Su Y, Cao B, Yang Jj Xing Q. Serum extracellular vesicle-derived mir-124–3p as a diagnostic and predictive marker for early-stage acute ischemic stroke. *Front Mol Biosci.* (2021) 8:685088. doi: 10.3389/fmolb.2021.685088

119. Geng W, Tang H, Luo S, Lv Y, Liang D, Kang X, et al. Exosomes from miRNA-126-modified ADSCs promotes functional recovery after stroke in rats by improving neurogenesis and suppressing microglia activation. *Am J Transl Res.* (2019) 11:780–92.

120. Yang J, Cao LL, Wang XP, Guo W, Guo RB, Sun YQ, et al. Neuronal extracellular vesicle derived miR-98 prevents salvageable neurons from microglial phagocytosis in acute ischemic stroke. *Cell Death Dis.* (2021) 12:23. doi: 10.1038/s41419-020-03310-2

121. Xin H, Li Y, Liu Z, Wang X, Shang X, Cui Y, et al. MiR-133b promotes neural plasticity and functional recovery after treatment of stroke with multipotent mesenchymal stromal cells in rats via transfer of exosome-enriched extracellular particles. *Stem Cells.* (2013) 31:2737–746. doi: 10.1002/stem.1409

122. Li G, Xiao L, Qin H, Zhuang Q, Zhang W, Liu L, et al. Exosomes-carried microRNA-26b-5p regulates microglia M1 polarization after cerebral ischemia/reperfusion. *Cell Cycle.* (2020) 19:1022–35. doi: 10.1080/15384101.2020.1743912

123. Zhang Y, Liu J, Su M, Wang X, Xie C. Exosomal microRNA-22–3p alleviates cerebral ischemic injury by modulating KDM6B/BMP2/BMF axis. *Stem Cell Res Ther.* (2021) 12:111. doi: 10.1186/s13287-020-02091-x

124. Hou Z, Chen J, Yang H, Hu X, Yang F. microRNA-26a shuttled by extracellular vesicles secreted from adipose-derived mesenchymal stem cells reduce neuronal damage through KLF9-mediated regulation of TRAF2/KLF2 axis. *Adipocyte.* (2021) 10:378–93. doi: 10.1080/21623945.2021.1938829

125. Lv H, Li J, Che Y. miR-31 from adipose stem cell-derived extracellular vesicles promotes recovery of neurological function after ischemic stroke by inhibiting TRAF6 and IRF5. *Exp Neurol.* (2021) 342:113611. doi: 10.1016/j.expneurol.2021.113611

126. Wu W, Liu J, Yang C, Xu Z, Huang J, Lin J. Astrocyte-derived exosome-transported microRNA-34c is neuroprotective against cerebral ischemia/reperfusion injury via TLR7 and the NF-κB/MAPK pathways. *Brain Res Bull.* (2020) 163:84–94. doi: 10.1016/j.brainresbull.2020.07.013

127. Xu L, Cao H, Xie Y, Zhang Y, Du M, Xu X, et al. Exosome-shuttled miR-92b-3p from ischemic preconditioned astrocytes protects neurons against oxygen and glucose deprivation. *Brain Res.* (2019) 1717:66–73. doi: 10.1016/j.brainres.2019.04.009

128. Li Z, Song Y, He T, Wen R, Li Y, Chen T, et al. viaM2 microglial small extracellular vesicles reduce glial scar formation the miR-124/STAT3 pathway after ischemic stroke in mice. *Theranostics.* (2021) 11:1232–48. doi: 10.7150/thno.48761

129. Yang Y, Cai Y, Zhang Y, Liu J, Xu Z. Exosomes secreted by adipose-derived stem cells contribute to angiogenesis of brain microvascular endothelial cells following oxygen-glucose deprivation *in vitro* through MicroRNA-181b/TRPM7 Axis. *J Mol Neurosci.* (2018) 65:74–83. doi: 10.1007/s12031-018-1071-9

130. Zhang H, Wu J, Wu J, Fan Q, Zhou J, Wu J, et al. Exosome-mediated targeted delivery of miR-210 for angiogenic therapy after cerebral ischemia in mice. *J Nanobiotechnol.* (2019) 17:29. doi: 10.1186/s12951-019-0461-7

131. Xin H, Katakowski M, Wang F, Qian Jy Liu Xs Ali Mm Buller B, Zhang Zg Chopp M. MicroRNA cluster miR-17–92 cluster in exosomes enhance neuroplasticity and functional recovery after stroke in rats. *Stroke.* (2017) 48:747–53. doi: 10.1161/STROKEAHA.116.015204

132. Ling X, Zhang G, Xia Y, Zhu Q, Zhang J, Li Q, et al. Exosomes from human urine-derived stem cells enhanced neurogenesis via miR-26a/HDAC6 axis after ischaemic stroke. *J Cell Mol Med.* (2020) 24:640–54. doi: 10.1111/jcmm.14774

133. Yang J, Zhang X, Chen X, Wang L, Yang G. Exosome mediated delivery of miR-124 promotes neurogenesis after ischemia. *Mol Ther Nucleic Acids.* (2017) 7:278–87. doi: 10.1016/j.omtn.2017.04.010

134. Song H, Zhang X, Chen R, Miao J, Wang L, Cui L, et al. Cortical neuron-derived exosomal MicroRNA-181c-3p inhibits neuroinflammation by downregulating CXCL1 in astrocytes of a rat model with ischemic brain injury. *Neuroimmunomodulation.* (2019) 26:217–33. doi: 10.1159/000502694

135. Zhong Y, Luo L. Exosomes from human umbilical vein endothelial cells ameliorate ischemic injuries by suppressing the RNA component of mitochondrial RNA-processing endoribonuclease via the induction of miR-206/miR-1–3p levels. *Neuroscience.* (2021) 476:34–44. doi: 10.1016/j.neuroscience.2021.08.026

136. Zhao Y, Gan Y, Xu G, Hua K, Liu D. Exosomes from MSCs overexpressing microRNA-223–3p attenuate cerebral ischemia through inhibiting microglial M1 polarization mediated inflammation. *Life Sci.* (2020) 260:118403. doi: 10.1016/j.lfs.2020.118403

137. Bu X, Li D, Wang F, Sun Q, Zhang Z. microRNA-361 Protective role of astrocyte-derived exosomal in cerebral ischemic-reperfusion injury by regulating the signaling pathway and targeting. *Neuropsychiatr Dis Treat.* (2020) 16:1863–77. doi: 10.2147/NDT.S260748

138. Yue KY, Zhang PR, Zheng MH, Cao XL, Cao Y, Zhang YZ, et al. Neurons can upregulate Cav-1 to increase intake of endothelial cells-derived extracellular vesicles that attenuate apoptosis via miR-1290. *Cell Death Dis.* (2019) 10:869. doi: 10.1038/s41419-019-2100-5

139. Ye Z, Hu J, Xu H, Sun B, Jin Y, Zhang Y, et al. Serum exosomal microRNA-27–3p aggravates cerebral injury and inflammation in patients with acute cerebral infarction by targeting PPARγ. *Inflammation.* (2021) 44:1035–48. doi: 10.1007/s10753-020-01399-3

140. Cui J, Liu N, Chang Z, Gao Y, Bao M, Xie Y, et al. Exosomal microRNA-126 from RIPC serum is involved in hypoxia tolerance in SH-SY5Y cells by downregulating DNMT3B. *Mol Ther Nucleic Acids.* (2020) 20:649–60. doi: 10.1016/j.omtn.2020.04.008

141. Liu Y, Li YP, Xiao LM, Chen LK, Zheng SY, Zeng EM, et al. Extracellular vesicles derived from M2 microglia reduce ischemic brain injury through microRNA-135a-5p/TXNIP/NLRP3 axis. *Lab Investig.* (2021) 101:837–50. doi: 10.1038/s41374-021-00545-1

142. Zhang D, Cai G, Liu K, Zhuang Z, Jia K, Pei S, et al. Microglia exosomal miRNA-137 attenuates ischemic brain injury through targeting Notch1. *Aging.* (2021) 13:4079–95. doi: 10.18632/aging.202373

143. Guo Y, Peng Y, Zeng H, Chen G. Progress in mesenchymal stem cell therapy for ischemic stroke. *Stem Cells Int.* (2021) 2021:9923566. doi: 10.1155/2021/9923566

144. Xiang E, Han B, Zhang Q, Rao W, Wang Z, Chang C, et al. Human umbilical cord-derived mesenchymal stem cells prevent the progression of early diabetic nephropathy through inhibiting inflammation and fibrosis. *Stem Cell Res Ther.* (2020) 11:336. doi: 10.1186/s13287-020-01852-y

145. Mohapatra S, Pioppini C, Ozpolat B, Calin GA. Non-coding RNAs regulation of macrophage polarization in cancer. *Mol Cancer.* (2021) 20:24. doi: 10.1186/s12943-021-01313-x

146. Panni S, Lovering RC, Porras P, Orchard S. Non-coding RNA regulatory networks. *Biochim Biophys Acta Gene Regul Mech.* (2020) 1863:194417. doi: 10.1016/j.bbagrm.2019.194417

147. Smolle Ma Prinz F, Calin Ga Pichler M. Current concepts of non-coding RNA regulation of immune checkpoints in cancer. *Mol Aspects Med.* (2019) 70:117–126. doi: 10.1016/j.mam.2019.09.007

148. Mercer TR, Dinger ME, Mattick JS. Long non-coding RNAs: insights into functions. *Nat Rev Genet.* (2009) 10:155–9. doi: 10.1038/nrg2521

149. Rinn JL, Chang HY. Genome regulation by long noncoding RNAs. *Ann Rev Biochem.* (2012) 81:145–66. doi: 10.1146/annurev-biochem-051410-092902

150. Chen LL. Linking long noncoding RNA localization and function. *Trends Biochem Sci.* (2016) 41:761–72. doi: 10.1016/j.tibs.2016.07.003

151. Wu P, Mo Y, Peng M, Tang T, Zhong Y, Deng X, et al. Emerging role of tumor-related functional peptides encoded by lncRNA and circRNA. *Mol Cancer.* (2020) 19:22. doi: 10.1186/s12943-020-1147-3

152. Ashwal-Fluss R, Meyer M, Pamudurti NR, Ivanov A, Bartok O, Hanan M, et al. circRNA biogenesis competes with pre-mRNA splicing. *Mol Cell.* (2014) 56:55–66. doi: 10.1016/j.molcel.2014.08.019

153. Meng S, Zhou H, Feng Z, Xu Z, Tang Y, Li P, et al. CircRNA: functions and properties of a novel potential biomarker for cancer. *Mol Cancer.* (2017) 16:94. doi: 10.1186/s12943-017-0663-2

154. Yang L, Han B, Zhang Z, Wang S, Bai Y, Zhang Y, et al. Extracellular vesicle-mediated delivery of circular RNA SCMH1 promotes functional recovery in rodent and nonhuman primate ischemic stroke models. *Circulation.* (2020) 142:556–74. doi: 10.1161/CIRCULATIONAHA.120.045765

155. Law ZK, Tan HJ, Chin SP, Wong CY, Yahya WN, Muda AS, et al. The effects of intravenous infusion of autologous mesenchymal stromal cells in patients with subacute middle cerebral artery infarct: a phase 2 randomized controlled trial on safety, tolerability and efficacy. *Cytotherapy.* (2021) 23:833–40. doi: 10.1016/j.jcyt.2021.03.005

156. Chung JW, Chang WH, Bang OY, Moon GJ, Kim SJ, Kim SK, et al. Efficacy and safety of intravenous mesenchymal stem cells for ischemic stroke. *Neurology.* (2021) 96:e1012–23. doi: 10.1212/WNL.0000000000011440

157. Ottoboni L, Von Wunster B, Martino G. Therapeutic plasticity of neural stem cells. *Front Neurol.* (2020) 11:148. doi: 10.3389/fneur.2020.00148

158. El Bassit G, Patel RS, Carter G, Shibu V, Patel AA, Song S, et al. MALAT1 in human adipose stem cells modulates survival and alternative splicing of PKCδII in HT22 cells. *Endocrinology.* (2017) 158:183–95. doi: 10.1210/en.2016-1819

159. Huang B, Jiang XC, Zhang TY, Hu YL, Tabata Y, Chen Z, et al. Peptide modified mesenchymal stem cells as targeting delivery system transfected with miR-133b for the treatment of cerebral ischemia. *Int J Pharm.* (2017) 531:90–100. doi: 10.1016/j.ijpharm.2017.08.073

160. Wagenaar N, De Theije CGM, De Vries LS, Groenendaal F, Benders Mjnl Nijboer CHA. Promoting neuroregeneration after perinatal arterial ischemic stroke: neurotrophic factors and mesenchymal stem cells. *Pediatr Res.* (2018) 83:372–84. doi: 10.1038/pr.2017.243

161. Tanaka E, Ogawa Y, Mukai T, Sato Y, Hamazaki T, Nagamura-Inoue T, et al. Dose-dependent effect of intravenous administration of human umbilical cord-derived mesenchymal stem cells in neonatal stroke mice. *Front Neurol.* (2018) 9:133. doi: 10.3389/fneur.2018.00133

162. Zhang Y, Dong N, Hong H, Qi J, Zhang S, Wang J. Mesenchymal stem cells: therapeutic mechanisms for stroke. *Int J Mol Sci.* (2022) 23:2550. doi: 10.3390/ijms23052550

163. Binder DK, Scharfman HE. Brain-derived neurotrophic factor. *Growth Fact.* (2004) 22:123–31. doi: 10.1080/08977190410001723308

164. Li L, Wu W, Lin LF, Lei M, Oppenheim RW, Houenou LJ. Rescue of adult mouse motoneurons from injury-induced cell death by glial cell line-derived neurotrophic factor. *Proc Natl Acad Sci USA.* (1995) 92:9771–5. doi: 10.1073/pnas.92.21.9771

165. Zhou L, Zhu H, Bai X, Huang J, Chen Y, Wen J, et al. Potential mechanisms and therapeutic targets of mesenchymal stem cell transplantation for ischemic stroke. *Stem Cell Res Ther.* (2022) 13:195. doi: 10.1186/s13287-022-02876-2

166. Bhatia V, Gupta V, Khurana D, Sharma Rr Khandelwal N. Randomized assessment of the safety and efficacy of intra-arterial infusion of autologous stem cells in subacute ischemic stroke. *Am J Neuroradiol.* (2018) 39:899–904. doi: 10.3174/ajnr.A5586

167. Chen DC, Lin SZ, Fan JR, Lin CH, Lee W, Lin CC, et al. Intracerebral implantation of autologous peripheral blood stem cells in stroke patients: a randomized phase II study. *Cell Transpl.* (2014) 23:1599–612. doi: 10.3727/096368914X678562

168. Fang J, Guo Y, Tan S, Li Z, Xie H, Chen P, et al. Autologous endothelial progenitor cells transplantation for acute ischemic stroke: a 4-year follow-up study. *Stem Cells Transl Med.* (2019) 8:14–21. doi: 10.1002/sctm.18-0012

169. Hess DC, Wechsler LR, Clark WM, Savitz SI, Ford GA, Chiu D, et al. Safety and efficacy of multipotent adult progenitor cells in acute ischaemic stroke (MASTERS): a randomised, double-blind, placebo-controlled, phase 2 trial. *Lancet Neurol.* (2017) 16:360–8. doi: 10.1016/S1474-4422(17)30046-7

170. Jin Y, Ying L, Yu G, Nan G. Analysis of the long-term effect of bone marrow mononuclear cell transplantation for the treatment of cerebral infarction. *Int J Clin Exp Med.* (2017) 10:3059–68.

171. Lee JS, Hong JM, Moon GJ, Lee PH, Ahn YH, et al. A long-term follow-up study of intravenous autologous mesenchymal stem cell transplantation in patients with ischemic stroke. *Stem Cells.* (2010) 28:1099–106. doi: 10.1002/stem.430

172. Prasad K, Sharma A, Garg A, Mohanty S, Bhatnagar S, Johri S, et al. Intravenous autologous bone marrow mononuclear stem cell therapy for ischemic stroke: a multicentric, randomized trial. *Stroke.* (2014) 45:3618–624. doi: 10.1161/STROKEAHA.114.007028

173. Savitz SI, Yavagal D, Rappard G, Likosky W, Rutledge N, Graffagnino C, et al. A phase 2 randomized, sham-controlled trial of internal carotid artery infusion of autologous bone marrow–derived ALD-401 cells in patients with recent stable ischemic stroke (RECOVER-Stroke). *Circulation.* (2019) 139:192–205. doi: 10.1161/CIRCULATIONAHA.117.030659

174. Bhasin A, Srivastava MV, Bhatia R, Mohanty S, Kumaran SS, Bose S. Autologous intravenous mononuclear stem cell therapy in chronic ischemic stroke. *J Stem Cells Regen Med.* (2012) 8:181. doi: 10.46582/jsrm.0803011

175. Bhasin Ashu, Srivastava Mv Padma, Mohanty Sujata, Bhatia Rohit, Kumaran Senthil S, Bose Sushmita. Stem cell therapy: a clinical trial of stroke. *Clin Neurol Neurosurg.* (2013) 115:1003–8. doi: 10.1016/j.clineuro.2012.10.015

176. Bhasin A, Srivastava MP, Mohanty S, Bhatia R, Kumaran SS, Bose S. Paracrine mechanisms of intravenous bone marrow-derived mononuclear stem cells in chronic ischemic stroke. *Cerebrovasc Dis Extra.* (2016) 6:107–19. doi: 10.1159/000446404

177. Bhasin A, Kumaran SS, Bhatia R, Mohanty S, Srivastava MP. Safety and feasibility of autologous mesenchymal stem cell transplantation in chronic stroke in Indian patients. A four-year follow up. *J Stem Cells Regen Med.* (2017) 13:14. doi: 10.46582/jsrm.1301003

178. Ghali AA, Yousef MK, Ragab OA, ElZamarany EA. Intra-arterial infusion of autologous bone marrow mononuclear stem cells in subacute

ischemic stroke patients. *Front Neurol.* (2016) 7:228. doi: 10.3389/fneur.2016.00228

179. Meng XG, Zhu SW, Gao H, Li YZ, Shi Q, Hou HS, et al. Treatment of cerebral infarction using autologous marrow mesenchymal stem cells transplantation: a six-month follow-up. *J Clin Rehabil Tissue Eng Res.* (2009) 13:6374–8. doi: 10.3969/j.issn.1673-8225.2009.32.036

180. Moniche F, Gonzalez A, Gonzalez-Marcos JR, Carmona M, Pinero P, Espigado I, et al. Intra-arterial bone marrow mononuclear cells in ischemic stroke: a pilot clinical trial. *Stroke.* (2012) 43:2242–4. doi: 10.1161/STROKEAHA.112.659409

181. Bang OY, Lee JS, Lee PH, Lee G. Autologous mesenchymal stem cell transplantation in stroke patients. *Ann Neurol.* (2005) 57:874–82. doi: 10.1002/ana.20501

182. Zhao T, Zhu T, Xie L, Li Y, Xie R, Xu F, et al. Neural stem cells therapy for ischemic stroke: progress and challenges. *Transl Stroke Res.* (2022) 13:665–75. doi: 10.1007/s12975-022-00984-y

183. Li Y, Wu H, Jiang X, Dong Y, Zheng J, Gao J. New idea to promote the clinical applications of stem cells or their extracellular vesicles in central nervous system disorders: combining with intranasal delivery. *Acta Pharm Sin B.* (2022) 12:3215–32. doi: 10.1016/j.apsb.2022.04.001

frontiers | Frontiers in Neurology

TYPE Review
PUBLISHED 09 March 2023
DOI 10.3389/fneur.2023.1118843

OPEN ACCESS

EDITED BY
Xia Wang,
University of New South Wales, Australia

REVIEWED BY
Lianchun Wang,
University of South Florida, United States
Julie Rayes,
University of Birmingham, United Kingdom

*CORRESPONDENCE
Chunyuan Zhang
✉ zcyself@sina.com
Yongjun Cao
✉ yongjuncao@126.com
Xia Zhang
✉ stefence1025@163.com

†These authors share first authorship

SPECIALTY SECTION
This article was submitted to Stroke, a section of the journal Frontiers in Neurology

RECEIVED 08 December 2022
ACCEPTED 22 February 2023
PUBLISHED 09 March 2023

CITATION
Huang Y, Lu M, Wang Y, Zhang C, Cao Y and Zhang X (2023) Podoplanin: A potential therapeutic target for thrombotic diseases. *Front. Neurol.* 14:1118843. doi: 10.3389/fneur.2023.1118843

Podoplanin: A potential therapeutic target for thrombotic diseases

Yaqian Huang[1†], Manli Lu[1†], Yi Wang[1], Chunyuan Zhang[2*], Yongjun Cao[1*] and Xia Zhang[1*]

[1]Department of Neurology, Clinical Research Center of Neurological Disease, The Second Affiliated Hospital of Soochow University, Suzhou, China, [2]Department of Rehabilitation, The Second Affiliated Hospital of Soochow University, Suzhou, China

As a specific lymphatic marker and a key ligand of C-type lectin-like receptor 2 (CLEC-2), podoplanin (Pdpn) is involved in various physiological and pathological processes such as growth and development, respiration, blood coagulation, lymphangiogenesis, angiogenesis, and inflammation. Thrombotic diseases constitute a major cause of disability and mortality in adults, in which thrombosis and inflammation play a crucial role. Recently, increasing evidence demonstrates the distribution and function of this glycoprotein in thrombotic diseases such as atherosclerosis, ischemic stroke, venous thrombosis, ischemic-reperfusion injury (IRI) of kidney and liver, and myocardial infarction. Evidence showed that after ischemia, Pdpn can be acquired over time by a heterogeneous cell population, which may not express Pdpn in normal conditions. In this review, the research progresses in understanding the roles and mechanisms of podoplanin in thromobotic diseases are summarized. The challenges of podoplanin-targeted approaches for disease prognosis and preventions are also discussed.

KEYWORDS

podoplanin, thrombotic, inflammation, CLEC-2, platelet activation, epithelial-mesenchymal transition

Introduction

Podoplanin (Pdpn), named according to its expression in renal podocytes, is a type I transmembrane glycoprotein containing a large number of O-glycoside chains, which makes it a member of mucin-type proteins. Due to its expression in human and several mammal species in various cells and tissues, it has many different names. In human it is also called gp36 and T1α (1), however, in mice which is also known as Aggrus, OTS-8, gp38, and antigen PA2.26 (2–4). Pdpn is mainly involved in growth and development, respiration, blood coagulation, lymphangiogenesis, angiogenesis, and inflammation (5–7). Especially the interaction with its receptor C-type lectin-like receptor 2 (CLEC-2) has been shown to play an important role in thromboinflammation (8, 9). Pdpn expression is upregulated in both epithelial and mesenchymal cell compartments during thrombosis and inflammation, and a growing body of evidence indicates its prominence in these pathologies of thrombotic diseases.

Structure, protein partners and cell expression

Pdpn consists of a heavily O-glycosylated ectodomain, a hydrophobic membrane spanning domain, and a short cytoplasmic tail (CT) of only nine amino acids. Besides C-type lectin-like receptor 2 (CLEC-2), there are variable proteins interacting with Pdpn,

such as CCL21, galectin-8, and heat-shock protein A9 (HSPA9) binding its ectodomain; CD9 and CD44 interacting with its transmenbrane domain; and ezrin, radixin, and moesin (ERM) binding to its CT. Through these interactions, Pdpn exerts various functions like platelet aggregation/activation, platelet biogenesis, immune surveillance, cytoskeleton rearrangement, and epithelial-mesenchymal transitions (EMTs) by protein–protein interactions for the lack of obvious enzymatic motifs (10–12) (Figure 1). Mostly, Pdpn is expressed on various cells, or at plasma membrane extensions, such as microvilli, filopodia, and ruffles, linking to the actin cytoskeleton to rearrange cytoskeleton and regulate cell motility. A fraction of Pdpn is localized in detergent-resistant membrane domains or raft platforms regulated by its CT and transmembrane domains, which appears to be necessary for Pdpn-mediated EMT and cell migration (13, 14). Besides, a soluble form of Pdpn (sPdpn) has recently been detected and investigated (15, 16). Cells ectopically or endogenously expressing Pdpn has been found to release extracellular vesicles (EVs) that contain Pdpn mRNA and protein. Pdpn incorporates into membrane shed microvesicles (MVs) and endosomal-derived exosomes (EXOs), and immunoelectron microscopy revealed its colocalization with the classical EV marker CD63 (15). Ovarian cancer cells express Pdpn themselves and also release Pdpn-rich EVs, both causing platelet aggregation, leading to venous thrombosis (16). Those Pdpn-EXO may contribute to sPdpn in circulating body fluid for $Pdpn^{+}$ microparticles were detected in human body fluids including plasma and other liquids, which were quantitated using surface plasmon resonance, immunohistochemistry, and a double-antibody sandwich ELISA (17–20).

The Pdpn research was originally started from the cloning of highly metastatic NL-17 subclone from mouse colon 26 cancer cell lines and the establishment of 8F11 monoclonal antibody (mAb) that could neutralize NL-17-induced platelet aggregation and hematogenous metastasis. Pdpn was identified as the antigen of 8F11 mAb, whose ectopic expression brought cells the platelet-aggregating abilities and hematogenous metastasis phenotypes. From the 8F11 mAb recognition epitopes, Pdpn is found to contain tandemly repeated, highly conserved motifs, designated platelet aggregation-stimulating (PLAG) domains, which are associated with the CLEC-2 binding (21). Pdpn was discovered for the first time in rat and mice lungs, and on the surface of stromal cells in lymph nodes (LNs) in mice, which has been found to be expressed in a wide variety of cells later, such as lymphatic endothelial cells, tumor cells, osteocytes, choroid plexus epithelial cells, glial cells, and cancer-associated fibroblasts for its pleiotropic functions (7, 22).

Pdpn signaling pathways

Among the many protein ligands of Pdpn, CLEC-2, and ERM proteins are studied comprehensively. CLEC-2 is a main receptor for Pdpn. The PLAG3 and PLAG4 domains of Pdpn are required for its binding to CLEC-2 (23, 24). The combination of CLEC-2 with the PLAG domains in the extracellular domain of Pdpn induces platelet activation and regulates inflammation through the Src, Syk, and SLP-76 kinase pathway (25, 26). Additionally, the interaction of Pdpn with CLEC-2 enhanced the interaction between Pdpn and ERM proteins and CD44, which activated Rho GTPase signaling pathway (27, 28). Both the interaction of Pdpn with CLEC-2 and with ERM are the two main pathways of cytoskeleton reorganization and inflammation regulation, which have been demonstrated to contribute to the occurrence and development of thrombotic diseases (29, 30). Studies show that Pdpn plays an important role in the functional regulation of immune cells. Following inflammatory or ischemic stimulation, Pdpn expression was upregulated in macrophages, microglia, and other immune cells, which influenced their motility and functionally phenotype transformation (31–33).

Pdpn in atherosclerosis

Atherosclerosis is usually considered as a chronic inflammatory disease, which is the main root cause of thrombotic diseases characterized by lipid deposition in parts of the artery accompanied by smooth muscle cell (SMC) and fibrous matrix proliferation. Unstable atherosclerotic plaque rupture and following thrombus formation, or vascular stenosis lead to arteriosclerotic cardiovascular disease (ASCVD) resulting in high rate of mortality in the population (34). Platelet activation and aggression has a well-established role in the development and manifestation of atherosclerosis (35–37). Both CLEC-2 and Pdpn have been shown to bind to atherosclerotic lesions. CLEC-2 co-localized with vascular SMCs, while Pdpn was localized to SMCs and macrophages (38). Besides, Pdpn expression in SMCs and macrophages increased with atherosclerotic progression. However, in a rat model similar to the plaque erosion in human which contains relatively few inflammatory cells and more SMCs compared with plaque rupture, Pdpn was found to be overexpressed in endothelial cells, not in SMCs. Further exploration showed that vascular endothelial growth factor (VEGF)-A, which is expressed in SMCs, macrophages, and endothelial cells in the advanced atherosclerotic lesions, induced Pdpn expression. Therefore, it is speculated that VEGF-A from superficial SMCs stimulates endothelial Pdpn expression, which interacts with CLEC-2 to induce platelet aggregation and thrombus formation (39). The results remind us that at different stages of atherosclerosis, Pdpn expression varies in different cells and plays different roles. This partly might be explained by the fact that inflammatory stimulation upregulated Pdpn expression in macrophages, and Pdpn was expressed on inflammatory but not tissue-resident macrophages (31). Toll-like receptor (TLR) stimulation and some inflammatory cytokines activates Pdpn expression. Additionally, in advanced atherosclerotic plaque, Pdpn was detected in a membranous or cytoplasmic staining pattern, suggesting Pdpn may contribute to atherosclerosis development in both CLEC-2-dependent and independent manners (38). Pdpn is expressed in stromal myofibroblasts, which contribute to cell migration and invasion, suggesting a role of Pdpn in vascular remodeling and atherosclerotic progression in atherosclerotic plaques. On the other hand, inflammatory cytokines in plaque progression promote Pdpn expression in stromal cells and endothelial cells. Besides, adventitial lymphatics in the arterial walls protect against atherosclerosis, which are important in reverse cholesterol transport from atherosclerotic lesions (40). Pdpn was specifically associated with lymphatic endothelium number of adventitial lymphatics of human internal

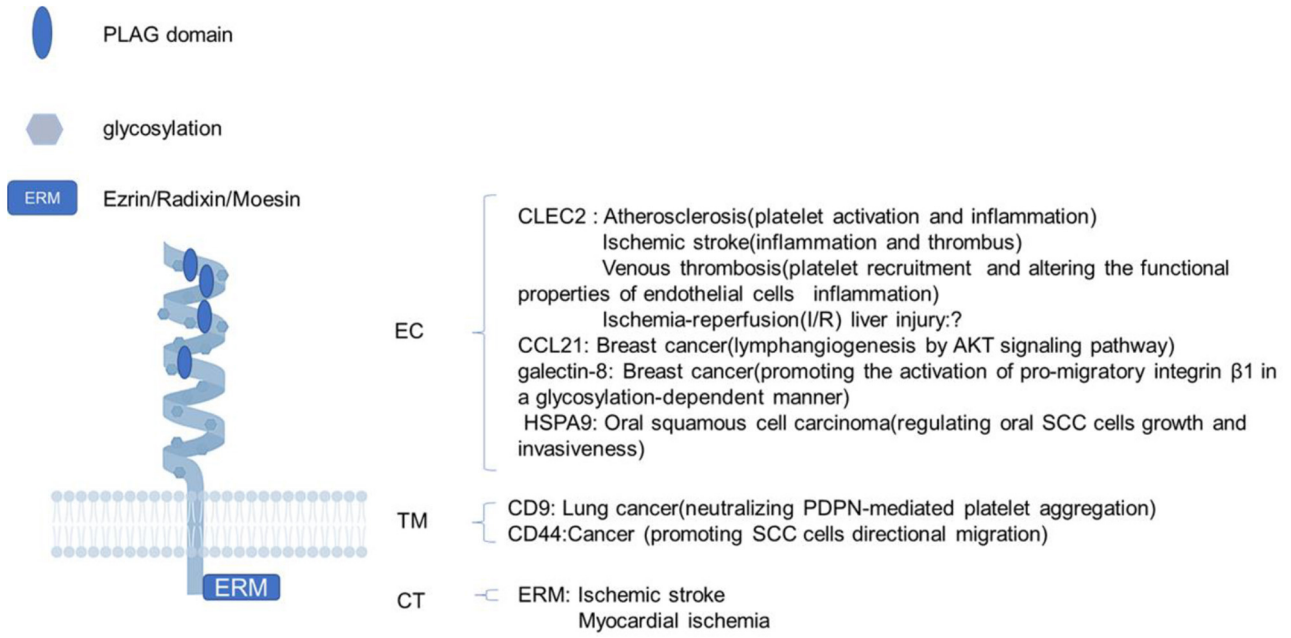

FIGURE 1
The structure of podoplanin and its functions with interacting proteins. Schematic representation of the molecular structure of podoplanin with a heavily glycosylated extracellular domain, a single transmembrane domain, and a short 9-amino acid cytoplasm. The ligands and biological processes during which the identified molecules interacting with podoplanin are presented. EC, ectodomain; TM, transmembrane region; CT, cytosolic domain; PLAG, platelet aggregation-stimulating.

carotid artery, which demonstrated Pdpn may participate in atherosclerosis *via* regulating functions and regeneration of adventitial lymphatic vessels in atherosclerotic lesions (41). In a disturbed blood flow (d-flow) model, monocyte Pdpn was upregulated by d-flow, and the myeloid-specific Pdpn deletion mitigated the subendothelial accumulation of platelets and monocytes/macrophages, which ameliorated vascular inflammation (42) (Table 1).

Much evidence confirmed the role of Pdpn in the development and manifestation of atherosclerosis mainly through inflammation and lymphatic vessel functional regulation pathways. CLEC-2 is the important partner for the role of Pdpn in atherosclerosis, however, other receptors and signaling pathways need to be explored.

Ischemic stroke

Ischemic stroke is one of the most common thrombotic diseases, caused by a blood clot occluding one or multiple cerebral arteries, which means rapid recanalization of the occluded blood vessel is necessary for the treatment of acute ischemic stroke (AIS). However, even recanalization is successful, symptoms can still aggravate. This is called ischemia/reperfusion (I/R) injury, in which thrombotic and inflammatory pathways play a crucial role. Thus, ischemic stroke is recognized as a thromboinflammation disease (85). The Pdpn/CLEC-2 axis is thought to be a major regulator of thrombo-inflammatory disorders (86, 87). Therefore, we previously conducted a prospective observational study, including 352 AIS patients and 112 healthy controls. The results showed that plasma CLEC-2 (pCLEC-2) levels were associated with stroke progression and poor prognosis at 90 days. During 1 year follow-up, pCLEC-2 levels were also predictive for higher incidence of death and vascular events (43, 44). Further we examined the mechanism of Pdpn/CLEC-2 axis in cerebral ischemia injury using a mouse middle cerebral artery occlusion (MCAO) model. In this study, the expression of CLEC-2 and Pdpn increased after ischemia/reperfusion (I/R) injury and anti-Pdpn antibody pretreatment reduced infarct volume and attenuated the neurological deficits with a significant decrease of IL-18 and IL-1β, indicating a possible role of the Pdpn/CLEC-2 axis in the regulation of inflammation in ischemic stroke *via* modulating NLRP3 inflammasome (45). An upregulated Pdpn expression in reactive astrocytes in the ischemic model was observed, which might be a part of compensatory response to ischemic brain injury. This implied a remarkable role of Pdpn in astrocytes in ischemic brain injury, and cellular interactions among astrocytes, neurons, and microglia await to be elucidated further (20). Qian et al. reported the molecular mechanism of Pdpn neutralization inhibiting I/R-induced microglial activation using transcriptome sequencing analysis and found numerous inflammation-related signaling pathways were regulated by the anti-Pdpn treatment (46). Some upper proteins such as TRPM7 kinase might downregulate CLEC-2 to protect mice from acute ischemic disease without developing intracranial hemorrhage, which could provide us some clues on the mechanism of Pdpn/CLEC-2 axis in ischemic stroke (88). Both vascular and neurovascular interaction mechanisms may be involved, awaiting to be elucidated. Moreover, the interaction of the CT of Pdpn with the ERM protein family activates Rho GTPases. RhoA/ROCK signaling pathway in astrocytes is suggested to be crucial in neurogenesis and angiogenesis after cerebral

TABLE 1 Pdpn in thrombotic diseases.

Diseases	Species	Trend	Outcomes	Potential molecules	References
Atherosclerosis	Human/Mouse	↑	Contributing to atherosclerosis development in both CLEC-2-dependent and independent manners.	CLEC-2, VEGF-A, inflammatory cytokines	Torres et al. (34), Kutkut et al. (40), Drozdz et al. (41)
Ischemic stroke	Human/Mouse	↑	High risk of stroke progression, poor prognosis, and death. Increased expression of CLEC-2 and Pdpn after I/R injury and protective effect of anti-Pdpn against I/R injury. Regulation of inflammatory cytokines through NLRP3? and thrombosis	CLEC-2, NLRP3?, RhoA/ROCK?	Zhang et al. (43), Wu et al. (44), Meng et al. (45), Zhao et al. (20), Qian et al. (46)
Venous thrombosis	Human/Mouse	↑	Anti-Pdpn antibody treatment and CLEC-2 deletion resulted in a reduction of thrombus formation. Pdpn overexpression was strongly associated with the amount of intratumoral thrombotic vessels and increased VTE risk in cancer patients. Anti-Pdpn antibody treatment inhibited platelet activation *in vitro* and decreased the incidence of VTE in mice.	CLEC-2	von Brühl et al. (47), Brill et al. (48, 49), Payne et al. (50), Kolenda et al. (51), Mir Seyed Nazari et (52, 53), Riedl et al. (54), Suzuki-Inoue (55), Wang et al. (56), Lee et al. (57), Sasano et al. (16), Sun et al. (58), Watanabe et al. (59), Tawil et al. (60), Zwicker (61)
Kidney ischemic injury	Human/Rats/Mouse	Glomeruli↓ renal interstitium↑	The increasing of urine Pdpn-to-creatinine ratio correlates with the onset of renal IRI. Significant decrease Pdpn expression in the renal glomerulus of diabetic kidney disease mice with an underlying chronic renal ischemia.	NF-κB?, mTOR?	Breiteneder-Geleff et al. (62), Weichhart et al. (63), Kezic et al. (64, 65), Zhang et al. (66), Chuang et al. (67), Kasinath et al. (68, 69), Yu et al. (70), Gao et al. (71)
Myocardial ischemia	Human/Mouse	↑	Upregulation of Pdpn in a heterogeneous cell population. Pdpn-neutralizing antibodies reduces inflammation post-MI without full suppression leading to heart function and scar composition improvement.	?	Mahtab et al. (72, 73), Douglas et al. (74), Cui (75), Loukas et al. (76), Noseda et al. (77), Popescu et al. (78), Aspelund et al. (79), Díaz-Flores et al. (80), Caporali et al. (81), Cimini et al. (82), Wakai et al. (83)
Ischemia-reperfusion liver injury	Mouse	↑	Activation of platelets.		Nakata et al. (84)

10.3389/fneur.2023.1118843

ischemia, which indicates the crosstalk among podoplanin, ERM protein family, and astrocytes in ischemic stroke needs to be further studied (Table 1).

Pdpn contributes to the cerebral ischemia injury mainly through thrombosis and inflammation pathways. Its expression is upregulated after brain ischemia in various kinds of cells, some of which may not express Pdpn in normal conditions. However, the exact cellular interactions, vascular and neurovascular interaction mechanisms, and molecular signaling pathways remains to be elucidated.

Venous thrombosis

Deep vein thrombosis (DVT) is a type of blood clot within deep veins, which is one of the most common venous thromboembolic disorders with a high mortality. Its underlying mechanisms still remain unclear, however, recent evidence has demonstrated that immune cells and inflammatory processes are involved in DVT initiation besides blood coagulation disorder (89). DVT is rich in red cells and fibrin, the formation of which involves the interaction of von Willebrand factor (vWF), platelets, neutrophils, and mast cells (47–49). In a murine DVT model of inferior vena cava (IVC) stenosis, it has been demonstrated that general inducible deletion of CLEC-2 or platelet-specific deficiency in CLEC-2 are protected against DVT. Also, anti-Pdpn antibody treatment resulted in a reduction of thrombus formation (50). The mechanisms have been suspected that the interaction of CLEC-2 in platelets and overexpressed Pdpn in the IVC wall induced venous thrombus formation. Highly distorted flow caused by IVC stenosis and following hypoxia led to upregulated Pdpn expression (51). However, Pdpn upregulation cannot only be a cause for thrombosis but might also be triggered by thrombus formation, which indicates both mechanisms may operate in parallel forming a positive feedback (Table 1). A recent study has demonstrated a role of CLEC-2 in cerebral venous thrombosis (CVT), an unusual manifestation of venous thrombosis. The results showed antibody (INU1-fab)-induced cooperative signaling of CLEC-2 and GPIIb/IIIa triggered a CVT-like thrombotic syndrome in mice. The authors speculated that INU1-fab alters the conformation of CLEC-2 and facilitates its interaction with an unknown ligand enriched in cerebral veins (90). Thus, Pdpn, a main ligand of CLEC-2 for platelet activation, was thought to be a candidate partner, as it is obviously upregulated in different inflammatory tissues including the brain, and can be shed from the cell surface to circulate in plasma (20, 91). However, it needs to be further explored.

A crucial role of the interaction between CLEC-2 and Pdpn in venous thrombosis has been revealed. Upregulated Pdpn expression was observed in DVT. The exact cellular expression and molecular signaling pathway remains to be uncovered, especially for CVT. Also, whether there are interactions between Pdpn and other receptors in venous thrombosis needs to be explored.

Cancer-associated thrombosis

Moreover, Pdpn-associated platelet activation has been demonstrated to contribute to cancer-associated thrombosis, which are based on the upregulation of Pdpn on the cell surface of brain tumor cells. CATS trial reported that Pdpn overexpression was strongly associated with the amount of intratumoral thrombotic vessels and increased VTE risk in cancer patients. Platelet counts were lower and plasma D-dimer levels were higher in those with Pdpn-expressing brain tumors (52). Increased Pdpn expression in glioma cells coincides with the development of venous thrombo-embolism, which is correlated with laboratory evidence of coagulation activation by elevated D-dimer levels (54). CLEC-2-Pdpn interaction has been suggested to stimulate cancer-associated thrombosis in which thromboinflammation plays a crucial role. One hand, thromboinflammation induces ectopic podoplanin expression in vascular endothelial cells or macrophages; on the other hand, CLEC-2 depletion reduces levels of plasma inflammatory cytokines (55). Anti-Pdpn antibody treatment inhibited platelet activation *in vitro* and decreased the incidence of VTE in mice (56). In oral squamous cell carcinoma and ovarian cancer, the same results have been reported (16, 57). Hypermethylation of CpG islands in the Pdpn promoter was regulated by mutant isocitrate dehydrogenase (IDH) in glioma, which resulted in decreased Pdpn expression (58). Indeed, combination of IDH1 mutation and Pdpn expression in brain tumors can help identify patients at high risk of VTE (53, 59). Further exploration found Pdpn was released with exosome-like EVs shed from cells (60). Additionally, in a mouse model of systemic Salmonella Typhimurium infection, Pdpn was upregulated in monocyets and Kupffer cells (KCs) and its combination with CLEC-2 promoted the formation of infection-driven thrombosis in the liver (61, 92) (Table 1). Different forms of Pdpn participate in the formation of cancer-associated thrombosis, to which pdpn-mediated thrombosis, inflammation, and intratumoral vessel generation contributes. Besides CLEC-2, there may be other partners interacting with Pdpn in cancer-associated thrombosis.

Kidney ischemic injury

Ischemia-reperfusion injury (IRI) is one of the most common causes of acute kidney injury (AKI), a serious and often deadly condition. Kidney IRI accounts for almost 50% of AKI cases, which is mediated by free radicals and reactive oxygen species (ROS) after periods of disrupted blood flow (68). Pdpn was named according to its expression in podocytes, mainly along their urinary surfaces, indicating a potentially functional role of Pdpn in kidney IRI (62). In a mouse model of kidney IRI, decreased Pdpn expression in the glomerulus and increased expression in the tubulointerstitial compartment of the kidney shortly after IRI was demonstrated. And the intensity of Pdpn in the tubulointerstitial compartment increased with the severity of ischemia, and the distribution of its expression changed over time (68). Moreover, an increase in the urine Pdpn-to-creatinine ratio was found to correlate with the onset of renal IRI. The researchers speculated that Pdpn was shed from the podocytes in an extracellular-vesicle form and expelled into the urine, which might be internalizated by the proximal tubule epithelium. Another hypothesis was spindle-shaped cells expressing Pdpn in the interstitium of the medulla might migrate to kidney from another organ, playing an important role in

neovascularization during processes of kidney IRI. However, the exact mechanisms need to be further explored. Pdpn expression was significantly decreased in the renal glomerulus of diabetic kidney disease mice with an underlying chronic renal ischemia (70).

During the process, the activation of NF-κB signaling pathway in podocytes downregulated the expression of Pdpn, leading to increased podocyte apoptosis. Moreover, rapamycin, a kind of mTOR inhibitor, had a controversial role in the treatment of acute ischemic kidney injury. Some studies indicated a damage-promoting role of rapamycin during kidney IR injury (64, 65), while some reported a protective role of rapamycin against kidney IR injury (63, 65, 66). However, there was evidence on correlation between phosphorylated mTOR expression and Pdpn expression in esophageal squamous cell carcinoma and traumatic brain injury, which indicated Pdpn might participated in kidney IRI *via* mTOR pathway, awaiting to be explored (67, 71). Immune responses are involved in the pathophysiology of ischemic acute kidney injury (AKI) (93). In some immune diseases of kidney such as rescentic glomerulonephritis (GN), membrane Pdpn on fibroblastic reticular cells (FRCs) may play an important role in the pathogenesis. The effect of treatment with anti-Pdpn antibody was similar to that of FRC depletion by decreasing T-cell activation in the lymph node (LN), resulting in reduction of kidney injury (69). Fibroblastic reticular cells also maintain the integrity of high endothelial venules (HEVs) through interactions between Pdpn on the FRCs and CLEC-2 on platelets (9). Anti-Pdpn treatment led to disorganization of laminin fibers in the kidney LN, which was associated with remarkably reduced expansion of the lymphatic vasculature (69). Therefore, it is hypothesized that Pdpn on FRCs may contribute to ischemic kidney injury by immune regulation, which may be the future research contents (Table 1).

The role of Pdpn in kidney IRI remains unclear. Its mechanisms are complex. Both sPdpn and cellular form participate in the pathogenesis, in which NF-κB and mTOR signaling pathways have been implicated. Moreover, the role of Pdpn on FRCs in activation of T-cells and maintenance of the integrity of HEVs in kidney IRI needs to be explored.

Myocardial ischemia (MI)

Myocardial ischemia (MI) is the commonest cardiovascular disease and one of the major causes of morbidity and mortality worldwide, in the pathogenesis of which inflammation and following heart tissue evolution play an important role. In the process, the growth and expansion of cardiac lymphatic vasculature in response to MI, is crucial for the transportation of extravasated proteins and lipids, inflammatory, and immune responses, as well as fluid balance (75, 76, 79). Therefore, Pdpn as a specific lymphatic marker, is thought to be vital in the cardiac development as well as the pathogenesis of MI. The function of Pdpn is crucial for epicardiac development and myocardial differentiation and its knockout shows a hypoplastic myocardium, atrioventricular valve abnormalities, and coronary artery abnormalities, which is partly correlated with reduced epithelial-mesenchymal transformation (EMT) caused by down-regulation of Pdpn (72, 74). Moreover, Pdpn deficiency results in hypoplastic sinus venosus myocardium including the sinoatrial node, which is also related to abnormal EMT due to up-regulated E-cadherin and down-regulated RhoA controlled by Pdpn (73). In the adult heart, Pdpn-positive cells only constitute <5% of the myocardial small cell population, which is only expressed by cardiac lymphatic endothelial cells in homeostatic conditions (94). However, after myocardial infarction (MI), Pdpn is upregulated in a heterogeneous cell population such as PDGFRα-, PDGFRβ-, and CD34-positive cells, besides lymphatic endothelial cells. Therefore, researchers thought Pdpn might be a sign of activation of a cohort of progenitor cells in different phases of post-ischemic myocardial wound repair. Inhibition of Pdpn by Pdpn-neutralizing antibodies reduces inflammation post-MI without full suppression leading to heart function and scar composition improvement. The increase of Pdpn-positive cells last from the acute (2 days) to the chronic phase of MI (2 weeks to 1 month) (82), which indicates a vital role of Pdpn in inflammation and wound repair after MI. Cimini et al. identified Pdpn as a potential cellular mediator of the lymphangiogenic and fibrogenic responses during different stages of myocardial wound repair after infarction (82). After injury, Pdpn is co-expressed by four kinds of cells such as PDGFRα-, PDGFRβ-, CD34-positive cells, and lymphatic endothelial cells which are responsible for regeneration, fibrosis, and inflammatory processes of the same pathologies. In the process, inflammation was thought to contribute to the recruitment of Pdpn-bearing LYVE-1-negative cells to the site of myocardial repair or the activation of Pdpn expression in responsive cell cohorts, which started the myocardial wound repair after infarction. At different stages of MI, Pdpn is expressed on various kinds of cells, for example, PDGFRα-positive cells during the whole process and PDGFRβ and CD34-positive cells at later stages of infarct healing in the mature scar. This means Pdpn plays multiple roles in the pathogenesis of MI. Cimini et al. reported the inhibition of the interaction between Pdpn and CLEC-2 expressing immune cells in the heart improved the cardiac performance, regeneration, and angiogenesis. In the model, Pdpn neutralizing antibody treatment induced recruitment of anti-inflammatory monocytes/macrophages and increased expression of anti-inflammatory cytokines (95).

Pericytes with PDGFR-β is very connected with Pdpn expression and transplantation of allogenic pericytes improves myocardial vascularization after MI resulting from the regulation of the endothelium in angiogenesis (81, 96). While mesenchymal stem cells (MSCs) expressing PDGFRα in the heart showed cardiomyocyte, endothelial, and smooth muscle lineage potential (77). *In vitro* differentiation of cardiac PDGFRα-positive cells brings out a lot of SMCs and endothelial cells only, indicating a predominant role of Pdpn in cardiac MSCs PDGFRα-positive cells in the vascular and mesenchymal compartments. CD34+telocytes expressed Pdpn after 15 days of MI, which supports cardiac growth, regeneration, renovation of connective tissue, and repair due to the unique communication with cardiac stem and progenitor cells (78, 80). Moreover, Pdpn expression significantly enhanced the migration of mesenchymal stromal cells (MSCs) and Pdpn-expressing MSCs extended processes into the endothelial cell layer, which could interact with circulating platelets (83) (Table 1).

In conclusion, cardiac ischemic injury induces upregulated and ectopic expression of Pdpn. The interaction of Pdpn and CLEC-2 or ERM proteins may participate in post-MI inflammatory response and cardiac repair through inflammation regulation, cytoskeleton

reorganization, and lymphangiogenic and fibrogenic responses. The exact mechanisms remain unclear. And the interaction of Pdpn with other partners in cardiac ischemic injury needs to be further explored.

Ischemia-reperfusion (I/R) liver injury

Hepatic I/R injury is usually associated with surgical procedures, trauma, liver transplantation, or resection as a consequence of interrupted blood supply to the liver, which leads to liver dysfunction and failure, as well as multiple organ failure (97, 98). Kupffer cells (KCs) and platelets were reported as two main roles in the procedure (99–101). Nakata et al. revealed Pdpn expression in the cytosol of hepatocytes in the post-ischemic liver and KC depletion weakened the Pdpn expression, which suggested that activated KCs regulate the expression of Pdpn in hepatocytes after I/R without clear mechanisms (84). Moreover, the authors demonstrated in the acute phase of hepatic I/R injury, the binding of CLEC-2 on the cell surface of platelets to Pdpn in hepatocytes activated platelets in the hepatic sinusoid (84). Therefore, the crosstalk among podoplanin, KCs, and platelets in hepatic I/R injury needs to be further studied (Table 1).

Conclusions and perspectives

Pdpn, as an important glyprotein, has multiple interacting proteins in various tissues and organs, demonstrating its pleiotropic functions, especially a role in thrombosis and inflammation. Thrombosis and inflammation contribute to the pathogenesis of thrombotic diseases, such as atherosclerosis, ischemic stroke, venous thrombosis, acute kidney and liver ischemic injury, and myocardial ischemia. Evidence showed that after ischemia, Pdpn can be acquired over time by a heterogeneous cell population such as SMCs, endothelial cells, astrocytes, pericytes, MSCs, telocytes, and so on, which may not express Pdpn in normal conditions. However, the exact mechanisms of Pdpn in such ischemic diseases have not clearly been demonstrated. Pdpn in different cells plays different roles such as thrombosis, inflammation, vascularization, lymphagiogenesis, growth, and regeneration. However, many issues remain to be elucidated further; for instance, cell/stage-specific effects of Pdpn and according molecular mechanisms, and the relevance of anti-Pdpn treatment on ischemic diseases, especially ischemic stroke, venous thrombosis, and myocardial ischemia. The solutions to these issues can provide a new target of treating thrombotic diseases from bench to clinical translation.

Author contributions

YH: writing-original draft, visualization, and data curation. ML and YW: data curation, visualization, and resources. CZ: validation, investigation, and resources. YC: writing—review, editing, and funding acquisition. XZ: conceptualization, methodology, project administration, writing—review, editing, funding acquisition, and supervision. All authors have carefully read and confirmed the final manuscript. All authors contributed to the article and approved the submitted version.

Funding

The study was supported by the opening project of Jiangsu Key Laboratory of Neurological and Psychiatric Diseases (KJS2030), Key Talent Project of Nuclear Technology Medical Application of the Second Affiliated Hospital of Soochow University (XKTJ-HRC2021006), the China National Natural Fund Project (No. 82171296), and Discipline Construction Program of the Second Affiliated Hospital of Soochow University (XKTJ-TD202004).

Conflict of interest

The authors declare that the research was conducted in the absence of any commercial or financial relationships that could be construed as a potential conflict of interest.

Publisher's note

References

1. Zimmer G, Oeffner F, Von Messling V, Tschernig T, Gröness HJ, Klenk HD, et al. Cloning and characterization of gp36, a human mucin-type glycoprotein preferentially expressed in vascular endothelium. *Biochem J.* (1999) 341(Pt 2):277–84. doi: 10.1042/bj3410277

2. Toyoshima M, Nakajima M, Yamori T, Tsuruo T. Purification and characterization of the platelet-aggregating sialoglycoprotein gp44 expressed by highly metastatic variant cells of mouse colon adenocarcinoma 26. *Cancer Res.* (1995) 55:767–73.

3. Nose K, Saito H, Kuroki T. Isolation of a gene sequence induced later by tumor-promoting 12-O-tetradecanoylphorbol-13-acetate in mouse osteoblastic cells (MC3T3-E1) and expressed constitutively in ras-transformed cells. *Cell Growth Differ.* (1990) 1:511–8.

4. Gandarillas A, Scholl FG, Benito N, Gamallo C, Quintanilla M. Induction of PA2.26, a cell-surface antigen expressed by active fibroblasts, in mouse epidermal keratinocytes during carcinogenesis. *Mol Carcinog.* (1997) 20:10–8. doi: 10.1002/(sici)1098-2744(199709)20:1<10::aid-mc3>3.0.co;2-m

5. Lee JY, Park C, Cho YP, Lee E, Kim H, Kim P, et al. Podoplanin-expressing cells derived from bone marrow play a crucial role in postnatal lymphatic neovascularization. *Circulation.* (2010) 122:1413–25. doi: 10.1161/CIRCULATIONAHA.110.941468

6. Tsukiji N, Inoue O, Morimoto M, Tatsumi N, Nagatomo H, Ueta K, et al. Platelets play an essential role in murine lung development through Clec-2/podoplanin interaction. *Blood.* (2018) 132:1167–79. doi: 10.1182/blood-2017-12-823369

7. Quintanilla M, Montero-Montero L, Renart J, Martín-Villar E. Podoplanin in inflammation and cancer. *Int J Mol Sci.* (2019) 20:707. doi: 10.3390/ijms20030707

8. Boulaftali Y, Hess PR, Getz TM, Cholka A, Stolla M, Mackman N, et al. Platelet ITAM signaling is critical for vascular integrity in inflammation. *J Clin Invest.* (2013) 123:908–16. doi: 10.1172/JCI65154

9. Herzog BH, Fu J, Wilson SJ, Hess PR, Sen A, McDaniel JM, et al. Podoplanin maintains high endothelial venule integrity by interacting with platelet CLEC-2. *Nature.* (2013) 502:105–9. doi: 10.1038/nature12501

10. Kaneko MK, Kato Y, Kameyama A, Ito H, Kuno A, Hirabayashi J, et al. Functional glycosylation of human podoplanin: glycan structure of platelet aggregation-inducing factor. *FEBS Lett.* (2007) 581:331–6. doi: 10.1016/j.febslet.2006.12.044

11. Martín-Villar E, Scholl FG, Gamallo C, Yurrita MM, Muñoz-Guerra M, Cruces J, et al. Characterization of human PA226 antigen (T1alpha-2, podoplanin), a small membrane mucin induced in oral squamous cell carcinomas. *Int J Cancer.* (2005) 113:899–910. doi: 10.1002/ijc.20656

12. Scholl FG, Gamallo C, Vilaró S, Quintanilla M. Identification of PA226 antigen as a novel cell-surface mucin-type glycoprotein that induces plasma membrane extensions and increased motility in keratinocytes. *J Cell Sci.* (1999) 112:4601–13. doi: 10.1242/jcs.112.24.4601

13. Barth K, Bläsche R, Kasper M. T1alpha/podoplanin shows raft-associated distribution in mouse lung alveolar epithelial E10 cells. *Cell Physiol Biochem.* (2010) 25:103–12. doi: 10.1159/000272065

14. Fernández-Muñoz B, Yurrita MM, Martín-Villar E, Carrasco-Ramírez P, Megías D, Renart J, et al. The transmembrane domain of podoplanin is required for its association with lipid rafts and the induction of epithelial-mesenchymal transition. *Int J Biochem Cell Biol.* (2011) 43:886–96. doi: 10.1016/j.biocel.2011.02.010

15. Carrasco-Ramírez P, Greening DW, Andrés G, Gopal SK, Martín-Villar E, Renart J, et al. Podoplanin is a component of extracellular vesicles that reprograms cell-derived exosomal proteins and modulates lymphatic vessel formation. *Oncotarget.* (2016) 7:16070–89. doi: 10.18632/oncotarget.7445

16. Sasano T, Gonzalez-Delgado R, Muñoz NM, Carlos-Alcade W, Cho MS, Sheth RA, et al. Podoplanin promotes tumor growth, platelet aggregation, and venous thrombosis in murine models of ovarian cancer. *J Thromb Haemost.* (2022) 20:104–14. doi: 10.1111/jth.15544

17. Roca E, Lacroix R, Judicone C, Laroumagne S, Robert S, Cointe S, et al. Detection of EpCAM-positive microparticles in pleural fluid: a new approach to mini-invasively identify patients with malignant pleural effusions. *Oncotarget.* (2016) 7:3357–66. doi: 10.18632/oncotarget.6581

18. Sankiewicz A, Guszcz T, Mena-Hortelano R, Zukowski K, Gorodkiewicz E. Podoplanin serum and urine concentration in transitional bladder cancer. *Cancer Biomark.* (2016) 16:343–50. doi: 10.3233/CBM-160572

19. Bai B, Ma W, Wang K, Ha S, Wang JB, Tan BX, et al. Detection of D2-40 monoclonal antibody-labeled lymphatic vessel invasion in esophageal squamous cell carcinoma and its clinicopathologic significance. *Cancer Biol Med.* (2013) 10:81–5. doi: 10.7497/j.issn.2095-3941.2013.02.003

20. Zhao X, Pan Y, Ren W, Shen F, Xu M, Yu M, et al. Plasma soluble podoplanin is a novel marker for the diagnosis of tumor occurrence and metastasis. *Cancer Sci.* (2018) 109:403–11. doi: 10.1111/cas.13475

21. Takemoto A, Miyata K, Fujita N. Platelet-activating factor podoplanin: from discovery to drug development. *Cancer Metastasis Rev.* (2017) 36:225–34. doi: 10.1007/s10555-017-9672-2

22. Renart J, Carrasco-Ramírez P, Fernández-Muñoz B, Martín-Villar E, Montero L, Yurrita MM, et al. New insights into the role of podoplanin in epithelial-mesenchymal transition. *Int Rev Cell Mol Biol.* (2015) 317:185–239. doi: 10.1016/bs.ircmb.2015.01.009

23. Kato Y, Kaneko MK, Kunita A, Ito H, Kameyama A, Ogasawara S, et al. Molecular analysis of the pathophysiological binding of the platelet aggregation-inducing factor podoplanin to the C-type lectin-like receptor CLEC-2. *Cancer Sci.* (2008) 99:54–61. doi: 10.1111/j.1349-7006.2007.00634.x

24. Nagae M, Morita-Matsumoto K, Kato M, Kaneko MK, Kato Y, Yamaguchi Y, et al. A platform of C-type lectin-like receptor CLEC-2 for binding O-glycosylated podoplanin and nonglycosylated rhodocytin. *Structure.* (2014) 22:1711–21. doi: 10.1016/j.str.2014.09.009

25. Suzuki-Inoue K, Fuller GL, García A, Eble JA, Pöhlmann S, Inoue O, et al. A novel Syk-dependent mechanism of platelet activation by the C-type lectin receptor CLEC-2. *Blood.* (2006) 107:542–9. doi: 10.1182/blood-2005-05-1994

26. Suzuki-Inoue K, Inoue O, Ozaki Y. Novel platelet activation receptor CLEC-2: from discovery to prospects. *J Thromb Haemost.* (2011) 9(Suppl 1):44–55. doi: 10.1111/j.1538-7836.2011.04335.x

27. Bourne JH, Beristain-Covarrubias N, Zuidscherwoude M, Campos J, Di Y, Garlick E, et al. CLEC-2 prevents accumulation and retention of inflammatory macrophages during murine peritonitis. *Front Immunol.* (2021) 12:693974. doi: 10.3389/fimmu.2021.693974

28. Martín-Villar E, Megías D, Castel S, Yurrita MM, Vilaró S, Quintanilla M. Podoplanin binds ERM proteins to activate RhoA and promote epithelial-mesenchymal transition. *J Cell Sci.* (2006) 119(Pt 21):4541–53. doi: 10.1242/jcs.03218

29. Zhang Z, Zhang N, Yu J, Xu W, Gao J, Lv X, et al. The role of podoplanin in the immune system and inflammation. *J Inflamm Res.* (2022) 15:3561–72. doi: 10.2147/JIR.S366620

30. Cheok YY, Tan GMY, Fernandez KC, Chan YT, Lee CYQ, Cheong HC, et al. Podoplanin drives motility of active macrophage *via* regulating filamin C during *Helicobacter pylori* infection. *Front Immunol.* (2021) 12:702156. doi: 10.3389/fimmu.2021.702156

31. Kerrigan AM, Navarro-Nuñez L, Pyz E, Finney BA, Willment JA, Watson SP, et al. Podoplanin-expressing inflammatory macrophages activate murine platelets *via* CLEC-2. *J Thromb Haemost.* (2012) 10:484–6. doi: 10.1111/j.1538-7836.2011.04614.x

32. Fei M, Wang H, Zhou M, Deng C, Zhang L, Han Y. Podoplanin influences the inflammatory phenotypes and mobility of microglia in traumatic brain injury. *Biochem Biophys Res Commun.* (2020) 523:361–7. doi: 10.1016/j.bbrc.2019.12.003

33. Nylander AN, Ponath GD, Axisa PP, Mubarak M, Tomayko M, Kuchroo VK, et al. Podoplanin is a negative regulator of Th17 inflammation. *JCI Insight.* (2017) 2:e92321. doi: 10.1172/jci.insight.92321

34. Torres N, Guevara-Cruz M, Velázquez-Villegas LA, Tovar AR. Nutrition and atherosclerosis. *Arch Med Res.* (2015) 46:408–26. doi: 10.1016/j.arcmed.2015.05.010

35. Davì G, Patrono C. Platelet activation and atherothrombosis. *N Engl J Med.* (2007) 357:2482–94. doi: 10.1056/NEJMra071014

36. Marx C, Novotny J, Salbeck D, Zellner KR, Nicolai L, Pekayvaz K, et al. Eosinophil-platelet interactions promote atherosclerosis and stabilize thrombosis with eosinophil extracellular traps. *Blood.* (2019) 134:1859–72. doi: 10.1182/blood.2019000518

37. Wang N, Tall AR. Cholesterol in platelet biogenesis and activation. *Blood.* (2016) 127:1949–53. doi: 10.1182/blood-2016-01-631259

38. Inoue O, Hokamura K, Shirai T, Osada M, Tsukiji N, Hatakeyama K, et al. Vascular smooth muscle cells stimulate platelets and facilitate thrombus formation through platelet CLEC-2: implications in atherothrombosis. *PLoS ONE.* (2015) 10:e0139357. doi: 10.1371/journal.pone.0139357

39. Furukoji E, Yamashita A, Nakamura K, Hirai T, Asada Y. Podoplanin expression on endothelial cells promotes superficial erosive injury and thrombus formation in rat carotid artery: implications for plaque erosion. *Thromb Res.* (2019) 183:76–9. doi: 10.1016/j.thromres.2019.10.015

40. Kutkut I, Meens MJ, McKee TA, Bochaton-Piallat ML, Kwak BR. Lymphatic vessels: an emerging actor in atherosclerotic plaque development. *Eur J Clin Invest.* (2015) 45:100–8. doi: 10.1111/eci.12372

41. Drozdz K, Janczak D, Dziegiel P, Podhorska M, Patrzałek D, Ziółkowski P, et al. Adventitial lymphatics of internal carotid artery in healthy and atherosclerotic vessels. *Folia Histochem Cytobiol.* (2008) 46:433–6. doi: 10.2478/v10042-008-0083-7

42. Tang C, Wang L, Sheng Y, Zheng Z, Xie Z, Wu F, et al. CLEC-2-dependent platelet subendothelial accumulation by flow disturbance contributes to atherogenesis in mice. *Theranostics.* (2021) 11:9791–804. doi: 10.7150/thno.64601

43. Zhang X, Zhang W, Wu X, Li H, Zhang C, Huang Z, et al. Prognostic significance of plasma CLEC-2 (C-Type Lectin-Like Receptor 2) in patients with acute ischemic stroke. *Stroke.* 2018:STROKEAHA118022563. doi: 10.1161/STROKEAHA.118.022563

44. Wu X, Zhang W, Li H, You S, Shi J, Zhang C, et al. Plasma C-type lectin-like receptor 2 as a predictor of death and vascular events in patients with acute ischemic stroke. *Eur J Neurol.* (2019) 26:1334–40. doi: 10.1111/ene.13984

45. Meng D, Ma X, Li H, Wu X, Cao Y, Miao Z, et al. A role of the podoplanin-CLEC-2 axis in promoting inflammatory response after ischemic stroke in mice. *Neurotox Res.* (2021) 39:477–88. doi: 10.1007/s12640-020-00295-w

46. Qian S, Qian L, Yang Y, Cui J, Zhao Y. Transcriptome sequencing analysis revealed the molecular mechanism of podoplanin neutralization inhibiting ischemia/reperfusion-induced microglial activation. *Ann Transl Med.* (2022) 10:638. doi: 10.21037/atm-22-1952

47. von Brühl ML, Stark K, Steinhart A, Chandraratne S, Konrad I, Lorenz M, et al. Monocytes, neutrophils, and platelets cooperate to initiate and propagate venous thrombosis in mice *in vivo*. *J Exp Med.* (2012) 209:819–35. doi: 10.1084/jem.20112322

48. Brill A, Fuchs TA, Chauhan AK, Yang JJ, De Meyer SF, Köllnberger M, et al. von Willebrand factor-mediated platelet adhesion is critical for deep vein thrombosis in mouse models. *Blood.* (2011) 117:1400–7. doi: 10.1182/blood-2010-05-287623

49. Brill A, Fuchs TA, Savchenko AS, Thomas GM, Martinod K, De Meyer SF, et al. Neutrophil extracellular traps promote deep vein thrombosis in mice. *J Thromb Haemost.* (2012) 10:136–44. doi: 10.1111/j.1538-7836.2011.04544.x

50. Payne H, Ponomaryov T, Watson SP, Brill A. Mice with a deficiency in CLEC-2 are protected against deep vein thrombosis. *Blood.* (2017) 129:2013–20. doi: 10.1182/blood-2016-09-742999

51. Kolenda J, Jensen SS, Aaberg-Jessen C, Christensen K, Andersen C, Brünner N, et al. Effects of hypoxia on expression of a panel of stem cell and chemoresistance markers in glioblastoma-derived spheroids. *J Neurooncol.* (2011) 103:43–58. doi: 10.1007/s11060-010-0357-8

52. Mir Seyed Nazari P, Riedl J, Pabinger I, Ay C. The role of podoplanin in cancer-associated thrombosis. *Thromb Res.* (2018) 164(Suppl 1):S34–9. doi: 10.1016/j.thromres.2018.01.020

53. Mir Seyed Nazari P, Riedl J, Preusser M, Posch F, Thaler J, Marosi C, et al. Combination of isocitrate dehydrogenase 1 (IDH1) mutation and podoplanin expression in brain tumors identifies patients at high or low risk of venous thromboembolism. *J Thromb Haemost.* (2018) 16:1121–7. doi: 10.1111/jth.14129

54. Riedl J, Preusser M, Nazari PM, Posch F, Panzer S, Marosi C, et al. Podoplanin expression in primary brain tumors induces platelet aggregation and increases risk of venous thromboembolism. *Blood.* (2017) 129:1831–9. doi: 10.1182/blood-2016-06-720714

55. Suzuki-Inoue K. Platelets and cancer-associated thrombosis: focusing on the platelet activation receptor CLEC-2 and podoplanin. *Blood.* (2019) 134:1912–8. doi: 10.1182/blood.2019001388

56. Wang X, Liu B, Xu M, Jiang Y, Zhou J, Yang J, et al. Blocking podoplanin inhibits platelet activation and decreases cancer-associated venous thrombosis. *Thromb Res.* (2021) 200:72–80. doi: 10.1016/j.thromres.2021.01.008

57. Lee HY, Yu NY, Lee SH, Tsai HJ, Wu CC, Cheng JC, et al. Podoplanin promotes cancer-associated thrombosis and contributes to the unfavorable overall survival in an ectopic xenograft mouse model of oral cancer. *Biomed J.* (2020) 43:146–62. doi: 10.1016/j.bj.2019.07.001

58. Sun C, Xiao L, Zhao Y, Shi J, Yuan Y, Gu Y, et al. Wild-type IDH1 and mutant IDH1 opposingly regulate podoplanin expression in glioma. *Transl Oncol.* (2020) 13:100758. doi: 10.1016/j.tranon.2020.100758

59. Watanabe J, Natsumeda M, Okada M, Kanemaru Y, Tsukamoto Y, Oishi M, et al. Podoplanin expression and IDH-wildtype status predict venous thromboembolism in patients with high-grade gliomas in the early postoperative period. *World Neurosurg.* (2019) 128:e982–8. doi: 10.1016/j.wneu.2019.05.049

60. Tawil N, Bassawon R, Meehan B, Nehme A, Montermini L, Gayden T, et al. Glioblastoma cell populations with distinct oncogenic programs release podoplanin as procoagulant extracellular vesicles. *Blood Adv.* (2021) 5:1682–94. doi: 10.1182/bloodadvances.2020002998

61. Zwicker JI. Risking thromboembolism: podoplanin and glioma. *Blood.* (2017) 129:1742–3. doi: 10.1182/blood-2017-02-763524

62. Breiteneder-Geleff S, Matsui K, Soleiman A, Meraner P, Poczewski H, Kalt R, et al. Podoplanin, novel 43-kd membrane protein of glomerular epithelial cells, is down-regulated in puromycin nephrosis. *Am J Pathol.* (1997) 151:1141–52.

63. Weichhart T, Säemann MD. The multiple facets of mTOR in immunity. *Trends Immunol.* (2009) 30:218–26. doi: 10.1016/j.it.2009.02.002

64. Kezic A, Becker JU, Thaiss F. The effect of mTOR-inhibition on NF-κB activity in kidney ischemia-reperfusion injury in mice. *Transplant Proc.* (2013) 45:1708–14. doi: 10.1016/j.transproceed.2013.02.110

65. Kezic A, Thaiss F, Becker JU, Tsui TY, Bajcetic M. Effects of everolimus on oxidative stress in kidney model of ischemia/reperfusion injury. *Am J Nephrol.* (2013) 37:291–301. doi: 10.1159/000348496

66. Zhang C, Zheng L, Li L, Wang L, Li L, Huang S, et al. Rapamycin protects kidney against ischemia reperfusion injury through recruitment of NKT cells. *J Transl Med.* (2014) 12:224. doi: 10.1186/s12967-014-0224-z

67. Chuang WY, Chang YS, Chao YK, Yeh CJ, Ueng SH, Chang CY, et al. Phosphorylated mTOR expression correlates with podoplanin expression and high tumor grade in esophageal squamous cell carcinoma. *Int J Clin Exp Pathol.* (2015) 8:12757–65.

68. Kasinath V, Yilmam OA, Uehara M, Yonar M, Jiang L, Li X, et al. Urine podoplanin heralds the onset of ischemia-reperfusion injury of the kidney. *Am J Physiol Renal Physiol.* (2019) 316:F957–65. doi: 10.1152/ajprenal.00538.2018

69. Kasinath V, Yilmam OA, Uehara M, Jiang L, Ordikhani F, Li X, et al. Activation of fibroblastic reticular cells in kidney lymph node during crescentic glomerulonephritis. *Kidney Int.* (2019) 95:310–20. doi: 10.1016/j.kint.2018.08.040

70. Yu J, Zong GN, Wu H, Zhang KQ. Podoplanin mediates the renoprotective effect of berberine on diabetic kidney disease in mice. *Acta Pharmacol Sin.* (2019) 40:1544–54. doi: 10.1038/s41401-019-0263-3

71. Gao C, Wang H, Wang T, Luo C, Wang Z, Zhang M, et al. Platelet regulates neuroinflammation and restores blood-brain barrier integrity in a mouse model of traumatic brain injury. *J Neurochem.* (2020) 154:190–204. doi: 10.1111/jnc.14983

72. Mahtab EA, Wijffels MC, Van Den Akker NM, Hahurij ND, Lie-Venema H, Wisse LJ, et al. Cardiac malformations and myocardial abnormalities in podoplanin knockout mouse embryos: correlation with abnormal epicardial development. *Dev Dyn.* (2008) 237:847–57. doi: 10.1002/dvdy.21463

73. Mahtab EA, Vicente-Steijn R, Hahurij ND, Jongbloed MR, Wisse LJ, DeRuiter MC, et al. Podoplanin deficient mice show a RhoA-related hypoplasia of the sinus venosus myocardium including the sinoatrial node. *Dev Dyn.* (2009) 238:183–93. doi: 10.1002/dvdy.21819

74. Douglas YL, Mahtab EA, Jongbloed MR, Uhrin P, Zaujec J, Binder BR, et al. Pulmonary vein, dorsal atrial wall and atrial septum abnormalities in podoplanin knockout mice with disturbed posterior heart field contribution. *Pediatr Res.* (2009) 65:27–32. doi: 10.1203/PDR.0b013e31818bc11a

75. Cui Y. Impact of lymphatic vessels on the heart. *Thorac Cardiovasc Surg.* (2010) 58:1–7. doi: 10.1055/s-0029-1240553

76. Loukas M, Abel N, Tubbs RS, Grabska J, Birungi J, Anderson RH. The cardiac lymphatic system. *Clin Anat.* (2011) 24:684–91. doi: 10.1002/ca.21104

77. Noseda M, Harada M, McSweeney S, Leja T, Belian E, Stuckey DJ, et al. PDGFRα demarcates the cardiogenic clonogenic Sca1+ stem/progenitor cell in adult murine myocardium. *Nat Commun.* (2015) 6:6930. doi: 10.1038/ncomms7930

78. Popescu LM, Curici A, Wang E, Zhang H, Hu S, Gherghiceanu M. Telocytes and putative stem cells in ageing human heart. *J Cell Mol Med.* (2015) 19:31–45. doi: 10.1111/jcmm.12509

79. Aspelund A, Robciuc MR, Karaman S, Makinen T, Alitalo K. Lymphatic system in cardiovascular medicine. *Circ Res.* (2016) 118:515–30. doi: 10.1161/CIRCRESAHA.115.306544

80. Díaz-Flores L, Gutiérrez R, Díaz-Flores L Jr, Goméz MG, Sáez FJ, Madrid JF. Behaviour of telocytes during physiopathological activation. *Semin Cell Dev Biol.* (2016) 55:50–61. doi: 10.1016/j.semcdb.2016.01.035

81. Caporali A, Martello A, Miscianinov V, Maselli D, Vono R, Spinetti G. Contribution of pericyte paracrine regulation of the endothelium to angiogenesis. *Pharmacol Ther.* (2017) 171:56–64. doi: 10.1016/j.pharmthera.2016.10.001

82. Cimini M, Cannatá A, Pasquinelli G, Rota M, Goichberg P. Phenotypically heterogeneous podoplanin-expressing cell populations are associated with the lymphatic vessel growth and fibrogenic responses in the acutely and chronically infarcted myocardium. *PLoS ONE.* (2017) 12:e0173927. doi: 10.1371/journal.pone.0173927

83. Wakai T, Fissore RA. Constitutive IP(3)R1-mediated Ca(2+) release reduces Ca(2+) store content and stimulates mitochondrial metabolism in mouse GV oocytes. *J Cell Sci.* (2019) 132:jcs225441. doi: 10.1242/jcs.225441

84. Nakata Y, Kono H, Akazawa Y, Hirayama K, Wakana H, Fukushima H, et al. Role of podoplanin and Kupffer cells in liver injury after ischemia-reperfusion in mice. *Surg Today.* (2022) 52:344–53. doi: 10.1007/s00595-021-02378-3

85. Schuhmann MK, Stoll G, Bieber M, Vögtle T, Hofmann S, Klaus V, et al. CD84 links T cell and platelet activity in cerebral thrombo-inflammation in acute stroke. *Circ Res.* (2020) 127:1023–35. doi: 10.1161/CIRCRESAHA.120.316655

86. Rayes J, Watson SP, Nieswandt B. Functional significance of the platelet immune receptors GPVI and CLEC-2. *J Clin Invest.* (2019) 129:12–23. doi: 10.1172/JCI122955

87. Martin EM, Zuidscherwoude M, Morán LA Di Y, García A, Watson SP. The structure of CLEC-2: mechanisms of dimerization and higher-order clustering. *Platelets.* (2021) 32:733–43. doi: 10.1080/09537104.2021.1906407

88. Gotru SK, Chen W, Kraft P, Becker IC, Wolf K, Stritt S, et al. TRPM7 kinase controls calcium responses in arterial thrombosis and stroke in mice. *Arterioscler Thromb Vasc Biol.* (2018) 38:344–52. doi: 10.1161/ATVBAHA.117.310391

89. Budnik I, Brill A. Immune factors in deep vein thrombosis initiation. *Trends Immunol.* (2018) 39:610–23. doi: 10.1016/j.it.2018.04.010

90. Stegner D, Göb V, Krenzlin V, Beck S, Hemmen K, Schuhmann MK, et al. Foudroyant cerebral venous (sinus) thrombosis triggered through CLEC-2 and GPIIb/IIIa dependent platelet activation. *Nat Cardiovasc Res.* (2022) 1:132–41. doi: 10.1038/s44161-021-00017-1

91. Lax S, Rayes J, Wichaiyo S, Haining EJ, Lowe K, Grygielska B, et al. Platelet CLEC-2 protects against lung injury *via* effects of its ligand podoplanin on inflammatory alveolar macrophages in the mouse. *Am J Physiol Lung Cell Mol Physiol.* (2017) 313:L1016–l29. doi: 10.1152/ajplung.00023.2017

92. Hitchcock JR, Cook CN, Bobat S, Ross EA, Flores-Langarica A, Lowe KL, et al. Inflammation drives thrombosis after Salmonella infection *via* CLEC-2 on platelets. *J Clin Invest.* (2015) 125:4429–46. doi: 10.1172/JCI79070

93. Kinsey GR, Sharma R, Okusa MD. Regulatory T cells in AKI. *J Am Soc Nephrol.* (2013) 24:1720–6. doi: 10.1681/ASN.2013050502

94. Pinto AR, Ilinykh A, Ivey MJ, Kuwabara JT, D'Antoni ML, Debuque R, et al. Revisiting cardiac cellular composition. *Circ Res.* (2016) 118:400–9. doi: 10.1161/CIRCRESAHA.115.307778

95. Lee PY, Nelson-Maney N, Huang Y, Levescot A, Wang Q, Wei K, et al. High-dimensional analysis reveals a pathogenic role of inflammatory monocytes in experimental diffuse alveolar hemorrhage. *JCI Insight.* (2019) 4:e129703. doi: 10.1172/jci.insight.129703

96. Alvino VV, Fernández-Jiménez R, Rodriguez-Arabaolaza I, Slater S, Mangialardi G, Avolio E, et al. Transplantation of allogeneic pericytes improves myocardial vascularization and reduces interstitial fibrosis in a swine model of reperfused acute myocardial infarction. *J Am Heart Assoc.* (2018) 7:e006727. doi: 10.1161/JAHA.117.006727

97. Huguet C, Gavelli A, Bona S. Hepatic resection with ischemia of the liver exceeding one hour. *J Am Coll Surg.* (1994) 178:454–8.

98. Lemasters JJ, Thurman RG. Reperfusion injury after liver preservation for transplantation. *Annu Rev Pharmacol Toxicol.* (1997) 37:327–38. doi: 10.1146/annurev.pharmtox.37.1.327

99. Colletti LM, Cortis A, Lukacs N, Kunkel SL, Green M, Strieter RM. Tumor necrosis factor up-regulates intercellular adhesion molecule 1, which is important in the neutrophil-dependent lung and liver injury associated with hepatic ischemia and reperfusion in the rat. *Shock.* (1998) 10:182–91. doi: 10.1097/00024382-199809000-00006

100. Devey L, Ferenbach D, Mohr E, Sangster K, Bellamy CO, Hughes J, et al. Tissue-resident macrophages protect the liver from ischemia reperfusion injury *via* a heme oxygenase-1-dependent mechanism. *Mol Ther.* (2009) 17:65–72. doi: 10.1038/mt.2008.237

101. Anitua E, Andia I, Ardanza B, Nurden P, Nurden AT. Autologous platelets as a source of proteins for healing and tissue regeneration. *Thromb Haemost.* (2004) 91:4–15. doi: 10.1160/TH03-07-0440

frontiers | Frontiers in Neurology

TYPE Original Research
PUBLISHED 22 March 2023
DOI 10.3389/fneur.2023.1093993

OPEN ACCESS

EDITED BY
Yanlin Zhang,
Second Affiliated Hospital of Soochow University, China

REVIEWED BY
Ali Sazci,
Okan University, Türkiye
Wenqiang Xin,
University Medical Center Göttingen, Germany

*CORRESPONDENCE
Addisu Melake
✉ addismelak@gmail.com

SPECIALTY SECTION
This article was submitted to Stroke, a section of the journal Frontiers in Neurology

RECEIVED 09 November 2022
ACCEPTED 01 March 2023
PUBLISHED 22 March 2023

CITATION
Melake A and Berhane N (2023) Angiotensin-converting enzyme gene insertion/deletion polymorphism and risk of ischemic stroke complication among patients with hypertension in the Ethiopian population. *Front. Neurol.* 14:1093993. doi: 10.3389/fneur.2023.1093993

Angiotensin-converting enzyme gene insertion/deletion polymorphism and risk of ischemic stroke complication among patients with hypertension in the Ethiopian population

Addisu Melake[1,2]* and Nega Berhane[2]

[1]Department of Biomedical Science, College of Health Science, Debre Tabor University, Debre Tabor, Ethiopia, [2]Department of Medical Biotechnology, Institute of Biotechnology, University of Gondar, Gondar, Ethiopia

Background: Ischemic stroke is a complicated, multifaceted condition brought on by a confluence of vascular, environmental, and genetic variables. The burden of ischemic stroke is currently rising in terms of death, morbidity, and disability worldwide. Genetic variables also play significant roles in the pathophysiology of hypertension and ischemic stroke in addition to the greatest effects of demographic, clinical, and behavioral risk factors. The key functional variation of the ACE gene that has drawn the most interest is the ACE I/D variant. Even though the ACE gene I/D polymorphism has been widely studied, the findings of investigations on the involvement of this polymorphism in ischemic stroke were contradictory and provide conflicting data. The goal of this study was to look into the effect of the ACE gene I/D polymorphism on the risk of ischemic stroke in patients with hypertension.

Methods: A hospital-based case–control study was carried out in 36 cases of patients with hypertensive IS and 36 age- and sex-matched healthy controls. Clinical and biochemical parameters were measured to assess the associated risk factors. The DNA was isolated from blood samples, and the ACE I/D genotypes were identified using polymerase chain reaction and analyzed by agarose gel electrophoresis.

Results: The ACE-DD genotype (OR = 3.71, 95% CI = 1.02–13.5; $P < 0.05$) and D allele (OR = 2.07, 95% CI = 1.06–4.03; P <0.05) were significantly more common in patients than in controls, indicating that it is a risk factor for the development of ischemic stroke in hypertensive individuals.

Conclusion: There is a significant correlation between the ACE gene I/D polymorphism and the development of ischemic stroke in patients with a history of hypertension in the Ethiopian population.

KEYWORDS

angiotensin-converting enzyme, genotype, hypertension, ischemic stroke, polymerase chain reaction

1. Introduction

Ischemic stroke (IS) is the loss of brain tissue caused by a cessation of blood supply to a region of the brain brought on by an obstruction of a carotid or vertebral artery, or distal branches of the anterior, middle, or posterior cerebral arteries (1). It is the primary cause of adult disability and the second-leading cause of mortality in the world, accounting for ∼ 10% of all deaths with 5.5 million people dying annually (2). According to data from the 2010 Global Burden of Diseases, Injuries, and Risk Factors Study (GBD), stroke is the most common cardiovascular disease (CVD) that results in death and disability in sub-Saharan Africa (SSA) and other low- and middle-income countries (LMICs) (3). Risk factors of IS may be divided into two categories: modifiable and non-modifiable. Age, sex, family history, and race/ethnicity are risk factors that cannot be modified, but hypertension, smoking, diet, and physical inactivity are some of the risk factors that can be modified (4). Due to health changes associated with constantly evolving social, economic, and demographic trends, the SSA and LMICs may be more impacted by the high burden of IS and other vascular illnesses. The population's shifting exposure to risk factors and their inability to pay the high cost of IS treatment are two additional reasons why the poor are becoming more and more impacted by this illness (5).

The 2017 WHO data reported that 6.23% of all fatalities in Ethiopia were due to stroke. In addition, the nation's age-adjusted stroke death rate is 89.82 per 100,000 of the population. The stroke burden will increase in the upcoming years as a result of poor healthcare-seeking behavior and insufficient neurologic therapies, according to previous data on the stroke trend (6). According to hospital-based research, stroke accounts for 24% of all neurologic hospitalizations in Ethiopia, making it one of the major causes of morbidity and death. Furthermore, due to changes in lifestyle and demographics that have an impact on the population's epigenetic makeup, the incidence of risk factors for stroke has been rising in the Ethiopian population (7).

Hypertension is the most significant modifiable risk factor for IS, increasing the relative risk by 3.1 times for men and 2.9 times for women, where the incidence of stroke rises proportionately with both systolic and diastolic blood pressure (8). Since HTN and IS share fundamental physiological regulatory systems, the causes of elevated blood pressure that operate through RAAS may be linked to IS. In addition, the atherosclerotic process involves RAAS in vascular remodeling, the production of oxidative stress, and inflammation that have shown a potential relationship with the condition (9). A number of RAAS gene polymorphisms, including those in the aldosterone synthase (CYP11B2), angiotensinogen (AGT), angiotensin II type 1 receptor (AT1R), and angiotensin-converting enzyme (ACE) genes, have been found to be strongly linked to hypertension and ischemic stroke. The most well-known and extensively researched variants of these polymorphisms are the ACE I/D polymorphisms (10).

The ACE is a membrane-bound dipeptidyl carboxypeptidase ectoenzyme found in the endothelium lining of blood arteries throughout the body, where it plays a crucial role in the proliferation of vascular smooth muscle cells by converting angiotensin I to angiotensin II (11). The human ACE gene, which spans 21 kb and has 26 exons and 25 introns, is located on the long arm (q) of chromosome 17 (17q23.3). The ACE gene's I/D polymorphism results from the insertion (I) or deletion (D) of a 287-base pair (bp) Alu sequence in intron 16, resulting in three genotypes: II homozygote, ID heterozygote, and DD homozygote (12). The ACE insertion/deletion (I/D) gene polymorphism (rs4646994) was shown to have a high association with the level of plasma ACE since it accounted for 47% of the overall phenotypic variance of ACE activity. According to some studies, those with the II genotype had lower ACE concentrations than people with the DD genotype (13). The DD genotype was linked to elevated ACE levels and activity, which consequently caused a spike in blood pressure by increasing the production of angiotensin II, starting the constriction of blood vessels, and also increasing the reabsorption of water and sodium by the kidneys, along with elevating blood volume and blood pressure that causes HTN-induced IS (14).

Numerous case–control studies on ACE I/D polymorphism and the risk of IS in various ethnic populations had been conducted. This led to the hypothesis that ACE I/D may be a candidate gene and that the DD genotype is correlated with IS (10). However, the findings of investigations on the involvement of this polymorphism in IS are contradictory and provide conflicting data as certain studies established a link while others did not (15). Furthermore, though a number of studies were conducted to estimate the prevalence, risk factors, and outcome of IS in the Ethiopian population (16), there are no reported data about the effect of ACE gene polymorphism on the occurrence and progression of the disease. Keeping all the aforementioned factors in mind, the purpose of this study was to determine the relationship between ACE gene I/D polymorphism and the risk of ischemic stroke complications among patients with hypertension in the Ethiopian population.

2. Methods

2.1. Study participants

A hospital-based matched case–control study was conducted from May to August 2022 in Debre Tabor Referral Hospital. It has a follow-up medical referral clinic (MRC) for major chronic illnesses, including IS and HTN, in which treatment and follow-up for those patients take place. All patients who visit MRC were the source population, and patients who are under follow-up for HTN with IS complications were study subjects. The study included a total of 72 participants of both sexes, consisting of 36 patients with

Abbreviations: ACE, angiotensin-converting enzyme; BMI, body mass index; DNA, deoxyribonucleic acid; DBP, diastolic blood pressure; FBG, fasting blood glucose; HDL, high-density lipoprotein; HTN, hypertension; LDL, low-density lipoprotein; PCR, polymerase chain reaction; RAAS, renin–angiotensin–aldosterone system; SBP, systolic blood pressure; TC, total cholesterol; TG, triglycerol.

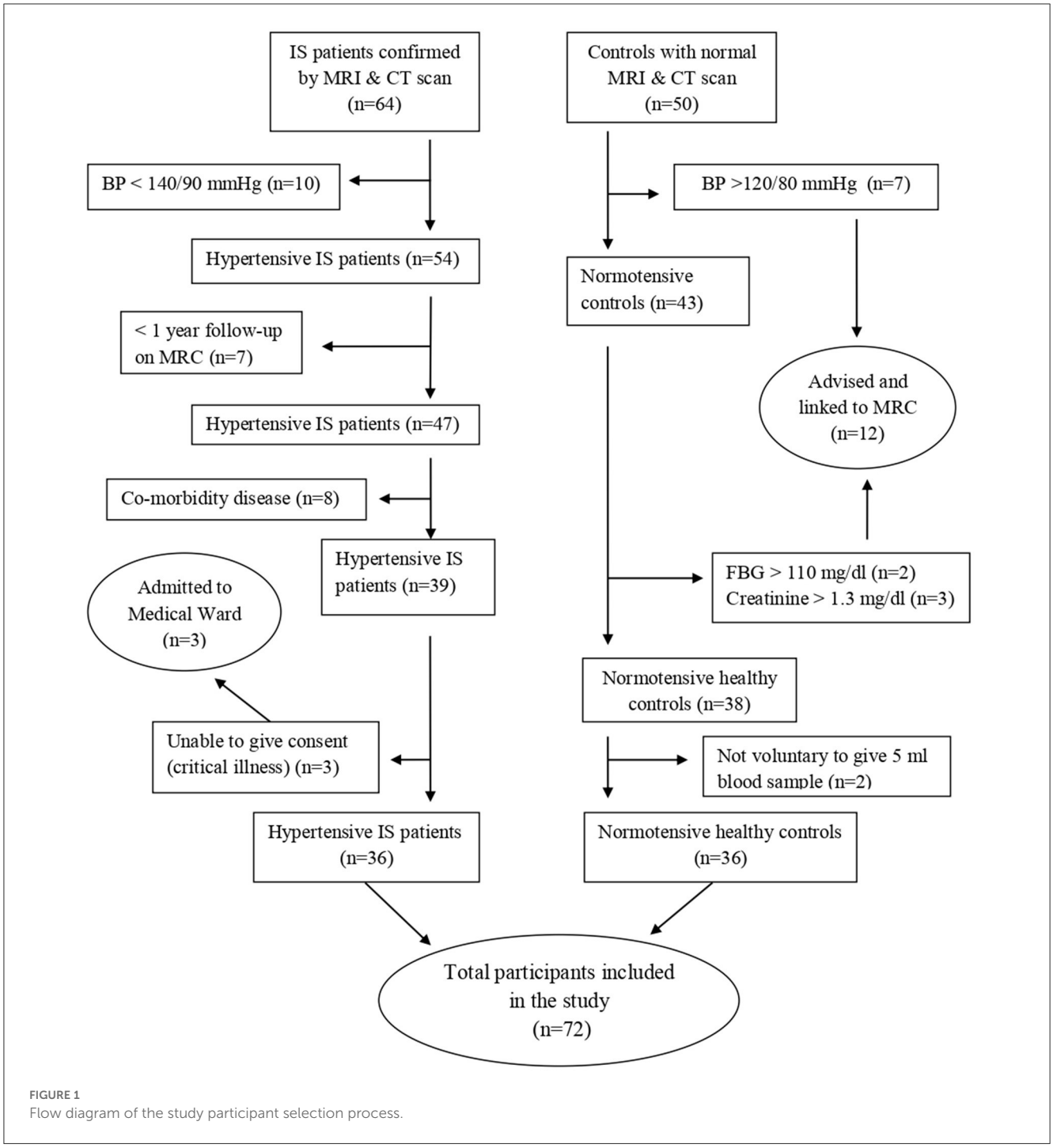

FIGURE 1
Flow diagram of the study participant selection process.

hypertensive IS and 36 normotensive healthy control groups (Figure 1).

2.2. Inclusion and exclusion criteria

Patients with IS secondary to HTN, who had been confirmed by computed tomography (CT) scans and magnetic resonance imaging (MRI), were recruited into this study. The study included patients who had been receiving follow-up care at MRC for at least 1 year. Controls were age- and sex-matched normotensive volunteers who were available during the study period. They were healthy individuals with normal brain imaging from the same geographical location and social status (Figure 1).

Patients who are diagnosed with hemorrhagic stroke, transient ischemic attack, hepatic and renal disease, cardiac source of embolization, secondary HTN, or chronic bacterial or viral infection were excluded. Patients who are unable to respond or are not willing to sign informed consent were also excluded from this study.

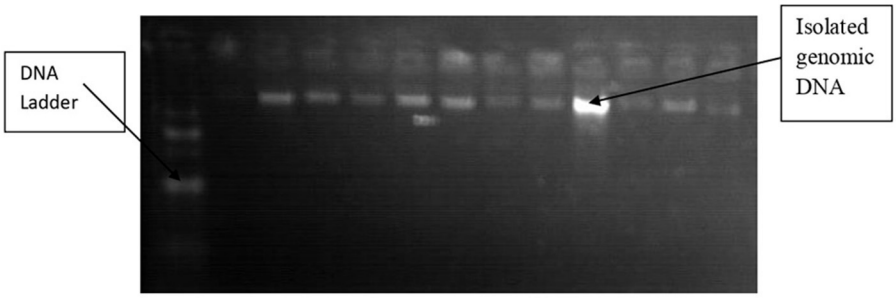

FIGURE 2
Agarose gel (1%) electrophoresis showing the quality of isolated genomic DNA.

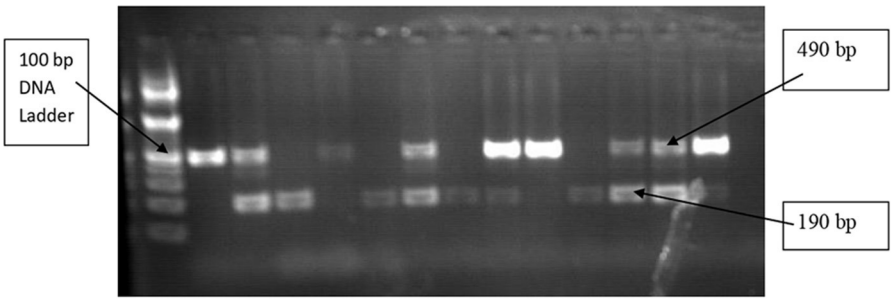

FIGURE 3
Agarose gel (2%) electrophoresis showing PCR products of the ACE I/D gene.

2.3. Data collection methods

The socio-demographic characteristics of both patients and healthy control subjects were obtained through a semi-structured questionnaire. Portable digital scales and portable stadiometers were used to determine body weight and height, respectively. Body mass index (BMI) is computed by dividing weight (in kilograms) by height (in meters square). Participants were classified as underweight (BMI $<$ 18.5 kg/m^2), healthy (18.5–25 kg/m^2), overweight (25.0–29.9 kg/m^2), or obese ($\geq$30 kg/m^2) based on their BMI (17). A digital instrument was used to measure blood pressure in the sitting stance after 5 min of rest, and the mean of three readings was used to compute SBP and DBP. Participants were categorized as hypertensive if their SBP was 140–159 mmHg and/or DBP was 90–99 mmHg (grade 1) or SBP was $\geq$ 160 mmHg and/or DBP was $\geq$ 100 mmHg (grade 2) or if they used antihypertensive medication; as having high normal BP, if SBP was 130–139 mmHg and/or DBP was 85–89 mmHg; and as having normal BP, if SBP was $<$130 mmHg and DBP was $<$ 85 mmHg (18).

2.4. Sample collection and laboratory methods

All participants, including patients and healthy controls, had a blood sample of 5 ml taken from the median cubital vein by laboratory staff under safety procedures. From the 5 ml sample, 3 ml was retained in the test tube without anticoagulants to allow the blood to clot. The tubes were then centrifuged to extract the serum, which was then collected into new tubes for biochemical tests. Enzymatic analyses of TC, TG, LDL, HDL, creatinine, and glucose were performed on each test in the Debre Tabor Referral Hospital diagnostic laboratory using the Dimension EXL 200 fully automated analyzer. The results were then scored by an investigator blinded to the sample withdrawal condition and experimental groups. If the fasting plasma glucose concentration is $>$126 mg/dl, then diabetes mellitus has been identified (19). Dyslipidemia can be defined if TC, TG, and LDL levels are above 200 mg/dl, 150 mg/dl, and 100 mg/dl, respectively, and the HDL level is below 60 mg/dl (20). Kidney disease is diagnosed if the blood creatinine concentration is $>$1.3 mg/dl for men and $>$1.1 mg/dl for women (21).

In the molecular biology laboratory at the University of Gondar, genomic DNA was extracted from the remaining 2 ml of samples collected in EDTA-containing tubes from each participant. The non-enzymatic salting-out approach (22) was used to isolate DNA from EDTA-anticoagulated blood from both patients and controls. The blood was then put into a clean 1.5 ml Eppendorf tube. By lysing and eliminating them with a buffer solution, red blood cells were removed. To lyse white blood cells, a nuclear lysis buffer solution was used. Thereafter, to precipitate and remove proteins, 6 M NaCl of a highly concentrated salt was applied. After freezing with isopropanol and washing with 70% ice-cold ethanol, the DNA was precipitated. Thereafter, Tris-EDTA (TE) buffer was used to

TABLE 1 Demographic, clinical, and behavioral characteristics of the study participants in Debre Tabor Referral Hospital, Northwest Ethiopia, 2022.

Variables	IS ($n = 36$)	Control ($n = 36$)	*P*-value
Sex (M/F)	19/17	18/18	0.8136
Age (yr)	59.4 ±12.1	58.2 ± 6.9	0.6177
Family history of HTN (%)	27.8 %	19.4 %	0.4051
Family history of IS (%)	16.7 %	8.3 %	0.2850
BMI (Kg/m^2)	23.6 ± 4.7	23.1 ± 4.2	0.6471
SBP (mmHg)	147.4 ± 6.0	116.2 ± 3.9	< 0.001*
DBP (mmHg)	91.3 ± 3.8	76.0 ± 4.0	< 0.001*
FBS (mg/dl)	91.0 ± 18.9	89.9 ± 5.7	0.7503
Total Cholesterol (mg/dl)	190.5 ± 47.6	153.4 ± 46.2	< 0.001*
Triglyceride (mg/dl)	135.4 ± 37.3	105.5 ± 37.1	< 0.001*
LDL-Cholesterol (mg/dl)	94.7 ± 32.6	68.5 ± 28.2	< 0.001*
HDL-Cholesterol (mg/dl)	43.8 ± 8.2	55.5 ± 11.5	< 0.001*
Creatinine (mg/dl)	0.79 ± 0.13	0.75 ± 0.12	0.2214
Smoking habit (yes/no)	6/30	2/34	0.1336
Alcohol intake (yes/no)	20/16	17/19	0.4793
Salt intake (yes/no)	35/1	32/4	0.1613
Physical exercise (yes/no)	3/33	7/29	0.1728
Stress (yes/no)	24/12	19/17	0.2296

*A P-value of < 0.05 is considered statistically significant. BMI, body mass index; SBP, systolic blood pressure; DBP, diastolic blood pressure; FBG, fasting blood glucose; LDL, low-density lipoprotein; HDL, high-density lipoprotein; HTN, hypertension; IS, ischemic stroke.

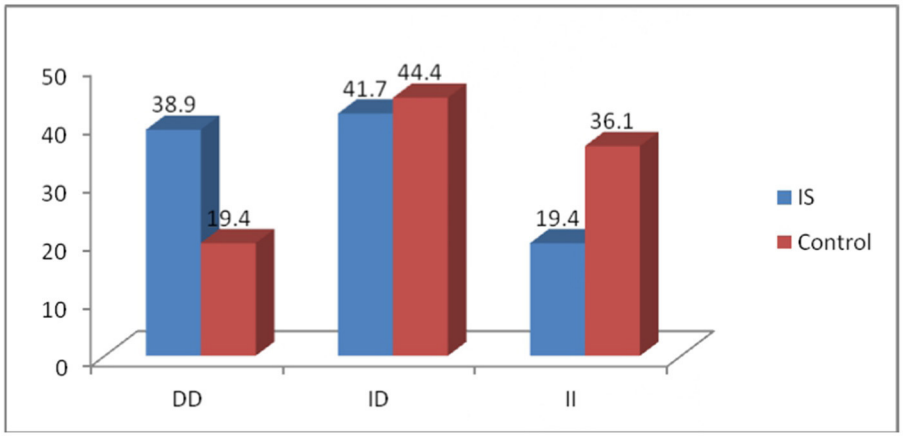

FIGURE 4
Distribution of the ACE I/D genotype in cases and controls.

dissolve genomic DNA. The quality of isolated genomic DNA was verified utilizing 1% agarose gel electrophoresis (Figure 2), and the sample was kept at −20 °C until it was needed (23).

Using specific primers (5′- CTG GAG ACC ACT CCC ATC CTT TCT-3′ and 5′- GAT GTG GCC ATC ACA TTC GTC AGA T-3′, respectively), direct PCR was used to identify the I/D alleles of the ACE gene polymorphism (24). A final volume (25 µl) of the PCR reaction mixture was prepared by combining 12.5 µl of master mix (MgCl2, dNTPs, PCR buffer, and Taq polymerase), 1 µl of forward primer, 1 µl of reverse primer, 2 µl of each sample, and 8.5 µl of PCR-grade water. The first denaturation step of the PCR amplification was set at 95°C for 5 min. The DNA was then amplified for 35 cycles with denaturation at 94°C for 30 s, annealing at 58°C for 30 s, extension at 72°C for 1 min, and a final extension at 72°C for 5 min (25).

ACE I/D genotypes of 490 bp band (II), 190 bp band (DD), and both 490 bp and 190 bp band (ID) PCR products were electrophoretically separated for 50 min at 120 V on a 2% agarose

gel (Figure 3). The PCR-amplified products (12 μl) were mixed with 3 μl of loading dye before being injected into the agarose gel wells. DNA ladders, which are molecular weight markers, were electrophoresed along with the DNA fragments to estimate the sizes of fragments of interest, and 3 μl of 2% ethidium bromide was also used for staining. In 1X tris acetate EDTA (TAE) buffer, electrophoresis was performed, and a UV transilluminator was used to visualize the gel (26).

2.5. Statistical analysis

The data were analyzed using STATA version 14. The means and standard deviations (x + s) were used to show quantitative data. A *t*-test for independent samples was applied to compare continuous variables between patients with hypertensive IS and healthy controls. The chi-square test was used to compare the distribution of genotype and allele frequencies. The risk correlations of ACE gene I/D polymorphisms with hypertensive IS were evaluated using logistic regression with a 95% confidence interval (CI). A one-way ANOVA was used to compare the relationships between ACE genotypes and clinical factors. Statistical significance was defined as a p-value of < 0.05.

3. Results

3.1. Socio-demographic and clinical characteristics

The distribution by sex and age was similar between hypertensive IS cases and normotensive control groups. Of the total 36 participants with hypertensive IS, 19 (52.8%) were male patients and 17 (47.2%) were female patients. Similarly, among the 36 healthy control groups, 18 (50 %) were male patients and 18 (50%) were female patients. The mean ages of the study groups were 59.4 ± 12.1 and 58.2 ± 6.9 for cases and controls, respectively. The clinical risk factors of IS such as systolic blood pressure (SBP), diastolic blood pressure (DBP), total cholesterol (TC), triglycerol (TG), LDL-cholesterol, and HDL-cholesterol levels were significantly higher in patients when compared to controls. However, there were no appreciable variations in blood creatinine levels, fasting blood glucose (FBG), or body mass index (BMI) between the two groups (Table 1).

3.2. Distribution of ACE genotypes and allele frequencies

The frequencies of the DD, ID, and II genotypes were 38.9, 41.7, and 19.4%, respectively, in the patient group, whereas they were 19.4, 44.4, and 36.1%, respectively, in the control group (Figure 4). Genotype distributions in the case and control groups were consistent with the Hardy–Weinberg equilibrium ($P > 0.05$). The D and I allele frequencies in patients were 0.60 and 0.40, respectively, while they were 0.42 and 0.58 in controls. The distribution of ACE genotype polymorphism between the two groups shows a significant difference ($P < 0.05$). Furthermore, compared to the control group, patients had a greater frequency of the homozygous DD genotype (odds ratio [OR] = 3.71; 95% confidence interval [CI] = 1.02–13.5; $P < 0.05$). The allelic frequencies showed high significance between the two groups, in which the D allele was two times higher than the I allele in patients (OR = 2.07; 95% CI = 1.06–4.03; $P < 0.05$) compared to controls. However, compared to healthy controls, ACE genotype II was less common in patients with hypertension (Table 2).

3.3. Association between ACE genotypes and clinical parameters

Table 3 shows the association of the ACE I/D genotype with the clinical parameters of patients with hypertensive IS and normotensive healthy controls. The ACE genotypes (DD, ID, and II) in the study groups were assessed with FBG, blood pressure, and lipid profiles. All the aforementioned clinical variables were not found to be significant with the genotypes in the study groups ($P > 0.05$). However, the SBP and DBP are higher in the ACE-DD genotype than in the ID and II genotypes.

4. Discussion

Ischemic stroke is a complex and heterogeneous disease with multiple etiologies and significant clinical manifestations (27). Even though conventional risk factors like diabetes, smoking, hypertension, and dyslipidemia were thought to be more important than inherited risk factors, recent case–control studies and meta-analyses have shown that genetic risk factors and genetic background have a significant impact on IS susceptibility (28). In the present study, the DD genotype and D allele had significantly higher frequencies in patients than in controls (Table 2, Figure 4). This finding is consistent with a meta-analysis conducted in a Caucasian population that included 22 case–control studies and discovered that patients with the DD genotype were more likely to have IS than those with the II genotypes (OR = 1.28, 95% CI = 1.05 to 1.55; $P < 0.001$) (29). Another meta-analysis with an encouraging result found that there was a substantial link between the D allele and IS in 105 relevant studies, encompassing 18,258 IS cases and 28,768 healthy controls (OR = 1.354; 95% CI = 1.272-1.440; $P < 0.001$). This meta-analysis suggests that although the statistical relevance for Caucasians is questionable, the ACE I/D polymorphism may be a genetic risk factor for IS, especially in Asians (30). Other research studies revealed that ACE-DD was connected to a high occurrence of IS in people from India (31), Iraq (32), and North India (33).

The exact mechanism by which the insertion/deletion mutation in the ACE gene increases the risk of HTN and IS was unknown (30). Extracellular volume and the homeostasis of the vascular wall are mediated by ACE, a crucial enzyme in the RAAS, which catalyzes the conversion of decapeptide angiotensin I into octapeptide angiotensin II. Numerous studies have shown that angiotensin II influences atherosclerotic changes and plaque rupture through a variety of mechanisms, including vasoconstriction and the expansion of vascular smooth muscle cells, which promote peripheral resistance of blood vessels (34). It

TABLE 2 Distribution of ACE genotypes and allele frequencies of the study participants in Debre Tabor Referral Hospital, Northwest Ethiopia, 2022.

Genotype	IS ($n = 36$)	Control ($n = 36$)	OR (95% CL)	p-value
DD	14 (38.9 %)	7 (19.4 %)	3.71 (1.02–13.5)	0.046*
ID	15 (41.7 %)	16 (44.4 %)	1.74 (0.54–5.54)	0.348
II	7 (19.4 %)	13 (36.1 %)	Ref	
Allele Frequency				
D	43 (59.7 %)	30 (41.7 %)	2.07 (1.52–3.22)	0.031*
I	29 (40.3 %)	42 (58.3 %)	Ref	

*A P-value of < 0.05 is considered to be statistically significant. Ref, reference; CL, confidence level; OR, odds ratio.

TABLE 3 Association of ACE I/D genotype with clinical characteristics in Debre Tabor Referral Hospital, Northwest Ethiopia, 2022.

Variables	Genotypes			p-value
	DD ($n = 21$)	ID ($n = 31$)	II ($n = 20$)	
Sex (M/F)	57/44	36/39	30/30	0.6479
Age (yr)	58.2 ± 11.8	58.9 ± 9.7	59.1 ± 8.1	0.2947
BMI (Kg/m^2)	23.7 ± 4.3	23.4 ± 4.1	22.8 ± 5.1	0.8263
SBP (mmHg)	135.6 ± 16.0	131.5 ± 17.8	128.2 ± 14.7	0.2167
DBP (mmHg)	85.4 ± 8.7	83.4 ± 9.4	82.2 ± 7.3	0.2280
FBS (mg/dl)	86.8 ± 9.8	90.9 ± 14.2	93.7 ± 16.6	0.5799
TC (mg/dl)	164.7 ± 41.1	179.8 ± 54.1	167.3 ± 53.5	0.7213
TG (mg/dl)	111.1 ± 41.1	128.4 ± 49.5	117.9 ± 30.2	0.6339
LDL-C (mg/dl)	90.8 ± 40.2	78.9 ± 32.7	76.2 ± 23.6	0.6194
HDL-C (mg/dl)	50.5 ± 11.3	48.2 ± 11.7	51.1 ± 11.7	0.8025
Creatinine (mg/dl)	0.79 ± 0.16	0.77 ± 0.12	0.75 ± 0.12	0.2451

*A P-value of < 0.05 is considered to be statistically significant.

has been shown that human RAAS activation worsens ischemia-induced brain injury mainly by stimulating atherosclerosis, reducing cerebral blood flow, and increasing oxidative stress, which results in a hypertension-induced IS complication (35). In addition, ACE-DD carriers have a higher level of angiotensin II than non-carriers, which affects the function of endothelial cells in a number of ways, including promoting endothelial cell apoptosis, raising vascular endothelial growth factor, and impairing the production of nitric oxide. This results in a higher risk of HTN and its associated IS complications (36).

Furthermore, the findings of this study disagree with the case–control study conducted in North Sumatra, Indonesia, which included a total of 78 patients with IS of both sexes, consisting of 43 patients with hypertension and 35 patients with normotension. Based on the allele and its genotype, there is no significant correlation between the ACE gene polymorphism and HTN in patients with IS. In this study, the I allele (72.1%) of the ACE gene polymorphism was more dominant than the D allele (27.9%) in patients with hypertensive IS (37). In addition, research conducted in South India (38) showed a link between the ACE II genotype and the I allele, which was exacerbated by factors such as smoking and diabetes among patients with IS. Other studies conducted in populations from Turkey (39) discovered no link between the ACE gene's I/D polymorphism and IS. The varying distribution frequencies of the ACE I/D polymorphism, which are impacted by regional and racial characteristics as well as ethnic variances, may be the reason for the controversial findings among the various ethnic communities (40). Different study methodologies, bias in selection, various matching criteria, or the kind of stroke might all be contributing variables (41).

In addition to the association between ACE polymorphism and IS, the contribution of other risk factors, such as the relation between ACE gene I/D polymorphism and patients with HTN without known histories of stroke, was studied in different populations (42). However, there are conflicting results regarding ACE polymorphisms and HTN risk (43). Studies conducted in populations from Pakistan (42) and Brazil (44) showed that ACE-DD was associated with a high incidence of HTN. Contradictory results were found from a study conducted in Afro-Brazilian and Caucasian populations (45) and the Peruvian elderly population (43), which showed no association between the ACE gene I/D polymorphism and HTN. Therefore, the controversial results about the association of ACE with hypertension and other cerebrovascular diseases in different populations may be due to interactions between genetic and some environmental factors that explain the complexity of genetic architecture (46). Inconsistencies were still visible between researchers about the ACE gene I/D polymorphism in hypertension and ischemic stroke complications.

Therefore, further research is still required; for instance, a third group would be needed to conclusively show the relationship between patients with HTN without a known history of ischemic stroke, patients with hypertension with IS complications, and normotensive healthy controls.

5. Conclusion

The current study found that the ACE I/D gene of the DD genotype and D allele is associated with a high risk of IS complications in patients with hypertension. As a result, the ACE I/D gene polymorphism can be used as a biomarker for the early diagnosis and detection of IS. Further studies with a large sample size are required to comprehend the correlation between the ACE gene and IS.

Data availability statement

The raw data supporting the conclusions of this article will be made available by the authors, without undue reservation.

Ethics statement

The studies involving human participants were reviewed and approved by the University of Gondar Ethical Rievew Board. The patients/participants provided their written informed consent to participate in this study.

Author contributions

AM prepared the final draft of the manuscript. NB critically reviewed the article and gave final approval for the version to be published. Both authors contributed to the article and approved the submitted version.

Acknowledgments

We would like to express our sincere gratitude to the Debre Tabor Referral Hospital diagnostic laboratory and the University of Gondar molecular biology laboratory staff for providing us with the assistance we required to conduct this study.

Conflict of interest

The authors declare that the research was conducted in the absence of any commercial or financial relationships that could be construed as a potential conflict of interest.

Publisher's note

References

1. Wang J, Sun Z, Yang Y, Wu J, Quan W, Chen X, Ni P, Li D. Association of laboratory parameters and genetic polymorphisms with ischemic stroke in Chinese Han population. *Exp Ther Med.* (2021) 21:1–9 doi: 10.3892/etm.2021.9921

2. Asres AK, Cherie A, Bedada T, Gebrekidan H. Frequency, nursing managements and stroke patients' outcomes among patients admitted to Tikur Anbessa specialized hospital, Addis Ababa, Ethiopia a retrospective, institution based cross-sectional study. *Int J Afr Nurs Sci.* (2020) 13:100228. doi: 10.1016/j.ijans.2020.100228

3. Fekadu G, Chelkeba L, Kebede A. Risk factors, clinical presentations and predictors of stroke among adult patients admitted to stroke unit of Jimma university medical center, south west Ethiopia: prospective observational study. *BMC Neurol.* (2019) 19:1–11. doi: 10.1186/s12883-019-1409-0

4. Yu JG, Zhou RR, Cai GJ. From hypertension to stroke: mechanisms and potential prevention strategies. *CNS Neurosci. Ther.* (2011) 17:577–84. doi: 10.1111/j.1755-5949.2011.00264.x

5. Agazhe M, Eshetu D, Arsicha A, Hamato A, Petros A, Dabaro D, et al. Incidence and pattern of stroke among patients admitted to medical ward at Yirgalem General Hospital, Sidama Regional State, Southern-Ethiopia. *SAGE Open Med.* (2021) 9:20503121211001154. doi: 10.1177/20503121211001154

6. Alene M, Assemie MA, Yismaw L, Ketema DB. Magnitude of risk factors and in-hospital mortality of stroke in Ethiopia: a systematic review and meta-analysis. *BMC Neurol.* (2020) 20:1–10. doi: 10.1186/s12883-020-01870-6

7. Abdu H, Tadese F, Seyoum G. Comparison of Ischemic and hemorrhagic stroke in the medical ward of Dessie Referral Hospital, Northeast Ethiopia: a retrospective study. *Neurol Res Int.* (2021). doi: 10.1155/2021/9996958

8. Cipolla MJ, Liebeskind DS, Chan SL. The importance of comorbidities in ischemic stroke: impact of hypertension on the cerebral circulation. *J Cereb Blood Flow Metab.* (2018) 38:2129–49. doi: 10.1177/0271678X18800589

9. Su C, Liu WC Li GM, Huang Y. Association between the angiotensin-converting enzyme I/D polymorphism and risk of cerebral small vessel disease: a meta-analysis based on 7186 subjects. *J Stroke Cerebrovas Dis.* (2021) 30:105579. doi: 10.1016/j.jstrokecerebrovasdis.2020.105579

10. Wang B, Guo Q, Peng Y, Lu J, Singh B, Hua B. Association of AGT M235T and ACE I/D polymorphisms with the risk of ischemic stroke: meta-analysis in Han Chinese population. *J Neurol Sci.* (2012) 320:79–84. doi: 10.1016/j.jns.2012.06.022

11. Prabhakar P, De T, Nagaraja D, Christopher R. Angiotensin-converting enzyme gene insertion/deletion polymorphism and small vessel cerebral stroke in Indian population. *Int J Vasc Med.* (2014). doi: 10.1155/2014/305309

12. Ollomo B, Mouélé LY, Bivigou-Mboumba B, Ondo BM, Lendoye E, Mezui J, et al. Allele and DD Genotype of I /D Polymorphism in The ACE gene in patients with hypertension, stroke and cancer prostate in Libreville: a concern given the high frequencies of these signatures in Gabonese population. *J Proteomics Genomics Res.* (2018) 2:31–59.

13. Pjević MD, Bumbaširevic LB, Vojvodic L, Grk M, Maksimović N, Damnjanović T, et al. Analysis of the association between polymorphisms within PAI-1 and ACE genes and ischemic stroke outcome after rt-PA therapy. *J Pharm Pharm Sci.* (2019) 22:142–9. doi: 10.18433/jpps30339

14. Malueka RG, Dwianingsih EK, Sutarni S, Bawono RG, Bayuangga HF, Gofir A, et al. The D allele of the angiotensin-converting enzyme (ACE) insertion/deletion (I/D) polymorphism is associated with worse functional outcome of ischaemic stroke. *Int J Neurosci.* (2018) 128:697–704. doi: 10.1080/00207454.2017.1412962

15. Mostafa MA, El-Nabiel LM, Fahmy NA, Aref H, Shreef E, Abd El-Tawab F, et al. gene in Egyptian ischemic stroke patients. *J Stroke Cereb Dis.* (2016) 25:2167–71. doi: 10.1016/j.jstrokecerebrovasdis.2015.05.015

16. Abate TW, Zeleke B, Genanew A, Abate BW. The burden of stroke and modifiable risk factors in Ethiopia: a systemic review and meta-analysis. *PLoS ONE.* (2021) 16:e0259244. doi: 10.1371/journal.pone.0259244

17. Gadekar T, Dudeja P, Basu I, Vashisht S, Mukherji S. Correlation of visceral body fat with waist–hip ratio, waist circumference and body mass index in healthy adults: a cross sectional study. *Med J Armed Forces India*. (2020) 76:41–6 doi: 10.1016/j.mjafi.2017.12.001

18. Unger T, Borghi C, Charchar F, Khan NA, Poulter NR, Prabhakaran D, et al. 2020 International society of hypertension global hypertension practice guidelines. *Hypertension*. (2020) 75:1334–5. doi: 10.1161/HYPERTENSIONAHA.120.15026

19. American Diabetes Association. 2. Classification and diagnosis of diabetes: standards of medical care in diabetes-—2020. *Diabetes Care*. (2020) 43:S14–31. doi: 10.2337/dc20-S002

20. Al Quran TM, Bataineh ZA, Al-Mistarehi AH, Zein Alaabdin AM, Allan H. Al Qura'an A, et al. Prevalence and pattern of dyslipidemia and its associated factors among patients with type 2 diabetes mellitus in Jordan: a cross-sectional study. *Int J Gen Med*. (2022) 1:7669–83. doi: 10.2147/IJGM.S377463

21. Komala G, Geetha K, Kishwanth DM, Nagendran R. Establishment of reference range for serum creatinine by IDMS and NIST SRM 967 traceable calibrator in government Kilpauk medical college hospital laboratory. *Int J Clin Chem Lab Med*. (2017) 3:23–32. doi: 10.20431/2455-7153.0303005

22. Birhan TA, Molla MD, Abdulkadir M, Tesfa KH. Association of angiotensin-converting enzyme gene insertion/deletion polymorphisms with risk of hypertension among the Ethiopian population. *PLoS ONE*. (2022) 17:e0276021. doi: 10.1371/journal.pone.0276021

23. Al-Hassani OM. Detection of AGT gene polymorphism in patient with hypertension in Mosul City. *J Biotechnol*. (2019) 4:18.

24. Ghanie A, Partan RU, Indrajaya T, Ali Z, Saleh MI, Hidayat R. The effect of angiotensin-converting enzyme gene polymorphisms in the coronary slow flow phenomenon at south sumatra, Indonesia population. *Open Access Maced J Med Sci*. (2020) 8:225–30. doi: 10.3889/oamjms.2020.3802

25. Borai IH, Hassan NS, Shaker OG, Ashour E, Badrawy ME, Fawzi OM, et al. Synergistic effect of ACE and AGT genes in coronary artery disease. *Univ J Basic Appl Sci*. (2018) 7:111–7. doi: 10.1016/j.bjbas.2017.09.003

26. Mocan O, Radulescu D, Buzdugan E, Cozma A, Leucuta DC, Procopciuc LM. Association between M235T-AGT and I/D-ACE polymorphisms and carotid atheromatosis in hypertensive patients: a cross-sectional study. *In vivo*. (2020) 34:2811–9. doi: 10.21873/invivo.12107

27. Della-Morte D, Guadagni F, Palmirotta R, Testa G, Caso V, Paciaroni M, et al. Genetics of ischemic stroke, stroke-related risk factors, stroke precursors and treatments. *Pharmacogenomics*. (2012) 13:595–613. doi: 10.2217/pgs.12.14

28. Salem GM, Gab-Allah GK. Angiotensin converting enzyme polymorphism and ischemic stroke. *Neurosci J*. (2020) 25:176–81. doi: 10.17712/nsj.2020.3.20190117

29. Yuan H, Wang X, Xia Q, Ge P, Wang X, Cao X. Angiotensin converting enzyme (I/D) gene polymorphism contributes to ischemic stroke risk in Caucasian individuals: a meta-analysis based on 22 case-control studies. *Int J Neurosci*. (2016) 126:488–98. doi: 10.3109/00207454.2015.1036421

30. Zhao J, Qin X, Li S, Zeng Z. Association between the ACE I/D polymorphism and risk of ischemic stroke: an updated meta-analysis of 47,026 subjects from 105 case–control studies. *J Neurol Sci*. (2014) 345:37–47. doi: 10.1016/j.jns.2014.07.023

31. A Goyal A, Saluja A, Saraswathy KN, Bansal P, Dhamija RK. Role of ACE polymorphism in acute ischemic stroke. *Neurology India*. (2021) 69:1217. doi: 10.1016/j.jns.2021.118676

32. Al-Gazally ME, Obed AF, Al-Saadi AH. Effect of ACE gene polymorphism of Iraqi patients on ischemic stroke. *Int J Chem Tech Res*. (2016) 9:424–9.

33. Kumar A, Vivekanandhan S, Srivastava A, Tripathi M, Padma Srivastava MV, Saini N, et al. Association between angiotensin converting enzyme gene insertion/deletion polymorphism and ischemic stroke in north Indian population: a case–control study and meta-analysis. *Neurol Res*. (2014) 36:786–94. doi: 10.1179/1743132814Y.0000000335

34. Tascilar N, Dursun A, Ankarali HA, Mungan G, Ekem S, Baris S. Angiotensin-converting enzyme insertion/deletion polymorphism has no effect on the risk of atherosclerotic stroke or hypertension. *J Neurol Sci*. (2009) 285:137–41. doi: 10.1016/j.jns.2009.06.016

35. Isordia-Salas I, Santiago-Germán D, Cerda-Mancillas MC, Hernández-Juárez J, Bernabe-García M, Leaños-Miranda A, et al. Gene polymorphisms of angiotensin-converting enzyme and angiotensinogen and risk of idiopathic ischemic stroke. *Gene*. (2019) 688:163–70. doi: 10.1016/j.gene.2018.11.080

36. Tuncer N, Tuglular S, Kiliç G, Sazci A, Us Ö, Kara I. Evaluation of the angiotensin-converting enzyme insertion/deletion polymorphism and the risk of Ischaemic stroke. *J Clin Neurosci*. (2006) 13:224–7. doi: 10.1016/j.jocn.2005.08.005

37. Alexander V, Siregar Y, Arina CA. Correlation of ACE gene polymorphism and hypertension in stroke ischemic patients. *Sumatera Med J*. (2020) 3:41–7. doi: 10.32734/sumej.v3i1.3310

38. Vijayan M, Chinniah R, Ravi PM, Joseph AK, Vellaiappan NA, Krishnan JI, et al. genotype and I allele predicts ischemic stroke among males in south India. *Meta Gene*. (2014) 2:661–9. doi: 10.1016/j.mgene.2014.09.003

39. Handan AK, Cengiz N, Bedir A, Onar MK. The relationship between angiotensin converting enzyme gene polimorphism and lacunar infarction. *Harran Üniversitesi Tip Fakültesi Dergisi*. (2013) 10:131–6.

40. Rong C, Xing Y, Jiang X, Wang J, Gao B, Zhao J, et al. Angiotensin-converting enzyme gene polymorphism and middle cerebral artery stenosis in a Chinese Han population. *Neural Regeneration Research*. (2013) 8:1410.

41. Yadav S, Hasan N, Marjot T, Khan MS, Prasad K, Bentley P, et al. Detailed analysis of gene polymorphisms associated with ischemic stroke in South Asians. *PLoS ONE*. (2013) 8:e57305. doi: 10.1371/journal.pone.0057305

42. Hussain M, Awan FR, Gujjar A, Hafeez S, Islam M, A. case control association study of ACE gene polymorphism (I/D) with hypertension in Punjabi population from Faisalabad, Pakistan. *Clin Exp Hypertens*. (2018) 40:186–91. doi: 10.1080/10641963.2017.1356842

43. Oscanoa TJ, Cieza EC, Lizaraso-Soto FA, Guevara ML, Fujita RM, Romero-Ortuno R. Lack of association between angiotensin-converting enzyme (ACE) genotype and essential hypertension in Peruvian older people. *Art Hypertension*. (2020) 24:115–9. doi: 10.5603/AH.a2020.0011

44. Pinheiro DS, Santos RS, Jardim PC, Silva EG, Reis AA, Pedrino GR, et al. The combination of ACE I/D and ACE2 G8790A polymorphisms revels susceptibility to hypertension: a genetic association study in Brazilian patients. *PLoS ONE*. (2019) 14:e0221248. doi: 10.1371/journal.pone.0221248

45. Bonfim-Silva R, Guimaraes LO, Santos JS, Pereira JF, Leal Barbosa AA, Souza Rios DL. Case–control association study of polymorphisms in the angiotensinogen and angiotensin-converting enzyme genes and coronary artery disease and systemic artery hypertension in African-Brazilians and Caucasian-Brazilians. *J Genet*. (2016) 95:63–9. doi: 10.1007/s12041-015-0599-5

46. Singh M, Singh AK, Singh S, Pandey P, Chandra S, Gambhir IS. Angiotensin-converting enzyme gene I/D polymorphism increases the susceptibility to hypertension and additive diseases: A study on North Indian patients. *Clin Exp Hypertens*. (2016) 38:305–11. doi: 10.3109/10641963.2015.1107085

frontiers | Frontiers in Neurology

TYPE Original Research
PUBLISHED 26 May 2023
DOI 10.3389/fneur.2023.1189746

OPEN ACCESS

EDITED BY
Yanlin Zhang,
Second Affiliated Hospital of Soochow University, China

REVIEWED BY
Bor-Sen Chen,
National Tsing Hua University, Taiwan
Wenqiang Xin,
University Medical Center Göttingen, Germany
Ali Sazci,
Okan University, Türkiye

*CORRESPONDENCE
Yu Feng
819270809@qq.com

†These authors have contributed equally to this work and share first authorship

RECEIVED 20 March 2023
ACCEPTED 02 May 2023
PUBLISHED 26 May 2023

CITATION
Shen J, Feng Y, Lu M, He J and Yang H (2023) Predictive model, miRNA-TF network, related subgroup identification and drug prediction of ischemic stroke complicated with mental disorders based on genes related to gut microbiome.
Front. Neurol. 14:1189746.
doi: 10.3389/fneur.2023.1189746

Predictive model, miRNA-TF network, related subgroup identification and drug prediction of ischemic stroke complicated with mental disorders based on genes related to gut microbiome

Jing Shen[1†], Yu Feng[2,3*†], Minyan Lu[1†], Jin He[1†] and Huifeng Yang[1†]

[1]The Affiliated Jiangsu Shengze Hospital of Nanjing Medical University, Nanjing, China, [2]The University of New South Wales, Sydney, NSW, Australia, [3]The University of Melbourne, Parkville, VIC, Australia

Background: Patients with comorbid schizophrenia, depression, drug use, and multiple psychiatric diagnoses have a greater risk of carotid revascularization following stroke. The gut microbiome (GM) plays a crucial role in the attack of mental illness and IS, which may become an index for the diagnosis of IS. A genomic study of the genetic commonalities between SC and IS, as well as its mediated pathways and immune infiltration, will be conducted to determine how schizophrenia contributes to the high prevalence of IS. According to our study, this could be an indicator of ischemic stroke development.

Methods: We selected two datasets of IS from the Gene Expression Omnibus (GEO), one for training and the other for the verification group. Five genes related to mental disorders and GM were extracted from Gene cards and other databases. Linear models for microarray data (Limma) analysis was utilized to identify differentially expressed genes (DEGs) and perform functional enrichment analysis. It was also used to conduct machine learning exercises such as random forest and regression to identify the best candidate for immune-related central genes. Protein–protein interaction (PPI) network and artificial neural network (ANN) were established for verification. The receiver operating characteristic (ROC) curve was drawn for the diagnosis of IS, and the diagnostic model was verified by qRT-PCR. Further immune cell infiltration analysis was performed to study the IS immune cell imbalance. We also performed consensus clustering (CC) to analyze the expression of candidate models under different subtypes. Finally, miRNA, transcription factors (TFs), and drugs related to candidate genes were collected through the Network analyst online platform.

Results: Through comprehensive analysis, a diagnostic prediction model with good effect was obtained. Both the training group (AUC 0.82, CI 0.93–0.71) and the verification group (AUC 0.81, CI 0.90–0.72) had a good phenotype in the qRT-PCR test. And in verification group 2 we validated between the two groups with and without carotid-related ischemic cerebrovascular events (AUC 0.87, CI 1–0.64). Furthermore, we investigated cytokines in both GSEA and immune infiltration and verified cytokine-related responses by flow cytometry, particularly IL-6, which played an important role in IS occurrence and progression. Therefore, we speculate that mental illness may affect the development of IS in B cells and IL-6 in T cells. MiRNA (hsa-mir-129-2-3p, has-mir-335-5p, and has-mir-16-5p) and TFs (CREB1, FOXL1), which may be related to IS, were obtained.

Conclusion: Through comprehensive analysis, a diagnostic prediction model with good effect was obtained. Both the training group (AUC 0.82, CI 0.93–0.71) and the verification group (AUC 0.81, CI 0.90–0.72) had a good phenotype in the qRT-PCR test. And in verification group 2 we validated between the two groups with and without carotid-related ischemic cerebrovascular events (AUC 0.87, CI 1–0.64). MiRNA (hsa-mir-129-2-3p, has-mir-335-5p, and has-mir-16-5p) and TFs (CREB1, FOXL1), which may be related to IS, were obtained.

KEYWORDS

ischemic stroke, mental disorders, gut microbiome, machine learning, qRT-PCR, diagnostic model, drug prediction, transcription factors ischemic stroke

1. Introduction

Stroke is one of the leading causes of death and disability globally, of which about 87 percent is ischemic stroke (IS) (1). Most IS patients have one or more comorbidities (2). IS patients with comorbidities experience more severe defects, increased disability and hospitalization rates, and higher mortality rates (3). Post-stroke cognitive impairment and dementia (PSCID) are the main sources of post-stroke morbidity and mortality worldwide (4). Current studies have shown that 25–30 percent of IS survivors develop vascular cognitive impairment (VCI) or vascular dementia (VaD) immediately or later (5). Post-stroke depression (PSD) is a general mental health problem affecting about 33 % of IS survivors. PSD adversely affects recovery and rehabilitation of cognitive and motor impairment after stroke, significantly increasing recurrence chances of neurovascular problems (6). Anxiety disorders affect about 1/4 of IS patients (7), which hinders IS rehabilitation and prevents patients from resuming daily activities (8), but clinical trials have not produced any clear evidence to guide the treatment of post-stroke anxiety disorders (9). There is a corresponding association between obsessive–compulsive disorder and IS. According to a national longitudinal study by Chen et al., patients with obsessive–compulsive disorder have a higher risk of developing IS during follow-up compared with non-obsessive–compulsive disorder controls (10), but the correlation between the two is not clear. Odds of carotid revascularization after stroke are lower in patients with psychiatric disorders, especially those with schizophrenia, depression, substance use disorders, and multiple psychiatric diagnoses (11). In patients with schizophrenia, the presence of atopic disease increases the risk of ischemic stroke. The increased the number of atopic comorbidities, the heightened the risk of ischemic stroke (11). We require more clinical data to clarify the causal relationship between SC, gut microbes, and IS. However, our findings will help predict IS early through clinical genetic testing, as well as to predict the high incidence of IS in specific populations, such as schizophrenia. Additionally, our research will contribute to a better understanding of the genetic, immunological, and metabolic mechanisms underlying IS's high incidence and dangerous prognosis.

Human body's gut microbiome (GM) is the largest microbiome that plays an important role in regulating the immune system (12). In the mouse model, GM is also associated with the occurrence and sequelae of IS (13, 14). IS usually causes intestinal dysfunction, GM imbalance, intestinal bleeding, and intestinal septicemia, thus affecting the poor prognosis (15). More and more evidence shows that there is a correlation between GM and mental disorders, such as anxiety disorder, depression (16), schizophrenia (17), and so on. However, there is a lack of research on the relationship between GM and IS complicated with mental disorders. Therefore, this study is mainly through the analysis of five kinds of mental disorders (schizophrenia, depression, anxiety disorder, obsessive–compulsive disorder, and dementia) and IS in GM.

2. Materials and methods

2.1. Datasets

The IS datasets GSE22255, and GSE66724 from the GEO database were selected as the training group (18).[1] Merging multiple datasets required the use of the 'inSilicoMerging' algorithm from the R-software package (19). We utilized the Johnson et al. (20) method to eliminate the batch effect, to select GSE58294 and GSE198600 as the test group. Five genes related to mental disorders and GM were collected from Genecards, the NCBI database, and related literature. Finally, 710 genes related to mental disorders and 434 genes related to GM were obtained and sorted out according to different types (Supplementary Tables S1, S2). The process specific to this method is presented in Figure 1.

2.2. Differentially expressed gene screening

We used Limma (21), a generalized linear equation model to use as a difference table screening method. R-based Limma was utilized to analyze the differences in order to derive the DEGs among control and comparison groups. The criteria for identifying DEGs in this study were$|\log2$ Fold Change (FC)$| > 1$ and $p < 0.05$, and the heat map and volcano plot of IS DEGs were visualized by sangerBox (22).

1 www.ncbi.nlm.nih.gov/geo/

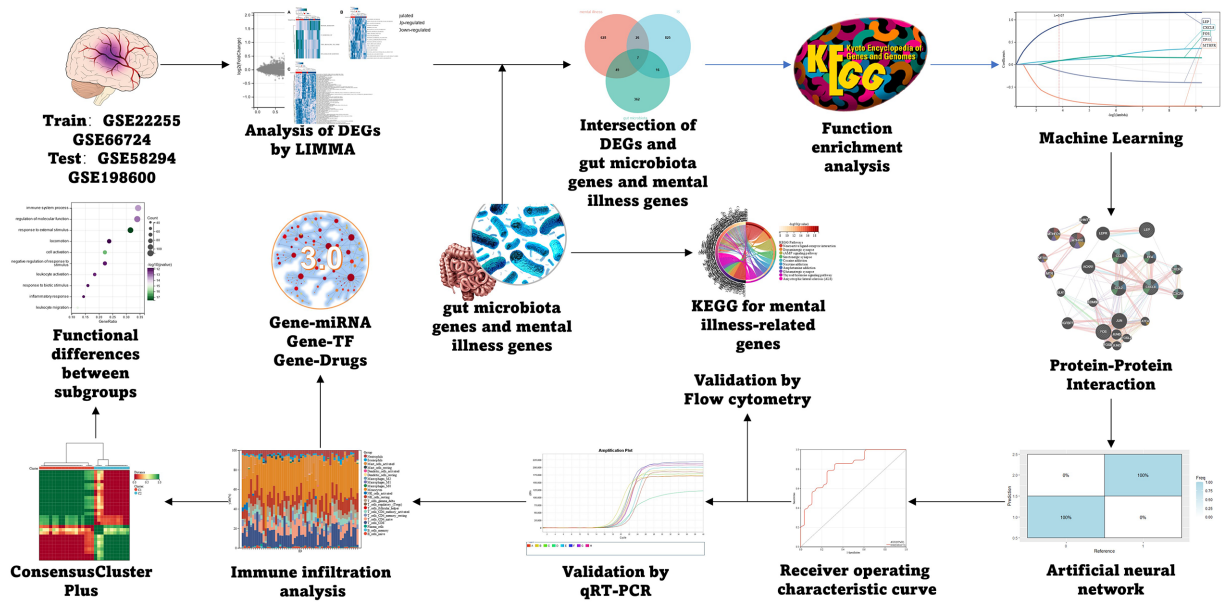

FIGURE 1
Flow chart.

2.3. Gene Set function enrichment analysis

The DEGs of IS and related genes of mental disorders and GM were cross-screened by Venn plot. For functional enrichment analysis, the genes related to mental disorders of IS were obtained. Further, KEGG rest API[2] and gene set function enrichment analysis (GSEA), were utilized to obtain the KEGG pathway's latest gene annotation. Moreover, the GO annotation of the gene "org.Hs.eg.db:" in the R-package (vs. 3.1.0) (23) was used as the gene map background. The clusterProfiler from the R-package was utilized for enrichment analysis (24) to obtain gene enrichment results. For GSEA analysis (25), GSEA software (vs. 3.0) was used to divide the sample into two groups. Also "c2.cp.kegg.v7.4.symbols.gmt" subset from Molecular Signatures Database (26) was used to assess the molecular mechanisms and the related pathways. We preset the minimum gene set to 5 on the basis of gene expression profile and phenotypes groupings. The value of the maximum gene set was 5,000, and a p-value<0.05 and an FDR < 0.1was kept as indices of statistical significance.

2.4. Screening candidate genes related to is and mental disorders by machine learning and constructing a protein–protein interaction network

"Glmnet" (27) and "RandomForest" (28) in the R software package were used to integrate gene expression data with survival time and survival status. Further lasso-cox and Random Forest methods were utilized for regression analysis. Moreover, 10%-fold cross-validation was set up to derive the optimal model. The final diagnosis prediction model was obtained by cross-screening the outcomes of the two machine-learning techniques through the Venn plot. Protein–protein interaction (PPI) network was built using the Gene MANIA database. The latter is a user-friendly, flexible website for deriving assumptions about gene function, gene prioritization for functional analysis, and gene list analysis (29).

2.5. Validation of predictive models for diagnosis and prognosis

pROC (30) from the R package was used for ROC analysis to obtain AUC. Also, pROC's CI function was utilized to assess the confidence interval (CI) and AUC so as to obtain the AUC result. Further, for visualization, sangerBox was used. Finally, we observed the expression of training set characteristic genes (GSE22255, GSE66724) and test group (GSE58294, GSE198600). In addition, a neuralnet (31) in the R software package was used to build an ANN for the characteristic genes obtained by the above method, thereby building a high-precision diagnostic model.

2.6. qRT-PCR and flow cytometry verification

Patients with acute IS hospitalized in Jiangsu Shengze Hospital, which is affiliated with the NMU (Nanjing Medical University) from January 1st, 2023, to January 15th, 2023, were enrolled retrospectively. Inclusion criteria: (1) the time of onset was within 7 days; (2) it met the diagnostic criteria revised by the Chinese Cerebrovascular Disease Classification 2015 of the Chinese Medical Association and was confirmed by head CT and/or MRI; (3) the medical records were complete. This research was conducted in accordance with the HD (Helsinki Declaration) and permitted by the Jiangsu Shengze Hospital's Ethics Committee (Lun No.: 2022–017-01).

2 https://www.kegg.jp/kegg/rest/keggapi.html

The qPCR gene of mRNA was detected in the PBMC samples of five patients with IS and five physical examiners. PBMC was extracted by the ficoll separation method (tbdscience, Tianjin, China), samples were anticoagulated by EDTA, and mRNA was extracted by magnetic beads method (BioPerfectus, Jiangsu, China). We used a one-step reverse transcription fluorescence quantitative PCR kit (BBI Lifesciences, Shanghai, China) for sybr green quantitative PCR amplification of mRNA. The primers were shown in Supplementary Table S3, and the amplification instrument was Applied Biosystems 7,500. The specificity of cDNA amplification was analyzed by melt curve, and the difference in gene expression was analyzed by Amplification Data.

We performed immunocytokine flow cytometry detection on the EDTA anticoagulated whole blood of 5 IS-confirmed patients and 5 physical examiners. An 8-item cytokine detection kit (multiplex microsphere flow immunofluorescence luminescence) (RAISEcare, Shandong, China) was used as the detection reagent, and BD FACSCanto II (Bccton, Dickinson and Company) was used as the cytokine detection instrument. The detection operation process is strictly in accordance with the kit instruction manual. We utilized flow cytometry to analyze the differences in the performance of the eight cytokines in the verification group.

2.7. Animal model and cell verification

Victoria G. Hernandez et al. induced stroke by distal middle cerebral artery occlusion (dMCAO) in an animal model and used RiboTag technology to obtain mRNA transcripts derived from astrocytes and microglia in the hyperacute phase (4 h) and acute phase (3 days) after stroke. The expression and log2 fold data for all sequenced genes are available on a user-friendly website (32).[3]

2.8. Immune infiltration analysis

The immune cell infiltration was analyzed by Cibersort (33) in R statistical package, and the correlation was evaluated by the

3 https://buckwalterlab.shinyapps.io/AstrocyteMicrogliaRiboTag/

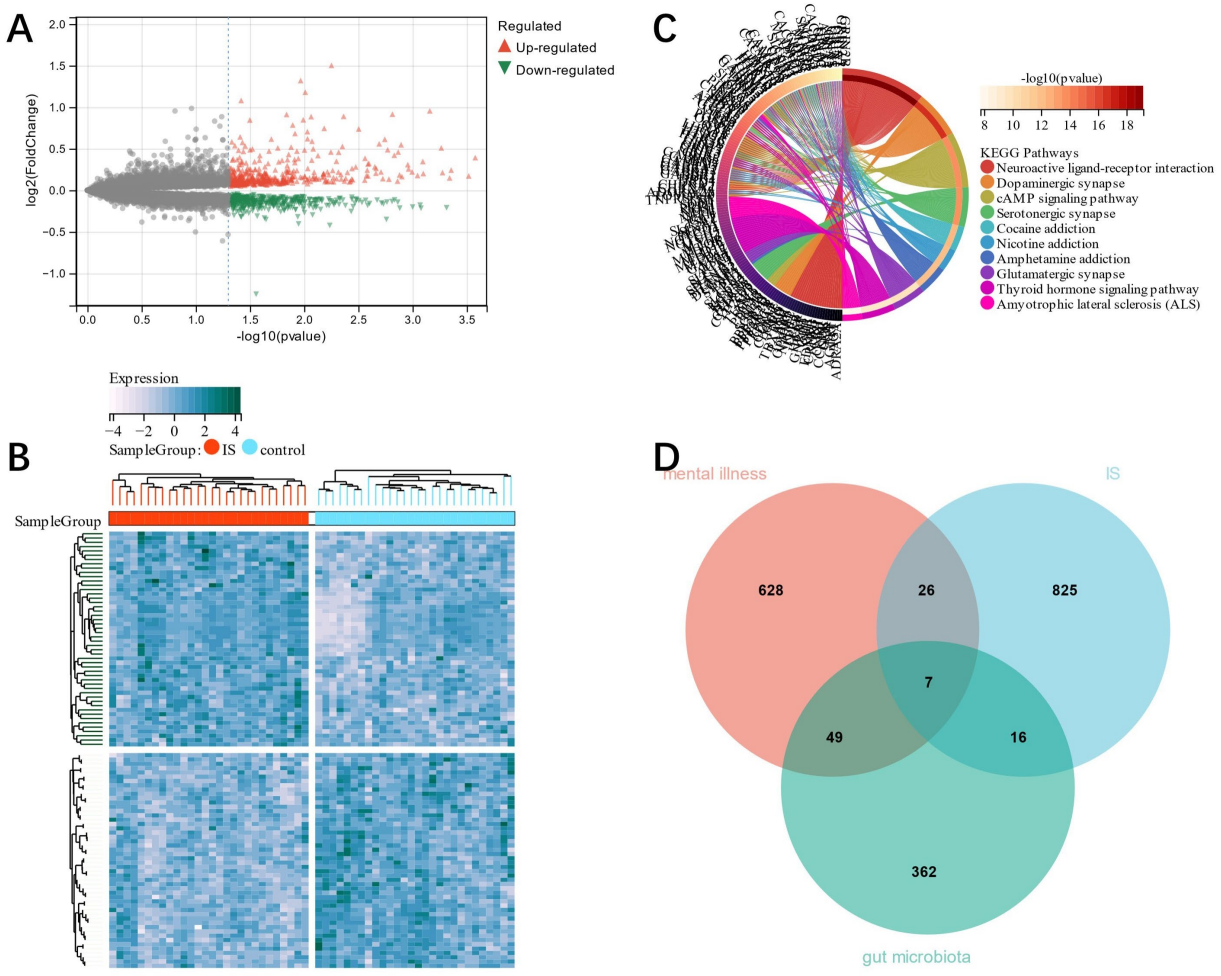

FIGURE 2
(A) volcano plot; **(B)** heat map of DEGs in IS; **(C)**, KEGG analysis corresponding to mental disorder-related genes; **(D)**, candidate genes were obtained by cross screening of mental disorder-related genes and GM in DEGs of IS.

spearman coefficient (34). The heat map of infiltrating immune cell correlation was drawn by corrplot (35) in the R software package.

2.9. Construction of miRNA and TF-hub gene network and drug prediction

The network of gene miRNA, gene-TFs, and gene-drug interaction was established by Network analyst (36).[4]

2.10. Subgroup analysis by candidate genes

Unsupervised hierarchical clustering analysis of IS samples was carried out utilizing the "ConsensusClusterPlus" of R (37) and the candidate genes' expression as input information. For Gene Set Variation Analysis (GSVA), the R statistical package was utilized to assess each sample's enrichment score in the gene set (38). The gene rank was predefined, and to evaluate the molecular mechanisms and related pathways, we downloaded the subsets c2.cp.kegg.v7.4.symbols.gmt, h.all.v7.4.symbols.gmt, and c2.cp.v7.4.symbols.gmt from Molecular Signatures Database. The minimum gene set was 5, and 5,000 was the maximum gene set. Each sample's enrichment score in each gene set was evaluated, and finally, the enrichment score matrix was obtained. The DEGs of subgroups were obtained by Limma analysis, and the functional differences between subgroups were analyzed by KEGG and GO.

3. Results

3.1. Is differentially expressed genes' screening

Combining GSE22255 and GSE66724 as training group datasets, 874 DEGs were identified in IS training group dataset by the Limma method, from which 417 were down-regulated and 457 up-regulated (Figures 2A,B). The genes' functional enrichment analysis that relates them to mental disorders was conducted. KEGG showed that genes related to mental disorders were mainly enriched in the interaction known as the Neuroactive ligand-receptor type (Figure 2C). This proved that there was a correlation between mental disorders and IS (39). Seven candidate genes related to mental disorders and GM were cross-screened by Venn plot (Figure 2D).

3.2. Functional enrichment analysis (FEA) of related candidate genes

FEA of candidate genes was carried out, and KEGG analysis showed that the "Toll-like receptor signaling pathway," "Rheumatoid arthritis,"

4 https://www.networkanalyst.ca/

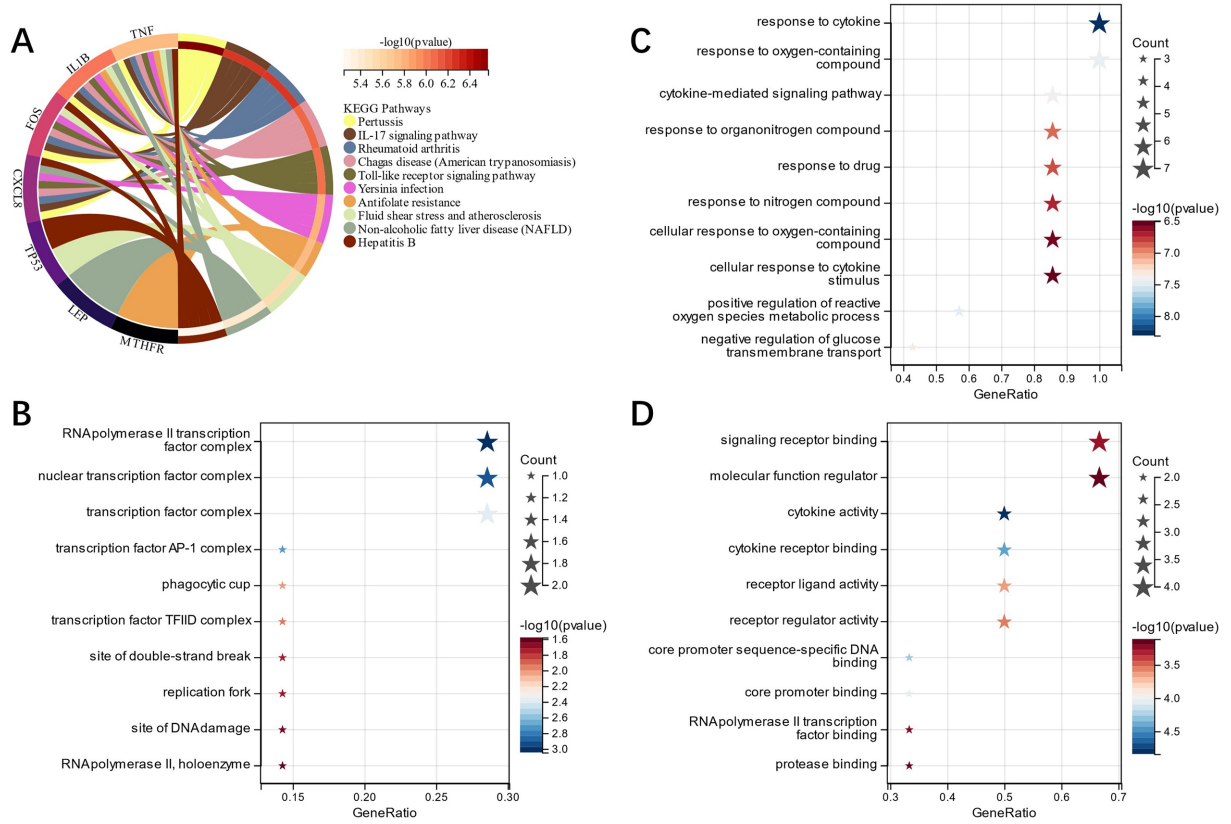

FIGURE 3
(A): KEGG analysis of candidate genes; **(B)**: GO analysis of the cell component of candidate genes; **(C)**: GO analysis of biological process of candidate genes; **(D)**: GO analysis of the molecular function of candidate genes.

"IL-17 signaling pathway," and other pathways had enrichment of candidate genes (Figure 3A). GO analysis showed that in terms of cell composition (CC), the candidate genes were primarily located in the "RNA polymerase II transcription factor complex" and "nuclear transcription factor complex" (Figure 3B). The main biological processes (BP) of candidate genes included "response to cytokine," "response to oxygen-containing compound," and "cytokine-mediated signaling pathway" (Figure 3C). Molecular function (MF) analysis depicted that the most crucial processes among the candidate genes were "signaling receptor binding," "cytokine receptor binding," and "cytokine activity" (Figure 3D). Accordingly, our candidate genes may be involved in immune infiltration as well as pathways related to cytokines in IS.

3.3. Screening of candidate genes related to is and construction of PPI network and PCD By machine learning

Candidate genes were identified by LASSO regression, and the results depicted that five potential candidate genes were identified (Figures 4A,B). We also used RF regression to identify candidate genes and showed four potential biomarkers (Figure 4C). Then the results selected by the two kinds of machine learning were cross-analyzed, and ultimately four candidate genes (CXCL8, FOS, LEP, MTHFR) were obtained (Figure 4D). And the PPI network was established through these four candidate genes, of which Physical Interactions occupied 77.64%, Coexpression occupied 8.01%, and Predicted occupied 5.37% (Figure 4E).

3.4. Diagnostic model's verification

The diagnostic value of the four candidate genes was verified by the ROC curve when all candidate genes were used as joint indicators (AUC 0.82, CI 0.93–0.71) (Figure 5A). We also put the diagnostic model into the verification group (GSE58294, GSE198600). It was shown that the diagnostic ROC (AUC 0.81, CI 0.90–0.72) of the positive and negative control groups in GSE58294 and the prognosis prediction ROC (AUC 0.87, CI 1–0.64) of the two groups in GSE198600 had a good predictive value (Figures 5B,C). The candidate genes were utilized to construct the neural network, and the outcomes depicted that the four candidate genes were able to distinguish the IS samples from the control samples, and the accuracy could reach 100% in the training group (Figures 5D,E). We also evaluated the expression profiles of the four candidate genes (Figures 5F–I), and the outcomes showed that there were statistically significant differences in candidate genes. GSEA analysis revealed that all four candidate genes were heavily enriched in immune-related pathways, such as the MAPK signaling pathway (Figures 6A–D). A relationship between candidate genes and pathways related to immune infiltration and cytokine production was further established by this study.

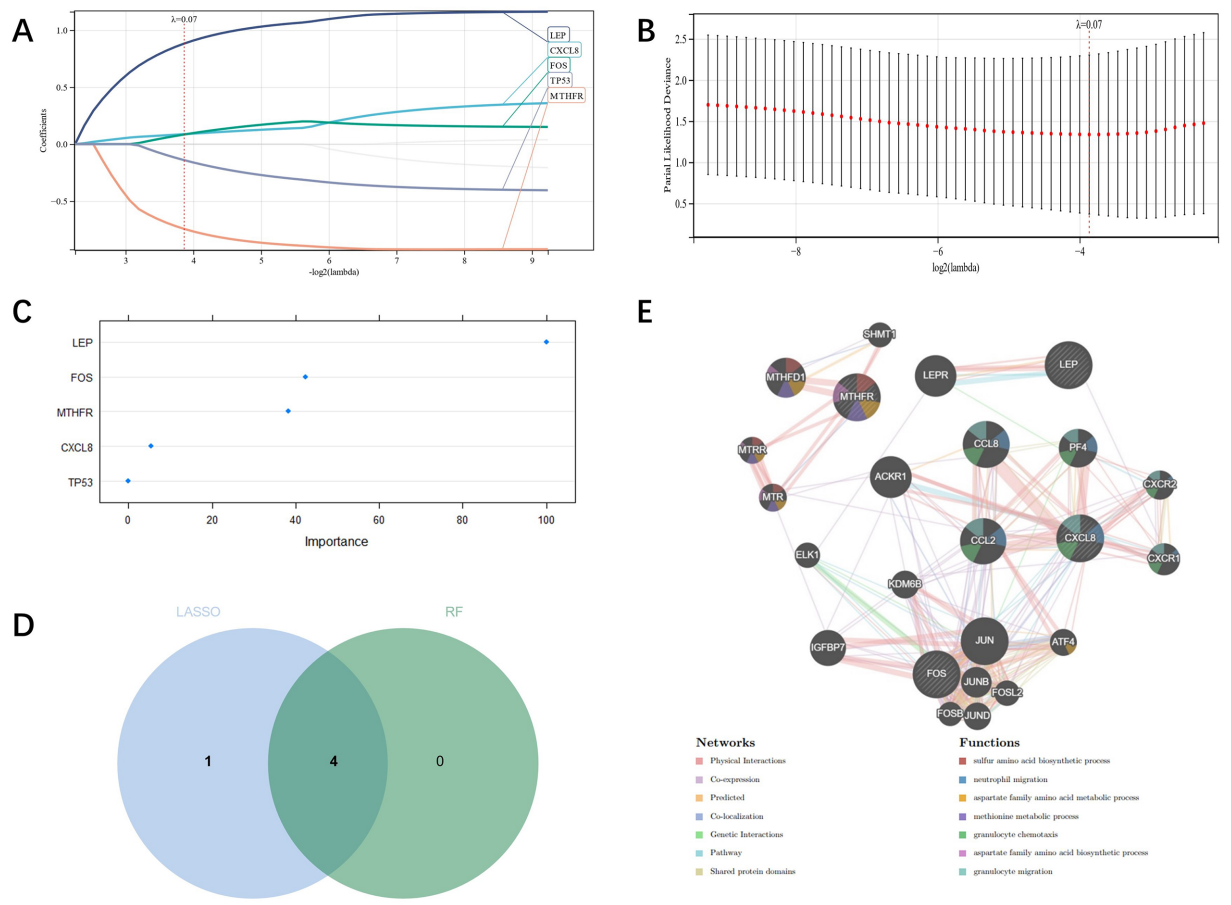

FIGURE 4
(A,B): candidate genes' screening through LASSO regression; **(C)**: Screening of candidate genes through RF regression; **(D)**: candidate genes cross screening through Venn plot and machine learning; **(E)**: PPI network construction of candidate genes.

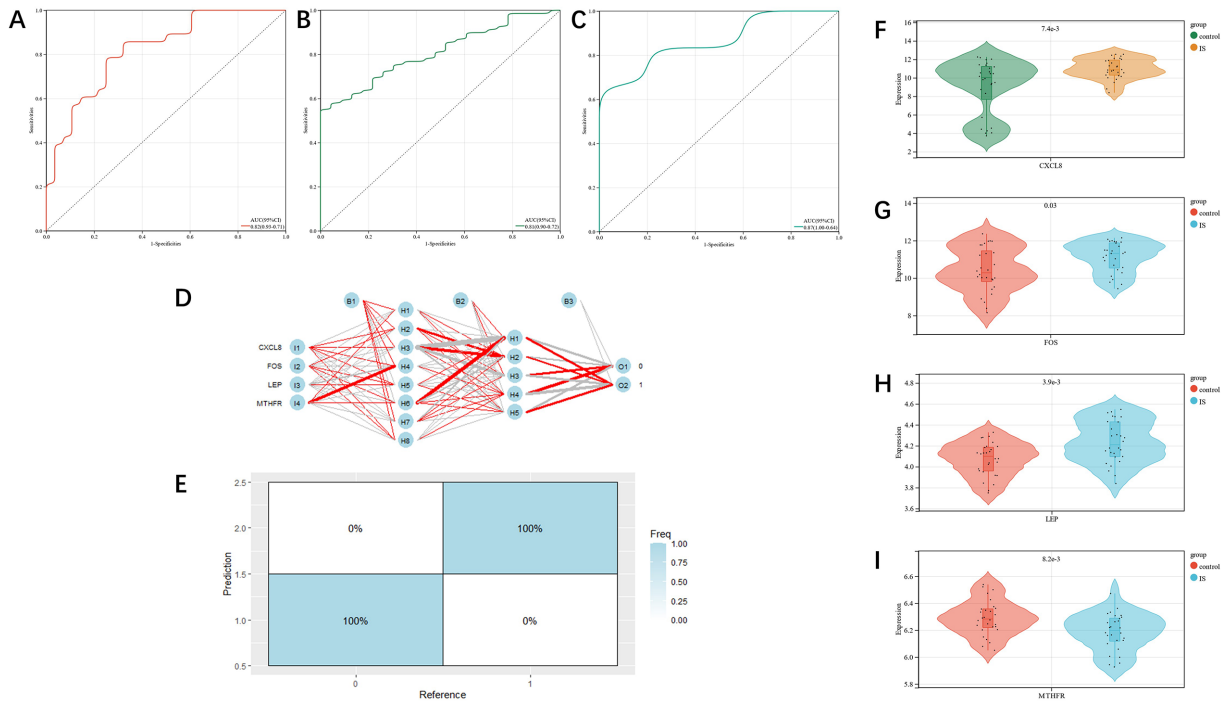

FIGURE 5
(A): training group's ROC curve; **(B,C)**: test group's ROC curve; **(D,E)**: artificial neural network verification of training group; **(F–I)**: analysis of candidate gene expression profile in the training group (CXCL8, FOS, LEP, MTHFR, respectively).

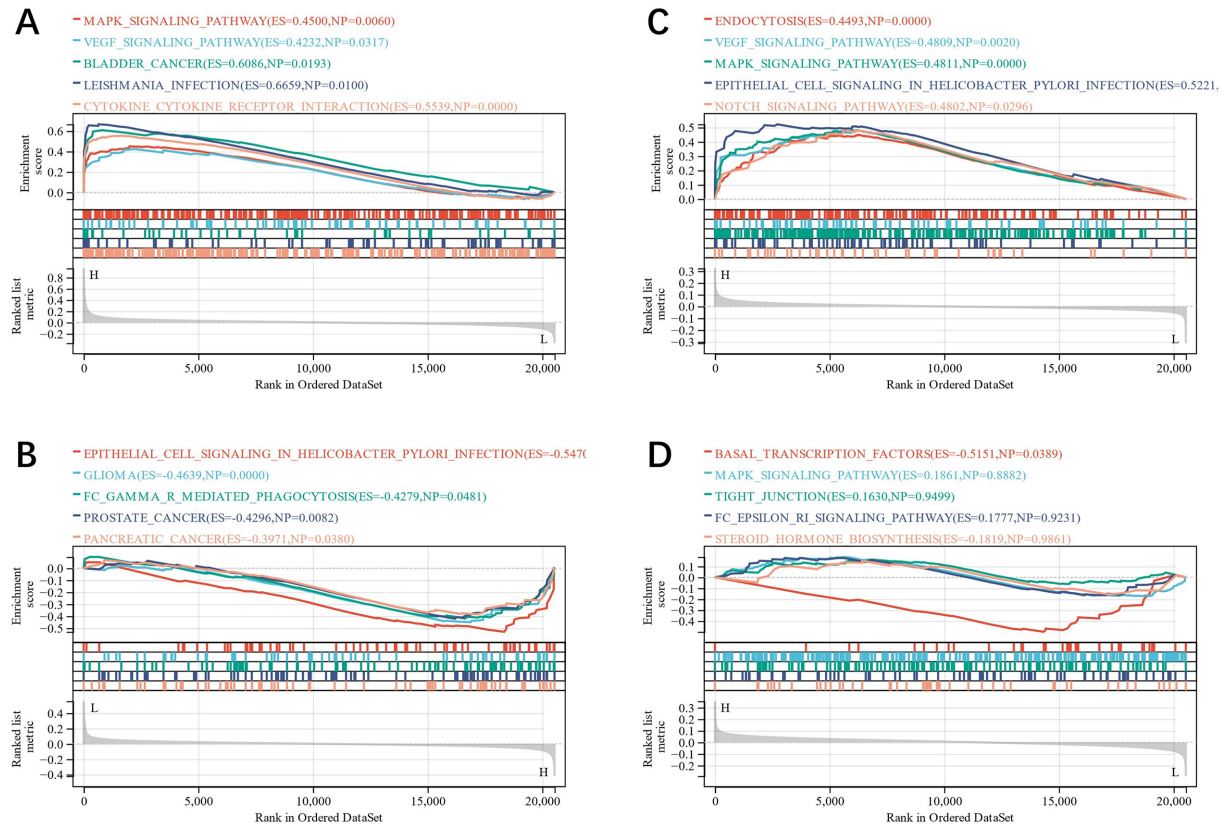

FIGURE 6
(A–D): GSEA analysis of CXCL8, FOS, LEP and MTHFR.

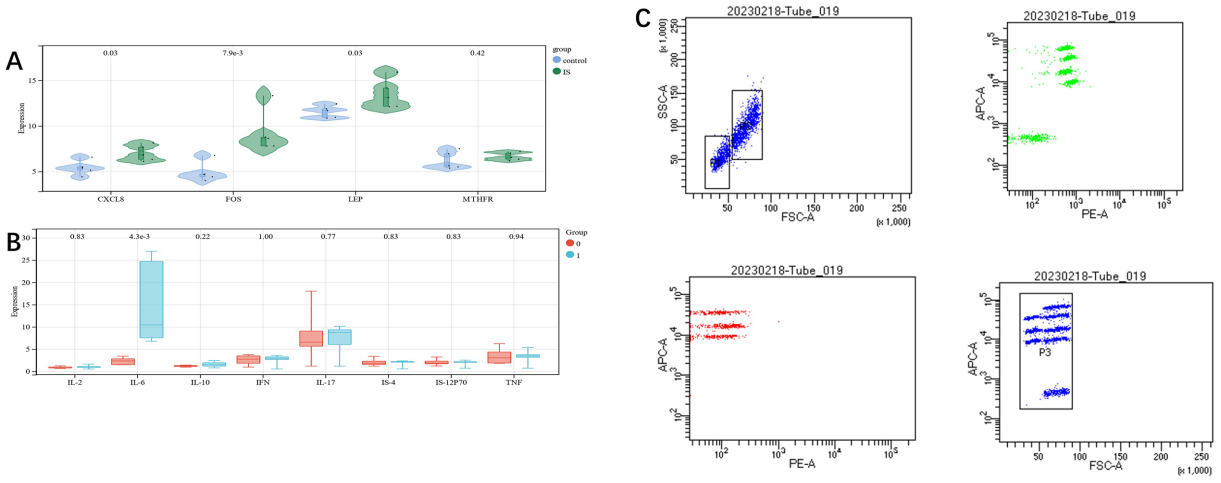

FIGURE 7
(A): measuring the RNA expression of candidate genes in blood samples using qRT-PCR; **(B,C)**: differences of eight cytokines in the two groups.

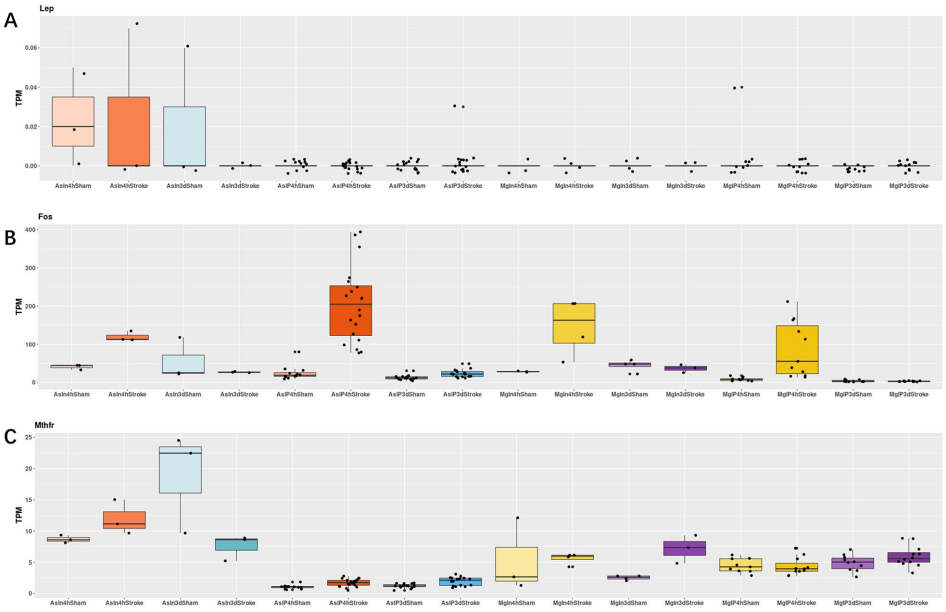

FIGURE 8
As=Astrocyte, Mg=icroglia, In=Input, IP=Immunoprecipitated, 4h=4h, 3d=3days. **(A–C)**: the expressions of Lep, Fos and Mthfr in astrocyte cells and microglia cells of stroke group and sham group, respectively.

3.5. Qrt-PCR-based verification of candidate genes, cytokines validated by flow cytometry

In order to verify the reliability of the dataset, clinical samples were taken, and the expression level of candidate genes was further identified by qRT-PCR (see Supplementary Table S3 for specific data). CXCL8, FOS, and LEP revealed statistically significant differences ($p < 0.05$), but similar differences were not found in MTHFR, which may be due to the less number of samples. The overall results were similar to those of mRNA chips (Figure 7A).

Flow cytometry was used to detect cytokines in the two groups of cases.， we found a significant difference in IL-6 between the two groups ($p < 0.05$). This is consistent with the conclusion we predicted based on the GSEA analysis (Figures 7B,C).

3.6. Cell expression in animal models

Regarding the Mthfr gene, we observed that in Astrocyte cells, the differences between the Stroke and Sham groups were 0.66 and 0.66 (Log2Foldchange) at 4 h and 3 days, respectively, with the Stroke

TABLE 1 Lep, Fos and Mthfr in astrocyte cells and microglia cells of stroke group and sham group, respectively.

Gene	Log2Foldchange	FDR	Contrast	Sample	Timepoint	Cell
Mthfr	0.658273148	0.0015194	Stroke vs Sham	IP	4 hours	Astrocyte
Mthfr	0.666646781	9.739E-05	Stroke vs Sham	IP	3 days	Astrocyte
Mthfr	0.016733677	0.99996073	Stroke vs Sham	Input	4 hours	Astrocyte
Mthfr	−1.042966608	0.00022618	Stroke vs Sham	Input	3 days	Astrocyte
Mthfr	−0.052261005	0.92826721	Stroke vs Sham	IP	4 hours	Microglia
Mthfr	0.613049601	0.00128746	Stroke vs Sham	IP	3 days	Microglia
Mthfr	0.040883082	0.99999794	Stroke vs Sham	Input	4 hours	Microglia
Mthfr	0.532884857	0.16583881	Stroke vs Sham	Input	3 days	Microglia
Lep	−0.000231797	0.99996073	Stroke vs Sham	Input	4 hours	Astrocyte
Lep	−0.01781688		Stroke vs Sham	Input	3 days	Astrocyte
Fos	3.007177925	2.48E-34	Stroke vs Sham	IP	4 hours	Astrocyte
Fos	0.883801901	0.00049238	Stroke vs Sham	IP	3 days	Astrocyte
Fos	0.914864058	0.27297506	Stroke vs Sham	Input	4 hours	Astrocyte
Fos	−0.260105863	0.39797136	Stroke vs Sham	Input	3 days	Astrocyte
Fos	3.353981233	6.10E-13	Stroke vs Sham	IP	4 hours	Microglia
Fos	−0.021996332	0.97666485	Stroke vs Sham	IP	3 days	Microglia
Fos	1.902812386	0.00033217	Stroke vs Sham	Input	4 hours	Microglia
Fos	−0.247118725	0.43279267	Stroke vs Sham	Input	3 days	Microglia
Lep	−0.000231797	0.999960729	Stroke vs Sham	Input	4 hours	Astrocyte
Lep	−0.01781688		Stroke vs Sham	Input	3 days	Astrocyte
Fos	3.007177925	2.48E-34	Stroke vs Sham	IP	4 hours	Astrocyte
Fos	0.883801901	0.000492377	Stroke vs Sham	IP	3 days	Astrocyte
Fos	0.914864058	0.272975062	Stroke vs Sham	Input	4 hours	Astrocyte
Fos	-0.260105863	0.397971358	Stroke vs Sham	Input	3 days	Astrocyte
Fos	3.353981233	6.10E-13	Stroke vs Sham	IP	4 hours	Microglia
Fos	-0.021996332	0.976664854	Stroke vs Sham	IP	3 days	Microglia
Fos	1.902812386	0.000332169	Stroke vs Sham	Input	4 hours	Microglia
Fos	-0.247118725	0.432792674	Stroke vs Sham	Input	3 days	Microglia

As, Astrocyte, Mg = microglia, In = Input, IP=Immunoprecipitated, 4 h = 4 h, 3d = 3 days.

group showing higher expression. In Microglia cells, there was no significant difference between the Stroke and Sham groups at 4 h, with a difference of −0.05, but at 3 days, the Stroke group showed higher expression with a difference of 0.61. For the Lep gene, there was no significant difference in expression at 4 h and 3 days in Astrocyte cells, with differences of −0.00 and − 0.02, respectively. For the Fos gene, in Astrocyte cells, there was a significant difference between the Stroke and Sham groups at 4 h, with a difference of 3.01, and at 3 days, with a difference of 0.88, both showing higher expression in the Stroke group. In Microglia cells, there was a significant difference between the Stroke and Sham groups at 4 h and 3 days, with differences of 3.35 and − 0.02, respectively, with the Stroke group showing higher expression (See Figure 8 and Table 1 for details).

3.7. Immune cell infiltration analysis

In this study, using the Cibersort algorithm, the concentration of 22 immune cells in IS samples and control samples in the training group was estimated (Figures 9A,B). The immune cell infiltration of IS and the control group was compared in the box plot (Figure 9C). The results revealed that there were statistically significant differences in memory B cells and resting mast cells in IS patients, and both were substantially compared to the control group. In the prognostic group of GSE198600, we found similar immune infiltration B lineage between the groups with and without carotid-related ischemic cerebrovascular events ($p < 0.05$) (Figure 8D).

3.8. Gene-miRNA, gene-TF, and gene-drug network diagram

The interaction networks of genes and miRNA, genes and TF with genes and drugs were generated by Network analyst. Four candidate genes-miRNA networks were constructed, and it was found that hsa-mir-129-2-3p, has-mir-335-5p, and has-mir-16-5p could regulate the expression of CXCL8, FOS and MTHFR simultaneously (Figure 10A). Four candidate genes-TF networks were constructed, and the results revealed that CREB1 could regulate the expression of CXCL8,

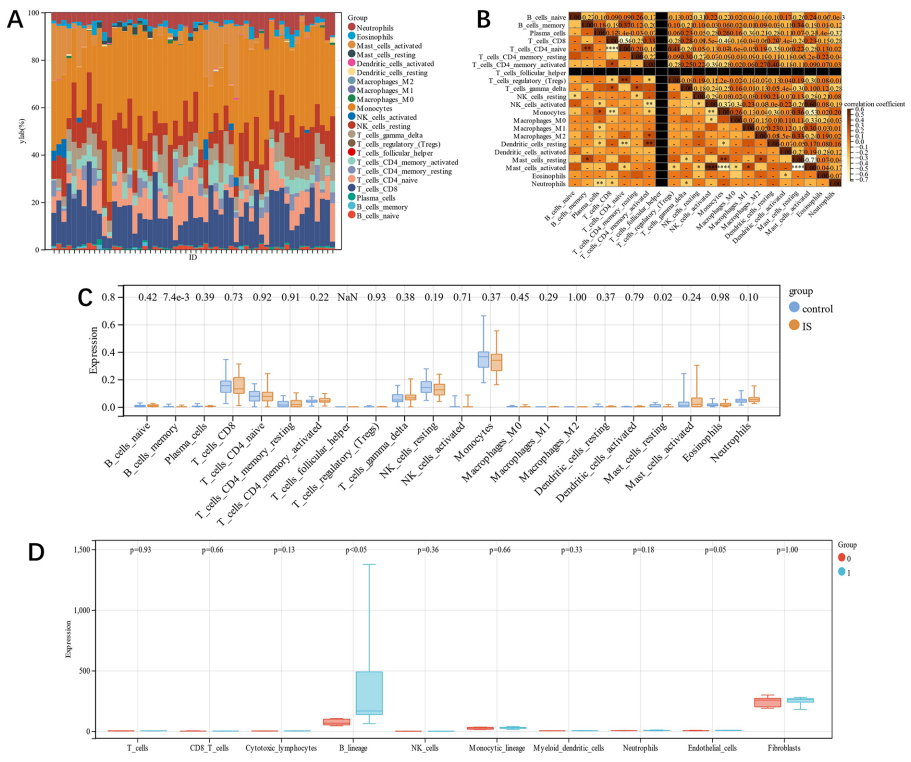

FIGURE 9
(A): each sample's relative percentage of 22 immune cells; **(B)**: The correlation among the 22 immune cells; **(C)**: immune infiltration difference between IS and control samples; **(D)**: Immune infiltration difference between the groups with and without carotid-related ischemic cerebrovascular events.

FOS, and MTHFR simultaneously, and FOXL1 could regulate the expression of CXCL8, LEP, and MTHFR simultaneously (Figure 10B).

Based on Drug Bank (40) and Comparative Toxicogenomics Database (41), a gene-drug interaction network was established (Figure 10C), and four of the most relevant drugs (Nickel, Arsenic, Aflatoxin B1, and sodium arsenite) were selected.

3.9. Candidate gene clusters' consensus clustering (CC) analysis

By CC analysis of four related candidate gene models, we observed that there were the most substantial differences among different groups (Figures 11A,B), so they were divided into C1 and C2 categories. Using the PCA diagram, it was revealed that the gene expression patterns of different clusters were different (Figure 11C). The expression levels of related genes in the two subgroups were visualized by a violin diagram (Figure 11D). There was a statistically significant difference among the CXCL8 and FOS ($p < 0.05$).

3.10. GSVA of biological pathway among subsets of candidate genes

We found that TNFA signaling *via* NFKB, UV response up, and inflammatory response in group C1 was lesser compared to group C2, but protein secretion in group C1 was greater as compared to group C2 (Figure 12A). The KEGG pathways, including amino sugar, galactose metabolism, beta-alanine metabolism, and nucleotide sugar metabolism in group C1, were greater compared to group C2. However, the pathways of type I diabetes mellitus and Circadian rhythm in group C1 were lesser than those in group C2 (Figure 12B). In the Reatcome pathway, HuR (ELAVL1) binds and stabilizes mRNA, MET receptor recycling, and TP53 Regulates Transcription of Caspase Activators and Caspases in group C1 were significantly greater compared to group C2, but Cytokine Network and p75NTR negatively regulate cell cycle *via* SC1 were lower than those in group C2 (Figure 12C). The GSVA analysis of the two groups with different prognoses in the verification group GSE198600 revealed that they were very similar to the CC group, and they were significantly enriched in several pathways of the glycan metabolism (Figure 12D). Target genes are predictive of IS risk grouping in unknown situations, and the reasons for such grouping criteria may be related to psychiatric disorders, especially schizophrenia, and gut microbiota.

3.11. Functional differences among subgroups

Through Limma analysis, 375 DEGs were obtained, from which 237 were down-regulated and 138 were up-regulated (Figure 13A). FEA and KEGG analysis revealed that the enrichment of differential

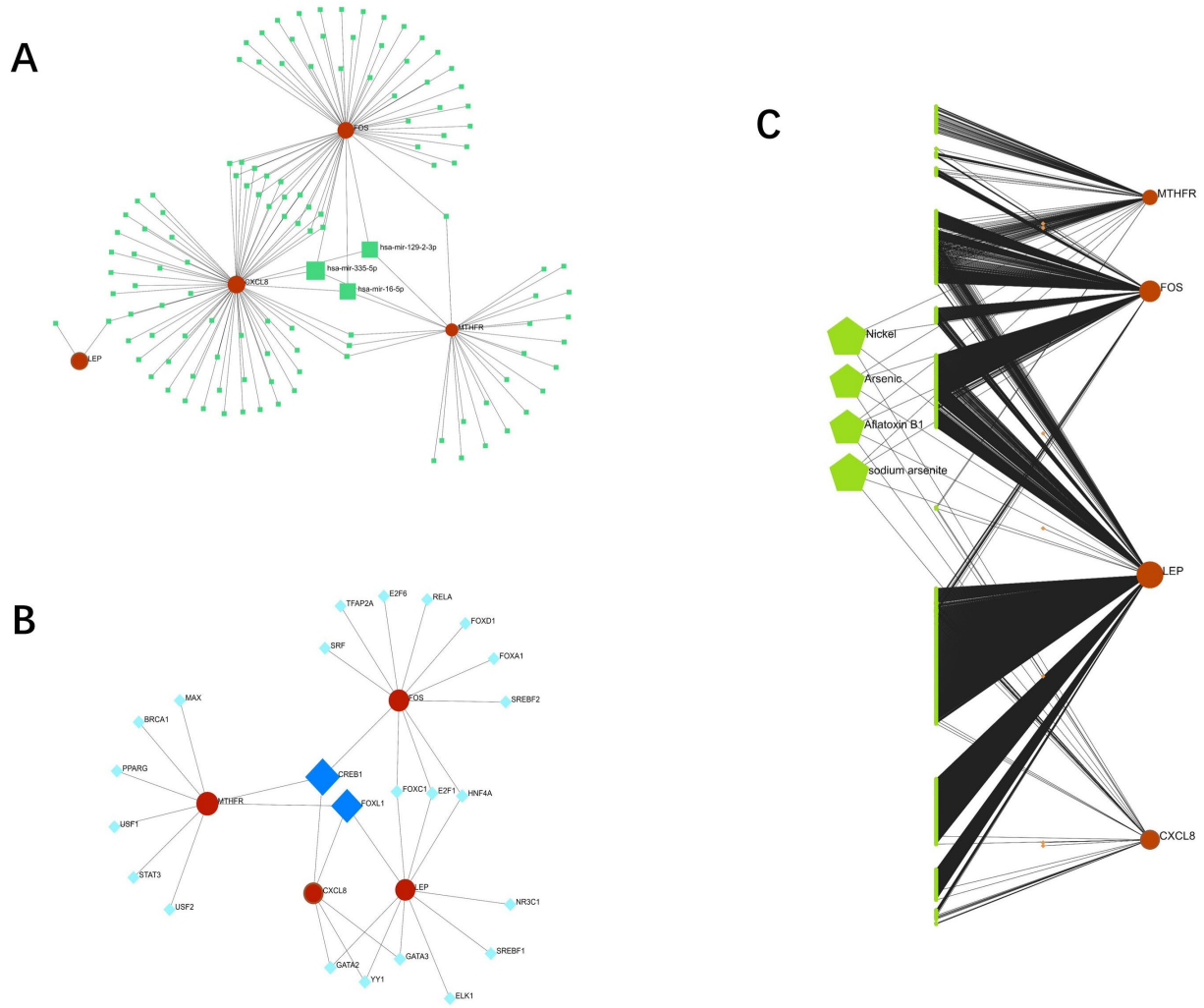

FIGURE 10
(A): interaction between candidate genes and miRNA; **(B)**: Interaction between candidate genes and TFs; **(C)**: gene-drug interaction network (red represents candidate genes, orange data comes from DrugBank, green data comes from Comparative Toxicogenomics Database).

genes was primarily in the pathways "TNF signaling pathway," "il-17 signaling pathway," and "Cytokine-cytokine receptor interaction" (Figure 13B). GO analysis showed the differential genes were chiefly located in the "intrinsic component of plasma membrane" and "secretory granule" on the basis of CC (Figure 13C). The primary biological processes (BP) of differential genes include the "immune system process" and "regulation of molecular function" (Figure 13D). MF analysis revealed that the main processes of the differential genes were "identical protein binding" and "signaling receptor binding" (Figure 13E). Through GO enrichment and the KEGG analysis, we observed that these differential genes were primarily enriched in immune system-related pathways.

4. Discussion

Existing studies have shown that ischemic stroke (IS) with dementia, depression, and other mental illness symptoms are common. The gut microbiome (GM) plays a critical role in mental illness and IS (42). However, this study aimed to identify the differences between genes related to ischemic stroke (IS) and mental disorders in the gut microbiome (GM) through bioinformatics analysis and qRT-PCR verification, and to predict drugs related to IS through candidate genes. Four candidate genes (CXCL8, FOS, LEP, MTHFR), three miRNA (hsa-mir-129-2-3p, has-mir-335-5p, and has-mir-16-5p), and two TFs (CREB1, FOXL1) were identified, and the four most related drugs (Nickel, Arsenic, AflatoxinB1, and sodium arsenite) were obtained.

The results of this study suggest that the gut microbiome may play a critical role in mental illness and IS. CXCL8, FOS, LEP, and MTHFR were found to be potential candidate genes for IS. These genes have been previously linked to other diseases and pathways, including chemokine activity, interleukin-8 receptor binding, and metabolism of water-soluble vitamins and cofactors. In addition, several studies have shown a significant correlation between FOS and IS, and MTHFR gene polymorphism and the increased risk of IS. Our study

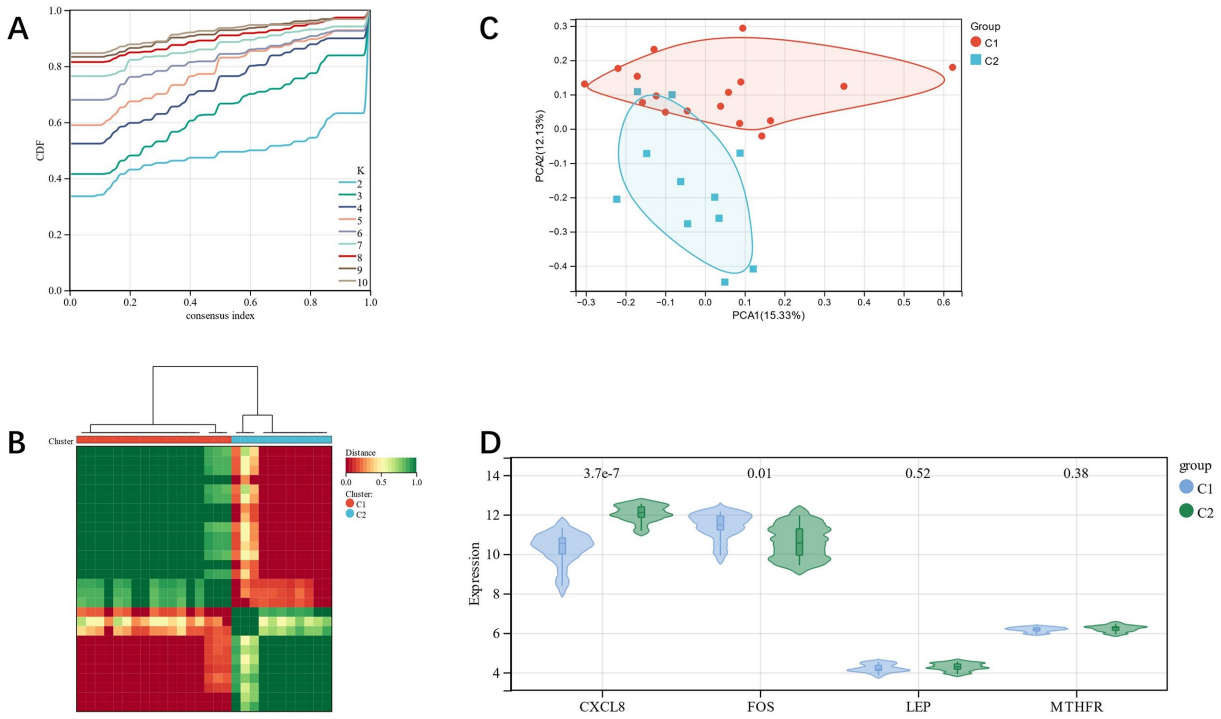

FIGURE 11
(A,B): CC analysis of related candidate genes; **(C)**: PCA diagram shows subclusters' distribution; **(D)**: violin diagram shows the differential expression of related candidate genes among subgroups.

supports these findings and provides further evidence of the role of these genes in IS.

Moreover, we found that IL-6, glucose metabolism, and B cell infiltration may be common pathways between schizophrenia and IS. This suggests that there may be a genetic correlation between these two diseases, and further studies are needed to clarify this relationship.

CXCL8 is a gene that codes for a protein and has been linked to diseases such as adult respiratory distress syndrome and melanoma. Pathways related to CXCL8 include TGF-pathway and MIF-mediated glucocorticoid regulation, as well as gene ontology annotations for chemokine activity and interleukin-8 receptor binding. Mouse experiments conducted by Hui Lv et al. suggest that CXCL8 may affect the development of IS by regulating the PI3K/Akt/NF-κB signaling pathway. Silencing CXCL8 led to a significant decrease in the deflection index, improved the size of the infarct, neurological function, and inhibited apoptosis index and glial cell loss (43). FOS is a gene that codes for a protein and is linked to diseases such as osteoblastoma and congenital systemic lipodystrophy. Pathways related to FOS include MyD88-dependent cascades initiated by endosomal and prolactin signal transduction. Gene ontology annotations for FOS include DNA binding to transcription factor activity and binding. Multiple bioinformatics analysis studies (44) have suggested a correlation between FOS and IS, and qRT-PCR verification has shown a statistically significant difference in IS-related FOS ($p < 0.01$).MTHFR is a gene that codes proteins. MTHFR is a gene that codes for proteins and is linked to diseases such as homocystinuria and folate-sensitive neural tube defects caused by a lack of N-methylenetetrahydrofolate reductase activity. Pathways related to MTHFR include the metabolism of water-soluble vitamins and cofactors, the methotrexate pathway (cancer cells), pharmacodynamics, and pharmacokinetics. Meta-analyses have shown a significant relationship between the C677T mutation of the MTHFR gene and the increased risk of IS. The MTHFR gene polymorphism is related to an increased IS risk, with a higher correlation observed in the Asian population (45). Ali Sazci et al. found that the MTHFR 1298C allele, C1298C genotype, and C677C/C1298C compound genotype are closely associated with ischemic stroke (46).

This study not only identified a genetic correlation between schizophrenia and IS, but also suggests that IL-6, glucose metabolism, and B cell infiltration are likely to be common pathways between these diseases. Four candidate genes were predicted, and the four most related drugs (Nickel, Arsenic, AflatoxinB1, and sodium arsenite) were obtained. Several studies have suggested a correlation between heavy metal levels and IS, with higher plasma concentrations of arsenic, aluminum, and cadmium and lower concentrations of iron and selenium increasing the risk of IS (47). Therefore, drugs containing Nickel, Arsenic, and sodium arsenite should be avoided in drug selection.

Further clinical data, particularly regarding schizophrenia and IS comorbidities and their follow-ups, are needed to clarify the causal relationship between SC, gut microbes, and IS. Relevant case collections and a large amount of clinical data and information will be needed to verify the conclusions of this study.

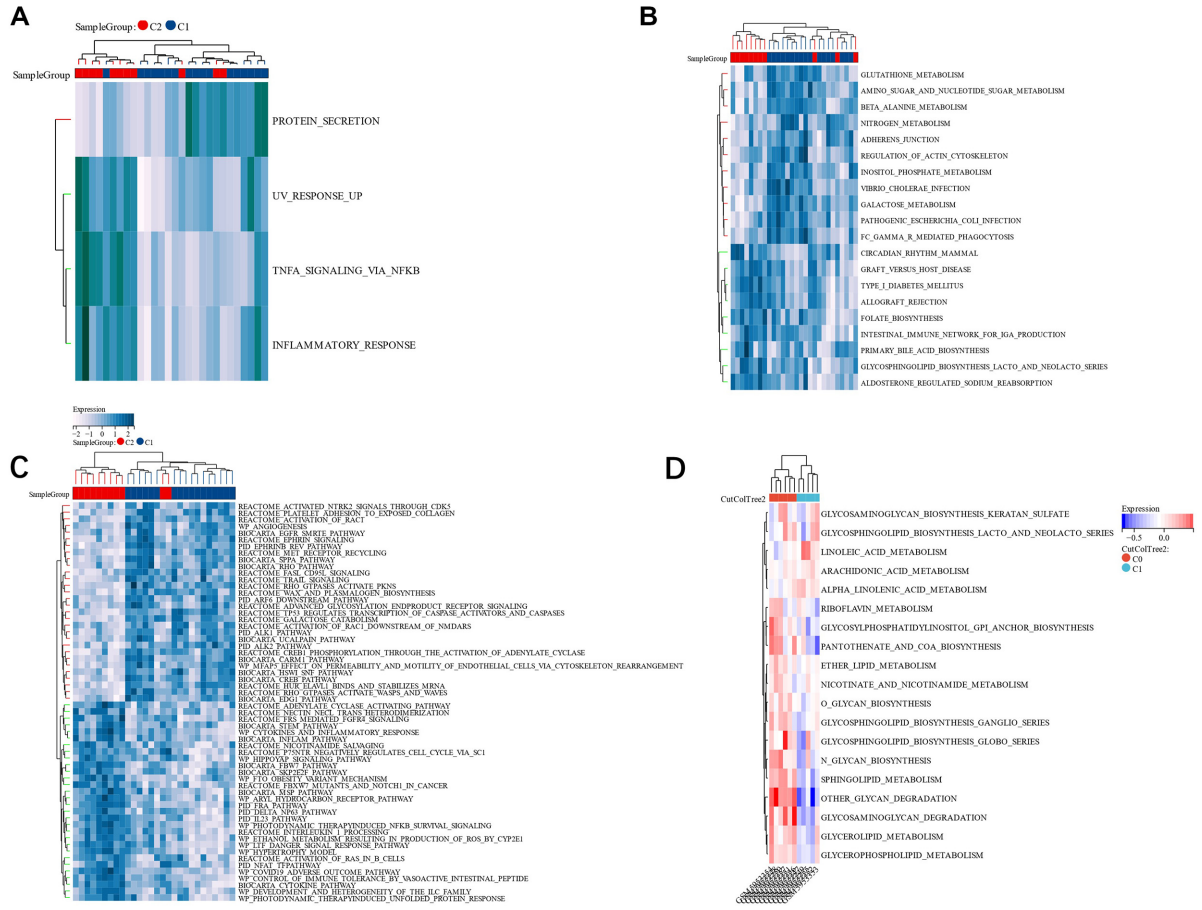

FIGURE 12
(A): HALLMARK pathway's GSVA; **(B)**: KEGG pathway's GSVA; **(C)**: Reatcome pathway's GSVA; **(D)**: A GSVA analysis of two groups in the validation set GSE198600 with different prognoses.

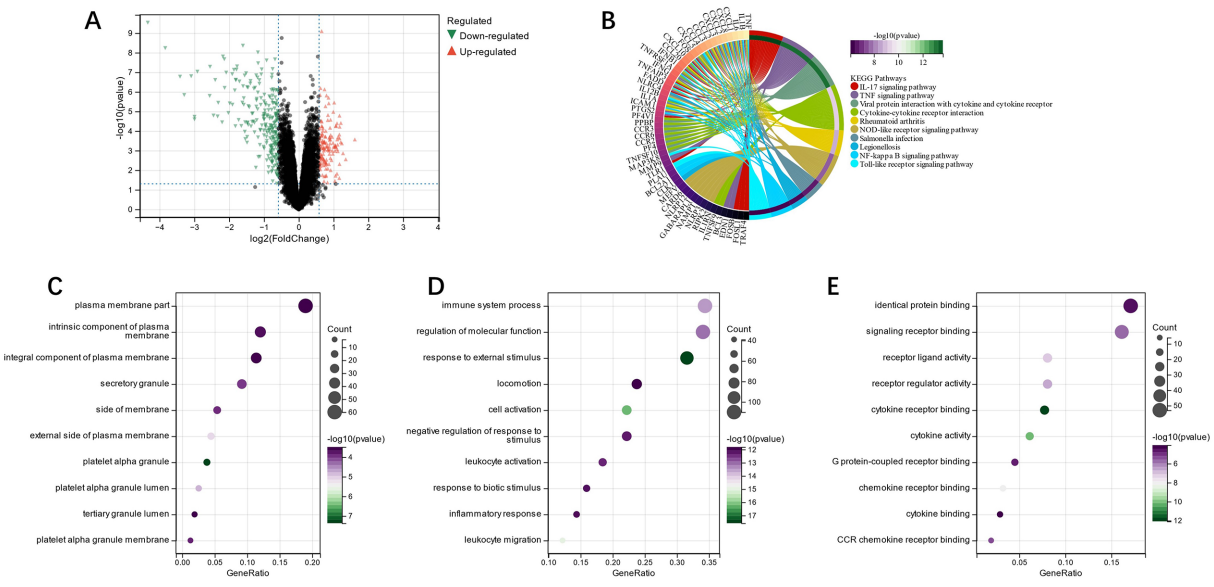

FIGURE 13
(A): subgroup DEGs' Volcano plot; **(B)**: differential genes' KEGG analysis; **(C)**: differential genes' GO analysis of cell composition; **(D)**: differential genes' GO analysis of the biological process (BP); **(E)**: differential genes' GO analysis of molecular function (MF).

5. Conclusion

Through comprehensive analysis, a diagnostic prediction model with good effect was obtained. Both the training group (AUC 0.82, CI 0.93–0.71) and the verification group (AUC 0.81, CI 0.90–0.72) had a good phenotype in the qRT-PCR test. And in verification group 2 we validated between the two groups with and without carotid-related ischemic cerebrovascular events (AUC 0.87, CI 1–0.64). Furthermore, we investigated cytokines in both GSEA and immune infiltration and verified cytokine-related responses by flow cytometry, particularly IL-6, which played an important role in IS occurrence and progression. Therefore, we speculate that mental illness may affect the development of IS in B cells and IL-6 in T cells. MiRNA (hsa-mir-129-2-3p, has-mir-335-5p, and has-mir-16-5p) and TFs (CREB1, FOXL1), which may be related to IS, were obtained.

Data availability statement

The original contributions presented in the study are included in the article/Supplementary material, further inquiries can be directed to the corresponding author.

Ethics statement

The studies involving human participants were reviewed and approved by Jiangsu Shengze Hospital clinical laboratory. Written informed consent for participation was not required for this study in accordance with the national legislation and the institutional requirements.

Author contributions

YF and JS wrote the article, ML, JH, and HY provided experimental help. All authors contributed to the article and approved the submitted version.

Acknowledgments

In the vastness of space and immensity of time, it is my joy to spend a planet and an epoch with Maggie.

Conflict of interest

The authors declare that the research was conducted in the absence of any commercial or financial relationships that could be construed as a potential conflict of interest.

Publisher's note

Supplementary material

The Supplementary material for this article can be found online at: https://www.frontiersin.org/articles/10.3389/fneur.2023.1189746/full#supplementary-material

References

1. Saini V, Guada L, Yavagal DR. Global epidemiology of stroke and access to acute ischemic stroke interventions. *Neurology*. (2021) 97:S6–s16. doi: 10.1212/wnl.0000000000012781

2. Qian Y, Chopp M, Chen J. Emerging role of Micrornas in ischemic stroke with comorbidities. *Exp Neurol*. (2020) 331:113382. doi: 10.1016/j.expneurol.2020.113382

3. Reeves MJ, Bushnell CD, Howard G, Gargano JW, Duncan PW, Lynch G, et al. Sex differences in stroke: epidemiology, clinical presentation, medical care, and outcomes. *Lancet Neurol*. (2008) 7:915–26. doi: 10.1016/s1474-4422(08)70193-5

4. Rost NS, Brodtmann A, Pase MP, van Veluw SJ, Biffi A, Duering M, et al. Post-stroke cognitive impairment and dementia. *Circ Res*. (2022) 130:1252–71. doi: 10.1161/circresaha.122.319951

5. Kalaria RN, Akinyemi R, Ihara M. Stroke injury, cognitive impairment and vascular dementia. *Biochim Biophys Acta*. (2016) 1862:915–25. doi: 10.1016/j.bbadis.2016.01.015

6. Das J, Rajanikant GK. Post stroke depression: the Sequelae of cerebral stroke. *Neurosci Biobehav Rev*. (2018) 90:104–14. doi: 10.1016/j.neubiorev.2018.04.005

7. Campbell Burton CA, Murray J, Holmes J, Astin F, Greenwood D, Knapp P. Frequency of anxiety after stroke: a systematic review and Meta-analysis of observational studies. *Int J Stroke*. (2013) 8:545–59. doi: 10.1111/j.1747-4949.2012.00906.x

8. Burvill PW, Johnson GA, Jamrozik KD, Anderson CS, Stewart-Wynne EG, Chakera TM. Anxiety disorders after stroke: results from the Perth community stroke study. *Br J Psychiatry*. (1995) 166:328–32. doi: 10.1192/bjp.166.3.328

9. Chun HY, Whiteley WN, Dennis MS, Mead GE, Carson AJ. Anxiety after stroke: the importance of subtyping. *Stroke*. (2018) 49:556–64. doi: 10.1161/strokeaha.117.020078

10. Chen MH, Tsai SJ, Su TP, Li CT, Lin WC, Chen TJ, et al. Increased risk of stroke in patients with obsessive-compulsive disorder: a Nationwide longitudinal study. *Stroke*. (2021) 52:2601–8. doi: 10.1161/strokeaha.120.032995

11. Bongiorno DM, Daumit GL, Gottesman RF, Faigle R. Patients with stroke and psychiatric comorbidities have lower carotid revascularization rates. *Neurology*. (2019) 92:e2514–21. doi: 10.1212/wnl.0000000000007565

12. Li N, Wang X, Sun C, Wu X, Lu M, Si Y, et al. Change of intestinal microbiota in cerebral ischemic stroke patients. *BMC Microbiol*. (2019) 19:191. doi: 10.1186/s12866-019-1552-1

13. Benakis C, Brea D, Caballero S, Faraco G, Moore J, Murphy M, et al. Commensal microbiota affects ischemic stroke outcome by regulating intestinal Γδ T cells. *Nat Med*. (2016) 22:516–23. doi: 10.1038/nm.4068

14. Houlden A, Goldrick M, Brough D, Vizi ES, Lénárt N, Martinecz B, et al. Brain injury induces specific changes in the Caecal microbiota of mice via altered autonomic activity and Mucoprotein production. *Brain Behav Immun*. (2016) 57:10–20. doi: 10.1016/j.bbi.2016.04.003

15. Pluta R, Januszewski S, Czuczwar SJ. The role of gut microbiota in an ischemic stroke. *Int J Mol Sci*. (2021) 22:915. doi: 10.3390/ijms22020915

16. Simpson CA, Diaz-Arteche C, Eliby D, Schwartz OS, Simmons JG, Cowan CSM. The gut microbiota in anxiety and depression – a systematic review. *Clin Psychol Rev*. (2021) 83:101943. doi: 10.1016/j.cpr.2020.101943

17. Zhuang Z, Yang R, Wang W, Qi L, Huang T. Associations between gut microbiota and Alzheimer's disease, major depressive disorder, and schizophrenia. *J Neuroinflammation*. (2020) 17:288. doi: 10.1186/s12974-020-01961-8

18. Barrett T, Wilhite SE, Ledoux P, Evangelista C, Kim IF, Tomashevsky M, et al. Ncbi geo: archive for functional genomics data sets—update. *Nucleic Acids Res*. (2012) 41:D991–5. doi: 10.1093/nar/gks1193

19. Taminau J, Meganck S, Lazar C, Steenhoff D, Coletta A, Molter C, et al. Unlocking the potential of publicly available microarray data using Insilicodb and Insilicomerging R/bioconductor packages. *BMC Bioinformatics*. (2012) 13:335. doi: 10.1186/1471-2105-13-335

20. Johnson WE, Li C, Rabinovic A. Adjusting batch effects in microarray expression data using empirical Bayes methods. *Biostatistics*. (2007) 8:118–27. doi: 10.1093/biostatistics/kxj037

21. Sokhansanj BA, Fitch JP, Quong JN, Quong AA. Linear fuzzy gene network models obtained from microarray data by exhaustive search. *BMC Bioinformatics*. (2004) 5:108. doi: 10.1186/1471-2105-5-108

22. Shen W, Song Z, Zhong X, Huang M, Shen D, Gao P, et al. Sangerbox: a comprehensive, interaction-friendly clinical bioinformatics analysis platform. *iMeta*. (2022) 1:e36. doi: 10.1002/imt2.36

23. R CMoHedGwafH, 3.15.0. pv. Carlson M (2022). _Org.Hs.Eg.Db: Genome wide annotation for Human_. R package version 3.15.0.

24. Yu G, Wang LG, Han Y, He QY. Clusterprofiler: an R package for comparing biological themes among gene clusters. *OMICS*. (2012) 16:284–7. doi: 10.1089/omi.2011.0118

25. Subramanian A, Tamayo P, Mootha VK, Mukherjee S, Ebert BL, Gillette MA, et al. Gene set enrichment analysis: a knowledge-based approach for interpreting genome-wide expression profiles. *Proc Natl Acad Sci U S A*. (2005) 102:15545–50. doi: 10.1073/pnas.0506580102

26. Liberzon A, Subramanian A, Pinchback R, Thorvaldsdóttir H, Tamayo P, Mesirov JP. Molecular signatures database (Msigdb) 3.0. *Bioinformatics*. (2011) 27:1739–40. doi: 10.1093/bioinformatics/btr260

27. Zhang M, Zhu K, Pu H, Wang Z, Zhao H, Zhang J, et al. An immune-related signature predicts survival in patients with lung adenocarcinoma. *Front Oncol*. (2019) 9:1314. doi: 10.3389/fonc.2019.01314

28. Yasir M, Karim AM, Malik SK, Bajaffer AA, Azhar EI. Prediction of antimicrobial minimal inhibitory concentrations for *Neisseria Gonorrhoeae* using machine learning models. *Saudi J Biol Sci*. (2022) 29:3687–93. doi: 10.1016/j.sjbs.2022.02.047

29. Franz M, Rodriguez H, Lopes C, Zuberi K, Montojo J, Bader GD, et al. Genemania Update 2018. *Nucleic Acids Res*. (2018) 46:W60–4. doi: 10.1093/nar/gky311

30. Robin X, Turck N, Hainard A, Tiberti N, Lisacek F, Sanchez JC, et al. Proc: an open-source package for R and S+ to analyze and compare roc curves. *BMC Bioinformatics*. (2011) 12:77. doi: 10.1186/1471-2105-12-77

31. Beck MW. Neuralnettools: visualization and analysis tools for neural networks. *J Stat Softw*. (2018) 85:1–20. doi: 10.18637/jss.v085.i11

32. Hernandez VG, Lechtenberg KJ, Peterson TC, Zhu L, Lucas TA, Owah JO, et al. Translatome analysis reveals microglia and astrocytes to be distinct regulators of inflammation in the Hyperacute and acute phases after stroke. *bio Rxiv*. (2023) 02, :520351. doi: 10.1101/2023.02.14.520351

33. Zhou S, Lu H, Xiong M. Identifying immune cell infiltration and effective diagnostic biomarkers in rheumatoid arthritis by bioinformatics analysis. *Front Immunol*. (2021) 12:726747. doi: 10.3389/fimmu.2021.726747

34. Pripp AH. Pearson's or Spearman's correlation coefficients. *Tidsskr Nor Laegeforen*. (2018) 138. doi: 10.4045/tidsskr.18.0042

35. Xie L, Huang G, Gao M, Huang J, Li H, Xia H, et al. Identification of atrial fibrillation-related Lncrna based on Bioinformatic analysis. *Dis Markers*. (2022) 2022:8307975. doi: 10.1155/2022/8307975

36. Zhou G, Soufan O, Ewald J, Hancock REW, Basu N, Xia J. Networkanalyst 3.0: a visual analytics platform for comprehensive gene expression profiling and Meta-analysis. *Nucleic Acids Res*. (2019) 47:W234–41. doi: 10.1093/nar/gkz240

37. Wilkerson MD, Hayes DN. Consensusclusterplus: a class discovery tool with confidence assessments and item tracking. *Bioinformatics*. (2010) 26:1572–3. doi: 10.1093/bioinformatics/btq170

38. Hänzelmann S, Castelo R, Guinney J. Gsva: gene set variation analysis for microarray and Rna-Seq data. *BMC Bioinformatics*. (2013) 14:7. doi: 10.1186/1471-2105-14-7

39. Lin W, Wang Y, Chen Y, Wang Q, Gu Z, Zhu Y. Role of calcium signaling pathway-related gene regulatory networks in ischemic stroke based on multiple Wgcna and single-cell analysis. *Oxidative Med Cell Longev*. (2021) 2021:8060477. doi: 10.1155/2021/8060477

40. Wishart DS, Feunang YD, Guo AC, Lo EJ, Marcu A, Grant JR, et al. Drugbank 5.0: a major update to the Drugbank database for 2018. *Nucleic Acids Res*. (2018) 46:D1074–82. doi: 10.1093/nar/gkx1037

41. Davis AP, Wiegers TC, Johnson RJ, Sciaky D, Wiegers J, Mattingly CJ. Comparative Toxicogenomics database (Ctd): update 2023. *Nucleic Acids Res*. (2022) 51:D1257–62. doi: 10.1093/nar/gkac833

42. Zeng J, Yang K, Nie H, Yuan L, Wang S, Zeng L, et al. The mechanism of intestinal microbiota regulating immunity and inflammation in ischemic stroke and the role of natural botanical active ingredients in regulating intestinal microbiota: a review. *Biomed Pharmacother*. (2023) 157:114026. doi: 10.1016/j.biopha.2022.114026

43. Lv H, Li J, Che YQ. Cxcl 8 gene silencing promotes Neuroglial cells activation while inhibiting Neuroinflammation through the Pi3k/Akt/Nf-Kb-signaling pathway in mice with ischemic stroke. *J Cell Physiol*. (2019) 234:7341–55. doi: 10.1002/jcp.27493

44. Ma Z, Liu CF, Zhang L, Xiang N, Zhang Y, Chu L. The construction and analysis of immune infiltration and competing endogenous Rna network in acute ischemic stroke. *Front Aging Neurosci*. (2022) 14:806200. doi: 10.3389/fnagi.2022.806200

45. Kumar P, Mishra A, Prasad MK, Verma V, Kumar A. Relationship of Methylenetetrahydrofolate Reductase (Mthfr) C677t variation with susceptibility of patients with ischemic stroke: a Meta-analysis. *Cureus*. (2022) 14:e28218. doi: 10.7759/cureus.28218

46. Sazci A, Ergul E, Tuncer N, Akpinar G, Kara I. Methylenetetrahydrofolate Reductase gene polymorphisms are associated with ischemic and hemorrhagic stroke: dual effect of Mthfr polymorphisms C677t and A1298c. *Brain Res Bull*. (2006) 71:45–50. doi: 10.1016/j.brainresbull.2006.07.014

47. Wen Y, Huang S, Zhang Y, Zhang H, Zhou L, Li D, et al. Associations of multiple plasma metals with the risk of ischemic stroke: a case-control study. *Environ Int*. (2019) 125:125–34. doi: 10.1016/j.envint.2018.12.037

frontiers | Frontiers in Neurology

TYPE Original Research
PUBLISHED 08 June 2023
DOI 10.3389/fneur.2023.1174711

OPEN ACCESS

EDITED BY
Yanlin Zhang,
Second Affiliated Hospital of Soochow University, China

REVIEWED BY
Jun Chen,
Zhejiang University, China
Dongsheng Cai,
Zhejiang University, China

*CORRESPONDENCE
Xiaoyang Gong
✉ rowlandgxy@163.com
Yong Liu
✉ fuwa52008@126.com

RECEIVED 27 February 2023
ACCEPTED 19 May 2023
PUBLISHED 08 June 2023

CITATION
Hu X, Liang J, Hao W, Zhou J, Gao Y, Gong X and Liu Y (2023) Prognostic value of inflammatory markers for in-hospital mortality in intensive care patients with acute ischemic stroke: a retrospective observational study based on MIMIC-IV.
Front. Neurol. 14:1174711.
doi: 10.3389/fneur.2023.1174711

Prognostic value of inflammatory markers for in-hospital mortality in intensive care patients with acute ischemic stroke: a retrospective observational study based on MIMIC-IV

Xuyang Hu[1,2], Jiaru Liang[2], Wenjian Hao[2], Jiaqi Zhou[1], Yuling Gao[1], Xiaoyang Gong[1]*and Yong Liu[1,2]*

[1]Department of Rehabilitation Medicine, The First Affiliated Hospital of Dalian Medical University, Dalian, China, [2]Institute (College) of Integrative Medicine, Dalian Medical University, Dalian, China

Background: Acute ischemic stroke (AIS) is a primary cause of death and disability worldwide. Four markers that can be readily determined from peripheral blood, namely, the systemic immune-inflammation index (SII), neutrophil-to-lymphocyte ratio (NLR), platelet-to-lymphocyte ratio (PLR), and total bilirubin, were measured in this study. We examined the relationship between the SII and in-hospital mortality after AIS and evaluated which of the above four indicators was most accurate for predicting in-hospital mortality after AIS.

Methods: We selected patients from the Medical Information Mart for Intensive Care-IV (MIMIC-IV) database who were aged >18years and who were diagnosed with AIS on admission. We collected the patients' baseline characteristics, including various clinical and laboratory data. To investigate the relationship between the SII and in-hospital mortality in patients with AIS, we employed the generalized additive model (GAM). Differences in in-hospital mortality between the groups were summarized by the Kaplan–Meier survival analysis and the log-rank test. The receiver operating characteristic (ROC) curve analysis was used to assess the accuracy of the four indicators (SII, NLR, PLR, and total bilirubin) for predicting in-hospital mortality in patients with AIS.

Results: The study included 463 patients, and the in-hospital mortality rate was 12.31%. The GAM analysis showed a positive correlation between the SII and in-hospital mortality in patients with AIS, but the correlation was not linear. Unadjusted Cox regression identified a link between a high SII and an increased probability of in-hospital mortality. We also found that patients with an SII of >1,232 (Q2 group) had a considerably higher chance of in-hospital mortality than those with a low SII (Q1 group). The Kaplan–Meier analysis demonstrated that patients with an elevated SII had a significantly lower chance of surviving their hospital stay than those with a low SII. According to the results of the ROC curve analysis, the in-hospital mortality of patients with AIS predicted by the SII had an area under the ROC curve of 0.65, which revealed that the SII had a better discriminative ability than the NLR, PLR, and total bilirubin.

Conclusion: The in-hospital mortality of patients with AIS and the SII were positively correlated, but not linearly. A high SII was associated with a worse prognosis in patients with AIS. The SII had a modest level of discrimination for forecasting in-hospital mortality. The SII was slightly better than the NLR and

significantly better than the PLR and total bilirubin for predicting in-hospital mortality in patients with AIS.

KEYWORDS

acute ischemic stroke, in-hospital mortality, MIMIC-IV, SII, inflammatory marker, predictor

Introduction

Stroke, which is the third leading cause of disability and the second leading cause of mortality worldwide, is a common and damaging disease, and the majority of stroke cases are ischemic stroke due to arterial occlusive disease (1). According to data from China's Hospital Quality Monitoring System, 2,466,785 patients with ischemic stroke were hospitalized in 2018, accounting for 81.9% of all stroke cases, placing a huge burden on society (2). Therefore, it is of great significance to identify convenient and efficient biomarkers to predict disease prognosis, which could reduce the adverse outcomes of patients with stroke.

The mechanisms of acute ischemic stroke (AIS) are complex and multifactorial. Scientific evidence links inflammation, which exacerbates brain damage, to the occurrence, progression, and outcome of AIS (3, 4). During the early stages of ischemic stroke, peripheral immune populations, including neutrophils, monocytes, T cells, and macrophages, infiltrate the brain parenchyma (5). Therefore, the assessment of inflammatory indicators is helpful to evaluate the prognosis of AIS. It is well known that AIS is closely associated with many inflammatory markers, including interleukin, high-sensitivity C-reactive protein, tumor necrosis factor, and homocysteine, amongst others (6, 7). In addition to the abovementioned indicators, several composite inflammatory markers have been used to predict the prognosis of patients with AIS. The neutrophil-to-lymphocyte ratio (NLR), which reflects the balance between circulating neutrophils and lymphocytes, is strongly associated with short-term functional outcomes in patients with AIS (8). Moreover, the platelet-to-lymphocyte ratio (PLR) is a strong predictor of AIS prognosis and could be used to assess platelet activation due to inflammation-coagulation interactions and other factors (9, 10). The systemic-immune inflammation index (SII) is also associated with poor outcomes in patients with AIS, reflecting thrombotic and immune dysregulation (11). Furthermore, once cerebral ischemia occurs, excessive oxidative stress ensues, resulting in structural and functional damage to the brain (12). As two early events of cerebral ischemic injury, inflammation and oxidative stress are closely related (13). Moreover, bilirubin is the most effective endogenous antioxidant and plays a neuroprotective role in stroke. Many studies have revealed a correlation between bilirubin and poor outcomes in patients with AIS, but there is still some controversy (12, 14–16).

The abovementioned four markers (SII, NLR, PLR, and bilirubin) can be readily determined from peripheral blood and are strongly associated with poor outcomes in patients with AIS. Therefore, this study sought to investigate the relationship between the SII and in-hospital mortality in intensive care patients with AIS and to examine which of these four inflammatory markers is most effective at predicting short-term mortality from AIS.

Methods

Medical information mart for intensive care-IV (MIMIC-IV) database

This retrospective and observational study was conducted based on primary data obtained from the comprehensive MIMIC-IV database. MIMIC-IV comprises numbers for each medical record relating to patients who were admitted to the intensive care unit (ICU) or emergency room at the Beth Israel Deaconess Medical Center between 2008 and 2019 (17). The first author (Xuyang Hu, certification ID: 51415516) was authorized to use the MIMIC-IV database after completing the National Institutes of Health's online education program. The BIDMC Institutional Review Board assessed the gathering of patient data and the development of the research resource, authorized the data-sharing project, and waived the requirement for informed consent. To ensure patient privacy, all processes were completed in compliance with the applicable regulations.

Patient selection

Using the International Classification of Diseases (ICD) codes ICD-9: 433, ICD-9: 434, ICD-9: 436, and ICD-10: I63, we selected 1,605 patients who were admitted to the ICU and who were diagnosed with AIS from the MIMIC-IV database. The inclusion criteria were as follows: (I) patients aged >18 years; (II) patients diagnosed with AIS; and (III) patients admitted to the ICU. The exclusion criteria were as follows: (I) patients with incomplete or difficult-to-find documentation or other important medical records; (II) patients with missing survival outcome data; and (III) patients with missing data on white blood cell count, neutrophil count, lymphocyte count, platelet count, or bilirubin concentration.

Patients' baseline characteristics

Patients' baseline characteristics were collected, including general information, vital signs, comorbidity history, laboratory parameters, and scoring system results. We extracted the first record of various data for patients diagnosed with AIS on admission. The vital signs included heart rate, mean blood pressure, systolic blood pressure, diastolic blood pressure, respiratory rate, body temperature, and pulse oximetry-derived oxygen saturation (SpO_2). The anion gap, blood urea nitrogen, bicarbonate, creatinine, chloride, glucose, hematocrit, hemoglobin, bilirubin, chloride, neutrophil count, serum sodium, lymphocyte count, serum potassium, prothrombin time, white blood

cell count, and platelet count were among the laboratory parameters that were recorded.

Both the Sequential Organ Failure Assessment (SOFA) score and Simplified Acute Physiology Score (SAPS) II for each patient were also calculated. In-hospital mortality was the endpoint of the study, as assessed by in-hospital survival.

The formula used to determine the SII was SII = platelet × neutrophil count ÷ lymphocyte count. The neutrophil count divided by the lymphocyte count was used to determine the NLR, while the platelet count divided by the lymphocyte count was used to determine the PLR.

Statistical analysis

We used the generalized additive model (GAM) to examine the association between the SII and in-hospital mortality in patients with AIS. According to the GAM analysis results, the patients were divided into two groups. Normally distributed continuous variables are presented as the mean ± standard deviation, whereas non-normally distributed continuous variables are presented as the median. Categorical variables are expressed as frequency and percentage. The groups were compared using the chi-square test, Kruskal–Wallis test, and one-way analysis of variance. Differences in in-hospital mortality between the groups were summarized using the Kaplan–Meier survival analysis and the log-rank test. Due to the possibility of confounding effects of variables based on laboratory tests and epidemiology, we utilized three quartile-based Cox proportional hazards regression models, the first of which was used as the reference model.

We adjusted the covariates of comorbidities and vital sign data, including age, sex, heart rate, mean blood pressure, SpO_2, congestive heart failure, renal failure, and temperature, in Model I. Model II was mostly modified for laboratory data, including creatinine, anion gap, hemoglobin, prothrombin time, glucose, and chloride. Based on Model II, the variables were further modified for the severity of illness scoring (SOFA score, SAPS II). Through the receiver operating characteristic (ROC) curve analysis, the discriminative ability of the four inflammatory indicators (SII, NLR, PLR, and total bilirubin) for predicting in-hospital mortality in patients with AIS was determined using the area under the ROC curve (AUC). Discrimination was considered good if the AUC exceeded 0.7 and moderate if the AUC was between 0.65 and 0.70. Statistical information was displayed as hazard ratios (HRs) and 95% confidence intervals (CIs). Each statistical test was conducted using a two-tailed design. R version 4.2.2 was used for the statistical analysis, and a p value of ≤ 0.05 was considered statistically significant.

Results

Baseline characteristics

In total, 463 suitable patients with a mean age of 71.68 ± 16.29 years (221 men and 242 women) were included in the study. Supplementary Tables S1, S2 provide further details on the data extraction procedure and missing data. The study yielded an in-hospital mortality rate of 12.31%, with 57 patients dying during hospitalization. According to the findings of the GAM analysis of the SII and in-hospital mortality, the patients were divided equally into two groups. In Table 1, the baseline characteristics of the groups are broken down according to the SII. The values for temperature, anion gap, blood glucose, and SAPS II were higher among patients with a high SII.

Relationship between the SII and in-hospital mortality in patients with AIS

According to the results of the GAM analysis, the in-hospital mortality of patients with AIS was positively correlated with the SII, but not linearly (Figure 1). A high SII was associated with a higher risk of in-hospital mortality according to the unadjusted Cox regression analysis (HR 1.75, 95% CI 1.02–3.02, $p = 0.044$). We further explored the relationship between the SII and in-hospital mortality in patients with AIS using three Cox regression models to account for the influence of other confounding variables (Table 2). After adjusting for vital signs and comorbidities, a high SII was associated with increased in-hospital mortality in Model I (HR 1.97, 95% CI 1.13–3.44, $p = 0.016$). After adjusting for laboratory data on the basis of Model I, the HR of high SII was 1.96 in Model II (95% CI 1.11–3.48, $p = 0.020$). Based on Model II, the variables were further modified in Model III for the severity of illness scoring (SAPS II and SOFA score). The high SII group still had a considerably higher likelihood of in-hospital mortality (HR 2.06, 95% CI 1.15–3.72, $p = 0.016$). The Kaplan–Meier survival plot for patients with various SII values is shown in Figure 2. The results demonstrate that patients with an elevated SII had a significantly lower chance of surviving their hospital stay than those with a low SII (log-rank test: $p = 0.041$).

The discriminative ability of the SII to predict in-hospital mortality in patients with AIS compared with the other indicators

According to the ROC curve analysis results, the AUC of in-hospital mortality in patients with AIS predicted by the SII was 0.65 (95% CI 0.62–0.68), the AUC of the NLR was 0.64 (95% CI 0.61–0.67), the AUC of the PLR was 0.60 (95% CI 0.53–0.67), and the AUC of total bilirubin was 0.55 (95% CI 0.52–0.58). The SII had a better discriminative ability for predicting in-hospital mortality in patients with AIS than the NLR, PLR, and total bilirubin. Overall, the SII had a modest discriminative ability for predicting in-hospital mortality (Figures 3–5).

Discussion

This study revealed a positive correlation between the in-hospital mortality of patients with AIS and the SII, but this correlation was not linear. The overall in-hospital mortality rate of patients with AIS was 12.31%, which is similar to the value of 13.9% from the Get With The Guidelines-Stroke database of the American Heart Association (18). We found that (1) a high SII was independently associated with a high risk of in-hospital mortality in patients with AIS; (2) hospitalized

TABLE 1 Patients' characteristics.

Characteristic	Total (*n*=463)	Q1 (*n*=231)	Q2 (*n*=232)	*p*-value
Age (years)	71.68 ± 16.29	71.58 ± 15.80	71.77 ± 16.81	0.901
Male	221 (47.73%)	117 (50.65%)	104 (44.83%)	0.246
SBP (mmHg)	134.63 ± 18.20	135.32 ± 18.43	133.97 ± 17.99	0.424
DBP (mmHg)	73.66 ± 12.22	73.68 ± 12.32	73.64 ± 12.14	0.972
MBP (mmHg)	90.53 ± 12.46	90.89 ± 12.42	90.17 ± 12.52	0.534
Heart rate (beats/min)	79.32 ± 14.98	78.46 ± 14.64	80.17 ± 15.30	0.218
Respiratory rate (breaths/min)	19.31 ± 3.12	19.37 ± 3.34	19.25 ± 2.89	0.671
Temperature (°C)	36.94 ± 0.34	36.90 ± 0.32	36.97 ± 0.35	**0.044**
SpO_2 (%)	96.78 ± 1.91	96.79 ± 2.03	96.78 ± 1.79	0.935
Comorbidities, *n* (%)				
Diabetes mellitus	151 (32.61%)	80 (34.63%)	71 (30.60%)	0.389
Myocardial infarction	57 (12.31%)	32 (13.85%)	25 (10.78%)	0.386
Congestive heart failure	119 (25.70%)	52 (22.51%)	67 (28.88%)	0.144
Chronic pulmonary disease	60 (12.96%)	29 (12.55%)	31 (13.36%)	0.904
Dementia	40 (8.64%)	21 (9.09%)	19 (8.19%)	0.857
Renal disease	89 (19.22%)	51 (22.08%)	38 (16.38%)	0.150
Malignancy	36 (7.78%)	20 (8.66%)	16 (6.90%)	0.593
Laboratory parameters				
Anion gap (mEq/L)	14.92 ± 3.10	14.56 ± 3.18	15.27 ± 2.98	**0.014**
BUN (mg/dL)	21.05 ± 15.15	21.05 ± 13.75	21.05 ± 16.45	0.999
Bicarbonate (mmol/L)	22.86 ± 3.14	23.05 ± 3.17	22.68 ± 3.12	0.210
Creatinine (mg/dL)	1.19 ± 1.34	1.26 ± 1.47	1.12 ± 1.20	0.260
Chloride (mmol/L)	103.51 ± 4.53	103.94 ± 4.40	103.70 ± 4.62	**0.038**
Glucose (mg/dL)	131.88 ± 47.24	126.82 ± 44.59	136.92 ± 49.32	**0.021**
Hematocrit (%)	37.20 ± 5.80	37.40 ± 5.88	37.00 ± 5.73	0.466
Hemoglobin (g/dL)	12.12 ± 2.12	12.18 ± 2.13	12.06 ± 2.10	0.533
Total bilirubin (mg/dL)	1.21 (2.26)	1.50 (2.82)	0.91 (1.46)	**0.005**
Neutrophil count (10^9/L)	7.66 ± 3.92	5.79 ± 2.56	9.52 ± 4.15	<0.001
Lymphocyte count (10^9/L)	1.67 ± 2.34	2.21 ± 3.19	1.13 ± 0.53	<0.001
Platelet count (10^9/L)	211.00 ± 83.00	196 ± 66.00	231.00 ± 90.00	<0.001
Potassium (mmol/L)	4.24 ± 0.53	4.24 ± 0.54	4.24 ± 0.53	0.979
PT (s)	13.34 ± 3.99	13.10 ± 3.42	13.57 ± 4.49	0.205
Sodium (mmol/L)	139.91 ± 3.88	140.20 ± 3.78	139.61 ± 3.97	0.101
WBC count (10^9/L)	10.28 ± 4.53	9.45 ± 5.00	10.36 ± 4.02	0.702
SOFA score	3.54 ± 0.06	3.75 ± 3.03	3.39 ± 2.53	0.165
SAPS II	32.64 ± 11.89	31.67 ± 11.21	33.61 ± 12.48	0.078
NLR	5.08 ± 6.75	3.62 ± 3.50	10.26 ± 7.54	<0.001
SII	1084.24 ± 1628.66	628.67 ± 259.37	2369.75 ± 1928.50	<0.001
ICU LOS (days)	4.55 ± 5.00	4.66 ± 4.86	4.45 ± 5.14	0.646
HOS LOS (days)	10.55 ± 11.61	10.18 ± 10.50	10.92 ± 12.64	0.494
In-hospital mortality	57 (12.31%)	20 (8.66%)	37 (15.95%)	0.025

SBP, systolic blood pressure; DBP, diastolic blood pressure; MBP, mean blood pressure; SpO_2, pulse oximetry-derived oxygen saturation; BUN, blood urea nitrogen; PT, prothrombin time; WBC, white blood cell; SOFA, Sequential Organ Failure Assessment; SAPS II, Simplified Acute Physiology Score II; NLR, neutrophil-to-lymphocyte ratio; SII, systemic immune-inflammation index; ICU, intensive care unit; HOS, hospital; LOS, length of stay.

The data are presented as the mean ± standard deviation and median or *n* (%).

The bold values for temperature, anion gap, blood glucose, and SAPS II were higher among patients with a high SII.

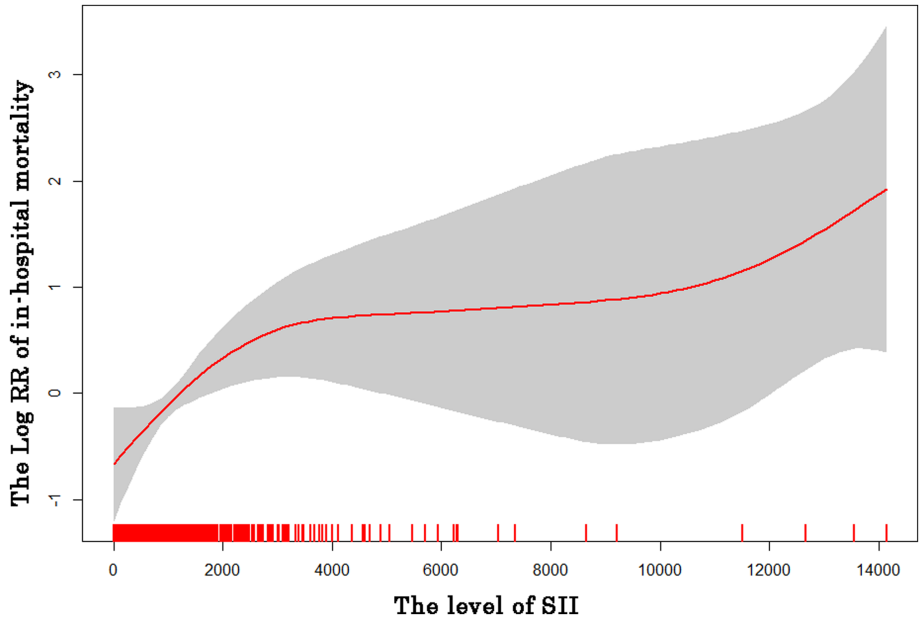

FIGURE 1
Cubic spline plot of relation of SII to risk of in-hospital patients' mortality.

TABLE 2 The SII and in-hospital mortality of patients with AIS.

Variable	Unadjusted model		Model I		Model II		Model III	
SII	HR (95% CI)	*p*-value	HR (95% CI)	*p*-value	HR (95% CI)	*p*-value	HR (95% CI)	*p*-value
Q1	1.0 (ref)		1.0 (ref)		1.0 (ref)			
Q2	1.75 (1.02–3.02)	0.044	1.97 (1.13–3.44)	0.016	1.96 (1.11–3.48)	0.020	2.06 (1.15–3.72)	0.016

HR, hazard ratio; SII, systemic immune-inflammation index.
Model I was adjusted for age, sex, heart rate, mean blood pressure, SpO_2, congestive heart failure, renal failure, and temperature.
Model II was adjusted for the variables adjusted in Model I, as well as creatinine, anion gap, hemoglobin, prothrombin time, glucose, and chloride.
Model III was adjusted for the variables adjusted in Model I and Model II, as well as the SAPS II and SOFA scores.

patients with AIS with a high SII were less likely to survive than patients with a low SII; (3) SII had a modest discriminative ability for forecasting in-hospital mortality in patients with AIS; and (4) the SII was marginally superior to the NLR and significantly better than the PLR and total bilirubin in forecasting in-hospital mortality in patients with AIS.

We also found that the values for temperature, anion gap, blood glucose, and SAPS II were higher among patients with a high SII, indicating that these indicators are strongly associated with poor outcomes in patients with AIS, as demonstrated in several previous studies. For example, a previous study showed that elevated body temperature was associated with increased mortality and poor functional outcome in patients with AIS (19). Another study showed that patients with an elevated plasma anion gap had worse clinical outcomes and were at a greater risk of in-hospital mortality (20). Moreover, hyperglycemia on admission has been linked to worse post-stroke outcomes (21). SAPS II, which was created to assess disease severity in patients in the ICU, is also linked to poor outcomes in patients with AIS (22).

The pathophysiological process after AIS is complex, and inflammation plays a key role, starting in the vascular compartment immediately after arterial blockage (23). Neutrophils, which are the earliest cells to react during ischemic stroke and are clinically associated with a poor functional outcome, begin to enter the brain parenchyma 12 h after stroke onset, causing neuronal death by producing elastase, matrix metalloproteinase-1, interleukin-7β, and reactive oxygen species. This in turn destroys the blood–brain barrier and induces damage to the ischemic area (5, 24). Additionally, neutrophils express inducible nitric oxide synthase, which is an enzyme that catalyzes the generation of nitric oxide and causes bigger infarcts during middle cerebral artery occlusion (25). Therefore, the increase in neutrophils is a key mediator of ischemic brain damage. Platelets interact with neutrophils and are key players in thrombotic inflammation and stroke pathogenesis (26). Similar to neutrophils, activated platelets interact with the endothelium and release mediators that promote inflammation after stroke, aggravating the inflammatory immune response (27). A previous study revealed that platelet P-selectin and glycoprotein Ib, which bind neutrophil P-selectin glycoprotein-1 and MAC-1 (CD11b/CD18), facilitate this interaction (28). Lymphocytes also play an important role in the inflammatory response in AIS, although the pathogenic role of lymphocytes is controversial. T cells play a key role in the exacerbation of ischemic brain injury (5); however, regulatory T cells are a major protective modulator of post-ischemic

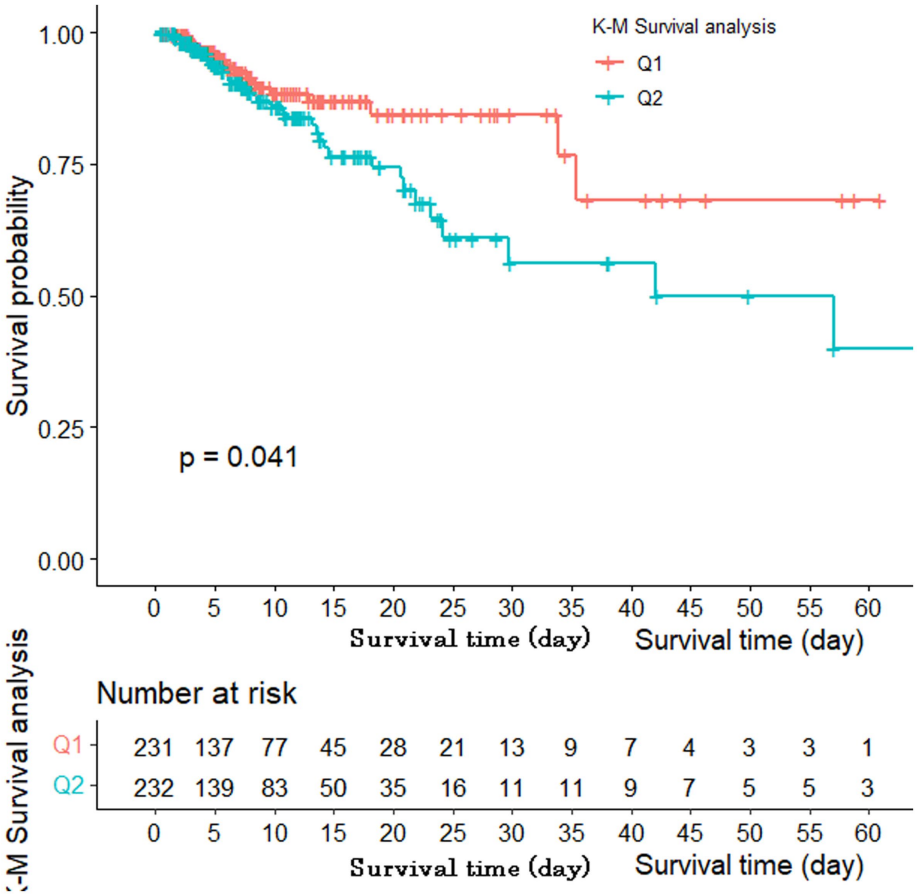

FIGURE 2
Kaplan–Meier survival curve of SII.

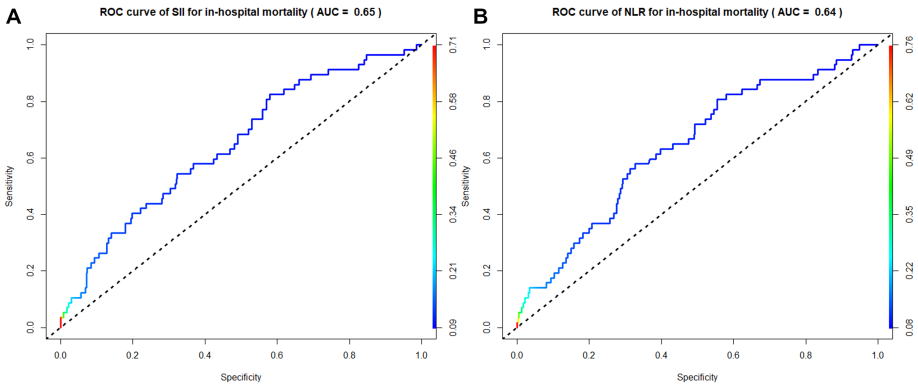

FIGURE 3
Receiver operating characteristic (ROC) curve of SII and NLR.

brain injury (29). For example, in a mouse experiment, regulatory T cell-treated mice had smaller infarcts and improved neurological function after stroke (30).

The SII, which is a novel comprehensive inflammatory index, is calculated based on three inflammatory immune cell types (lymphocytes, neutrophils, and platelets) that reflect the balance between the immunological and inflammatory states of the host. The SII was initially used to predict tumor prognosis and identify patients at a high risk of death (31). The SII has reportedly been linked to increased disease severity and a poor prognosis in various illnesses and could be used to anticipate fatality in patients with various cancers, heart failure, and cardiovascular disease (32). Thus far, the value of the SII in cerebrovascular illnesses has been demonstrated in several studies. For example, studies by Zhou et al. (33) and Wang et al. (34) showed that a high SII increases the risk of death from AIS. Moreover, Zhang's study

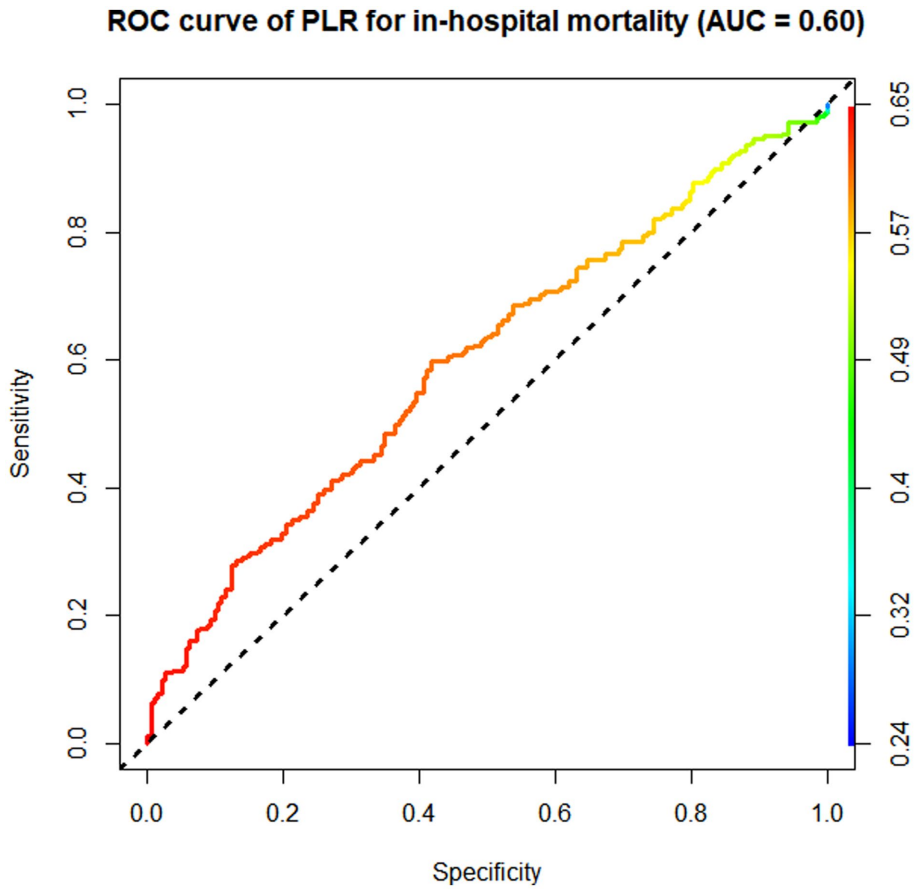

FIGURE 4
Receiver operating characteristic (ROC) curve of PLR.

showed that a high SII may adversely affect carotid plaque vulnerability. Specifically, patients with fragile plaques with burst fibrous caps may experience a considerable impact, which might worsen the severity of AIS (35). A previous study based on the MIMIC-IV database showed that a high SII increased 30-day all-cause mortality (36). Chen investigated the difference between four inflammatory immune markers in predicting the outcome of patients with ischemic stroke (37). Moreover, in a meta-analysis, high SII was strongly associated with poor ischemic stroke outcomes and a high mortality rate (38). However, more research is needed to ascertain the association between the SII and in-hospital mortality in patients with AIS.

According to our literature review, this may be the first study to assess the relationship between markers of both inflammation and oxidative stress and in-hospital mortality in patients with AIS. Focusing on the SII, we assessed the predictive power of four markers (SII, NLR, PLR, and total bilirubin) simultaneously. The study demonstrated that an elevated SII was significantly associated with the risk of in-hospital mortality in patients with AIS. However, whether the SII predicts in-hospital mortality in patients with AIS better than the NLR is less reported. We found that the SII was a greater prognosticator of in-hospital mortality than the NLR (AUC 0.65 vs. 0.64, respectively). Therefore, compared with the NLR, the SII might be a more reasonable and valid reflection of the overall change and regression status of the immune system in patients with stroke. The NLR mainly suggests inflammatory injury, the PLR demonstrates an impact on hemostasis and thrombosis, and SII can be thought of as a combination of the NLR and PLR. Therefore, an elevated SII may reflect thrombosis, the inflammatory response, and the adaptive immunological response (11).

In this study, we adjusted for the mixed effects of several factors based on rigorous study principles. We confirmed that the SII measured within 24 h of admission was significantly associated with adverse clinical outcomes. These data revealed an independent relationship between the SII and the risk of in-hospital mortality in patients with AIS. Few studies have explored the importance of the SII in predicting in-hospital mortality in patients with AIS. Our findings are based on a large sample; therefore, data from a more diverse group of patients in the clinical setting were included. The findings imply that the SII could be utilized to forecast prognosis in patients with AIS. According to this study, patients with an SII of >1,232 (Q2 group) had a considerably higher chance of dying in the hospital than patients with a low SII (Q1 group). Therefore, for patients with AIS with an elevated SII, there is a need to clarify the cause of the high SII and to provide more appropriate treatment. The value of the SII for identifying high-risk subgroups with AIS needs to be further explored in the future to provide more valuable guidance for early targeted treatment. In addition, blood analysis is available at the time of admission. As such, the SII is readily available, can be performed at no additional cost, and has relatively high patient compliance. The SII can therefore be used as a supplement to blood gas analysis.

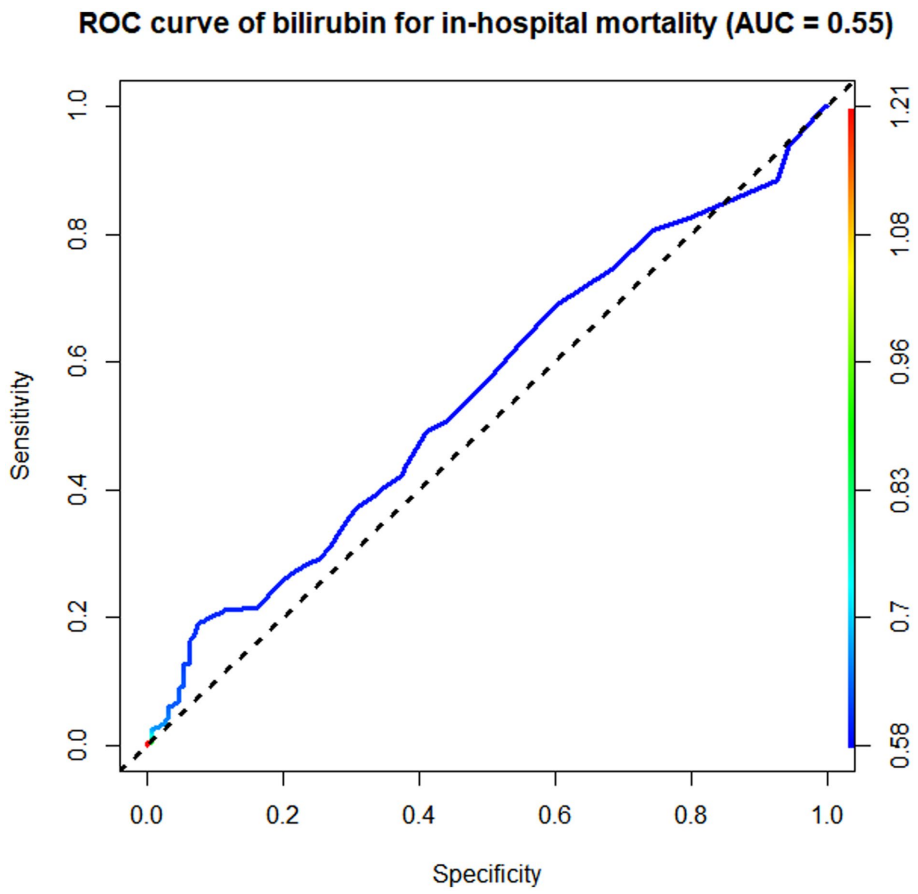

FIGURE 5
Receiver operating characteristic (ROC) curve of bilirubin.

Conclusion

In this study, the in-hospital mortality of patients with AIS and the SII were positively correlated, but not linearly. A high SII was associated with a worse prognosis in patients with AIS. The SII had a modest discriminative ability for predicting in-hospital mortality in patients with AIS. The SII was slightly better than the NLR and significantly better than the PLR and total bilirubin at forecasting in-hospital mortality in patients with AIS.

Limitations

This study has several limitations that should be noted. First, this study did not categorize the patients who died based on whether they had undergone surgery. Therefore, future research should analyze different patient subgroups. Second, this was a single-center study, so the study could contain selection bias. Third, this study lacked some blood indicators, including interleukin, high-sensitivity C-reactive protein, and other cytokines. Finally, only the in-hospital mortality of patients with AIS was studied. As such, additional research is needed to determine how useful the SII is for predicting the long-term prognosis of patients with AIS.

Data availability statement

The original contributions presented in the study are included in the article/Supplementary material, further inquiries can be directed to the corresponding authors.

Author contributions

XH developed the study protocol's design, gathered and analyzed the data, and wrote the majority of the original draft text for publication. JL and WH provided support for editing the manuscript. A specialist clinical analysis was provided by YL and XG. The data were examined and the data confirmation was finished by JZ and YG. All authors contributed to the article and approved the submitted version.

Funding

The authors received funding for this project from the Natural Science Fund of Liaoning Province (2021-MS-282) and the National Backbone of TCM Innovation [TCM Education Letter (2019) No. 128].

Acknowledgments

The MIMIC-IV database was created and is kept updated by a team from the Massachusetts Institute of Technology, for which we are extremely appreciative. The authors would like to thank TopEdit (www.topeditsci.com) for the English language editing of this manuscript.

Conflict of interest

The authors declare that the research was conducted in the absence of any commercial or financial relationships that could be construed as a potential conflict of interest.

Publisher's note

All claims expressed in this article are solely those of the authors and do not necessarily represent those of their affiliated organizations, or those of the publisher, the editors and the reviewers. Any product that may be evaluated in this article, or claim that may be made by its manufacturer, is not guaranteed or endorsed by the publisher.

Supplementary material

The Supplementary material for this article can be found online at: https://www.frontiersin.org/articles/10.3389/fneur.2023.1174711/full#supplementary-material

References

1. Campbell BCV, Khatri P. Stroke. *Lancet*. (2020) 396:129–42. doi: 10.1016/S0140-6736(20)31179-X

2. Wang YJ, Li ZX, Gu HQ, Zhai Y, Jiang Y, Zhao XQ, et al. China stroke statistics 2019: a report from the National Center for healthcare quality Management in Neurological Diseases, China National Clinical Research Center for neurological diseases, the Chinese Stroke Association, National Center for chronic and non-communicable disease control and prevention, Chinese Center for Disease Control and Prevention and institute for global neuroscience and stroke collaborations. *Stroke Vasc Neurol*. (2020) 5:211–39. doi: 10.1136/svn-2020-000457

3. Shi K, Tian DC, Li ZG, Ducruet AF, Lawton MT, Shi FD. Global brain inflammation in stroke. *Lancet Neurol*. (2019) 18:1058–66. doi: 10.1016/S1474-4422(19)30078-X

4. Anrather J, Iadecola C. Inflammation and stroke: an overview. *Neurotherapeutics*. (2016) 13:661–70. doi: 10.1007/s13311-016-0483-x

5. DeLong JH, Ohashi SN, O'Connor KC, Sansing LH. Inflammatory responses after ischemic stroke. *Semin Immunopathol*. (2022) 44:625–48. doi: 10.1007/s00281-022-00943-7

6. Coveney S, Murphy S, Belton O, Cassidy T, Crowe M, Dolan E, et al. Inflammatory cytokines, high-sensitivity C-reactive protein, and risk of one-year vascular events, death, and poor functional outcome after stroke and transient ischemic attack. *Int J Stroke*. (2022) 17:163–71. doi: 10.1177/1747493021995595

7. Zhang H, Huang J, Zhou Y, Fan Y. Association of homocysteine level with adverse outcomes in patients with acute ischemic stroke: a meta-analysis. *Curr Med Chem*. (2021) 28:7583–91. doi: 10.2174/0929867328666210419131016

8. Kim MS, Heo MY, Joo HJ, Shim GY, Chon J, Chung SJ, et al. Neutrophil-to-lymphocyte ratio as a predictor of short-term functional outcomes in acute ischemic stroke patients. *Int J Environ Res Public Health*. (2023) 20:898. doi: 10.3390/ijerph20020898

9. Chen C, Gu L, Chen L, Hu W, Feng X, Qiu F, et al. Neutrophil-to-lymphocyte ratio and platelet-to-lymphocyte ratio as potential predictors of prognosis in acute ischemic stroke. *Front Neurol*. (2020) 11:525621. doi: 10.3389/fneur.2020.525621

10. Wang RH, Wen WX, Jiang ZP, du ZP, Ma ZH, Lu AL, et al. The clinical value of neutrophil-to-lymphocyte ratio (NLR), systemic immune-inflammation index (SII), platelet-to-lymphocyte ratio (PLR) and systemic inflammation response index (SIRI) for predicting the occurrence and severity of pneumonia in patients with intracerebral hemorrhage. *Front Immunol*. (2023) 14:1115031. doi: 10.3389/fimmu.2023.1115031

11. Huang L. Increased systemic immune-inflammation index predicts disease severity and functional outcome in acute ischemic stroke patients. *Neurologist*. (2023) 28:32–8. doi: 10.1097/NRL.0000000000000464

12. Li P, Stetler RA, Leak RK, Shi Y, Li Y, Yu W, et al. Oxidative stress and DNA damage after cerebral ischemia: potential therapeutic targets to repair the genome and improve stroke recovery. *Neuropharmacology*. (2018) 134:208–17. doi: 10.1016/j.neuropharm.2017.11.011

13. He J, Liu J, Huang Y, Tang X, Xiao H, Hu Z. Oxidative stress, inflammation, and autophagy: potential targets of mesenchymal stem cells-based therapies in ischemic stroke. *Front Neurosci*. (2021) 15:641157. doi: 10.3389/fnins.2021.641157

14. Wang X, Wu D, Zhong P. Serum bilirubin and ischaemic stroke: a review of literature. *Stroke Vasc Neurol*. (2020) 5:198–204. doi: 10.1136/svn-2019-000289

15. Sheng X, Du H, Tang Y. Decreased serum Total bilirubin level predicts early neurological deterioration in patients with acute ischemic stroke. *Neuropsychiatr Dis Treat*. (2021) 17:1977–82. doi: 10.2147/NDT.S315330

16. Zhong P, Wu D, Ye X, Wang X, Zhou Y, Zhu X, et al. Association of circulating total bilirubin level with ischemic stroke: a systemic review and meta-analysis of observational evidence. *Ann Transl Med*. (2019) 7:335. doi: 10.21037/atm.2019.06.71

17. Johnson A, Bulgarelli L, Pollard T, Horng S, Celi LA, Mark R. Mimic-iv version 2.0. *PhysioNet*. (2022). doi: 10.13026/rrgf-xw32

18. Cumbler E, Wald H, Bhatt DL, Cox M, Xian Y, Reeves M, et al. Quality of care and outcomes for in-hospital ischemic stroke. *Stroke*. (2014) 45:231–8. doi: 10.1161/STROKEAHA.113.003617

19. Tiainen M, Meretoja A, Strbian D, Suvanto J, Curtze S, Lindsberg PJ, et al. Body temperature, blood infection parameters, and outcome of thrombolysis-treated ischemic stroke patients. *Int J Stroke*. (2013) 8:632–8. doi: 10.1111/ijs.12039

20. Jhou HJ, Chen PH, Yang LY, Chang SH, Lee CH. Plasma anion gap and risk of in-hospital mortality in patients with acute ischemic stroke: analysis from the MIMIC-IV database. *J Pers Med*. (2021) 11:1004. doi: 10.3390/jpm11101004

21. Gentile NT, Seftchick MW, Huynh T, Kruus LK, Gaughan J. Decreased mortality by normalizing blood glucose after acute ischemic stroke. *Acad Emerg Med*. (2006) 13:174–80. doi: 10.1197/j.aem.2005.08.009

22. Papamichalis P, Karagiannis S, Dardiotis E, Chovas A, Papadopoulos D, Zafeiridis T, et al. Predictors of need for critical care support, adverse events, and outcome after stroke thrombolysis. *J Stroke Cerebrovasc Dis*. (2018) 27:591–8. doi: 10.1016/j.jstrokecerebrovasdis.2017.09.042

23. Vidale S, Consoli A, Arnaboldi M, Consoli D. Postischemic inflammation in acute stroke. *J Clin Neurol*. (2017) 13:1–9. doi: 10.3988/jcn.2017.13.1.1

24. Choi YH, Laaker C, Hsu M, Cismaru P, Sandor M, Fabry Z. Molecular mechanisms of Neuroimmune crosstalk in the pathogenesis of stroke. *Int J Mol Sci*. (2021) 22:9486. doi: 10.3390/ijms22179486

25. Garcia-Bonilla L, Moore JM, Racchumi G, Zhou P, Butler JM, Iadecola C, et al. Inducible nitric oxide synthase in neutrophils and endothelium contributes to ischemic brain injury in mice. *J Immunol*. (2014) 193:2531–7. doi: 10.4049/jimmunol.1400918

26. Lisman T. Platelet-neutrophil interactions as drivers of inflammatory and thrombotic disease. *Cell Tissue Res*. (2018) 371:567–76. doi: 10.1007/s00441-017-2727-4

27. Denorme F, Rustad JL, Campbell RA. Brothers in arms: platelets and neutrophils in ischemic stroke. *Curr Opin Hematol*. (2021) 28:301–7. doi: 10.1097/MOH.0000000000000665

28. Denorme F, Manne BK, Portier I, Eustes AS, Kosaka Y, Kile BT, et al. Platelet necrosis mediates ischemic stroke outcome in mice. *Blood*. (2020) 135:429–40. doi: 10.1182/blood.2019002124

29. Liesz A, Suri-Payer E, Veltkamp C, Doerr H, Sommer C, Rivest S, et al. Regulatory T cells are key cerebroprotective immunomodulators in acute experimental stroke. *Nat Med*. (2009) 15:192–9. doi: 10.1038/nm.1927

30. Li P, Gan Y, Sun BL, Zhang F, Lu B, Gao Y, et al. Adoptive regulatory T-cell therapy protects against cerebral ischemia. *Ann Neurol*. (2013) 74:458–71. doi: 10.1002/ana.23815

31. Hu B, Yang XR, Xu Y, Sun YF, Sun C, Guo W, et al. Systemic immune-inflammation index predicts prognosis of patients after curative resection for hepatocellular carcinoma. *Clin Cancer Res*. (2014) 20:6212–22. doi: 10.1158/1078-0432.CCR-14-0442

32. Acar BA, Acar T, Vatan MB, Aras YG, Ulaş SB, Eryılmaz HA, et al. Predictive value of systemic immune-inflammation index for cerebral reperfusion and clinical outcomes in patients with acute ischemic stroke undergoing endovascular treatment. *Eur Rev Med Pharmacol Sci*. (2022) 26:5718–28. doi: 10.26355/eurrev_202208_29507

33. Zhou YX, Li WC, Xia SH, Xiang T, Tang C, Luo JL, et al. Predictive value of the systemic immune inflammation index for adverse outcomes in patients with acute ischemic stroke. *Front Neurol*. (2022) 13:836595. doi: 10.3389/fneur.2022.836595

34. Wang N, Yang Y, Qiu B, Gao Y, Wang A, Xu Q, et al. Correlation of the systemic immune-inflammation index with short- and long-term prognosis after acute ischemic stroke. *Aging (Albany NY)*. (2022) 14:6567–78. doi: 10.18632/aging.204228

35. Zhang L, Lyu Q, Zhou W, Li X, Ni Q, Jiang S, et al. High systemic immune-inflammation index is associated with carotid plaque vulnerability: new findings based on carotid ultrasound imaging in patients with acute ischemic stroke. *Front Neurol*. (2022) 13:959531. doi: 10.3389/fneur.2022.959531

36. Wu S, Shi X, Zhou Q, Duan X, Zhang X, Guo H. The association between systemic immune-inflammation index and all-cause mortality in acute ischemic stroke patients: analysis from the MIMIC-IV database. *Emerg Med Int*. (2022) 2022:4156489–10. doi: 10.1155/2022/4156489

37. Chen PY, Chen GC, Hsiao CL, Hsu PJ, Yang FY, Liu CY, et al. Comparison of clinical features, immune-inflammatory markers, and outcomes between patients with acute in-hospital and out-of-hospital ischemic stroke. *J Inflamm Res*. (2022) 15:881–95. doi: 10.2147/JIR.S342830

38. Huang YW, Yin XS, Li ZP. Association of the systemic immune-inflammation index (SII) and clinical outcomes in patients with stroke: a systematic review and meta-analysis. *Front Immunol*. (2022) 13:1090305. doi: 10.3389/fimmu.2022.1090305

frontiers | Frontiers in Neurology

TYPE Original Research
PUBLISHED 09 June 2023
DOI 10.3389/fneur.2023.1167549

OPEN ACCESS

EDITED BY
Yanlin Zhang,
Second Affiliated Hospital of Soochow University, China

REVIEWED BY
Felix Schlachetzki,
University of Regensburg, Germany
Kazuo Yamashiro,
Juntendo University Urayasu Hospital, Japan

*CORRESPONDENCE
Tom Finck
✉ tom.finck@tum.de

†These authors have contributed equally to this work and share first authorship

RECEIVED 16 February 2023
ACCEPTED 08 May 2023
PUBLISHED 09 June 2023

CITATION
Finck T, Sperl P, Hernandez-Petzsche M, Boeckh-Behrens T, Maegerlein C, Wunderlich S, Zimmer C, Kirschke J and Berndt M (2023) Inflammation in stroke: initial CRP levels can predict poor outcomes in endovascularly treated stroke patients. *Front. Neurol.* 14:1167549. doi: 10.3389/fneur.2023.1167549

Inflammation in stroke: initial CRP levels can predict poor outcomes in endovascularly treated stroke patients

Tom Finck[1*†], Philipp Sperl[1†], Moritz Hernandez-Petzsche[1], Tobias Boeckh-Behrens[1], Christian Maegerlein[1], Silke Wunderlich[2], Claus Zimmer[1], Jan Kirschke[1] and Maria Berndt[1]

[1]Department of Diagnostic and Interventional Neuroradiology, School of Medicine, Klinikum Rechts der Isar, Technical University of Munich, Munich, Germany, [2]Department of Neurology, School of Medicine, Klinikum Rechts der Isar, Technical University of Munich, Munich, Germany

Background and purpose: Inflammation has been linked to poor prognoses in cardio- and cerebrovascular conditions. As it is known to increase after ischemia, C-reactive protein (CRP) may serve as a surrogate for systemic inflammation and thus be a hallmark of increased tissue vulnerability. The question arises whether CRP in the acute phase of ischemic stroke, prior to mechanical thrombectomy (MT), might help predict outcomes.

Materials and methods: A single-center collective of patients with large-vessel occlusion, who were treated via MT, was analyzed in this observational case–control study. Univariate and multivariate models were designed to test the prognostic value of inflammatory markers (CRP and leukocytosis) in predicting clinical outcomes (modified Rankin score >2) and all-cause mortality 90 days after MT.

Results: A total of 676 ischemic stroke patients treated with MT were included. Of these, 313 (46.3%) showed elevated CRP levels (≥5 mg/l) on admission. Poor clinical outcome and mortality at 90 days occurred in 113 (16.7%) and 335 (49.6%) patients and significantly more frequently when initial CRP levels were elevated [213 (64.5%) vs. 122 (42.1%), $p < 0.0001$, and 79 (25.2%) vs. 34 (9.4%), $p < 0.0001$, respectively]. CRP levels were highly predictive for impaired outcomes, especially in patients with atrial fibrillation, in both univariate and multivariate models. Interestingly, patients with initially elevated CRP levels also showed more pronounced increases in CRP post-MT.

Conclusion: Poor outcome and death occur significantly more often in stroke patients with elevated CRP levels before MT. Our findings suggest that stroke patients with atrial fibrillation and elevated inflammatory markers are of particular risk for poor outcomes.

KEYWORDS

inflammation, stroke, thrombectomy, C-reactive protein, stroke outcome, neuroinflammation

Introduction

Outcomes in ischemic stroke have improved greatly over the last decades in large part due to the wider availability of specialized stroke units as well as the establishment of endovascular therapy as the standard of care for patients who present with acute large-vessel occlusions (LVOs) (1–5). In recent years, the indication for mechanical thrombectomy (MT) has been extended, e.g., to later time windows and smaller vessels, with procedural techniques being continuously improved (6, 7).

Nonetheless, ischemic stroke continues to pose a significant burden as it remains a main cause of morbidity and mortality worldwide and accounts for a large proportion of quality-adjusted life years lost (8). Many multiparametric models for predicting good clinical outcomes after endovascularly treated stroke include obvious confounders, such as time to treatment or the success of revascularization. However, despite successful reperfusion in good time windows, the long-term clinical trajectory is not always as favorable as expected. Some mechanisms conveying adverse outcomes remain ill-explained, especially as complex markers such as neuronal damage serum proteins may also play an important and yet poorly understood role in influencing outcomes (9, 10).

Pro-inflammatory systemic environments have recently been identified to independently predict poor outcomes in a panoply of conditions, from ischemic heart disease to carotid atherosclerosis progression, as well as ischemic stroke treated via intravenous thrombolysis (11–15). Moreover, the more delayed cellular inflammation conveyed by leukocytosis has been shown to correlate with poor outcome after MT (16). All these observations are hinting at the role that neuro-inflammation could have in post-ischemic brain remodeling.

High-sensitivity C-reactive protein (CRP) is an accessible serum protein known to be a reliable marker for systemic inflammation but also mediate pro-inflammatory downstream cascades, making it a suitable candidate to assess the level of intra-individual inflammation (17, 18). Moreover, the observation that most stroke patients showcase high-CRP levels is noteworthy given that activation of the secondary complement system and subsequent secondary brain damage through CRP has been shown experimentally (19).

It remains unclear whether CRP is elevated in response to ischemia-induced neuronal damage or whether pro-inflammatory mechanisms themselves are causing a time-delayed injury of ischemic brain tissue, analogous to phenomena seen after thermic tissue shock (20). As inflammatory markers have been associated with atrial fibrillation and thromboembolic complications, it may also be conceivable that inflammation influences the pathogenesis of ischemic stroke (21).

Our assumption is that CRP levels in the very-early stage of ischemic stroke could be a hallmark of systemic inflammation and increase the *ad hoc* vulnerability of the brain tissue to ischemic stress as well as promote subsequent neuronal damage through mediation of a post-ischemic ischemia-inflammation cascade. Identification of this association would add to current knowledge in stroke care, identify patients at risk benefitting from the most intensified and early anti-inflammatory therapy regimes, and advocate for future interventional studies (22).

To address those questions, the present study aims to investigate an association of inflammatory blood markers (CRP and leukocytosis) with neurological outcome and mortality in a large cohort of ischemic stroke patients with LVO treated with MT.

Methods

Study design

Prospectively collected clinical, interventional, and outcome parameters of a large collective of endovascular treated stroke patients in a comprehensive stroke center were analyzed for this retrospective single-center case–control study. The association of inflammatory markers with outcome parameters was tested as outcomes.

The study was approved by the local ethics committee, and the need for patient consent was waived. The observational, retrospective study design did not interfere with the routine clinical workflow and did not influence therapeutic decision-making. The results were reported in adherence to the STROBE statement guidelines.

Study population

This retrospective, single-center study included all consecutive patients with ischemic stroke due to LVO who were admitted at a single comprehensive stroke center and treated by MT between January 2017 and March 2021 ($n = 1{,}012$).

Patients with an unclear onset of symptoms (wake-up stroke) or a concurring cause of infection at both admission or during the first 7 days of hospital stay were excluded. Furthermore, we only included patients for whom inflammatory serum markers on admission and outcome data at 90-day follow-up were available.

The prospectively collected clinical and imaging data were retrospectively analyzed. Basic demographic, clinical, and interventional data of patients were gathered. NIHSS-certified neurologists assessed the National Institutes of Health Stroke Scale (NIHSS) score at the time of admission and discharge. Substantial neurological improvement (SNI) was defined as the difference between admission and discharge, with an NIHSS score of $\geq$8 or a discharge NIHSS score of $\leq$1.

The mRS score was used to measure disability premorbid at discharge and at follow-up, while a poor clinical outcome in the 90-day follow-up was defined as mRS $>$ 2.

Outcome values such as mRS and mortality in the follow-up were assessed either through routine follow-up in-house visits or, if the patient was not present for various reasons, by phone call through an experienced study nurse.

Stroke pathogeneses were determined according to the international TOAST (Trial of ORG 10172 in Acute Stroke Treatment) classification based on diagnostic and clinical

Abbreviations: LVO, large-vessel occlusion; MT, mechanical thrombectomy; CRP, C-reactive protein; NIHSS, National Institutes of Health Stroke Scale; SNI, substantial neurological improvement; mRS, modified Rankin scale; TOAST, Trial of ORG 10172 in Acute Stroke Treatment; tPA, tissue-type plasminogen activator; CTP, CT perfusion; SD, standard deviation; ROC, receiver operator characteristic; OR, odds ratio; CI, confidence interval.

information available for each patient (23). Further variables that are relevant for the present study included the presence of atrial fibrillation as well as documentation of cardiovascular risk factors such as active smoking, hypertension, hyperlipidemia, and diabetes mellitus. Pre-existing treatment with platelet-inhibiting drugs or lipid-lowering therapies was documented. Administration of pre-interventional intravenous tissue-type plasminogen activator (tPA) thrombolysis was assessed. At the end of the endovascular procedure, successful recanalization was defined as mTICI 2b-3 (24). Time of symptom onset, time of admission, time of reperfusion, and corresponding procedure times were taken from the existing database. Time to admission was defined between symptom onset and admission. Reperfusion time was defined between symptom onset and mTICI $\geq$ 2b. In cases, when recanalization was not successful (TICI $<$ 2b), the control series after the last maneuver was used as the time endpoint.

Assessment of inflammation markers

In patients with elevated CRP levels (defined as >5 mg/l), hospital records were retrospectively screened to determine whether any cause of infection was apparent prior to stroke onset or became uncovered during the acute-care hospital stay.

Levels of CRP and leukocyte counts were determined from the emergency blood panel taken upon referral, prior to MT, as well as blood panels drawn within the first 7 days after MT. This allowed for the analysis of three models: (i) outcome prediction based on the level of inflammatory markers at the time of admission, (ii) subgroup analysis in patients for whom serum inflammatory markers were available in the hyper-acute phase (<4 h after symptom onset), with an aim to exclude the effects of CRP release secondary to brain ischemia, and (iii) subgroup analysis of prognostic effects linked to the CRP dynamics in the first 7 days after MT.

Imaging analysis

The volume of brain tissue necrosis at the time of admission was quantitatively estimated from CT perfusion (CTP) data [RAPID software (iSchemaView, Menlo Park, CA, USA)] (25). Acquisition of CTP is part of an in-house stroke neuroimaging standard operating procedure and was thus available for all patients, irrespective of the timing of symptom onset. The infarct core at admission was defined as the volumetric sum of voxels showcasing cerebral blood flow < 30% to the contralateral hemisphere. Alberta Stroke Program Early CT Score (ASPECTS) was automatically assessed from admission CT imaging (iSchemaView, Inc., Menlo Park, CA, USA) for patients with occlusion of the MCA.

Statistical analysis

Continuous and categorical variables are given as mean and standard deviation (SD) and frequencies if not indicated otherwise. Variables were compared using the Mann–Whitney *U*-test and unpaired student *t*-test, as appropriate. Receiver operator characteristic (ROC) curve analysis was used to determine the association of continuously measured CRP levels and outcomes. The Youden index was subsequently determined to find optimal cutoff values for CRP levels. The relationship between outcomes and elevated CRP levels (defined cutoff of 5 mg/L according to in-house laboratory standards) was expressed as an odds ratio (OR), with a corresponding 95% confidence interval (CI) through logistic regression.

To correct for confounders, adjustments for the impact of age, sex, atrial fibrillation, hypertension, diabetes mellitus, estimated CTP infarct volume, premorbid mRS levels, and reperfusion success were made with multiple logistic regression. A moderation analysis was performed to check the interaction of the subgroups with/without atrial fibrillation on the association between CRP levels and outcomes under consideration of the abovementioned covariates (26).

Statistical analyses were performed using IBM SPSS Statistics version 28.0.0. for macOS (IBM, USA).

Results

Patient demographics and clinical data

Over the retrieval period, 1,012 patients were referred for MT of a LVO. Of these, 62 were lost to follow-up. Furthermore, 274 patients were either "wake-up" strokes or had an infection either pre-existing or developing within the first 7 days of in-clinic stay (mean diagnosis at 4.3 days post-MT) and were thus excluded, leading to a study collective of 676 patients at a mean age of 74 $\pm$ 13 years (48.5% men). Mean CRP levels at admission were 1.7 $\pm$ 3.2 mg/l and elevated in 313 patients (46.3%). Patients with elevated CRP levels experienced higher frequencies of atrial fibrillation (57.5 vs. 41.3%, $p < 0.001$), hypertension (64.9 vs. 60.6%, $p = 0.01$), and diabetes mellitus (26.2 vs. 16.8%, $p = 0.003$), as well as leukocyte counts (10.46 $\pm$ 6.79 G/l vs. 9.79 vs. 3.39 G/l, $p < 0.001$). Apart from this, both groups had similar clinical profiles (Table 1).

Stroke- and MT-related parameters

In descending frequency, the most commonly occluded vessels were middle cerebral artery ($n = 384$, 56.8%), distal segment of the internal carotid artery ($n = 73$, 10.8%), combination of >1 occluded intracranial vessel ($n = 59$, 8.7%), tandem occlusions ($n = 53$, 7.8%), basilar artery ($n = 44$, 6.5%), proximal segment of the internal carotid artery ($n = 37$, 5.5%), posterior cerebral artery ($n = 11$, 1.6%), anterior cerebral artery ($n = 8$, 1.2%), and the vertebral artery ($n = 7$, 1.0%). Symptom severity was moderate on average with mean NIHSS scores of 13 $\pm$ 6.8. Counting from the onset of clinical symptoms, the time to admission (52 $\pm$ 41 min vs. 58 $\pm$ 72 min, $p = 0.19$) and the time to reperfusion (191 $\pm$ 144 min vs. 189 $\pm$ 146 min, $p = 0.79$) were similar for both groups. I.v. thrombolysis was performed significantly less frequently in the cohort with elevated CRP levels (37.1 vs. 47.7%, $p = 0.006$). Moreover, patients with elevated CRP levels demonstrated larger

TABLE 1 Patient demographics for the study cohort and dichotomized according to CRP levels.

	Subgroups			
	All ($n = 676$)	CRP $\geq$ 5 mg/l ($n = 313$)	CRP $<$ 5 mg/l ($n = 363$)	*P*
Age	73.87 ± 13.37	75.4 ± 13.2	72.5 ± 13.3	0.005
%Male	328 (48.5%)	152 (48.6%)	176 (48.5%)	0.98
NIHSS at admission	13 ± 6.76	13 ± 6.64	13 ± 6.87	0.92
Hypertension	439 (64.9%)	219 (70.0%)	220 (60.6%)	0.01
Diabetes	143 (21.2%)	82 (26.2%)	61 (16.8%)	0.003
Smoking*	157 (23.2%)	78 (24.9%)	79 (21.8%)	0.34
Hyperlipidemia	143(21.2%)	72 (23.0%)	71 (19.6%)	0.28
LLT	173 (25.6%)	90 (28.8%)	83 (22.9%)	0.08
Anticoagulation	195 (28.8%)	90(28.8%)	105 (28.9%)	0.98
Atrial fibrillation	330 (48.8%)	180 (57.5%)	150 (41.3%)	<0.001
TOAST 1	94 (13.9%)	41 (13.1%)	53 (14.6%)	0.57
TOAST 2	324 (47.6%)	168 (53.4%)	155 (42.7%)	0.006
TOAST 3	0 (0%)	0 (0%)	1 (0%)	0.99
TOAST 4	42 (6.2%)	20 (6.4%)	22 (6.1%)	0.87
TOAST 5	216 (32.0%)	84 (26.9%)	132 (36.4%)	0.008
CRP levels (mg/l) (admission)	1.71 ± 3.15	31.0 ± 37.7	2.0 ± 1.5	<0.001
Leukocytes (G/l) (admission)	10.46 ± 6.79	11.24 ± 9.27	9.79 ± 3.39	0.009
Time to admission (min)	55 ± 62	52 ± 41	58 ± 72	0.19
Time to reperfusion	191 ± 144	192 ± 138	189 ± 146	0.79
i.v. thrombolysis	289 (42.8%)	116 (37.1%)	173 (47.7%)	0.006
ASPECTS	4.97 ± 4.10	4.95 ± 4.00	5.0 ± 4.2	0.87
Infarct core at admission (ml)	20.2 ± 37.1	24.2 ± 41.2	17.3 ± 29.4	0.014
% mTICI 2b or better	590 (87.3%)	283 (90.4%)	307 (84.6%)	0.02

LLT, lipid-lowering therapy. ASPECTS are provided for patients with occlusion of the middle cerebral artery, only ($n = 384$). *Current smoker. TOAST 1, large artery atherosclerosis; TOAST 2, cardioembolism; TOAST 3, small-vessel occlusion; TOAST 4, stroke of other determined etiology; TOAST 5, stroke of undetermined etiology.

estimated infarct cores on CTP (24.2 ± 41.2 ml vs. 17.3 ± 29.4 ml, $p = 0.014$) albeit comparable infarct areas as estimated by ASPECTS (4.95 ± 4.0 vs. 5.0 ± 4.2, $p = 0.0.87$) in the subgroup with MCA occlusion. Moreover, the thrombectomy results were better in patients whose initial CRP levels were elevated with 90.4 % (against 84.6%, $p = 0.02$) of final thrombectomy scores being mTICI 2b or better.

Outcomes

After 90 days of thrombectomy, a total of 113 patients (16.7%) were deceased with death occurring significantly more often in patients showcasing high-CRP levels *ad initio* (25.2 vs. 9.4%, $p < 0.0001$) (Figure 1). Median mRS after 90 days was 3 (IQR: 2; 5) and at a disadvantage in the high-CRP group with 4 (2; 6) vs. 2 (1; 4) ($p < 0.0001$). Brain hemorrhage up until the day of discharge, as verified by CT or MR imaging, was noted in a total of 15/460 patients (3.3%) for whom postprocedural imaging was available and at comparable rates in both groups (3.7 vs. 3.0%, $p = 0.69$). NIHSS values at discharge were available for 460/676 patients. A SNI at discharge could be noted in 206 of these patients. The frequency of SNI showed a trend to be higher in patients with normal initial CRP values (141/297, 47.5%) than in patients with elevated initial CRP values (65/163, 39.9%) ($p = 0.11$). Refer to Table 2 for a detailed outcome analysis.

Association of inflammatory markers with outcomes

Odds ratios for death or poor outcome (mRS > 2) 90 days after thrombectomy have been calculated for all investigated parameters in univariate models, as shown in Figures 2A, B. In the decreasing order, CTP-estimated infarct volumes, elevated initial CRP levels, poor thrombectomy results (TICI < 2b), and pre-existing neurological impairments (mRS > 0) showed the highest association with poor outcomes after 90 days. On the other hand,

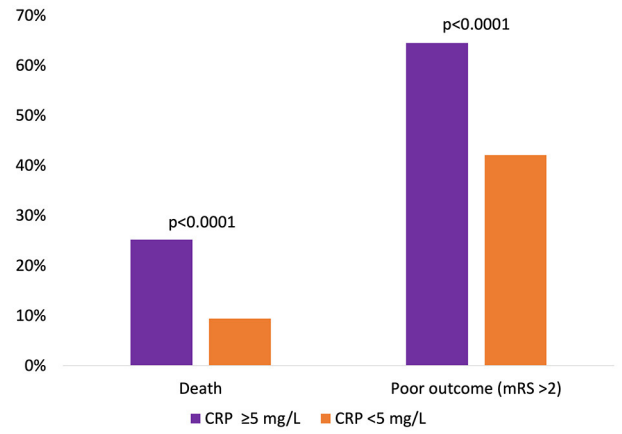

FIGURE 1
Relative occurrence of death or poor clinical outcome 90 days after mechanical thrombectomy, dichotomized according to initial CRP levels.

TABLE 2 Occurrence of primary outcomes 90 days after mechanical thrombectomy, as well as secondary endpoint occurrence ICH and re-occlusion, as verified by CT or MRI, up until discharge.

Primary outcomes	Subgroups			
	All ($n = 676$)	CRP $\geq$ 5 mg/l ($n = 313$)	CRP $<$ 5 mg/l ($n = 363$)	*P*
Mortality	113 (16.7%)	79 (25.2%)	34 (9.4%)	<0.001
mRS	3 (2; 5)	4 (2; 6)	2 (1; 4)	<0.001
Poor outcome (mRS > 2)	335 (49.6%)	213 (68.1%)	122 (33.6%)	<0.001
Secondary outcomes	**Subgroups**			
	All ($n = 460$)	CRP $\geq$ 5 mg/l ($n = 163$)	CRP $<$ 5 mg/l ($n = 297$)	*P*
SNI	206 (44.8%)	65 (39.9%)	141 (47.5)	0.11
ICH	15 (3.3%)	6 (3.7%)	9 (3.0%)	0.69
Re-occlusion	31 (6.7%)	14 (8.6%)	17 (5.7%)	0.24

mRS, modified Rankin scale; SNI, substantial neurological improvement; ICH, intracranial hemorrhage.

poor thrombectomy outcomes (TICI < 2b), elevated CRP levels, CTP-estimated infarct volumes, and elevated leukocyte counts were most predictive for death at 90 days.

Due to the partial unavailability of confounding covariates, multivariate analysis and moderation analysis were calculated for a patient subset of $n = 212$.

Multivariate logistic regression, after correction for the effects of age, sex, atrial fibrillation, hypertension, diabetes mellitus, infarct volumes, pre-existing neurological impairments, and thrombectomy outcomes, highlights that initial CRP levels remained predictive for both mortality and poor mid-term outcome with respective odds ratios of 2.72 (95% CI: 1.43; 5.21) and 3.85 (95% CI: 2.49; 5.94), as shown in Figure 2C.

In a second step, the impact of the etiological subgroups with and without atrial fibrillation on the association between initial CRP levels and poor mid-term outcomes was tested in a moderation analysis under consideration of the abovementioned covariates. The conditional effect of initial CRP levels on poor outcomes remained significant for the atrial fibrillation group ($p < 0.001$). For the patient subgroup without atrial fibrillation, the conditional effect was lowered and lost its significance on the 5% level ($p = 0.06$), which implies that the importance of CRP levels for clinical outcomes is predominantly seen in patients with atrial fibrillation.

Multivariate logistic regression analyses for leukocyte counts lost their predictive power with respective odds ratios to predict mortality and poor mid-term outcomes of 0.92 (95% CI: 0.41, 2.05) and 0.73 (95% CI: 0.44, 1.23), respectively.

CRP values were further validated as a binary classifier for poor outcomes as a predictive model containing the above-referenced risk factors benefitted significantly from the inclusion of CRP measurements. As such, the AUC under the ROC increased from 0.74 (95% CI: 0.67, 0.81) to 0.81 (95% CI: 0.76, 0.87), as illustrated in Supplementary Figure 1. Calculation of the Youden Index yielded an optimal cutoff CRP level of 3.5 mg/l (sensitivity of 81.4% and specificity of 61%) and 8.5 mg/l (sensitivity of 69.0% and specificity of 69.0%) to predict poor outcomes and mortality, respectively.

Endpoint-dependent CRP analysis

Post-hoc determination of CRP levels as a function of outcome showed that patients who reached the endpoint of mortality or mRS > 2 did not only have higher CRP levels *ad initio* but also experienced prolonged increases in CRP levels over the first 7 days post-MT. Endpoint-dependent CRP trajectories and values are given in Figure 3.

Subgroup analysis for very-early inflammatory markers

In patients where initial blood sampling took place earlier than 4 h after symptom onset ($n = 430$), CRP levels were predictive for both poor outcomes [OR: 3.13 (95% CI, 2.06, 5.95)] and mortality [OR: 3.41 (95% CI, 2.11, 5.65)]. This effect remained intact in a multivariate model after correction for age, sex, atrial fibrillation, hypertension, diabetes mellitus, CTP-estimated infarct volume, premorbid mRS levels, NIHSS, and thrombectomy outcome for both poor clinical outcomes [OR: 2.59 (95% CI, 1.08, 6.41)] and mortality [OR: 2.94 (95% CI, 1.06, 9.07)]. Leukocyte counts, on the other hand, lost their predictive power for poor clinical outcomes after multivariate correction (Table 3).

Discussion

The present study validates systemic inflammation markers, especially CRP levels, for predicting clinical outcomes in a large collective of endovascularly treated stroke patients. Our results show that (i) poor outcome and death occur significantly more

10.3389/fneur.2023.1167549

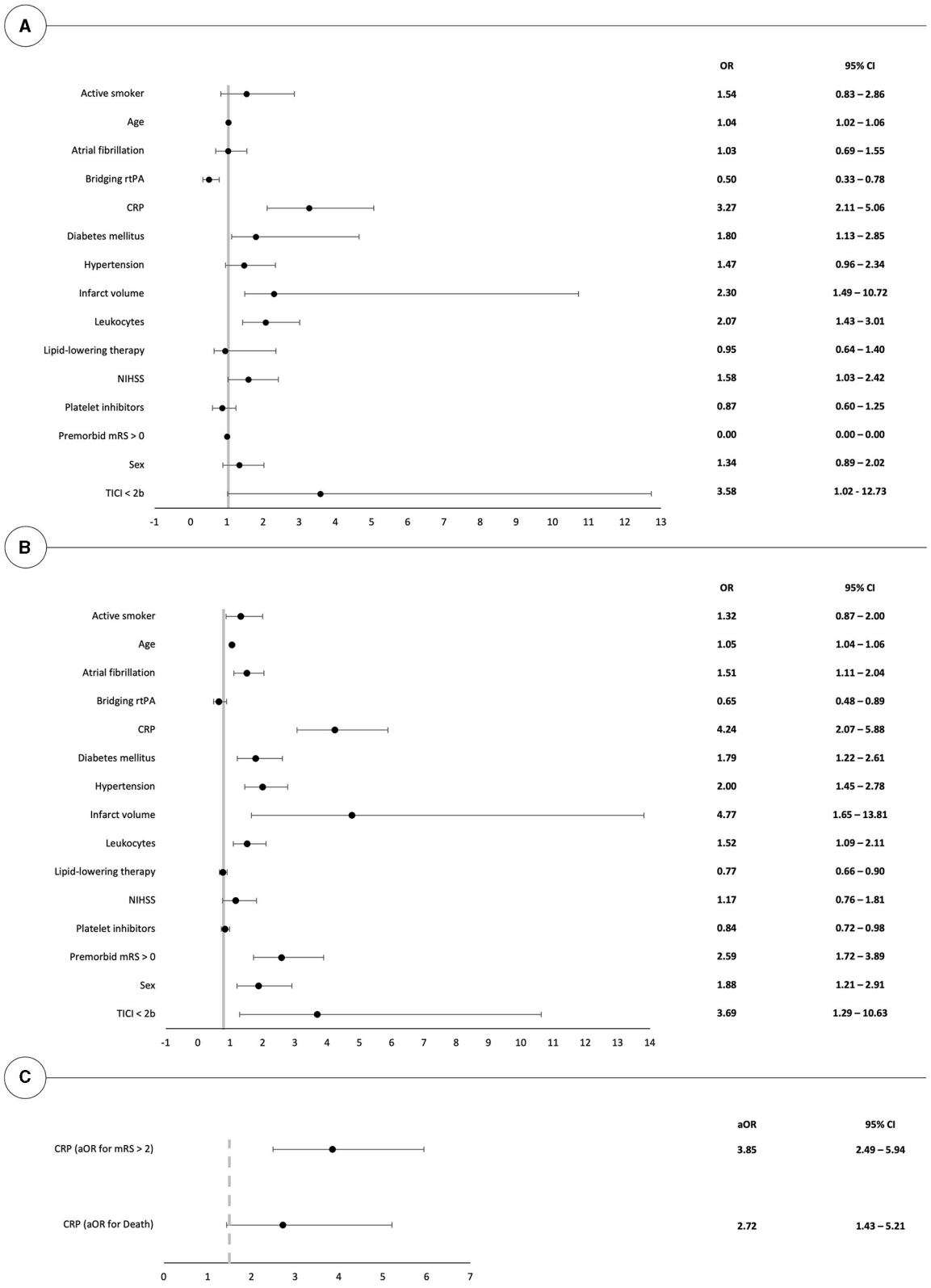

FIGURE 2
Forest plot illustrating the univariate risk for poor clinical outcome (mRS > 2) and death at 90 days after mechanical thrombectomy in **(A, B)**. **(C)** depicts the respective odds ratios in a multivariate model in patients with elevated CRP values. OR, odds ratio.

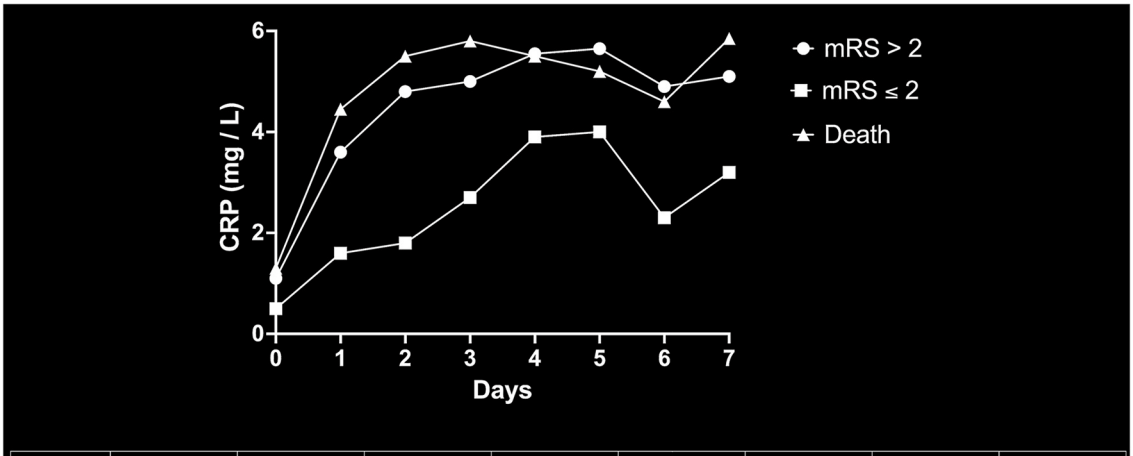

	0	1	2	3	4	5	6	7
mRS ≤ 2	0.5 (0.2; 0.7)	1.6 (0.2; 3.6)	1.8 (1.0; 4.2)	2.7 (1.4; 5.7)	3.9 (1.5; 7.4)	4.0 (1.4; 7.3)	2.3 (1.2; 5.0)	3.2 (0.7; 6.5)
mRS > 2	1.1 (0.4; 1.3)*	3.6 (2.0; 6.2)*	4.8 (2.6; 7.8)*	5.0 (2.6; 9.0)*	5.6 (3.3; 9.8)*	5.7 (3.2; 9.9)*	4.9 (3.2; 10.6)*	5.1 (2.7; 10.5)*
Death	1.3 (0.5; 3.2)*	4.5 (2.3; 6.5)*	5.5 (2.6; 7.3)*	5.8 (3.2; 9.0)*	5.5 (4.1; 8.4)*	5.2 (3.4; 8.8)*	4.6 (3.3; 9.4)*	5.9 (2.9; 10.0)*

FIGURE 3
Post-hoc determination of CRP dynamics as a function of outcomes. Beyond the initial increase of inflammatory markers in patients with poor outcomes, the trajectory of CRP values continued to steepen over the consecutive 7 days after MT as compared to the cohort with favorable outcomes. The upper panel depicts the respective trajectories of CRP values for patients with good outcomes (mRS ≤ 2), poor outcomes (mRS > 2), and mortality. The corresponding median values and respective 95% CI are given in the lower panel. *Significantly above mRS ≤ 2 at the respective timepoint.

often in stroke patients with elevated CRP levels before MT, particularly in patients with atrial fibrillation, (ii) these effects seem to be mediated by a systemic inflammatory environment and not as a response to brain tissue ischemia, and (iii) the ischemia-inflammation cascade in MT patients is more pronounced if CRP levels are elevated *ad initio*.

Evidence is growing that systemic inflammation has a pivotal role in many pathophysiological processes from cardiovascular disease to cancer progression and cognitive decline (27–29). CRP has already been identified as a sensible serum marker to predict adverse outcomes in cardiovascular events, and its levels are known to be influenced by genetic polymorphisms, an observation that could further deepen our understanding of the development and progression of vascular disease (30). CRP as an inflammatory marker has been associated with atrial fibrillation, including development, recurrence, and total burden, as well as associated with thromboembolic complications (21). It thus seems plausible that inflammation also influences the pathogenesis of ischemic stroke.

In this study, we are interested in finding out whether CRP levels in the acute phase of ischemic stroke can help explain the outcome disparities in patients with endovascularly treated LVO.

Our data show that CRP levels at admission are strongly and independently associated with an increased risk of mortality and poor clinical outcomes. In a broad, prospectively acquired collective of 676 patients, we thus noted that 70% of deaths at 90-day follow-up occurred in patients with initially elevated CRP levels. Moreover, after multivariate correction for confounding factors

TABLE 3 Subgroup analysis for very-early (<4 h after symptom onset) CRP levels and leukocyte counts to predict mortality or poor clinical outcomes.

Endpoint	Inflammatory marker	OR	
		Univariate	Multivariate
MRS > 2	CRP	3.13 (2.06; 5.95)	2.59 (1.08; 6.41)
	Leukocytes	1.44 (0.94; 2.22)	1.51 (0.51; 4.60)
Mortality	CRP	3.41 (2.11; 5.65)	2.94 (1.06; 9.07)
	Leukocytes	2.26 (1.42; 3.59)	1.86 (1.07; 2.63)

known to carry a negative prognostic value such as reperfusion failure or large volumes of estimated infarct cores, the relative risk of death or poor clinical outcomes remains significant if CRP levels were elevated *ad initio*. This observation held true even as patients with elevated CRP levels had smaller infarct volumes as well as more favorable thrombectomy results than those with no signs of systemic inflammation. The influence of etiology was also deliberated while atrial fibrillation was chosen as a covariate. Despite the known association between atrial fibrillation and elevated CRP levels, the inflammation marker has independently impacted outcomes. In a moderation analysis, it was shown that the importance of CRP levels for clinical outcomes is predominantly seen in patients with atrial fibrillation. This fits the known association of CRP levels in atrial fibrillation with burden and severity of thromboembolic events. It may have an impact

on clinical practice as special focus should be placed on patients with cardioembolic stroke and elevated CRP levels regarding rehabilitation and secondary prevention.

Furthermore, our observation that CRP trajectories post-MT diverge in a way that initially high levels tend to further increase over the course of 7 days is of particular interest. One could speculate that CRP promotes a cascade where first-hit tissue damage promotes inflammatory mechanisms, again worsening tissue damage through known effects such as complement activation or T-cell platelet interaction (15, 31). Secondary burn progression in thermic injuries, where cell necrosis advances beyond the initial stress area in a time-delayed manner, could thus be a blueprint for some of the pathophysiological processes in brain ischemia. Moreover, the fact that injury in myocardial infarction has been mitigated by blocking CRP synthesis hints at the plausibility of such a cascade and causative role that CRP could have in the time-delayed cellular damage (32).

Validation of our findings in a multicentric setting could pave the way for interventional studies exploring CRP apheresis as a possible tool to break this ischemia-inflammation cascade in stroke patients (32, 33). Elegantly, this could potentially be achieved through intensified statin use, as one of the lipid-lowering agent properties is to dose-dependently reduce levels of not only LDL—known to also negatively impact the prognosis of ischemic stroke patients—but also CRP and other inflammatory markers (34). The hypothesis that in adjunct to reducing established cardio- and cerebrovascular risk factors, mitigating low-level systemic inflammation as a means of primary and secondary prevention gains momentum as a promising future avenue in stroke care (35).

Although CRP has been validated as an independent predictor of poor outcomes in patients with ICH (36), we found no correlation between early CRP levels and brain hemorrhage or repeated LVO after MT. At first sight, this may seem counterintuitive given the vast evidence that links low-level inflammation to endothelial dysfunction and might be due to the overall low rates of these secondary endpoints in our study cohort (37). Moreover, leukocyte counts on admission carried less prognostic weight as this marker reacts more slowly to a pro-inflammatory stimulus and might thus be less well suited as an early predictive marker.

Testing for CRP-related genetic polymorphisms would have provided a significant value to our analysis as this could have clarified if CRP is really the hallmark agent linked to poor outcomes after MT or just a surrogate marker for low-level systemic inflammation.

The study design in its very nature was retrospective with all inherent limitations. A further limitation is the monocentric study setting, calling for prospective multicentric studies to validate our findings, as well as the multivariate analysis with less power due to the partial unavailability of confounding variables. All-cause mortality after 90 days was chosen as an endpoint due to the common impossibility to determine a specific cause of death, especially in a cohort of elderly patients. It can, however, be assumed that the large cohort size flattens out potential inequalities in the rates of confounding co-morbidities among both groups. Body temperatures were not available although this metric might have provided further information on the potential onset of a latent infection during the clinical stay. Moreover, definite volumes of the infarcted tissue were not quantitatively assessed. Finally, patients with elevated CRP levels were on average 3 years older, with intuitive prognostic implications, a confounder mitigated by the multivariate correction we performed in our analysis.

To conclude, our study provides evidence for the negative prognostic value of acute-stage CRP levels in stroke patients treated via MT. In a set of more than 600 patients, we show that mid-term clinical outcomes and mortality are significantly and independently associated with initial CRP levels, particularly in patients suffering from atrial fibrillation. Our findings encourage the theory that mitigating low-level systemic inflammation could be a promising step to improve the prognosis of stroke patients. Based on this, data questions on acute vs. chronic and systemic inflammation should be further investigated in larger studies.

Data availability statement

The datasets presented in this article are not readily available because of ethical and privacy restrictions. Requests to access the datasets should be directed to TF, tom.finck@tum.de.

Ethics statement

The studies involving human participants were reviewed and approved by Local Ethics Committee. Written informed consent for participation was not required for this study in accordance with the national legislation and the institutional requirements.

Author contributions

All authors listed have made a substantial, direct, and intellectual contribution to the work and approved it for publication.

Conflict of interest

The authors declare that the research was conducted in the absence of any commercial or financial relationships that could be construed as a potential conflict of interest.

Publisher's note

Supplementary material

The Supplementary Material for this article can be found online at: https://www.frontiersin.org/articles/10.3389/fneur.2023.1167549/full#supplementary-material

References

1. Goyal M, Demchuk AM, Menon BK, Eesa M, Rempel JL, Thornton J, et al. Randomized assessment of rapid endovascular treatment of ischemic stroke. *N Engl J Med.* (2015) 372:1019–30. doi: 10.1056/NEJMoa1414905

2. Saver JL, Goyal M, Bonafe A, Diener HC, Levy EI, Pereira VM, et al. Stent-retriever thrombectomy after intravenous t-PA vs. t-PA alone in stroke. *N Engl J Med.* (2015) 372:2285–95. doi: 10.1056/NEJMoa1415061

3. Campbell BCV, Mitchell PJ, Kleinig TJ, Dewey HM, Churilov L, Yassi N, et al. Endovascular therapy for ischemic stroke with perfusion-imaging selection. *N Engl J Med.* (2015) 372:1009–18. doi: 10.1056/NEJMoa1414792

4. Jovin TG, Chamorro A, Cobo E, de Miquel MA, Molina CA, Rovira A, et al. Thrombectomy within 8 hours after symptom onset in ischemic stroke. *N Engl J Med.* (2015) 372:2296–306. doi: 10.1056/NEJMoa1503780

5. Berkhemer OA, Fransen PS, Beumer D, Van Den Berg LA, Lingsma HF, Yoo AJ, et al. A randomized trial of intraarterial treatment for acute ischemic stroke. *N Engl J Med.* (2015) 372:11–20. doi: 10.1056/NEJMx140064

6. Albers GW, Marks MP, Kemp S, Christensen S, Tsai JP, Ortega-Gutierrez S, et al. Thrombectomy for stroke at 6 to 16 hours with selection by perfusion imaging. *N Engl J Med.* (2018) 378:708–18. doi: 10.1056/NEJMoa1713973

7. Menon BK, Hill MD, Davalos A, Roos YBWEM, Campbell BCV, Dippel DWJ, et al. Efficacy of endovascular thrombectomy in patients with M2 segment middle cerebral artery occlusions: meta-analysis of data from the HERMES Collaboration. *J Neurointerv Surg.* (2019) 11:1065–9. doi: 10.1136/neurintsurg-2018-014678

8. Mensah GA, Norrving B, Feigin VL. The global burden of stroke. *Neuroepidemiology.* (2015) 45:143–5. doi: 10.1159/000441082

9. Rha JH, Saver JL. The impact of recanalization on ischemic stroke outcome: a meta-analysis. *Stroke.* (2007) 38:967–73. doi: 10.1161/01.STR.0000258112.14918.24

10. Pedersen A, Stanne TM, Nilsson S, Klasson S, Rosengren L, Holmegaard L, et al. Circulating neurofilament light in ischemic stroke: temporal profile and outcome prediction. *J Neurol.* (2019) 266:2796–806. doi: 10.1007/s00415-019-09477-9

11. Kent SM, Taylor AJ. Usefulness of lowering low-density lipoprotein cholesterol to <70 mg/dl and usefulness of C-reactive protein in patient selection. *Am J Cardiol.* (2003) 92:1224–7. doi: 10.1016/j.amjcard.2003.07.040

12. Arthurs ZM, Andersen C, Starnes BW, Sohn VY, Mullenix PS, Perry J. A prospective evaluation of C-reactive protein in the progression of carotid artery stenosis. *J Vasc Surg.* (2008) 47:744–50; discussion 751 doi: 10.1016/j.jvs.2007.11.066

13. Montaner J, Fernandez-Cadenas I, Molina CA, et al. Poststroke C-reactive protein is a powerful prognostic tool among candidates for thrombolysis. *Stroke.* (2006) 37:1205–10. doi: 10.1161/01.STR.0000217744.89208.4e

14. Ridker PM, Rifai N, Rose L, Buring JE, Cook NR. Comparison of C-reactive protein and low-density lipoprotein cholesterol levels in the prediction of first cardiovascular events. *N Engl J Med.* (2002) 347:1557–65. doi: 10.1056/NEJMoa021993

15. Stoll G, Nieswandt B. Thrombo-inflammation in acute ischaemic stroke - implications for treatment. *Nat Rev Neurol.* (2019) 15:473–81. doi: 10.1038/s41582-019-0221-1

16. Huber T, Kleine JF, Kaesmacher J, Bette S, Poppert H, Zimmer C, et al. Blood leukocytes as prognostic parameter in stroke thrombectomy. *Cerebrovasc Dis.* (2016) 42:32–40. doi: 10.1159/000444369

17. Kaplan MH, Volanakis JE. Interaction of C-reactive protein complexes with the complement system. I Consumption of human complement associated with the reaction of C-reactive protein with pneumococcal C-polysaccharide and with the choline phosphatides, lecithin and sphingomyelin. *J Immunol.* (1974) 112:2135–47. doi: 10.4049/jimmunol.112.6.2135

18. Zimmerman MA, Selzman CH, Cothren C, Sorensen AC, Raeburn CD, Harken AH. Diagnostic implications of C-reactive protein. *Arch Surg.* (2003) 138:220–4. doi: 10.1001/archsurg.138.2.220

19. Hsuchou H, Kastin AJ, Mishra PK, Pan W. C-reactive protein increases BBB permeability: implications for obesity and neuroinflammation. *Cell Physiol Biochem.* (2012) 30:1109–19. doi: 10.1159/000343302

20. Laggner M, Lingitz M-T, Copic D, Direder M, Klas K, Bormann D, et al. Severity of thermal burn injury is associated with systemic neutrophil activation. *Sci Rep.* (2022) 12:1654. doi: 10.1038/s41598-022-05768-w

21. Korantzopoulos P, Letsas KP, Tse G, Fragakis N, Goudis CA, Liu T. Inflammation and atrial fibrillation: a comprehensive review. *J Arrhythm.* (2018) 34:394–401. doi: 10.1002/joa3.12077

22. Hill MD, Goyal M, Menon BK, Nogueira RG, McTaggart RA, Demchuk AM, et al. Efficacy and safety of nerinetide for the treatment of acute ischaemic stroke (ESCAPE-NA1): a multicentre, double-blind, randomised controlled trial. *Lancet.* (2020) 395:878–87. doi: 10.1016/S0140-6736(20)30258-0

23. Adams HP, Jr., Bendixen BH, Kappelle LJ, et al. Classification of subtype of acute ischemic stroke. Definitions for use in a multicenter clinical trial. TOAST. Trial of Org. 10172 in Acute Stroke Treatment. *Stroke.* (19943) 24:35–41. doi: 10.1161/01.STR.24.1.35

24. Zaidat OO, Yoo AJ, Khatri P, Tomsick TA, von Kummer R, Saver JL, et al. Recommendations on angiographic revascularization grading standards for acute ischemic stroke: a consensus statement. *Stroke.* (2013) 44:2650–63. doi: 10.1161/STROKEAHA.113.001972

25. Mokin M, Levy EI, Saver JL, Siddiqui AH, Goyal M, Bonafé A, et al. Predictive value of RAPID assessed perfusion thresholds on final infarct volume in SWIFT PRIME (solitaire with the intention for thrombectomy as primary endovascular treatment). *Stroke.* (2017) 48:932–8. doi: 10.1161/STROKEAHA.116.015472

26. Hayes AF, Rockwood NJ. Regression-based statistical mediation and moderation analysis in clinical research: observations, recommendations, and implementation. *Behav Res Ther.* (2017) 98:39–57. doi: 10.1016/j.brat.2016.11.001

27. Tao Q, Ang TFA, Akhter-Khan SC, Itchapurapu IS, Killiany R, Zhang X, et al. Impact of C-reactive protein on cognition and Alzheimer disease biomarkers in homozygous apolipoprotein E varepsilon4 carriers. *Neurology.* (2021) 97:e1243–52. doi: 10.1212/WNL.0000000000012512

28. Hart PC, Rajab IM, Alebraheem M, Potempa LA. C-reactive protein and cancer-diagnostic and therapeutic insights. *Front Immunol.* (2020) 11:595835. doi: 10.3389/fimmu.2020.595835

29. Blake GJ, Ridker PM. C-reactive protein, subclinical atherosclerosis, and risk of cardiovascular events. *Arterioscler Thromb Vasc Biol.* (2002) 22:1512–3. doi: 10.1161/01.ATV.0000038145.59548.85

30. Brull DJ, Serrano N, Zito F, Jones L, Montgomery HE, Rumley A, et al. Human CRP gene polymorphism influences CRP levels: implications for the prediction and pathogenesis of coronary heart disease. *Arterioscler Thromb Vasc Biol.* (2003) 23:2063–9. doi: 10.1161/01.ATV.0000084640.21712.9C

31. Suresh MV, Singh SK, Ferguson DA Jr, Agrawal A. Role of the property of C-reactive protein to activate the classical pathway of complement in protecting mice from pneumococcal infection. *J Immunol.* (2006) 176:4369–74. doi: 10.4049/jimmunol.176.7.4369

32. Ries W, Torzewski J, Heigl F, Pfluecke C, Kelle S, Darius H, et al. C-reactive protein apheresis as anti-inflammatory therapy in acute myocardial infarction: results of the CAMI-1 study. *Front Cardiovasc Med.* (2021) 8:591714. doi: 10.3389/fcvm.2021.591714

33. Boljevic D, Nikolic A, Rusovic S, Lakcevic J, Bojic M, Balint B, et al. Promising innovative treatment for ST-elevation myocardial infarction: the use of C-reactive protein selective apheresis: case report. *Blood Purif.* (2020) 49:753–7. doi: 10.1159/000506176

34. Nissen SE, Tuzcu EM, Schoenhagen P, Crowe T, Sasiela WJ, Tsai J, et al. Statin therapy, LDL cholesterol, C-reactive protein, and coronary artery disease. *N Engl J Med.* (2005) 352:29–38. doi: 10.1056/NEJMoa042000

35. Ishikawa J, Tamura Y, Hoshide S, Eguchi K, Ishikawa S, Shimada K, et al. Low-grade inflammation is a risk factor for clinical stroke events in addition to silent cerebral infarcts in Japanese older hypertensives: the Jichi Medical School ABPM Study, wave 1. *Stroke.* (2007) 38:911–7. doi: 10.1161/01.STR.0000258115.46765.f1

36. Löppönen P, Qian C, Tetri S, Juvela S, Huhtakangas J, Bode MK, et al. Predictive value of C-reactive protein for the outcome after primary intracerebral hemorrhage. *J Neurosurg.* (2014) 121:1374–9. doi: 10.3171/2014.7.JNS132678

37. Teoh H, Quan A, Lovren F, Wang G, Tirgari S, Szmitko PE, et al. Impaired endothelial function in C-reactive protein overexpressing mice. *Atherosclerosis.* (2008) 201:318–25. doi: 10.1016/j.atherosclerosis.2008.02.034

frontiers | Frontiers in Neurology

TYPE Original Research
PUBLISHED 05 July 2023
DOI 10.3389/fneur.2023.1173276

OPEN ACCESS

EDITED BY
Yanlin Zhang,
Second Affiliated Hospital of Soochow University, China

REVIEWED BY
Chengyan Chu,
Dalian Municipal Central Hospital, China
Alina Gonzalez-Quevedo,
Instituto de Neurología y Neurocirugía, La Habana, Cuba

*CORRESPONDENCE
Xiangying Du
✉ duxying_xw@163.com

RECEIVED 24 February 2023
ACCEPTED 19 June 2023
PUBLISHED 05 July 2023

CITATION
Bao J, Wang C, Zhang Y, Su Z, Du X and Lu J (2023) Evaluating cardiac function with chest computed tomography in acute ischemic stroke: feasibility and correlation with short-term outcome.
Front. Neurol. 14:1173276.
doi: 10.3389/fneur.2023.1173276

Evaluating cardiac function with chest computed tomography in acute ischemic stroke: feasibility and correlation with short-term outcome

Jie Bao[1], Chen Wang[1], Yimeng Zhang[1], Zhuangzhi Su[1,2], Xiangying Du[1,2]* and Jie Lu[1,2]

[1]Department of Radiology, Xuanwu Hospital, Capital Medical University, Beijing, China, [2]Beijing Key Laboratory of Magnetic Resonance Imaging and Brain Informatics, Beijing, China

Background: The outcomes of patients with acute ischemic stroke (AIS) are related to cardiac function. Cardiac insufficiency can manifest as hydrostatic changes in the lungs. Computed tomography (CT) of the chest is commonly used for screening pulmonary abnormalities and provides an opportunity to assess cardiac function.

Purpose: To evaluate the correlation between hydrostatic lung manifestations on chest CT and cardiac function with its potential to predict the short-term outcome of AIS patients.

Methods: We retrospectively analyzed AIS patients who had undergone chest CT at admission and echocardiogram within 48h. Morphological and quantitative hydrostatic changes and left ventricular dimensions were assessed using chest CT. Improvement in the National Institutes of Health Stroke Scale (NIHSS) score on the seventh day determined short-term outcomes. Multivariate analysis examined the correspondence between hydrostatic lung manifestations, left ventricular dimension, and left ventricle ejection fraction (LVEF) on echocardiography, and the correlation between hydrostatic changes and short-term outcomes.

Results: We included 204 patients from January to December 2021. With the progression of hydrostatic changes on chest CT, the LVEF on echocardiography gradually decreased ($p<0.05$). Of the 204, 53 patients (26%) with varying degrees of hypostatic lung manifestations had less improvement in the NIHSS score ($p<0.05$). The density ratio of the anterior/posterior lung on CT showed a significant negative correlation with improvement in the NIHSS score ($r=-5.518$, $p<0.05$). Additionally, patients with a baseline NIHSS ≥4 with left ventricular enlargement had significantly lower LVEF than that of patients with normal NIHSS scores.

Conclusion: Hydrostatic lung changes on chest CT can be used as an indicator of cardiac function and as a preliminary reference for short-term outcome in AIS patients.

KEYWORDS

acute ischemic stroke, hydrostatic lung, cardiac function, chest CT, computed tomography, NIHSS, outcome

1. Introduction

Although acute ischemic stroke (AIS) mostly results from direct occlusion of the carotid-cerebral arteries, cardiac abnormalities play an important role in the pathogenesis and evolution of strokes. As the second most common risk factor for cardiogenic stroke after atrial fibrillation (AF), decreased left ventricular function is a major risk factor for functional outcomes of strokes (1). Heart failure is an important independent variable influencing stroke mortality when controlling for other factors such as AF, age, and stroke syndromes (2). The identification of impaired ejection fraction may aid in timely recognition of stroke patients who are at a higher risk of early and long-term adverse outcomes (3, 4). On the other hand, sympathetic overstimulation and the release of catecholamines following an ischemic stroke can lead to toxic injury of the myocardium and weaken the myocardial contractility. High levels of catecholamines stimulate adrenergic receptors to cause systemic vasoconstriction and increase the systemic vascular resistance, subsequently elevating the ventricular filling pressure (5, 6). Cardiac function progressively deteriorates, ultimately leading to heart failure. The interaction between AIS and impaired cardiac function may accelerate deterioration in AIS patients.

In addition to decreased left ventricular ejection fraction (LVEF) and hypertensive cardiac remodeling, decreased left ventricular function can lead to elevated pulmonary artery pressure and microvascular filtration pressure in the lungs, which cause lung injury and promote fluid formation through hydrostatic mechanisms and changes in permeability (7–9). These processes culminate in hydrostatic changes in the lungs, which may be more apparent than the cardiac changes.

Computed tomography (CT) of the chest plays a valuable role in clinical screening, especially in emergency patients with unclear clinical histories (10, 11). CT was more widely used in many institutions during the pandemic for screening of COVID-19 infection (12). Although precise assessment of cardiac function with chest CT is difficult, preliminary evaluation of cardiac function based on pulmonary involvement and gross measurements of left ventricle size can be achieved, which can potentially aid in the global evaluation of and strategic decision-making for AIS patients.

This study aimed to evaluate the correlation between hydrostatic lung manifestations and cardiac changes on chest CT and the short-term outcomes for AIS patients to assess the efficacy of chest CT as a prognostic indicator.

2. Materials and methods

2.1. Patient selection

We retrospectively analyzed the medical records of AIS patients who had been admitted to our institution between January to December 2021. All patients underwent a standard set of brain CT scans (non-contrast CT alone or multimodal CT, including perfusion and computed tomography angiography) and chest CT immediately upon admission. Inclusion criteria for this study were as follows: (1) the diagnosis of ischemic stroke met the national and international criteria for acute stroke and the time of stroke onset was less than 6 hours (from the hyperacute period), and for patients who underwent echocardiography this occurred within 48 h after admission to rule out structural abnormality; (2) patients with first-ever ischemic stroke or no legacy effects of their previous ischemic stroke; and (3) patients who had received recanalization therapy (thrombolysis or thrombectomy) and no complications or adverse effects were noted. The exclusion criteria were as follows: (1) patients with chronic obstructive pulmonary disease, bilateral diffuse emphysema, pulmonary fibrosis, severe intrapulmonary infection, or lung cancer; and (2) patients with coronary stents, prosthetic heart valves, prior coronary artery bypass graft surgery, or metal artifacts in the region of the cardiac silhouette that affected image quality.

On hospital admission, demographic data [age, sex, body mass index (BMI), and laboratory examinations] were collected, and cardiovascular risk factors (smoking, arterial hypertension, diabetes mellitus, hypercholesterolemia, atrial fibrillation, and recanalization therapy) were recorded. The National Institutes of Health Stroke Scale (NIHSS) was assessed at admission (baseline) and 7 days later. The water swallow test (WST) score was performed at admission to assess the degree of dysphagia (1) for ability to swallow the water continuously, (2) for ability to swallow the water more than twice without coughing or choking, (3) for voice quality or breathing pattern change, (4) for ability to swallow the water more than twice with coughing or choking, and (5) for inability to swallow (13, 14).

2.2. Measurements and outcome

All chest CT examinations were performed using a 256-detector row CT scanner (Revolution CT; GE Healthcare, Milwaukee, WI, United States). Chest CT was performed using a tube voltage of 100 kV and tube current modulation. Routine reconstruction of the chest CT images included axial images of 5 mm thickness with a high resolution and soft tissue algorithm, and axial images of 0.625 mm thickness with a high-resolution algorithm. The coronal images of the lung window were also reformatted. All the images were transferred to the picture archiving and communication system (PACS) server for image reading and further analysis.

Image evaluation was performed by two experienced radiologists (with at least 3 years of experience in chest radiology). The radiologists were blinded to the clinical information and study outcomes. Dedicated monitors and workstations for image reading with multiplanar reformation capacity were used for image analysis.

The imaging features of the lungs related to hydrostatic changes and other signs were evaluated and recorded, including small ill-defined opacities, interlobular septal thickening, ground-glass attenuation, airspace consolidation, and pleural effusion (Figure 1) (15). For quantitative analysis, we used the sector method to measure the density of a peripheral area of lung parenchyma (16, 17). We manually drew regions of interest (ROIs) on the axial images in 12 regions, including the right and left upper lobes, left lingula and right middle lobe, and left and right lower lobes (size, 2 cm × 1 cm), and recorded CT Hounsfield unit (HU) of every ROI. The central vasculature, including the main and lobar pulmonary arteries, pulmonary veins, and airways, were excluded from the ROIs (Figure 2). The mean anterior/posterior lung density ratio (ΔA/P) for the patients was determined as follows: the density values in the ROIs at the peripheral one-third of the right and left anterior and posterior lung fields were arithmetically averaged.

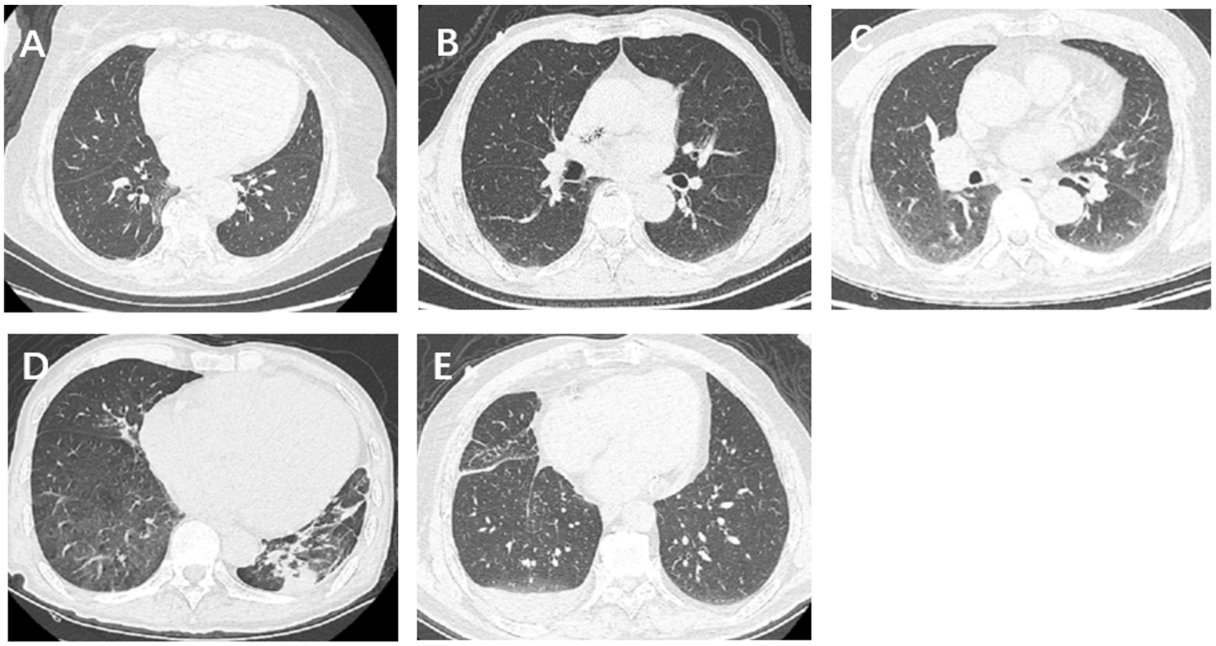

FIGURE 1
Imaging features of lungs related to hydrostatic changes, including small ill-defined opacities, interlobular septal thickening, ground-glass attenuation, airspace consolidation, and pleural effusion.

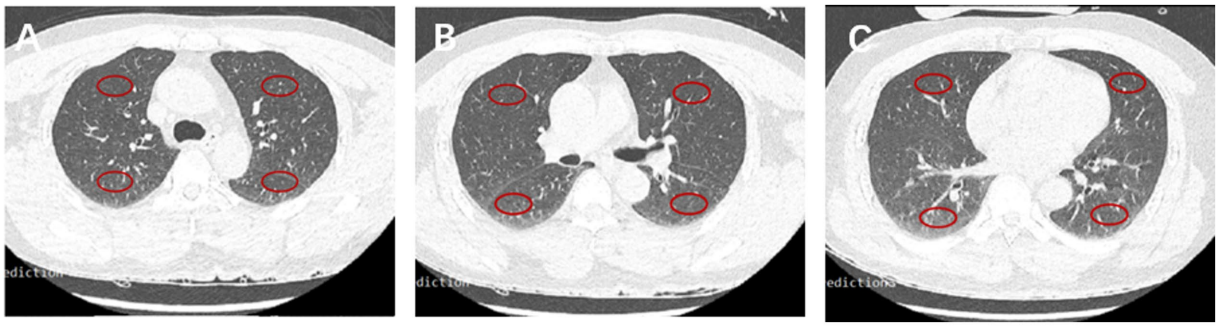

FIGURE 2
CT HU in 12 fields of the lung. Representative ROIs in different lobes in the carina **(A)**, main stem bronchi **(B)**, and bottom **(C)** levels.

To assess the left ventricular (LV) dimensions, short-axis images of the left ventricle were reformatted using thin-slice images on the workstation. The maximum transverse diameter of the left ventricle, including the interventricular septum and lateral wall, was measured (Figure 3). LV enlargement was defined as >66 mm deviation in men and >64 mm deviation in women from normal cardiac magnetic resonance imaging (MRI) data (18). Stroke severity was assessed using the NIHSS score at admission and 7 days later. The short-term recovery was rated as follows: not improved (NIHSS score improvement ≤30%) or improved (NIHSS score improvement >30%). Based on initial NIHSS score, stroke patients were divided into two groups, namely the mild stroke group (baseline NIHSS score ≤4) and the severe stroke group (NIHSS score >4) (19).

Measurement of cardiac dimension and function was performed with trans-thoracic echocardiography using a clinical scanner (Philips IE33 or GE Vivid E95) by certified cardiologists or sonologists. LVEF and LV dimensions were recorded for comparison with chest CT features. Left ventricular internal diameter in diastole (LVIDd) >56 mm is defined as LV enlargement in males and LVIDd >51 mm in females (20).

2.3. Statistical analyses

Interobserver agreement and various parameters measured using echocardiography or chest CT were assessed using the kappa coefficient statistical test. Differences in characteristics between patients with or without imaging signs were assessed by χ^2 analysis or Mann–Whitney test in both mild and severe stroke groups. Frequency of hydrostatic signs in the lungs on the chest CT in AIS patients were

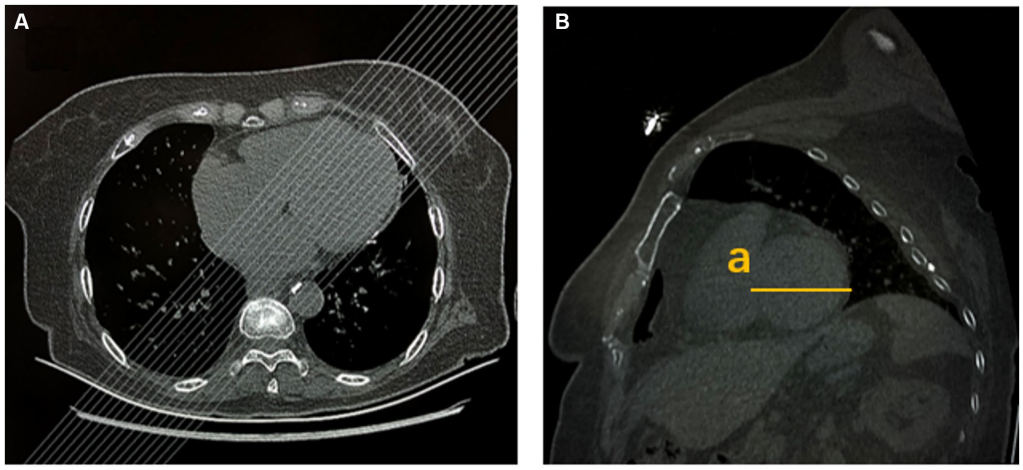

FIGURE 3
Left ventricular size was measured by chest CT. **(A)** Multiplanar reformation (MPR) after chest axial CT scans. **(B)** MPR after chest sagittal CT scans (a: maximum transverse diameter of left ventricular short axis, including interventricular septum and lateral wall).

calculated. Polyserial correlation coefficients were used to evaluate the association between continuous CT HU measurements, LV widest short-axis dimensions, and poor outcomes at 7 days. Multiple linear regression analysis was used to assess the related factors on the improvement of the NIHSS score. Receiver operating characteristic (ROC) curve analysis was performed to determine the cut-off value of CT HU measurements for differentiation between improvement of ≤30% of the NIHSS score from admission to the seventh day.

3. Results

3.1. Study population

A total of 204 patients were included in this study, with 81 and 123 in the mild and severe stroke groups, respectively. The demographic and clinical data of the two groups are presented in Table 1. Notably, the number of patients who did not show improvement was significantly lower in the mild stroke group than in the severe stroke group. Moreover, the LVEF measured by echocardiography was significantly higher in the mild stroke group. The time from stroke onset to CT, history of diabetes mellitus, acute treatment, and laboratory examinations were also different between the two groups.

3.2. Morphological analysis of the lung CT

Among the included patients, 146 (72%) had abnormal lung CT findings and tended to have a lower proportion of NIHSS improvement in both the mild and severe stroke groups, both of which were statistically significant (Table 2). The frequency of each morphological finding is presented in Table 3. The ground-glass attenuation areas in the inferior and middle lobes were the most frequent presentation of hydrostatic changes in the lungs. The number of patients with ground-glass attenuation in the lungs was significantly higher in the severe stroke group (52.8%) than in the mild stroke group (25.9%). Additionally, the patients with ground-glass attenuation areas in the lungs showed a lower LVEF measured by echocardiography ($p < 0.001$) and a lower improvement in NIHSS on the seventh day ($p < 0.001$) compared to patients without lung changes or with only interlobular septal thickening (Figures 4A–D).

3.3. Quantitative analysis of the lung CT

There were strong correlations between ΔA/P and LVEF measured using echocardiography, especially in the severe stroke group (Figure 5). In the multivariate linear regression adjusted for recanalization therapy (thrombolysis or thrombectomy), NIHSS score on admission, and WST score, which had a greater impact on the improvement of outcome, ΔA/P showed a strong negative correlation with the improvement of outcome within 7 days between the two groups (Table 4).

The ROC analysis results of ΔA/P for determining an improvement of ≤30% of the NIHSS score from admission to the seventh day are shown in Figure 6. The largest area under the curve in the mild stroke group was 0.928, with a cutoff value of 1.135 (sensitivity = 100% and specificity = 78.8%), and the largest area under the curve in the severe stroke group was 0.775, with a cutoff value of 1.235 (sensitivity = 80.6% and specificity = 67.5%).

3.4. Quantification of left ventricular size

Excellent agreement between the two radiologists was achieved for the LV measurements (kappa = 0.807). The kappa statistic showed excellent agreement between CT and echocardiography for the definition of LV enlargement in both the mild and severe stroke groups (kappa = 0.633/kappa = 0.604). As shown in Figures 4E–F, patients in the severe stroke group with LV enlargement had a significantly lower LVEF than those of patients with a normal LV ($p < 0.001$). However, this difference was not significant in the mild stroke group ($p = 0.962$). Furthermore, ΔA/P measured on CT and the

TABLE 1 Demographic and clinical characteristics of the patients.

	Mild stroke (NIHSS ≤4)	Severe stroke (NIHSS >4)	*p*-value
Characteristic			
Sex (male)	60	92	0.908
Age, years	63 (56, 70)	66 (62, 71)	0.091
BMI	25 (23, 26)	25 (22, 27)	0.905
Smoking, (*n*)	48	61	0.431
Water swallow test	1 (1, 3)	1 (1, 4)	0.08
Time stroke to CT, min	198 (145, 245)	219 (166, 285)	0.035
Medical history			
Atrial fibrillation	5 (6.2%)	18 (14.6%)	0.072
Diabetes mellitus	18 (22.8%)	50 (40.7%)	0.01
Hypercholesteremia	60 (74.1%)	79 (64.2%)	0.168
Hypertension	58 (71.6%)	78 (63.4%)	0.288
Laboratory examination			
WBC	7.0 (5.7, 8.3)	8.1 (6.5, 10.1)	0.000
Neutrophils	4.3 (3.5, 5.6)	6.2 (4.6, 7.7)	0.000
NEUT%	63.8% (57.6, 72.6%)	76.6% (68.2, 83.0%)	0.000
Acute treatment			
IVT	57 (70%)	68 (55.3%)	0.04
MT	5 (6.2%)	30 (24.4%)	0.01
Location of stroke			
Left	33 (40.7%)	58 (47.2%)	0.669
Right	39 (48.1%)	53 (43.1%)	
Posterior	9 (11.1%)	12 (9.8%)	
Echocardiographic			
LVEF (%)	67 (64, 69)	63 (55, 67)	0.000
The outcome of stroke			
>30%	65 (80.2%)	82 (66.7%)	0.034
≤30%	16 (19.8%)	41 (33.3%)	

WBC, white blood cell; NEUT, neutrophil; IVT, intravenous thrombolysis; MT, mechanical thrombectomy; LVEF, left ventricular ejection fraction.

improvement of NIHSS score in seven days had no correlation with LV maximum short-axis dimension in both the mild and severe stroke groups ($p = 0.233$, $p = 0.137$), but patients with LV enlargement showed a higher ΔA/P ($p < 0.001$) and a lower NIHSS improvement ($p < 0.001$) in the severe stroke group (Figures 4I,J). Similarly, a non-significant trend was observed in the mild stroke group ($p = 0.793$, $p = 0.872$), as shown in Figures 4G,H.

4. Discussion

Cardiac function is associated with stroke occurrence and mortality (3, 21). Preexisting cardiac failure has an adverse influence on stroke mortality independent of other known factors (2). These findings suggest the possible benefits of evaluating cardiac function in AIS patients. Echocardiography is commonly used to assess cardiac function and structure, even in emergency settings. However, it was not recommended in AIS patients according to the guidelines, unless severe heart failure presented or pre-existing severe cardiac abnormality was acknowledged (22). Other cardiac imaging modalities, including CT and MRI, are seldom performed at presentation. Chest CT has been widely used to screen hospitalized patients to prevent possible in-hospital catastrophic transmission over the last few years, although its cost-effectiveness has been debated (12, 23, 24). In addition to native pulmonary abnormalities, intrapulmonary changes related to cardiac function and dimensions can be assessed using chest CT. The development of high pulmonary capillary pressure based on decreased cardiac function results in hydrostatic gradients for fluid flux out of capillaries into the interstitial and alveolar spaces, presenting visible hydrostatic changes in the lung on CT (25). In addition, the overall LV dimension can be measured using multiplanar reformation of the heart. These findings provide an initial assessment to detect impaired cardiac function in AIS patients.

The primary findings of this study are as follows: (1) we observed a difference between improvement in early outcome among patients with and without presentation of morphological changes due to

TABLE 2 Baseline characteristics.

	Mild stroke (NIHSS ≤4)			Severe stroke (NIHSS >4)		
	Normal CT scan	Abnormal CT scan	*p*-value	Normal CT scan	Abnormal CT scan	*p*-value
Characteristic						
Sex (male)	26 (72.2%)	34 (75.6%)	0.734	18 (81.8%)	74 (73.3%)	0.403
Age, years	64 (55, 74)	63 (57, 68)	0.558	62 (57, 66)	66 (62, 72)	0.009
BMI	24 (23, 26)	25 (24, 27)	0.451	24 (22, 27)	25 (22, 27)	0.341
Smoking, (*n*)	21 (58.3%)	27 (60%)	0.879	11 (50%)	56 (55.4%)	0.642
Water swallow test	1 (1, 1)	1 (1, 1)	0.811	1 (1, 3)	2 (1, 4)	0.072
Atrial fibrillation	2 (5.6%)	3 (6.7%)	0.606	3 (13.6%)	15 (14.9%)	0.593
Time stroke to CT, min	170.5 (131, 214)	216 (159, 264)	0.011	188 (145, 283)	220 (174, 288)	0.275
Medical history						
Diabetes mellitus	10 (27.8%)	23 (51.1%)	0.034	5 (22.7%)	23 (22.8%)	0.996
Hypercholesteremia	26 (72.2%)	34 (75.6%)	0.734	18 (81.8%)	61 (60.4%)	0.057
Hypertension	26 (72.2%)	32 (71.1%)	0.912	16 (72.7%)	68 (67.3%)	0.622
Laboratory examination						
WBC	6.4 (5.2, 8.3)	7.1 (6.0, 8.2)	0.204	7.3 (6.1, 9.3)	8.2 (6.5, 10.3)	0.173
Neutrophils	3.9 (3.0, 5.5)	4.4 (3.8, 5.7)	0.1	4.9 (4.6, 6.9)	6.3 (4.7, 8.3)	0.123
NEUT%	61.3% (56.7, 72.1%)	64.8% (60.4, 73.6%)	0.139	69.7% (65.3, 78.9%)	76.2% (69.0, 83.3%)	0.061
The outcome of stroke						
>30%	32 (88.9%)	31 (73.3%)	0.031	20 (90.9%)	62 (61.4%)	0.008
≤30%	4 (11.1%)	14 (26.7%)		2 (9.1%)	39 (38.6%)	

TABLE 3 Frequency of each morphological finding in the mild/severe stroke group.

Morphological findings	Mild stroke (NIHSS ≤4)	Severe stroke (NIHSS >4)	*p*-value
Small ill-defined opacities	1 (1.2%)	0 (0%)	0.4
Interlobular septal thickening	23 (28.4%)	31 (25.2%)	0.613
Ground-glass attenuation	21 (25.9%)	65 (52.8%)	0.000
Airspace consolidation	0 (0%)	2 (1.6%)	0.519
Pleural effusion	0 (0%)	3 (2.4%)	0.411
None	36 (44.4%)	22 (17.9%)	0.000

hydrostatic pressure, especially ground-glass attenuation in the lungs; (2) the ΔA/P showed a strong association with LVEF along with the improvement of outcome in 7 days. Moreover, ΔA/P had high sensitivity and specificity for differentiating patients with the potential to demonstrate >30% of baseline NIHSS score; and (3) patients from the severe stroke group demonstrating LV dilation had a higher ΔA/P and a poorer improvement in NIHSS score compared to patients without LV dilation (baseline NIHSS score >4).

Typical morphological changes due to hydrostatic pressure of the lung mainly include small ill-defined opacities, interlobular septal thickening, ground-glass attenuation, airspace consolidation, and pleural effusion. Previous studies have reported ground-glass attenuation in 25%–100% patients with hydrostatic edema. The lesions are mostly peribronchovascular owing to gravity (26, 27). In our study, patients in the severe stroke group had bilateral ground-glass attenuation areas in the inferior and middle lobes more frequently than the mild stroke group. Our study demonstrated a moderately strong correlation between hydrostatic changes in the lungs and LVEF measured by echocardiography after 48 h. Patients with ground-glass attenuation had a lower LVEF and less improvement compared to patients without morphological changes in the lung or with only interlobular septal thickening ($p < 0.001$). AIS patients showing ground-glass attenuation or more severe hydrostatic changes suggestive of decreased cardiac function at presentation showed poor short-term improvement in the NIHSS score on the seventh day.

Previous studies support our findings of quantitative analysis of CT HU measurements in AIS patients, which suggest an altered cardiac function (28–31). Rosenblum et al. (16) first used the sector method to measure the density of a peripheral area of lung parenchyma, which could detect the subtle changes in lung density including either high- or low-density lung disease and increase the

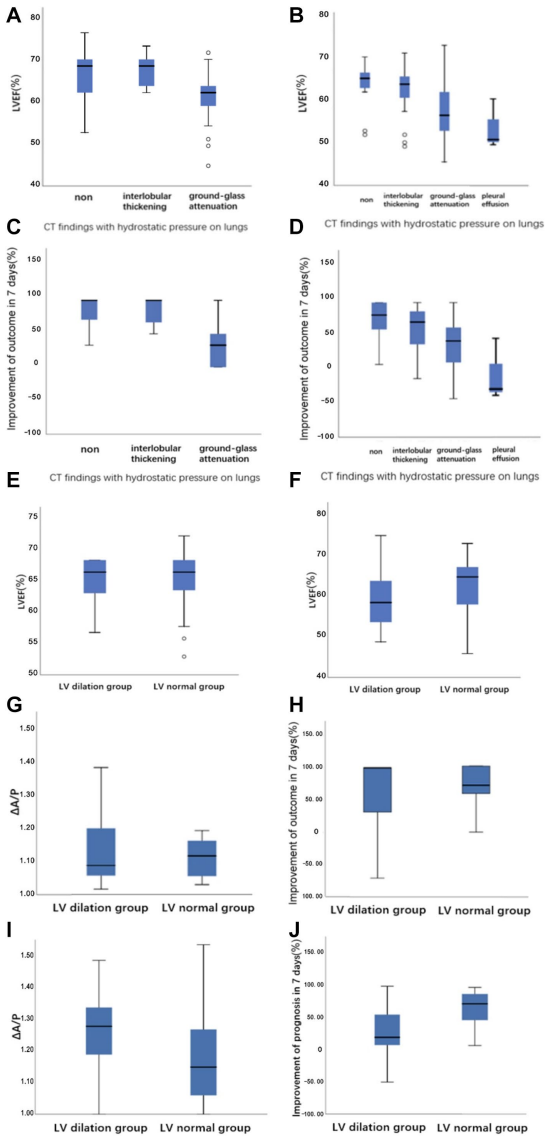

FIGURE 4
Boxplots demonstrating **(A,B)** the relationship between LVEF versus CT findings with hydrostatic pressure on lungs in the mild stroke group and the severe stroke group, respectively. **(C,D)** The relationship between the improvement of outcome in 7days versus CT findings with hydrostatic pressure on lungs in the mild stroke group and the severe stroke group, respectively. **(E,F)** The raw data for LVEF at LV dilation and LV normal groups defined with CT image in the mild stroke group and the severe stroke group, respectively. **(G–J)** The ΔA/P and the improvement of NIHSS score in 7days at LV dilation and LV normal groups defined with CT image in the mild stroke and the severe stroke groups, respectively.

likelihood that such diagnoses can be made earlier than they can from plain radiographs. Then, Slutsky et al. used the same method to relate density changes to the alteration in left ventricular filling pressure. The results showed the ratio of pulmonary density in the anterior and posterior segments (A/P) is related with heart failure (17). The dependent lung is always denser; this is attributed to the effect of gravity on the lower lobes (32). The ΔA/P may more reliably reflect changes in total lung water given the absence of additional factors that may confound density measurements. We found that ΔA/P was strongly correlated with LVEF, especially in the severe stroke group. In addition, we observed a robust association between ΔA/P and improved outcome. Evaluation of pulmonary hydrostatic changes using ΔA/P demonstrated excellent accuracy in differentiating short-term improvements of >30%, with areas under the curve as high as 0.928 in the mild stroke group and 0.775 in the severe stroke group. Moreover, ΔA/P cutoff of 1.135 in the mild stroke group and 1.235 in the severe stroke group showed high sensitivity (100% and 80.6%, respectively) and specificity (78.8% and 67.5%, respectively) for ≤30% NIHSS score improvement at 7 days. Increased ΔA/P might lead to an increased suspicion of hydrostatic pneumonia and subsequent treatments, which further affects the patients' short-term results. Patients in the mild stroke group presented higher sensitivity and specificity, which could be attributed to the severe stroke group having a higher severity of lung disease and more influencing factors in the short term. In sum, quantitative analysis of CT HU measurements can provide first handed information of cardiac function during the acute stage of stroke. It is also useful for providing a preliminary indication of short-term outcome.

In addition to pulmonary manifestations, CT can provide information on cardiac structures that can reflect cardiac function. Previous studies have shown that LV dilation is an independent adverse predictor of cardiac function from other risk factors and is associated with an increased risk of clinical heart failure (33, 34). In our study, the results of LV evaluation using chest CT were consistent with those of echocardiography. Meanwhile, in the severe stroke group, we observed that patients with LV dilation had a higher ΔA/P and a poorer improvement in the NIHSS score than those of patients without LV dilation.

4.1. Advantages and limitations

The major advantage of this study was that chest CT is an easily achievable tool for excluding coexisting pulmonary conditions without a significant delay in patient management. However, due to the preliminary nature of this study, it also entailed several limitations. First, our study only included patients with hyperacute AIS; therefore, pulmonary manifestations were less affected by other factors such as subsequent infection. Evaluation of patients at other stages should be conducted in future studies. Second, chest CT can only be used for the gross evaluation of cardiac function, and the parameters are mostly indirect indicators. However, previous studies have established a linear correlation between CT HU measurements and pulmonary capillary wedge pressure measurements, as well as the New York Heart Association functional classification of heart failure (22). Third, our study was retrospective and only short-term outcomes were included in the analysis. It remains unknown whether subsequent treatment decisions based on this information can improve clinical outcomes. Therefore, further follow-up studies are required to confirm these findings.

5. Conclusion

A preliminary assessment of cardiac function can be achieved with qualitative and quantitative analyses of chest CT features, which can be used to predict short-term outcome in AIS patients.

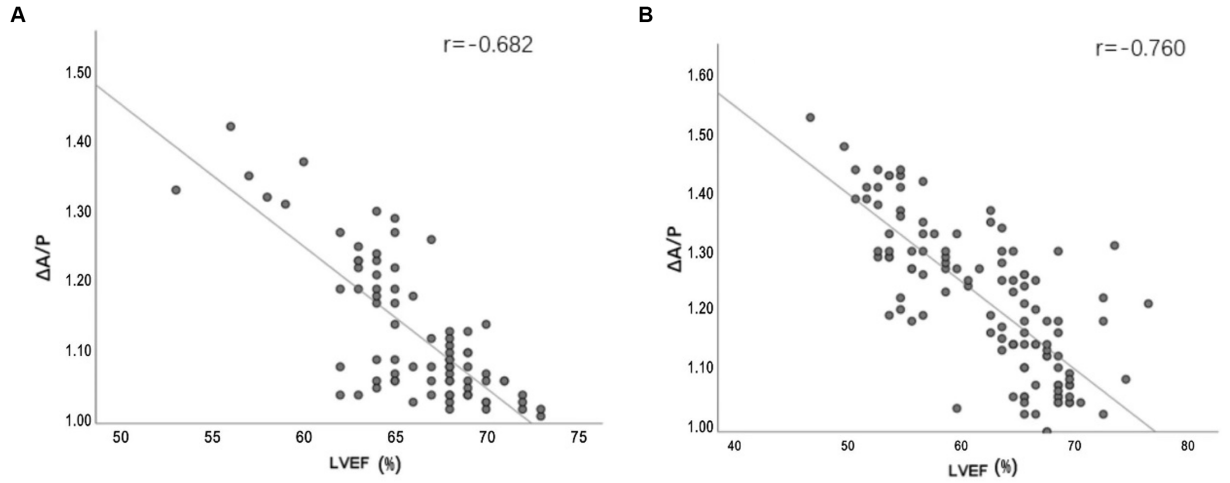

FIGURE 5
(A,B) Line plots demonstrating the relationship between ΔA/P measured by CT HU measurements and LVEF measured by echocardiograph in the mild stroke and the severe stroke groups, respectively.

TABLE 4 Prediction of the improvement in outcome from admission until the seventh day from quantitative analysis of lung CT and clinical factors.

Variables	β	95% CI	*p*-value
NIHSS score on admission	−0.047	(0.911, 0.995)	0.033
Water swallow test	−0.013	(0.976, 0.999)	0.030
Recanalization therapy	0.333	(0.003, 0.662)	0.048
ΔA/P	−5.518	(−6.930, −4.107)	0.000

Factors that were statistically significant ($p < 0.05$) in the multiple linear regression analysis were presented.

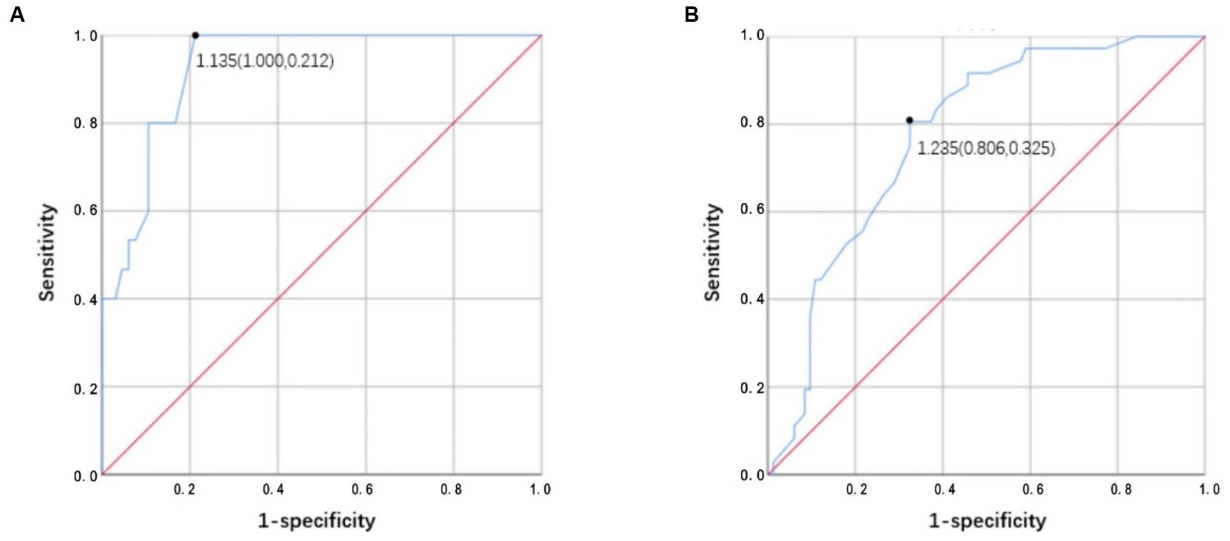

FIGURE 6
(A,B) Receiver operator characteristic (ROC) analysis results of ΔA/P by CT HU measurements for determining improvement <30% of NIHSS score from admission to the seventh day in the mild stroke and the severe stroke groups, respectively.

Data availability statement

The raw data supporting the conclusions of this article will be made available by the authors, without undue reservation.

Ethics statement

Ethical review and approval was not required for the study on human participants in accordance with the local legislation and institutional requirements. Written informed consent from the patients/participants or patients/participants' legal guardian/next of kin was not required to participate in this study in accordance with the national legislation and the institutional requirements.

Author contributions

XD and JL conceived and designed the experiments. JB, CW, YZ, and ZS performed the experiments. JB, CW, and YZ analyzed the data. JB wrote the manuscript. All authors contributed to the article and approved the submitted version.

Conflict of interest

The authors declare that the research was conducted in the absence of any commercial or financial relationships that could be construed as a potential conflict of interest.

Publisher's note

All claims expressed in this article are solely those of the authors and do not necessarily represent those of their affiliated organizations, or those of the publisher, the editors and the reviewers. Any product that may be evaluated in this article, or claim that may be made by its manufacturer, is not guaranteed or endorsed by the publisher.

References

1. Lozano Villanueva JL, Torres Zafra JF, Cortés Muñoz F, Mendoza Beltrán FDC, Sánchez Casas JC, Barragán Pedraza LA. Association between heart failure and clinical prognosis in patients with acute ischemic stroke: a retrospective cohort study. *J Clin Neurol.* (2021) 17:200–5. doi: 10.3988/jcn.2021.17.2.200

2. Sharma JC, Fletcher S, Vassallo M, Ross I. Cardiovascular disease and outcome of acute stroke: influence of pre-existing cardiac failure. *Eur J Heart Fail.* (2000) 2:145–50. doi: 10.1016/s1388-9842(00)00067-2

3. Milionis H, Faouzi M, Cordier M, D'Ambrogio-Remillard S, Eskandari A, Michel P. Characteristics and early and long-term outcome in patients with acute ischemic stroke and low ejection fraction. *Int J Cardiol.* (2013) 168:1082–7. doi: 10.1016/j.ijcard.2012.11.036

4. Miller J, Chaudhry F, Tirgari S, Calo S, Walker AP, Thompson R, et al. Cardiac stroke volume index is associated with early neurological improvement in acute ischemic stroke patients. *Front Physiol.* (2021) 12:689278. doi: 10.3389/fphys.2021.689278

5. Finsterer J. Neurological perspectives of neurogenic pulmonary edema. *Eur Neurol.* (2019) 81:94–102. doi: 10.1159/000500139

6. Zhao J, Xuan NX, Cui W, Tian BP. Neurogenic pulmonary edema following acute stroke: the progress and perspective. *Biomed Pharmacother.* (2020) 130:110478. doi: 10.1016/j.biopha.2020.110478

7. Guazzi M, Phillips SA, Arena R, Lavie CJ. Endothelial dysfunction and lung capillary injury in cardiovascular diseases. *Prog Cardiovasc Dis.* (2015) 57:454–62. doi: 10.1016/j.pcad.2014.11.003

8. Doyle IR, Nicholas TE, Bersten AD. Serum surfactant protein-a levels in patients with acute cardiogenic pulmonary edema and adult respiratory distress syndrome. *Am J Respir Crit Care Med.* (1995) 152:307–17. doi: 10.1164/ajrccm.152.1.7599839

9. Nugent K, Dobbe L, Rahman R, Elmassry M, Paz P. Lung morphology and surfactant function in cardiogenic pulmonary edema: a narrative review. *J Thorac Dis.* (2019) 11:4031–8. doi: 10.21037/jtd.2019.09.02

10. Tækker M, Kristjánsdóttir B, Andersen MB, Fransen ML, Greisen PW, Laursen CB, et al. Diagnostic accuracy of ultra-low-dose chest computed tomography in an emergency department. *Acta Radiol.* (2022) 63:336–44. doi: 10.1177/0284185121995804

11. Kristjánsdóttir B, Taekker M, Andersen MB, Bentsen LP, Berntsen MH, Dahlin J, et al. Ultra-low dose computed tomography of the chest in an emergency setting: a prospective agreement study. *Medicine.* (2022) 101:e29553. doi: 10.1097/MD.0000000000029553

12. Machnicki S, Patel D, Singh A, Talwar A, Mina B, Oks M, et al. The usefulness of chest CT imaging in patients with suspected or diagnosed COVID-19: a review of literature. *Chest.* (2021) 160:652–70. doi: 10.1016/j.chest.2021.04.004

13. Chen PC, Chuang CH, Leong CP, Guo SE, Hsin YJ. Systematic review and meta-analysis of the diagnostic accuracy of the water swallow test for screening aspiration in stroke patients. *J Adv Nurs.* (2016) 72:2575–86. doi: 10.1111/jan.13013

14. Tohara H, Saitoh E, Mays KA, Kuhlemeier K, Palmer JB. Three tests for predicting aspiration without video fluorography. *Dysphagia.* (2003) 18:126–34. doi: 10.1007/s00455-002-0095-y

15. Hansell DM, Bankier AA, MacMahon H, McLoud TC, Müller NL, Remy J. Fleischner society: glossary of terms for thoracic imaging. *Radiology.* (2008) 246:697–722. doi: 10.1148/radiol.2462070712

16. Rosenblum LJ, Mauceri RA, Wellenstein DE, Thomas FD, Bassano DA, Raasch BN, et al. Density patterns in the normal lung as determined by computed tomography. *Radiology.* (1980) 137:409–16. doi: 10.1148/radiology.137.2.7433674

17. Slutsky RA, Peck WW, Higgins CB, Mancini GBJ. Pulmonary density distribution in experimental and clinical cardiogenic pulmonary edema evaluated by computed transmission tomography. *Am Heart J.* (1984) 108:401–7. doi: 10.1016/0002-8703(84)90632-X

18. Hudsmith LE, Petersen SE, Francis JM, Robson MD, Neubauer S. Normal human left and right ventricular and left atrial dimensions using steady state free precession magnetic resonance imaging. *J Cardiovasc Magn Reson.* (2005) 7:775–82. doi: 10.1080/10976640500295516

19. Fischer U, Baumgartner A, Arnold M, Nedeltchev K, Gralla J, De Marchis GM, et al. What is a minor stroke? *Stroke.* (2010) 41:661–6. doi: 10.1161/STROKEAHA.109.572883

20. Harkness A, Ring L, Augustine DX, Oxborough D, Robinson S, Sharma V, et al. Normal reference intervals for cardiac dimensions and function for use in echocardiographic practice: a guideline from the British Society of Echocardiography. *Echo Res Pract.* (2020) 7:G1–G18. doi: 10.1530/ERP-19-0050

21. Kim WJ, Nah HW, Kim DH, Cha JK. Association between left ventricular dysfunction and functional outcomes at three months in acute ischemic stroke. *J Stroke Cerebrovasc Dis.* (2016) 25:2247–52. doi: 10.1016/j.jstrokecerebrovasdis.2016.05.004

22. Powers WJ, Rabinstein AA, Ackerson T, Adeoye OM, Bambakidis NC, Becker Ket alOn Behalf of The American Heart Association Stroke Council. Guidelines for the early management of patients with acute ischemic stroke: 2019 update to the 2018 guidelines for the early management of acute ischemic stroke: a guideline for healthcare professionals from the American Heart Association/American Stroke Association. *Stroke* (2019);50:e344–e418, Doi: 10.1161/STR.0000000000000211

23. Khatami F, Saatchi M, Zadeh SST, Aghamir ZS, Shabestari AN, Reis LO, et al. A meta-analysis of accuracy and sensitivity of chest CT and RT-PCR in COVID-19 diagnosis. *Sci Rep.* (2020) 10:22402. doi: 10.1038/s41598-020-80061-2

24. Hope MD, Raptis CA, Henry TS. Chest computed tomography for detection of coronavirus disease 2019 (COVID-19): don't rush the science. *Ann Intern Med.* (2020) 173:147–8. doi: 10.7326/M20-1382

25. Wheatley-Guy CM, Sajgalik P, Cierzan BS, Wentz RJ, Johnson BD. Validation of radiofrequency determined lung fluid using thoracic CT: findings in acute decompensated heart failure patients. *Int J Cardiol Heart Vasc.* (2020) 30:100645. doi: 10.1016/j.ijcha.2020.100645

26. Ribeiro CMC, Marchiori E, Rodrigues R, Gasparetto E, Souza AS, Escuissato D, et al. Hydrostatic pulmonary edema: high-resolution computed tomography aspects. *J Bras Pneumol.* (2006) 32:515–22. doi: 10.1590/S1806-37132006000600008

27. Cardinale L, Priola AM, Moretti F, Volpicelli G. Effectiveness of chest radiography, lung ultrasound and thoracic computed tomography in the diagnosis of congestive heart failure. *World J Radiol*. (2014) 6:230–7. doi: 10.4329/wjr.v6.i6.230

28. Barile M, Hida T, Hammer M, Hatabu H. Simple quantitative chest CT for pulmonary edema. *Eur J Radiol Open*. (2020) 7:100273. doi: 10.1016/j.ejro.2020.100273

29. Morooka N, Watanabe S, Masuda Y, Inagaki Y. Estimation of pulmonary water distribution and pulmonary congestion by computed tomography. *Jpn Heart J*. (1982) 23:697–709. doi: 10.1536/ihj.23.697

30. Kato S, Nakamoto T, Iizuka M. Early diagnosis and estimation of pulmonary congestion and edema in patients with left-sided heart diseases from histogram of pulmonary CT number. *Chest*. (1996) 109:1439–45. doi: 10.1378/chest.109.6.1439

31. Jain CC, Tschirren J, Reddy YNV, Melenovsky V, Redfield M, Borlaug BA. Subclinical pulmonary congestion and abnormal hemodynamics in heart failure with preserved ejection fraction. *JACC Cardiovasc Imaging*. (2022) 15:629–37. doi: 10.1016/j.jcmg.2021.09.017

32. Vergani G, Cressoni M, Crimella F, L'Acqua C, Sisillo E, Gurgitano M, et al. A morphological and quantitative analysis of lung CT scan in patients with acute respiratory distress syndrome and in cardiogenic pulmonary edema. *J Intensive Care Med*. (2020) 35:284–92. doi: 10.1177/0885066617743477

33. Vasan RS, Larson MG, Benjamin EJ, Evans JC, Levy D. Left ventricular dilatation and the risk of congestive heart failure in people without myocardial infarction. *N Engl J Med*. (1997) 336:1350–5. doi: 10.1056/NEJM199705083361903

34. Yeboah J, Bluemke DA, Hundley WG, Rodriguez CJ, Lima JA, Herrington DM. Left ventricular dilation and incident congestive heart failure in asymptomatic adults without cardiovascular disease: multi-ethnic study of atherosclerosis (MESA). *J Card Fail*. (2014) 20:905–11. doi: 10.1016/j.cardfail.2014.09.002

frontiers | Frontiers in Neurology

TYPE Original Research
PUBLISHED 17 August 2023
DOI 10.3389/fneur.2023.1207795

OPEN ACCESS

EDITED BY
Yanlin Zhang,
Second Affiliated Hospital of Soochow University, China

REVIEWED BY
Manoj Kumar Mahata,
Belle Vue Clinic, India
Shuhong Luo,
RayBiotech, United States

*CORRESPONDENCE
Yihua An
✉ riveran@ccmu.edu.cn

RECEIVED 29 April 2023
ACCEPTED 26 July 2023
PUBLISHED 17 August 2023

CITATION
Wang S, Tan S, Chen F and An Y (2023) Identification of immune-related biomarkers co-occurring in acute ischemic stroke and acute myocardial infarction.
Front. Neurol. 14:1207795.
doi: 10.3389/fneur.2023.1207795

Identification of immune-related biomarkers co-occurring in acute ischemic stroke and acute myocardial infarction

Shan Wang[1], Shengjun Tan[2], Fangni Chen[3] and Yihua An[4]*

[1]Emergency Station, Dougezhuang Community Health Service Center, Beijing, China, [2]Key Laboratory of Zoological Systematics and Evolution, Institute of Zoology, Chinese Academy of Sciences, Beijing, China, [3]Department of Nuclear Medicine, The Fifth Medical Center of the General Hospital of the People's Liberation Army, Beijing, China, [4]Department of Neurosurgery, Sanbo Brain Hospital, Capital Medical University, Beijing, China

Background: Acute ischemic stroke (AIS) and acute myocardial infarction (AMI) share several features on multiple levels. These two events may occur in conjunction or in rapid succession, and the occurrence of one event may increase the risk of the other. Owing to their similar pathophysiologies, we aimed to identify immune-related biomarkers common to AIS and AMI as potential therapeutic targets.

Methods: We identified differentially expressed genes (DEGs) between the AIS and control groups, as well as AMI and control groups using microarray data (GSE16561 and GSE123342). A weighted gene co-expression network analysis (WGCNA) approach was used to identify hub genes associated with AIS and/or AMI progression. The intersection of the four gene sets identified key genes, which were subjected to functional enrichment and protein–protein interaction (PPI) network analyses. We confirmed the expression levels of hub genes using two sets of gene expression profiles (GSE58294 and GSE66360), and the ability of the genes to distinguish patients with AIS and/or AMI from control patients was assessed by calculating the receiver operating characteristic values. Finally, the investigation of transcription factor (TF)-, miRNA-, and drug–gene interactions led to the discovery of therapeutic candidates.

Results: We identified 477 and 440 DEGs between the AIS and control groups and between the AMI and control groups, respectively. Using WGCNA, 2,776 and 2,811 genes in the key modules were identified for AIS and AMI, respectively. Sixty key genes were obtained from the intersection of the four gene sets, which were used to identify the 10 hub genes with the highest connection scores through PPI network analysis. Functional enrichment analysis revealed that the key genes were primarily involved in immunity-related processes. Finally, the upregulation of five hub genes was confirmed using two other datasets, and immune infiltration analysis revealed their correlation with certain immune cells. Regulatory network analyses indicated that *GATA2* and hsa-mir-27a-3p might be important regulators of these genes.

Conclusion: Using comprehensive bioinformatics analyses, we identified five immune-related biomarkers that significantly contributed to the pathophysiological mechanisms of both AIS and AMI. These biomarkers can be used to monitor and prevent AIS after AMI, or vice versa.

KEYWORDS

acute ischemic stroke, acute myocardial infarction, immune response, neutrophils, CIBERSORT, weighted gene co-expression network analysis, bioinformatics

Introduction

Cardiovascular diseases (CVDs)—including stroke and ischemic heart diseases—pose a significant global health burden, affecting millions of people and causing substantial morbidity and mortality (1). Two of the most severe CVDs, acute ischemic stroke (AIS) and acute myocardial infarction (AMI), frequently become a heavy burden on families and society (2). Although the causes of AIS and AMI are unclear, their pathophysiologies are similar in principle: deficient blood and oxygen supply to the brain or heart. They are typically caused by sudden arterial blockage, which can be caused by the formation of a blood clot (thrombus) or plaque buildup (atherosclerosis). This blockage results in the deprivation of oxygen and nutrients to the surrounding tissues, leading to ischemia and necrosis of the affected tissues (3). The concurrence of AIS and AMI has also been reported in one patient (4, 5). They can occur simultaneously or in close temporal succession and are risk factors for one another (6). For example, the incidence of ischemic stroke (IS) after AMI is 4–5% (7, 8), while patients with AMI who concomitantly experience AIS are at a substantially higher risk of both in-hospital (>8-fold increase) and 1-year mortality (>3-fold increase) than patients with AMI alone (9). Similar treatments, such as reperfusion therapy or catheter-based thrombectomy, are used to treat AIS and AMI; however, these diseases occur suddenly and have a narrow therapeutic window. To improve patient outcomes, attempts, e.g., faster and more convenient diagnoses, are needed to shorten the treatment delay.

Inflammation is a key contributor to the development and progression of both cardiac and brain ischemia, and immune cells play a crucial role in the pathophysiology of CVDs as they are involved in inflammation and tissue injury (10–13). The systematic inflammatory response is activated after AIS or AMI and is involved in the entire process of these two diseases (14, 15). The neuroinflammatory response disrupts the blood–brain barrier in AIS, leading to the migration of macrophages, monocytes, lymphocytes, and other inflammatory cells to the ischemic site (16, 17). Studies have also shown that peripheral immune cells can contribute to secondary neurodegeneration after AIS by infiltrating the brain and interacting with resident brain cells (18). For AMI, various immune cells and genes participate in immunomodulation after an acute event, working together to rebuild injured areas and remove necrotic tissue (15). Chronic inflammation can also contribute to the development of atherosclerosis, which is a major risk factor for both conditions. Therefore, exploring the immune microenvironment and inflammatory mechanisms of AIS and AMI may identify potential immunoregulatory therapies as alternative treatment methods.

Genetic factors can influence the expression and activity of various immune and inflammatory molecules, which in turn can affect the severity and outcome of AIS and AMI. Certain genetic variants have been associated with an increased risk of AIS (19). Several studies have shown that dysregulated genes, long non-coding RNAs, and miRNAs are potential biomarkers of either AIS or AMI (20–22). For example, elevated expression of *MMP9* has been detected in patients with AMI when compared with controls, and plasma levels of *MMP9* and *NT-proBNP* have a time-dependent relationship (23). Understanding the genetic basis of immunoinflammatory mechanisms involved in AIS and AMI may help identify new therapeutic targets and improve patient outcomes. However, only a limited number of studies have focused on identifying biomarkers for the diagnosis of these diseases (14, 24). According to a family study, AIS and AMI share several genetic characteristics (25); therefore, there is an urgent need to screen for immune-related biomarkers of both diseases.

In our study, we acquired two datasets (GSE16561 and GSE123342) for identifying differentially expressed genes (DEGs) between individuals diagnosed with AIS or AMI and their respective control groups. Using weighted gene co-expression network analysis (WGCNA), we aimed to identify hub genes associated with AIS/AMI progression. Important genes were further analyzed using gene ontology (GO) and protein–protein interaction (PPI) network analyses, and CIBERSORT was used to analyze immune cell infiltration in AIS and AMI. Finally, the investigation of transcription factor (TF)-, miRNA-, and drug–gene interactions discovered the possible therapeutic candidates.

Materials and methods

Acquisition of expression data

Figure 1 shows the basic workflow of our study for identifying potential biomarkers of AIS and/or AMI. By searching for expression data related to AIS and AMI in the Gene Expression Omnibus (GEO) database (http://www.ncbi.nlm.nih.gov/geo/), we decided to focus on two datasets that contain sufficient samples to perform a comparative study: GSE16561 was acquired using the GPL6883 platform and contained a total of 39 AIS samples and 24 control samples; GSE123342 was obtained using the GPL17586 platform and consisted of 67 AMI samples and 22 control samples with stable coronary heart disease. These two datasets were used to identify key biomarkers of AIS and AMI.

We downloaded another two datasets from GEO to validate gene expression. GSE58294, which included 69 IS and 23 control samples, was created using the GPL570 platform. Onset among the 69 IS samples included three time points (3 h, 5 h, and 24 h). In this study, the 23 IS samples in the 3 h group were treated as AIS, while the 5 h and 24 h groups were treated as post-AIS. GSE66360, which included 49 patients with AMI and 50 healthy controls, was also created using the GPL570 platform.

GSE123342 contained additional myocardial infarction (MI) samples 30 days ($n = 64$) and 365 days ($n = 37$) after AMI. We used this dataset in conjunction with GSE66360 to investigate the temporal expression patterns of key genes identified in AIS and/or AMI.

Data pre-processing and screening of DEGs

The microarray data were pre-processed before analysis. We found that the series matrix file of GSE16561 contained numerous NA values; therefore, we downloaded the raw profiling file. Expression values were then log2 transformed. For genes targeted by more than one probe, the median expression levels were calculated. We only retained protein-coding genes with a stable

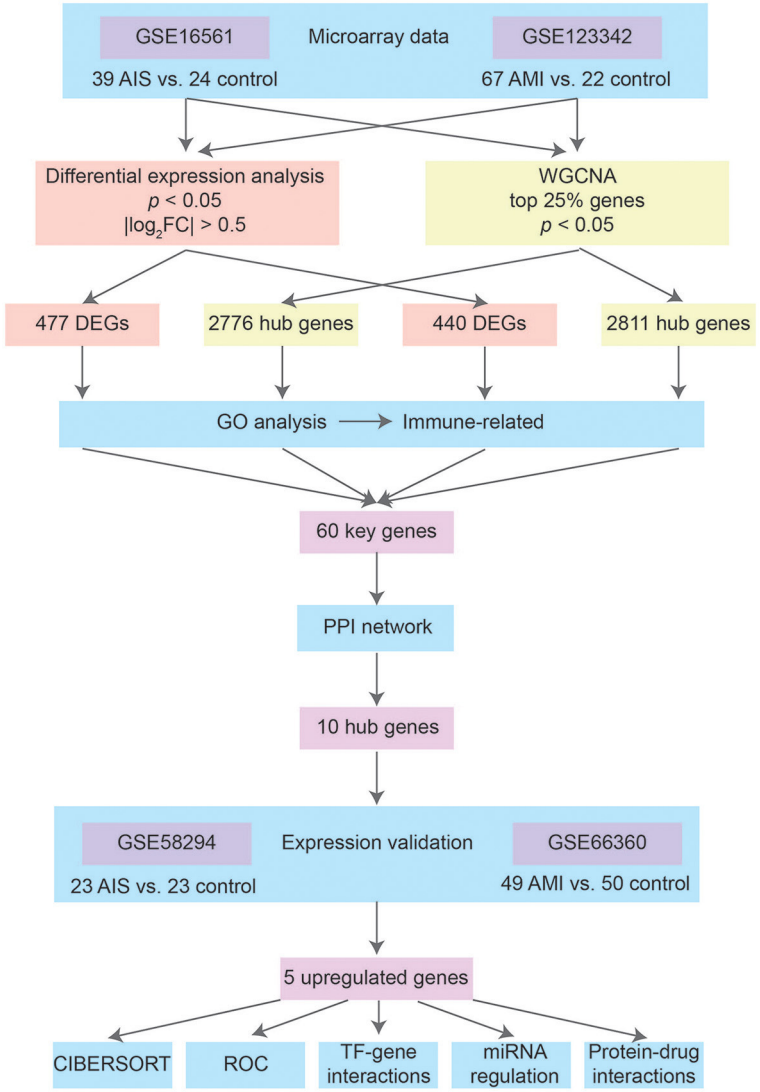

FIGURE 1
Workflow of the study.

gene symbol and the Ensembl gene id; other genes, such as long non-coding RNAs and pseudogenes, were excluded.

The identification of DEGs in GSE16561 and GSE123342 was based on the limma package in R. DEGs in AIS and AMI were filtered using the following cutoff criteria: an adjusted *p*-value of <0.05 and $|\log_2 FC| > 0.5$.

Construction of WGCNA

The gene expression matrix was standardized by scaling after pre-processing. Subsequently, the WGCNA package in R was used to identify hub genes. The initial dataset consisted of the highest variance genes, which comprised the top 25% of genes in the normalized gene expression matrix file. The samples were clustered using the average linkage method in WGCNA. The scale independence and average connectivity were calculated and used to obtain a scale-free network. The similarity matrix was converted into an adjacency matrix, which was then used to calculate the topological overlap matrix (TOM) values. Genes were hierarchically clustered based on the dissimilarity measure (1-TOM) derived from the TOM values, and the dynamic tree-cut (DTC) method was used to identify modules. The minimum module size for the resulting dendrogram was set to 30 genes. Close modules with a threshold of 0.25 were merged.

Functional enrichment analysis

After retrieving four gene sets, the DEGs of AIS and AMI and hub genes of AIS and AMI in the key modules of WGCNA, the clusterProfiler R package was used to perform functional enrichment analysis, i.e., GO. Significantly enriched terms were identified based on an adjusted *p*-value of <0.01. GO enrichment analysis included biological processes (BPs), cellular components (CCs), and molecular functions (MFs). Common GO terms

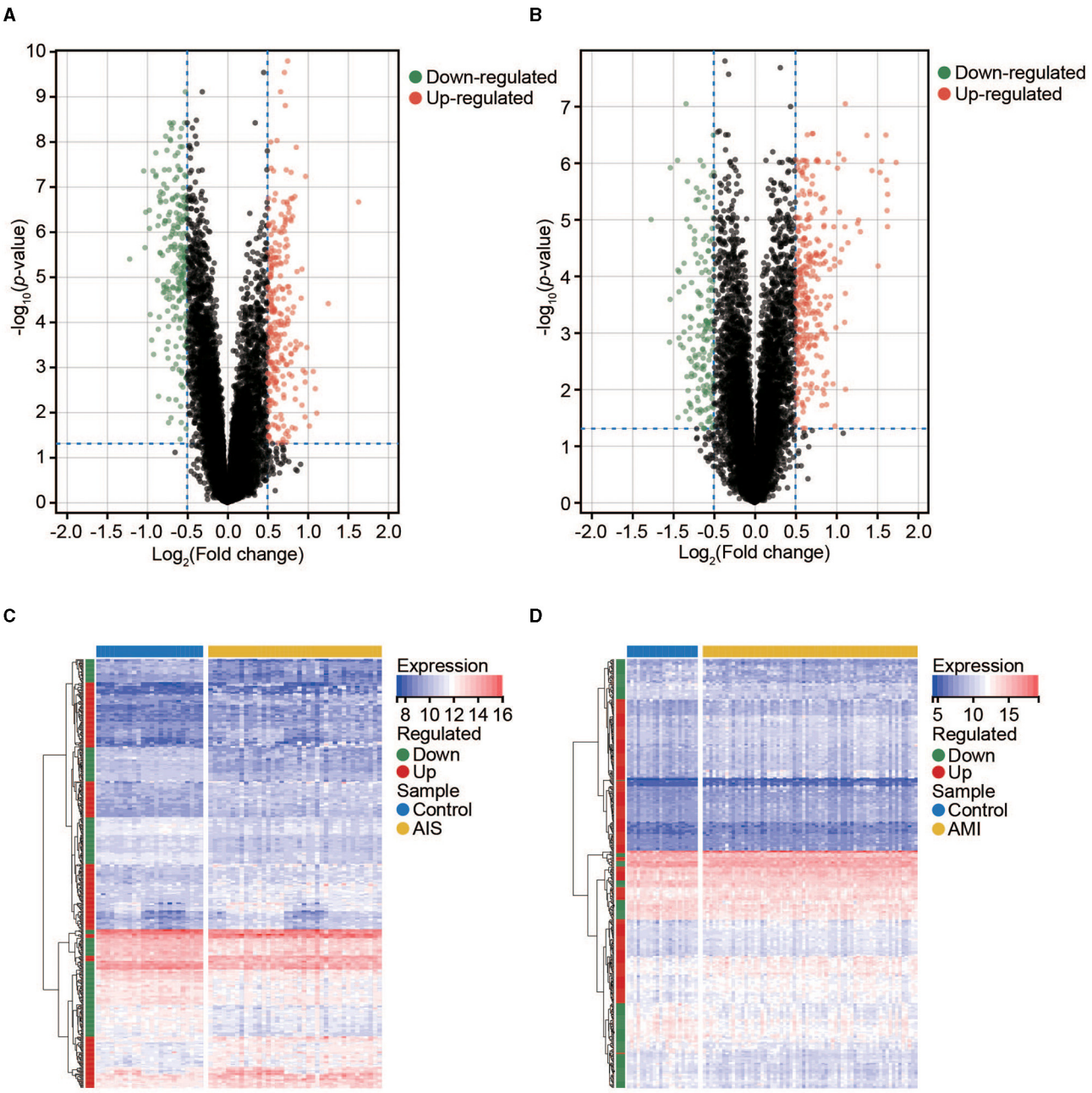

FIGURE 2
Expression profile of DEGs in AIS and AMI. **(A)** Volcano map of DEGs in AIS. **(B)** Volcano map of DEGs in AMI. **(C)** Clustered heatmap of DEGs in AIS. **(D)** Clustered heatmap of DEGs in AMI.

among the four gene sets were identified by overlapping the aforementioned results.

PPI network

From the four gene sets, 60 key genes were identified and subjected to the construction of the PPI network in the STRING database (26), where a threshold of 0.4 was set as the minimum confidence interaction score. The PPI network was visualized and analyzed using Cytoscape 3.9.1 (27). Functional enrichment analyses of the PPI network, including BP analysis, Reactome pathway analysis, and annotated keywords in UniProt were conducted using STRING. The MCC method in Cytoscape was employed to identify the 10 hub genes with the highest connection scores.

Immune cell infiltration analysis

The CIBERSORT algorithm is a widely used computational tool that enables the estimation of the infiltration levels of 22

10.3389/fneur.2023.1207795

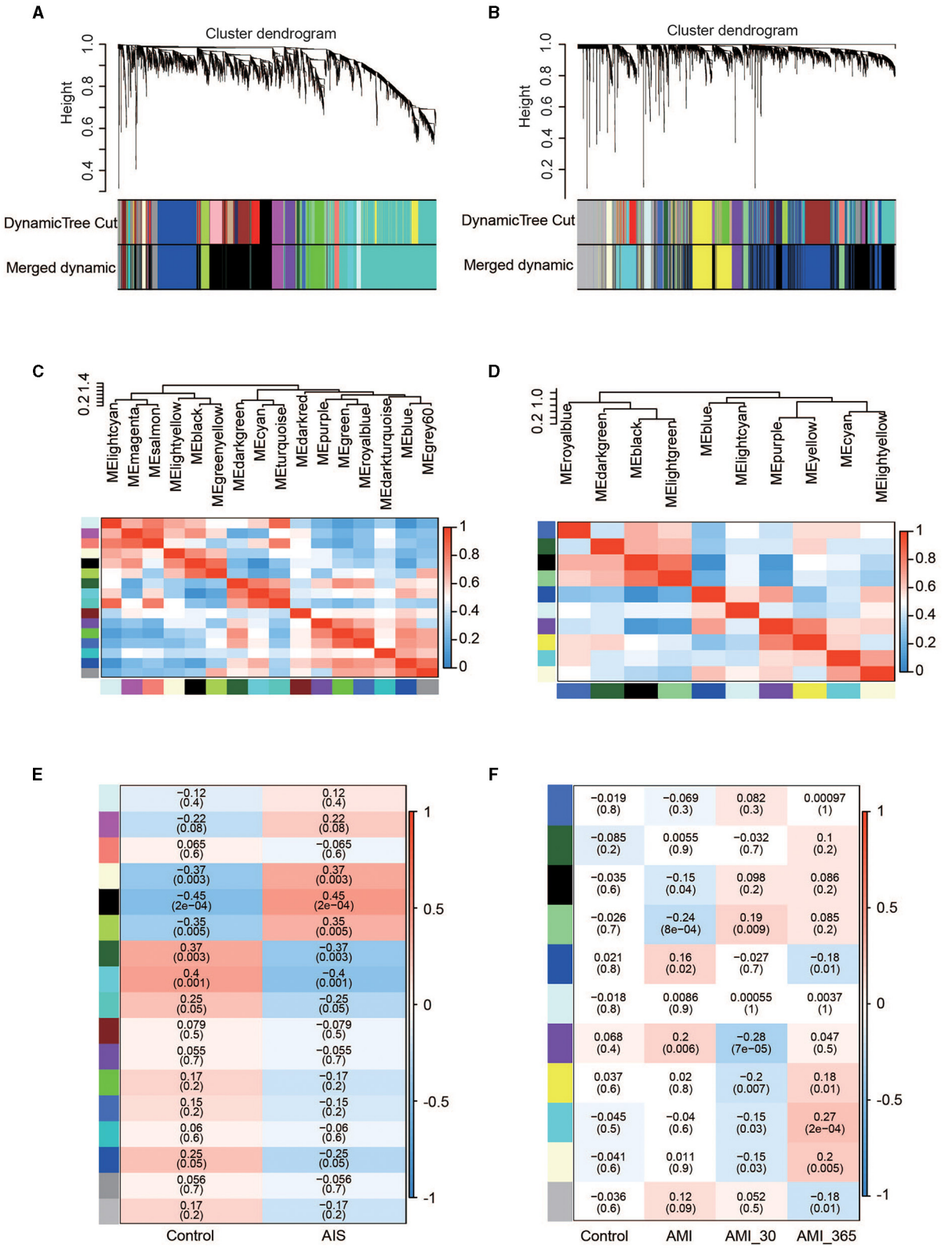

FIGURE 3
Co-expression networks in AIS and AMI. **(A)** Gene dendrogram obtained by average linkage hierarchical clustering in AIS. The row underneath the dendrogram shows the module assignment determined by the dynamic tree cut. **(B)** Gene dendrogram obtained by average linkage hierarchical clustering in AMI. **(C)** Relationship among all modules in AIS. **(D)** Relationship among all modules in AMI. **(E)** Correlation coefficients of the WGCNA modules between the control and AIS groups. **(F)** Correlation coefficients of the WGCNA modules between the control, AMI, and post-AMI groups.

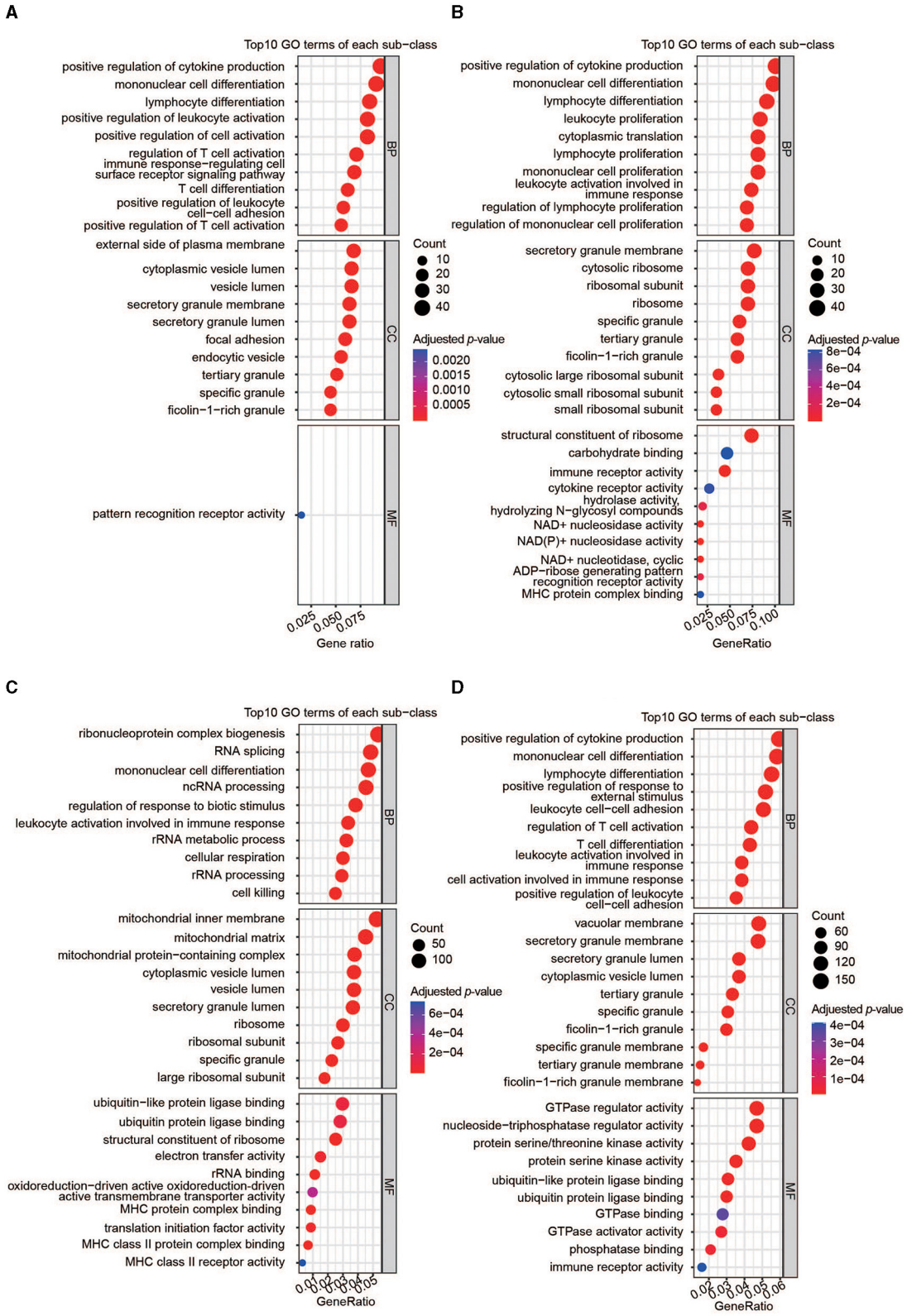

FIGURE 4
Functional analyses of the important genes. **(A)** GO enrichment analysis of DEGs in AIS. **(B)** GO enrichment analysis of DEGs in AMI. **(C)** GO enrichment analysis of hub genes in AIS. **(D)** GO enrichment analysis of hub genes in AMI.

different immune cell types in various diseases. We downloaded the default LM22 signature matrix file and R package according to the instructions on the CIBERSORT website. The relative proportion of immune cells was calculated for AIS and AMI samples, and Spearman's correlation coefficient was used to determine the strength and direction of the relationship between genes and immune cells.

TF-, miRNA-, and drug–gene interaction analyses

After validation, five upregulated genes in AIS and AMI were selected as target genes. Three networks—including the TF-gene, miRNA-gene, and drug–protein interaction networks—were analyzed for the target genes in NetworkAnalyst using the JASPAR, TarBase (version 8.0), and DrugBank (version 5.0) software packages.

Results

DEGs in AIS and AMI

We used the limma package in R to conduct DEG analysis on the microarray transcriptome data of the AIS and control samples or AMI and control samples. In total, 477 and 440 DEGs were identified in the AIS and AMI samples, respectively (Figures 2A, B). The expression profiles of these DEGs are shown in Figures 2C, D; among them, 225 were downregulated and 252 were upregulated in the AIS samples, whereas 165 were downregulated and 275 were upregulated in the AMI samples (Figures 2A, B). These DEGs were further considered to be candidate transcriptional signatures.

Key modules and hub genes

To identify groups of genes with highly correlated expression patterns across the AIS and AMI samples, we performed a co-expression analysis of all genes using the WGCNA R package. As no obvious outlier samples were detected in the sample clustering, we did not exclude any samples from the subsequent WGCNA. The top 25% of genes with the highest degree of variation in both datasets were subsequently chosen as the input. We selected soft thresholds of 7 for AIS and 10 for AMI when $R^2 >$ 0.85 (Supplementary Figure 1) and identified 16 and 10 modules, respectively (Figures 3A–D). Based on the correlation coefficients between the sample groups and modules, we selected the key modules as those significantly related to AIS and AMI (Figures 3E, F). A total of 2,776 and 2,811 genes were incorporated into these key modules, respectively.

Functional enrichment analysis

Four gene sets were included for gene enrichment analysis: the DEGs and hub genes identified through WGCNA in AIS and AMI. Generally, the most important genes are enriched in immune-related processes (Figures 4A–D). We then selected the most common GO terms among the four gene lists, with a p-value of <0.01 as the cutoff. Among the 77 BP terms shared by all four datasets, 54 (70.1%) were related to immunity (Supplementary Table 1), for example, positive regulation of cytokine production, lymphocyte differentiation, positive regulation of leukocyte activation, regulation of T-cell activation, and leukocyte-mediated immunity. CC outcomes showed that most proteins were located on the membrane (Supplementary Table 1), suggesting that they may participate in immune responses.

PPI of the key genes

Overlaps between the four datasets identified 60 key genes (Figure 5A), with 60 nodes and 63 edges in the PPI network (Figure 5B and Supplementary Figure 1). Functional enrichment in the network also demonstrated that the key genes were immune-related. The top five BP terms were T-cell differentiation involved in immune response, positive T-cell selection, triglyceride biosynthetic process, response to oleic acid, and positive regulation of myeloid dendritic cell activation (Figure 5C). The significantly enriched Reactome pathways included the immune system, innate immune system, neutrophil degranulation, immunoregulatory interactions between a lymphoid and a non-lymphoid cell, and toll-like receptor 4 (TLR4) cascade (Figure 5D). Significantly enriched annotated keywords in UniProt were transmembrane helix, glycoprotein, disulfide bond, innate immunity, immunity, and adaptive immunity (Figure 5E). Finally, a topological analysis helped identify the top 10 hub genes: *ITGAM*, *CD2*, *CD3E*, *CD163*, *GZMK*, *ARG1*, *CD3G*, *HIF1A*, *ACSL1*, and *CD96* (Figure 5F).

Validation of the hub genes

We found that five hub genes were upregulated (expressed at a significantly higher level in patients with AIS/AMI than in control samples), whereas five other genes were significantly downregulated in patients with AIS/AMI (Figures 6A, B). The expression patterns of these genes were validated using two other microarray transcriptome datasets from patients with AIS and AMI. The upregulated expression patterns of *ITGAM*, *CD163*, *ARG1*, *HIF1A*, and *ACSL1* were confirmed in both datasets (Figures 6C, D). Moreover, samples from GSE58294 were classified into three time groups: 3 h, 5 h, and 24 h after AIS. The results showed that these genes were consistently upregulated in all three IS groups compared with the control group; the highest expression level was usually reached at 5 h post-AIS (Figure 6E). Similarly, samples from GSE123342 were classified into three time groups: acute phase, 30 days after AMI, and 365 days after AMI. Five genes were upregulated in the acute phase, and their expression levels decreased to normal after 30 days when compared with the control group (Figure 6F). Combining these results, we concluded that the high expression of these genes can last up to 24 h, after which their expression levels begin to decrease to normal levels.

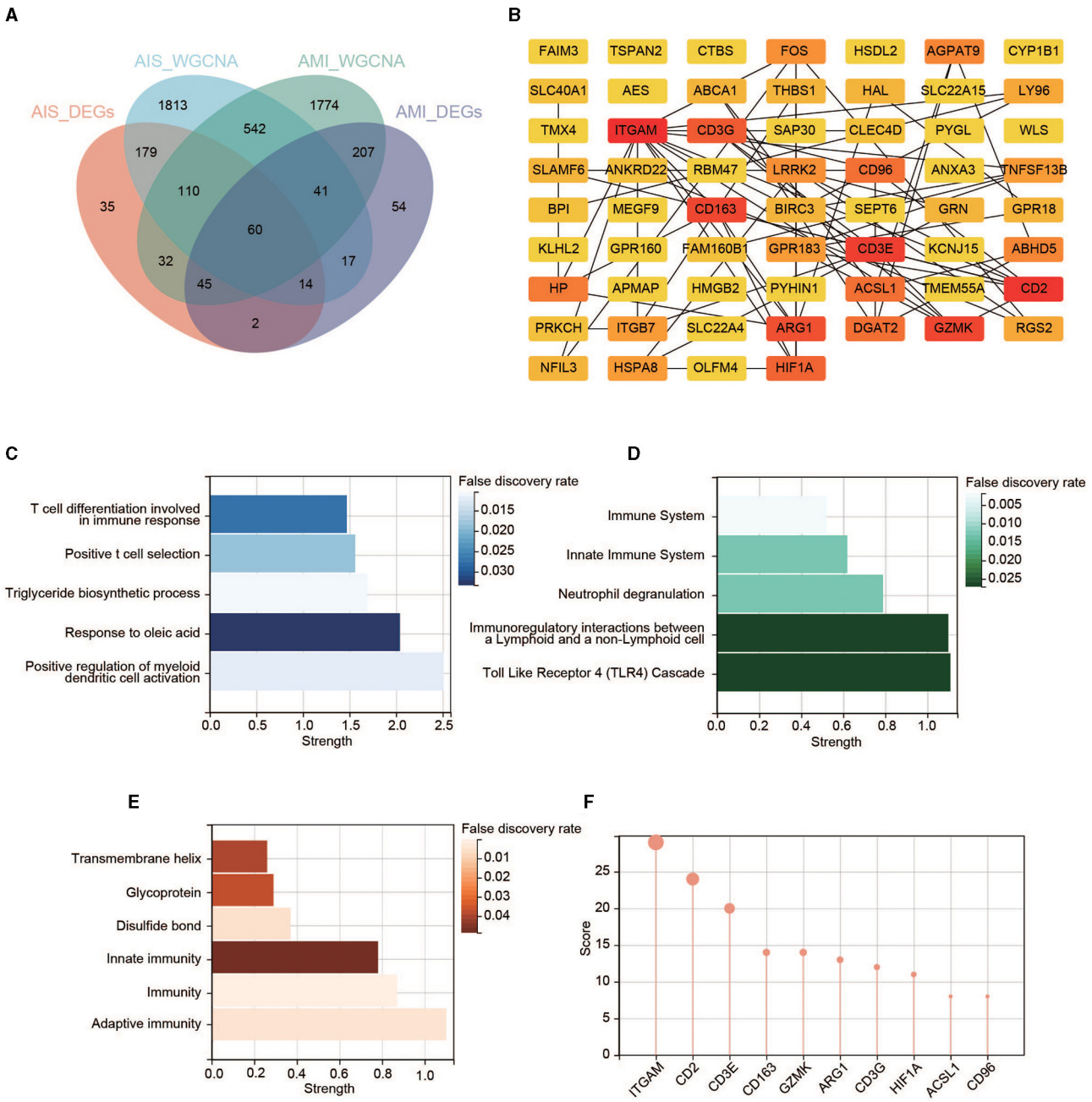

FIGURE 5
Identification of the key genes. **(A)** Venn diagram of the four gene sets. **(B)** PPI network of the 60 key genes. Colors from yellow to red represent the low-to-high MCC score. **(C)** GO enrichment analysis in the PPI network. **(D)** Reactome pathway analysis in the PPI network. **(E)** Annotated keywords in UniProt enrichment analysis in the PPI network. **(F)** Top 10 genes in the PPI network ranked by the MCC method.

The potential of hub genes as diagnostic markers

To evaluate the diagnostic power of the five immune-related biomarkers for AIS and AMI, receiver operating characteristic (ROC) analysis was performed on multiple datasets. The AUC values were then obtained for ITGAM, CD163, ARG1, HIF1A, and ACSL1, which were 0.89, 0.97, 0.94, 0.79, and 0.79 in GSE16561 (Figure 7A); 0.78, 0.78, 0.80, 0.77, and 0.73 in GSE58294 (Figure 7B); 0.75, 0.90, 0.89, 0.72, and 0.85 in GSE123342 (Figure 7C); and 0.72, 0.85, 0.66, 0.77, and 0.88 in GSE66360 (Figure 7D), respectively.

Immune infiltration analysis

To further investigate the significance of the identified genes, we examined the levels of infiltrating immune cells in AIS and AMI as suggested by GO analysis, highlighting their immune-related functionality. In the AIS samples, the most prominent

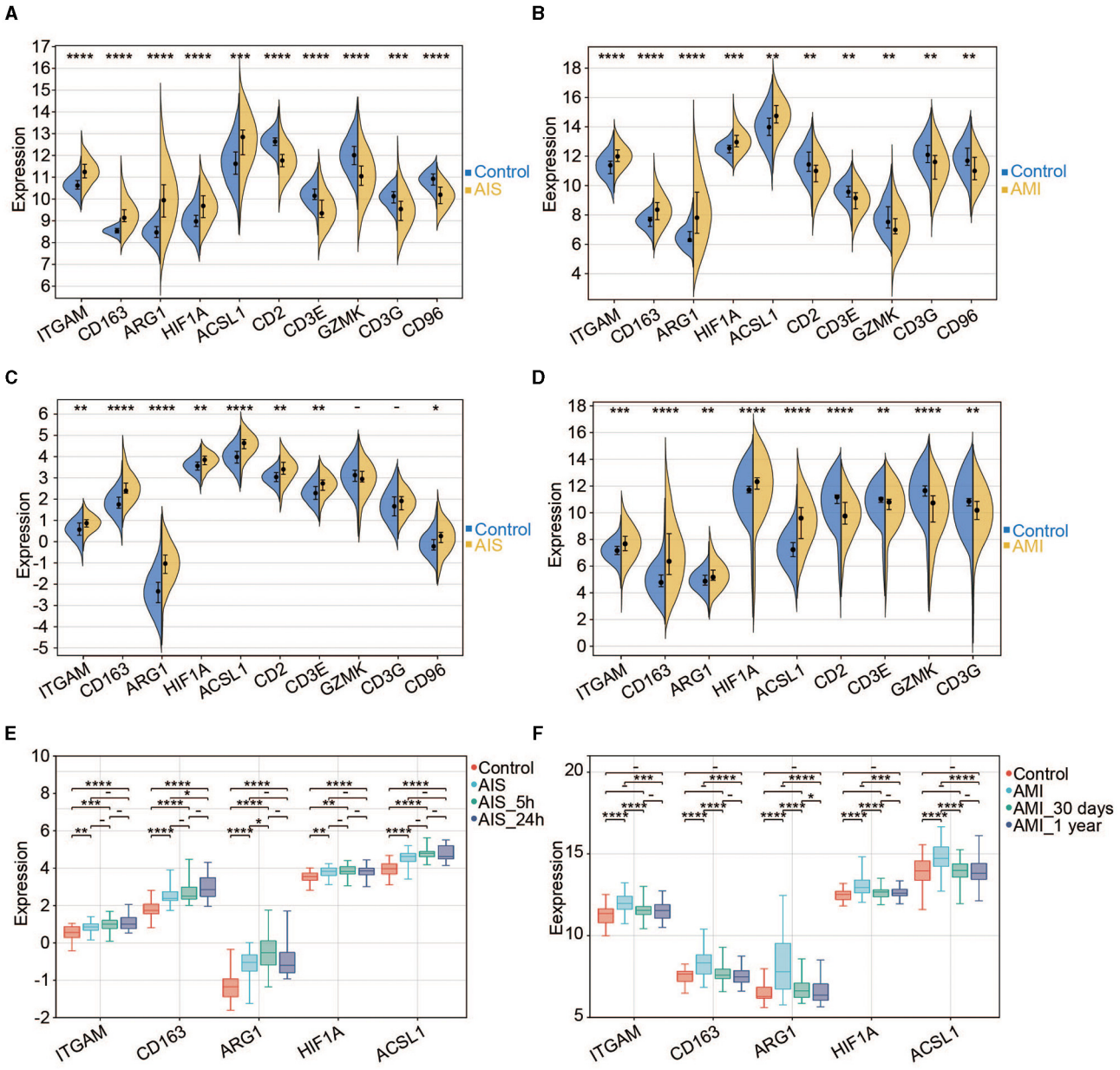

FIGURE 6
Expression pattern of the hub genes. **(A)** Expression profiles of the 10 hub genes in the control and AIS groups (GSE16561). **(B)** Expression profiles of the 10 hub genes in the control and AMI groups (GSE123342). **(C)** Expression profiles of the 10 hub genes in the control and AIS groups (GSE58294). **(D)** Expression profiles of the nine hub genes in the control and AIS groups (GSE66360). *CD96* does not have a probe in GSE66360. **(E)** Expression profiles of the five hub genes among different time points for AIS (GSE58294). **(F)** Expression profiles of the five hub genes among different time points for AMI (GSE123342). $^{*}P < 0.05$, $^{**}P < 0.01$, $^{***}P < 0.001$, and $^{****}P < 0.0001$.

infiltrating immune cells were monocytes, neutrophils, and CD8+ T cells (Figure 8A); the AMI samples were characterized by an abundance of neutrophils (Figure 8B). Compared with the control group, patients with AIS and AMI exhibited significantly elevated levels of neutrophils and lower levels of memory B cells and CD8+ T cells (Figures 8C, D). Investigation of the relationship between the five genes and immune cells revealed that all genes exhibited a significantly positive correlation with neutrophils and a significantly negative correlation with CD8+ T cells in both the AIS and AMI samples (Figures 8E, F).

Construction of TF-, miRNA-, and drug–gene interactions

We identified 34 TFs that targeted the five hub genes using the JASPAR software package in NetworkAnalyst. Nine key TFs—*GATA2*, *NR2F1*, *FOXC1*, *YY1*, *MEF2A*, *NFIC*, *SRF*, *NFKB1*, and *IRF2*—have a node degree value of ≥2 (Figure 9A).

One hundred and thirty-eight miRNAs targeting the five hub genes were obtained from NetworkAnalyst using TarBase. Hsa-mir-27a-3p and hsa-mir-1-3p targeted three genes, whereas

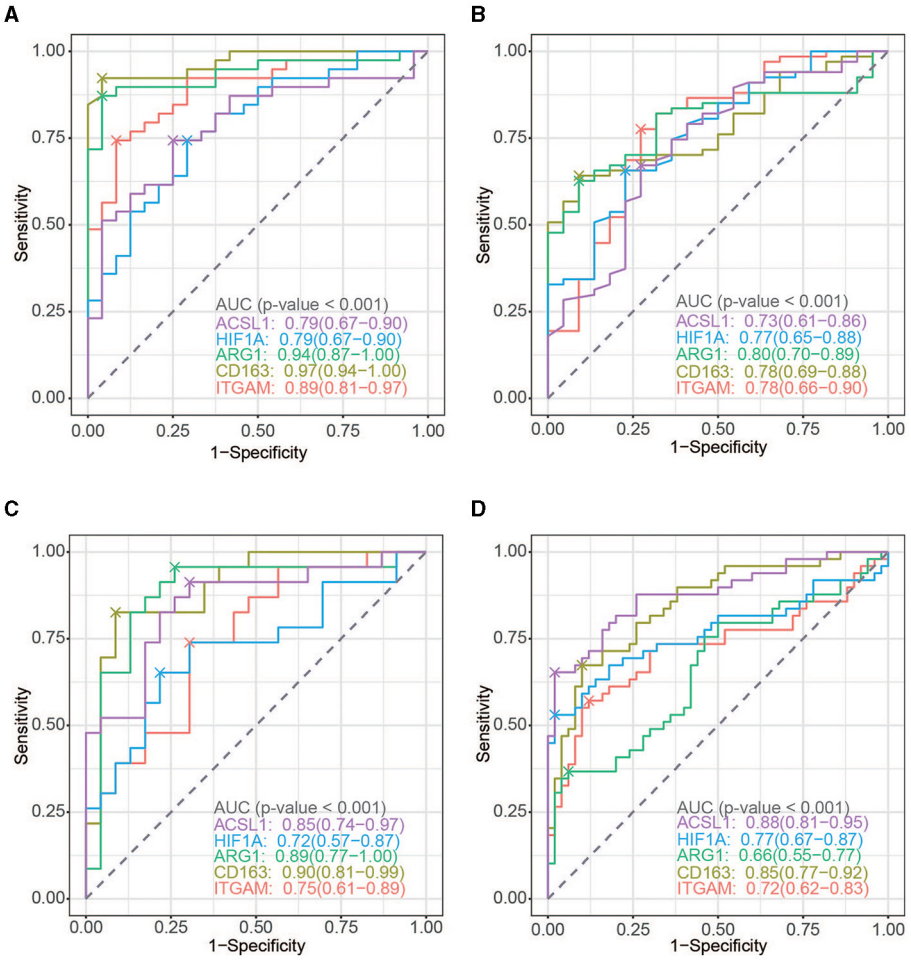

FIGURE 7
ROC curve analysis. **(A)** ROC curve of the five hub genes in AIS (GSE16561). **(B)** ROC curve of the five hub genes in AMI (GSE123342). **(C)** ROC curve of the five hub genes in AIS (GSE58294). **(D)** ROC curve of the five hub genes in AIS (GSE66360).

hsa-mir-30a-5p, hsa-mir-107, hsa-mir-7-5p, hsa-mir-34a-5p, hsa-mir-191-5p, hsa-mir-429, hsa-mir-10b-5p, hsa-mir-373-3p, hsa-mir-124-3p, hsa-mir-16-5p, hsa-mir-27a-5p, and hsa-mir-26a-5p targeted two genes (Figure 9B).

Drug-targeting proteins encoded by *ARG1* and *HIF1A* were identified in NetworkAnalyst using DrugBank (version 5.0). Eleven therapeutic drugs interacted with ARG1 (Figure 9C), and three drugs interacted with HIF1A (Figure 9D); no drugs targeted ITGAM, CD163, or ACSL1.

Discussion

As two of the most prominent causes of mortality and disability worldwide, AIS and AMI share several genetic characteristics (25). A growing consensus has been reached regarding the importance of early prevention of AIS and AMI. Microarray analysis is a valuable tool for identifying susceptibility genes for AIS and AMI and may ultimately lead to improved diagnosis, prevention, and treatment of the disease. In the present study, we identified five hub genes (*ITGAM*, *CD163*, *ARG1*, *HIF1A*, and *ACSL1*) using integrated analyses of AIS and AMI datasets, including DEG, WGCNA, GO enrichment, PPI network, and regulatory network analyses. We also verified the upregulation of these five genes in AIS and AMI samples. On the one hand, these identified genes have the potential to serve as biomarkers for the diagnosis of patients with AIS or AMI. On the other hand, studies have shown that these diseases could be risk factors for one another. Therefore, these biomarkers can be used to monitor and prevent AIS after AMI or vice versa.

Atherosclerosis, characterized by inflammatory cell accumulation in the arterial walls, is a well-known instance of chronic arterial inflammation and is commonly regarded as the pathological foundation for both AIS and AMI (28). The arterial narrowing can result in decreased blood flow and oxygen supply to the heart muscle, ultimately leading to the development of AIS and/or AMI. Immune cells play a fundamental role in the pathophysiology of atherosclerosis (10), and there is a genetic basis for the inflammatory pathogenesis of AIS and/or AMI. For example, the plasma levels of specific immune-inflammatory markers were reduced with atorvastatin treatment in AIS (29). Certain KIR genes and HLA alleles may modulate cytokine and cell-mediated inflammatory activation, which could contribute

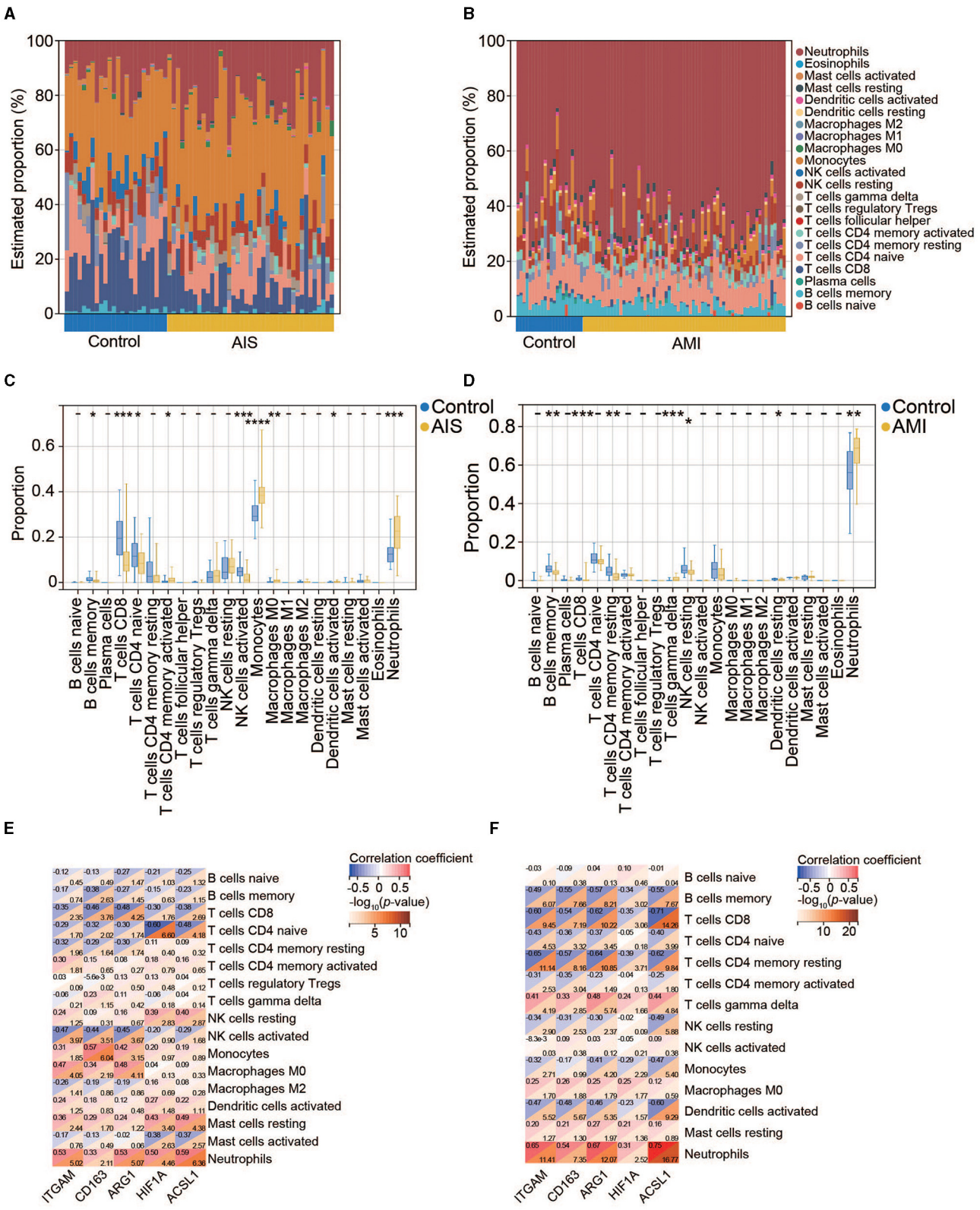

FIGURE 8
Immune cell infiltration analysis. **(A)** Percentage distribution of 22 immune cell subtypes in GSE16561. **(B)** Percentage distribution of 22 immune cell subtypes in GSE123342. **(C)** The difference in immune cell infiltration between the control and AIS groups. **(D)** The difference in immune cell infiltration between the control and AMI groups. **(E)** Correlation between the five hub genes and immune cells in AIS. **(F)** Correlation between the five hub genes and immune cells in AMI.

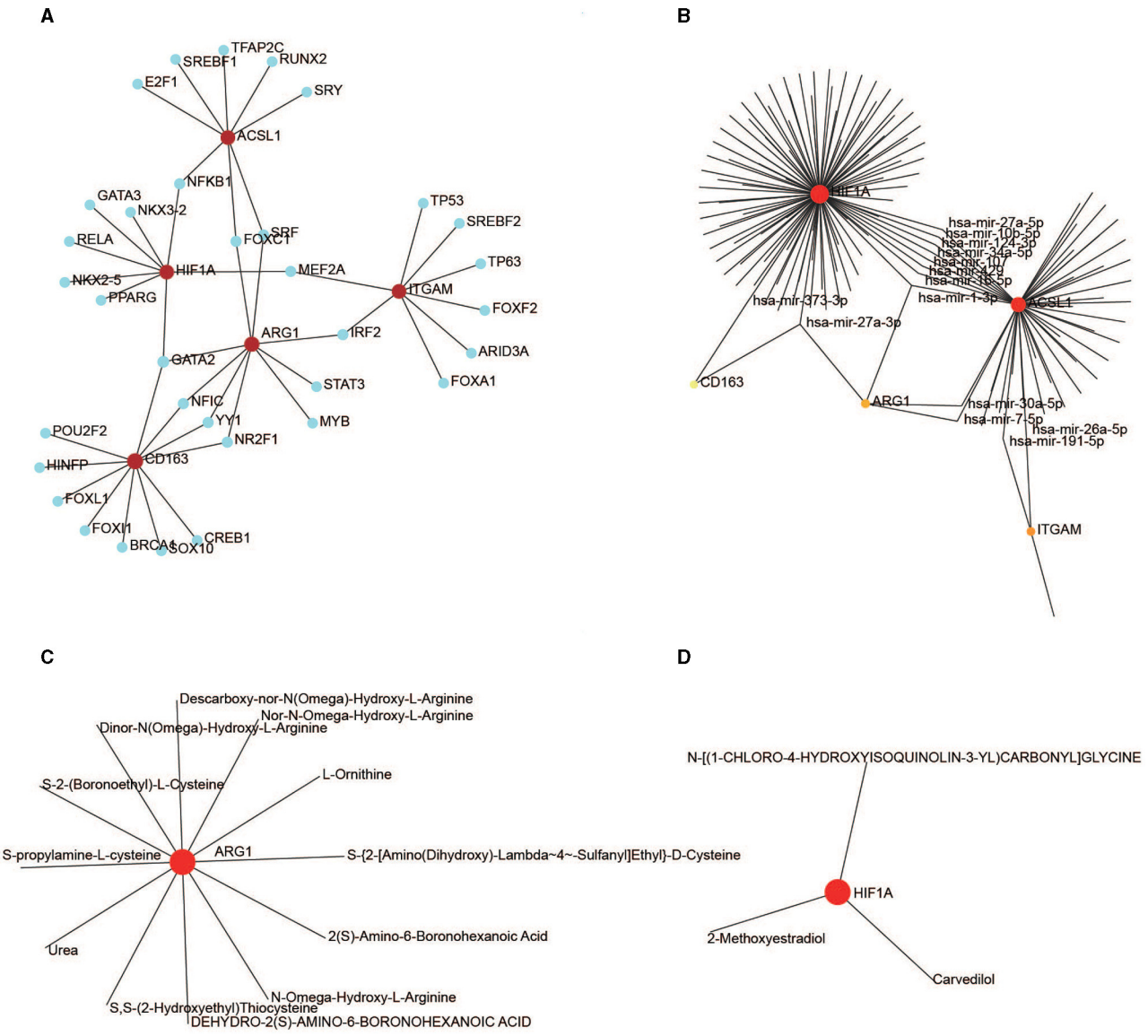

FIGURE 9
Regulation of the hub genes. **(A)** TF-gene interaction for the five hub genes. **(B)** MiRNA-gene interaction for the five hub genes. **(C)** Drug-ARG1 interaction. **(D)** Drug-HIF1A interaction.

to stroke occurrence and severity after AIS (19, 30). Similarly, we found that important genes (DEG and WGCNA) were always enriched in immune responses, representing an important medium between inflammation and atherosclerosis. They are involved in the regulation of multiple immune cell types, such as B cells, T cells, lymphocytes, and leukocytes (Figure 4), suggesting that the migration of these cells to AIS and AMI sites may release pro-inflammatory factors and help disrupt the blood barrier.

When concentrating on the Reactome enrichment of the PPI network, several signaling pathways were detected, such as the TLR4 cascade and neutrophil degranulation (Figure 5D). Activation of TLR4 triggers the biosynthesis of diverse mediators of inflammation (31), and neutrophil degranulation is a common feature of many inflammatory disorders, including AIS and AMI (32). Coincidentally, we found a significantly greater proportion of neutrophils in the AIS/AMI group than in the control group (Figures 8C, D). Neutrophils are the first to be recruited to AIS and AMI sites (33, 34) and have pathophysiological relevance in AIS and AMI; for example, the presence of neutrophils in the brain can exacerbate impairment of the blood–brain barrier. We found that gene expression levels were significantly positively correlated with the proportion of neutrophils among the 22 immune cells (Figures 8E, F). For the first time, we demonstrated that immune modulation by neutrophils in AIS and AMI could potentially target ITGAM, CD163, ARG1, HIF1A, and ACSL1, thereby establishing a theoretical rationale for immune-targeted interventions in AIS and AMI.

The immune functions of these five genes in AIS and AMI were partially elucidated in previous studies. *ITGAM* encodes the integrin alpha M chain, which binds neutrophils and monocytes

to the stimulated endothelium; additionally, it was demonstrated to function as a receptor for complement component 3, thereby contributing to the inflammatory response (35). In particular, the upregulation of *ITGAM* expression, which indicates increased inflammatory activation of immune cells, has been observed in patients with thrombus (36) and is thus associated with AIS and AMI (37, 38).

CD163, which is primarily expressed by monocytes and macrophages, serves as a scavenger of haptoglobin–hemoglobin complexes. Specifically, CD163 is considered a marker of alternatively activated or anti-inflammatory macrophages. Studies have shown that the soluble form of CD163 could be a potential biomarker in AIS and AMI (39, 40).

ARG1 is an enzyme that can modulate the synthesis of nitric oxide (NO) in the immune system. By suppressing the release of NO from macrophages, ARG1 can inhibit the production of pro-inflammatory cytokines (41). Similar bioinformatics-based approaches identified ARG1 as a potential biomarker in AIS and AMI (24, 42).

HIF1A is a TF that governs oxygen availability during inflammatory responses in the pathogenesis of AIS. Moreover, it is responsible for NLRP3 inflammasome-initiated pyroptosis following IS (43). An experiment in transgenic mice demonstrated that overexpression of *HIF1A* led to reduced infarct size and enhanced cardiac function 4 weeks after AMI (44).

Elevated triglyceride levels were observed in the peripheral white blood cells of patients with AMI. This finding can be attributed to the upregulation of *ACSL1*, which suppresses fatty acid β-oxidation via the PPARγ pathway, resulting in increased triglyceride levels (45). However, the functional role of *ACSL1* in AIS remains still unclear.

Our investigation revealed that gene expression levels increased within the first 3–24 h of AIS onset (Figure 6E). Consistently, another study based on microarray data showed that a comprehensive alteration in the gene expression profile, including that of *ARG1*, was discernible in the peripheral blood cells of patients with AIS within 3–24 h after onset (46). Subsequently, the gene expression decreased to normal levels after 30 days (Figure 6F), indicating an instantaneous role of these genes after AMI. In the future, sequencing data of both AIS and AMI at more time points should be obtained to reveal clearer molecular dynamics and physiological details during IS and MI development.

In our study, we found that GATA2 interacts with three biomarkers: ARG1, CD163, and HIF1A. Similarly, hsa-mir-27a-3p regulates these three biomarkers. As a vital TF in multilineage hematopoiesis, mutations in *GATA2* induce several hematological diseases (47). *GATA2* is upregulated in ischemia-reperfusion injury (48); additionally, there is a link between GATA2 deficiency and AIS (49). Interestingly, hsa-mir-27a-3p alleviates cerebral ischemia-reperfusion injury by targeting FOXO1 (50), therefore playing a significant therapeutic role in the management of AIS. According to our results, both GATA2 and hsa-mir-27a-3p can target ARG1, CD163, and HIF1A; thus, it is possible that they may function in the same pathway in AIS and AMI. Further investigations are required to elucidate the mechanism by which GATA2 and hsa-mir-27a-3p co-modulate ARG1, CD163, and HIF1A expression in AIS and AMI.

We identified 12 drugs targeting HIF1A, and three drugs targeting ARG1, which have therapeutic potential to treat patients with AIS and AMI. Conducting a range of laboratory-based trials can thus facilitate the determination of the efficacy of a compound and offer alternative solutions to immunotherapy for AIS and AMI.

In conclusion, we have addressed the scarcity of studies investigating common biomarkers derived from the shared pathological characteristics of both AIS and AMI using comprehensive bioinformatics analyses. Second, we have delved into potential targets for five biomarkers in the immune microenvironment of AIS and AMI, such as neutrophils, which expanded our understanding of these diseases. Third, while previous studies have provided partial elucidation of these five biomarkers primarily through experiments, we not only confirmed their importance in the pathophysiology of AIS and AMI but also established the value of microarray analysis for identifying susceptibility genes associated with both conditions. Finally, the identification of GATA2 and hsa-mir-27a-3p as agents capable of targeting ARG1, CD163, and HIF1A suggest that these two elements may function within the same pathway in both AIS and AMI.

There are limitations in our study as well. The analysis was conducted using data from public databases that originated from various platforms, which had different inclusion criteria and lacked corresponding clinical data in general. Additionally, it is important to note that our study is confined to the transcriptome level, and further validation of the findings is necessary through prospective clinical and basic experiments.

Data availability statement

The original contributions presented in the study are included in the article/Supplementary material, further inquiries can be directed to the corresponding author.

Ethics statement

Ethical review and approval was not required for the study on human participants in accordance with the local legislation and institutional requirements. Written informed consent from the patients/participants or patients/participants' legal guardian/next of kin was not required to participate in this study in accordance with the national legislation and the institutional requirements.

Author contributions

YA and SW designed the study and wrote the manuscript. ST performed the data analysis. FC revised the manuscript. All authors contributed to the article and approved the submitted version.

Acknowledgments

We thank GEO for providing the sequencing data.

Conflict of interest

The authors declare that the research was conducted in the absence of any commercial or financial relationships

that could be construed as a potential conflict of interest.

Publisher's note

All claims expressed in this article are solely those of the authors and do not necessarily represent those of their affiliated organizations, or those of the publisher, the editors and the reviewers. Any product that may be evaluated in this article, or claim that may be made by its manufacturer, is not guaranteed or endorsed by the publisher.

Supplementary material

The Supplementary Material for this article can be found online at: https://www.frontiersin.org/articles/10.3389/fneur.2023.1207795/full#supplementary-material

References

1. Morovatdar N, Avan A, Azarpazhooh MR, Di Napoli M, Stranges S, Kapral MK, et al. Secular trends of ischaemic heart disease, stroke, and dementia in high-income countries from 1990 to 2017: the global burden of disease study 2017. *Neurol Sci.* (2022) 43:255–64. doi: 10.1007/s10072-021-05259-2

2. Tsao CW, Aday AW, Almarzooq ZI, Alonso A, Beaton AZ, Bittencourt MS, et al. Heart disease and stroke statistics—2022 update: a report from the American heart association. *Circulation.* (2022) 145:e153–639. doi: 10.1161/CIR.0000000000001052

3. Widimský P, Kožnar B, Vaško P, Peisker T, Štětkářová I. Acute myocardial infarction and acute stroke: what are the differences? Focus on reperfusion therapy. *Cor et Vasa.* (2013) 55:e111–6. doi: 10.1016/j.crvasa.2013.02.002

4. Bao CH, Zhang C, Wang XM, Pan YB. Concurrent acute myocardial infarction and acute ischemic stroke: Case reports and literature review. *Front Cardiovasc Med.* (2022) 9:1012345. doi: 10.3389/fcvm.2022.1012345

5. Chin PL, Kaminski J, Rout M. Myocardial infarction coincident with cerebrovascular accidents in the elderly. *Age Ageing.* (1977) 6:29–37. doi: 10.1093/ageing/6.1.29

6. Boyanpally A, Cutting S, Furie K. Acute ischemic Stroke associated with myocardial infarction: challenges and management. *In Seminars Neurol.* (2021) 41:331–9. doi: 10.1055/s-0041-1726333

7. Ulvenstam A, Kajermo U, Modica A, Jernberg T, Söderström L, Mooe T. Incidence, trends, and predictors of ischemic stroke 1 year after an acute myocardial infarction. *Stroke.* (2014) 45:3263–8. doi: 10.1161/STROKEAHA.114.005770

8. Loh E, Sutton MS, Wun CC, Rouleau JL, Flaker GC, Gottlieb SS, et al. Ventricular dysfunction and the risk of stroke after myocardial infarction. *New Eng J Med.* (1997) 336:251–7. doi: 10.1056/NEJM199701233360403

9. Al Suwaidi J, Al Habib K, Asaad N, Singh R, Hersi A, Al Falaeh H, et al. Immediate and one-year outcome of patients presenting with acute coronary syndrome complicated by stroke: findings from the 2ndgulf registry of acute coronary events (Gulf RACE-2). *BMC Cardiovasc Disord.* (2012) 12:1–9. doi: 10.1186/1471-2261-12-64

10. Hansson GK. Inflammation, atherosclerosis, and coronary artery disease. *New Eng J Med.* (2005) 352:1685–95. doi: 10.1056/NEJMra043430

11. Zotova L. Immune checkpoint inhibitors-related myocarditis: a review of reported clinical cases. *Diagnostics.* (2023) 13:1243. doi: 10.3390/diagnostics13071243

12. Schiffer WB, Deych E, Lenihan DJ, Zhang KW. Coronary and aortic calcification are associated with cardiovascular events on immune checkpoint inhibitor therapy. *Int J Cardiol.* (2021) 322:177–82. doi: 10.1016/j.ijcard.2020.08.024

13. Hu JR, Florido R, Lipson EJ, Naidoo J, Ardehali R, Tocchetti CG, et al. Cardiovascular toxicities associated with immune checkpoint inhibitors. *Cardiovasc Res.* (2019) 115:854–68. doi: 10.1093/cvr/cvz026

14. Zheng PF, Liao FJ, Yin RX, Chen LZ Li H, Nie RJ, Wang Y, et al. Genes associated with inflammation may serve as biomarkers for the diagnosis of coronary artery disease and ischaemic stroke. *Lipids Health Dis.* (2020) 19:1–0. doi: 10.1186/s12944-020-01217-7

15. Ong SB, Hernández-Reséndiz S, Crespo-Avilan GE, Mukhametshina RT, Kwek XY, Cabrera-Fuentes HA, et al. Inflammation following acute myocardial infarction: multiple players, dynamic roles, and novel therapeutic opportunities. *Pharmacol Ther.* (2018) 186:73–87. doi: 10.1016/j.pharmthera.2018.01.001

16. Amantea D, Micieli G, Tassorelli C, Cuartero MI, Ballesteros I, Certo M, et al. Rational modulation of the innate immune system for neuroprotection in ischemic stroke. *Front Neurosci.* (2015) 9:147. doi: 10.3389/fnins.2015.00147

17. Yang C, Hawkins KE, Doré S, Candelario-Jalil E. Neuroinflammatory mechanisms of blood-brain barrier damage in ischemic stroke. *Am J Physiol Cell Physio.* (2019) 316:C135–53. doi: 10.1152/ajpcell.00136.2018

18. Jones KA, Maltby S, Plank MW, Kluge M, Nilsson M, Foster PS, et al. Peripheral immune cells infiltrate into sites of secondary neurodegeneration after ischemic stroke. *Brain Behav Immun.* (2018) 67:299–307. doi: 10.1016/j.bbi.2017.09.006

19. Tuttolomondo A, Di Raimondo D, Pecoraro R, Casuccio A, Di Bona D, Aiello A, et al. HLA and killer cell immunoglobulin-like receptor (KIRs) genotyping in patients with acute ischemic stroke. *J Neuroinflammation.* (2019) 16:1–5. doi: 10.1186/s12974-019-1469-5

20. Tiedt S, Prestel M, Malik R, Schieferdecker N, Duering M, Kautzky V, et al. RNA-Seq identifies circulating miR-125a-5p, miR-125b-5p, and miR-143-3p as potential biomarkers for acute ischemic stroke. *Circ Res.* (2017) 121:970–80. doi: 10.1161/CIRCRESAHA.117.311572

21. He GD, Huang YQ, Liu L, Huang JY, Lo K, Yu YL, et al. Association of circulating, inflammatory-response exosomal mRNAs with acute myocardial infarction. *Front Cardiovas Med.* (2021) 8:712061. doi: 10.3389/fcvm.2021.712061

22. Yin X, Wang X, Wang S, Xia Y, Chen H, Yin L, et al. Screening for regulatory network of miRNA–inflammation, oxidative stress and prognosis-related mrna in acute myocardial infarction: an in silico and validation study. *Int J Gen Med.* (2022) 3:1715–31. doi: 10.2147/IJGM.S354359

23. Orn S, Manhenke C, Squire IB, Ng L, Anand I, Dickstein K. Plasma MMP-2, MMP-9 and N-BNP in long-term survivors following complicated myocardial infarction: relation to cardiac magnetic resonance imaging measures of left ventricular structure and function. *J Card Fail.* (2007) 13:843–9. doi: 10.1016/j.cardfail.2007.07.006

24. Feng S, Li R, Zhou Q, Qu F, Hu W, Liu X. Bioinformatics analysis to identify potential biomarkers and therapeutic targets for ST-segment–elevation myocardial infarction-related ischemic stroke. *Front Neurol.* (2022) 13:894289. doi: 10.3389/fneur.2022.894289

25. Banerjee A, Lim CC, Silver LE, Welch SJ, Banning AP, Rothwell PM. Familial history of stroke is associated with acute coronary syndromes in women. *Circulation: Cardiovascular Genetics.* (2011) 4:9–15. doi: 10.1161/CIRCGENETICS.110.957688

26. Szklarczyk D, Gable AL, Lyon D, Junge A, Wyder S, Huerta-Cepas J, et al. STRING v11: protein–protein association networks with increased coverage, supporting functional discovery in genome-wide experimental datasets. *Nucleic Acids Res.* (2019) 47:D607–13. doi: 10.1093/nar/gky1131

27. Shannon P, Markiel A, Ozier O, Baliga NS, Wang JT, Ramage D, et al. Cytoscape: a software environment for integrated models of biomolecular interaction networks. *Genome Res.* (2003) 13:2498–504. doi: 10.1101/gr.1239303

28. Holmstedt CA, Turan TN, Chimowitz MI. Atherosclerotic intracranial arterial stenosis: risk factors, diagnosis, and treatment. *The Lancet Neurology.* (2013) 12:1106–14. doi: 10.1016/S1474-4422(13)70195-9

29. Tuttolomondo A, Di Raimondo D, Pecoraro R, Maida C, Arnao V, Della Corte V, et al. Early high-dosage atorvastatin treatment improved serum immune-inflammatory markers and functional outcome in acute ischemic strokes classified as large artery atherosclerotic stroke: a randomized trial. *Medicine.* (2016) 95:e3186. doi: 10.1097/MD.0000000000003186

30. Di Bona D, Scafidi V, Plaia A, Colomba C, Nuzzo D, Occhino C, et al. HLA and killer cell immunoglobulin-like receptors influence the natural course of CMV infection. *J Infect Dis.* (2014) 210:1083–9. doi: 10.1093/infdis/jiu226

31. Zughaier SM, Zimmer SM, Datta A, Carlson RW, Stephens DS. Differential induction of the toll-like receptor 4-MyD88-dependent and-independent signaling pathways by endotoxins. *Infect Immun.* (2005) 73:2940–50. doi: 10.1128/IAI.73.5.2940-2950.2005

32. Lacy P. Mechanisms of degranulation in neutrophils. *Allergy Asthma Clin Immunol.* (2006) 2:1–1. doi: 10.1186/1710-1492-2-3-98

33. Carbone F, Nencioni A, Mach F, Vuilleumier N, Montecucco F. Pathophysiological role of neutrophils in acute myocardial infarction. *Thromb Haemost.* (2013) 110:501–14. doi: 10.1160/TH13-03-0211

34. Zhao Z, Pan Z, Zhang S, Ma G, Zhang W, Song J, et al. Neutrophil extracellular traps: a novel target for the treatment of stroke. *Pharmacol Ther.* (2022) 6:108328. doi: 10.1016/j.pharmthera.2022.108328

35. Lavi S, Gruberg L, Kapeliovich M, Hammerman H, Boulos M, Grenadier E, et al. The impact of GP IIb/IIIa inhibitors during primary percutaneous coronary intervention in acute myocardial infarction patients. *J Invasive Cardiol.* (2005) 17:296–9.

36. Pfluecke C, Tarnowski D, Plichta L, Berndt K, Schumacher P, Ulbrich S, et al. Monocyte–platelet aggregates and CD11b expression as markers for thrombogenicity in atrial fibrillation. *Clin Res Cardiol.* (2016) 105:314–22. doi: 10.1007/s00392-015-0922-4

37. Wen S, Yan W, Wang L. mRNA expression disturbance of complement system related genes in acute arterial thrombotic and paroxysmal atrial fibrillation patients. *Ann Palliat Med.* (2020) 9:835–46. doi: 10.21037/apm.2020.04.18

38. Zhu X, Liu X, Liu Y, Chang W, Song Y, Zhu S. Uncovering the potential differentially expressed miRNAs and mRNAs in ischemic stroke based on integrated analysis in the gene expression omnibus database. *Eur Neurol.* (2020) 83:404–14. doi: 10.1159/000507364

39. Sun H, Zhang X, Ma J, Liu Z, Qi Y, Fang L, et al. Circulating soluble CD163: a potential predictor for the functional outcome of acute ischemic stroke. *Front Neurol.* (2021) 12:740420. doi: 10.3389/fneur.2021.740420

40. Shao X, Wu B, Chen P, Hua F, Cheng L, Li F, et al. Circulating CX3CR1+ CD163+ M2 monocytes markedly elevated and correlated with cardiac markers in patients with acute myocardial infarction. *Annals Translat Med.* (2020) 8:383. doi: 10.21037/atm-20-383

41. Murray PJ. Macrophage polarization. *Annu Rev Physiol.* (2017) 79:541–66. doi: 10.1146/annurev-physiol-022516-034339

42. Zhang R, Ji Z, Qu Y, Yang M, Su Y, Zuo W, et al. Clinical value of ARG1 in acute myocardial infarction patients: Bioinformatics-based approach. *Biomed Pharmacotherapy.* (2020) 121:109590. doi: 10.1016/j.biopha.2019.109590

43. Jiang Q, Geng X, Warren J, Cosky EE, Kaura S, Stone C, et al. Hypoxia inducible factor-1α (HIF-1α) mediates NLRP3 inflammasome-dependent-pyroptotic and apoptotic cell death following ischemic stroke. *Neuroscience.* (2020) 448:126–39. doi: 10.1016/j.neuroscience.2020.09.036

44. Kido M, Du L, Sullivan CC Li X, Deutsch R, Jamieson SW, Thistlethwaite PA. Hypoxia-inducible factor 1-alpha reduces infarction and attenuates progression of cardiac dysfunction after myocardial infarction in the mouse. *J Am Coll Cardiol.* (2005) 46:2116–24. doi: 10.1016/j.jacc.2005.08.045

45. Li T, Li X, Meng H, Chen L, Meng F. ACSL1 affects triglyceride levels through the PPARγ pathway. *Int J Med Sci.* (2020) 17:720. doi: 10.7150/ijms.42248

46. Tang Y, Xu H, Du XL, Lit L, Walker W, Lu A, et al. Gene expression in blood changes rapidly in neutrophils and monocytes after ischemic stroke in humans: a microarray study. *J Cereb Blood Flow Metabol.* (2006) 26:1089–102. doi: 10.1038/sj.jcbfm.9600264

47. Bresnick EH, Jung MM, Katsumura KR. Human GATA2 mutations and hematologic disease: how many paths to pathogenesis? *Blood Adv.* (2020) 4:4584–92. doi: 10.1182/bloodadvances.2020002953

48. Huang D, Chen D, Hu T, Liang H. GATA2 promotes oxidative stress to aggravate renal ischemia-reperfusion injury by up-regulating Redd1. *Mol Immunol.* (2023) 153:75–84. doi: 10.1016/j.molimm.2022.09.012

49. Bierman-Chow S, Holland SM, Hsu AP, Palmer C, Lynch J, Mina Y, et al. Clinical, Imaging, and laboratory findings in patients with GATA2 deficiency presenting with early-onset ischemic stroke. *Neurology.* (2023) 100:338–41. doi: 10.1212/WNL.0000000000201569

50. Li W, Zhu Q, Xu X, Hu X. MiR-27a-3p suppresses cerebral ischemia-reperfusion injury by targeting FOXO1. *Aging.* (2021) 13:11727. doi: 10.18632/aging.202866

frontiers | Frontiers in Neurology

TYPE Original Research
PUBLISHED 04 October 2023
DOI 10.3389/fneur.2023.1255524

OPEN ACCESS

EDITED BY
Yanlin Zhang,
Second Affiliated Hospital of Soochow University, China

REVIEWED BY
Rizaldy Taslim Pinzon,
Duta Wacana Christian University, Indonesia
Veronica Olavarria,
Clínica Alemana, Chile

*CORRESPONDENCE
Xiuquan Lin
✉ linxiuquan@fjmu.edu.cn
Xiaoxin Zheng
✉ xiaoxinzheng@whu.edu.cn
Min Chen
✉ minchen@fjmu.edu.cn

†These authors have contributed equally to this work

RECEIVED 09 July 2023
ACCEPTED 12 September 2023
PUBLISHED 04 October 2023

CITATION
Liang D, Guan Q, Huang M, He Y, Ou Y, Chen M, Zheng X and Lin X (2023) Changing trends of disease burden of stroke from 1990 to 2019 and its predictions among the Chinese population. *Front. Neurol.* 14:1255524. doi: 10.3389/fneur.2023.1255524

Changing trends of disease burden of stroke from 1990 to 2019 and its predictions among the Chinese population

Dong Liang[1,2†], Qing Guan[1†], Minqing Huang[2†], Yiyu He[3,4,5], Yangjiang Ou[6], Min Chen[1*], Xiaoxin Zheng[3,4,5*] and Xiuquan Lin[7,2*]

[1]The School of Health Management, Fujian Medical University, Fuzhou, Fujian, China, [2]The School of Public Health, Fujian Medical University, Fuzhou, Fujian, China, [3]Department of Cardiology, Renmin Hospital of Wuhan University, Wuhan, Hubei, China, [4]Cardiovascular Research Institute, Wuhan University, Wuhan, Hubei, China, [5]Hubei Key Laboratory of Cardiology, Wuhan, Hubei, China, [6]"The 14th Five-Year Plan" Application Characteristic Discipline of Hunan Province (Clinical Medicine), Hunan Provincial Key Laboratory of the Traditional Chinese Medicine Agricultural Biogenomics, Changsha Medical University, Changsha, Hunan, China, [7]Department for Chronic and Noncommunicable Disease Control and Prevention, Fujian Provincial Center for Disease Control and Prevention, Fuzhou, Fujian, China

Objective: This study aimed to understand the temporal trends in the disease burden of stroke and its attributable risk factors in China, along with the future trends in the next 25 years, that is important for effective prevention strategies and improvement, and to provide new insights into the age- and sex-specific incidence, prevalence, mortality, disability-adjusted life-years (DALYs) and their trends from 1990 to 2019, and the prediction in the next 25 years.

Methods: The Global Burden of Disease Study (2019) was used to extract the data on age- and sex-specific incidence, mortality, and disability-adjusted life-years (DALYs) of stroke in China, 1990–2019. We estimated the estimated annual percentage change (EAPC) to access the temporal trends of the disease burden of stroke. The R package called Nordpred was used to perform an age-period-cohort analysis to predict the prevalence of stroke.

Results: The number of incidence cases, deaths, and DALYs of stroke increased from 1990 to 2019. Overall downward trends were observed in the age-standardized incidence rate (ASIR) from 1990 to 2019. Significant temporal trends in mortality and DALYs of stroke were observed. High systolic blood pressure, smoking, and high-sodium diet were the main driving forces for stroke. The DALYs lost attributable to smoking were different for male and female patients. In the next 25 years, the number of new cases and deaths from stroke should continue to increase. The ASIR and age-standardized mortality rate (ASMR) should show a downward trend among male and female patients.

Conclusion: Despite the overall rates of stroke declined over the period from 1990 to 2019, the absolute number of people affected by stroke has substantially increased. There has been a substantial increase in the burden of stroke due to risk factors and will continue to increase in the next 25 years.

KEYWORDS

stroke, disease burden, temporal trend, risk factor, prediction

Introduction

Stroke is a global health issue, which can either be hemorrhagic (a rupture of a blood vessel) or ischemic (an occlusion of a blood vessel). Annually, 15 million people suffer a stroke worldwide, of which 5 million die, making it the second leading cause of death globally (1) and another 5 million are left permanently disabled. Stroke becomes the leading

cause of longtime disability, especially in low-income and middle-income countries (2). The Global Burden of Disease Study (GBD) 2019 estimated that deaths caused by stroke in China reached ∼4 million in 2019, and the incidence of stroke, including hemorrhagic stroke (IS) and ischemic stroke (HS), showed a general increasing trend in the past years (3). The number of stroke patients in China is likely to rise as a result of lifestyle and demographic changes, as well as inadequate control of major risk factors for stroke (4). Despite its implications and comorbidities, stroke still receives relatively less research or public attention. Stroke prevention and treatment are urgently needed in China due to its high incidence.

Both environmental and genetic factors contribute to ischemic and hemorrhage stroke disease. Some of these factors are not modifiable, such as age, gender, and family history, while others are potentially modifiable, such as hypertension, smoking, and higher sodium intake. It is possible to control and prevent strokes by modifying these potentially modifiable factors. There is a continuous, consistent, and independent relationship between blood pressure and the risk of developing stroke. Observational studies indicate that the risk of death from both ischemic heart disease and stroke increases beginning at systolic blood pressure as low as 115 mmHg. The mortality from stroke doubles with each increment of 20 mmHg systolic blood pressure (5). In a plethora of studies over the years, smoking has been identified as an independent risk factor for stroke. The relative risk for stroke ascribed to cigarette smoking is 1.5 (6). Dietary salt increases the risk of death from stroke, especially in overweight individuals, and higher sodium intake is associated with ∼89% increased risk for stroke mortality (7).

The latest Global Burden of Diseases (GBD) study (2019) has provided new epidemiological data on the incidence, mortality, and disability-adjusted life-years (DALYs) of stroke from 1990 to 2019, enabling us to provide updated estimates of the prevalence and risk factors for stroke in China. However, to the best of our knowledge, no published article has yet described the disease burden and attributable risk factors of stroke by age, sex, and year, and the future trends in the next 25 years of the disease burden of stroke in China. Therefore, we conducted a comprehensive and rigorously designed assessment of stroke incidence, mortality, and DALYs, stratified by age and gender. We also analyzed primary risk factors for stroke and forecasted its incidence and mortality rates in China over the next 25 years. The analysis of epidemiological trends and major risk factors of stroke as well as the prediction of future epidemiological trends in our study will be of great significance in reducing the incidence and mortality of stroke.

Materials and methods

The data of age- and sex-specific incidence, mortality, and disability-adjusted life-years (DALYs) of ischemic and hemorrhage stroke in China, 1990–2019, were derived from the Global Burden of Disease Study (2019). The estimated annual percentage change (EAPC) was estimated to access the temporal trends of disease burden of ischemic and hemorrhage stroke, and the R package called Nordpred was used to perform an age-period-cohort analysis to predict the numbers and rates of incidence and mortality for ischemic and hemorrhage stroke in the next 25 years.

Data sources

The data on incidence, mortality, and DALYs of ischemic and hemorrhage stroke were downloaded from the website of Institute for Health Metrics and Evaluation (IHME) (http://ghdx.healthdata.org/gbd-results-tool), and the rules of this selecting data were as follows: location name was "China," the cause was "stroke," and measures were "incidence," "mortality," and "DALYs." These indicators were calculated with 95% uncertainty intervals (95% UIs).

The WHO World Standard Population Distribution (2000–2025) was used as the standard population. The United Nations World Population Prospects 2019 Revision (https://population.un.Org/WPP/Download/Standard/Population/) was used as the prediction population. Ethics approval was not required as this study was based on publicly available data (GBD, 2019), and no personal data were collected.

Evaluation of ischemic and hemorrhage stroke burden

Estimates of the incidence and prevalence of ischemic and hemorrhage stroke were calculated with the DisMod-MR2.1 (disease-model-Bayesian meta-regression) modeling tool. DisMOd-MR is a Bayesian geospatial disease modeling software that uses various disease parameters, the epidemiological relationships between these parameters, and geospatial relationships to estimate incidence and prevalence. All available high-quality data on incidence, prevalence, and mortality were used to estimate the non-fatal ischemic and hemorrhage stroke burden. All-cause and cause-specific mortality for ischemic and hemorrhage stroke were estimated using the Cause of Death Ensemble modeling. DALYs were the sum of years lived with disabilities (YLDs) and years of life lost (YLLs). YLDs were calculated by multiplying the prevalence with the corresponding disability weights. YLLs were calculated by multiplying observed deaths for a specific age by global age-specific reference life expectancy. In the study, 95% UIs capturing both random and systematic error in statistical modeling were calculated for all estimates. For the risk factors, the comparative risk assessment (CRA) framework was used to estimate the proportion of DALYs attributable to three well-established risk factors for ischemic and hemorrhage stroke by age and sex: high fasting glucose, high systolic blood pressure, and smoking. The detailed study methods of GBD 2019 have been reported in previous studies (8–10).

Statistical analysis

The incidence, mortality, and DALYs of ischemic and hemorrhage stroke were performed by age group, sex, and year. The temporal trends for these indicators from 1990 to 2019 were plotted. The age was divided into 18 age groups at 5 years, and 0–39 years were combined into one age group. The time trends of age-standardized incidence (ASIR), age-standardized mortality (ASMR), and age-standardized DALY rates were described by the

estimated annual percentage change (EAPC) which was calculated from a regression model with the natural logarithm of the rate, that is, $\ln(\text{rate}) = \alpha + \beta \times (\text{calendar year}) + \varepsilon$. EAPC was defined as $100 \times (\exp(\beta) - 1)$. Its 95% confidence interval (95% CI) was also generated from the fitted model.

The power5 APC model of the R package called Nordpred which has been shown to perform well in predicting the trend of disease incidence and mortality (11, 12) was used to predict the number and rate of ischemic and hemorrhage stroke incidence and mortality in the next 25 years. Moreover, we estimated the number and rates of ischemic and hemorrhage stroke events by assuming that the events for ischemic and hemorrhage stroke remained stable, decreased, and increased by 1% per year based on the observed data of ischemic and hemorrhage stroke in 2019 in order to facilitate comparison with predicted results. We used the ggplot2 packages from the R program (Version 4.1.2; R core team, R Foundation for Statistical Computing, Vienna, Austria) to perform the visualization of the results.

Results

Incidence, mortality, and DALYs of ischemic and hemorrhage stroke in 2019

In 2019, the number of incidence cases and ASIR of ischemic and hemorrhage stroke among the total Chinese population were 3935.18 thousand (95% UI: 3431.72, 4579.87) and 200.84 per 100,000 (95% UI: 176.95, 230.84), respectively (Table 1). Ischemic and hemorrhage stroke contributed to 2189.18 thousand (95% UI: 1885.90, 2513.77) deaths in 2019, and ASMR was 127.25 per 100,000 (95% UI: 110.21, 144.89) among the total Chinese population (Table 2). Ischemic and hemorrhage stroke caused 45949.13 thousand (95% UI: 39813.51, 52335.53) DALYs in 2019, and the age-standardized rate of DALYs was 2412.52 per 100,000 (95% UI: 2102.92, 2742.48) (Table 3). The number and age-standardized rates of incidence, mortality, and DALYs are about the same for male and female patients (Tables 1–3).

Among the total population in 2019, the numbers of incidence cases, deaths, and DALYs of ischemic and hemorrhage stroke reached a peak aged 65–69 years, 80–84 years, and 70–74 years, respectively (Tables 1–3), and these trends were similar for males and female patients (Figure 1). In contrast, the number of incidence cases, deaths, and DALYs was lower among men than women over 90 years old (Figure 1).

A peak in incidence, mortality, and DALYs was observed among the total population aged 80–84 years, 95+ years, and 85–89 years, respectively (Tables 1–3). The trends of age-specific rates of incidence among female patients were similar to the trends for the total population, whereas the trends of age-specific rates of incidence among male patients increased with increasing age. In male patients, the age-specific rates of mortality and DALYs peaked at 90–94 years old. In female patients, the age-specific rates of mortality and DALYs increased with increasing age. In addition, the numbers and rates of incidence, deaths, and DALYs were concentrated in the elderly population (≥60 years old) (Figure 1).

Temporal trends of incidence, mortality, and DALYs of ischemic and hemorrhage stroke from 1990 to 2019

There has been a significant increase in the number of incidence of cases, deaths, and DALYs of ischemic and hemorrhage stroke among the total population from 1990 to 2019 (Tables 1–3). The number of incidence cases increased by more than two times among men ≥60 years old and women ≥50 years old during the study period (Figure 2A). The ASIR was 221.51 per 100,000 (95% UI: 196.81, 249.61) in 1990, which decreased in 2019, with an EAPC of −1.31 (95% CI: −3.41, 0.85) in the total population (Table 1). The ASIR of female patients decreased more significantly than that of male patients during this period [EAPC = −1.43, 95% CI: (−3.51, 0.69) vs. EAPC = −1.20, 95% CI: (−3.35, 1.01), respectively] (Table 1). Additionally, overall downward trends in the incidence rates were observed among both sexes in most age-specific groups, while short-term upward trends were observed between 1990 and 2000 among male patients (Figure 2B).

The ASMR decreased from 1990 [211.44 per 100,000 (95% UI: 187.68, 243.80)] to 2019, with an EAPC of −2.85 (95% CI: −4.68, −0.98) (Table 2). A decreasing trend of age-standardized DALYs was also observed during this period, and the EAPC was −2.83 (95%CI: −4.60, −1.02) (Table 3). Overall downward trends in mortality and DALY rate were observed in most age-specific groups and both sexes from 1990 to 2019 (Figures 2C, D).

Mortality and DALY rates of ischemic and hemorrhage stroke attributable to risk factors and their temporal trends from 1990 to 2019

The mortality that was attributed to high systolic blood pressure was the highest among men and women in all age-specific groups (Figure 3A). Trends of ischemic and hemorrhagic stroke mortality attributable to smoking were seen to grow at first and then decline, while decreasing trends of ischemic and hemorrhage stroke mortality attributable to smoking were observed in men in most age-specific groups. The overall downward trends attributable to high systolic blood pressure and a high-sodium diet were observed in most age-specific groups and both sexes (Figure 3A). Moreover, the temporal trends of the rates of DALYs attributable to smoking, high systolic blood pressure, and a high-sodium diet exposure were similar to those mortality (Figure 3B).

There was a difference between male and female patients in the proportion of DALYs attributable to risk factors (high systolic blood pressure, smoking, and high-sodium diet). High systolic blood pressure was the most significant contribution among both sexes, accounting for more than 43.9% of DALYs in male patients and more than 45.4% of DALYs in female patients, and the proportions of DALYs attributed to high systolic blood pressure increased over

TABLE 1 Number of incidence cases and incidence rate of ischemic and hemorrhage stroke in China in 1990 and 2019 and EAPC from 1990 to 2019.

Characteristics	1990		2019		1990–2019
	Incidence cases [$\times 10^3$ (95% UI)]	Incidence rate [per 1, 00, 000 (95% UI)]	Incidence cases [$\times 10^3$ (95% UI)]	Incidence rate [per 1, 00, 000 (95% UI)]	EAPC in incidence rate [% (95% CI)]
Overall[a]	1760.44 (1560.97, 2005.21)	221.51 (196.81, 249.61)	3935.18 (3431.72, 4579.87)	200.84 (176.95, 230.84)	−1.31 (−3.41, 0.85)
Sex[a]					
Male	868.03 (769.11, 993.05)	227.92 (202.83, 257.34)	1950.98 (1713.53, 2260.51)	209.75 (185.84, 239.39)	−1.20 (−3.35, 1.01)
Female	892.41 (791.42, 1019.26)	216.45 (192.14, 245.19)	1984.2 (1719.09, 2322.54)	194.53 (169.65, 225.19)	−1.43 (−3.51, 0.69)
Age at diagnosis[b] (year)					
0–14	52.23 (33.77, 76.41)	16.17 (10.46, 23.66)	31.02 (19.76, 46.63)	13.80 (8.79, 20.74)	−0.35 (−2.42, 1.76)
15–19	17.88 (10.91, 27.05)	14.09 (8.60, 21.32)	9.29 (5.41, 14.68)	12.36 (7.20, 19.54)	−0.81 (−2.21, 0.61)
20–24	23.21 (16.22, 32.60)	17.53 (12.25, 24.62)	12.32 (8.22, 18.28)	15.05 (10.04, 22.33)	−1.15 (−2.47, 0.20)
25–29	27.28 (18.89, 38.75)	24.75 (17.14, 35.17)	22.82 (14.78, 34.81)	20.61 (13.35, 31.44)	−1.37 (−2.73, 0.00)
30–34	33.15 (25.16, 43.19)	37.45 (28.42, 48.79)	38.97 (28.41, 53.07)	30.19 (22.01, 41.11)	−1.51 (−2.90, −0.10)
35–39	50.16 (36.26, 68.44)	54.81 (39.62, 74.79)	43.79 (32.31, 58.53)	43.41 (32.02, 58.01)	−1.54 (−2.98, −0.08)
40–44	67.15 (53.49, 83.15)	99.86 (79.55, 123.65)	79.26 (63.82, 98.76)	77.97 (62.79, 97.16)	−1.55 (−3.14, 0.05)
45–49	89.45 (66.09, 115.75)	172.94 (127.78, 223.80)	162.49 (121.27, 213.82)	133.88 (99.92, 176.18)	−1.55 (−3.25, 0.19)
50–54	135.62 (108.49, 164.95)	283.72 (226.96, 345.07)	304.26 (247.94, 369.49)	243.20 (198.19, 295.34)	−1.25 (−3.14, 0.68)
55–59	186.22 (140.48, 244.07)	428.47 (323.23, 561.57)	386.79 (286.65, 508.44)	407.83 (302.25, 536.1)	−0.96 (−3.04, 1.16)
60–64	223.72 (178.07, 278.53)	631.62 (502.72, 786.36)	505.13 (398.15, 635.25)	643.03 (506.84, 808.66)	−0.91 (−3.15, 1.38)
65–69	244.78 (177.31, 325.91)	894.41 (647.9, 1190.87)	663.85 (468.8, 903.16)	943.19 (666.07, 1283.19)	−0.98 (−3.35, 1.44)
70–74	231.55 (183.45, 293.70)	1227.95 (972.86, 1557.56)	612.33 (477.76, 794.97)	1279.53 (998.33, 1661.17)	−1.05 (−3.41, 1.37)
75–79	186.56 (144.17, 235.81)	1635.02 (1263.5, 2066.59)	498.40 (389.29, 627.74)	1669.87 (1304.31, 2103.22)	−1.11 (−3.45, 1.28)
80–84	122.25 (97.6, 150.43)	2168.07 (1730.89, 2667.74)	357.78 (282.01, 449.01)	1876.40 (1479.02, 2354.85)	−1.59 (−3.88, 0.76)
85–89	53.92 (43.03, 68.19)	2812.1 (2243.81, 3556.03)	159.43 (130.38, 192.61)	1874.60 (1533.11, 2264.80)	−2.30 (−4.53, −0.02)
90–94	12.78 (9.49, 17.23)	3428.42 (2545.6, 4623.93)	39.80 (30.54, 49.49)	1773.69 (1360.92, 2205.35)	−3.06 (−5.24, −0.82)
95+	2.53 (1.70, 3.59)	4068.08 (2735.78, 5762.46)	7.46 (4.97, 10.14)	1671.05 (1111.93, 2270.55)	−3.61 (−5.77, −1.40)

EAPC, estimated annual percentage change; 95% UI, 95% uncertainty interval; 95% CI, 95% confidence interval; [a]age-standardized incidence rate; [b]crude incidence rate in each age group.

time from 1990 to 2019. For male patients, the proportion of DALYs attributable to ischemic and hemorrhage strokes was ∼5 times higher than for female patients (Figure 3C).

Furthermore, the proportion of DALYs attributable to high systolic blood pressure, smoking, and a high-sodium diet shows a notable difference between sexes in most age-specific groups during this period, and there was a higher proportion of DALYs attributable to three risk factors among male than female patients. The proportion of DALYs attributable to high systolic blood pressure, smoking, and a high-sodium diet was observed having a relatively flat increase but then a drastic decrease in >65 years old among male and female patients (Figure 3D).

Predictions of incidence and mortality of ischemic and hemorrhage stroke from 2020 to 2044

Based on GBD data of ischemic and hemorrhage stroke from 1990 to 2019 in China, we further predicted the number and rate of incidence and mortality in the next 25 years (Figure 4). In the next 25 years, the rates of incidence among both sexes should show a stable trend (Figure 4A), and the mortality among both sexes should decline (Figure 4A), while the numbers of new cases and deaths of ischemic and hemorrhage stroke should rise steadily from 2020 to 2044 (Figures 4B, C). There should

TABLE 2 Number of deaths and mortality rate of ischemic and hemorrhage stroke in China in 1990 and 2019 and EAPC from 1990 to 2019.

Characteristics	1990		2019		1990–2019
	Deaths cases [$\times 10^3$ (95% UI)]	Mortality rate [per 100, 000 (95% UI)]	Deaths cases [$\times 10^3$ (95% UI)]	Mortality rate [per 1, 00, 000 (95% UI)]	EAPC in mortality rate [% (95% CI)]
Overall[a]	1377.09 (1220.67, 1564.24)	211.44 (187.68, 243.80)	2189.18 (1885.90, 2513.77)	127.25 (110.21, 144.89)	−2.85 (−4.68, −0.98)
Sex[a]					
Male	712.83 (599.05, 837.93)	246.30 (212.62, 286.86)	1261.12 (1035.32, 1509.29)	170.32 (141.87, 200.18)	−2.26 (−4.14, −0.34)
Female	664.26 (567.00, 792.33)	188.28 (161.70, 224.20)	928.06 (747.28, 1117.12)	97.44 (78.87, 117.01)	−3.40 (−5.18, −1.59)
Age at diagnosis [b] (year)					
0–14	10.93 (7.46, 13.40)	3.39 (2.31, 4.15)	0.69 (0.55, 0.96)	0.31 (0.24, 0.43)	−7.43 (−9.24, −5.59)
15–19	3.32 (2.74, 3.96)	2.61 (2.16, 3.12)	0.90 (0.73, 1.09)	1.20 (0.98, 1.45)	−3.27 (−5.20, −1.31)
20–24	4.54 (3.69, 5.47)	3.43 (2.79, 4.13)	1.78 (1.44, 2.12)	2.18 (1.76, 2.59)	−2.72 (−4.57, −0.83)
25–29	5.47 (4.65, 6.53)	4.96 (4.22, 5.93)	3.20 (2.62, 3.75)	2.89 (2.37, 3.39)	−2.76 (−4.61, −0.88)
30–34	7.82 (6.66, 9.34)	8.84 (7.53, 10.55)	7.31 (5.82, 8.59)	5.66 (4.51, 6.65)	−2.59 (−4.45, −0.70)
35–39	16.75 (14.26, 19.89)	18.31 (15.59, 21.74)	11.19 (9.03, 13.16)	11.09 (8.95, 13.04)	−2.70 (−4.59, −0.77)
40–44	26.77 (22.71, 31.77)	39.81 (33.77, 47.24)	21.70 (17.63, 25.84)	21.35 (17.35, 25.42)	−2.97 (−4.85, −1.06)
45–49	36.65 (31.1, 43.01)	70.86 (60.13, 83.15)	39.73 (32.41, 47.66)	32.73 (26.71, 39.27)	−3.28 (−5.16, −1.37)
50–54	70.02 (59.63, 81.20)	146.48 (124.75, 169.88)	76.23 (62.36, 91.74)	60.94 (49.84, 73.33)	−3.85 (−5.70, −1.96)
55–59	107.97 (92.14, 125.02)	248.42 (212, 287.66)	97.94 (80.24, 117.13)	103.27 (84.61, 123.5)	−3.77 (−5.60, −1.90)
60–64	141.16 (121.88, 163.80)	398.53 (344.10, 462.45)	146.60 (122.63, 172.89)	186.62 (156.11, 220.09)	−3.56 (−5.40, −1.70)
65–69	183.60 (161.28, 211.35)	670.86 (589.30, 772.27)	238.92 (201.75, 280.32)	339.46 (286.65, 398.28)	−3.42 (−5.27, −1.53)
70–74	228.07 (201.52, 269.60)	1209.52 (1068.72, 1429.76)	327.72 (278.88, 379.93)	684.81 (582.74, 793.90)	−3.36 (−5.23, −1.47)
75–79	227.78 (203.91, 266.13)	1996.22 (1787.07, 2332.29)	362.57 (312.72, 416.05)	1214.77 (1047.76, 1393.98)	−2.99 (−4.91, −1.03)
80–84	183.02 (162.01, 216.05)	3245.67 (2873.12, 3831.38)	417.37 (360.79, 470.96)	2188.93 (1892.2, 2469.96)	−2.62 (−4.56, −0.63)
85–89	94.90 (82.73, 113.52)	4948.81 (4314.41, 5919.86)	311.31 (269.92, 350.65)	3660.48 (3173.88, 4123.02)	−2.32 (−4.27, −0.33)
90–94	23.61 (19.99, 28.37)	6336.52 (5363.56, 7612.73)	99.59 (81.82, 114.88)	4438.08 (3646.14, 5119.37)	−2.61 (−4.56, −0.61)
95+	4.71 (3.88, 5.53)	7573.85 (6228.16, 8884.52)	24.43 (19.27, 28.39)	5469.91 (4316.36, 6358.26)	−2.36 (−4.33, −0.35)

EAPC, estimated annual percentage change; 95% UI, 95% uncertainty interval; 95% CI, 95% confidence interval; [a]age-standardized mortality rate; [b]crude mortality rate in each age group.

be 7570.95 thousand new ischemic and hemorrhage stroke cases (Figure 4B) and 3954.71 thousand deaths of NVHD (Figure 4C) in 2044. In 2044, among male patients, the number of incidence cases and deaths should increase to 3645.09 thousand and 2409.47 thousand, respectively (Figures 4B, C). Among female patients, the number of incidence cases and deaths should increase to 3946.26 thousand and 1582.75 thousand in 2044, respectively (Figures 4B, C).

Discussion

The analysis of epidemiological trends and major risk factors of stroke as well as the prediction of future epidemiological trends in our study will be of great significance in reducing the incidence and mortality of stroke.

Prevalence and prediction of disease burden of stroke in China

New epidemiological data of the Global Burden of Disease (GBD) 2019 study on stroke at macro- and meso-level geographic scales enable us to offer the most consistent, up-to-date, and comprehensive overview of the prevalence and risk factors for stroke nationally. First, our study has shown that this synthetical

TABLE 3 Number of DALYs and DALY rate of ischemic and hemorrhage stroke in China in 1990 and 2019 and EAPC from 1990 to 2019.

Characteristics	1990		2019		1990–2019
	DALYs [$\times 10^3$ (95% UI)]	DALY rate [per 100, 000 (95% UI)]	DALYs [$\times 10^3$ (95% UI)]	DALY rate [per 100, 000 (95% UI)]	EAPC in DALY rate [% (95% CI)]
Overall[a]	33621.26 (29916.11, 38026.59)	4134.28 (3697.14, 4674.62)	45949.13 (39813.51, 52335.53)	2412.52 (2102.92, 2742.48)	−2.83 (−4.60, −1.02)
Sex[a]					
Male	18106.11 (15236.54, 21193.12)	4656.60 (3971.22, 5403.45)	27103.24 (22271.00, 32864.28)	3052.05 (2535.20, 3643.00)	−2.34 (−4.17, −0.48)
Female	15515.14 (13247.44, 18060.26)	3707.97 (3178.76, 4330.48)	18845.89 (15670.19, 22244.53)	1876.80 (1566.50, 2204.53)	−3.38 (−5.09, −1.64)
Age at diagnosis[b] (year)					
0–14	1000.60 (690.22, 1222.39)	309.87 (213.75, 378.56)	93.76 (74.16, 120.52)	41.71 (32.99, 53.62)	−2.81 (−4.63, −0.95)
15–19	289.79 (245.68, 338.60)	228.39 (193.63, 266.86)	93.73 (77.37, 110.31)	124.75 (102.98, 146.82)	−2.35 (−4.12, −0.55)
20–24	374.54 (313.19, 440.18)	282.89 (236.55, 332.46)	160.53 (130.96, 187.44)	196.08 (159.97, 228.95)	−2.35 (−4.10, −0.56)
25–29	416.25 (357.58, 484.11)	377.73 (324.49, 439.32)	271.18 (225.86, 313.11)	244.92 (203.99, 282.80)	−2.30 (−4.06, −0.50)
30–34	525.67 (456.13, 607.14)	593.90 (515.33, 685.94)	524.96 (430.75, 606.95)	406.64 (333.66, 470.15)	−2.46 (−4.27, −0.62)
35–39	979.04 (850.75, 1146.58)	1069.89 (929.70, 1252.97)	691.39 (568.48, 801.40)	685.26 (563.44, 794.29)	−2.74 (−4.57, −0.89)
40–44	1365.92 (1176.16, 1600.83)	2031.34 (1749.13, 2380.68)	1170.00 (968.13, 1360.51)	1151.05 (952.46, 1338.48)	−3.00 (−4.83, −1.13)
45–49	1662.60 (1422.57, 1934.50)	3214.62 (2750.53, 3740.35)	1929.92 (1601.52, 2278.78)	1590.16 (1319.57, 1877.61)	−3.52 (−5.34, −1.67)
50–54	2777.62 (2380.68, 3195.08)	5810.68 (4980.29, 6683.98)	3251.20 (2711.66, 3834.61)	2598.81 (2167.53, 3065.15)	−3.44 (−5.27, −1.59)
55–59	3755.79 (3257.84, 4306.20)	8641.45 (7495.75, 9907.84)	3706.89 (3103.92, 4384.77)	3908.59 (3272.81, 4623.36)	−3.26 (−5.09, −1.39)
60–64	4231.52 (3697.27, 4871.95)	11946.49 (10438.21, 13754.57)	4784.67 (4064.31, 5578.26)	6090.79 (5173.78, 7101.01)	−3.12 (−4.98, −1.24)
65–69	4606.71 (4074.41, 5244)	16832.80 (14887.77, 19161.43)	6532.17 (5620.85, 7479.65)	9280.79 (7986.01, 10626.96)	−3.12 (−4.99, −1.22)
70–74	4646.28 (4126.91, 5428.97)	24640.29 (21885.99, 28791.10)	7184.06 (6205.01, 8192.53)	15011.86 (12966.02, 17119.15)	−2.80 (−4.73, −0.83)
75–79	3660.84 (3305.67, 4225.99)	32083.10 (28970.44, 37035.99)	6241.81 (5440.97, 7098.04)	20913.03 (18229.85, 23781.80)	−2.49 (−4.44, −0.49)
80–84	2247.42 (1997.41, 2608.97)	39855.85 (35422.06, 46267.55)	5414.79 (4721.75, 6047.91)	28398.18 (24763.50, 31718.61)	−2.23 (−4.18, −0.23)
85–89	883.80 (774.71, 1045.89)	46089.93 (40400.56, 54542.74)	3014.92 (2630.56, 3360.95)	35450.59 (30931.16, 39519.39)	−2.50 (−4.45, −0.51)
90–94	170.58 (145.01, 203.47)	45771.85 (38910.70, 54598.58)	746.28 (623.15, 852.31)	33257.45 (27770.13, 37982.52)	−6.41 (−7.76, −5.04)
95+	26.27 (21.78, 30.70)	42215.02 (34991.08, 49324.92)	136.90 (108.76, 157.39)	30657.65 (24356.42, 35247.24)	−2.36 (−4.32, −0.35)

DALYs, disability-adjusted life-years; EAPC, estimated annual percentage change; 95% UI, 95% uncertainty interval; 95% CI, 95% confidence interval; [a]age-standardized DALY rate; [b]crude DALY rate in each age group.

assessment of the numbers of incidence cases and DALYs lost from PAD demonstrates that there has been a remarkable increase among the total Chinese population over the past 30 years. The number of incidence cases will increase with aging and economic development, and China becomes one of the countries with the highest burden of stroke in the world. Advanced age, hypertension, smoking, and diet high in sodium were proved to be associated with a higher risk of stroke. With the global aging process continuing in the next several decades, the burden of stroke will probably increase substantially in the next several decades. This is consistent with the results predicted by our prediction model. For the next 25 years, it indicates that the

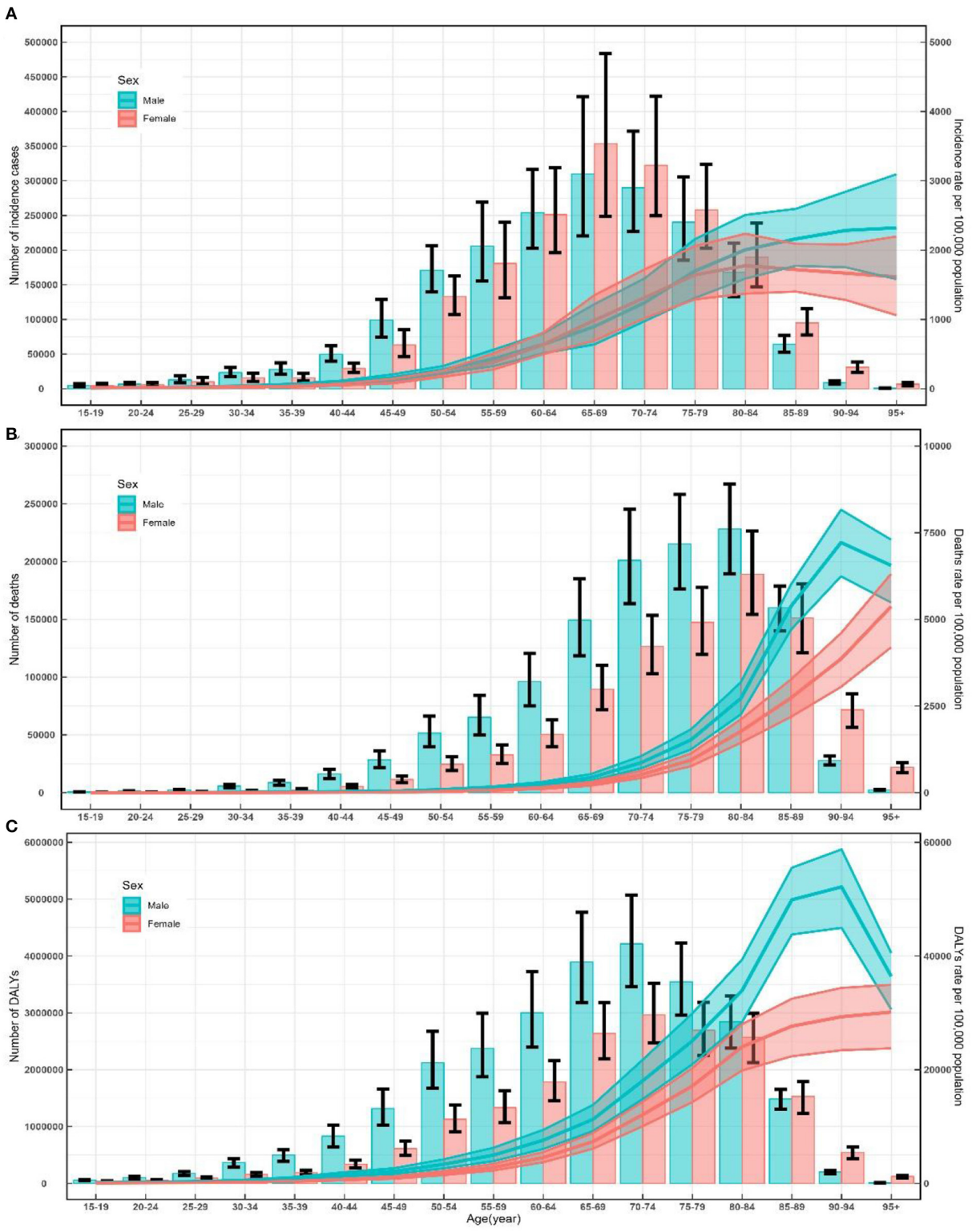

FIGURE 1
Number and rate of incidence **(A)**, death **(B)** and DALY **(C)** of ischemic and hemorrhage stroke by age and sex in 2019 in China. Shading represents the upper and lower limits of the 95% uncertainty intervals (95% UIs). DALYs, disability-adjusted life-years.

number of new cases, deaths, and DALYs of stroke should keep on increasing among male and female patients. Meanwhile, all the incidence rates, mortality rates, and DALY rates showed an overall increasing trend. Despite the improvement of clinical professional level and current policies to reduce the burden of stroke morbidity, it is clear that the continued heavy burden

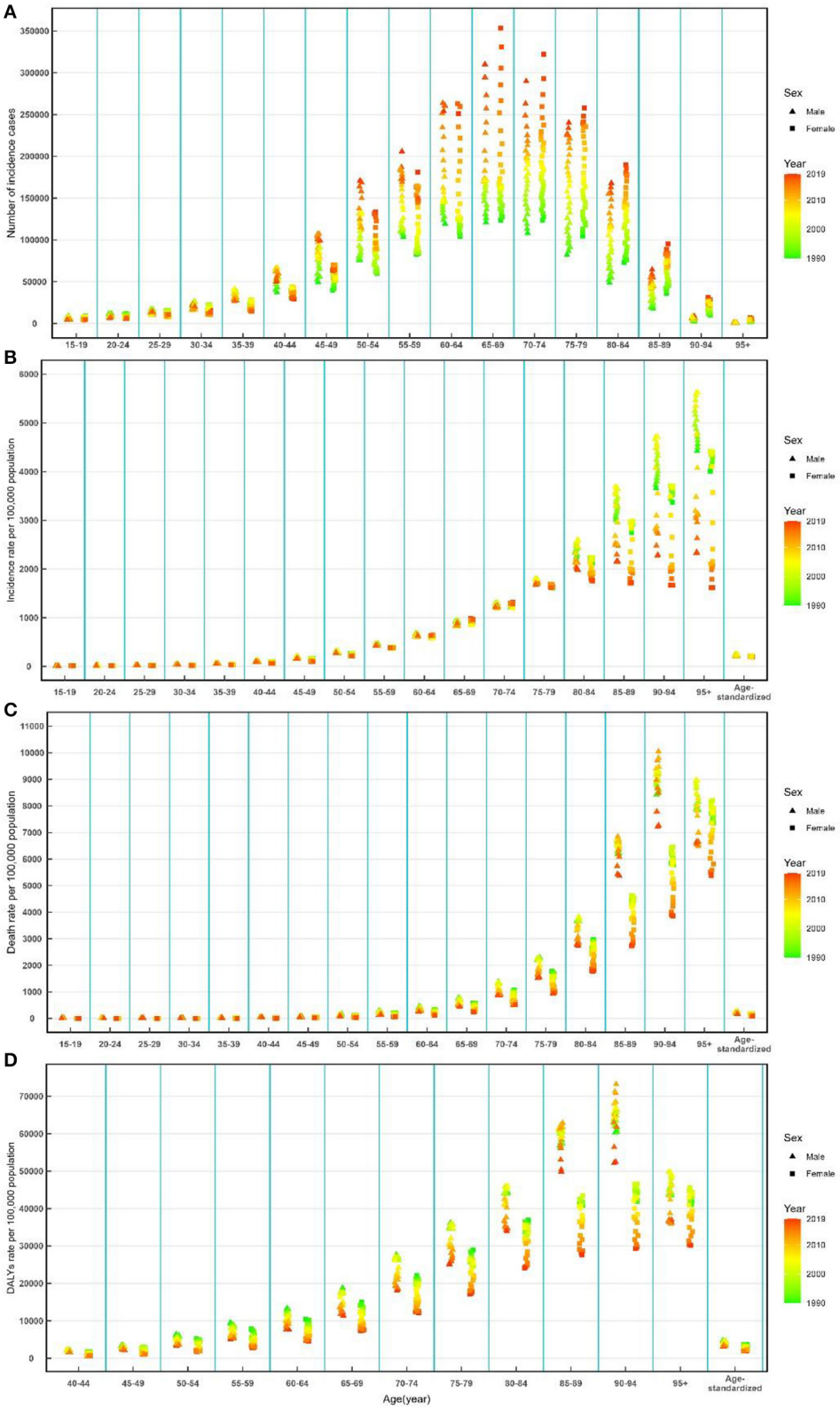

FIGURE 2
Number of incidence cases **(A)**, incidence rate **(B)**, death rate **(C)**, and DALY rate **(D)** of ischemic and hemorrhage stroke by age and sex from 1990 to 2019 in China. DALYs, disability-adjusted life-years.

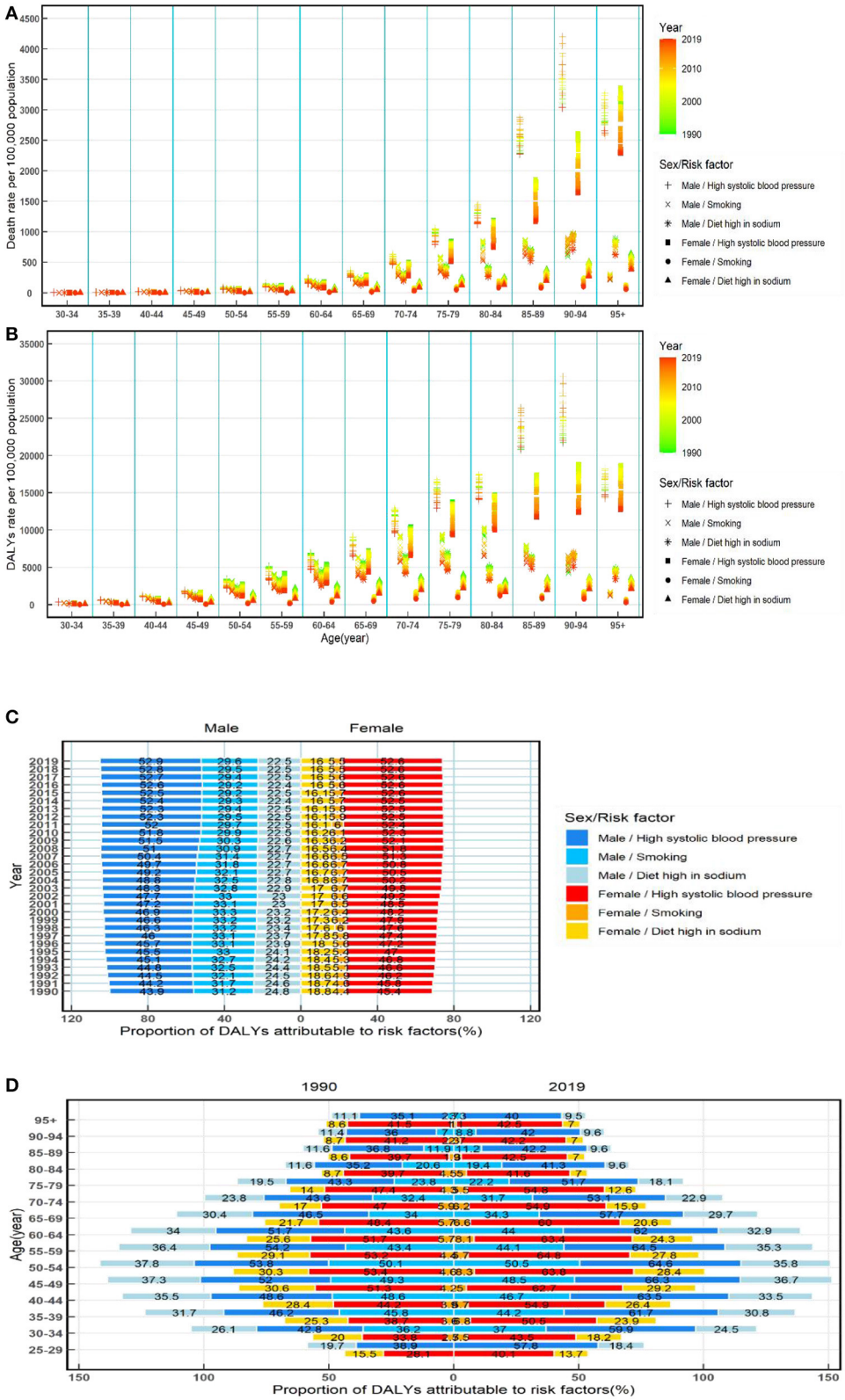

FIGURE 3
Rates of death and also rates and proportions of DALYs attributable to risk factors by age and sex from 1990 to 2019 in China. Rates of death **(A)** and DALYs **(B)** of ischemic and hemorrhage stroke attributable to risk factors by age and sex from 1990 to 2019 in China; proportions of DALYs attributable to risk factors by sex from 1990 to 2019 in China **(C)**; and proportions of DALYs attributable to risk factors by age and sex in 1990 and 2019 in China **(D)**. DALYs, disability-adjusted life-years.

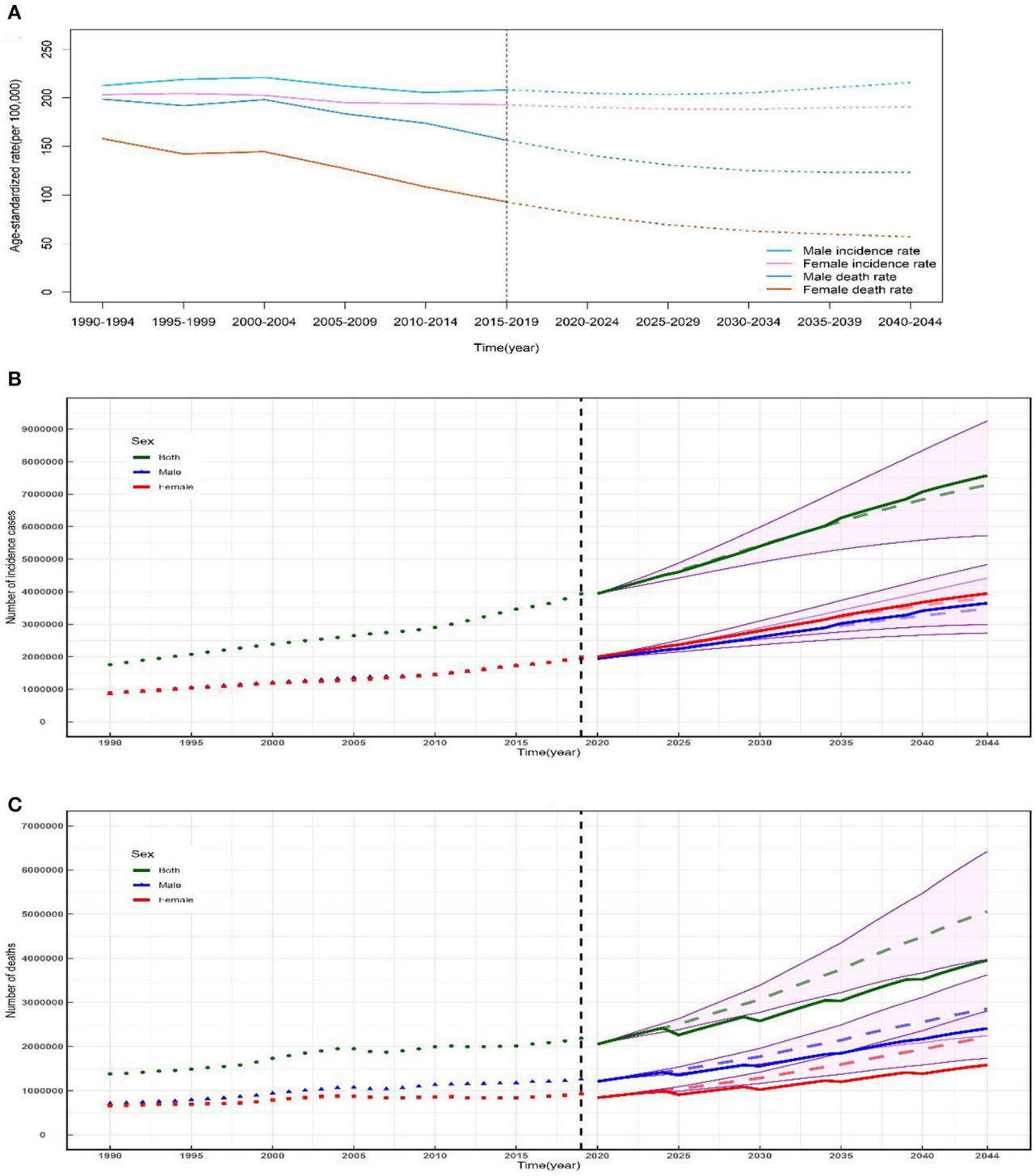

FIGURE 4
Temporal trends and forecasted rates of incidence and death **(A)** and number of incidence cases **(B)** and deaths **(C)** of ischemic and hemorrhage stroke by sex from 2020 to 2044 in China. Solid lines and dash lines represent the observed and the predicted number of incidence cases and deaths of ischemic and hemorrhage stroke; shading represents a 1% decrease and increase interval based on the 2019 rate. DALYs, disability-adjusted life-years.

of stroke in China may be shifting from chronic morbidity to mortality.

Cause of increased prevalence of stroke disease

Our study indicates that the age-standardized prevalence and DALY rates of stroke are prevalent among the Chinese population based on the data from GBD 2019, which is similar to the level worldwide. Although the age-standardized prevalence and DALY rates decreased in China basically, the significant increase in stroke cases and DALYs in China draws more attention. The increased prevalence of stroke results from manifold reasons. First, recent studies have shown that the elderly population aged ≥60 years is estimated to increase to 300 million by the end of 2025. Such an increase in absolute numbers of stroke-related new cases, deaths, and DALYs from the data in our study can be explained by the ever-growing population of elderly people and longer life expectancies. Second, some projects were implemented by Chinese authorities for the populations with a high risk of stroke. In 2011, the National Stroke Screening and Prevention Project promoted stroke emergency interventions, including stroke screening, acute stroke units, emergency green channels, and early rehabilitation services. The number of basic hospitals offering emergency stroke interventions increased from 58 to 224 from 2010 to 2016 (13). These improvements have undoubtedly contributed to the declining case fatality rates and increasing newly detected cases that have been witnessed. Third, other primary drivers include medical techniques, while concurrent declining CVD mortality and improved cardiovascular care are also the major contributors. The popularization of image diagnosis technology such as CT and MRI and new technologies such as computed tomography perfusion imaging (CTPI) and diffusion-weighted imaging (DWI) may increase the incidence of stroke (14). Increased stroke prevalence can also be explained by notably different lifestyles compared with previous generations. The past 3 decades have seen an economic boom in China, with unhealthy lifestyles, such as smoking, high-fat diets, and sedentary lifestyles, being increasingly adopted. Consequently, metabolic risk factors among younger populations have also increased (15, 16). With the improvement of the changing public health awareness and lifestyles in China, there has been a decline in the rates of incidence, mortality, and DALYs.

Risk factors of stroke disease

Many pathological and behavioral conditions have been shown to lead to a higher risk of experiencing a stroke. Targeting risk factors include, but are not limited to, hypertension, smoking, diet high in sodium, obesity, and lack of physical activity. Traditional risk factors remain highly prevalent in stroke survivors, among which high systolic blood pressure was the most common. High systolic blood pressure is the most important modifiable risk factor for stroke, with a direct, strong, continuous, and linear relationship between blood pressure and stroke risk. Overall, 23.2% (estimated 244.5 million) of the Chinese residents aged ≥18 years had hypertension and another 41.3% (estimated 435.3 million) had pre-hypertension according to the Chinese guidelines (17). A meta-analysis of 147 trials stated that blood pressure increase of 5 mm Hg diastolic or 10 mm Hg systolic was associated with a 40% increase in stroke risk (18). Even among those who are not defined as hypertensive, the higher the blood pressure, the higher the risk of stroke (19). These could explain the result of our study, and we found that the proportion of DALYs attributable to high systolic blood pressure was more than 52.9% in China in 2019 among both sexes. Since 2009, the Chinese government has incorporated hypertension management into community public service projects, and ∼100 million hypertensive patients are under management; training covers 31 provinces, 3,90,000 primary medical institutions, and 1.84 million medical staff; quality control covers 15,000 institutions and 1.71 million patients; 26.66 million people completed the mission (17). The benefits of hypertension management in reducing the risk of stroke have also been supported in our results. Among both male and female patients, the proportions of DALYs attributable to high systolic blood pressure decreased in nearly all age groups from 2000 to 2019.

In addition to high systolic blood pressure, smoking and diet high in sodium were two significant contributions to stroke from 1990 to 2019. The precision of our estimation for risk factors of stroke prevalence in our study is consistent with former data, which is consistent with former data (20), implying the importance of proper control of these two risk factors. However, among Chinese adults, the current rate of smoking is as high as 28.3% (21), and giving up smoking is associated with a considerable reduction in risk of stroke, and the benefit seems to be apparent within 5 years (22–24). On the other hand, China belongs to a country with a high-salt diet (25). The "Report on Nutrition and Chronic Disease Status of Chinese Residents (2020)" shows that the average daily cooking salt of Chinese households in 2019 can reach 9.3 g, and the daily individual intake in the North of China is about twice of that in the South. Compared with lower salt intake, higher salt intake was associated with a 24% higher rate of stroke (26). In our study, the proportions of DALYs attributable to smoking and diet high in sodium were higher in male patients than in female patients, and smoking contributed to more than six times higher in the proportion of DALYs in male patients than female patients. The China Adult Tobacco Investigation Report (2015) shows that 52.1% of men and 2.7% of women smoke, contributing to the gender differences. For diet, the biological plausibility of the association between sodium chloride intake and stroke risk shows that an elevated sodium chloride intake induced a negative effect on endothelial function (27), oxidative stress (28), platelet aggregation (29), arterial stiffness (30, 31), left ventricular mass and function (32), and the development of vascular damage (33). The Chinese government announced the Implementation Rules for the Regulations on Hygiene Management in Public Places, which clearly stipulates that smoking is prohibited in indoor public places. Meanwhile, the authorities have also responded positively and put forward salt reduction targets in China's Medium- and Long-Term Plan for the Prevention and Treatment of Chronic Diseases (2017–2025) and the National Nutrition Plan (2017–2030). The benefits of smoking cessation and salt restriction have also been shown in our

results. Among both male and female patients, all the ASIR, AMIR, and DALY rates decreased in the past 3 decades, and this trend will remain the same in the next 25 years.

Actions for stroke disease prevention in China

Although the overall decreasing trends in the rates of incidence, deaths, and DALYs were observed in all age-specific groups and both sexes, the numbers of new cases, deaths, and DALYs lost showed an upward trend from 1990 to 2019. The total expenses of healthcare and treatment for CVD have increased rapidly since 2004, which is much faster than the increase in gross domestic product. Furthermore, a large number of individuals with stroke hospitalization have caused huge economic burden. A multifarious approach is recommended to alter this condition. The 2019 edition of China's guidelines for the prevention and treatment of hypertension proposes antihypertensive treatment to reduce the total risk of morbidity and mortality of stroke. In 2016, the State Council issued the protocol of "healthy China 2030" plan (34), which forcefully put forward "comprehensively promote the implementation of tobacco control." In 2019, the authorities promulgated the implementation of healthy China action, requiring that the proportion of people protected by comprehensive smoke-free regulations should be no <30 and 80%, respectively, by 2022 and 2030, and smoking rate of people over 15 years old should be <24.5 and 20%. Additionally, healthy China 2030 put forward that it is urgent to guide a reasonable diet (34). Even so, greater efforts and special attention should be paid to targeted public health strategy making for stroke control.

Limitations

Our investigation has several limitations to be announced. First, we only evaluated the disease burden of stroke at the national level but did not conduct some more details provincially. Additionally, one of these limitations was that the accurate assessment of stroke-related mortality could be challenged by the complexity of differentiating between deaths directly attributed to stroke and those resulting from its coexisting health conditions. Second, the inclusion of more data on risk factors for stroke would contribute to a deep insight into the epidemiology of stroke and a more scientific preventive policy. We could not evaluate the stroke burden caused by other important risk factors such as high fasting plasma glucose and obesity because of incomplete or missing corresponding data in the GBD database. Third, it has been described previously how the inevitable limitations of the GBD methodology affect related studies (35, 36). The GBD study cannot capture the most recent changes in health status, because of the time lags in the reporting of health information by the authorities. In this study, although the data used to estimate the prevalence were corrected, fitted, and filled through multifarious models, non-determinacy still needs to be under consideration when interpreting our results.

Conclusion

This study has demonstrated that stroke is continuing to be a major healthcare challenge in China in the past 3 decades, especially in the elderly. An even larger number of stroke cases are to be expected, while the ASIR, ASMR, and DALY rate should show a downward trend among both sexes. It may lead to high care and treatment costs in the next 25 years. Traditional risk factors remain highly prevalent in stroke survivors, among which high systolic blood pressure was the most common. Our study results are valuable in drawing attention to the control and treatment of stroke, and more preventative, therapeutic, and rehabilitative strategies for stroke are needed to reduce negative health outcomes.

Data availability statement

Publicly available datasets were analyzed in this study. This data can be found at: Institute for Health Metrics and Evaluation (IHME), Global Health Data Exchange (GHDx), 2019 Global Burden of Disease (GBD) study, https://vizhub.healthdata.org/gbd-results/.

Ethics statement

Ethical review and approval was not required for the study on human participants in accordance with the local legislation and institutional requirements. Written informed consent from the patients/participants or patients/participants' legal guardian/next of kin was not required to participate in this study in accordance with the national legislation and the institutional requirements.

Author contributions

DL: Writing—original draft, Writing—review and editing. QG: Writing—original draft, Writing—review and editing. MH: Writing—original draft, Writing—review and editing. YH: Writing—original draft. YO: Writing—review and editing. MC: Writing—review and editing. XZ: Writing—review and editing. XL: Writing—review and editing, Methodology, Software, Writing—original draft.

Funding

This study was supported by the National Natural Science Foundation of China (grant numbers 81800431 and 81800444), Fujian Provincial Natural Science Foundation (no. 2018J01121), Fujian Provincial Health Technology Project (no. 2020GGA026), the Natural Science Foundation of Hubei Province (grant number 2018CFB415), the Medical humanities research project of Fujian Medical University (grant number RW202206), and

the Fujian Province civil policy theory research topic (grant number FMZD202303).

Conflict of interest

The authors declare that the research was conducted in the absence of any commercial or financial relationships that could be construed as a potential conflict of interest.

Publisher's note

References

1. Zhao HL, Huang Y. Lifetime risk of stroke in the global burden of disease study. *N Engl J Med.* (2019) 380:1377–8. doi: 10.1056/NEJMc1900607

2. Kim J, Thayabaranathan T, Donnan GA, Howard G, Howard VJ, Rothwell PM. Global stroke statistics 2019. *Int J Stroke.* (2020) 15:819–38. doi: 10.1177/1747493020909545

3. Wang Y, Zhou L, Guo J, Yang Y, Peng Q, Gao Y, et al. Secular trends of stroke incidence and mortality in China, 1990 to 2016: the global burden of disease study 2016. *J Stroke Cerebrovasc Dis.* (2020) 29:104959. doi: 10.1016/j.jstrokecerebrovasdis.2020.104959

4. Lou H, Dong Z, Zhang P, Shao X, Li T, Zhao C. Interaction of diabetes and smoking on stroke: a population-based cross-sectional survey in China. *BMJ Open.* (2018) 8:e017706. doi: 10.1136/bmjopen-2017-017706

5. Chobanian AV, Bakris GL, Black HR, Cushman WC, Green LA, Izzo JL. The seventh report of the joint national committee on prevention, detection, evaluation, and treatment of high blood pressure: the JNC 7 report. *JAMA.* (2003) 289:2560–72. doi: 10.1001/jama.289.19.2560

6. Grysiewicz RA, Thomas K, Pandey DK. Epidemiology of ischemic and hemorrhagic stroke: Incidence, prevalence, mortality, and risk factors. *Neurol Clin.* (2008) 26:871–95. doi: 10.1016/j.ncl.2008.07.003

7. Nagata C, Takatsuka N, Shimizu N, Shimizu H. Sodium intake and risk of death from stroke in Japanese men and women. *Stroke.* (2004) 35:1543–7. doi: 10.1161/01.STR.0000130425.50441.b0

8. GBD 2019 Diseases and Injuries Collaborators. Global burden of 369 diseases and injuries in 204 countries and territories, 1990-2019: a systematic analysis for the global burden of disease study 2019. *Lancet.* (2020) 396:1204–22. doi: 10.1016/S0140-6736(20)30925-9

9. GBD 2019 Risk Factors Collaborators. Global burden of 87 risk factors in 204 countries and territories, 1990-2019: a systematic analysis for the global burden of disease study 2019. *Lancet.* (2020) 396:1223–49. doi: 10.1016/S0140-6736(20)30752-2

10. GBD 2019 Stroke Collaborators. Global, regional, and national burden of stroke and its risk factors, 1990-2019: a systematic analysis for the global burden of disease study 2019. *The Lancet Neurol.* (2021) 20:795–820. doi: 10.1016/S1474-4422(21)00252-0

11. Zhang T, Chen H, Yin X, He Q, Man J, Yang X. Changing trends of disease burden of gastric cancer in China from 1990 to 2019 and its predictions: findings from global burden of disease study. *Chin J Cancer Res.* (2021) 33:11–26. doi: 10.21147/j.issn.1000-9604.2021.01.02

12. Torres-Roman JS, Valcarcel B, Guerra-Canchari P, Santos CAD, Barbosa IR, La Vecchia C. Leukemia mortality in children from Latin America: trends and predictions to 2030. *BMC Pediatr.* (2020) 20:511. doi: 10.1186/s12887-020-02408-y

13. Chao BH, Yan F, Hua Y, Liu JM, Yang Y, Ji XM. Stroke prevention and control system in China: CSPPC-stroke program. *Int J Stroke Off J Int Stroke Soc.* (2021) 16:265–72. doi: 10.1177/1747493020913557

14. He G, Wei L, Lu H, Li Y, Zhao Y, Zhu Y. Advances in imaging acute ischemic stroke: Evaluation before thrombectomy. *Rev Neurosci.* (2021) 32:495–512. doi: 10.1515/revneuro-2020-0061

15. Wu YF, Ma GS, Hu YH Li YP, Li X, Cui ZH. The current prevalence status of body overweight and obesity in China: data from the China national nutrition and health survey. *Chin J Prev Med.* (2005) 39:316–20.

16. Huang Y, Gao L, Xie X, Tan SC. Epidemiology of dyslipidemia in Chinese adults: meta-analysis of prevalence, awareness, treatment, and control. *Popul Health Metr.* (2014) 12:28. doi: 10.1186/s12963-014-0028-7

17. Wang Z, Chen Z, Zhang L, Wang X, Hao G, Zhang Z. Status of hypertension in China: Results from the China hypertension survey, 2012-2015. *Circulation.* (2018) 137:2344–56. doi: 10.1161/CIRCULATIONAHA.117.032380

18. Moon JR, Capistrant BD, Kawachi I, Avendano M, Subramanian SV, Bates LM. Stroke incidence in older us hispanics: is foreign birth protective? *Stroke.* (2012) 43:1224–9. doi: 10.1161/STROKEAHA.111.643700

19. Stansbury JP, Jia H, Williams LS, Vogel WB, Duncan PW. Ethnic disparities in stroke: epidemiology, acute care, and postacute outcomes. *Stroke.* (2005) 36:374–86. doi: 10.1161/01.STR.0000153065.39325.fd

20. Wang J, Wen X, Li W, Li X, Wang Y, Lu W. Risk factors for stroke in the Chinese population: a systematic review and meta-analysis. *J Stroke Cerebrovasc Dis.* (2017) 26:509–17. doi: 10.1016/j.jstrokecerebrovasdis.2016.12.002

21. Ding L, Xu Y, Wang LM, Jiang Y, Zhang M, Li YC. Smoking and its relation to metabolic status among Chinese adults: analysis ofoverweight and obesity in China a nationwide survey. *Biomed Environ Sci.* (2016) 29:619–27. doi: 10.3967/bes2016.084

22. Wannamethee SG, Shaper AG, Whincup PH, Walker M. Smoking cessation and the risk of stroke in middle-aged men. *JAMA.* (1995) 274:155–60. doi: 10.1001/jama.274.2.155

23. Svetkey LP, Sacks FM, Obarzanek E, Vollmer WM, Appel LJ. The dash diet, sodium intake and blood pressure trial (dash-sodium): rationale and design. *J Am Dietet Assoc.* (1999) 99:S96–104. doi: 10.1016/S0002-8223(99)00423-X

24. MacGregor GA, Markandu ND, Sagnella GA, Singer DR, Cappuccio FP. Double-blind study of three sodium intakes and long-term effects of sodium restriction in essential hypertension. *Lancet.* (1989) 2:1244–7. doi: 10.1016/S0140-6736(89)91852-7

25. Anderson CA, Appel LJ, Okuda N, Brown IJ, Chan Q, Zhao L. Dietary sources of sodium in China, japan, the united kingdom, and the united states, women and men aged 40 to 59 years: the intermap study. *J Am Diet Assoc.* (2010) 110:736–45. doi: 10.1016/j.jada.2010.02.007

26. Aburto NJ, Ziolkovska A, Hooper L, Elliott P, Cappuccio FP, Meerpohl JJ. Effect of lower sodium intake on health: systematic review and meta-analyses. *BMJ.* (2013) 346:f1326. doi: 10.1136/bmj.f1326

27. Dickinson KM, Keogh JB, Clifton PM. Effects of a low-salt diet on flow-mediated dilatation in humans. *Am J Clin Nutr.* (2009) 89:485–90. doi: 10.3945/ajcn.2008.26856

28. Koga Y, Hirooka Y, Araki S, Nozoe M, Kishi T, Sunagawa K. High salt intake enhances blood pressure increase during development of hypertension via oxidative stress in rostral ventrolateral medulla of spontaneously hypertensive rats. *Hypertens Res.* (2008) 31:2075–83. doi: 10.1291/hypres.31.2075

29. Somova L, Mufunda J. Platelet activity and salt sensitivity in the pathogenesis of systemic (essential) hypertension in black Africans. *Clin Exp Hypertens.* (1993) 15:781–96. doi: 10.3109/10641969309041641

30. Partovian C, Benetos A, Pommies JP, Mischler W, Safar ME. Effects of a chronic high-salt diet on large artery structure: role of endogenous bradykinin. *Am J Physiol.* (1998) 274:H1423–1428. doi: 10.1152/ajpheart.1998.274.5.H1423

31. Gates PE, Tanaka H, Hiatt WR, Seals DR. Dietary sodium restriction rapidly improves large elastic artery compliance in older adults with systolic hypertension. *Hypertension.* (2004) 44:35–41. doi: 10.1161/01.HYP.0000132767.74476.64

32. Schmieder RE, Messerli FH, Garavaglia GE, Nunez BD. Dietary salt intake. A determinant of cardiac involvement in essential hypertension. *Circulation.* (1988) 78:951–6. doi: 10.1161/01.CIR.78.4.951

33. Oberleithner H, Riethmuller C, Schillers H, MacGregor GA, de Wardener HE, Hausberg M. Plasma sodium stiffens vascular endothelium and reduces nitric oxide release. *Proc Natl Acad Sci U S A.* (2007) 104:16281–6. doi: 10.1073/pnas.0707791104

34. State Council. *Tutorial for Outline of the Healthy China 2030 Plan.* (2016). Available online at: http://www.Gov.Cn/zhengce/2016-10/25/content_5124174.Htm (accessed November 15, 2011).

35. Zhou M, Wang H, Zeng X, Yin P, Zhu J, Chen W. Mortality, morbidity, and risk factors in China and its provinces, 1990-2017: a systematic analysis for the global burden of disease study 2017. *Lancet.* (2019) 394:1145–58. doi: 10.1016/S0140-6736(19)30427-1

36. Rudd KE, Johnson SC, Agesa KM, Shackelford KA, Tsoi D, Kievlan DR. Global, regional, and national sepsis incidence and mortality, 1990-2017: Analysis for the global burden of disease study. *Lancet.* (2020) 395:200–11. doi: 10.1016/S0140-6736(19)32989-7

frontiers | Frontiers in Neurology

TYPE Brief Research Report
PUBLISHED 12 October 2023
DOI 10.3389/fneur.2023.1230141

OPEN ACCESS

EDITED BY
Yanlin Zhang,
Second Affiliated Hospital of Soochow University, China

REVIEWED BY
Ali Sazci,
Okan University, Türkiye
Manabesh Nath,
All India Institute of Medical Sciences, India

*CORRESPONDENCE
Seong Hye Choi
✉ seonghye@inha.ac.kr

†These authors have contributed equally to this work

RECEIVED 06 June 2023
ACCEPTED 03 October 2023
PUBLISHED 12 October 2023

CITATION
Yoon CW, Kim J, Suh YJ, Kim BC, Youn YC, Jeong JH, Han HJ and Choi SH (2023) Angiotensin-converting enzyme insertion/deletion gene polymorphism and the progression of cerebral microbleeds. *Front. Neurol.* 14:1230141. doi: 10.3389/fneur.2023.1230141

Angiotensin-converting enzyme insertion/deletion gene polymorphism and the progression of cerebral microbleeds

Cindy W. Yoon[1†], Jonguk Kim[1†], Young Ju Suh[2], Byeong C. Kim[3], Young Chul Youn[4], Jee Hyang Jeong[5], Hyun Jeong Han[6] and Seong Hye Choi[1*]

[1]Department of Neurology, Inha University School of Medicine, Incheon, Republic of Korea, [2]Department of Biomedical Sciences, Inha University School of Medicine, Incheon, Republic of Korea, [3]Department of Neurology, Chonnam National University Medical School, Gwangju, Republic of Korea, [4]Department of Neurology, Chung-Ang University College of Medicine, Seoul, Republic of Korea, [5]Department of Neurology, Ewha Womans University School of Medicine, Seoul, Republic of Korea, [6]Department of Neurology, Myongji Hospital, Hanyang University College of Medicine, Goyang, Republic of Korea

Background and purpose: The angiotensin-converting enzyme (ACE) insertion (I)/deletion (D) polymorphism has been studied as a genetic candidate for cerebral small vessel disease (CSVD). However, no previous study has evaluated the relationship between the ACE I/D polymorphism and cerebral microbleed (CMB), an important CSVD marker. We evaluated the association between ACE I/D polymorphisms and 2-year changes in CMBs.

Methods: The CHALLENGE (Comparison Study of Cilostazol and Aspirin on Changes in Volume of Cerebral Small Vessel Disease White Matter Changes) database was analyzed. Of 256 subjects, 186 participants who underwent a 2-year follow-up brain scan and ACE genotyping were included. Our analysis was conducted by dividing the ACE genotype into two groups (DD vs. ID/II) under the assumption of the recessive effects of the D allele. A linear mixed-effect model was used to compare the 2-year changes in the number of CMBs between the DD and combined ID/II genotypes.

Results: Among 186 patients included in this study, 24 (12.9%) had the DD genotype, 91 (48.9%) had the ID genotype, and 71 (38.2%) had the II genotype. Baseline clinical characteristics and cerebral small vessel disease markers were not different between the two groups (DD vs. ID/II) except for the prevalence of hypertension (DD 66.7% vs. ID/II 84.6%; $p = 0.04$). A multivariate linear mixed-effects model showed that the DD carriers had a greater increase in total CMB counts than the ID/II carriers after adjusting for the baseline number of CMBs, age, sex, and hypertension (estimated mean of difference [standard error (SE)] = 1.33 [0.61]; $p = 0.03$). When we performed an analysis of cases divided into deep and lobar CMBs, only lobar CMBs were significantly different between the two groups (estimated mean of difference [SE] = 0.94 [0.42]; $p = 0.02$).

Conclusion: The progression of CMBs over 2 years was greater in the ACE DD carriers compared with the combined II/ID carriers. The results of our study indicate a possible association between the ACE I/D polymorphism and CMB. A study with a larger sample size is needed to confirm this association.

KEYWORDS

cerebral microbleeds (CMB), cerebral small vessel disease (CSVD), angiotensin-converting enzyme, polymorphism, insertion/deletion polymorphism

Introduction

Cerebral small vessel disease (CSVD) is a disorder of the small perforating arterioles, capillaries, and venules of the brain (1). Clinically, CSVD is a major contributor to stroke (both ischemic and hemorrhagic) and dementia. CSVD causes about a quarter of ischemic strokes and most hemorrhagic strokes, is the most common cause of vascular dementia, and often co-occurs with Alzheimer's disease (1). CSVD is associated with aging and vascular risk factors, especially hypertension (HTN) (2). Neuroimaging markers of CSVD include lacunes, white matter hyperintensities (WMH), cerebral microbleeds (CMBs), and enlarged perivascular spaces (3).

Angiotensin-converting enzyme (ACE) is a key regulator of the renin-angiotensin system that converts inactive angiotensin-I (Ang-I) to active angiotensin-II (Ang-II), which causes vasoconstriction and increases sodium and water retention, leading to increased blood pressure. The gene encoding ACE is located on the long arm of chromosome 17 (17q23) (4). The ACE insertion (I)/deletion (D) polymorphism is known to influence ACE levels, and the D allele is associated with higher ACE level and activity (4). The ACE I/D polymorphism has been studied as a genetic candidate for CSVD because Ang-II has a critical role in HTN, a major risk factor for CSVD, and can affect cerebral circulation by promoting oxidative stress, leading to vascular damage and dysfunction (5).

Although results have not been consistent across studies, an association between the ACE I/D polymorphism and CSVD markers including WMH or lacunar infarct has been suggested (6–9). CMB is a clinically important CSVD marker of a bleeding-prone microangiopathy that is related to the risk of hemorrhagic stroke (10). A recent meta-analysis indicated that the ACE I/D polymorphism is associated with a risk of hemorrhagic stroke (11). However, no previous study has evaluated the relationship between the ACE I/D polymorphism and CMB. This study investigated the impact of the ACE I/D polymorphism on the progression of CMBs.

Methods

Study participants

This study was a sub-analysis of the CHALLENGE (Clinicaltrials.gov; Unique identifier: NCT01932203) trial, a multicenter, double-blind, randomized controlled trial that enrolled participants aged 50–85 years with CSVD (12). A diagnosis of CSVD was established based on the presence of at least one lacune and moderate to severe WMH, according to the modified Fazekas criteria for periventricular WMH with a cap or rim of ≥5 mm and deep WMH with a maximum diameter of ≥10 mm (13). The main objective of the trial was to compare the effects of cilostazol and aspirin on changes in the WMH volume over 2 years. Between July 2013 and August 2016, 282 participants were screened for eligibility, of whom 256 were randomly assigned to the cilostazol or aspirin group using a permuted block randomization method (12). Out of 256 CHALLENGE subjects, 186 participants who underwent a 2-year follow-up magnetic resonance imaging (MRI) and ACE I/D genotyping were included. A comparison between the included and excluded subjects is shown in Supplementary Table S1. There were no significant differences between the two groups.

The Institutional Review Boards of the participating centers approved this study. The approval number of the affiliated center of the corresponding author (SC) was 2013–03-006. Written informed consent was obtained from all potential participants prior to enrollment.

Genotyping of the ACE I/D polymorphism

DNA was extracted from a 2 mL blood sample from each participant. To isolate the buffy coat from the 2 mL blood sample, blood collected in an EDTA-containing tube was centrifuged at 1500 × g for 10 min. The buffy coat was carefully extracted using a fine-tipped pipette and stored at −80°C for further analysis. A QuickGene DNA Whole Blood Kit S (Kurabo, Osaka, Japan) was used to extract DNA from the buffy coat according to the manufacturer's instructions. The genotyping analysis was performed after the CHALLENGE study was completed.

Genotyping of the ACE I/D polymorphism was performed by DNA direct sequencing. PCR was used to amplify the ACE fragments using UCSC In-Silico PCR.[1] The final volume of the PCR test sample was 10 μL, consisting of 10 ng of DNA, 0.5 nM of each primer pair, 0.25 mM dNTPs, 3 mM $MgCl_2$, 1 μL 1× reaction buffer, and 0.25 U Taq DNA polymerase (Intron Biotechnology, Seongnam-Si, Gyeonggi-do, Korea). The region of intron 16 was amplified using PCR primers (forward; 5′-GAGAGGAGAGAGACTCAAGC-3′, reverse; 5′-AGCCTGGTTGATGAGTTC-3′) designed by DNA LINK Inc. The PCR conditions used were as follows: initial denaturation at 95°C for 10 min, followed by 35 cycles of denaturation at 95°C for 30 s, annealing at 60°C for 1 min, initial extension at 72°C for 1 min, and final extension at 72°C for 10 min. The PCR products were purified using a MultiScreen384-PCR Filter Plate (Millipore, Billerica, MA, United States). The purified products were then sequenced using a BigDye Terminator Cycle Sequencing Kit and an ABI 3730xl automated sequencer (Applied Biosystems, Foster City, CA, United States). The sequencing primers were the same as those used for the PCR amplification. Mutation analyzes were performed using Phred, Phrap, Consed, and Polyphred 5.04 software.[2]

1 http://genome.ucsc.edu/cgi-bin/hgPcr?command=start

2 http://droog.mbt.washington.edu/PolyPhred.html

TABLE 1 Comparison of the baseline characteristics according to the angiotensin-converting enzyme (ACE) gene insertion (I)/deletion (D) polymorphism.

	DD (n = 24)	ID/II (n = 162)	p-value
Age, years	75.1 (7.5)	73.1 (6.6)	0.16
Female	15 (62.5)	106 (65.4)	0.82
Hypertension	16 (66.7)	137 (84.6)	0.04
Diabetes	9 (37.5)	63 (38.9)	1.00
Hyperlipidemia	10 (41.7)	81 (50.6)	0.51
Current Smoking	1 (4.2)	11 (6.8)	1.00
Body mass index, kg/m^2	24.7 (2.6)	24.7 (3.1)	0.99
Antiplatelet medication			0.27
Aspirin	10 (41.7)	90 (55.6)	
Cilostazol	14 (58.3)	72 (44.4)	
Follow-up, years	1.96 (0.22)	1.97 (0.17)	0.58
Baseline CSVD markers			
WMH volume, mL	45.6 (31.6–52.1)	33.7 (23.6–47.6)	0.07
Number of lacunes	6 (2–12)	5 (2–10)	0.53
Number of CMBs			
Total	1 (1–12)	2 (0–7)	0.49
Deep	1 (0–8)	1 (0–4)	0.55
Lobar	1 (0–4)	0 (0–2)	0.36

The values are presented as percentages (%), mean (standard deviation), or median (interquartile range).
CSVD, cerebral small vessel disease; WMH, white matter hyperintensities; CMB, cerebral microbleed.

Imaging markers

Brain MRI data including an axial T2∗-weighted gradient-echo sequence (4-mm slice thickness with no interslice gap) were acquired using a 3.0 Tesla MR scanner. The same scanner and sequence were used for the baseline and follow-up MRI. CMBs were defined as lesions with a diameter ≤ 10 mm and rated using the Microbleed Anatomical Rating Scale (14). Two experienced neurologists blinded to the clinical information counted the number of CMBs on gradient-echo MRI images. Pearson's correlation coefficient of agreement on the number of CMBs between the two neurologists was 0.958 (95% confidence interval 0.809–0.989; $p < 0.001$). The two neurologists reached a consensus after discussing cases where there was an initial disagreement. CMBs were categorized as deep (basal ganglia, thalamus, internal/external capsule, corpus callosum, deep/periventricular white matter, and brainstem) or lobar (frontal, parietal, temporal, occipital, and insular cortices). The decision on CMB progression was made in a blind manner without access to any other clinical information.

Statistical analysis

Referring to previous research results (7, 15), our analysis was conducted by dividing the ACE I/D genotype into two groups (DD vs. ID/II) under the assumption of the recessive effects of the D allele. The baseline characteristics were compared between the DD and combined ID/II genotypes using the chi-square test for categorical variables and the Student's t-test or the Mann–Whitney U-test for continuous variables. The change in the number of CMBs and the proportion of patients with CMB progression (defined as an increase in the number of CMBs ≥1) during the 2-year follow-up period were compared using the Mann–Whitney U-test and the chi-square test. We used a linear mixed-effects model with a random subject effect to estimate and compare changes in the number of CMBs over 2 years. To assess the trend in each group, linear mixed-model analyzes were performed separately using time (baseline and 2-year follow-up visit) as a predictor. To determine the impact of the ACE I/D genotype on the longitudinal changes in CMB counts, we explored the interaction between the ACE I/D genotype and time (ACE I/D genotype × time) adjusted for the baseline number of CMBs, age, sex, and HTN.

Results

Among 186 included patients, 24 (12.9%) had the DD genotype, 91 (48.9%) had the ID genotype, and 71 (38.2%) had the II genotype. We compared the DD genotype with the combined ID/II genotypes assuming the recessive effect of the D allele. The baseline clinical characteristics were not different between the two groups except for the prevalence of HTN (DD 66.7% vs. ID/II 84.6%; $p = 0.04$) (Table 1). There was no difference in baseline CSVD markers, including baseline number of CMBs, between the two groups. After 2 years of follow-up, the proportion of patients with CMB progression (defined as an increase in the number of CMBs by ≥1) was 54.2% (13/24) for the DD genotype and 48.8% (79/162) for the ID/II genotype ($p = 0.67$). The median (interquartile range) increase in the number of CMBs over 2 years was 1 (0–3) for the DD genotype and 0 (0–1) for the ID/II genotype ($p = 0.38$).

In the linear mixed-effect model, which tested the effect of the ACE I/D genotype × time interaction on changes in CMB counts, the DD carriers had a much greater increase in total CMB counts than the ID/II carriers after adjusting for the baseline number of CMBs, age, sex, and HTN (estimated mean of difference [standard error (SE)] = 1.33 [0.61]; $p = 0.03$) (Table 2). Figure 1 shows the estimated effect of the ACE I/D genotype on the longitudinal changes in the number of total CMBs over a 2-year follow-up period. In the analysis using CMBs divided into deep and lobar CMBs, only lobar CMBs showed a significant difference between the two groups (estimated mean of difference [SE] = 0.94 [0.42]; $p = 0.02$) (Table 2).

Discussion

CMB is an important CSVD marker associated with the risk of stroke, cognitive decline, and depression (10, 16–19). In this longitudinal study, we compared the progression of CMBs according to the ACE I/D polymorphism. This is the first study to investigate the relationship between the ACE I/D polymorphism and CMBs. Our

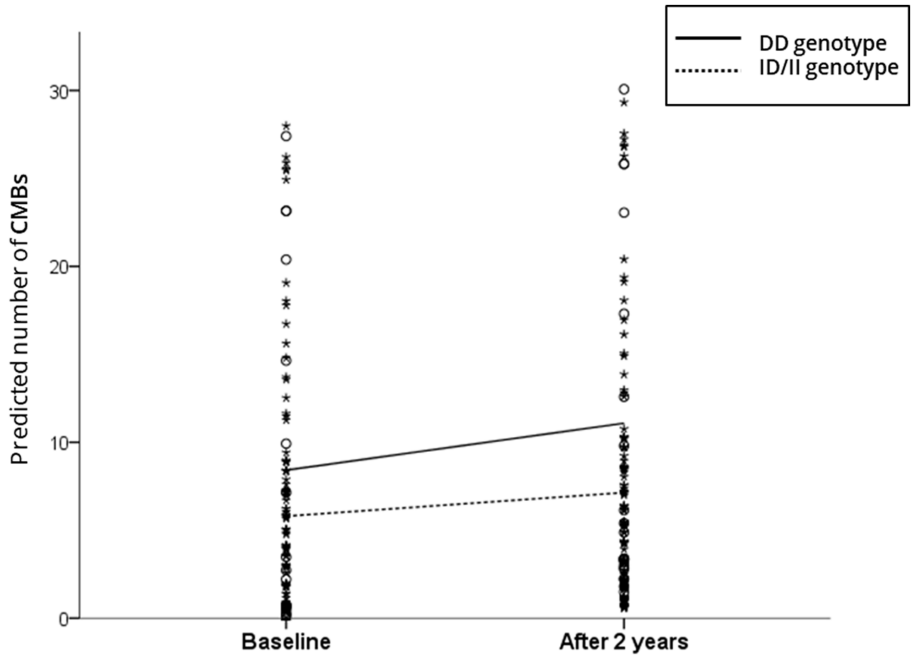

FIGURE 1
Scatterplot of the predicted number of cerebral microbleeds (CMBs) according to the angiotensin-converting enzyme (ACE) gene insertion (I)/deletion (D) polymorphism. The solid and dotted lines indicate the linear regression model of patients with the DD and ID/DD genotypes, respectively. The analysis controlled for the baseline number of CMBs, age, sex, and hypertension.

TABLE 2 Comparison of the longitudinal changes in the number of cerebral microbleeds according to the angiotensin-converting enzyme (ACE) gene insertion (I)/deletion (D) polymorphism.

Changes in the number of CMBs over the 2-year follow-up period[a]				
	DD	ID/II	Differences between DD and ID/II (ID/II as a reference)	
	Estimated mean (SE)	Estimated mean (SE)	Estimated mean (SE)	*P*-value
Total	2.67 (0.93)	1.34 (0.18)	1.33 (0.61)	0.03
Deep	1.04 (0.36)	0.60 (0.10)	0.44 (0.29)	0.14
Lobar	1.63 (0.77)	0.69 (0.11)	0.94 (0.42)	0.02

CMBs, cerebral microbleeds; SE, standard error.
[a]Results of a linear mixed model adjusted for the baseline number of CMBs, age, sex, and hypertension.

major finding was that the progression of CMBs over 2 years was greater in the DD homozygote carriers compared with the combined II/ID carriers.

The ACE I/D polymorphism affects the level and activity of ACE, which converts Ang-I to Ang-II (4). The formation of CMB is caused by the structural weakening and endothelial dysfunction of the microvasculature (20). Ang-II promotes oxidative stress in the cerebral vasculature, which leads to endothelial dysfunction, increased blood–brain barrier permeability, inflammation, and vascular structural damage (5). These effects of Ang-II on the cerebral microvasculature can cause vascular leakage from vulnerable small vessels, which leads to the formation of CMB. Because the ACE level and activity are known to be higher in the DD genotype than in the other two genotypes (4), this could be a possible mechanism for the more pronounced CMB progression in the DD carriers.

HTN is a major risk factor for CMB formation (10) and Ang-II plays a role in increasing the blood pressure. However, in our study, the prevalence of HTN was higher in the II/ID carriers, but the progression of CMBs was more pronounced in the DD carriers. This suggested that the more pronounced CMB progression in DD carriers was not due to the influence of the D allele on HTN incidence. However, even in patients with HTN, the progression of CMBs may differ depending on the actual blood pressure control status and blood pressure variability (21, 22). One of the limitations of our study was that we did not have detailed information on the level of blood pressure control and blood pressure variability.

The DD homozygote carriers had a significantly greater increase in the number of total and lobar CMBs than the ID/II carriers, but no significant difference in the number of deep CMBs. The deep perforating arteries are affected in deep CMBs, whereas the cortical and leptomeningeal arteries are affected in lobar CMBs. Regarding the inconsistent results between the deep and lobar CMBs, the effect of Ang-II on the vasculature might differ depending on the vascular location. However, it should be noted that the prevalence of HTN was significantly higher in the ID/II carriers compared with the DD carriers (84.6% vs. 66.7%) in our study. Although HTN was adjusted for in the analysis, the higher prevalence of HTN in the ID/II carriers might offset the impact of the DD genotype on the progression of CMBs because HTN has a strong influence, especially on the formation of deep MBs.

Our data should be interpreted with caution due to the small sample size. A study with a larger sample size is needed to test and

confirm the genetic association. Furthermore, only Koreans were included, which could limit the generalizability of our results. Also, because our patient group consisted of older individuals with relatively severe pre-existing CSVD, this limits the generalization of our results. Finally, although an adjustment for confounding factors was made in the multivariate analyzes, differences in the prevalence of HTN between the genotypes were also an important limitation of our study. Finally, as mentioned earlier, we did not have detailed information on the level of blood pressure control or blood pressure variability.

Conclusion

In this study, the progression of CMBs over 2 years was greater in the ACE DD carriers compared with the combined II/ID carriers. Our results suggest that the ACE I/D polymorphism is associated with CMBs. Further studies with larger multiethnic samples are needed to confirm this association.

Data availability statement

The raw data supporting the conclusions of this article will be made available by the authors, without undue reservation.

Ethics statement

The studies involving humans were approved by Inha University Hospital Institutional Review Board. The studies were conducted in accordance with the local legislation and institutional requirements. Written informed consent for participation in this study was provided by the participants' legal guardians/next of kin.

Author contributions

CY, JK, and SC contributed to the conception and design of the study. CY, JK, BK, YY, JJ, HH, and SC collected the data and organized the database. CY and YS performed the statistical analysis. CY and JK wrote the first draft of the manuscript. SC reviewed and edited the manuscript. All authors contributed to the article and approved the submitted version.

Funding

This study was supported by grants from the National Research Council of Science and Technology (NST) Aging Convergence Research Center (CRC22011-600), the Institute of Information and Communications Technology Planning and Evaluation (IITP) (2022-0-00448), and the Basic Science Research Program through the National Research Foundation of Korea (NRF) (NRF-2020M3E5D2A01084721) funded by the Ministry of Science and ICT, Republic of Korea, from the Korea Health Technology R&D Project through the Korea Health Industry Development Institute (KHIDI), and Korea Dementia Research Center (KDRC) funded by the Ministry of Health and Welfare and Ministry of Science and ICT, Republic of Korea (HU21C0016), and from Inha University and the Korea Otsuka Pharmaceutical Company. The funders were not involved in the study design, collection, analysis, interpretation of data, the writing of this article or the decision to submit it for publication.

Conflict of interest

The authors declare that the research was conducted in the absence of any commercial or financial relationships that could be construed as a potential conflict of interest.

Publisher's note

All claims expressed in this article are solely those of the authors and do not necessarily represent those of their affiliated organizations, or those of the publisher, the editors and the reviewers. Any product that may be evaluated in this article, or claim that may be made by its manufacturer, is not guaranteed or endorsed by the publisher.

Supplementary material

The Supplementary material for this article can be found online at: https://www.frontiersin.org/articles/10.3389/fneur.2023.1230141/full#supplementary-material

References

1. Wardlaw JM, Smith C, Dichgans M. Small vessel disease: mechanisms and clinical implications. *Lancet Neurol.* (2019) 18:684–96. doi: 10.1016/S1474-4422(19)30079-1

2. Wang Z, Chen Q, Chen J, Yang N, Zheng K. Risk factors of cerebral small vessel disease: a systematic review and meta-analysis. *Medicine*. (2021) 100:e28229. doi: 10.1097/MD.0000000000028229

3. Wardlaw JM, Smith EE, Biessels GJ, Cordonnier C, Fazekas F, Frayne R, et al. Neuroimaging standards for research into small vessel disease and its contribution to ageing and neurodegeneration. *Lancet Neurol.* (2013) 12:822–38. doi: 10.1016/S1474-4422(13)70124-8

4. Sayed-Tabatabaei F, Oostra B, Isaacs A, Van Duijn C, Witteman J. ACE polymorphisms. *Circ Res*. (2006) 98:1123–33. doi: 10.1161/01.RES.0000223145.74217.e7

5. De Silva TM, Faraci FM. Effects of angiotensin II on the cerebral circulation: role of oxidative stress. *Front Physiol.* (2013) 3:484. doi: 10.3389/fphys.2012.00484

6. Paternoster L, Chen W, Sudlow CL. Genetic determinants of white matter hyperintensities on brain scans: a systematic assessment of 19 candidate gene polymorphisms in 46 studies in 19 000 subjects. *Stroke*. (2009) 40:2020–6. doi: 10.1161/STROKEAHA.108.542050

7. Zhang Z, Xu G, Liu D, Fan X, Zhu W, Liu X. Angiotensin-converting enzyme insertion/deletion polymorphism contributes to ischemic stroke risk: a meta-analysis of 50 case-control studies. *PLoS One*. (2012) 7:e46495. doi: 10.1371/journal.pone.0046495

8. Su C, Liu W-C, Li G-M, Huang Y. Association between the angiotensin-converting enzyme I/D polymorphism and risk of cerebral small vessel disease: a Meta-analysis based on 7186 subjects. *J Stroke Cerebrovasc Dis*. (2021) 30:105579. doi: 10.1016/j.jstrokecerebrovasdis.2020.105579

9. Hassan A, Lansbury A, Catto A, Guthrie A, Spencer J, Craven C, et al. Angiotensin converting enzyme insertion/deletion genotype is associated with leukoaraiosis in lacunar syndromes. *J Neurol Neurosurg Psychiatry*. (2002) 72:343–6. doi: 10.1136/jnnp.72.3.343

10. Kim BJ, Lee S-H. Cerebral microbleeds: their associated factors, radiologic findings, and clinical implications. *J Stroke*. (2013) 15:153–63. doi: 10.5853/jos.2013.15.3.153

11. Nath M, Misra S, Talwar P, Vibha D, Srivastava AK, Prasad K, et al. Association between angiotensin converting enzyme insertion/deletion gene polymorphism with the risk of hemorrhagic stroke: a systematic review and Meta-analysis of 53 studies. *Gene*. (2021) 790:145696. doi: 10.1016/j.gene.2021.145696

12. Kim BC, Youn YC, Jeong JH, Han HJ, Kim JH, Lee J-H, et al. Cilostazol versus aspirin on white matter changes in cerebral small vessel disease: a randomized controlled trial. *Stroke*. (2022) 53:698–709. doi: 10.1161/STROKEAHA.121.035766

13. Noh Y, Lee Y, Seo SW, Jeong JH, Choi SH, Back JH, et al. A new classification system for ischemia using a combination of deep and periventricular white matter hyperintensities. *J Stroke Cerebrovasc Dis*. (2014) 23:636–42. doi: 10.1016/j.jstrokecerebrovasdis.2013.06.002

14. Gregoire S, Chaudhary U, Brown M, Yousry T, Kallis C, Jäger H, et al. The microbleed anatomical rating scale (MARS): reliability of a tool to map brain microbleeds. *Neurology*. (2009) 73:1759–66. doi: 10.1212/WNL.0b013e3181c34a7d

15. Slowik A, Dziedzic T, Pera J, Wloch D, Kopec G, Szczudlik A. ACE genotype, risk and causal relationship to stroke: implications for treatment. *Curr Treat Options Cardiovasc Med*. (2007) 9:198–204. doi: 10.1007/s11936-007-0013-6

16. Akoudad S, Wolters FJ, Viswanathan A, de Bruijn RF, van der Lugt A, Hofman A, et al. Association of cerebral microbleeds with cognitive decline and dementia. *JAMA Neurol*. (2016) 73:934–43. doi: 10.1001/jamaneurol.2016.1017

17. Charidimou A, Kakar P, Fox Z, Werring DJ. Cerebral microbleeds and recurrent stroke risk: systematic review and meta-analysis of prospective ischemic stroke and transient ischemic attack cohorts. *Stroke*. (2013) 44:995–1001. doi: 10.1161/STROKEAHA.111.000038

18. Wang R, Liu K, Ye X, Yan S. Association between cerebral microbleeds and depression in the general elderly population: a meta-analysis. *Front Psych*. (2018) 9:94. doi: 10.3389/fpsyt.2018.00094

19. Yates PA, Villemagne VL, Ellis KA, Desmond PM, Masters CL, Rowe CC. Cerebral microbleeds: a review of clinical, genetic, and neuroimaging associations. *Front Neurol*. (2014) 4:205. doi: 10.3389/fneur.2013.00205

20. Ungvari Z, Tarantini S, Kirkpatrick AC, Csiszar A, Prodan CI. Cerebral microhemorrhages: mechanisms, consequences, and prevention. *Am J Phys Heart Circ Phys*. (2017) 312:H1128–43. doi: 10.1152/ajpheart.00780.2016

21. Henskens LH, Van Oostenbrugge RJ, Kroon AA, De Leeuw PW, Lodder J. Brain microbleeds are associated with ambulatory blood pressure levels in a hypertensive population. *Hypertension*. (2008) 51:62–8. doi: 10.1161/HYPERTENSIONAHA.107.100610

22. Chen YK, Liang WC, Yuan SL, Ni ZX, Li W, Liu YL, et al. Circadian rhythms of blood pressure in hypertensive patients with cerebral microbleeds. *Brain Behav*. (2022) 12:e2530. doi: 10.1002/brb3.2530

frontiers | Frontiers in Neurology

TYPE Original Research
PUBLISHED 12 October 2023
DOI 10.3389/fneur.2023.1271391

OPEN ACCESS

EDITED BY
Yanlin Zhang,
Second Affiliated Hospital of Soochow University, China

REVIEWED BY
Shubham Misra,
Yale University, United States
Fei Peng,
Capital Medical University, China

*CORRESPONDENCE
Weiqiang Chen
✉ 15397370948@163.com
Junqiang Ma
✉ 736247781@qq.com

†These authors share first authorship

RECEIVED 02 August 2023
ACCEPTED 19 September 2023
PUBLISHED 12 October 2023

CITATION
Zhong Y, Sun H, Chen H, Jing W, Chen W and Ma J (2023) Association between lactate/albumin ratio and 28-day all-cause mortality in ischemic stroke patients without reperfusion therapy: a retrospective analysis of the MIMIC-IV database.
Front. Neurol. 14:1271391.
doi: 10.3389/fneur.2023.1271391

Association between lactate/albumin ratio and 28-day all-cause mortality in ischemic stroke patients without reperfusion therapy: a retrospective analysis of the MIMIC-IV database

Yuan Zhong[1†], Hao Sun[1†], Hongzhuang Chen[2], Wenjuan Jing[3], Weiqiang Chen[1*] and Junqiang Ma[1*]

[1]Department of Neurosurgery, First Affiliated Hospital of Shantou University Medical College, Shantou, Guangdong, China, [2]Department of Critical Care Medicine, First Affiliated Hospital of Shantou University Medical College, Shantou, Guangdong, China, [3]Department of Dermatology, First Affiliated Hospital of Shantou University Medical College, Shantou, Guangdong, China

Objective: The lactate/albumin ratio (LAR) has been used as a novel prognostic indicator for aneurysmal subarachnoid hemorrhage, traumatic brain injury, sepsis, heart failure, and acute respiratory failure. However, its potential in predicting all-cause mortality in patients with ischemic stroke (IS) has not been evaluated. Therefore, this study aimed to elucidate the correlation between LAR and 28-day all-cause mortality in IS patients without reperfusion therapy.

Methods: This retrospective cohort study used data from the Medical Information Mart for Intensive Care (MIMIC-IV) (v2.0) database. It included 568 IS adult patients admitted to the intensive care unit (ICU). The correlation between LAR and ICU 28-day all-cause mortality rate was analyzed using multiple COX regression analysis and Kaplan–Meier survival analysis. Restricted cubic spline (RCS) curves were used to assess the relationship between LAR and 28-day mortality. In addition, a subgroup analysis was performed to investigate the impact of other influencing factors on outcomes. The primary outcome was the ability of LAR to predict 28-day mortality in IS patients.

Results: Among the 568 patients with IS, 370 survived (survival group) and 198 died (non-survival group) within 28 days of admission (mortality rate: 34.9%). A multivariate COX regression analysis indicated that LAR was an independent predictor of all-cause mortality within 28 days after admission for patients with IS (hazard ratio: 1.32; 95% confidence interval: 1.03–1.68; $P = 0.025$). We constructed a model that included LAR, age, race, sex, white blood cell count, Sequential Organ Failure Assessment (SOFA) score, and anion gap (AG) and established a prediction model with an area under the curve (AUC) value of 71.5% (95% confidence interval: 67.1%–75.8%). The optimal cutoff value of LAR that separated the survival group and the non-survival group based on the Youden index was 0.55. The Kaplan-Meier survival curves plotted using this critical value showed that patients with LAR $\geq$ 0.55 had a significantly higher 28-day all-cause mortality rate than patients with LAR $<$ 0.55 ($P = 0.0083$).

Conclusion: LAR can serve as an independent predictor of all-cause mortality within 28 days after admission for patients with IS.

KEYWORDS

lactate/albumin ratio, ischemic stroke, all-cause mortality, 28-day, prognosis

1. Introduction

Ischemic stroke (IS) is a grave condition that affects the blood vessels in the brain and endangers the life of patients. It is the second most common cause of disability and death across the globe (1). Approximately 15% of IS patients die within 30 days (1). In recent years, the emergence of venous thrombolysis and endovascular thrombectomy has ushered us into a new era of IS treatment, wherein efficient reperfusion therapy is widely employed (2). However, numerous patients cannot be treated with reperfusion therapy in time, especially in developing countries. Therefore, there is an urgent need for simple and practical risk indicators that can inform the clinical management of IS patients without reperfusion therapy.

Lactate, a by-product of anaerobic metabolism, indicates the degree of tissue underperfusion and cellular oxygen deprivation (3). It can also forecast organ dysfunction and death in critically ill patients (4). Besides, it plays a crucial role in IS prognosis because it accumulates rapidly due to impaired diffusion of ischemic brain tissue, and its excess causes acidosis, which activates specific ion channels, leading to neurotoxic calcium accumulation and cytotoxic swelling (5). However, protein hydrolysis metabolism and metformin intake in patients with liver dysfunction or abnormalities can lead to abnormal lactate levels (6, 7). Therefore, relying solely on lactate levels for prediction may not guarantee reliable results.

Albumin is a vital protein that regulates blood osmotic pressure and influences the physiological function of the circulatory system. It also exhibits anti-inflammatory, antioxidant, and antithrombotic effects. However, serum albumin levels are influenced by kidney disease or nutritional status and therefore have limited value on their own in predicting IS outcomes (8, 9).

Some studies have explored the lactate/albumin ratio (LAR) as a potential predictor of acute pancreatitis, severe pneumonia, traumatic brain injury, and aneurysm subarachnoid hemorrhage (10–13). However, the link between LAR and mortality in IS patients remains unknown. Therefore, we obtained and analyzed data on IS patients admitted between 2008 and 2019 from the MIMIC-IV (v2.0) database. The current study aims to analyze the relationship between LAR and all-cause mortality within 28 days of admission in IS patients.

2. Methods

2.1. Data collection

We obtained our data from the MIMIC-IV (v2.0), a large-scale, open-source database created and maintained by the MIT Computational Physiology Laboratory (https://physionet.org/content/mimiciv/2.0/). This database contains the records of all the patients hospitalized at the Beth Israel Deaconess Medical Center (BIDMC) between 2008 and 2019. It provides comprehensive data, such as length of stay, laboratory results, medication administration, vital signs, etc., for each patient. The data was anonymized by replacing personal information with random codes to protect patient privacy, so we did not require patient consent or ethical approval. The MIMIC-IV (v2.0) database is available for download from the PhysioNet online platform (https://physionet.org/). To access the database, the second author of this study, Chen HongZhuang, completed the Collaborative Institutional Training Initiative (CITI) course and passed the exams on "Conflict of Interest" and "Data or Sample Only Research" (ID: 52748910). The research team was then authorized to use the database and extract data.

2.2. Population selection criteria

We selected patients from the MIMIC-IV database using the following criteria: (1) age above 18 years, and (2) IS diagnosis based on ICD-9 codes 433, 434, 436, 437.0, and 437.1 or ICD-10 codes I63 and I65 (Figure 1). We excluded patients who underwent reperfusion therapy and those without lactate or albumin measurements. If patients had multiple ICU admissions, we only used clinical data from the first ICU admission. Ultimately, 568 patients were included in this study.

2.3. Data extraction

We selected LAR as the primary variable of interest. We used the first blood lactate and serum albumin levels measured after admission to reduce the influence of subsequent treatments on these values. Potential confounders, such as demographics (age, sex, and race), vital signs (heart rate, systolic blood pressure, and diastolic blood pressure), comorbidities (myocardial infarction, congestive heart failure, peripheral vascular disease, dementia, chronic pulmonary disease, rheumatic disease, peptic ulcer disease, liver disease, diabetes, paraplegia, renal disease, AIDS, and hemorrhage), laboratory tests (red blood cell, white blood cell, and red blood cell distribution width, platelet, hemoglobin, and lymphocyte percentage, hematocrit, serum glucose level, anion gap, prothrombin time, and international normalized ratio), and sequential organ failure assessment (SOFA) scores were also extracted. Data extraction was performed using PostgreSQL (v13.7.1) and Navicate Premium (version 15) with structured query language. All the code for computing demographic features, laboratory tests, comorbidities, and severity scores were obtained from the GitHub website (GitHub - MIT-LCP/mimic-iv: Deprecated. For the latest MIMIC-IV code see: https://github.com/MIT-LCP/mimic-code).

2.4. Grouping and endpoint events

This study classified the patients into two groups: those who survived in the hospital for 28 days (survival group, $n = 370$) and

Abbreviations: AUC, area under the curve; AG, anion gap; CI, confidence interval; DBP, Diastolic Blood Pressure; HR, hazard ratio; IS, ischemic stroke; ICU, intensive care unit; LAR, lactate/albumin ratio; MIMIC-IV, Medical Information Mart for Intensive Care; RCS, Restricted cubic spline; SBP, Systolic Blood Pressure; SOFA, Sequential Organ Failure Assessment; WBC count, white blood cell count.

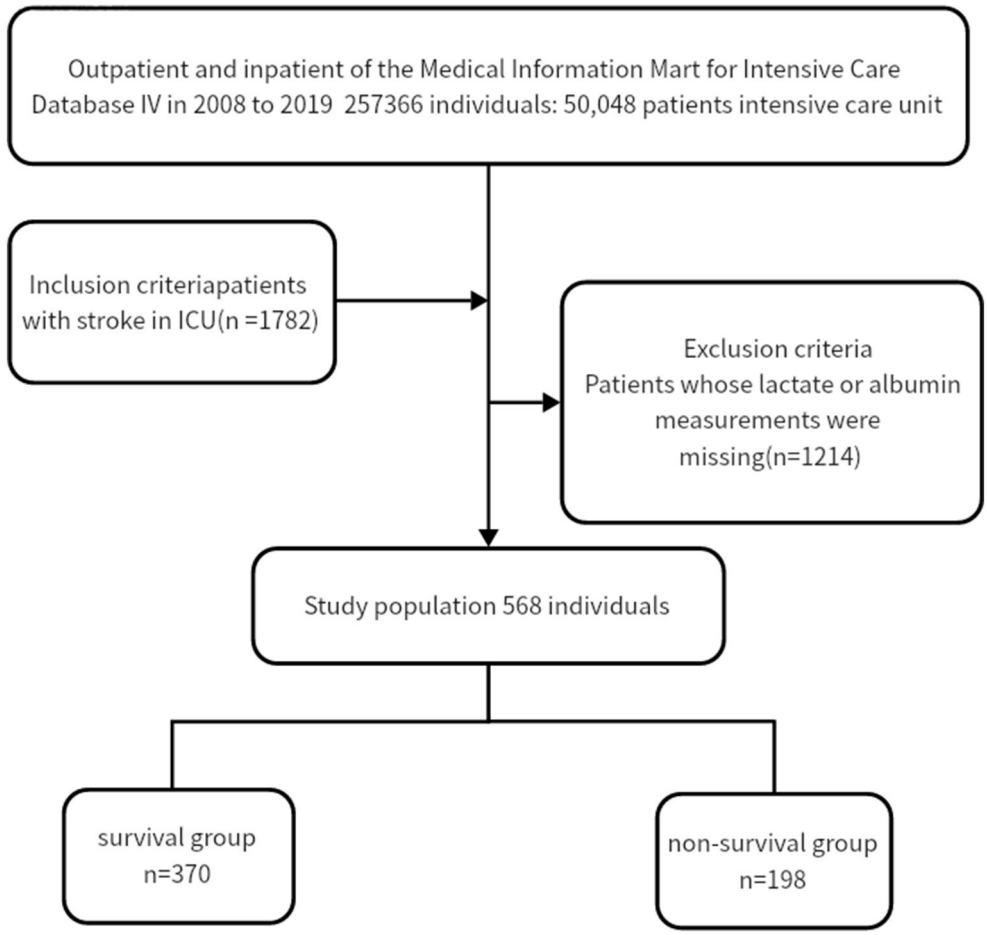

FIGURE 1
Flowchart of patient inclusion.

those who died in the hospital within 28 days (non-survival group, $n = 198$). The primary outcome of interest was all-cause mortality within 28 days of admission.

2.5. Management of missing data and outliers

Variables with more than 15% missing values, such as blood cholesterol, triglycerides, high-density lipoprotein, low-density lipoprotein, and C-reactive protein, were omitted to reduce bias. For variables with <15% missing values (lymphocyte, monocyte, and neutrophil counts), multiple imputation was applied to choose the best possible data set to impute the missing values (14).

2.6. Statistical analysis

The Kolmogorov-Smirnov test evaluated the normality of continuous variables. Continuous variables were reported as mean ± SD for normal distributions, median (IQR) for skewed distributions, and frequencies (%) for categorical variables. In the baseline characteristics analysis, continuous variables were compared using T-test or one-way ANOVA, while categorical variables were compared using Pearson's $\chi 2$ test and Fisher's test. A univariate COX regression analysis identified potential risk factors and a multivariate COX regression analysis determined the independent risk factors for in-hospital mortality with p-values below 0.05. A receiver operating characteristic (ROC) analysis assessed the model's predictive performance for 28-day in-hospital mortality by calculating the area under the curve (AUC), sensitivity, and specificity of the models. The Youden index was utilized to determine the optimal cutoff value.

Restricted cubic spline (RCS) analysis was employed to depict the non-linear relationship between LAR and 28-day all-cause mortality in IS subjects.

Kaplan–Meier curves were used to observe the relationship between LAR and mortality rate in IS patients. Subgroup analysis examined the effect of LAR on different characteristics, such as age, sex, race, SOFA scores, white blood cell (WBC) count, anion gap, ventilation status, and cerebral hemorrhage, and their p-values for interactions were also tested. All analyses were performed with free statistical software version 1.6 and R 4.1.3 (R Foundation for Statistical Computing, Vienna, Austria). $P < 0.05$ from two-tailed tests indicated statistical significance.

10.3389/fneur.2023.1271391

TABLE 1 Baseline characteristics between survivors(0) and non-survivors(1).

Variables	Total ($n = 568$)	0 ($n = 370$)	1 ($n = 198$)
Sex: male, *n* (%)	309 (54.4)	199 (53.8)	110 (55.6)
Age, mean ± SD	67.8 ± 15.7	66.1 ± 16.0	71.0 ± 14.5
Ethnicity, *n* (%)			
1 White	365 (64.3)	251 (67.8)	114 (57.6)
2 Black	71 (12.5)	47 (12.7)	24 (12.1)
3 Other	64 (11.3)	47 (12.7)	17 (8.6)
4 Unknown	68 (12.0)	25 (6.8)	43 (21.7)
SBP, mean ± SD	129.4 ± 27.8	129.4 ± 27.6	129.3 ± 28.3
DBP, mean ± SD	70.9 ± 20.0	70.5 ± 20.0	71.7 ± 20.2
SOFA, mean ± SD	7.4 ± 3.6	7.1 ± 3.4	7.9 ± 4.0
GCS, mean ± SD	9.1 ± 4.2	9.6 ± 4.1	8.1 ± 4.3
WBC, mean ± SD	13.1 ± 7.1	12.4 ± 6.6	14.4 ± 7.8
Neutrophils, mean ± SD	937.5 ± 735.7	904.9 ± 718.5	994.3 ± 763.5
Lymphocytes, mean ± SD	121.0 ± 208.1	109.8 ± 93.7	140.5 ± 321.5
Monocytes, mean ± SD	50.2 ± 61.2	47.1 ± 47.1	55.5 ± 79.9
Platelets, mean ± SD	229.3 ± 124.3	231.1 ± 131.0	225.8 ± 110.9
Hemoglobin, mean ± SD	11.5 ± 2.6	11.4 ± 2.6	11.6 ± 2.7
Glucose, mean ± SD	172.3 ± 99.9	171.0 ± 104.5	174.7 ± 90.9
Creatinine, mean ± SD	1.6 ± 1.5	1.6 ± 1.6	1.6 ± 1.4
Anion gap, mean ± SD	16.4 ± 5.1	15.8 ± 4.7	17.6 ± 5.6
PT, mean ± SD	17.4 ± 14.2	17.3 ± 13.8	17.5 ± 15.0
PTT, mean ± SD	36.4 ± 21.5	35.9 ± 20.3	37.2 ± 23.7
Phosphate, mean ± SD	3.8 ± 1.5	3.8 ± 1.4	3.9 ± 1.6
Lactate, mean ± SD	2.3 ± 2.0	2.1 ± 1.6	2.6 ± 2.5
Albumin, mean ± SD	3.2 ± 0.7	3.2 ± 0.7	3.1 ± 0.6
LAR, mean ± SD	0.8 ± 0.7	0.7 ± 0.6	0.9 ± 0.9
Myocardial infarct, *n* (%)	95 (16.7)	64 (17.3)	31 (15.7)
Congestive heart failure, *n* (%)	140 (24.6)	85 (23)	55 (27.8)
Peripheral vascular disease, *n* (%)	102 (18.0)	66 (17.8)	36 (18.2)
Cerebrovascular disease, *n* (%)	568 (100.0)	370 (100)	198 (100)
Dementia, *n* (%)	12 (2.1)	6 (1.6)	6 (3)
Chronic pulmonary disease, *n* (%)	129 (22.7)	91 (24.6)	38 (19.2)
Rheumatic disease, *n* (%)	15 (2.6)	10 (2.7)	5 (2.5)
Peptic ulcer disease, *n* (%)	12 (2.1)	7 (1.9)	5 (2.5)
Mild liver disease, *n* (%)	67 (11.8)	45 (12.2)	22 (11.1)
Severe liver disease, *n* (%)	16 (2.8)	11 (3)	5 (2.5)
Diabetes, *n* (%)	214 (37.7)	141 (38.1)	73 (36.9)
Paraplegia, *n* (%)	158 (27.8)	101 (27.3)	57 (28.8)
Renal disease, *n* (%)	129 (22.7)	84 (22.7)	45 (22.7)
Aids, *n* (%)	4 (0.7)	1 (0.3)	3 (1.5)
Charlson comorbidity index,	6.9 ± 2.7	6.7 ± 2.6	7.3 ± 2.8
Hemorrhage, *n* (%)	84	57	27
Atrial fibrillation, *n* (%)	254	162	92

DBP, Diastolic Blood Pressure; GCS, Glasgow coma scale; LAR, lactate-to-albumin ratio; SBP, Systolic Blood Pressure; SOFA, sequential organ failure assessment; WBC, white blood cell count.

3. Results

3.1. Baseline demographic and clinical characteristics

Table 1 shows the baseline characteristics of the survival and non-survival groups. Of the 568 patients who met the inclusion criteria, 309 (55.4%) were men and the median age was 67.8 (52.1, 83.5) years. The 28-day mortality rate was 34.9%. Non-survivors were older ($P < 0.01$) and had lower Glasgow Coma Scale scores, lower albumin levels ($P < 0.05$), higher SOFA scores, higher LAR [0.9 (0, 1.8) *vs.* 0.7 (0.1, 1.3), $P = 0.002$], and higher lactate levels ($P < 0.05$) than survivors. The other covariates were not significantly different between the groups ($P > 0.05$).

3.2. LAR is an independent risk factor for all-cause mortality within 28 days of hospital admission

Unadjusted LAR showed a significant association with all-cause mortality within 28 days of admission [hazard ratio (HR), 1.45; 95% confidence interval (CI), 1.15–1.83; $P = 0.002$] according to the results of the univariate COX regression analysis (Table 2). In the multivariate COX regression analysis (Table 3), LAR remained significantly associated with higher in-hospital 28-day all-cause mortality after adjusting for potential confounding factors such as age, sex, and race (HR, 1.55; 95% CI, 1.23–1.96; $P < 0.002$) in Model 1. Moreover, in Model 2, which included additional adjustments for WBC count, anion gap, and SOFA score, LAR remained an

10.3389/fneur.2023.1271391

TABLE 2 Univariate Cox regression models evaluating the association between LAR and 28-day all-cause mortality with IS.

Item	HR (95%CI)	*P* (Wald's test)
Sex	1.05 (0.79,1.39)	0.758
Age	1.02 (1.01,1.03)	0.001
Ethnicity: ref. = 1		
2	1.08 (0.7,1.68)	0.731
3	0.84 (0.5,1.39)	0.49
4	2.6 (1.83,3.69)	<0.001
SBP	1.0001 (0.9951, 1.0052)	0.957
DBP	1.0024 (0.9956, 1.0092)	0.485
SOFA	1.05 (1.01,1.09)	0.022
GCS	0.93 (0.9,0.97)	<0.001
WBC	1.03 (1.01,1.05)	<0.001
Neutrophils	1.0002 (1, 1.0004)	0.104
Lymphocytes	1.0005 (1, 1.0011)	0.042
Monocytes	1.0024 (1.0003, 1.0045)	0.026
Platelets	0.9998 (0.9987, 1.0009)	0.719
Hemoglobin	1.03 (0.98,1.09)	0.215
Glucose	1.0004 (0.9991, 1.0017)	0.564
Creatinine	1.01 (0.93,1.11)	0.752
Anion gap	1.05 (1.02,1.07)	<0.001
Sodium	1.03 (1.01,1.05)	0.011
Potassium	1.11 (0.96,1.28)	0.168
PT	0.9999 (0.9902, 1.0096)	0.982
PTT	1.0021 (0.9959, 1.0083)	0.514
Phosphate	1.08 (0.99,1.19)	0.099
Lactate	1.11 (1.05,1.18)	<0.001
Albumin	0.86 (0.7,1.05)	0.138
LAR	1.45 (1.15,1.83)	0.002
Myocardial infarction: 1 vs. 0	0.89 (0.61,1.31)	0.568
Congestive heart failure: 1 vs. 0	1.21 (0.88,1.65)	0.236
Peripheral vascular disease: 1 vs. 0	1.04 (0.73,1.5)	0.822
Dementia: 1 vs. 0	1.53 (0.68,3.46)	0.303
Chronic pulmonary disease: 1 vs. 0	0.76 (0.54,1.09)	0.132
Rheumatic disease: 1 vs. 0	0.9 (0.37,2.18)	0.813
Peptic ulcer disease: 1 vs. 0	1.21 (0.5,2.94)	0.676
Mild liver disease: 1 vs. 0	0.87 (0.56,1.36)	0.549
Severe liver disease: 1 vs. 0	0.8 (0.33,1.93)	0.613
Diabetes: 1 vs. 0	0.94 (0.71,1.26)	0.692
Paraplegia: 1 vs 0	1.07 (0.78,1.45)	0.681
Renal disease: 1 vs. 0	0.9963 (0.7146, 1.3891)	0.983
Aids: 1 vs. 0	3.39 (1.08,10.61)	0.036
Charlson comorbidity index	1.06 (1.01,1.11)	0.026
Hemorrhage: 1 vs. 0	0.89 (0.59,1.33)	0.556
Atrial fibrillation: 1 vs. 0	1.08 (0.82,1.43)	0.573

(Continued)

TABLE 2 (Continued)

DBP, Diastolic Blood Pressure; GCS, Glasgow coma scale; LAR, lactate-to-albumin ratio; SBP, Systolic Blood Pressure; SOFA, sequential organ failure assessment; WBC, white blood cell count.

independent predictor of increased mortality risk (HR, 1.32; 95% CI, 1.03–1.68; $P = 0.025$).

3.3. ROC curve analysis, RCS curves, and Kaplan–Meier curve

Figure 2 displays the ROC curves of Model 2 plotted for predicting all-cause mortality within 28 days after admission of IS patients, and the AUC of the model was 71.5% (95% CI: 67.1%−75.8%). Additionally, Model 2 had a sensitivity of 75.13% and a specificity of 58.81%. Based on the Youden index, we selected the optimal threshold value to divide the IS patients into a high LAR group (LAR $\geq$ 0.55, $n = 283$) and a low LAR group (LAR < 0.55, $n = 285$). An RCS analysis was employed to assess the non-linear relationship between LAR and 28-day mortality in IS subjects (Figure 3). The Kaplan–Meier survival curves (Figure 4) show that the mortality rate of the high LAR group was significantly higher than that of the low LAR group ($P = 0.0083$).

3.4. Subgroup analysis and forest plots

Figure 5 shows that the correlation between LAR and all-cause mortality within 28 days of admission of IS patients was stable across subgroups. The forest plot from the stratified analysis was performed for age, sex, race, SOFA score, WBC count, anion gap, ventilation status, and hemorrhagic transformation of cerebral infarction and showed that LAR had no significant interaction with each subgroup (interaction P: 0.073–0.735). These results prove that LAR was an independent prognostic factor.

4. Discussion

This is the first study examining the role of LAR in IS patients. The results of this retrospective study demonstrated that the LAR was an independent factor for all-cause mortality in IS patients without reperfusion therapy within 28 days of hospital

10.3389/fneur.2023.1271391

TABLE 3 Multivariable Cox regression models evaluating the association between LAR and 28-day all-cause mortality with IS.

Variable	Crude. HR_95CI	Crude_*p*-value	Adj. HR_95CI	Adj. _*p*-value
Model 1				
LAR	1.45 (1.15∼1.83)	0.002	1.55 (1.23∼1.96)	0.001
Sex: male	1.05 (0.79∼1.39)	0.758	1.18 (0.88∼1.58)	0.267
Age	1.02 (1.01∼1.03)	0.001	1.02 (1.01∼1.03)	0.001
Ethnicity 1	Ref			
Ethnicity 2	1.09 (0.7∼1.7)	0.687	1.13 (0.72∼1.76)	0.601
Ethnicity 3	0.85 (0.51∼1.41)	0.524	0.93 (0.55∼1.55)	0.773
Ethnicity 4	2.55 (1.78∼3.65)	0.001	3.01 (2.09∼4.33)	0.001
Model 2				
LAR	1.45 (1.15∼1.83)	0.002	1.32 (1.03∼1.68)	0.025
Sex: male	1.05 (0.79∼1.39)	0.758	1.18 (0.88∼1.58)	0.257
Age	1.02 (1.01∼1.03)	0.001	1.02 (1.01∼1.03)	<0.001
Ethnicity 1	Ref			
Ethnicity 2	1.09 (0.7∼1.7)	0.687	1.19 (0.76∼1.88)	0.452
Ethnicity 3	0.85 (0.51∼1.41)	0.524	0.94 (0.56∼1.59)	0.821
Ethnicity 4	2.55 (1.78∼3.65)	<0.001	3.01 (2.08∼4.35)	<0.001
WBC	1.03 (1.01∼1.05)	<0.001	1.03 (1.01∼1.05)	0.002
Anion gap	1.05 (1.02∼1.07)	0.001	1.04 (1.01∼1.07)	0.007
SOFA	1.05 (1.01∼1.09)	0.022	1.03 (0.99∼1.07)	0.2

Ethnicity 1, Wihte; Ethnicity 2, Black; Ethnicity 3, Others; Ethnicity 4, Unknown; LAR, lactate-to-albumin ratio; SOFA, sequential organ failure assessment; WBC, white blood cell count.

admission. Our study included 568 patients from the MIMIC-IV (2.0) database. We conducted COX regression analysis to determine the independent predictive factors for 28-day mortality before and after adjusting for confounding factors. We found that LAR was consistently identified as an independent predictor of 28-day mortality. Additionally, we identified an optimal cutoff point (0.55), allowing us to construct a Kaplan–Meier curve and demonstrate that LAR effectively differentiated patients who died within 28 days. Furthermore, we adjusted for all confounding factors and created a forest plot, which showed that LAR remained a stable indicator unaffected by other variables. Therefore, LAR is reliable for predicting the 28-day mortality of IS patients and can be used as a novel clinical biomarker.

Lactate is an important indicator of tissue oxygenation, blood perfusion, and metabolism in the body. Hypoxia-induced acidosis in brain tissue is a sensitive indicator of brain injury (5). Lactate is a biomarker of ischemia produced by anaerobic glycolysis (15). Sakal et al. found that hyperlactatemia was correlated with increased mortality at 1, 3, and 12 months in IS patients (16, 17). However, interpreting serum lactate levels is indeed complex. For example, patients with liver disease may have abnormal lactate metabolism. Under hypoxic conditions, lactate production may also increase. Some drugs, such as salbutamol and metformin, can also elevate lactate levels. In addition, some critically ill patients may have lower lactate levels in venous blood, which reduces the reliability of lactate levels alone in predicting patient outcomes (18).

Serum albumin is associated with the outcome of IS (19). Serum albumin extravasation into the ischemic brain may provide neuroprotection by limiting metal-catalyzed oxidative stress (20). Gao et al. found that a decline in serum albumin levels after 90 days of acute large vessel occlusive stroke was independently associated with poor prognosis (21). Dziedzic et al. and Babu et al. suggested that higher serum albumin levels in acute stroke patients could reduce the risk of adverse outcomes (22, 23).

A meta-analysis (24) including 13,618 patients with acute IS or transient ischemic attack concluded that low serum albumin levels could predict adverse functional outcomes and mortality in patients with these diseases. However, different albumin detection methods in different studies may have biased the results. In addition, serum albumin levels are influenced by underlying diseases, nutritional status, and inflammation, which may limit its prognostic value as a single measurement. In the present study, we took the ratio of blood lactate to serum albumin, reducing the influence of a single factor on the regulatory mechanism by causing inverse changes through two different mechanisms, thus more accurately predicting the outcome for IS patients.

Recently, researchers explored the predictive value of LAR in the prognosis of neurosurgical diseases. For example, Wang et al.'s cohort study (12) on the mortality of patients with moderate to severe traumatic brain injury showed that non-survivors had higher LAR than survivors (1.09 *vs.* 0.53, $P < 0.001$), which was close to our results. Zhang et al. (13) established a prediction model for

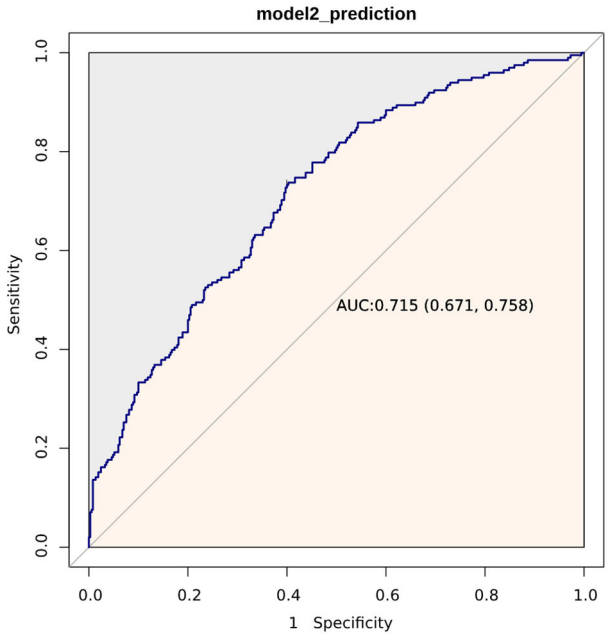

FIGURE 2
ROC curves of Model 2 for predicting 28-day mortality. Model 2 includes WBC count, anion gap, SOFA score, and LAR.

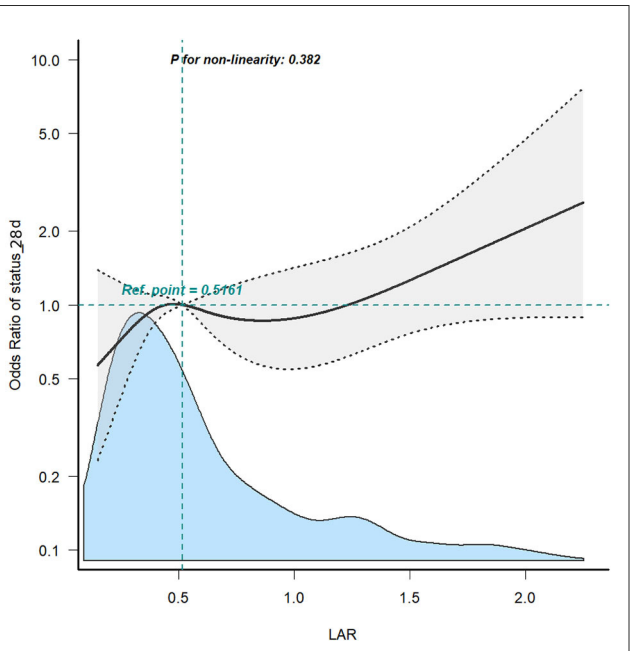

FIGURE 3
RCS curve for the LAR. Shaded ribbons denote 95% confidence intervals.

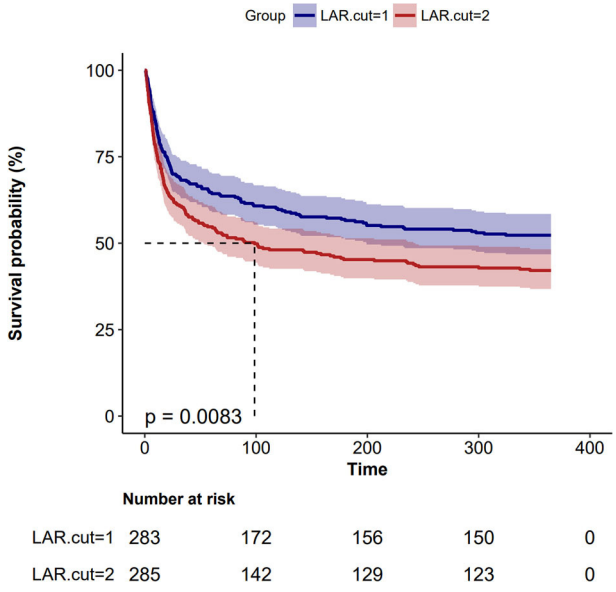

FIGURE 4
Kaplan–Meier survival analysis curves for 28-day all-cause mortality.

in-hospital mortality of patients with spontaneous subarachnoid hemorrhage. Independent predictors included age, LAR, anion gap, and Acute Physiology Score III, which was similar to our prediction model. Their results showed that LAR was closely related to increased in-hospital mortality of patients with spontaneous subarachnoid hemorrhage. However, studies using LAR to predict the outcome of ischemic stroke patients have yet to be reported.

Our results also confirmed previous research findings on the association between WBC count at admission and the prognosis of patients with ischemic stroke. Zheng et al. demonstrated that elevated WBC counts are correlated with stroke severity and adverse major and minor outcomes within a 3-month period (25). Furlan et al. reported that with each increase of $1 \times 10(-9)$/l in WBC count, there is a proportional rise in stroke severity, degree of disability at discharge, and 30-day mortality (26).

In addition to WBC count, our study also investigated the association between the anion gap and the prognosis of patients with ischemic stroke. Consistent with prior studies, Wang et al. observed a significant association between elevated AG values and increased all-cause mortality rates at 1 year, 4 years, and overall in patients with ischemic stroke who received rtPA treatment (27). Furthermore, Liu et al. demonstrated that high AG is an independent risk factor for all-cause mortality at 30 days, 60 days, and 180 days in patients with ischemic stroke (28). These collective study findings suggest that AG has the potential to serve as a biomarker for predicting the prognosis of patients with ischemic stroke.

Patients with IS admitted to the ICU have a higher mortality rate than other patients with IS. This may explain why the mortality rate of the patients included in our study was higher than the overall mortality rate of IS patients. In a study involving 370,386 ICU patients [including 7,046 (1.9%) stroke patients, with 4,072 having IS and 2,974 having intracerebral hemorrhage] (29), the short-term mortality rate of stroke patients admitted to the ICU was higher, with a 30-day mortality rate of 31% for IS patients, which is similar to our study.

In our study, LAR could be used as an independent predictor of 28-day all-cause mortality in IS patients without reperfusion

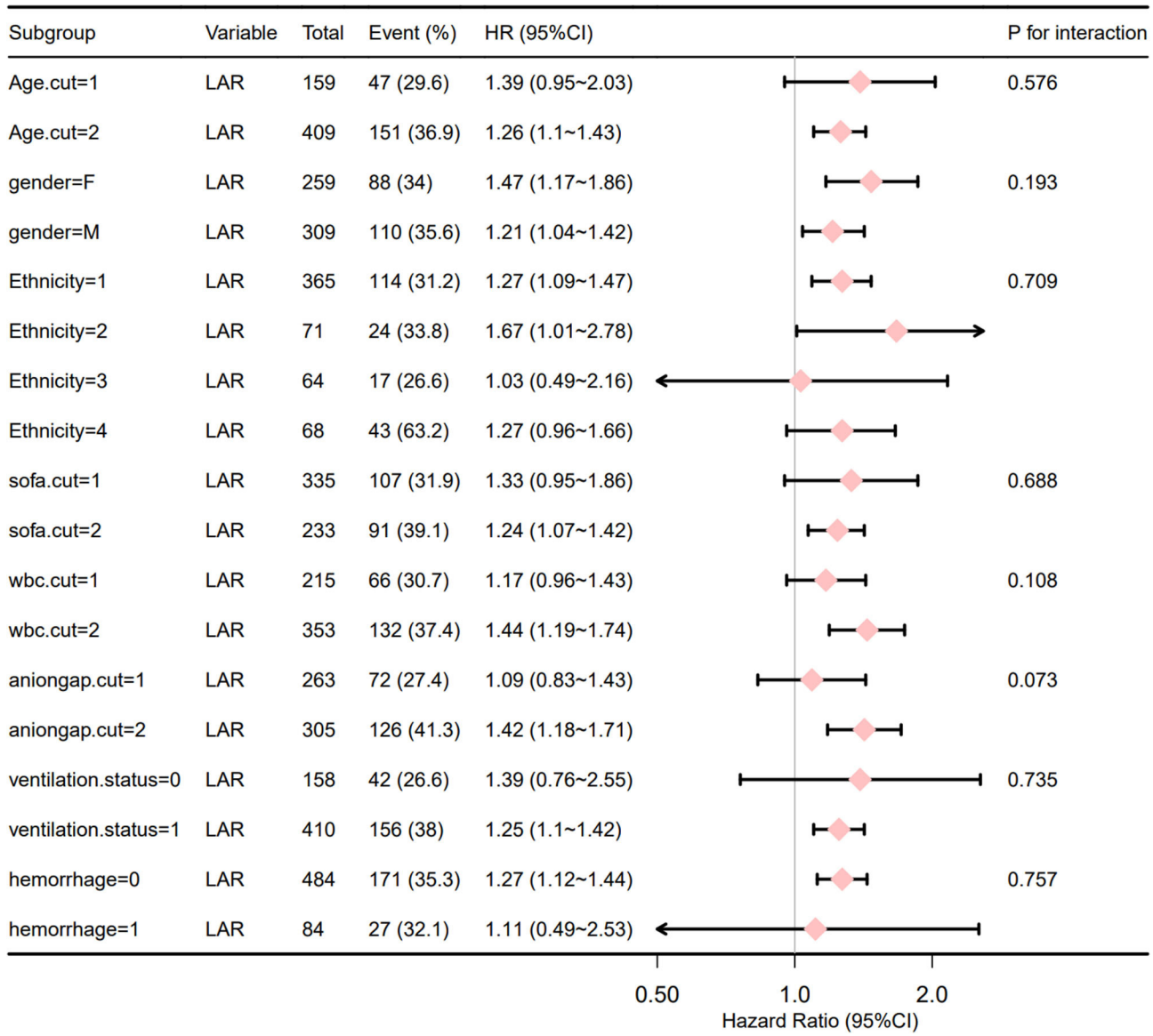

FIGURE 5
Forest plot for the subgroup analysis of the relationship between hospital mortality and LAR. Age.cut1, age < 67.8; Age.cut2, age > 67.8; Ethnicity1, White; Ethnicity2, Black; Ethnicity3, Other; Ethnicity4, Unknown; Sofa.cut1, sofa < 7; Sofa.cut2, sofa > 7; Wbc.cut1, WBC count < 13.1; Wbc.cut2, WBC count ≥ 13.1; aniogap.cut1, aniogap < 16.4; aniogap.cut2, aniogap > 16.4; for ventilation.status and hemorrhage, 0 means that the value does not exist and 1 means that it exists.

therapy; it yielded a more accurate prognosis than blood lactate or serum albumin alone. This will provide medical workers with a better tool for clinic planning for poor patient outcomes. Further validation of LAR as a readily available and objective biomarker is still needed in large-scale multicenter prospective studies.

Our study has some limitations. First, it is a single-center retrospective cohort study, which cannot elucidate the relationship between LAR and IS as prospective studies do, to the extent that our findings need more persuasive power. Second, the drugs and hospital medical care, which may affect the LAR of patients with IS, were not recorded, which might bias our results. Lastly, although potential confounding factors such as myocardial infarction, congestive heart failure, peripheral vascular disease, dementia, liver disease, and hemorrhage were not significantly present in our results, they should be considered and potentially excluded in future prospective studies.

5. Conclusion

LAR can serve as an independent predictor of all-cause mortality within 28 days after admission for IS patients without reperfusion therapy.

Data availability statement

The data analyzed in this study was obtained from the Medical Information Mart for Intensive Care IV (MIMIC-IV) database, the following licenses/restrictions apply: To access the files, users must be credentialed users, complete the required training (CITI Data or Specimens Only Research) and sign the data use agreement for the project. Requests to access these datasets should be directed to PhysioNet, https://physionet.org/, doi: 10.13026/6mm1-ek67.

Ethics statement

Ethical review and approval was not required for the study on human participants in accordance with the local legislation and institutional requirements. Written informed consent from the patients/participants or patients/participants' legal guardian/next of kin was not required to participate in this study in accordance with the national legislation and the institutional requirements.

Author contributions

YZ: Conceptualization, Data curation, Formal analysis, Funding acquisition, Investigation, Methodology, Project administration, Resources, Software, Supervision, Validation, Visualization, Writing—original draft, Writing—review and editing. HS: Conceptualization, Data curation, Formal analysis, Funding acquisition, Investigation, Methodology, Project administration, Resources, Software, Supervision, Validation, Visualization, Writing—original draft, Writing—review and editing. HC: Conceptualization, Data curation, Investigation, Methodology, Software, Supervision, Writing—review and editing. WJ: Data curation, Formal analysis, Methodology, Project administration, Supervision, Validation, Writing—review and editing. WC: Conceptualization, Data curation, Formal analysis, Funding acquisition, Investigation, Methodology, Project administration, Resources, Software, Supervision, Validation, Visualization, Writing—original draft, Writing—review and editing. JM: Conceptualization, Data curation, Formal analysis, Funding acquisition, Investigation, Methodology, Project administration, Resources, Software, Supervision, Validation, Visualization, Writing—original draft, Writing—review and editing.

Funding

The author(s) declare that no financial support was received for the research, authorship, and/or publication of this article. This work received no funding.

Acknowledgments

We gratefully appreciate all of the participants and staff for their contributions.

Conflict of interest

The authors declare that the research was conducted in the absence of any commercial or financial relationships that could be construed as a potential conflict of interest.

Publisher's note

References

1. Feigin VL, Forouzanfar MH, Krishnamurthi R, Mensah GA, Connor M, Bennett DA, et al. Global and regional burden of stroke during 1990–2010: findings from the global burden of disease study 2010. *Lancet.* (2014) 383:245–55. doi: 10.1016/S0140-6736(13)61953-4

2. Fisher M, Savitz SI. Pharmacological brain cytoprotection in acute ischaemic stroke — renewed hope in the reperfusion era. *Nat Rev Neurol.* (2022) 18:193–202. doi: 10.1038/s41582-021-00605-6

3. James JH, Luchette FA, McCarter FD, Fischer JE. Lactate is an unreliable indicator of tissue hypoxia in injury or sepsis. *Lancet.* (1999) 354:505–8. doi: 10.1016/S0140-6736(98)91132-1

4. Doenyas-Barak K, Beberashvili I, Marcus R, Efrati S. Lactic acidosis and severe septic shock in metformin users: a cohort study. *Critical Care.* (2016) 20:10. doi: 10.1186/s13054-015-1180-6

5. M. Tóth O, Menyhárt Á, Frank R, Hantosi D, Farkas E, Bari F. Tissue acidosis associated with ischemic stroke to guide neuroprotective drug delivery. *Biology.* (2020) 9:460. doi: 10.3390/biology9120460

6. Katopodis P, Pappas EM, Katopodis KP. Acid-base abnormalities and liver dysfunction. *Ann Hepatol.* (2022) 27:100675. doi: 10.1016/j.aohep.2022.100675

7. Park J, Hwang SY, Jo IJ, Jeon K, Suh GY, Lee TR, et al. Impact of metformin use on lactate kinetics in patients with severe sepsis and septic shock. *Shock.* (2017) 47:582–7. doi: 10.1097/SHK.0000000000000782

8. Manolis AA, Manolis TA, Melita H, Mikhailidis DP, Manolis AS. Low serum albumin: a neglected predictor in patients with cardiovascular disease. *Eur J Intern Med.* (2022) 102:24–39. doi: 10.1016/j.ejim.2022.05.004

9. Gillum RF, Ingram DD, Makuc DM. Relation between serum albumin concentration and stroke incidence and death: the nhanes i epidemiologic follow-up study. *Am J Epidemiol.* (1994) 140:876–88. doi: 10.1093/oxfordjournals.aje.a117176

10. Liu Q, Zheng H-L, Wu M-M, Wang Q-Z, Yan S-J, Wang M, et al. Association between lactate-to-albumin ratio and 28-days all-cause mortality in patients with acute pancreatitis: a retrospective analysis of the mimic-iv database. *Front Immunol.* (2022) 13:1076121. doi: 10.3389/fimmu.2022.1076121

11. Xu C, Liu H, Zhang H, Zeng J, Li Q, Yi Y, et al. Predictive value of arterial blood lactate to serum albumin ratio for in-hospital mortality of patients with community-acquired pneumonia admitted to the intensive care unit. *Postgrad Med.* (2022) 135:273–82. doi: 10.1080/00325481.2022.2110769

12. Wang R, He M, Qu F, Zhang J, Xu J. Lactate albumin ratio is associated with mortality in patients with moderate to severe traumatic brain injury. *Front Neurol.* (2022) 13:662385. doi: 10.3389/fneur.2022.662385

13. Zhang G-G, Hao J-H, Yong Q, Nie Q-Q, Yuan G-Q, Zheng Z-Q, et al. Lactate-to-albumin ratio is associated with in-hospital mortality in patients with spontaneous subarachnoid hemorrhage and a nomogram model construction. *Front Neurol.* (2022) 13:1009253. doi: 10.3389/fneur.2022.1009253

14. Austin PC, White IR, Lee DS, van Buuren S. Missing data in clinical research: A tutorial on multiple imputation. *Can J Cardiol.* (2021) 37:1322–31. doi: 10.1016/j.cjca.2020.11.010

15. Kraut JA, Madias NE. Lactic acidosis. *N Engl J Med.* (2014) 371:2309–19. doi: 10.1056/NEJMra1309483

16. Brouns R, Sheorajpanday R, Wauters A, De Surgeloose D, Mariën P, De Deyn PP. Evaluation of lactate as a marker of metabolic stress and cause of secondary damage in acute ischemic stroke or tia. *Clinica Chimica Acta.* (2008) 397:27–31. doi: 10.1016/j.cca.2008.07.016

17. Sakal C, Ak R, Taşçi A, Kirkpantur ED, Ünal Akoglu E, Cimilli Ozturk T. Admission blood lactate levels of patients diagnosed with cerebrovascular disease effects on short- and long-term mortality risk. *Int J Clin Pract.* (2021) 75:e14161. doi: 10.1111/ijcp.14161

18. Bou Chebl R, Geha M, Assaf M, Kattouf N, Haidar S, Abdeldaem K, et al. The prognostic value of the lactate/albumin ratio for predicting mortality in septic patients presenting to the emergency department: a prospective study. *Ann Med.* (2021) 53:2268–77. doi: 10.1080/07853890.2021.2009125

19. Wang A, Zhang Y, Xia G, Tian X, Zuo Y, Chen P, et al. Association of serum albumin to globulin ratio with outcomes in acute ischemic stroke. *CNS Neurosc Ther.* (2023) 29:1357–67. doi: 10.1111/cns.14108

20. Gum ET, Swanson RA, Alano C, Liu J, Hong S, Weinstein PR, et al. Human serum albumin and its n-terminal tetrapeptide (dahk) block oxidant-induced neuronal death. *Stroke.* (2004) 35:590–5. doi: 10.1161/01.STR.0000110790.05859.DA

21. Gao J, Zhao Y, Du M, Guo H, Wan T, Wu M, et al. Serum albumin levels and clinical outcomes among ischemic stroke patients treated with endovascular thrombectomy. *Neuropsychiatr Dis Treat.* (2021) 17:401–11. doi: 10.2147/NDT.S293771

22. Dziedzic T, Slowik A, Szczudlik A. Serum albumin level as a predictor of ischemic stroke outcome. *Stroke.* (2004) 35:e156–8. doi: 10.1161/01.STR.0000126609.18735.be

23. Babu MS, Kaul S, Dadheech S, Rajeshwar K, Jyothy A, Munshi A. Serum albumin levels in ischemic stroke and its subtypes: correlation with clinical outcome. *Nutrition.* (2013) 29:872–5. doi: 10.1016/j.nut.2012.12.015

24. Zhou H, Wang A, Meng X, Lin J, Jiang Y, Jing J, et al. Low serum albumin levels predict poor outcome in patients with acute ischaemic stroke or transient ischaemic attack. *Stroke Vasc Neurol.* (2021) 6:458–66. doi: 10.1136/svn-2020-000676

25. Zheng X, Zeng N, Wang A, Zhu Z, Zhong C, Xu T, et al. Prognostic value of white blood cell in acute ischemic stroke patients. *Curr Neurovasc Res.* (2018) 15:151–7. doi: 10.2174/1567202615666180626154857

26. Furlan JC, Vergouwen MDI, Fang J, Silver FL. White blood cell count is an independent predictor of outcomes after acute ischaemic stroke. *Eur J Neurol.* (2013) 21:215–22. doi: 10.1111/ene.12233

27. Wang H, Liu C, Xu H, Zhang Y, Gao P, Geng S, et al. The association between serum anion gap and all-cause mortality in cerebral infarction patients after treatment with rtpa: a retrospective analysis. *Dis Markers.* (2022) 2022:1–10. doi: 10.1155/2022/1931818

28. Liu X, Feng Y, Zhu X, Shi Y, Lin M, Song X, et al. Serum anion gap at admission predicts all-cause mortality in critically ill patients with cerebral infarction: evidence from the mimic-iii database. *Biomarkers.* (2020) 25:725–32. doi: 10.1080/1354750X.2020.1842497

29. van Valburg MK, Termorshuizen F, Brinkman S, Abdo WF, van den Bergh WM, Horn J, et al. Long-term mortality among icu patients with stroke compared with other critically ill patients. *Crit Care Med.* (2020) 48:e876–83. doi: 10.1097/CCM.0000000000004492

frontiers | Frontiers in Neurology

TYPE Brief Research Report
PUBLISHED 19 December 2023
DOI 10.3389/fneur.2023.1267136

OPEN ACCESS

EDITED BY
Yanlin Zhang,
Second Affiliated Hospital of Soochow University, China

REVIEWED BY
Manoj Kumar Tembhre,
All India Institute of Medical Sciences, India
Takashi Fujimoto,
Nagasaki University, Japan
Manovriti Thakur,
University of Bern, Switzerland

*CORRESPONDENCE
Tsuyoshi Izumo
✉ go-izumo@hotmail.co.jp

†These authors have contributed equally to this work

RECEIVED 26 July 2023
ACCEPTED 09 November 2023
PUBLISHED 19 December 2023

CITATION
Takahira R, Ujifuku K, Izumo T, Xie A, Okamura K, Morofuji Y and Matsuo T (2023) Do neutrophil extracellular traps implicate in atheromatous plaques from carotid endarterectomy? Re-analyzes of cDNA microarray data by surgeons. *Front. Neurol.* 14:1267136. doi: 10.3389/fneur.2023.1267136

Do neutrophil extracellular traps implicate in atheromatous plaques from carotid endarterectomy? Re-analyzes of cDNA microarray data by surgeons

Ryotaro Takahira†, Kenta Ujifuku†, Tsuyoshi Izumo*, Ang Xie, Kazuaki Okamura, Yoichi Morofuji and Takayuki Matsuo

Department of Neurosurgery, Graduate School of Biomedical Sciences, Nagasaki University, Nagasaki, Japan

Background: Carotid artery stenosis is the cause of 15% of strokes. Neutrophil extracellular traps (NETs) and peptidyl arginine deiminase 4 (PAD4) are believed to be involved in thrombosis. This pilot study described the differential expression profile of NETs between atheromatous plaques and surrounding tissues.

Methods: Microarray datasets of carotid plaques were obtained from Gene Expression Omnibus. The normalized data were processed into comma-separated value matrix files using spreadsheet software. Analyzes of microarray data were conducted using integrated differential expression and pathway analysis.

Result: The clustering results illustrated that the classifications of plaque and control had reasonable biological validity. Pathway analysis revealed the relevance of immune response, cell signaling, and other pathways. Differentially expressed genes were detected between carotid plaques and control specimens. However, enrichment analyzes did not reveal a difference in PAD4 expression between the groups and that NET implication was only found in one cDNA microarray dataset.

Discussion: This pilot study does not necessarily dismiss the possibility of a relationship between NETs and atherothrombotic stroke. Gene expression could differ between endothelial cells and atheromas, and further studies are needed.

KEYWORDS

atheromatous plaque, carotid endarterectomy, cDNA microarray, neutrophil extracellular traps, peptidyl arginine deiminase 4

1 Introduction

Carotid artery stenosis is the cause of 15% of strokes (1, 2). Based on early histopathologic studies, ischemic events are associated with intraplaque hemorrhage, ulceration, calcification, lipid-rich necrosis, plaque thrombus, macrophage infiltration, and high microvessel density (3–6).

Neutrophil extracellular traps (NETs) are specialized structures released by neutrophils. NETs were initially believed to form in response to stimuli such as infection and inflammation and contribute to the elimination of pathogens such as bacteria and viruses (7). Recently, they have been suggested to participate in the regulation of inflammatory responses, blood

TABLE 1 Reanalyzed microarray data of carotid endarterectomy specimens.

Authors and Year	GEO accession number	Examined specimens, number	Comparison specimens, number	Array
Manca et al. (2011) (18)	GSE28829	Advanced lesion (thin or thick fibrous cap atheroma), 16	Early lesion (intimal thickening and intimal xanthoma), 13	Affymetrix Human Genome U133 Plus 2.0 Array
Bricca et al. (2013) (17)	GSE43292	Atheroma plaque (stage IV and over of the Stary classification) containing the core and shoulders of the plaque, 32	Distant macroscopically intact tissue (stages I and II), 32	Affymetrix Human Gene 1.0 ST Array [transcript (gene) version]

GEO, Gene expression omnibus. The normalized data files are downloaded from GEO (https://www.ncbi.nlm.nih.gov/geo/).

coagulation, and pathological conditions such as autoimmune diseases and thrombosis (8–10). Elevated peptidyl arginine deiminase 4 (PAD4) levels have been detected in blood samples collected during carotid artery stenting, suggesting the involvement of NETs in the pathogenesis of atherothrombotic stroke (11).

Microarray and ribonucleic acid sequencing (RNAseq) allow comprehensive analyzes of transcriptomes. Genome-wide transcriptome analysis is often required in addition to individual gene expression analyzes. There are already re-analysis reports of existing microarray data (12, 13). However, big data analysis requires knowledge of statistics, informatics, and data science, which can pose difficulties for general biologists, physicians, and surgeons (14, 15).

In the absence of a bioinformatics expert, this study analyzed whether correlations related to NETs could be detected using historical carotid plaque-derived complementary deoxyribonucleic acid (cDNA) microarray data.

2 Materials and methods

Based on national ethical guidelines, this study did not originally fall under the category of research requiring written consent from study participants (16). This study was approved by the Institutional Review Board (number 23071016). The Gene Expression Omnibus[1] database was examined using the search terms human, carotid artery, and endarterectomy. Twelve data were found as of October 2023. GSE28829 and GSE43292 datasets, which appeared to compare plaque and normal to early atheromatous vessels, were selected for the present analysis (Table 1) (17, 18). The downloaded normalized data were converted to comma-separated value (CSV) matrix files using spreadsheet software. An outline of the strategy used for the GEO original data is provided in the Supplementary Files S1–S4. Analyzes of microarray data were conducted using integrated Differential Expression and Pathway analysis (iDEP) 1.1 (19).[2] The detailed methods and R session information are provided in the Supplementary File S5.

3 Results

3.1 Heatmap, principal component analysis, and differential expression analysis

The elimination q-value (false discovery rate [FDR]) was 0.10 in the iDEP computation. The clustering results indicated that the pre-specified classification of plaque and control specimens had more than moderate biological validity (Figures 1A,B). In PCA, principal component 1 (PC1) was mainly relevant to immune response, and PC2 was related to cell signaling, tissue development, neurogenesis, and other pathways (Figure 1C; Supplementary Figure S1). Differentially expressed genes (DEGs) of advanced carotid plaque were detected. Compared to microscopically normal artery, 87 upregulated and 60 downregulated DEGs were detected in advanced carotid plaque in the GSE43292 dataset ($q < 0.1$; Figure 2). In comparison with early plaques, 396 upregulated and 71 downregulated genes were detected in advanced carotid plaque in the GSE28829 dataset ($q < 0.1$; Supplementary Figure S1). See the Supplementary Files for detailed specific genes (Supplementary Files S6, S8).

3.2 Enrichment and pathway analyzes

Pathway analysis was performed using Generally Applicable Gene-set Enrichment for Pathway Analysis (20) and Gene Ontology (21), and the selected gene sets were obtained from the Kyoto Encyclopedia of Genes and Genomes (KEGG) (22). The pathway significance cutoff (FDR) was 0.2. The main results are summarized in Table 2. The NET formation was enriched as a significant pathway only in the GSE43292 dataset, and DEGs were presented on the KEGG graph. PAD4 was not identified as a DEG in the expression analyzes. The two datasets shared the same reduced expression of histone deacetylase (HDAC), but differences were observed for histone expression (Figure 3; Supplementary Figure S1). See the Supplementary Files for detailed specific pathways (Supplementary Files S7, S9).

1 GEO, https://www.ncbi.nlm.nih.gov/geo/.

2 http://ge-lab.org/idep/

Abbreviations: cDNA, complementary deoxyribonucleic acid; CSV, comma-separated value; DEGs, differentially expressed genes; FDR, false discovery rate; GEO, Gene Expression Omnibus; HDAC, histone deacetylase; iDEP, integrated Differential Expression and Pathway analysis; KEGG, Kyoto Encyclopedia of Genes and Genomes; NETs, neutrophil extracellular traps; PAD4, peptidyl arginine deiminase 4; PC, principal component; PCA, principal component analysis; RNAseq, ribonucleic acid sequencing.

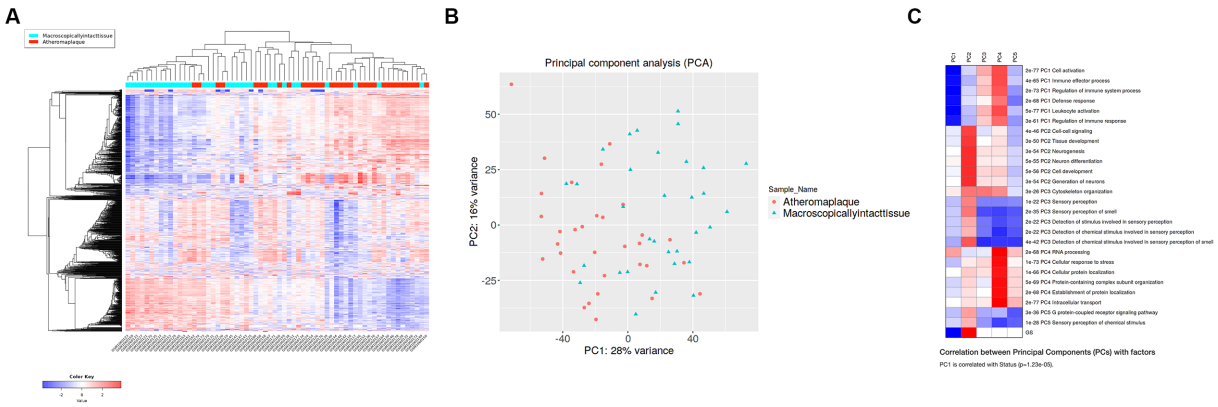

FIGURE 1
Hierarchical clustering heatmap **(A)** and principal component analysis **(B)** of advanced (unstable) and early (stable) atherosclerotic arteries from the GSE43292 dataset. The clusters are separated according to the pre-specified classification (plaque or normal), and the comparisons are likely to be meaningful. **(C)** GSE43292 pathway analysis of the PCA rotation matrix displays gene groups extracted using the results of principal component analysis. Inflammation, immune response, and other pathways were extracted.

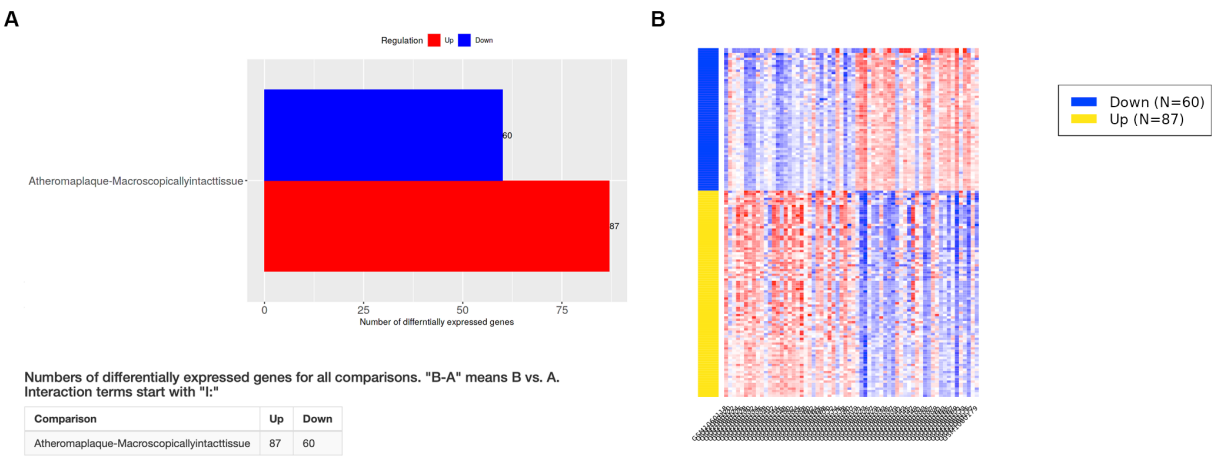

Numbers of differentially expressed genes for all comparisons. "B-A" means B vs. A. Interaction terms start with "I:"

Comparison	Up	Down
Atheromaplaque-Macroscopicallyintacttissue	87	60

FIGURE 2
Differentially expressed genes (DEGs) in the GSE43292 dataset. **(A)** Compared to the findings for control specimens (microscopically normal artery), 87 upregulated and 60 downregulated DEGs were detected in advanced carotid plaque ($q < 0.1$). **(B)** Heatmap of DEGs in the GSE43292 dataset. See the Supplementary Files for detailed data (Supplementary Files S6, S7).

4 Discussion

Existing cDNA microarray data on carotid plaques of human origin represent a valuable source of information as they can be repeatedly analyzed to reflect the latest research, depending on the researcher's interest. Nai et al. reported a re-analysis of the GSE43292 dataset and explored novel genes and pathways of carotid atheroma (12). Gao et al. examined immune cell infiltration between early and advanced carotid atheromatous plaque using the GSE28829 dataset (13). The cooperation of bioinformatics experts is considered essential for the former consideration. On the other hand, the latter report uses a web tool and does not necessarily require an expert, which could be another option from the present study. Our study presented a method for uploading normalized CSV matrix files to the iDEP web platform and analyzing the data (see legends in Supplementary Files S1–S4). All analyzes were performed on a

TABLE 2 **Enriched pathways in both GSE28829 and GSE 43292 datasets.**

Direction	Enriched pathway
Downregulated	Regulation of muscle contraction
Downregulated	Muscle contraction
Downregulated	Regulation of muscle system process
Upregulated	Immune response
Upregulated	Immune system process
Upregulated	Defense response
Upregulated	Response to other organism
Upregulated	Biological process involved in interspecies interaction between organisms
Upregulated	Inflammatory response
Upregulated	Cell activation

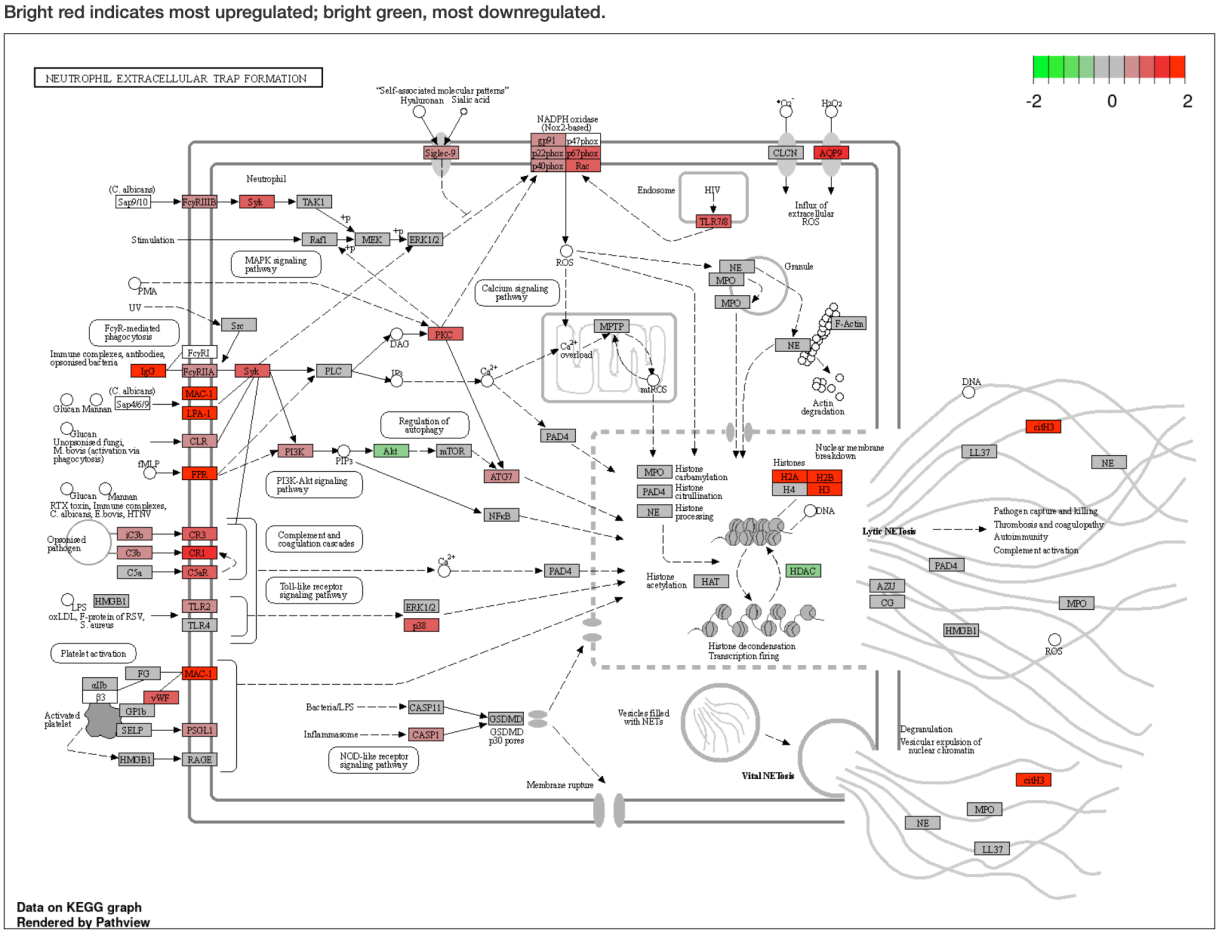

FIGURE 3
Pathway analysis of the GSE43292 dataset described in Kyoto Encyclopedia of Genes and Genomes graph. Neutrophil extracellular trap formation is enriched (false discovery rate < 0.2). Peptidyl arginine deiminase 4 (PAD4) expression was not significantly elevated. Histone deacetylase expression was reduced. Bright red indicates most upregulated; bright green, most downregulated. The KEGG pathway map (hsa04613 Neutrophil extracellular trap formation) is reprinted with permission from Kanehisa Laboratories (20).

graphical user interface such that the character user interface was avoided. As the analysis is performed online, a computer with standard performance was sufficient. Some typical cDNA microarray and RNAseq analysis methods are available and free of charge for scientific use (15, 19). We adopted this method in the present study because it allows visualization and display of the NETs' DEG information on the KEGG graph.

The organization of the controls was not consistent in the present study (Table 1). Data from GSE28829 compared advanced plaque with intimal thickening and intimal xanthoma, and advanced plaque and distant macroscopically intact tissues were compared in GSE43292. One possible reason for the discrepancies between the results of the two datasets in this study could be that the former detected mainly DEGs associated with plaque progression, while the latter detected mainly DEGs associated with plaque development. The lack of control samples compared to the number of validation samples in the GSE28829 data may have also affected the results. Conversely, it remains nearly impossible to obtain human-derived normal arterial tissue as control samples from an ethical viewpoint.

High PAD4 expression was not extracted as a DEG in our re-analysis of existing microarray data. This finding is inconsistent with that reported by Simonaga et al. (11). They collected blood samples from the luminal side, which could represent a different target from our study results, in which atheromas were analyzed. In other words, it is possible that different genes could be expressed in vascular endothelial cells and atheromas even though both contribute to a series of atherosclerotic processes. Therefore, we cannot exclude the possibility that NETs are involved in the development of carotid artery plaques and their rupture. Clinicopathological studies and single-cell comprehensive gene expression analyzes could be helpful for clarifying their pathogenesis.

Several limitations to this study warrant mention. Because of the inconsistency of the controls, whether they represented normal tissue may be debatable (Table 1). Next, microarrays are not chip-compatible, making integrated analysis extremely difficult. Then, although the results of analyzes of cDNA microarray and RNAseq data can suggest certain correlations, causal relationships cannot always be proven. Furthermore, scientists should consider the final biological interpretation as the results of big data and machine learning do not necessarily have biological relevance (15, 23). Finally, this research is an analysis that is only possible within the platform created by bioinformatics researchers. The need to rely on experts will continue to be necessary when detailed fine-tuning or new analysis methods are required.

Data availability statement

The original contributions presented in the study are included in the article/Supplementary material, further inquiries can be directed to the corresponding author.

Ethics statement

The studies involving humans were approved by the Nagasaki University Hospital Institutional Review Board. The studies were conducted in accordance with the local legislation and institutional requirements. The human samples used in this study were acquired from another research group. Written informed consent for participation was not required from the participants or the participants' legal guardians/next of kin in accordance with the national legislation and institutional requirements.

Author contributions

RT: Conceptualization, Data curation, Formal analysis, Methodology, Writing – original draft, Writing – review & editing. KU: Conceptualization, Data curation, Formal analysis, Funding acquisition, Methodology, Project administration, Resources, Software, Writing – original draft, Writing – review & editing. TI: Conceptualization, Formal analysis, Funding acquisition, Investigation, Project administration, Supervision, Validation, Visualization, Writing – original draft, Writing – review & editing. AX: Data curation, Writing – review & editing. KO: Writing – review & editing. YM: Funding acquisition, Writing – review & editing. TM: Funding acquisition, Supervision, Writing – review & editing.

Funding

The author(s) declare financial support was received for the research, authorship, and/or publication of this article. This study was supported by Grants-in-Aid for Scientific Research from JSPS KAKENHI (C) 20K09351 (to YM), (C) 21K09154 (to KU), (C) 21K09180 (to TI), and (C) 21K09129 (to TM) and from Fostering Joint International Research 20KK0254 (to YM).

Acknowledgments

The authors would like to pay tribute to the original plaque research teams (17, 18), the developers of bioinformatics tools (19–22, 24), and the sample donors to GEO. In this study, the authors referred to the Online Mendelian Inheritance in Man and Ensembl database (25, 26). The R logo is (C) 2016 The R Foundation, released under the terms of the Creative Commons Attribution-ShareAlike 4.0 International License (CC-BY-SA 4.0; https://www.r-project.org) (24). The copyright holder of the KEGG pathway map (hsa04613 Neutrophil extracellular trap formation) is Kanehisa Laboratories (22). We would also like to thank Enago for the English language review.

Conflict of interest

The authors declare that the research was conducted in the absence of any commercial or financial relationships that could be construed as a potential conflict of interest.

The reviewer TF declared a shared affiliation with the authors to the handling editor at the time of review.

Publisher's note

Supplementary material

The Supplementary material for this article can be found online at: https://www.frontiersin.org/articles/10.3389/fneur.2023.1267136/full#supplementary-material

SUPPLEMENTARY DATASHEET 1-4
Data for integrated Differential Expression and Pathway analysis. Matrix data were processed using spreadsheet software and saved as CSV files (Suppl1GSE28829_series_matrix, and Suppl3GSE43292_series_matrix). Attribute data were additionally attached (Suppl2GSE28829_series_attribute, and Suppl4GSE43292_series_attribute). When you process original Gene Expression Omnibus data, (1) the 1 × 1 cell must be blank data. (2) Paste the gene name or ID column from the 2 × 1 cell. Select the column, and specify the display format as a character string. (3) Provide the names of the specimens from the 1 × 2 cell. (4) Paste the expression data and complete the matrix data. (5) Remove the unnecessary description of statistics and other data. Unnecessary cells, columns, and rows should be removed. (6) Save the matrix as a CSV file. (15) See the Suppl1GSE28829_series_matrix and Suppl3GSE43292_series_matrix files for examples.

SUPPLEMENTARY DATASHEET 5
GSE43292 differentially expressed genes.

SUPPLEMENTARY DATASHEET 6
GSE43292 enriched phenomena.

SUPPLEMENTARY FILE 7
GSE28829 differentially expressed genes.

SUPPLEMENTARY FILE 8
GSE28829 enriched phenomena.

References

1. Rothwell PM, Eliasziw M, Gutnikov SA, Warlow CP, Barnett HJCarotid Endarterectomy Trialists Collaboration. Endarterectomy for symptomatic carotid stenosis in relation to clinical subgroups and timing of surgery. *Lancet*. (2004) 363:915–24. doi: 10.1016/S0140-6736(04)15785-1

2. Chaturvedi S, Bruno A, Feasby T, Holloway R, Benavente O, Cohen SN, et al. Carotid endarterectomy--an evidence-based review: report of the Therapeutics and Technology Assessment Subcommittee of the American Academy of Neurology. *Neurology*. (2005) 65:794–801. doi: 10.1212/01.wnl.0000176036.07558.82

3. Imparato AM, Riles TS, Gorstein F. The carotid bifurcation plaque: pathologic findings associated with cerebral ischemia. *Stroke*. (1979) 10:238–45. doi: 10.1161/01.STR.10.3.238

4. Fryer JA, Myers PC, Appleberg M. Carotid intraplaque hemorrhage: the significance of neovascularity. *J Vasc Surg*. (1987) 6:341–9. doi: 10.1016/0741-5214(87)90004-8

5. Virmani R, Kolodgie FD, Burke AP, Farb A, Schwartz SM. Lessons from sudden coronary death: a comprehensive morphological classification scheme for atherosclerotic lesions. *Arterioscler Thromb Vasc Biol*. (2000) 20:1262–75. doi: 10.1161/01.ATV.20.5.1262

6. Howard DP, Van Lammeren GW, Rothwell PM, Redgrave JN, Moll FL, De Vries JP, et al. Symptomatic carotid atherosclerotic disease: correlations between plaque composition and ipsilateral stroke risk. *Stroke*. (2015) 46:182–9. doi: 10.1161/STROKEAHA.114.007221

7. Brinkmann V, Reichard U, Goosmann C, Fauler B, Uhlemann Y, Weiss DS, et al. Neutrophil extracellular traps kill bacteria. *Science*. (2004) 303:1532–5. doi: 10.1126/science.1092385

8. Sorensen OE, Borregaard N. Neutrophil extracellular traps - the dark side of neutrophils. *J Clin Invest*. (2016) 126:1612–20. doi: 10.1172/JCI84538

9. Papayannopoulos V. Neutrophil extracellular traps in immunity and disease. *Nat Rev Immunol*. (2018) 18:134–47. doi: 10.1038/nri.2017.105

10. Franck G, Mawson TL, Folco EJ, Molinaro R, Ruvkun V, Engelbertsen D, et al. Roles of PAD4 and NETosis in experimental atherosclerosis and arterial injury: implications for superficial Erosion. *Circ Res*. (2018) 123:33–42. doi: 10.1161/CIRCRESAHA.117.312494

11. Shimonaga K, Matsushige T, Takahashi H, Hashimoto Y, Yoshiyama M, Ono C, et al. Peptidylarginine deiminase 4 as a possible biomarker of plaque instability in carotid artery stenosis. *J Stroke Cerebrovasc Dis*. (2021) 30:105816. doi: 10.1016/j.jstrokecerebrovasdis.2021.105816

12. Nai W, Threapleton D, Lu J, Zhang K, Wu H, Fu Y, et al. Identification of novel genes and pathways in carotid atheroma using integrated bioinformatic methods. *Sci Rep*. (2016) 6:18764. doi: 10.1038/srep18764

13. Gao J, Shi L, Gu J, Zhang D, Wang W, Zhu X, et al. Difference of immune cell infiltration between stable and unstable carotid artery atherosclerosis. *J Cell Mol Med*. (2021) 25:10973–9. doi: 10.1111/jcmm.17018

14. Ujifuku K, Fujimoto T, Sato K, Morofuji Y, Muto H, Masumoto H, et al. Exploration of Pericyte-derived factors implicated in lung Cancer brain metastasis protection: a pilot messenger RNA sequencing using the blood-brain barrier in vitro model. *Cell Mol Neurobiol*. (2022) 42:997–1004. doi: 10.1007/s10571-020-00988-y

15. Ujifuku K, Morofuji Y, Masumoto H. RNA sequencing data analysis on the maser platform and the tag-count comparison graphical userInterface. *Methods Mol Biol*. (2022) 2535:157–70. doi: 10.1007/978-1-0716-2513-2_13

16. Eba J, Nakamura K. Overview of the ethical guidelines for medical and biological research involving human subjects in Japan. *Jpn J Clin Oncol*. (2022) 52:539–44. doi: 10.1093/jjco/hyac034

17. Ayari H, Bricca G. Identification of two genes potentially associated in iron-heme homeostasis in human carotid plaque using microarray analysis. *J Biosci*. (2013) 38:311–5. doi: 10.1007/s12038-013-9310-2

18. Doring Y, Manthey HD, Drechsler M, Lievens D, Megens RT, Soehnlein O, et al. Auto-antigenic protein-DNA complexes stimulate plasmacytoid dendritic cells to promote atherosclerosis. *Circulation*. (2012) 125:1673–83. doi: 10.1161/CIRCULATIONAHA.111.046755

19. Ge SX, Son EW, Yao R. iDEP: an integrated web application for differential expression and pathway analysis of RNA-Seq data. *BMC Bioinformatics*. (2018) 19:534. doi: 10.1186/s12859-018-2486-6

20. Luo W, Friedman MS, Shedden K, Hankenson KD, Woolf PJ. GAGE: generally applicable gene set enrichment for pathway analysis. *BMC Bioinformatics*. (2009) 10:161. doi: 10.1186/1471-2105-10-161

21. Gene Ontology C, Aleksander SA, Balhoff J, Carbon S, Cherry JM, Drabkin HJ, et al. The Gene Ontology knowledgebase in 2023. *Genetics*. (2023) 224:31. doi: 10.1093/genetics/iyad031

22. Kanehisa M, Goto S. KEGG: Kyoto encyclopedia of genes and genomes. *Nucleic Acids Res*. (2000) 28:27–30. doi: 10.1093/nar/28.1.27

23. Ching T, Himmelstein DS, Beaulieu-Jones BK, Kalinin AA, Do BT, Way GP, et al. Opportunities and obstacles for deep learning in biology and medicine. *J R Soc Interface*. (2018) 15:20170387. doi: 10.1098/rsif.2017.0387

24. R Core Team. *R: A language and environment for statistical computing*. Vienna, Austria: R Core Team (2019).

25. Amberger J, Bocchini C, Hamosh A. A new face and new challenges for online Mendelian inheritance in man (OMIM(R)). *Hum Mutat*. 32:564–7. doi: 10.1002/humu.21466

26. Howe KL, Achuthan P, Allen J, Allen J, Alvarez-Jarreta J, Amode MR, et al. Ensembl 2021. *Nucleic Acids Res*. (2021) 49:D884–91. doi: 10.1093/nar/gkaa942

frontiers | Frontiers in Neurology

TYPE Original Research
PUBLISHED 29 December 2023
DOI 10.3389/fneur.2023.1308041

OPEN ACCESS

EDITED BY
Ulises Gomez-Pinedo,
Health Research Institute of Hospital Clínico San Carlos, Spain

REVIEWED BY
Ruxandra F. Sirbulescu,
Massachusetts General Hospital and Harvard Medical School, United States
Yanet Karina Gutierrez-Mercado,
University of Guadalajara, Mexico

*CORRESPONDENCE
Yanlin Zhang
✉ zhangyanlin0012006@163.com

†These authors have contributed equally to this work

RECEIVED 05 October 2023
ACCEPTED 01 December 2023
PUBLISHED 29 December 2023

CITATION
Zhang Y, Jiang Y, Zou Y, Fan Y, Feng P, Fu X, Li K, Zhang J, Dong Y, Yan S and Zhang Y (2023) Peripheral blood CD19 positive B lymphocytes increase after ischemic stroke and correlate with carotid atherosclerosis.
Front. Neurol. 14:1308041.
doi: 10.3389/fneur.2023.1308041

Peripheral blood CD19 positive B lymphocytes increase after ischemic stroke and correlate with carotid atherosclerosis

Yuhua Zhang[1†], Yu Jiang[1†], Yutian Zou[1,2†], Yinyin Fan[3], Ping Feng[3], Xiang Fu[1], Keru Li[1], Jinru Zhang[1], Yunlei Dong[1], Shuying Yan[1] and Yanlin Zhang[1*]

[1]Department of Neurology and Clinical Research Center of Neurological Disease, The Second Affiliated Hospital of Soochow University, Suzhou, China, [2]Department of Neurology, Affliated Changshu Hospital of Nantong University, Changshu, China, [3]Department of Clinical Laboratory, The Second Affiliated Hospital of Soochow University, Suzhou, China

Introduction: Atherosclerosis is the primary pathological basis of ischemic stroke, and dyslipidemia is one of its major etiological factors. Acute ischemic stroke patients exhibit imbalances in lymphocyte subpopulations, yet the correlation between these dynamic changes in lymphocyte subpopulations and lipid metabolism disorders, as well as carotid atherosclerosis in stroke patients remains poorly understood.

Methods: We retrospectively analyzed the demographic data, risk factors of cerebrovascular disease, laboratory examination (lymphocyte subsets, lipid indexes, etc.), clinical features and c;/]-sity from December 2017 to September 2019 and non-stroke patients with dizziness/vertigo during the same period.

Results: The results showed that peripheral B lymphocyte proportions are elevated in acute ischemic stroke patients compared with those of the control group (13.6 ± 5.3 vs. $11.7 \pm 4.4\%$, $p = 0.006$). Higher B lymphocyte proportions are associated with concurrent dyslipidemia, increased levels of vascular risk factors including triglycerides (TG), total cholesterol (TC), low-density lipoprotein cholesterol (LDL-C), and very-low-density lipoprotein cholesterol (VLDL-C), as well as decreased levels of the protective factor high-density lipoprotein cholesterol (HDL-C). Elevated B lymphocyte proportions are independently correlated with carotid atherosclerosis in stroke patients.

Discussion: We found CD19 positive B Lymphocytes increase after ischemic stroke and correlate with Carotid Atherosclerosis. Lymphocyte subpopulations should be highlighted in stroke patients.

KEYWORDS

B lymphocytes, CD19, lipid metabolism, carotid atherosclerosis, ischemic stroke

1 Introduction

Globally, stroke remained the second-leading cause of death and the third-leading cause of death and disability combined in 2019. Ischemic stroke constituted 62·4% of all incident strokes. Its high incidence, mortality, and disability rates impose a significant burden on families and society (1, 2). Ischemic stroke has many risk factors, with atherosclerosis being its primary pathological basis.

Timely and effective treatment within the time window is the key to preventing the progression of ischemic stroke and improving its prognosis. Currently, acute-phase treatments

for ischemic stroke primarily include ultra-early mechanical thrombectomy and intravenous thrombolysis (3), which benefit only a minority (<10%) of patients and may lead to hemorrhagic transformation (HT), potentially causing early deterioration in neurological function, early mortality, and poor prognosis (4). Furthermore, even in patients achieving vascular recanalization, 35% of them cannot restore effective perfusion and neurological function (5). The development of ischemic penumbra imaging techniques has made it an attractive and important strategy in the acute phase to salvage the ischemic penumbra and improve stroke outcomes (6). Research suggests that ischemic stress can activate immune cells, trigger inflammation, and programmatic cell death, playing a crucial role in the expansion of the ischemic core into the penumbral zone. Targeted immunomodulation is expected to improve outcomes in patients with ischemic stroke by salvaging ischemic penumbral tissue. S1P (Sphingosine 1-phosphate) signaling coordinates vascular functions in other organs, and S1P1 modulators including fingolimod show promise for the treatment of ischemic and hemorrhagic stroke. S1P coordinates lymphocyte trafficking, and lymphocytes are currently viewed as the principal therapeutic target for S1P1 modulation in stroke (7, 8). Professor Shi Fudong's team in China discovered in animal models that the lymphocyte modulator fingolimod can reduce infarct size, improve collateral circulation, and enhance blood–brain barrier integrity (9–11). Dr. Francisco Campos' team at Massachusetts General Hospital found in a mouse middle cerebral artery ischemia model that fingolimod treatment can alleviate ischemia-induced neurofunctional deficits, reduce infarct size, improve the neurofunctional outcome of thrombolysis therapy, and decrease the risk of hemorrhagic transformation when used in combination with t-PA. In patients with acute and anterior cerebral circulation occlusion stroke, oral fingolimod within 72 h of disease onset was safe, limited secondary tissue injury from baseline to 7 d, decreased microvascular permeability, attenuated neurological deficits, and promoted recovery. Extending the t-PA treatment window to 72 h (12, 13) suggests that targeted modulation of lymphocyte subpopulations in combination with thrombectomy/thrombolysis therapy holds promise as a prospective treatment strategy in the acute phase of ischemic stroke.

B Lymphocyte subpopulations play crucial regulatory roles by generating germinal centers, producing antibodies, and cytokines during both the acute and recovery phases of ischemic stroke (14). Atherosclerosis is the main pathological basis of ischemic stroke, and lipid metabolism disorders are the core link in the occurrence and progression of atherosclerosis. Monoclonal antibodies against B cell surface molecules (e.g., CD20) and survival factors (e.g., BAFF) have been shown to have a protective effect in atherosclerotic animal models (15–17), and targeting depletion of the B-cell surface co-stimulatory molecules CD80 and CD86 can slow the development of atherosclerosis (18).

Different B lymphocytes play different roles in the different stage of stroke. In the acute stage of stroke, using an anti-CD20 antibody Pharmacologic depletion of B cells, lack of circulating B cells in JHD−/− mice or reconstitution of Rag1−/− mice with B cells did not influence infarct volumes and functional outcome at day 1 and 3 after stroke (19), but cell adoptive transfer to mice reduced infarct volumes 3 and 7 d after transient middle cerebral artery occlusion. B cell depletion by rituximab reduced stroke-induced hippocampal neurogenesis and cell survival (20), IL-10-producing B-cells limit CNS inflammation and infarct volume in experimental stroke (21, 22). Whole-brain volumetric serial two-photon tomography (STPT) and a custom-developed image analysis pipeline visualized and quantified poststroke B cell diapedesis throughout the brain showed that B cells migrate into remote brain areas regulating motor and cognitive functions and support neurogenesis and functional recovery after focal stroke in mice (20). However, B lymphocytes are involved in the development of post-ischemic stroke cognitive impairment by producing antibodies, μ MT (B-cell deletion) mice do not have delayed cognitive deficits, and the B-cell-targeted drug rituximab can reduce post-stroke cognitive impairment (23, 24).

These foundation show that targeted B-cell therapy has the potential to improve the prognosis of patients by regulating atherosclerosis, reducing thrombolytic hemorrhagic transformation, prolonging the window period of thrombolytic therapy, alleviating cognitive impairment after stroke, and participating in the whole process of ischemic stroke. However, the dynamics of lymphocyte subsets after ischemia and the key lymphocyte subsets that regulate ischemic brain tissue are unclear. This study aims to analyze the changes of peripheral blood lymphocyte subsets in patients with acute ischemic stroke, focusing on the correlation between B-cell subsets and lipid metabolism disorders as well as carotid atherosclerosis, the key risk factors of stroke. In order to provide a reference for the promotion of immunointerventional therapy for ischemic stroke.

2 Materials and methods

2.1 General materials

Retrospective data collection was conducted on acute ischemic stroke patients admitted to the Department of Neurology, Second Affiliated Hospital of Soochow University, from December 2017 to September 2019. This study was approved by the Ethics Committee of the Second Affiliated Hospital of Soochow University (EC-AF(SQ)-12/20210601). Inclusion Criteria: Meet the diagnostic requirements of the "Chinese Guidelines for the Diagnosis and Treatment of Acute Ischemic Stroke 2018" (25), and confirm that there is a new cerebral infarction by MRI, and the onset is within 2 weeks. Exclusion criteria included: ① Concomitant autoimmune diseases, tumors, blood disorders, tuberculosis, or related conditions; ② History of infectious diseases or trauma within three months; ③ Use of antibiotics, hormones, or immunosuppressive agents within three months; and ④ Incomplete information.

2.2 Grouping

Based on the inclusion and exclusion criteria, 416 cases of acute ischemic stroke were included as the observation group. Additionally, 60 patients admitted during the same period with dizziness/vertigo but without vascular diseases were included as the control group. There were no significant differences in baseline characteristics, including age and gender, between the observation and control groups.

To investigate the dynamic changes of peripheral blood lymphocytes at different phases after ischemic stroke, sixty cases of acute ischemic stroke patients were randomly selected. The levels of their lymphocytes were compared with those of 55 cases of transient

ischemic attack patients (characterized by brief attacks that could recur and lack of imaging evidence of cerebral infarction), 21 cases of patients in the recovery phase of ischemic stroke (onset more than six months prior), and 47 cases of patients in the sequelae phase (onset more than one year prior).

2.3 Determination of clinical characteristics

Carotid atherosclerosis was defined as an intima-media thickness greater than or equal to 1 or the presence of plaques by carotid ultrasound. Additionally, several factors defined the risk of cerebrovascular diseases: ① Comorbidities: hypertension, diabetes, coronary heart disease, atrial fibrillation; ② Personal history: current smoking, current alcohol consumption; and ③ Medication history: antihypertensive drugs, antidiabetic drugs, statins, antiplatelet drugs. Medical history was defined as having a history, having no history but a history of medication, or being diagnosed during the current hospitalization. Current smoking was defined as smoking at least one cigarette per day for at least one year and currently reporting smoking. Current alcohol consumption was defined as consuming any type of alcoholic beverage at least once a week in the past three years.

2.4 Data collection

Demographic data, cerebrovascular disease risk factors, laboratory tests (lymphocyte subpopulations, lipid profiles), clinical characteristics, and carotid ultrasound results were collected. Laboratory tests were uniformly performed on the second day after admission. Venous blood was collected in the morning to measure the proportions of various lymphocyte subpopulations and lipid profiles. Lymphocyte subpopulations included T lymphocytes (CD3+), T helper/inducer lymphocytes (CD4+), T cytotoxic/suppressor lymphocytes (CD8+), natural killer (NK) lymphocytes (CD16 + CD56 + CD3-), and B lymphocytes (CD19+). Clinical characteristics included admission time, baseline systolic and diastolic blood pressure, National Institute of Health Stroke Scale (NIHSS) score at admission and on the third day, post-stroke infections, progressive stroke, and other data. Carotid ultrasound primarily assessed intima-media thickness and the presence of plaques in the left and right carotid arteries. Vascular recanalization treatment included intravenous thrombolysis or arterial thrombectomy. Functional assessments were performed using the modified Rankin Scale (mRS) at discharge and one year later to evaluate prognosis.

2.5 Statistical methods

Statistical analysis was conducted using SPSS 26 and GraphPad 8.0 software. Two-tailed tests were performed, and p-values less than 0.05 were considered statistically significant. Continuous data were presented as mean ± standard deviation or median (25th–75th percentile). The Shapiro–Wilk test was used to assess normality, and independent sample t-tests were applied for normally distributed data; otherwise, non-parametric tests were used. Count data were expressed as numbers (constituent ratios), and group comparisons were made using the chi-square test.

Single-factor logistic regression and binary logistic regression were used to analyze the correlation of atherosclerosis. B lymphocytes were grouped according to quartiles, and data were presented as odds ratios (OR) and 95% confidence intervals (CI). The Receiver Operating Characteristic (ROC) curve was used to calculate the optimal diagnostic threshold for adverse outcomes and carotid atherosclerosis.

3 Results

3.1 Clinical characteristics of acute ischemic stroke patients and dizziness/vertigo control group patients

Compared to the control group (patients with dizziness/vertigo), the observation group (acute ischemic stroke patients) showed no significant differences in age or gender. However, a significantly higher prevalence of hypertension, diabetes, smoking history, alcohol consumption history, and antiplatelet drug usage was observed in the observation group. Additionally, the proportion of B lymphocyte subpopulations (13.6 ± 5.3 vs. 11.7 ± 4.4%, $p = 0.006$) was significantly higher in the observation group than in the control group. There were no statistically significant differences in the proportions of other lymphocyte subpopulations, including T lymphocytes, T helper/inducer lymphocytes, T cytotoxic/suppressor lymphocytes, and NK lymphocytes (See Figure 1; Table 1). Furthermore, there were no significant differences in various lipid parameters (TG, TC, HDL-C, VLDL-C, and LDL-C).

3.2 Dynamic changes in peripheral blood lymphocyte subpopulations at different phases of cerebral ischemia

Based on the timing of cerebral ischemic events, patients were divided into the acute phase, recovery phase, and sequelae phase. A total of 60 patients with acute ischemic strokes were randomly selected. In addition, 55 patients with transient ischemic attacks, 21 patients in the recovery phase, and 47 patients in the sequelae phase were enrolled. The proportions of various lymphocyte subpopulations in these groups were compared to a control group of 60 patients with dizziness/vertigo. No significant differences were observed in the proportions of T lymphocytes, T helper/inducer lymphocytes, T cytotoxic/suppressor lymphocytes, or NK lymphocytes compared to the control group. However, the proportion of B lymphocytes was significantly higher in both transient ischemic attack (13.9 ± 5.1% vs. 11.7 ± 4.4%, $p = 0.019$) and acute ischemic stroke (14.1 ± 5.3% vs. 11.7 ± 4.4%, $p = 0.006$) groups compared to the control group, indicating statistical significance (see Figures 2A,B).

Subsequently, acute ischemic stroke patients were grouped based on hospital admission time: one day, three days, one week, and two weeks, consisting of 232 cases, 105 cases, 44 cases, and 35 cases, respectively. These groups were compared to the control group. The proportion of B lymphocytes was significantly higher in the first day (14.7 ± 4.9% vs. 11.7 ± 4.4%, $p = 0.006$), third day (14.4 ± 4.9% vs. 11.7 ± 4.4%, $p = 0.028$), and first week (13.7 ± 4.4% vs. 11.7 ± 4.4%, $p = 0.025$) compared to the control group. However, by the second

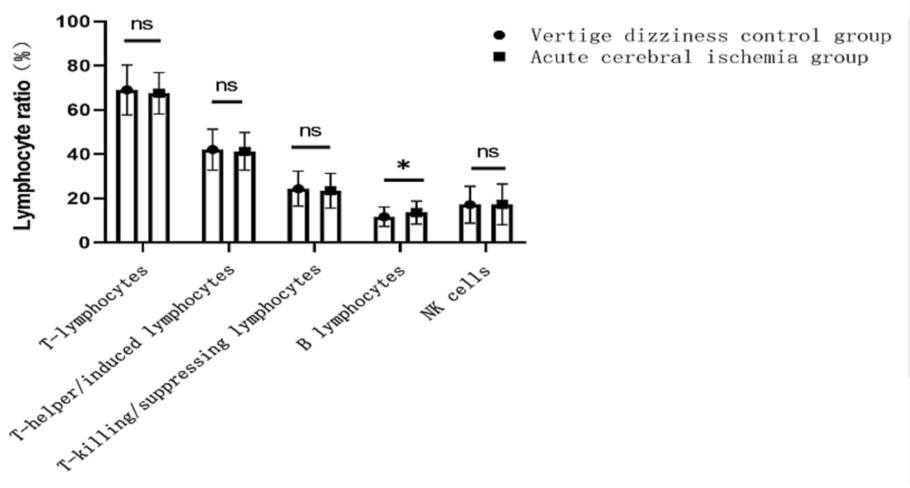

FIGURE 1
Changes in the proportion of lymphocyte subsets to controls in patients with acute ischemic stroke. ns indicates no difference, * indicates P less than 0.05 vs. control group.

week (13.4 ± 6.2% vs. 11.7 ± 4.4%, $p = 0.132$), the proportion had decreased to baseline levels (see Figure 2C).

3.3 Relationship between peripheral blood B lymphocyte proportions and clinical characteristics

Based on whether the proportion of peripheral blood B lymphocytes exceeded the control group's average of 11.7%, B lymphocytes were divided into two groups: "B^{low}" and "B^{high}." Clinical characteristics between these two groups were compared (see Table 2). Patients in the B lymphocyte low proportion group differed significantly from those in the high proportion group in terms of age (67 ± 13.2 vs. 63 ± 13.9, $p = 0.001$) and gender (126 (75%) vs. 153 (61%), $p = 0.003$), indicating that younger and female ischemic stroke patients had a higher proportion of B cells. Significant differences were observed in various blood lipid indicators, with the high B lymphocyte proportion group showing higher lipid levels. Specifically, the lipid indicators in the B^{low} and B^{high} groups were as follows: TG (1.63 ± 2.04 vs. 1.7 ± 1.08 mmol/L, $p = 0.001$), TC (4.59 ± 1.34 vs. 4.79 ± 1.10 mmol/L, $p = 0.028$), HDL-C (1.18 ± 0.32 vs. 1.09 ± 0.32 mmol/L, $p = 0.002$), VLDL-C (0.81 ± 0.87 vs. 0.82 ± 0.41 mmol/L, $p = 0.003$), and LDL-C (2.61 ± 0.89 vs. 2.88 ± 0.96 mmol/L, $p = 0.005$). The proportion of carotid artery atherosclerosis in the B^{high} group was significantly higher at 41% compared to the 16% in the B^{low} group.

3.4 Correlation analysis between B lymphocytes and carotid atherosclerosis

Among the included acute ischemic stroke patients, 208 cases underwent carotid ultrasound. They were divided into a carotid atherosclerosis group with 149 cases and a non-carotid atherosclerosis group with 59 cases. The correlation between lymphocyte subgroups and carotid atherosclerosis was analyzed. Single-factor analysis revealed that a decrease in the proportion of T lymphocytes (66.3 ± 8.5 vs. 69.4 ± 9.0%, $p = 0.032$), a decrease in the proportion of T cytotoxic/suppressor lymphocytes (22.4 ± 7.6 vs. 25.4 ± 8.6%, $p = 0.017$), and an increase in the proportion of B lymphocytes (14.9 ± 4.6 vs. 11.0 ± 4.7%, $p < 0.001$) were associated with carotid atherosclerosis, with p-values of 0.032, 0.017, and less than 0.001, respectively (see Table 3). The B lymphocyte proportions were divided into four groups based on quartiles, with the first quartile as the reference. Single-factor analysis showed that the second, third, and fourth quartile groups all had significant associations, indicating that an increased proportion of B lymphocytes increased the risk of carotid atherosclerosis. Even after adjusting for confounding factors, the results remained significant. The risk of carotid atherosclerosis in the third quartile group was 7.68 times that of the first quartile group (95% confidence interval 2.98–19.79, $p = 0.002$), and the risk in the fourth quartile group was 7.71 times that of the first quartile group (95% confidence interval 2.98–19.93, $p = 0.002$) (see Table 4). The OR decreases from group III to group IV, which indicated that as the proportion of B lymphocytes increases, the risk of atherosclerosis increases. ROC curve analysis showed that the optimal cutoff value for diagnosing carotid atherosclerosis based on the B lymphocyte proportion was 11.8, with a sensitivity of 79.8%, specificity of 70.9%, and an area under the curve of 0.745 (see Figure 3).

4 Discussion

Circulating lymphocytes changes following ischemic stroke are associated with increased susceptibility to infection and poor patient outcome due to their role in exacerbating the ischemic injury and long-term disability. Global understanding of early changes to systemic immunity is critical to identify immune targets to improve clinical outcome. However, changes in the number of immune cells at

TABLE 1 The demographic characteristics, risk factors, and clinical parameters of the study population.

	Acute ischemic stroke n = 416	Control n = 60	p value
Demographic information			
Age	64 ± 13.8	61 ± 14.3	0.120
Male (%)	279 (67)	38 (63)	0.566
Comorbidities n (%)			
Hypertension	307 (74)	35 (58)	**0.013**
Diabetes	115 (28)	7 (11)	**0.008**
Coronary heart disease	28 (7)	3 (5)	0.612
Personal history n (%)			
Smoking now	143 (34)	10 (17)	**0.006**
Drinking now	96 (23)	3 (5)	**0.001**
Medication history n (%)			
Antihypertensive drugs	245 (59)	31 (52)	0.289
Hypoglycemic drugs	94 (23)	7 (12)	0.053
Statins	53 (13)	3 (5)	0.082
Antiplatelet drugs	66 (16)	2 (3)	**0.010**
Laboratory examination (lymphatic n %, blood lipid mmol/L)			
T lymphocytes	67.7 ± 9.2	69.1 ± 11.3	0.255
T-helper/inducible lymphocytes	41.3 ± 8.4	42.1 ± 9.3	0.458
T-killing/suppressor lymphocytes	23.5 ± 7.9	24.4 ± 8.4	0.388
B lymphocytes	13.6 ± 5.3	11.7 ± 4.4	**0.006**
NK lymphocytes	17.1 ± 8.9	17.2 ± 8.4	0.994
TG	1.68 ± 1.54	1.76 ± 1.30	0.607
TC	4.71 ± 1.20	4.83 ± 0.95	0.425
HDL-C	1.13 ± 0.32	1.22 ± 0.43	0.054
VLDL-C	0.82 ± 0.64	0.87 ± 0.55	0.527
LDL-C	2.77 ± 0.94	2.77 ± 0.80	0.995
Clinical features			
Time of onset (h)	53 ± 61.9		
Baseline systolic blood pressure (mmHg)	150 ± 23.3		
Baseline diastolic blood pressure (mmHg)	83 ± 14.7		
Admission NIHSS score	4 (2–5)		

Bold: $p < 0.05$.

different stage after stroke remain controversial. Some evidence revealed a rapid decline in lymphocytes and NK cells in blood early after stroke (26), while other studies showed differential responses in different immune cell populations (27–29). A possible explanation is that signs of strong immunosuppression after stroke do not have the same effect on all lymphocyte subsets, which is related to lymphocyte subset specificity (30). In this study, we observed prominent increase in B cells after stroke. One interesting finding is that the proportion of B lymphocytes is related to age and gender, with higher proportions observed in young individuals and female patients. This correlation may be linked to the more active immune system in these two demographic groups, although the underlying mechanisms require further investigation.

Different B cell subsets have been proposed on the basis of expression levels of transcription factors as well as specific surface proteins. Peripheral blood B cells can be divided into 8 continuously differentiated subsets by the expression of immunoglobulin M (IgM), Ig D, CD10, CD19, CD24, CD27 and CD38, followed by Immature B, T1 Transitional B, T2 Transitional B, T3 Transitional B, Naive B, Unswitched Memory B, and Switched Memory B, Plasmablast. Different B cells play different roles in atherosclerosis and ischemic stroke (31–33). More and more findings allude to the potential candidacy of these subpopulations as therapeutic targets in the realm of ischemic stroke prevention and management.

Atherosclerosis constitutes a major pathological mechanism underlying ischemic stroke, wherein the accumulation of oxidized lipids associated with lipid metabolism abnormalities within the vascular wall is a central process in atherosclerotic development and progression (34). Analysis of genome-wide association and transcriptomic data suggests the involvement of B cells in the formation of atherosclerosis, and the activation and proliferation of B

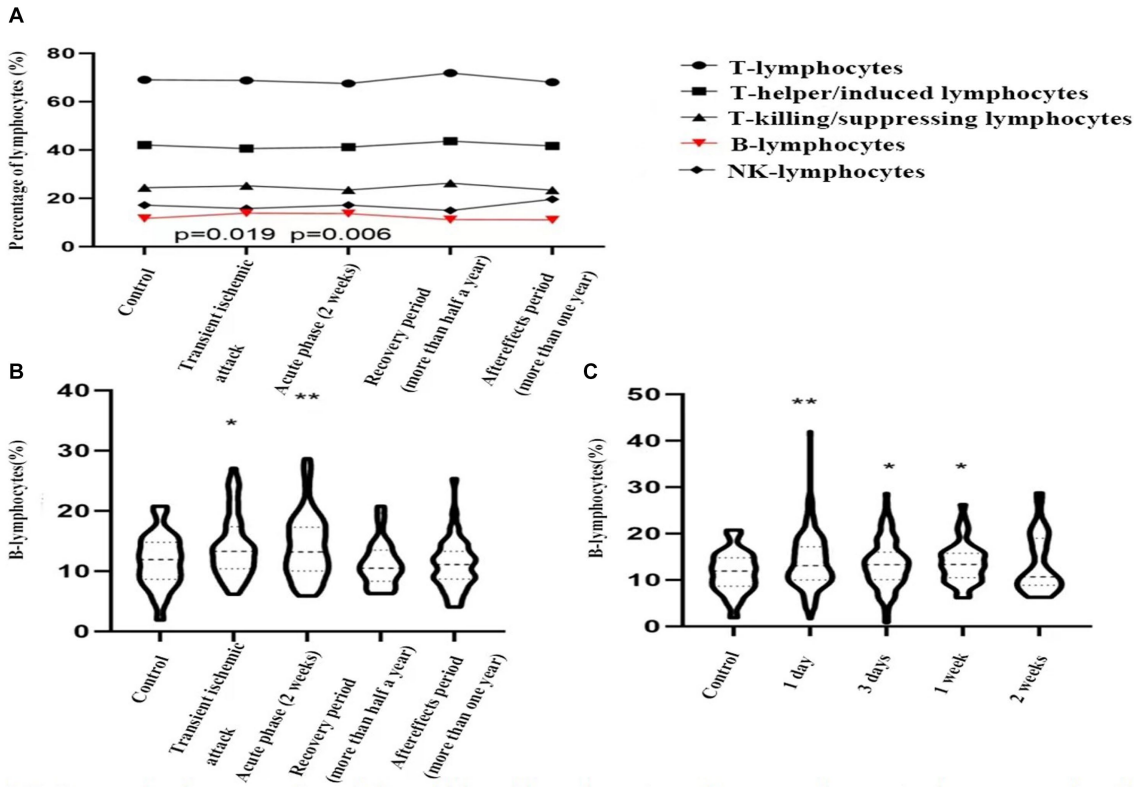

FIGURE 2
Dynamic changes of peripheral blood lymphocyte sub-groups in control group and patients with transient ischemic attack (TIA), acute ischemic stroke, stroke recovery period, stroke sequelae phase. **(A)** TIA vs. control group, $p = 0.019$; acute ischemic stroke vs. control group, $p = 0.006$; **(B,C)**. *indicates $p < 0.05$, **indicates $p < 0.01$ vs. control group.

cells are significant risk factors in the development of ischemic cerebrovascular diseases (35). This study revealed that among various lymphocyte subpopulations, elevated levels of B cell subsets in ischemic stroke patients are significantly correlated with atherosclerosis and lipid metabolism abnormalities. Patients with higher levels of B lymphocyte subsets exhibited an increased incidence of carotid artery sclerosis (41% vs. 16%), along with elevated levels of detrimental lipid parameters including triglycerides (TG), total cholesterol (TC), very low-density lipoprotein cholesterol (VLDL-C), and low-density lipoprotein cholesterol (LDL-C), accompanied by reduced levels of protective high-density lipoprotein cholesterol (HDL-C). As B lymphocyte levels rose, the occurrence and severity of atherosclerosis also increased. A higher proportion of B lymphocytes (optimal threshold at 11.8%) demonstrated elevated sensitivity (79.8%) and specificity (70.9%) in diagnosing atherosclerosis. Although the mechanism by which B cells regulate lipid metabolism and atherosclerosis remains to be investigated. These suggest that B cell subpopulations might participate in the regulation of atherosclerosis and contribute to the modulation of ischemic stroke. Thus, targeted therapies involving B cells could potentially play a significant regulatory role in both the prevention and treatment of ischemic stroke, benefiting patients.

However, animal experimentation results indicate that after receiving whole spleen B cell transplantation, mice with splenectomy and apolipoprotein E knockout (ApoE−/−) exhibited significantly reduced aortic root atherosclerotic plaques, showing a protective role of B cells in atherosclerosis. Employing univariate and multivariate Cox proportional hazard models to scrutinize the relationship between B cell subtypes, circulating antibodies, and secondary cardiovascular incidents over a 3-year follow-up period, it has been discerned that specific B cell subgroups possess inherent potential in prognosticating and preventing secondary cardiovascular events in patients afflicted by atherosclerosis (36, 37). These datas suggest that the main focus of work to find the immune intervention targets for prevention and treatment of atherosclerotic diseases should be to find the main pathogenic B-cell subsets.

Following an ischemic stroke event, B cells exhibit a sustained presence within cerebral tissues. In murine models, B cells have been identified in the brain up to 10 weeks post-stroke, while human ischemic stroke patients continue to exhibit elevated peripheral B cell levels beyond the 12-week mark post-ischemia. Furthermore, the synthesis of immunoglobulins in the cerebrospinal fluid of stroke patients persists for several months post-ischemia (38). Our study also found an increase in peripheral B cells after stroke, which increased continuously for at least 7 days, decreased to baseline levels by two weeks. Unfortunately, because this study was retrospective, the dynamic changes of lymphocytes in each patient could not be observed. Future prospective studies are expected to fill this gap.

Different B cell subpopulations exhibit distinct regulatory functions at various stages of the post-stroke period. On one hand, B

cells are a major source of brain-derived neurotrophic factor (BDNF), and their neurotrophic capabilities penetrate the post-stroke brain, inducing early antigen-independent protection against ischemic injury, participate in the restoration of neural plasticity in cerebral motor and cognitive regions, serving as a defense mechanism against potential recurrent immune injuries (20). On the other hand, they can adversely affect the hippocampus by generating antibodies, activating the complement system, leading to delayed cognitive impairments, and potentially infiltrating neighboring unaffected healthy tissues, thereby exacerbating the pathological condition (23, 24).

TABLE 2 Comparison of baseline information of lymphocytes in B^{low} and B^{high} groups.

	B^{low} $n = 167$	B^{high} $n = 249$	*p* value
Demographic information			
Age	67 ± 13.2	63 ± 13.9	**0.001**
Male (%)	126(75)	153(61)	**0.003**
Past history *n* (%)			
Stroke	40(24)	49(19)	0.297
Hypertension	131(78)	176(71)	0.078
Diabetes	45(27)	70(28)	0.794
Coronary heart disease	15(9)	13(5)	0.133
Atrial fibrillation	17(10)	23(9)	0.749
Personal History *n* (%)			
Smoking now	49(29)	94(37)	0.077
Drinking now	38(23)	58(23)	0.898
Medication history *n* (%)			
Antihypertensive drugs	104(62)	141(57)	0.251
Glucose-lowering drugs	36(22)	58(23)	0.678
Statin	26(16)	27(11)	0.156
Antiplatelet agents	28(17)	38(15)	0.680
Laboratory tests (mmol/L)			
TG	1.63 ± 2.04	1.7 ± 1.08	**0.001**
TC	4.59 ± 1.34	4.79 ± 1.10	**0.028**
HDL-C	1.18 ± 0.32	1.09 ± 0.32	**0.002**
VLDL-C	0.81 ± 0.87	0.82 ± 0.41	**0.003**
LDL-C	2.61 ± 0.89	2.88 ± 0.96	**0.005**
Clinical characteristics			
Time to onset of disease (h)	58 ± 69.6	50 ± 56.1	0.556
Baseline systolic blood pressure(mmHg)	150 ± 23.9	150 ± 23.0	0.807
Baseline diastolic blood pressure(mmHg)	82 ± 15.7	83 ± 14.1	0.480
Admission NIHSS score	4(2–6)	4(2–5)	0.428
Carotid ultrasound			
Carotid athe%	26(16)	103(41)	**<0.001**

Bold: $p < 0.05$.

Over the years, many scholars have done a lot of work in trying to discover disease-causing B cell subsets. CD19+CD86+B cells are associated with pro-inflammatory factor release, carotid artery stenosis, and high risk of stroke. CD19+CD40+ B cells are associated with a low risk of stroke (39). Depletion of B2 cells with monoclonal antibody against CD20 or BAFF receptor or BAFF receptor-deficient mice improves atherosclerosis. B2 cells can promote atherosclerosis by producing IgG, secreting pro-inflammatory cytokines, and activating CD4 T cells (15, 16). CD11 b^{high} B cells regulate microglia phenotype and increase microglia phagocytosis in both *ex vivo* and *in vivo* settings, likely by production of regulatory cytokines (e.g., TNF-α). As both APCs and adaptive immune cells with long-term memory function, B cells are uniquely positioned to regulate acute and chronic phases of the post-stroke immune response, and their influence is subset specific (40). B cells producing IL-10 and Treg cells exert their influence by modulating neutrophils, thereby mitigating inflammatory responses and reducing infarct size (41). Notably, memory B cells have demonstrated a positive correlation with improved postoperative outcomes in patients undergoing carotid endarterectomy (42).

In conclusion, B cell-targeted therapy emerges as a promising and complementary approach for the treatment of ischemic stroke. Its potential benefits lie in its ability to extend the therapeutic window, minimize hemorrhagic complications, and its relevance across the pre-onset, acute, and chronic phases of the disease. However, it's essential to recognize that different subpopulations of B cells exert distinct regulatory functions during various stages of ischemic stroke, driven by the dynamic changes in the immune milieu. This study, being retrospective and single-center with a relatively modest sample size, presents certain limitations. Furthermore, it lacks the dynamic tracking of lymphocyte subpopulation alterations in individual patients. Future research should focus on expanding the sample size and conducting comprehensive, systematic investigations into the dynamics of B cell subpopulations following ischemic stroke. This will entail gaining deeper insights into the dynamic changes in B lymphocyte subpopulations in acute ischemic stroke patients, conducting in-depth exploration of the roles played by diverse B cell subpopulations at different stages of ischemic stroke, and delving into the identification of key subgroups and core mechanisms through which B cells regulate ischemic stroke. In terms of intervention assessment, it is imperative to consider both short-term and long-term

TABLE 3 Univariate analysis of carotid atherosclerosis patients and lymphocyte subsets.

	Total	Non-atherosclerosis $n = 59$	Carotid atherosclerosis $n = 149$	*p* value
T lymphocyte	67.5 ± 8.9	69.4 ± 9.0	66.3 ± 8.5	**0.032**
T-helper/induced lymphocytes	41.1 ± 8.2	40.2 ± 9.6	41.6 ± 7.3	0.402
T kills/inhibits lymphocytes	23.6 ± 8.1	25.4 ± 8.6	22.4 ± 7.6	**0.017**
B lymphocytes	13.4 ± 5.0	11.0 ± 4.7	14.9 ± 4.6	**<0.001**
NK lymphocytes	17.7 ± 9.2	18.0 ± 9.2	17.4 ± 9.1	0.515

Bold: $p < 0.05$.

TABLE 4 Relationship between different levels of B lymphocytes and carotid atherosclerosis.

	Before adjustment			* After adjustment		
B lymphocyte%	OR value	95% confidence interval	*p*-value	OR value	95% confidence interval	*p*-value
Group I (≤9.9)	1			1		
Group II (9.9–13.1)	3.44	1.54–7.69	0.003	3.2	1.40–7.34	0.006
Group III (13.1–17.0)	9.84	3.93–24.61	0.001	7.68	2.98–19.79	0.002
Group IV (>17)	9.6	3.83–24.04	0.001	7.71	2.98–19.93	0.002

*Smoking, alcohol consumption, T lymphocytes, and T killer/suppressed lymphocytes were included in the regression model.

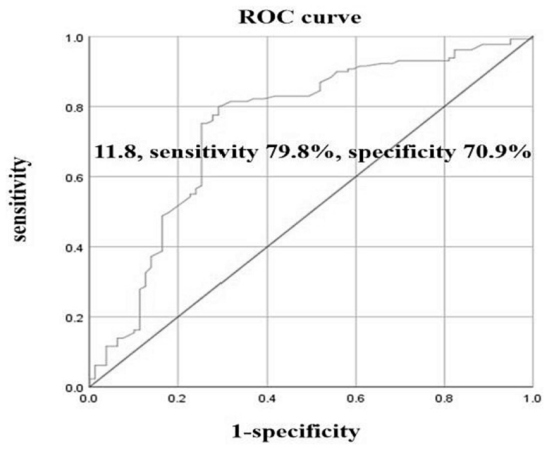

FIGURE 3
B lymphocytes predict ROC curves for carotid atherosclerosis.

outcomes, including cognitive function evaluations. Ultimately, if specific B cell subpopulations that play pivotal pathogenic roles in post-ischemic brain tissue damage can be pinpointed in clinical practice, and if targeted interventions are demonstrated to benefit stroke patients, this research may provide pivotal guidance for the clinical translation of immunomodulatory interventions as therapeutic targets in ischemic stroke.

Data availability statement

The original contributions presented in the study are included in the article/supplementary material, further inquiries can be directed to the corresponding author.

Ethics statement

The studies involving humans were approved by Ethics Committee of the Second Affiliated Hospital of Soochow University. The studies were conducted in accordance with the local legislation and institutional requirements. The ethics committee/institutional review board waived the requirement of written informed consent for participation from the participants or the participants' legal guardians/next of kin because this study is a retrospective clinical study, which does not involve any prospective observation or intervention, and the information obtained is only used for the study protocol to effectively protect the privacy of the subjects.

Author contributions

YuhZ: Conceptualization, Investigation, Software, Writing – original draft. YJ: Conceptualization, Data curation, Formal analysis, Software, Validation, Writing – original draft, Writing – review & editing. YutZ: Conceptualization, Data curation, Investigation, Software, Validation, Writing – original draft. YF: Conceptualization, Data curation, Validation, Visualization, Investigation, Software, Writing – review & editing. PF: Conceptualization, Data curation, Investigation, Validation, Writing – review & editing. XF: Data curation, Investigation, Validation, Writing – review & editing. KL: Data curation, Investigation, Software, Validation, Writing – review & editing. JZ: Conceptualization, Data curation, Investigation, Software, Validation, Writing – review & editing. YD: Conceptualization, Formal analysis, Resources, Software, Validation, Writing – review & editing. SY: Writing – review & editing, Data curation, Formal analysis, Validation. YanZ: Conceptualization, Data curation, Formal analysis, Funding acquisition, Investigation, Methodology, Project administration, Resources, Supervision, Validation, Visualization, Writing – original draft, Writing – review & editing.

Funding

The author(s) declare financial support was received for the research, authorship, and/or publication of this article. The Project of State Key Laboratory of Radiation Medicine and Protection, Soochow University (GZK12023052), The Key Young Medical Talents Project of Jiangsu Province (QNRC2016871), Jiangsu Province Capability Improvement Project through Science, Technology and Education (ZDXK202217), the Project of Suzhou Science and Technology (SKJY2021089), the Natural Science Foundation of the Jiangsu Higher Education Institutions of China.

Conflict of interest

The authors declare that the research was conducted in the absence of any commercial or financial relationships that could be construed as a potential conflict of interest.

Publisher's note

References

1. Wang W, Jiang B, Sun H, Ru X, Sun D, Wang L, et al. Prevalence, incidence, and mortality of stroke in China: results from a Nationwide population-based survey of 480, 687 adults. *Circulation*. (2017) 135:759–71. doi: 10.1161/CIRCULATIONAHA.116.025250

2. Global Burden of Disease Study 2019. Global, regional, and national burden of stroke and its risk factors, 1990-2019: a systematic analysis for the global burden of disease study 2019. *Lancet Neurol*. (2021) 20:795–820. doi: 10.1016/S1474-4422(21)00252-0

3. Prabhakaran S, Ruff I, Bernstein RA. Acute stroke intervention: a systematic review. *JAMA*. (2015) 313:1451–62. doi: 10.1001/jama.2015.3058

4. Yaghi S, Willey JZ, Cucchiara B, Goldstein JN, Gonzales NR, Khatri P, et al. Treatment and outcome of hemorrhagic transformation after intravenous Alteplase in acute ischemic stroke: a scientific statement for healthcare professionals from the American Heart Association/American Stroke Association. *Stroke*. (2017) 48:e343–61. doi: 10.1161/STR.0000000000000152

5. Goyal M, Menon BK, van Zwam WH, Dippel DWG, Mitchell PG, Demchuk AM, et al. Endovascular thrombectomy after large-vessel ischemic stroke: a meta-analysis of individual patient data from five randomized trials. *Lancet*. (2016) 387:1723–31. doi: 10.1016/S0140-6736(16)00163-X

6. Ma J, Zhang H, Gao Y, Huang J, Liang Z, Feng Q, et al. Iterative image reconstruction for cerebral perfusion CT using a pre-contrast scan induced edge-preserving prior. *Phys Med Biol*. (2012) 57:7519–42. doi: 10.1088/0031-9155/57/22/7519

7. Gauberti M, Martinez De Lizarrondo S, Vivien D. The "inflammatory penumbra" in ischemic stroke: from clinical data to experimental evidence. *Eur Stroke J*. (2016) 1:20–7. doi: 10.1177/2396987316630249

8. Nitzsche A, Poittevin M, Benarab A, Bonnin P, Faraco G, Uchida H, et al. Endothelial S1P1 signaling counteracts infarct expansion in ischemic stroke. *Circ Res*. (2021) 128:363–82. doi: 10.1161/CIRCRESAHA.120.316711

9. Fu Y, Zhang N, Ren L, Yan Y, Sun N, Li YJ, et al. Impact of an immune modulator fingolimod on acute ischemic stroke. *Proc Natl Acad Sci U S A*. (2014) 111:18315–20. doi: 10.1073/pnas.1416166111

10. Tian D-C, Shi K, Zhu Z, Yao J, Yang X, Su L, et al. Fingolimod enhances the efficacy of delayed alteplase administration in acute ischemic stroke by promoting anterograde reperfusion and retrograde collateral flow. *Ann Neurol*. (2018) 84:717–28. doi: 10.1002/ana.25352

11. Zhang S, Zhou Y, Zhang R, Zhang M, Campbell B, Lin L, et al. Rationale and design of combination of an immune modulator Fingolimod with Alteplase bridging with mechanical Thrombectomy in acute ischemic stroke (FAMTAIS) trial. *Int J Stroke*. (2017) 12:906–9. doi: 10.1177/1747493017710340

12. Diaz Diaz AC, Malone K, Shearer JA, Moore AC, Waeber C. Preclinical evaluation of Fingolimod in rodent models of stroke with age or atherosclerosis as comorbidities. *Front Pharmacol*. (2022) 13:920449. doi: 10.3389/fphar.2022.920449

13. Zhu Z, Fu Y, Tian D, Sun N, Han W, Chang G, et al. Combination of the immune modulator Fingolimod with alteplase in acute ischemic stroke: a pilot trial. *Circulation*. (2015) 132:1104–12. doi: 10.1161/CIRCULATIONAHA.115.016371

14. Iadecola C, Buckwalter MS, Anrather J. Immune responses to stroke: mechanisms, modulation, and therapeutic potential. *J Clin Investig*. (2020) 130:2777–88. doi: 10.1172/JCI135530

15. Ait-Oufella H, Herbin O, Bouaziz JD, Binder CJ, Uyttenhove C, Laurans L, et al. B cell depletion reduces the development of atherosclerosis in mice. *J Exp Med*. (2010) 207:1579–87. doi: 10.1084/jem.20100155

16. Kyaw T, Cui P, Tay C, Kanellakis P, Hosseini H, Liu E, et al. BAFF receptor mAb treatment ameliorates development and progression of atherosclerosis in hyperlipidemic ApoE(−/−) mice. *PLoS One*. (2013) 8:e60430. doi: 10.1371/journal.pone.0060430

17. Bernelot Moens SJ, van Leuven SI, Zheng KH, Havik SR, Versloot MV, van Duivenvoorde LM, et al. Impact of the B cell growth factor APRIL on the qualitative and immunological characteristics of atherosclerotic plaques. *PLoS One*. (2016) 11:e0164690. doi: 10.1371/journal.pone.0164690

18. Ewing MM. T-cell co-stimulation by CD28-CD80/86 and its negative regulator CTLA-4 strongly influence accelerated atherosclerosis development. *Int J Cardiol*. (2013) 168:1965–74. doi: 10.1016/j.ijcard.2012.12.085

19. Schuhmann MK, Langhauser F, Kraft P, Kleinschnitz C. B cells do not have a major pathophysiologic role in acute ischemic stroke in mice. *J Neuroinflammation*. (2017) 14:112. doi: 10.1186/s12974-017-0890-x

20. Ortega SB, Torres VO, Latchney SE, Whoolery CW, Noorbhai IZ, Poinsatte K, et al. B cells migrate into remote brain areas and support neurogenesis and functional recovery after focal stroke in mice. *Proc Natl Acad Sci U S A*. (2020) 117:4983–93. doi: 10.1073/pnas.1913292117

21. Bodhankar S, Chen Y, Vandenbark AA, Murphy SJ, Offner H. IL-10-producing B-cells limit CNS inflammation and infarct volume in experimental stroke. *Metab Brain Dis*. (2013) 28:375–86. doi: 10.1007/s11011-013-9413-3

22. Bodhankar S, Chen Y, Vandenbark AA, Murphy J, Offner H. Treatment of experimental stroke with IL-10-producing B-cells reduces infarct size and peripheral and CNS inflammation in wild-type B-cell-sufficient mice. *Metab Brain Dis*. (2014) 29:59–73. doi: 10.1007/s11011-013-9474-3

23. Malone MK, Ujas TA, Britsch DRS, Cotter KM, Poinsatte K, Stowe AM. The immunopathology of B lymphocytes during stroke induced injury and repair. *Semin Immunopathol*. (2023) 45:315–27. doi: 10.1007/s00281-022-00971-3

24. Doyle KP, Quach LN, Sole M, Axtell RC, Nguyen TV, Soler-Llavina GJ, et al. B-lymphocyte-mediated delayed cognitive impairment following stroke. *J Neurosci*. (2015) 35:2133–45. doi: 10.1523/JNEUROSCI.4098-14.2015

25. Chinese Medical Association, Neurology Branch, Cerebrovascular Disease Group. Guidelines for the diagnosis and treatment of acute ischemic stroke in China 2018. *Chin J Neurol*. (2018) 51:666–82.

26. Haeusler KG, Schmidt WU, Fohring F, Meisel C, Helms T, Jungehulsing GJ, et al. Cellular immunodepression preceding infectious complications after acute ischemic stroke in humans. *Cerebrovasc Dis*. (2008) 25:50–8. doi: 10.1159/000111499

27. Krishnan S, O'Boyle C, Smith CJ, Hulme S, Allan SM, Grainger JR, et al. A hyperacute immune map of ischemic stroke patients reveals alterations to circulating innate and adaptive cells. *Clin Exp Immunol*. (2021) 203:458–71. doi: 10.1111/cei.13551

28. Wang Y, Liu J, Wang X, Liu Z, Li F, Chen F, et al. Frequencies of circulating B- and T-lymphocytes as indicators for stroke outcomes. *Neuropsychiatr Dis Treat*. (2017) 13:2509–18. doi: 10.2147/NDT.S148073

29. Li S, Huang Y, Liu Y, Rocha M, Li X, Wei P, et al. Change and predictive ability of circulating immunoregulatory lymphocytes in long-term outcomes of acute ischemic stroke. *J Cereb Blood Flow Metab*. (2021) 41:2280–94. doi: 10.1177/0271678X21995694

30. Yan J, Greer JM, Etherington K, Cadigan GP, Cavanagh H, Henderson RD, et al. Immune activation in the peripheral blood of patients with acute ischemic stroke. *J Neuroimmunol*. (2009) 206:112–7. doi: 10.1016/j.jneuroim.2008.11.001

31. Huan T, Zhang B, Wang Z, Joehanes R, Zhu J, Johnson AD, et al. A systems biology framework identifies molecular underpinnings of coronary heart disease. *Arterioscler Thromb Vasc Biol*. (2013) 33:1427–34. doi: 10.1161/ATVBAHA.112.300112

32. Caligiuri G, Nicoletti A, Poirier B, Hansson GK. Protective immunity against atherosclerosis carried by B cells of hypercholesterolemic mice. *J Clin Investig*. (2002) 109:745–53. doi: 10.1172/JCI7272

33. Chen Y, Bodhankar S, Murphy SJ, Vandenbark AA, Alkayed NJ, Offner H. Intrastriatal B-cell administration limits infarct size after stroke in B-cell deficient mice. *Metab Brain Dis*. (2012) 27:487–93. doi: 10.1007/s11011-012-9317-7

34. Zou Y, Zhang Y, Cao Y. Research progress on the regulation of atherosclerotic stroke by B cells. *Chinese J Mod Neurol Dis*. (2020) 20:15–21.

35. Urra X, Cervera A, Villamor N, Planas AM, Chamorro A. Harms and benefits of lymphocyte subpopulations in patients with acute stroke. *Neuroscience*. (2009) 158:1174–83. doi: 10.1016/j.neuroscience.2008.06.014

36. Kyaw T, Tipping P, Bobik A, Toh BH. Opposing roles of B lymphocyte subsets in atherosclerosis. *Autoimmunity*. (2017) 50:52–6. doi: 10.1080/08916934.2017.1280669

37. Sage AP, Tsiantoulas D, Binder CJ, Mallat Z. The role of B cells in atherosclerosis. *Nat Rev Cardiol*. (2019) 16:180–96. doi: 10.1038/s41569-018-0106-9

38. Jian Z, Liu R, Zhu X, Smerin D, Zhong Y, Gu L, et al. The involvement and therapy target of immune cells after ischemic stroke. *Front Immunol*. (2019) 10:2167. doi: 10.3389/fimmu.2019.02167

39. Mantani PT, Ljungcrantz I, Andersson L, Alm R, Hedblad B, Björkbacka H, et al. Circulating CD40+ and CD86+ B cell subsets demonstrate opposing associations with risk of stroke. *Arterioscler Thromb Vasc Biol*. (2014) 34:211–8. doi: 10.1161/ATVBAHA.113.302667

40. Korf JM, Honarpisheh P, Mohan EC, Banerjee A, Blasco-Conesa MP, Honarpisheh P, et al. CD11b^{high} B cells increase after stroke and regulate microglia. *J Immunol*. (2022) 209:288–300. doi: 10.4049/jimmunol.2100884

41. Ren X, Akiyoshi K, Dziennis S, Vandenbark AA, Herson PS, Hurn PD, et al. Regulatory B cells limit CNS inflammation and neurologic deficits in murine experimental stroke. *J Neurosci*. (2011) 31:8556–63. doi: 10.1523/JNEUROSCI.1623-11.2011

42. Meeuwsen JAL, van Duijvenvoorde A, Gohar A, Kozma MO, van de Weg SM, Gijsberts CM, et al. High levels of (un)switched memory B cells are associated with better outcome in patients with advanced atherosclerotic disease. *J Am Heart Assoc*. (2017) 6:e005747. doi: 10.1161/JAHA.117.005747

frontiers | Frontiers in Neurology

TYPE Original Research
PUBLISHED 16 February 2024
DOI 10.3389/fneur.2024.1323878

OPEN ACCESS

EDITED BY
Yanlin Zhang,
Second Affiliated Hospital of Soochow University, China

REVIEWED BY
Xingguang Luo,
Yale University, United States
Qidi Ai,
Hunan University of Chinese Medicine, China

*CORRESPONDENCE
Fan Wang
✉ fanwang@bjmu.edu.cn
Yanlong Liu
✉ benjaminlyl@wmu.edu.cn
Cunbao Li
✉ 850984084@qq.com

†These authors have contributed equally to this work

RECEIVED 18 October 2023
ACCEPTED 07 February 2024
PUBLISHED 16 February 2024

CITATION
Zhou Y, Han X, Mu Q, Xing L, Wu Y, Li C, Liu Y and Wang F (2024) The effect of the interaction of sleep onset latency and age on ischemic stroke severity via inflammatory chemokines.
Front. Neurol. 15:1323878.
doi: 10.3389/fneur.2024.1323878

The effect of the interaction of sleep onset latency and age on ischemic stroke severity via inflammatory chemokines

Yuyu Zhou[1,2†], Xiaoli Han[3†], Qingshuang Mu[4†], Lifei Xing[5], Yan Wu[1], Cunbao Li[2*], Yanlong Liu[6*] and Fan Wang[1*]

[1]Beijing Hui-Long-Guan Hospital, Peking University, Beijing, China, [2]Medical Neurobiology Lab, Inner Mongolia Medical University, Huhhot, China, [3]Clinical Nutrition Department, Friendship Hospital of Urumqi, Urumqi, China, [4]Xinjiang Key Laboratory of Neurological Disorder Research, The Second Affiliated Hospital of Xinjiang Medical University, Urumqi, China, [5]Department of Neurology, Sinopharm North Hospital, Baotou, China, [6]School of Mental Health, Wenzhou Medical University, Wenzhou, China

Objective: Prolonged sleep onset latency (PSOL) and age have been linked to ischemic stroke (IS) severity and the production of chemokines and inflammation, both of which contribute to IS development. This study aimed to explore the relationship between chemokines, inflammation, and the interplay between sleep onset latency (SOL) and age in influencing stroke severity.

Methods: A cohort of 281 participants with mild to moderate IS was enrolled. Stroke severity was assessed using the National Institutes of Health Stroke Scale (NIHSS), and SOL was recorded. Serum levels of macrophage inflammatory protein-1alpha (MIP-1α), macrophage inflammatory protein-1beta (MIP-1β), monocyte chemoattractant protein-1 (MCP-1), interleukin-6 (IL-6), and tumor necrosis factor-alpha (TNF-α) were measured.

Results: NIHSS scores of middle-aged participants with PSOL were significantly higher than those with normal sleep onset latency (NSOL) ($p = 0.046$). This difference was also observed when compared to both the elderly with NSOL ($p = 0.022$), and PSOL ($p < 0.001$). Among middle-aged adults with PSOL, MIP-1β exhibited a protective effect on NIHSS scores ($\beta = -0.01$, $t = -2.11$, $p = 0.039$, $R^2 = 0.13$). MIP-1α demonstrated a protective effect on NIHSS scores in the elderly with NSOL ($\beta = -0.03$, $t = -2.27$, $p = 0.027$, $R^2 = 0.12$).

Conclusion: This study reveals a hitherto undocumented association between PSOL and IS severity, along with the potential protective effects of MIP-1β in mitigating stroke severity, especially among middle-aged patients.

KEYWORDS

sleep onset latency, age, ischemic stroke, inflammation, interaction

1 Introduction

Stroke is considered the second leading cause of death worldwide and remains a significant cause of disability in both developed and developing countries (1). Ischemic stroke accounts for almost 70% of all stroke cases (1). There is a rich literature available substantiating that prolonged sleep onset latency (PSOL) and age can determine stroke severity (2–4). However,

the precise mechanisms by which PSOL and age impact the development of ischemic stroke (IS) remain incompletely understood.

Sleep onset latency (SOL) is the amount of time it takes a person to fall asleep in bed, and represents an important marker for assessing sleep quality (5). PSOL is one of the main manifestations of sleep structural changes in ischemic stroke (6). Studies have demonstrated a positive correlation between PSOL and the prevalence of stroke; short SOL was associated with a 36% reduction in the risk of stroke, while PSOL was also related to the severity of IS symptoms (7), suggesting that shorter SOL may protect against stroke (2). In addition, it has been shown that sleep onset latency is prolonged with aging (8), and aging is a significant factor affecting stroke (3). Besides, stroke tends to occur predominantly in the elderly, and its incidence and severity are closely related to age (3, 9, 10). Consistently, a study revealed that the severity of strokes tended to increase with increasing age (10). In contrast, a growing body of evidence suggests the "younger stroke" phenomenon is gaining prominence as a pressing public health issue, marked by a rising occurrence of strokes among individuals considered "younger" (those under 50 years of age) (11, 12). Consequently, SOL and age have been established as risk factors for ischemic stroke. Nonetheless, the underlying pathophysiological mechanisms governing their interplay in influencing the severity of IS remain uncertain.

Prolonged sleep onset latency can lead to a series of sleep-related issues that exacerbate stroke severity by triggering a systemic inflammatory response (13–16). In addition, prior investigations have shown that PSOL is exacerbated with age (17). However, recent research has indicated prolonged sleep onset latency even among middle-aged individuals, indicating a close relationship between SOL and age (18). Interestingly, age also impacts stroke severity through its influence on inflammation (19). Chemokines, as small molecular proteins, play a crucial role in the immune and inflammatory responses after stroke, which are involved in the processing of neovascularization, neurogenesis, and neural network reconstruction (20). Chemokines are cytokines attracting selective leukocyte subsets and subgrouping into the four major subfamilies, CC, CXC, C, and CX3C. macrophage inflammatory protein-1 alpha (MIP-1α), macrophage inflammatory protein 1beta (MIP-1β), and monocyte chemoattractant protein-1 (MCP-1) are the three best-known and most extensively studied CC chemokines in primary and secondary inflammatory responses in humans (21, 22). An increasing body of literature suggests that chemokines and cytokines, such as high levels of MIP-1α, MIP-1β, MCP-1, interleukin-6 (IL-6) and tumor necrosis factor-alpha (TNF-α) are associated with poor subjective sleep quality characterized by PSOL (23–27). In this respect, animal experiments have demonstrated that older mice exhibit notably higher MIP-1α and MIP-1β levels than their younger counterparts (28), which indicate that the cytokines and chemokines are also closely related to age. The overexpression of chemokines MIP-1α and MCP-1 can promote the recruitment of inflammatory cytokines IL-6 and TNF-α (29), and the recruitment of pro-inflammatory factors accelerates the development of atherosclerotic plaques, which further aggravates blood–brain barrier injury (30) and leads to brain injury. The chemokine-induced inflammatory response is pivotal in exacerbating stroke outcomes (30, 31). These cumulative factors collectively contribute to the heightened severity of ischemic stroke (32, 33). In essence, the combined influence of sleep onset latency and age on these cytokines may provide insights into explaining the underlying pathophysiology of ischemic stroke.

As described above, most studies have shown that SOL and age are independently correlated with stroke severity (2, 3, 7), and these cytokines played roles in the severity of IS. However, the association between chemokines, inflammation, and the interaction of SOL and age with stroke severity remains elusive, yet it holds crucial significance for preventing ischemic stroke. Therefore, this study aimed to examine how the interplay between sleep onset latency and age impacts chemokine levels and inflammation, with a subsequent exploration of their combined role in determining the severity of strokes.

2 Materials and methods

2.1 Participants

A total of 281 participants with mild and moderate ischemic stroke admitted to Sinopharm North Hospital from June 2020 to December 2021 were recruited.

Sociodemographic data, such as age, years of education, occupation, and current body mass index (BMI), were collected. Clinical data, such as a history of substance abuse and dependence, were obtained according to medical records and self-reports and confirmed by the next of kin and family members. Data on SOL in the 1–3 months before stroke were collected by self-assessment and report.

The following criteria were used for participant inclusion: individuals aged 45–80 diagnosed with mild and moderate ischemic stroke based on clinical symptoms, physical examination, and imaging findings. Participants with a history of working night shifts, diagnosed with severe stenosis of the internal carotid artery, external carotid artery, subclavian artery, and vertebral artery as evident by cranial MRA and vascular color ultrasound, individuals diagnosed with tumors, those experiencing significant and persistent sleep problems along with diagnosed sleep disorders, or those taking medications and healthcare products known to affect sleep patterns were excluded. In addition, participants with severe and very severe ischemic stroke were excluded due to the high prevalence of altered consciousness, such as coma, which would hinder the accurate assessment of sleep patterns. The exclusion criteria also included a history of any substance abuse or dependence, as well as any neurological and psychiatric disorders diagnosed by the Statistical Manual of Mental Disorders-V (DSM-V).

The present study was approved by the Institutional Review Board of the Sinopharm North Hospital (Approval number: GYBFYY-LL-2020006) and was performed in accordance with the Declaration of Helsinki, and written informed consent was obtained. No financial compensation was provided to the subjects in this study.

2.2 Assessments and laboratory tests

The National Institutes of Health Stroke Scale (NIHSS) contains 15 items, a reliable, valid, and responsive tool for measuring stroke severity (34). The NIHSS includes the following domains: level of consciousness, eye movements, integrity of visual fields, facial movements, arm and leg muscle strength, sensation, coordination, language, speech, and neglect. Each impairment is scored on an ordinal scale ranging from 0 to 2, 0 to 3, or 0 to 4. The cumulative scores yield a total ranging from 0 to 42, with higher scores indicating

more severe strokes (35). Stroke severity was categorized as follows: mild (NIHSS score 0–5), moderate (NIHSS score 6–14), severe (NIHSS score 15–24), and very severe (NIHSS score 25) (36, 37).

Recognizing that sleep onset latencies exceeding 30 min are associated with sleep difficulties in middle-aged and older adults (38), the present study categorized participants based on this established criterion (38). Participants with a sleep onset latency of more than 30 min were grouped as the PSOL group ($n = 153$), and those who had an SOL of 30 min or less constituted the normal sleep onset latency (NOSL) group ($n = 127$).

High-density lipoprotein (HDL), low-density lipoprotein (LDL), total cholesterol (TC), and triglyceride (TG) levels were obtained from routine tests to assess the participants' physical condition in relation to ischemic stroke. SOL data and NIHSS scores were collected after peripheral metabolic markers were measured on the first day of admission. Participants were admitted to the hospital either on the day of the onset of physical symptoms or the next day.

Peripheral blood samples were obtained upon admission. The serum was separated and immediately frozen at −80°C. Analyses were performed to measure the serum levels of MIP1α, MIP1β, MCP1, IL-6, and TNFα using ELISA kits (Shanghai Xinle Biotechnology Co., LTD, Shanghai, China). Laboratory technicians conducting the analyses were blinded to clinical data.

2.3 Statistical analysis

Data were presented as mean ± standard deviation (SD) for continuous variables and as frequencies and percentages for categorical variables. The comparison of categorical variables was performed by the chi-squared test. The normality of all variables was assessed using the Shapiro–Wilk test. Levene's test verified the homoscedasticity of residual variances, confirming the equal distribution of residuals (all $p > 0.05$). As a result, an analysis of covariance (ANCOVA) was employed to compare differences in inflammatory markers between groups (see Table 1). Partial correlation analysis was used to examine the correlation between inflammatory markers and NIHSS scores.

In addition, general linear models (GLMs) were applied to test the significance of the interaction between SOL and age and their effect on NIHSS scores. Current BMI was included as a covariate in all models. Model comparisons and testing were carried out using an F-statistic.

All statistical analyses were performed using IBM SPSS Statistics for Windows, Version 22.0 (IBM Corp., Armonk, NY, United States). Figures were generated using GraphPad Prism version 8 (GraphPad Software Inc.). All tests were two-sided, and the significance threshold was set at $p < 0.05$.

3 Results

3.1 Demographic and clinical characteristics

An ANCOVA was conducted with BMI as the covariate to identify disparities in sociodemographic, clinical variables, and inflammatory markers across various groups (Table 1). In contrast to participants with NSOL, those with PSOL exhibited a higher proportion of females (50.7% vs. 27.1%, $p < 0.001$). Participants in the PSOL group reported lower rates of smoking than those in the NSOL group (39.5% vs. 60.5%, $p < 0.001$), while no difference was observed in other sociodemographic and clinical characteristics between both groups.

3.2 Analysis of differences between groups

The participants were divided into age groups [Middle-aged (aged 45–65) and Elderly (aged 65+)] and presence of PSOL/NSOL which resulted in four distinct groups:Middle-aged with PSOL ($n = 62$), Middle-aged with NSOL ($n = 59$), Elderly with PSOL ($n = 91$), and Elderly with NSOL ($n = 68$).

The homogeneity of variance for the NIHSS scores variable, determined through Levene's test, yielded a p-value greater than 0.05. Thus, ANCOVA was employed to compare differences in NIHSS scores between the groups. Taking current BMI as the covariate, the impacts of SOL and age on NIHSS scores were found to be significant ($F = 6.51$, $p = 0.011$). In this regard, the NIHSS scores in the Middle-aged with PSOL group were notably higher than those in both the Elderly with NSOL group and the Elderly with PSOL group ($p = 0.015$ and $p < 0.001$, respectively).

3.3 General linear models analysis

To explore potential interactions between SOL and age in relation to stroke severity, GLM analyses of NIHSS scores were performed while controlling for current BMI. GLM analysis revealed strong interactions for NIHSS scores between SOL and age within the dataset. Notably, the NIHSS scores of participants in the Middle-aged with PSOL group were significantly higher compared to the Middle-aged with NSOL group ($p = 0.046$). Furthermore, the NIHSS scores of participants in the Middle-aged with PSOL group were significantly elevated compared to those in both the Elderly with NSOL group ($p = 0.022$) and the Elderly with PSOL group ($p < 0.001$; Table 2, Figure 1).

3.4 Correlations analysis

After adjusting for current BMI, a partial correlation analysis was conducted to assess the relationship between NIHSS scores and inflammatory markers within each group. Notably, a negative correlation was observed between MIP-1β levels and NIHSS scores in the Middle-aged with PSOL group ($r = -0.30$, $p = 0.020$). Similarly, a negative correlation was found between MIP-1α levels and NIHSS scores in the Elderly with NSOL group ($r = -0.27$, $p = 0.029$; Table 3, Figure 2).

3.5 Hierarchical stepwise linear regression analysis

A hierarchical stepwise linear regression analysis revealed noteworthy findings, with BMI as the initial covariate and NIHSS score as the dependent variable. MIP-1β levels emerged as a protective

TABLE 1 The differences in clinical characteristics between groups.

Variables	PSOL (>30 min)		NSOL (≤30 min)		F/χ^2	p
	Middle-aged (n = 62)	Elderly (n = 91)	Middle-aged (n = 59)	Elderly (n = 68)		
Age (years)	57.29 ± 5.03	72.29 ± 4.65	57.24 ± 4.69	71.93 ± 4.06	283.60	**<0.001*****
Gender					24.64	**<0.001*****
Male	37 (59.7%)	39 (42.9%)	49 (83.1%)	44 (63.8%)		
Female	25 (40.3%)	52 (57.1%)	10 (16.9%)	25 (36.2%)		
BMI (Kg/m^2)	25.38 ± 2.76	24.88 ± 3.39	24.90 ± 3.05	25.00 ± 2.75	0.37	0.766
Education (years)	8.97 ± 2.90	6.35 ± 3.26	9.02 ± 3.16	7.06 ± 3.13	13.41	**<0.001*****
Active drinker					23.54	**<0.001*****
Yes	22 (35.5%)	15 (16.5%)	30 (50.8%)	15 (21.7%)		
No	40 (64.5%)	76 (83.5%)	29 (49.2%)	54 (78.3%)		
Active smoker					28.02	**<0.001*****
Yes	33 (53.2%)	28 (30.8%)	44 (74.6%)	33 (47.8%)		
No	29 (46.8%)	63 (69.2%)	15 (25.4%)	36 (52.2%)		
Hypertension					6.28	0.100
Yes	43 (69.4%)	65 (71.4%)	40 (67.8%)	36 (52.9%)		
No	19 (30.6%)	26 (28.6%)	19 (32.2%)	32 (47.1%)		
Diabetes					6.48	0.090
Yes	15 (24.2%)	33 (36.3%)	11 (18.6%)	17 (24.6%)		
No	47 (75.8%)	58 (63.7%)	48 (81.4%)	52 (75.4%)		
Hyperlipidemia					2.46	0.482
Yes	21 (33.9%)	22 (24.2%)	14 (23.7%)	21 (30.9%)		
No	41 (66.1%)	69 (75.8%)	45 (76.3%)	47 (69.1%)		
HDL (mmol/L)	1.14 ± 0.23	1.17 ± 0.27	1.16 ± 0.28	1.14 ± 0.26	0.18	0.913
LDL (mmol/L)	3.14 ± 0.74	3.27 ± 2.35	2.96 ± 0.94	2.96 ± 1.00	0.73	0.537
TC (mmol/L)	4.82 ± 1.04	4.61 ± 1.20	4.49 ± 1.22	4.44 ± 1.19	1.26	0.290
TG (mmol/L)	2.37 ± 1.59	1.60 ± 0.75	1.83 ± 0.86	1.88 ± 1.33	5.20	0.002**
MIP-1α (ng/L)	53.86 ± 28.11	49.90 ± 22.26	47.29 ± 19.83	48.80 ± 21.34	0.78	0.511
MIP-1β (ng/L)	158.43 ± 72.09	145.53 ± 66.19	142.80 ± 61.16	133.03 ± 53.19	1.61	0.188
MCP-1 (ng/L)	157.44 ± 69.21	141.55 ± 65.80	138.84 ± 59.92	141.21 ± 75.02	0.89	0.445
IL-6 (ng/L)	111.43 ± 47.92	107.55 ± 50.02	92.60 ± 32.78	99.37 ± 38.38	2.19	0.089
TNFα (ng/L)	97.71 ± 46.36	91.97 ± 41.65	87.96 ± 47.31	96.10 ± 42.04	0.55	0.645

PSOL, prolonged sleep onset latency; NSOL, normal sleep onset latency; BMI, body mass index; HDL, High-density lipoprotein; LDL, Low-density lipoprotein; TC, total cholesterol; TG, triacylglycerol; MIP-1α, macrophage inflammatory protein-1alpha; MIP-1β, macrophage inflammatory protein-1beta; MCP-1, monocyte chemoattractant protein-1; IL-6, interleukin-6; TNFα, tumor necrosis factor-alpha.
Data were presented as mean ± standard deviation (SD) for continuous variables and as frequencies and percentages for categorical variables. p value for analysis of covariance (ANCOVA) or chi-square test, *$p < 0.05$, **$p < 0.01$, ***$p < 0.001$.

factor for NIHSS scores in Middle-aged adults with PSOL (β = −0.01, 95%CI [−0.01 ~ 0.00], $t = -2.11$, $p = 0.039$, $R^2 = 0.13$). Additionally, MIP-1α levels were identified as a protective factor for NIHSS scores in the Elderly with NSOL group (β = −0.03, 95%CI [−0.05 ~ 0.00], $t = -2.27$, $p = 0.027$, $R^2 = 0.12$).

4 Discussion

This pioneering study aims to shed light on the hitherto underexplored relationship between sleep onset latency, age, and stroke severity by investigating the pathophysiological mechanisms potentially driving this association. Importantly, we substantiated the association between PSOL and the severity in middle-aged IS participants, with higher NIHSS scores associated with PSOL and lower levels of MIP-1β.

Our findings suggest that middle-aged stroke participants with PSOL are at greater risk of experiencing a severe stroke, and MIP-1β plays a protective role against IS. Over the years, studies have emphasized that high-risk factors for stroke occurrence (39) and increased stroke severity (5, 10, 40) include sleep difficulties and advanced age. Notably, while stroke has conventionally been linked to

TABLE 2 The interaction of SOL and age on NIHSS scores.

Variables	PSOL (>30 min)		NSOL (≤30 min)		MD	*p*
	Middle-aged ($n = 62$)	Elderly ($n = 91$)	Middle-aged ($n = 59$)	Elderly ($n = 68$)		
	Mean ± SD	Mean ± SD	Mean ± SD	Mean ± SD		
NIHSS scores	1.95 ± 0.21	–	1.31 ± 0.23	–	0.64	0.046*
	1.95 ± 0.21	–	–	1.26 ± 0.20	0.69	0.022*
	1.95 ± 0.21	0.90 ± 0.17	–	–	1.05	**<0.001*****

PSOL, prolonged sleep onset latency; NSOL, normal sleep onset latency; NIHSS, National Institutes of Health Stroke Scale; GLM, general linear models; MD, Mean differences; SD, standard deviation.
GLM was used to calculate the differences in levels between four groups with BMI as the covariate. The simple effect was calculated using GLM. Data were reported as mean ± SD, *$p < 0.05$, **$p < 0.01$, ***$p < 0.001$.

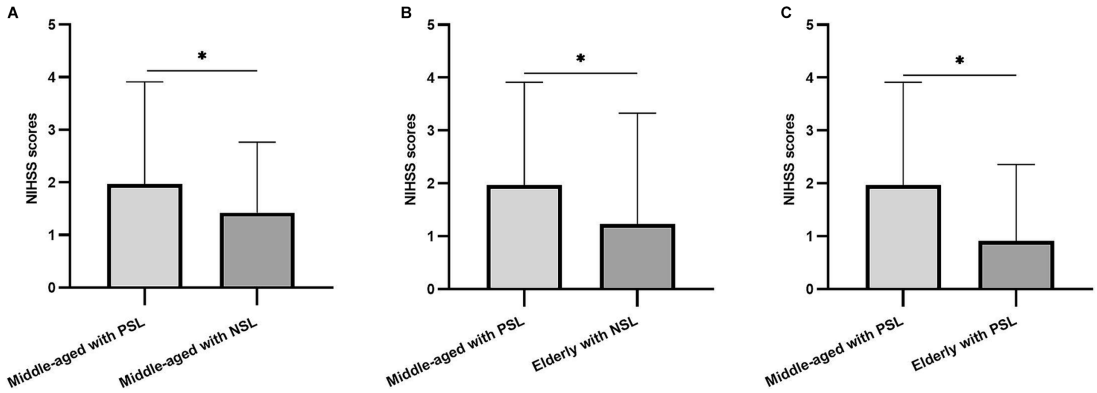

FIGURE 1
The difference in National Institutes of Health Stroke Scale (NIHSS) scores between groups. **(A)** The differences among the NIHSS scores of the participants in Middle-aged with prolonged sleep onset latency (PSOL) and Middle-aged with normal sleep onset latency (NSOL); **(B)** The differences among the NIHSS scores of the participants in Middle-aged with PSOL and Elderly with NSOL; **(C)** The differences among the NIHSS scores of the participants in Middle-aged with PSOL and Elderly with PSOL. *$p < 0.05$.

older age, recent years have witnessed a substantial decline in the average age of stroke onset, coupled with a rise in stroke incidence and hospitalization rates among middle-aged individuals. This phenomenon of "younger-age stroke" has emerged as a significant public health challenge (12, 41–43), consistent with the results of this study. Indeed, middle-aged people with PSOL face an elevated risk of more severe strokes, possibly attributable to several factors. Firstly, compared to older individuals, middle-aged individuals necessitate efficient and higher sleep quality to sustain bodily functions and metabolism (44–46). Hence, when middle-aged stroke patients with PSOL experience a range of sleep-related issues such as diminished sleep quality, insomnia, and inadequate sleep (15), their sleep requirements are unmet, significantly impeding the recovery from cerebral ischemia-induced reversible or irreversible synaptic and membrane failures, which, influences neuroplasticity and post-stroke recovery (47). Secondly, older individuals usually have more flexible morning routines due to retirement, alleviating the impact of PSOL-related sleep shortage (18). Conversely, middle-aged individuals contend with heightened work pressures, constrained wake-up times and are more prone to insufficient sleep and subpar sleep quality (18). Moreover, middle-aged individuals tend to engage in more social activities, potentially adopting unhealthy lifestyles like high-calorie diets, smoking, and alcohol consumption (48). Besides, the compounded effects of sleep deprivation, stress, and unhealthy habits are widely acknowledged to exacerbate stroke severity (49–51).

In addition, this study found that MIP-1β was negatively associated with NIHSS scores in the middle-aged group with PSOL, indicating that elevated levels of MIP-1β could protect against severe strokes in this cohort. Previous research has indicated the potential involvement of MIP-1β in monocyte recruitment within atherosclerotic plaques, where heightened serum MIP-1β levels have been associated with the progression of IS (52). Despite the established association between PSOL and stroke severity, our study suggests that elevated serum MIP-1β levels could potentially mitigate the severity of stroke events in middle-aged patients with PSOL. Several underlying mechanisms could account for this phenomenon. First, the mRNA and protein expression of the chemokine MIP-1β has been reported to be inhibited by prostaglandin E2 (PGE2) (53). PGE2, a pivotal endogenous anti-inflammatory mediator linked to sleep regulation, demonstrates wakefulness-promoting properties (53). Notably, its concentration is markedly higher during wakefulness compared to slow-wave sleep (54). In this context, participants grappling with PSOL are prone to extended periods of wakefulness (15), leading to heightened PGE2 levels and diminished MIP-1β levels. Intriguingly, PGE2's impact extends further, potentially playing a dual role. PGE2 has been identified as a disruptor of Na(+)-Ca(2+) exchange and Ca(2+) homeostasis through the EP1 receptor, thereby contributing to excessive Ca(2+) accumulation. This effect also extends to the induction of neuronal cell death and the augmentation of ischemic-induced neurodegeneration (55), ultimately amplifying

TABLE 3 Correlation between NIHSS scores and inflammatory cytokines in different groups.

Groups correlation		MIP-1α (ng/L)	MIP-1β (ng/L)	MCP-1 (ng/L)	IL-6 (ng/L)	TNFα (ng/L)
Middle-aged with NSOL	*r*	−0.15	−0.20	−0.05	0.13	0.06
	p	0.290	0.143	0.735	0.343	0.691
Middle-aged with PSOL	*r*	−0.22	−0.30	−0.09	−0.06	0.02
	p	0.096	0.020*	0.494	0.678	0.860
Elderly with NSOL	*r*	−0.27	−0.18	−0.22	0.08	0.07
	p	0.029*	0.152	0.087	0.525	0.609
Elderly with PSOL	*r*	−0.01	−0.14	0.05	0.07	0.18
	p	0.895	0.203	0.667	0.547	0.099

PSOL, prolonged sleep onset latency; NSOL, normal sleep onset latency; MIP-1α, macrophage inflammatory protein-1alpha; MIP-1β, macrophage inflammatory protein-1beta; MCP-1, monocyte chemoattractant protein-1; IL-6, interleukin-6; TNFα, tumor necrosis factor-alpha.
Correlations between MIP-1α, MIP-1β, MCP-1, IL-6, TNFα levels and NIHSS scores were calculated using Partial correlation. $^{*}p < 0.05$, $^{**}p < 0.01$.

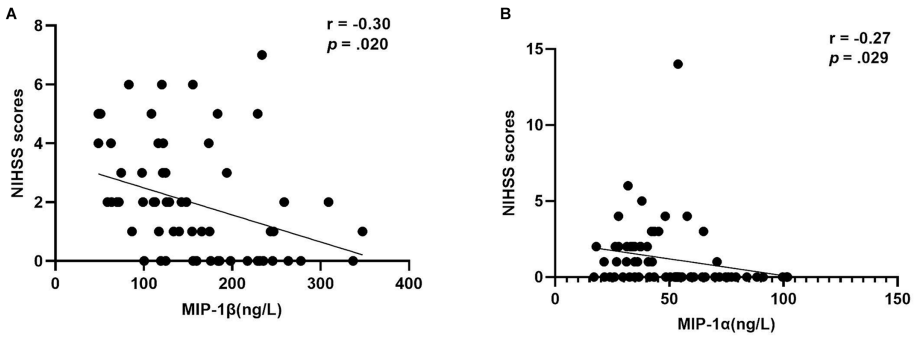

FIGURE 2
The correlation of MIP-1β levels and MIP-1α levels with NIHSS scores. **(A)** The negative correlation of macrophage inflammatory protein 1beta (MIP-1β) levels with the NIHSS scores ($r = -0.30$, $p = 0.020$) in group of middle-aged with PSOL; **(B)** The negative correlation of macrophage inflammatory protein-1 alpha (MIP-1α) levels with the NIHSS Scores ($r = -0.27$, $p = 0.029$) in the group of Elderly with NSOL.

stroke severity. Indeed, it is highly conceivable that the deleterious influence of MIP-1β on stroke severity in middle-aged individuals with PSOL might be attenuated by PGE2, potentially even manifesting as a protective function. However, this study did not observe a correlation between serum MIP-1β levels and NIHSS scores in older adults with PSOL, attributed to the confounding impact of age. In this regard, one animal study unveiled heightened expression of MIP-1β levels in older mice (28), while another investigation highlighted an accelerated decline in serum MIP-1β levels with aging (56). Consequently, aging appears to disrupt the relationship between MIP-1β and NIHSS scores in older individuals with PSOL. In essence, the protective role of MIP-1β against stroke severity seems to be confined to middle-aged patients with PSOL.

Besides, the NSOL group displayed a potential protective effect against stroke in the elderly, as evidenced by the negative association between MIP-1α and NIHSS scores. Previous studies have shown that, compared to middle-aged mice, chemokine MIP-1α levels are highly expressed in older mice (28). Interestingly, it has been found that MIP-1α levels were significantly reduced in the brain tissue of older patients with IS (57), and MIP-1α tended to decline with age in this patient population (56). At the same time, the NIHSS score at admission increased significantly with age (58). Therefore, the negative correlation between serum MIP-1α level and NIHSS score in senile stroke patients with NSOL may be due to aging. However, our study did not observe the correlation between serum MIP-1α and NIHSS score in elderly patients with PSOL, attributed to the fact that individuals suffering from PSOL exhibited suboptimal sleep quality, consequently experiencing extended periods of wakefulness, which led to an increase in PGE2. The increased PGE2 led to a decline in the chemokine MIP-1α level (59), thus disrupting the age-related negative correlation typically observed between serum MIP-1α levels and NIHSS scores.

Besides, we found no association between MCP-1, IL-6, and TNF-α and NIHSS scores across the four groups. However, prior research on individuals with severe IS demonstrated a correlation between elevated levels of these factors and the severity of IS (60–62). Discrepancies in outcomes might stem from the inclusion of subjects with mild to moderate IS in this current study. Moreover, a prior investigation examining stroke severity 7 days after admission demonstrated a positive association between elevated MCP-1 levels and heightened stroke severity at the same time point (61), Conversely, the present study did not reveal a connection between MCP-1 and stroke severity. This discrepancy may be attributable to the timing of MCP-1 measurement; in this study, samples were collected on day one after admission, whereas the previous study assessed MCP-1 levels 7 days post-stroke. The temporal dynamics of ischemic brain cell damage likely influence the correlation between MCP-1 and stroke severity. In cases where initial ischemic attack

results in more severe injury, cytokine and chemokine production may be suppressed. This offers a potential explanation for the absence of a correlation between MCP-1 and NIHSS scores in the current study (61).

Several limitations need consideration within this study. Firstly, the participant pool only comprised Chinese individuals residing in the northern inland region, regardless of whether they were experiencing their first episode or recurrence. Future research should prioritize geographically diverse recruitment and larger sample sizes to improve generalizability of results. Additionally, it is essential to differentiate between first-episode patients and those with recurrent episodes and to conduct stratification analyses based on the number of episodes to bolster result accuracy. Secondly, since sleep patterns influence IS over an extended duration, this study only retrospectively gathered SOL data from 1 to 3 months preceding the IS onset. While data from this brief interval might not comprehensively capture the impact, collecting recent-stage sleep data retrospectively was more feasible, and patient cooperation was facilitated. Lastly, most IS participants in this study exhibited mild to moderate stroke. Consequently, it is important to acknowledge that the generalizability of our study findings may be limited to cases of milder stroke severity. Nevertheless, the presented results provide valuable guidance for the development of targeted preventive interventions for individuals at risk of such strokes.

5 Conclusion

The present study provides strong evidence of the association between PSOL and the severity of IS and the potential protective effects of MIP-1β in reducing stroke severity, especially in middle-aged patients, suggesting that falling asleep quickly might contribute to low ischemic stroke severity. In the future, the role of other subfamilies of chemokines in the interaction of sleep onset latency and age on IS severity should be further explored to improve and supplement this study.

Data availability statement

The original contributions presented in the study are included in the article/supplementary material, further inquiries can be directed to the corresponding authors.

Ethics statement

The studies involving humans were approved by the Institutional Review Board of the Sinopharm North Hospital (Approval number: GYBFYY-LL-2020006). The studies were conducted in accordance with the local legislation and institutional requirements. The participants provided their written informed consent to participate in this study.

Author contributions

FW: Conceptualization, Funding acquisition, Writing – review & editing. YZ: Conceptualization, Data curation, Writing – original draft. XH: Writing – original draft. QM: Writing – original draft. LX: Methodology, Writing – review & editing. YW: Data curation, Funding acquisition, Writing – review & editing. CL: Conceptualization, Writing – review & editing, Methodology. YL: Conceptualization, Writing – review & editing, Methodology.

Funding

The author(s) declare financial support was received for the research, authorship, and/or publication of this article. This work was supported by the following grants: The Technology Support Project of Xinjiang (2017E0267), the 10th Inner Mongolia Autonomous Region "Prairie excellence" Project, Natural Science Foundation of Xinjiang Province (2018D01C228), Xinjiang Outstanding Youth Science Grant (2017Q007), Natural Science Foundation of China (81560229), Beijing Natural Science Foundation (7152074), the "Qingmiao" program of Beijing Municipal Hospital Management Center (QML20212003), and the Youth Scientific Research Foundation of Beijing Huilongguan Hospital (LY202106).

Acknowledgments

We thank all the participants for their willingness to participate in the study and the time that they devoted to the study.

Conflict of interest

The authors declare that the research was conducted in the absence of any commercial or financial relationships that could be construed as a potential conflict of interest.

Publisher's note

References

1. Song Y, Zhang X, Li C, Xu S, Zhou B, Wu X. Is bilirubin associated with the severity of ischemic stroke? A dose response Meta-analysis. *J Clin Med*. (2022) 11:3262. doi: 10.3390/jcm11123262

2. Kadier K, Qin L, Ainiwaer A, Rehemuding R, Dilixiati D, Du YY, et al. Association of Sleep-Related Disorders with cardiovascular disease among adults in the United States: a cross-sectional study based on National Health and nutrition examination survey 2005-2008. *Front Cardiovasc Med*. (2022) 9:954238. doi: 10.3389/fcvm.2022.954238

3. Guo Y, Wang H, Tian Y, Wang Y, Lip GY. Multiple risk factors and Ischaemic stroke in the elderly Asian population with and without atrial fibrillation. An analysis of

425,600 Chinese individuals without prior stroke. *Thromb Haemost*. (2016) 115:184–92. doi: 10.1160/TH15-07-0577

4. Terzoudi A, Vorvolakos T, Heliopoulos I, Livaditis M, Vadikolias K, Piperidou H. Sleep architecture in stroke and relation to outcome. *Eur Neurol*. (2009) 61:16–22. doi: 10.1159/000165344

5. Zhong X, Gou F, Jiao H, Zhao D, Teng J. Association between night sleep latency and hypertension: a cross-sectional study. *Medicine (Baltimore)*. (2022) 101:e31250. doi: 10.1097/MD.0000000000031250

6. Miano S, Fanfulla F, Nobili L, Heinzer R, Haba-Rubio J, Berger M, et al. Sas care 1: sleep architecture changes in a cohort of patients with ischemic stroke/Tia. *Sleep Med*. (2022) 98:106–13. doi: 10.1016/j.sleep.2022.06.002

7. Kim WH, Yoo YH, Lim JY, Kang SG, Jung HY, Bae JN, et al. Objective and subjective sleep problems and quality of life of rehabilitation in patients with mild to moderate stroke. *Top Stroke Rehabil*. (2020) 27:199–207. doi: 10.1080/10749357.2019.1673591

8. Habte-Gabr E, Wallace RB, Colsher PL, Hulbert JR, White LR, Smith IM. Sleep patterns in rural elders: demographic, health, and Psychobehavioral correlates. *J Clin Epidemiol*. (1991) 44:5–13. doi: 10.1016/0895-4356(91)90195-f

9. Wang F, Wang J, Han Y, Shi X, Xu X, Hou C, et al. Triglyceride-glucose index and stroke recurrence in elderly patients with ischemic stroke. *Front Endocrinol (Lausanne)*. (2022) 13:1005614. doi: 10.3389/fendo.2022.1005614

10. Chen RL, Balami JS, Esiri MM, Chen LK, Buchan AM. Ischemic stroke in the elderly: an overview of evidence. *Nat Rev Neurol*. (2010) 6:256–65. doi: 10.1038/nrneurol.2010.36

11. Aigner A, Grittner U, Rolfs A, Norrving B, Siegerink B, Busch MA. Contribution of established stroke risk factors to the burden of stroke in young adults. *Stroke*. (2017) 48:1744–51. doi: 10.1161/STROKEAHA.117.016599

12. Maaijwee NA, Rutten-Jacobs LC, Schaapsmeerders P, van Dijk EJ, de Leeuw FE. Ischaemic stroke in young adults: risk factors and long-term consequences. *Nat Rev Neurol*. (2014) 10:315–25. doi: 10.1038/nrneurol.2014.72

13. Petrov KK, Hayley A, Catchlove S, Savage K, Stough C. Is poor self-rated sleep quality associated with elevated systemic inflammation in healthy older adults? *Mech Ageing Dev*. (2020) 192:111388. doi: 10.1016/j.mad.2020.111388

14. Schloss MJ, Swirski FK, Nahrendorf M. Modifiable cardiovascular risk, hematopoiesis, and innate immunity. *Circ Res*. (2020) 126:1242–59. doi: 10.1161/CIRCRESAHA.120.315936

15. Hawes NJ, Wiggins AT, Reed DB, Hardin-Fanning F. Poor sleep quality is associated with obesity and depression in farmers. *Public Health Nurs*. (2019) 36:270–5. doi: 10.1111/phn.12587

16. Newton TL, Fernandez-Botran R. Promoting health by improving subjective sleep quality? Reduction in depressive symptoms and inflammation as potential mechanisms and implications for trauma-exposed persons. *Front Psych*. (2016) 7:76. doi: 10.3389/fpsyt.2016.00076

17. Ohayon MM, Carskadon MA, Guilleminault C, Vitiello MV. Meta-analysis of quantitative sleep parameters from childhood to old age in healthy individuals: developing normative sleep values across the human lifespan. *Sleep*. (2004) 27:1255–73. doi: 10.1093/sleep/27.7.1255

18. Myllyntausta S, Salo P, Kronholm E, Pentti J, Oksanen T, Kivimaki M, et al. Does removal of work stress explain improved sleep following retirement? The Finnish retirement and aging study. *Sleep*. (2019) 42:zsz109. doi: 10.1093/sleep/zsz109

19. Finger CE, Moreno-Gonzalez I, Gutierrez A, Moruno-Manchon JF, McCullough LD. Age-related immune alterations and cerebrovascular inflammation. *Mol Psychiatry*. (2022) 27:803–18. doi: 10.1038/s41380-021-01361-1

20. Lin YT, Chen HD, Ai QD, Yang YT, Zhang Z, Chu SF, et al. Characteristics and pathogenesis of chemokines in the post-stroke stage. *Int Immunopharmacol*. (2023) 116:109781. doi: 10.1016/j.intimp.2023.109781

21. Zaremba J, Ilkowski J, Losy J. Serial measurements of levels of the chemokines Ccl2, Ccl3 and Ccl5 in serum of patients with acute Ischaemic stroke. *Folia Neuropathol*. (2006) 44:282–9.

22. Florholmen J, Kristiansen MG, Steigen SE, Sorbye SW, Paulssen EJ, Kvamme JM, et al. A rapid chemokine response of macrophage inflammatory protein (Mip)-1alpha, Mip-1beta and the regulated on activation, Normal T expressed and secreted chemokine is associated with a sustained Virological response in the treatment of chronic hepatitis C. *Clin Microbiol Infect*. (2011) 17:204–9. doi: 10.1111/j.1469-0691.2010.03206.x

23. Liu X, Chen B, Huang Z, Duan R, Li H, Xie L, et al. Effects of poor sleep on the immune cell landscape as assessed by single-cell analysis. *Commun Biol*. (2021) 4:1325. doi: 10.1038/s42003-021-02859-8

24. Sprecher KE, Koscik RL, Carlsson CM, Zetterberg H, Blennow K, Okonkwo OC, et al. Poor sleep is associated with Csf biomarkers of amyloid pathology in cognitively Normal adults. *Neurology*. (2017) 89:445–53. doi: 10.1212/WNL.0000000000004171

25. Huang WY, Huang CC, Chang CC, Kor CT, Chen TY, Wu HM. Associations of self-reported sleep quality with circulating interferon gamma-inducible protein 10, interleukin 6, and high-sensitivity C-reactive protein in healthy menopausal women. *PLoS One*. (2017) 12:e0169216. doi: 10.1371/journal.pone.0169216

26. Milrad SF, Hall DL, Jutagir DR, Lattie EG, Ironson GH, Wohlgemuth W, et al. Poor sleep quality is associated with greater circulating pro-inflammatory cytokines and severity and frequency of chronic fatigue syndrome/Myalgic encephalomyelitis (Cfs/me) symptoms in women. *J Neuroimmunol*. (2017) 303:43–50. doi: 10.1016/j.jneuroim.2016.12.008

27. Prather AA, Epel ES, Cohen BE, Neylan TC, Whooley MA. Gender differences in the prospective associations of self-reported sleep quality with biomarkers of systemic inflammation and coagulation: findings from the heart and soul study. *J Psychiatr Res*. (2013) 47:1228–35. doi: 10.1016/j.jpsychires.2013.05.004

28. Porcher L, Bruckmeier S, Burbano SD, Finnell JE, Gorny N, Klett J, et al. Aging triggers an upregulation of a multitude of cytokines in the male and especially the female rodent Hippocampus but more discrete changes in other brain regions. *J Neuroinflammation*. (2021) 18:219. doi: 10.1186/s12974-021-02252-6

29. Wang Q, Tang XN, Yenari MA. The inflammatory response in stroke. *J Neuroimmunol*. (2007) 184:53–68. Epub 2006/12/26. doi: 10.1016/j.jneuroim.2006.11.014

30. Huang Y, Chen S, Luo Y, Han Z. Crosstalk between inflammation and the Bbb in stroke. *Curr Neuropharmacol*. (2020) 18:1227–36. doi: 10.2174/1570159X18666200620230321

31. Przykaza L. Understanding the connection between common stroke comorbidities, their associated inflammation, and the course of the cerebral ischemia/reperfusion Cascade. *Front Immunol*. (2021) 12:782569. doi: 10.3389/fimmu.2021.782569

32. Jones KL, Maguire JJ, Davenport AP. Chemokine receptor Ccr5: from aids to atherosclerosis. *Br J Pharmacol*. (2011) 162:1453–69. doi: 10.1111/j.1476-5381.2010.01147.x

33. Libby P. Inflammation in atherosclerosis. *Nature*. (2002) 420:868–74. doi: 10.1038/nature01323

34. Kasner SE. Clinical interpretation and use of stroke scales. *Lancet Neurol*. (2006) 5:603–12. doi: 10.1016/S1474-4422(06)70495-1

35. Kwah LK, Diong J. National Institutes of Health stroke scale (Nihss). *J Physiother*. (2014) 60:61. doi: 10.1016/j.jphys.2013.12.012

36. Reinholdsson M, Palstam A, Sunnerhagen KS. Prestroke physical activity could influence acute stroke severity (part of Papsigot). *Neurology*. (2018) 91:e1461–7. doi: 10.1212/WNL.0000000000006354

37. Lindley RI, Wardlaw JM, Whiteley WN, Cohen G, Blackwell L, Murray GD, et al. Alteplase for acute ischemic stroke: outcomes by clinically important subgroups in the third international stroke trial. *Stroke*. (2015) 46:746–56. doi: 10.1161/STROKEAHA.114.006573

38. Scinicariello F, Buser MC, Feroe AG, Attanasio R. Antimony and sleep-related disorders: Nhanes 2005-2008. *Environ Res*. (2017) 156:247–52. doi: 10.1016/j.envres.2017.03.036

39. Mai X, Liang X. Risk factors for stroke based on the National Health and nutrition examination survey. *J Nutr Health Aging*. (2020) 24:791–5. doi: 10.1007/s12603-020-1430-4

40. Zhang Y, Xia X, Zhang T, Zhang C, Liu R, Yang Y, et al. Relationship between sleep disorders and the prognosis of neurological function after stroke. *Front Neurol*. (2022) 13:1036980. doi: 10.3389/fneur.2022.1036980

41. Krishnamurthi RV, Moran AE, Feigin VL, Barker-Collo S, Norrving B, Mensah GA, et al. Stroke prevalence, mortality and disability-adjusted life years in adults aged 20-64 years in 1990-2013: data from the global burden of disease 2013 study. *Neuroepidemiology*. (2015) 45:190–202. doi: 10.1159/000441098

42. Kissela BM, Khoury JC, Alwell K, Moomaw CJ, Woo D, Adeoye O, et al. Age at stroke: temporal trends in stroke incidence in a large, biracial population. *Neurology*. (2012) 79:1781–7. doi: 10.1212/WNL.0b013e318270401d

43. George MG, Tong X, Kuklina EV, Labarthe DR. Trends in stroke hospitalizations and associated risk factors among children and young adults, 1995-2008. *Ann Neurol*. (2011) 70:713–21. doi: 10.1002/ana.22539

44. Taillard J, Gronfier C, Bioulac S, Philip P, Sagaspe P. Sleep in Normal aging, homeostatic and circadian regulation and vulnerability to sleep deprivation. *Brain Sci*. (2021) 11:1003. doi: 10.3390/brainsci11081003

45. Mander BA, Winer JR, Walker MP. Sleep and Human Aging. *Neuron*. (2017) 94:19–36. doi: 10.1016/j.neuron.2017.02.004

46. Hirshkowitz M, Whiton K, Albert SM, Alessi C, Bruni O, DonCarlos L, et al. National Sleep Foundation's updated sleep duration recommendations: final report. *Sleep Health*. (2015) 1:233–43. doi: 10.1016/j.sleh.2015.10.004

47. Hofmeijer J, van Kaam R, Vermeer SE, van Putten M. Severely disturbed sleep in patients with acute ischemic stroke on stroke units: a pilot study. *Front Neurol*. (2019) 10:1109. doi: 10.3389/fneur.2019.01109

48. Gao Y, Jia Z, Zhao L, Han S. The effect of activity participation in middle-aged and older people on the trajectory of depression in later life: National Cohort Study. *JMIR Public Health Surveill*. (2023) 9:e44682. doi: 10.2196/44682

49. Reddin C, Murphy R, Hankey GJ, Judge C, Xavier D, Rosengren A, et al. Association of Psychosocial Stress with risk of acute stroke. *JAMA Netw Open*. (2022) 5:e2244836. doi: 10.1001/jamanetworkopen.2022.44836

50. McDermott M, Brown DL, Chervin RD. Sleep disorders and the risk of stroke. *Expert Rev Neurother*. (2018) 18:523–31. doi: 10.1080/14737175.2018.1489239

51. Ding D, Rogers K, van der Ploeg H, Stamatakis E, Bauman AE. Traditional and emerging lifestyle risk behaviors and all-cause mortality in middle-aged and older adults: evidence from a large population-based Australian cohort. *PLoS Med*. (2015) 12:e1001917. doi: 10.1371/journal.pmed.1001917

52. Mirabelli-Badenier M, Braunersreuther V, Viviani GL, Dallegri F, Quercioli A, Veneselli E, et al. Cc and cxc chemokines are pivotal mediators of cerebral injury in Ischaemic stroke. *Thromb Haemost*. (2011) 105:409–20. doi: 10.1160/TH10-10-0662

53. Hayaishi O. Molecular mechanisms of sleep-wake regulation: roles of prostaglandins D2 and E2. *FASEB J*. (1991) 5:2575–81. doi: 10.1096/fasebj.5.11.1907936

54. Gerozissis K, De Saint HZ, Orosco M, Rouch C, Nicolaidis S. Changes in hypothalamic prostaglandin E2 may predict the occurrence of sleep or wakefulness as assessed by parallel Eeg and microdialysis in the rat. *Brain Res*. (1995) 689:239–44. doi: 10.1016/0006-8993(95)00583-c

55. Yagami T, Koma H, Yamamoto Y. Pathophysiological roles of cyclooxygenases and prostaglandins in the central nervous system. *Mol Neurobiol*. (2016) 53:4754–71. doi: 10.1007/s12035-015-9355-3

56. Swift ME, Burns AL, Gray KL, DiPietro LA. Age-related alterations in the inflammatory response to dermal injury. *J Invest Dermatol*. (2001) 117:1027–35. doi: 10.1046/j.0022-202x.2001.01539.x

57. Sieber MW, Claus RA, Witte OW, Frahm C. Attenuated inflammatory response in aged mice brains following stroke. *PLoS One*. (2011) 6:e26288. doi: 10.1371/journal.pone.0026288

58. Purroy F, Vena A, Forne C, de Arce AM, Davalos A, Fuentes B, et al. Age- and sex-specific risk profiles and in-hospital mortality in 13,932 Spanish stroke patients. *Cerebrovasc Dis*. (2019) 47:151–64. doi: 10.1159/000500205

59. Takayama K, Garcia-Cardena G, Sukhova GK, Comander J, Gimbrone MA Jr, Libby P. Prostaglandin E2 suppresses chemokine production in human macrophages through the Ep4 receptor. *J Biol Chem*. (2002) 277:44147–54. doi: 10.1074/jbc.M204810200

60. Xu P, Zhang S, Kan X, Shen X, Mao J, Fang C, et al. Changes and roles of Il-17a, Vegf-a and Tnf-alpha in patients with cerebral infarction during the acute phase and early stage of recovery. *Clin Biochem*. (2022) 107:67–72. doi: 10.1016/j.clinbiochem.2022.05.001

61. Bonifacic D, Toplak A, Benjak I, Tokmadzic VS, Lekic A, Kucic N. Monocytes and monocyte chemoattractant protein 1 (Mcp-1) as early predictors of disease outcome in patients with cerebral ischemic stroke. *Wien Klin Wochenschr*. (2016) 128:20–7. doi: 10.1007/s00508-015-0878-4

62. Shaafi S, Sharifipour E, Rahmanifar R, Hejazi S, Andalib S, Nikanfar M, et al. Interleukin-6, a reliable prognostic factor for ischemic stroke. *Iran J Neurol*. (2014) 13:70–6.

10.3389/fneur.2024.1323878

Glossary

BMI	Body mass index
GLM	General linear models
HDL	High-density lipoprotein
IL-6	Interleukin-6
IS	Ischemic stroke
LDL	Low-density lipoprotein
MIP-1α	Macrophage inflammatory protein-1alpha
MIP-1β	Macrophage inflammatory protein-1beta
MCP-1	Monocyte chemoattractant protein-1
MD	Mean differences
NIHSS	National Institutes of Health Stroke Scale
NSOL	Normal sleep onset latency
PSOL	Prolonged sleep onset latency
SOL	Sleep onset latency
SD	Standard deviation
TNFα	Tumor necrosis factor-alpha
TC	Total cholesterol
TG	Triacylglycerol

frontiers | Frontiers in Neurology

TYPE Original Research
PUBLISHED 21 August 2024
DOI 10.3389/fneur.2024.1321909

OPEN ACCESS

EDITED BY
Xia Wang,
University of New South Wales, Australia

REVIEWED BY
Cristofol Vives-Bauza,
University of the Balearic Islands, Spain
Karen M. Doyle,
University of Galway, Ireland

*CORRESPONDENCE
Jiyue Wang
✉ 13326356176@163.com
Liyong Zhang
✉ 13346256936@163.com

†These authors have contributed equally to this work and share first authorship

RECEIVED 15 October 2023
ACCEPTED 05 August 2024
PUBLISHED 21 August 2024

CITATION
Xu B, Yin T, Sun T, Lv H, Zhang W, Zan X, Hao J, Wang J and Zhang L (2024) Venous thrombolysis prior to mechanical thrombectomy reduces glycocalyx damage in patients with acute ischemic stroke. *Front. Neurol.* 15:1321909. doi: 10.3389/fneur.2024.1321909

Venous thrombolysis prior to mechanical thrombectomy reduces glycocalyx damage in patients with acute ischemic stroke

Bin Xu[1,2†], Tengkun Yin[1†], Tanggui Sun[1], Hang Lv[2,3], Wenyv Zhang[2], Xv Zan[2], Jiheng Hao[1], Jiyue Wang[1*] and Liyong Zhang[1,2*]

[1]Neurosurgery Department, Liaocheng People's Hospital, Liaocheng, China, [2]School of Clinical Medicine, Weifang Medical University, Weifang, China, [3]Joint Laboratory for Translational Medicine Research, Liaocheng People's Hospital, Liaocheng, Shandong, China

Introduction: The administration of intravenous thrombolysis (IVT) before mechanical thrombectomy (MT) in the treatment of acute ischemic stroke (AIS) has been a subject of debate, and its potential benefits remain uncertain. This retrospective study aimed to investigate the effect of preoperative IVT on glycocalyx damage in patients with cerebral ischemia-reperfusion injury (IRI).

Methods: A cohort of 106 patients with acute large vessel occlusion in the anterior circulation treated with mechanical thrombectomy was enrolled. The levels of the glycocalyx damage marker, syndecan-1, were measured in the peripheral blood of these patients to assess glycocalyx damage during IRI, and clinical outcomes were compared between patients receiving MT alone vs. combined IVT and MT.

Results: The study results indicate that thrombolytic drugs have a significant impact on syndecan-1 levels in the blood. Compared to patients who underwent direct MT, those who received preoperative IVT had significantly lower levels of syndecan-1 in their blood. Although preoperative IVT did not alter the final clinical outcomes, the levels of syndecan-1 shedding reflect the extent of damage to the endothelial glycocalyx.

Discussion: This suggests that using thrombolytic drugs before mechanical thrombectomy may reduce endothelial glycocalyx damage in patients with ischemia-reperfusion injury. These findings provide indirect clinical evidence supporting the preoperative use of intravenous thrombolysis in such patients.

KEYWORDS

thrombolysis, thrombectomy, glycocalyx, stroke, syndecan-1

Introduction

Stroke is a significant global health challenge, ranking as the second leading cause of disability and mortality worldwide (1). AIS is the most common form of stroke, accounting for ~87% of all stroke cases. It represents a critical medical emergency characterized by insufficient blood supply to the brain's blood vessels, resulting in damage to brain cells and potentially devastating consequences (2). Timely and effective treatment is crucial in managing AIS to minimize brain injury and improve patient outcomes.

In the management of AIS, IVT and MT are the primary first-line treatment approaches. IVT involves the use of fibrinolytic agents, such as recombinant tissue plasminogen activator (rt-PA), to promote fibrinolysis and dissolve blood clots, causing vessel occlusion. The rt-PA activates plasminogen to plasmin by cleaving the Arg^{561}-Val^{562} peptide bond (3). Plasminogen activation to plasmin plays a vital role in degrading fibrin and inhibiting clotting factors, which facilitates thrombus dissolution and restores blood flow (4, 5). Patients with AIS who do not ameliorate after IVT may benefit from transfer to a hospital where MT can be performed, which is known as bridging therapy (6).

MT is a minimally invasive procedure that employs endovascular instruments to directly remove the obstructive thrombus, thereby restoring blood flow in the brain tissue. However, the reestablishment of blood flow after a period of ischemia and hypoxia can lead to IRI, characterized by rapid tissue damage (7). This phenomenon triggers the production of excessive reactive oxygen species and nitrogen in the ischemic brain tissue, promoting the aggregation of pro-inflammatory immune cells at the injury site and causing endothelial glycocalyx dysfunction (8). The endothelial glycocalyx is a protective layer that lines the interior of blood vessels. It is composed of various components, including glycoproteins, proteoglycans such as heparan sulfate proteoglycans (including members of the syndecans family), and glycosaminoglycan side chains. This glycocalyx layer plays a critical role in preserving the integrity and functionality of blood vessels. In the field of stroke, it has also gained increasing attention as a novel marker of cerebral IRI.

Syndecan-1 is a transmembrane proteoglycan that is primarily expressed on the surface of endothelial cells. Under inflammatory and pathological conditions, proteases such as heparanase can cleave the extracellular domain of syndecan-1, causing it to shed into the extracellular matrix and enter the bloodstream. Elevated syndecan-1 levels in peripheral blood during IRI serve as a crucial marker of glycocalyx damage, indicating injury to this protective layer of endothelial cells (9). Our previous study highlighted a significant increase in syndecan-1 shedding during the hyperacute phase of AIS, and its dynamic changes are potentially linked to blood-brain barrier permeability (10). Currently, there is an ongoing controversy within the academic community regarding the effectiveness of bridging therapy with thrombolytic drugs before MT in AIS patients (11–15). However, it is worth noting that this approach is strongly recommended in the guidelines issued by European Stroke Organization (ESO)/European Society for Minimally Invasive Neurological Therapy (ESMINT) (16). The potential benefits of this treatment in preserving glycocalyx integrity and improving clinical outcomes require further investigation and clarification. In this study, our research objective is to observe syndecan-1 levels and evaluate whether preoperative treatment with conventional thrombolytic drugs preserves the integrity of the endothelial glycocalyx after IRI. Understanding the impact of preoperative thrombolytic therapy on glycocalyx preservation and patient prognosis could provide valuable insights for optimizing treatment strategies for IRI.

Abbreviations: IVT, Intravenous thrombolysis; MT, Mechanical thrombectomy; IRI, Ischemia-reperfusion injury; AIS, Acute ischemic stroke; rt-PA, Tissue plasminogen activator; NIHSS, National Institutes of Health Stroke Scale; mRS, Modified Rankin Scale; HPSE, Heparanase.

Materials and methods

Sample

Plasma samples were collected from eight healthy individuals aged 50–80 years and 106 AIS patients at Liaocheng People's Hospital between August 2020 and May 2022. Informed consent was obtained from all participants. The inclusion criteria were as follows: (1) age ≥18 years; (2) confirmation of anterior circulation cerebral vessel occlusion through computed tomography (CT) angiography or digital subtraction angiography (DSA); (3) all patients who underwent mechanical thrombectomy (MT) with retrieved stents and received standard medical therapy; (4) patients who received preoperative thrombolytic treatment after being treated with rt-PA; and (5) all patients who achieved successful reperfusion (modified treatment in cerebral infarction score ≥2b). The exclusion criteria included severe inflammatory disease, cancer, autoimmune disease, and cytostatic/immunosuppressive therapy within the past 3 months. Various data, including demographic characteristics, risk factors, occlusion position/cause, time from stroke onset to groin puncture/reperfusion success, stroke severity [National Institutes of Health Stroke Scale (NIHSS)], clinical outcome [modified Rankin Scale (mRS)], intracranial hemorrhage, malignant cerebral edema, and neurological deterioration, were prospectively collected. The NIHSS scores were obtained from patients at admission, 1 day post-operation, 7 days post-operation, and at discharge. Neurological deterioration was defined as an increase in the NIHSS score of ≥4 points during the patient's hospitalization (17).

Ethics approval was obtained from the local ethics committee.

In this retrospective study, due to the unclear association between thrombolytic drugs and syndecan-1 at a specific time point, we initially examined multiple time-point blood samples from 37 patients for a small-sample experiment. The levels of peripheral blood syndecan-1 were measured at different time points during IRI in 37 patients before MT, intraoperatively, and at 1 h, 1, 3, and 7 days after MT. The aim was to investigate the impact of thrombolytic drugs on syndecan-1 levels at various stages of IRI. Based on screening for the most sensitive time point (i.e., 1 h post-operation), the remaining 69 patients were further tested for syndecan-1 levels in peripheral blood at that time point to provide additional clarity to the research results. The total number of samples at this time is 106 (37 + 69).

Intraoperative blood was defined as the extraction of intracranial blood from the distal lesion vessels at the occlusion site using a microcatheter during surgery (18). During our intraoperative collection of distal blood, we relied on the research conducted by Kollikowski AM, which thoroughly delineates the technique for harvesting arterial blood from the core of occluded vessel lumens. For a comprehensive understanding of the procedural steps and accompanying videos, please refer to Kollikowski AM's study on local leukocyte invasion in hyperacute ischemic stroke (18). Before undertaking stent-embolus retrieval in conjunction with the distal aspiration technique, we initiated

the procedure with the insertion of micro guidewires and microcatheters, intricately maneuvering the microcatheter through the thrombotic occlusion site to obtain blood samples amid occlusive ischemic conditions. Upon successfully positioning the microcatheter, 1 mm of ischemic blood sample was extracted using a syringe for subsequent laboratory analysis.

All blood samples were centrifuged at 3,000 rpm for 10 min and promptly frozen at −80°C for subsequent analysis.

Syndecan-1 levels were measured using the Human Syndecan-1 ELISA kit (CD138) from Abcam (Cambridge, MA, USA, Cat No. ab46506).

Statistical analysis

The normality of each variable was tested using the Shapiro-Wilk test. Normally distributed continuous variables were presented as the ±mean standard deviation (SD), while non-normally distributed continuous variables were presented as the median with the interquartile range (IQR). Categorical variables were presented as numbers and percentages. The Student *t*-test or Mann-Whitney *U*-test was used for continuous variables, while the chi-squared test was used for categorical variables. The Wilcoxon rank-sum test was employed to analyze the dynamic changes in syndecan-1 levels at different time points. The primary objective was to compare syndecan-1 levels in the blood between patients who received thrombolytic drugs preoperatively and those who did not, as shown in Table 3. The comparison of syndecan-1 levels between the two groups was conducted using the Mann-Whitney *U*-test. For syndecan-1 levels detected 1 h post-operation, we included confounding factors in the generalized linear model analysis. Furthermore, clinical outcomes between the two groups were compared using odds ratios (OR) or β-coefficients with their 95% confidence intervals, which were analyzed using binary logistic regression models or generalized linear models. Multivariable models were adjusted for potential confounders such as age, sex, and admission NIHSS score.

Statistical analyses were performed using SPSS software (version 26.0), and significant differences were set at a *p*-value of ≤0.05.

Results

The study included 106 patients, with 66 patients in the IVT+MT group and 40 patients in the direct MT group. A study flowchart is shown in Figure 1. The mean age of the patients was 67 years (SD, ±11), and 74% of the participants were male. The median baseline NIHSS score was 19 points (IQR, 12–21). The median time from stroke onset to groin puncture was 294 min (IQR, 216–401), and the median time from stroke onset to recanalization was 400 min (IQR, 294–538). Among the 16 patients who received thrombolytic therapy at external hospitals, the median time from intravenous administration of thrombolytic drugs to femoral artery puncture was 393 min (IQR, 344–703). Excluding the patients treated at external hospitals, the median time from the intravenous administration of thrombolytic drugs to femoral artery puncture for the remaining patients was 61 min

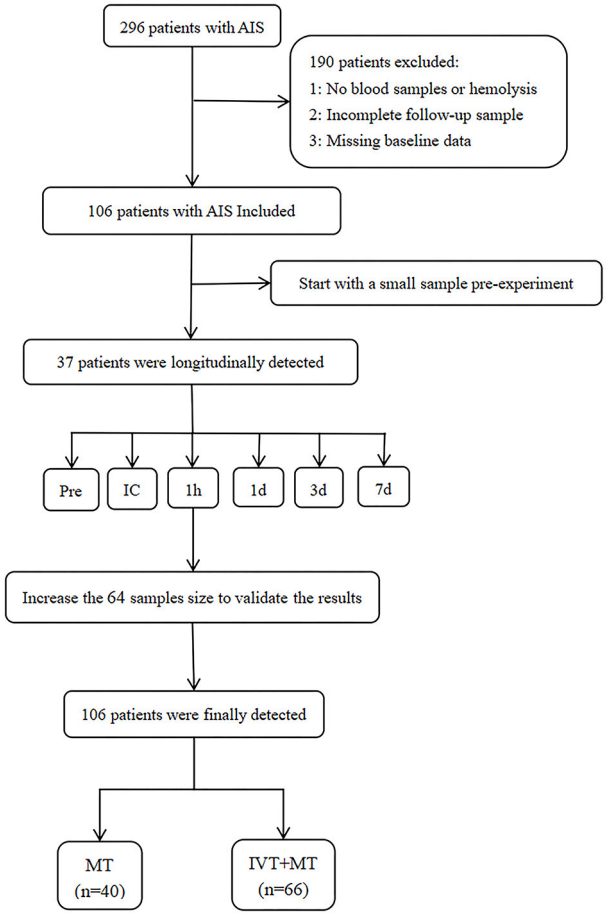

FIGURE 1
Study flowchart. AIS, Acute ischemic stroke; MT, Mechanical thrombectomy; IVT, Intravenous thrombolysis. Pre, preoperation; IC, intracranial; 1 h and 1 d =1 h and 1 day after MT.

(IQR, 40–109). Although the time from thrombolysis to femoral artery puncture was longer for patients who received thrombolysis at external hospitals than for those who were treated at our hospital, there was no significant difference in syndecan-1 levels between the two groups. The baseline characteristics of the study population are shown in Table 1. The median mRS follow-up score at 90 days was 3 (IQR, 0–5), and the mortality rate within 90 days was 21%. The baseline characteristics between the two groups are compared in Table 2. Baseline characteristics were counterbalanced between the two groups, except for the admission NIHSS score.

The longitudinal assessment of syndecan-1 levels in the peripheral blood of 37 patients at six time points showed a biphasic change after stroke occurrence, with the most significant increase observed at 1 h post-operation. Statistically significant changes were observed at each time point (Figure 2). There were also statistically significant differences in syndecan-1 levels between the two groups only during the intraoperative period and at 1 h post-operation ($p < 0.01$, Figure 3). Specifically, syndecan-1 levels in the blood of AIS patients who received preoperative thrombolysis were lower than those in the direct MT group (Table 3). At 1 h post-operation, the preoperative thrombolysis group showed

TABLE 1 Baseline characteristics of the study population ($n = 106$).

Sociodemographic characteristics	
Age, y	67 (11)
Male	78 (74)
Risk factors	
Smoking	33 (31)
Drinking	30 (28)
Previous stroke	20 (19)
Hypertension	62 (58)
Coronary artery disease	22 (21)
Atrial fibrillation	36 (34)
Diabetes	10 (19)
Hypercholesterolaemia	17 (16)
Cause of large-vessel occlusion	
Cardioembolism	51 (48)
Others/Unknown	55 (52)
Occlusion position	
Internal carotid artery occlusion	56 (43)
Middle cerebral artery occlusion	60 (57)
Clinical metrics	
Mean systolic blood pressure, mm Hg	153 (±23)
Mean diastolic blood pressure, mm Hg	88 (±12)
Admission NIHSS score	19 (13–29)
Time from stroke onset to groin puncture, min	294 (216–401)
Time from stroke onset to recanalization, min	400 (294–538)

Data are mean (±SD), n (%), median (IQR).
SD, Mean standard deviation; IQR, Interquartile range; NIHSS, National Institutes of Health Stroke Scale.

significantly lower levels of syndecan-1 compared to the direct MT group [median, 149 vs. 180 ng/ml; $\beta = -50.38$ [95% CI, −75.54 to −25.22]; $P < 0.001$; Figure 4]. The comparison of clinical outcomes between the two groups of patients is shown in Table 4.

Among the 106 patients who completed a 90-day follow-up, an adjusted binary logistic regression analysis showed no significant difference in the favorable clinical outcome (mRS score of 0–2) between the two groups [48 vs. 47%; adjusted OR, 0.655 [95% CI, 0.265–1.623]; $P = 0.361$]. There were no significant differences between the two groups regarding secondary and safety outcomes.

Discussion

In this study, we investigated the effect of preoperative IVT on glycocalyx damage in patients with IRI undergoing MT for AIS. For the first time, we discovered that preoperative thrombolytic drug administration before MT significantly reduced

TABLE 2 Baseline and procedural characteristics of patients treated with MT vs. those treated with IVT + MT.

Baseline and procedural characteristics	MT ($N = 40$)	IVT + MT ($N = 66$)	*P*-value
Sociodemographic characteristics			
Age, y	67 (10)	67 (11)	0.953
Sex, *n* (%)			0.515
Male	28 (70)	50 (76)	
Female	12 (30)	16 (24)	
Risk factors, *n* (%)			
Smoking	13 (33)	20 (30)	0.813
Drinking	14 (35)	16 (24)	0.233
Previous stroke	10 (25)	10 (15)	0.209
Hypertension	20 (50)	42 (64)	0.167
Coronary artery disease	5 (13)	17 (26)	0.103
Atrial fibrillation	15 (38)	21 (32)	0.549
Diabetes	4 (10)	11 (17)	0.505
Hypercholesterolaemia	8 (20)	9 (14)	0.387
The application of thrombolytic drug			
External hospital thrombolysis	-	16 (24)	
Median time from thrombolysis to groin puncture, min*	-	61 (40–109)	
Cause of large-vessel occlusion			0.762
Cardioembolism	20 (50)	31 (47)	
Others/unknown	20 (50)	35 (53)	
Occlusion position			0.885
Internal carotid artery occlusion	17 (42)	29 (44)	
Middle cerebral artery occlusion	23 (58)	37 (56)	
Clinical metrics			
Mean systolic blood pressure, mmHg	157 (±24)	150 (±22)	0.152
Mean diastolic blood pressure, mmHg	89 (±11)	87 (±12)	0.315
NIHSS score at admission	23 (15–33)	15 (12–22)	0.001
Median time from symptom onset to groin puncture, min	303 (222–523)	282 (208–362)	0.205
Median time from symptom onset to recanalization, min	432 (306–605)	383 (276–504)	0.164

Data are mean (±SD), n (%), and median (IQR).
SD, standard deviation; IQR, Interquartile range; MT, Mechanical thrombectomy; IVT+MT, Intravenous thrombolysis before mechanical thrombectomy; NIHSS, National Institutes of Health Stroke Scale.
*Median time from thrombolysis to groin puncture (N = 50): 16 patients who received thrombolytic treatment at external hospitals were excluded due to the inability to determine the exact timing of medication.

10.3389/fneur.2024.1321909

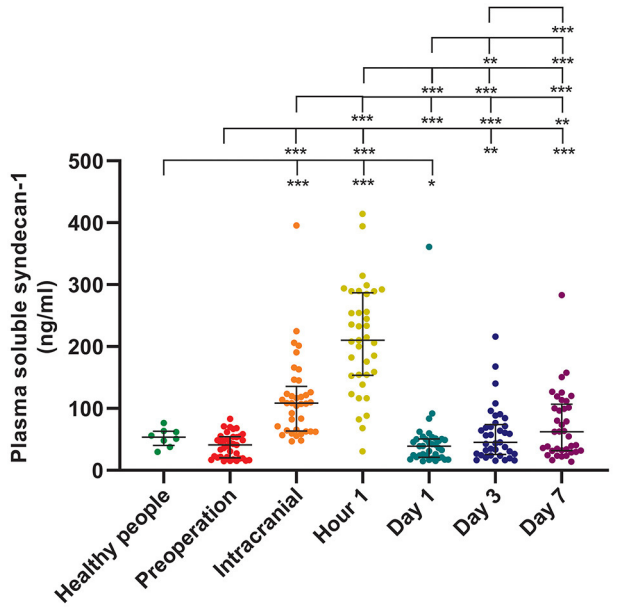

FIGURE 2
Syndecan-1 in the plasma of healthy individuals and longitudinally dynamics after AIS. Healthy individuals ($n = 8$); AIS patients ($n = 37$); *$p < 0.05$; **$p < 0.01$; ***$p < 0.001$. AIS, Acute ischemic stroke. Data presentation: median (line; 50th percentile) and whiskers (25–75th percentile).

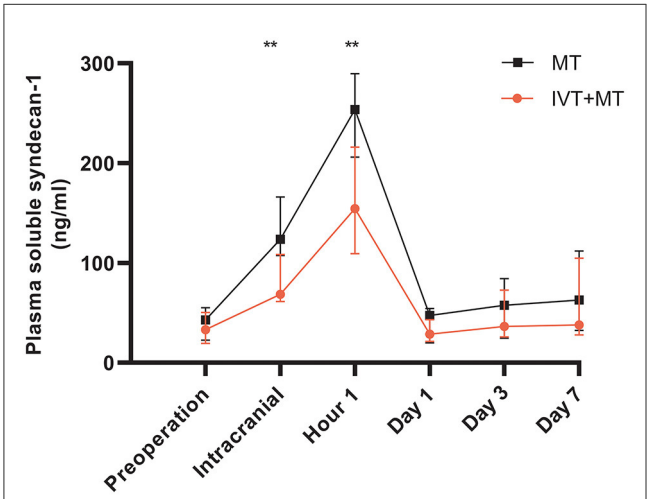

FIGURE 3
Longitudinally comparison of the MT and IVT+MT. MT, Mechanical thrombectomy ($n = 19$); IVT+MT, Intravenous thrombolysis before mechanical thrombectomy ($n = 18$); IQR, Interquartile range. **$P < 0.01$. Data presentation: median, IQR (whiskers).

the levels of syndecan-1, a marker of glycocalyx damage, in the blood.

Thrombolytic drugs were found to reduce syndecan-1 levels in the blood, with the most significant effect observed from the intraoperative period to 1 h post-operation. Alteplase exhibits specificity for fibrin, primarily targeting plasminogen and fibrin in the coagulation process, with relatively minimal impact on other biological molecules (pharmacokinetics of alteplase in treating ischemic stroke). The current literature does not explicitly suggest that alteplase directly degrades syndecan-1 after administration. Therefore, the likelihood of alteplase directly degrading syndecan-1 appears low. It may influence syndecan-1 shedding through indirect pathways, particularly impacting the shedding of glycocalyx on endothelial cell surfaces. This finding indicates that thrombolytic drugs may have a certain inhibitory effect on syndecan-1 shedding, thereby preserving the integrity of the endothelial glycocalyx. Thrombolytic drugs achieve their fibrinolytic effect by activating plasminogen to plasmin, which degrades fibrinogen and various coagulation factors such as Factor V (5, 19). Coagulation factor V serves as a cofactor and forms a prothrombinase complex with coagulation factor X, leading to the cleavage of prothrombin during endothelial or cerebral injury, ultimately activating thrombin (20, 21). The activated thrombin then releases heparanase (HPSE) from platelets and granulocytes into the blood by interacting with protease-activated receptor 1 (22).

HPSE is an endoglycosidase that specifically cleaves heparan sulfate chains in the endothelial glycocalyx, leading to the enhanced shedding of syndecan-1 (23, 24). Based on an extensive review of relevant literature, we suggest that thrombolytic drugs may inhibit the shedding of syndecan-1 through the thrombin-HPSE pathway. Existing research has confirmed that syndecan-1 is an important biomarker in response to glycocalyx damage caused by IRI (9). Consequently, thrombolytic drugs may alleviate glycocalyx damage caused by ischemia-reperfusion through the thrombin-HPSE pathway.

Moreover, we found that thrombolytic drugs have a significant effect on syndecan-1 levels from the intraoperative period to 1 h post-operation. However, after more than 24 h post-operation, there were no significant differences in syndecan-1 levels between the two groups. This observation is consistent with the pharmacokinetics of alteplase, which is a thrombolytic drug used in the study (25). In patients who underwent preoperative thrombolytic therapy in our hospital, the preoperative peripheral blood samples were collected ~61 min (40–109) after the administration of thrombolytic drugs. At this time point, syndecan-1 levels in the blood were not affected by the thrombolytic drugs, indicating that the effect of thrombolytic drugs on syndecan-1 was not immediate and could only be observed after a delay of at least 1 h. We compared preoperative syndecan-1 levels with data from healthy individuals and found no significant difference between them. The delayed effect of thrombolytic drugs on syndecan-1 may be because, at the time of preoperative blood collection, syndecan-1 on the surface of the endothelial glycocalyx has not yet undergone significant shedding (26), resulting in the limited observed drug efficacy. It could also simply be due to the fact that thrombolytic agents reduce thrombosis, thereby simplifying the thrombectomy process, alleviating endothelial stress, and resulting in lower syndecan-1 levels in the blood both during and after the procedure.

Furthermore, our study did not reveal any significant clinical benefits in bridging therapy patients when comparing the clinical outcomes between the two groups. While the DIRECT-SAFE (27) and SWIFT DIRECT (15) studies suggest that the combined strategy of IVT before MT is not associated with clinical benefits,

TABLE 3 The syndecan-1 levels of patients treated with MT vs. those treated with IVT + MT.

Syndecan-1 (ng/ml)	MT ($N = 40$)	IVT and MT ($N = 66$)	*P*-value*	Adjusted effect size (95% CI)**	*P*-value
1 h post-operation	180 (147–252)	149 (116–167)	0.001	−50.38 (−75.54 to −25.22)	0.000
Longitudinally syndecan-1 (ng/ml)	$N = 19$	$N = 18$			
Pre-operation	43 (23–55)	33 (19–50)	0.395	-	-
Intraoperative	124 (108–166)	68 (61–108)	0.001	-	-
1 h post-operation	254 (206–290)	154 (109–216)	0.001	-	-
1 day post-operation	47 (20–54)	29 (21–43)	0.095	-	-
3 days post-operation	57 (25–84)	36 (26–73)	0.584	-	-
7 days post-operation	63 (32–112)	38 (28–105)	0.584	-	-

Data are median (IQR).
IQR, Interquartile range.
*Mann-Whitney U-test.
**Adjusted for age, sex, and NIHSS score at admission. The β-coefficients were calculated using a generalized linear model.

the SWIFT DIRECT trial revealed a favorable prognosis rate of 65% in the IVT + MT group compared to the rate of 57% in the group undergoing direct MT. This finding suggests a trend favoring the adoption of a bridging treatment strategy in the SWIFT DIRECT trial, despite previous research indicating that elevated peripheral blood syndecan-1 levels could predict poor outcomes in AIS patients undergoing thrombolytic therapy (28). Our study found no predictive value of syndecan-1 levels in 106 patients for clinical outcomes. The lack of predictive value might be attributed to the inconsistency in the timing of the studies. It is worth noting that syndecan-1 plays a specific role in the pathophysiological processes at various stages of brain tissue injury after stroke. This finding suggests that the dynamics of syndecan-1 levels and their effects on clinical outcomes could be complex and multifactorial. We are conducting a prospective study with a substantial sample size, multiple time points, and an array of markers pertaining to glycocalyx injury. Our primary objective from a clinical perspective is to further validate the impact of thrombolytic drugs on glycocalyx and clinical outcomes in AIS patients. We also seek to confirm the involvement of the thrombin-HPSE pathway, which could shed light on the underlying mechanisms of thrombolytic drug effects on glycocalyx.

However, we must acknowledge certain limitations of this study. First, the sample size and the low proportion of female participants might not be sufficient to ensure the utmost statistical stability and generalizability of the results. There is a significant difference in NIHSS scores upon admission between the mechanical thrombectomy group and the bridging therapy group, which may affect the results. We could not obtain microcirculation vascular imaging data, which hinders our analysis of whether the IVT + MT bridging strategy also facilitates reperfusion of small brain vessels. Therefore, we remain committed to recruiting more patients and incorporating the evaluation of microcirculation vascular imaging data into subsequent clinical data, ensuring the availability of a robust dataset for analysis. Second, practical constraints hindered our ability to perform simultaneous measurements of syndecan-1, HPSE, and coagulation factors in the blood at the same time point for each patient. Addressing this limitation could provide valuable insights into their correlation and validate the thrombin-HPSE pathway. Finally, we recognize that relying solely on syndecan-1 as a single marker of glycan shedding might not offer comprehensive evidence of glycocalyx damage. To address this limitation, we plan to investigate multiple glycocalyx markers and conduct foundational research on relevant pathophysiological mechanisms in the future to further validate the safety and reliability of this conclusion.

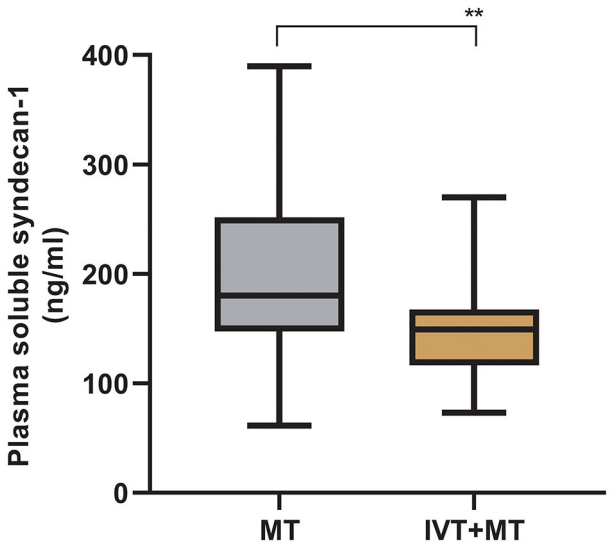

FIGURE 4
Comparison of syndecan-1 levels between MT and IVT+MT at 1-h post-operation. MT, Mechanical thrombectomy ($n = 66$); IVT+MT, Intravenous thrombolysis before mechanical thrombectomy ($n = 40$), $^{**}P < 0.01$. The "box" depicts the median and the 25 and 75th quartiles, and the "whisker" shows the 5 and 95th percentile.

TABLE 4 Clinical outcomes of patients treated with MT vs. those treated with IVT + MT.

Clinical outcomes	MT ($N = 40$)	IVT + MT ($N = 66$)	Effect size (95% CI)	*P*-value	Adjusted effect size (95% CI)*	*P*-value
Primary outcome						
90-day mRS (0–2)	19 (48)	31 (47)	0.979 (0.446–2.150)	0.958	0.655 (0.265–1.623)†	0.361
Secondary outcomes						
90-day mRS (0–1)	14 (35)	27 (41)	1.286 (0.570–2.902)	0.545	0.807 (0.317–2.053)†	0.652
90-day mRS (0–3)	24 (60)	37 (56)	0.851 (0.383–1.889)	0.691	0.539 (0.214–1.359)†	0.190
NIHSS score at 1 day	19 (12–25)	15 (10–23)	−2.646 (-6.471–1.178)	0.175	1.075 (-2.170–4.319)‡	0.516
NIHSS score at 7 days	17 (6–25)	12 (6–19)	−3.370 (-7.920–1.179)	0.146	0.405 (-3.581–4.390)‡	0.842
Discharge NIHSS score	15 (5–28)	11 (5–19)	−3.344 (-8.252–1.564)	0.182	−0.132 (-4.582–4.318)‡	0.954
Discharge mRS (0–2)	13 (33)	21 (32)	0.969 (0.418–2.246)	0.942	0.505 (0.183–1.394)†	0.187
Safety outcomes						
Death within 90 days	8 (20)	14 (21)	1.077 (0.407–2.852)	0.881	1.539 (0.479–4.947)†	0.470
Any ICH within 24 h	11 (28)	18 (27)	0.989 (0.410–2.384)	0.980	1.247 (0.472–3.297)†	0.656
Malignant brain edema	10 (25)	11 (17)	0.600 (0.229–1.575)	0.300	0.910 (0.306–2.704)†	0.865
Neurological deterioration	10 (25)	22 (33)	1.500 (0.622–3.616)	0.368	1.779 (0.693–4.568)†	0.231

Data are median (IQR), n (%).
IQR, Interquartile range; MT, Mechanical thrombectomy; IVT+MT, Intravenous thrombolysis before mechanical thrombectomy; mRS, modified Rankin Scale; NIHSS, National Institutes of Health Stroke Scale; ICH, Intracranial hemorrhage; NIHSS, National Institutes of Health Stroke Scale; OR, odds ratio.
*Adjusted for age, sex, and admission NIHSS score.
†The OR values were calculated using a binary logistic regression model.
‡The β-coefficients were calculated using a generalized linear model.

Conclusion

Our study indicates that administering pre-thrombectomy intravenous thrombolytics in AIS patients can effectively reduce the shedding of syndecan-1. This reduction may be attributed to the potential impact of thrombolytic drugs on the thrombin-HPSE pathway, thereby mitigating endothelial glycocalyx damage caused by IRI. This finding may indirectly support bridging therapy and provide a new research perspective on how thrombolytic drugs benefit AIS patients. However, further validation studies will be necessary to gain a deeper understanding of this mechanism and explore its potential therapeutic applications.

Data availability statement

The original contributions presented in the study are included in the article/supplementary material, further inquiries can be directed to the corresponding authors.

Ethics statement

The studies involving humans were approved by the Medical Ethics Committee of Liaocheng People's Hospital (No. 20191130016). The studies were conducted in accordance with the local legislation and institutional requirements. The participants provided their written informed consent to participate in this study. Written informed consent was obtained from the individual(s) for the publication of any potentially identifiable images or data included in this article.

Author contributions

BX: Conceptualization, Data curation, Formal analysis, Methodology, Project administration, Visualization, Writing – original draft, Writing – review & editing. TY: Conceptualization, Data curation, Supervision, Validation, Writing – review & editing. TS: Data curation, Formal analysis, Visualization, Writing – original draft. HL: Data curation, Supervision, Validation, Writing – review & editing. WZ: Conceptualization, Formal analysis, Visualization, Writing – review & editing. XZ: Data curation, Validation, Visualization, Writing – original draft. JH: Conceptualization, Funding acquisition, Project administration, Supervision, Writing – review & editing. JW: Formal analysis, Funding acquisition, Project administration, Supervision, Writing – review & editing. LZ: Conceptualization, Funding acquisition, Project administration, Supervision, Writing – review & editing.

Funding

The author(s) declare financial support was received for the research, authorship, and/or publication of

this article. This study was supported by the Clinical Research Team of Liaocheng People's Hospital, the 2020 Shandong Provincial Medical Association Umbilical Cord Blood Research Special Fund Project (grant number: YXH2020ZX002, LZ) and the Medical and Health Science and Technology Development Project of Shandong Province (grant number: 202104040390, TY).

Acknowledgments

We acknowledge the efforts of Yaming Fan, Conghui Tian, Xinxin Sun, and Xiaodong Jia.

Conflict of interest

The authors declare that the research was conducted in the absence of any commercial or financial relationships that could be construed as a potential conflict of interest.

Publisher's note

References

1. GBD 2016 Stroke Collaborators. Global, regional, and national burden of stroke, 1990–2016: a systematic analysis for the Global Burden of Disease Study 2016. *Lancet Neurol.* (2019) 18:439–58. doi: 10.1016/S1474-4422(19)30034-1

2. Saini V, Guada L, Yavagal DR. Global epidemiology of stroke and access to acute ischemic stroke interventions. *Neurology.* (2021) 97(20Suppl.2):S6–16. doi: 10.1212/WNL.0000000000012781

3. Schaller J, Gerber SS. The plasmin-antiplasmin system: structural and functional aspects. *Cell Mol Life Sci.* (2011) 68:785–801. doi: 10.1007/s00018-010-0566-5

4. Hur WS, Mazinani N, Lu XJD, Britton HM, Byrnes JR, Wolberg AS, et al. Coagulation factor XIIIa is inactivated by plasmin. *Blood.* (2015) 126:2329–37. doi: 10.1182/blood-2015-07-650713

5. Zeibdawi AR, Pryzdial EL. Mechanism of factor VA inactivation by plasmin. Loss of A2 and A3 domains from a Ca^{2+}-dependent complex of fragments bound to phospholipid. *J Biol Chem.* (2001) 276:19929–36. doi: 10.1074/jbc.M004711200

6. Walter K. What is acute ischemic stroke? *J Am Med Assoc.* (2022) 327:885. doi: 10.1001/jama.2022.1420

7. Kalogeris T, Baines CP, Krenz M, Korthuis RJ. Cell biology of ischemia/reperfusion injury. *Int Rev Cell Mol Biol.* (2012) 298:229–317. doi: 10.1016/B978-0-12-394309-5.00006-7

8. Kalogeris T, Baines CP, Krenz M, Korthuis RJ. Ischemia/reperfusion. *Compr Physiol.* (2016) 7:113–70. doi: 10.1002/cphy.c160006

9. Abassi Z, Armaly Z, Heyman SN. Glycocalyx degradation in ischemia-reperfusion injury. *Am J Pathol.* (2020) 190:752–67. doi: 10.1016/j.ajpath.2019.08.019

10. Yin T, Hao J, Jiang Q, Xu X, Xu B, Lv H, et al. Dynamics of intracranial and peripheral plasma Syndecan-1 after ischemic stroke with large vessel occlusion. *CNS Neurosci Ther.* (2022) 2022:13898. doi: 10.1111/cns.13898

11. Katsanos AH, Tsivgoulis G. Is intravenous thrombolysis still necessary in patients who undergo mechanical thrombectomy? *Curr Opin Neurol.* (2019) 32:3–12. doi: 10.1097/WCO.0000000000000633

12. Ahmed N, Mazya M, Nunes AP, Moreira T, Ollikainen JP, Escudero-Martínez I, et al. Safety and outcomes of thrombectomy in ischemic stroke with vs. without IV thrombolysis. *Neurology.* (2021) 97:e765–76. doi: 10.1212/WNL.0000000000012327

13. Du H, Lei H, Ambler G, Fang S, He R, Yuan Q, et al. Intravenous thrombolysis before mechanical thrombectomy for acute ischemic stroke: a meta-analysis. *J Am Heart Assoc.* (2021) 10:e022303. doi: 10.1161/JAHA.121.022303

14. Tong X, Wang Y, Fiehler J, Bauer CT, Jia B, Zhang X, et al. Thrombectomy versus combined thrombolysis and thrombectomy in patients with acute stroke: a matched-control study. *Stroke.* (2021) 52:1589–600. doi: 10.1161/STROKEAHA.120.031599

15. Fischer U, Kaesmacher JS, Plattner P, Bütikofer L, Mordasini P, Deppeler S, et al. SWIFT DIRECT: Solitaire™ with the intention for thrombectomy plus intravenous t-PA versus DIRECT SolitaireTM stent-retriever thrombectomy in acute anterior circulation stroke: methodology of a randomized, controlled, multicentre study. *Int J Stroke.* (2022) 17:698–705. doi: 10.1177/17474930211048768

16. Turc G, Tsivgoulis G, Audebert HJ, Boogaarts H, Bhogal P, De Marchis GM, et al. European Stroke Organisation (ESO)-European Society for Minimally Invasive Neurological Therapy (ESMINT) expedited recommendation on the indication for intravenous thrombolysis before mechanical thrombectomy in patients with acute ischemic stroke and anterior circulation large vessel occlusion. *J Neurointerv Surg.* (2022) 14:209. doi: 10.1136/neurintsurg-2021-018589

17. Saleem Y, Nogueira RG, Rodrigues GM, Kim S, Sharashidze V, Frankel M, et al. Acute neurological deterioration in large vessel occlusions and mild symptoms managed medically. *Stroke.* (2020) 51:1428–34. doi: 10.1161/STROKEAHA.119.027011

18. Kollikowski AM, Schuhmann MK, Nieswandt B, Müllges W, Stoll G, Pham M. Local leukocyte invasion during hyperacute human ischemic stroke. *Ann Neurol.* (2020) 87:466–79. doi: 10.1002/ana.25665

19. Murray V, Norrving B, Sandercock PaG, Terént A, Wardlaw JM, Wester P. The molecular basis of thrombolysis and its clinical application in stroke. *J Intern Med.* (2010) 267:191–208. doi: 10.1111/j.1365-2796.2009.02205.x

20. Dahlbäck B. Blood coagulation. *Lancet.* (2000) 355:1627–32. doi: 10.1016/S0140-6736(00)02225-X

21. Chen B, Cheng Q, Yang K, Lyden PD. Thrombin mediates severe neurovascular injury during ischemia. *Stroke.* (2010) 41:2348–52. doi: 10.1161/STROKEAHA.110.584920

22. Tatour M, Shapira M, Axelman E, Ghanem S, Keren-Politansky A, Bonstein L, et al. Thrombin is a selective inducer of heparanase release from platelets and granulocytes via protease-activated receptor-1. *Thromb Haemost.* (2017) 117:1391–401. doi: 10.1160/TH16-10-0766

23. Ramani VC, Pruett PS, Thompson CA, DeLucas LD, Sanderson RD. Heparan sulfate chains of syndecan-1 regulate ectodomain shedding. *J Biol Chem.* (2012) 287:9952–61. doi: 10.1074/jbc.M111.330803

24. Huang X, Reye G, Momot KI, Blick T, Lloyd T, Tilley WD, et al. Heparanase promotes syndecan-1 expression to mediate fibrillar collagen and mammographic density in human breast tissue cultured *ex vivo*. *Front Cell Dev Biol.* (2020) 8:599. doi: 10.3389/fcell.2020.00599

25. Tanswell P, Seifried E, Su PCAF, Feuerer W, Rijken DC. Pharmacokinetics and systemic effects of tissue-type plasminogen activator in normal subjects. *Clin Pharmacol Ther.* (1989) 46:155–62. doi: 10.1038/clpt.1989.120

26. Zhang YN, Wu Q, Zhang NN, Chen HS. Ischemic preconditioning alleviates cerebral ischemia-reperfusion injury by interfering with glycocalyx. *Transl Stroke Res.* (2022) 22:1081. doi: 10.1007/s12975-022-01081-w

27. Yang P, Zhang Y, Zhang L, Zhang Y, Treurniet KM, Chen W, et al. Endovascular thrombectomy with or without intravenous alteplase in acute stroke. *N Engl J Med.* (2020) 382: 1981–93. doi: 10.1056/NEJMoa2001123

28. Zhao F, Wang R, Huang Y, Li L, Zhong L, Hu Y, et al. Elevated plasma syndecan-1 as a glycocalyx injury marker predicts unfavorable outcomes after rt-PA intravenous thrombolysis in acute ischemic stroke. *Front Pharmacol.* (2022) 13:949290. doi: 10.3389/fphar.2022.949290

Frontiers in Neurology

Explores neurological illness to improve patient care

The third most-cited clinical neurology journal explores the diagnosis, causes, treatment, and public health aspects of neurological illnesses. Its ultimate aim is to inform improvements in patient care.

Discover the latest Research Topics

See more →

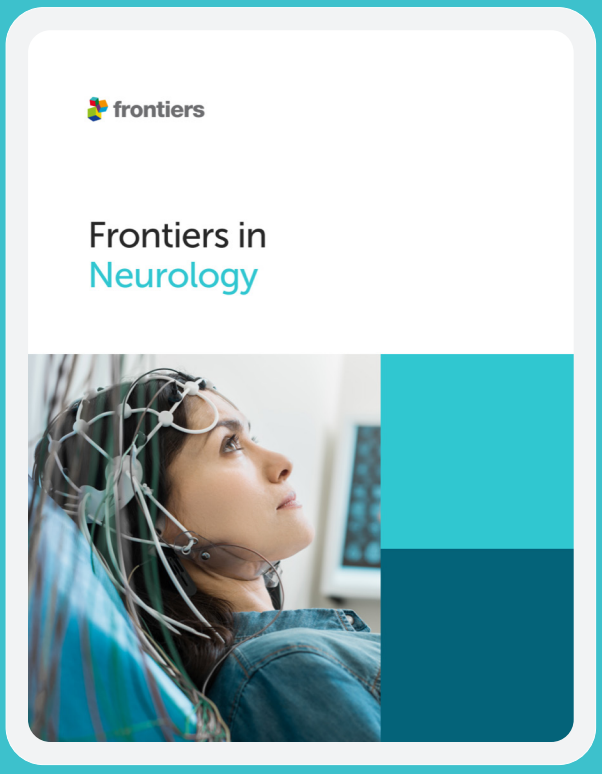

Frontiers

Avenue du Tribunal-Fédéral 34
1005 Lausanne, Switzerland
frontiersin.org

Contact us

+41 (0)21 510 17 00
frontiersin.org/about/contact